The efficacy of surface polishing clinically available internal fixation materials for ease of removal

Jessica Susan Hayes

Submitted for the degree of Ph.D. to the University of Wales, Cardiff, UK.

June 2008

AO Foundation

AO Research Institute
Clavadelerstrasse, 8
Davos Platz, CH7270
Switzerland.

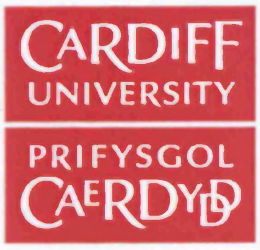

Cardiff School of Biosciences
Cardiff University
Museum Avenue
CF10 3US
Wales, UK.

ProQuest LLC
789 East Eisenhower Parkway
P.O. Box 1346
Ann Arbor, MI 48106-1346

Murphy's law:

Nothing is as easy as it looks.
Everything takes longer than you expect.
And if anything can go wrong,
It will, at the worst possible moment.

Thesis abstract:

Removal of fracture fixation devices due to symptomatic or asymptomatic reasons is a costly procedure which is further increased when complications are encountered. One of the main difficulties faced by a surgeon is a timely and successful removal of the device due to excessive bone overgrowth. Due to the increased time required for removal of the bone from the device, complications such as increased surgery time, excessive blood loss, debris contamination and implant breakage are often encountered. Practically all internal fixation systems such as locking compression plate constructs, and intramedullary nails, are fabricated for clinics with a micro-rough surface. However, it is well known, that surface micro-topography can be a major factor in determining the type, and extent of tissue integration. Despite the knowledge that surface microtopography can be a major determinant of osseointegration, this avenue has only been investigated for applications requiring accelerated bony integration and has not previously been explored as a potential resolution to issues involving device removal. Thus, we hypothesise that reducing the surface micro-topography of clinically available materials will reduce the incidence of excessive bony over-growth, and consequently will ease implant removal.

To investigate this hypothesis, we first characterised, using atomic force microscopy, scanning electron microscopy, contact angle, and white light profilometry, changes in the surface micro-topography of the clinically available materials commercially pure titanium (cpTi), titanium-6%aluminum-7%niobium (TAN), and titanium-15%molybdenum (Ti15Mo) in their standard micro-rough form, as well as in their experimental electropolished, and paste polished form. Stainless steel (Ss) was included as the orthopaedic grade 'smooth' surface control. Additionally, we employed X-ray photoelectron spectroscopy to examine the changes, if any, in the chemical composition of the surfaces. Overall, it was shown that both electropolishing and paste polishing techniques were successful at reducing the micro-roughness of the respective materials, as well as producing a smoothened surface morphologically. As all surfaces were anodised subsequent to polishing, alterations in the surface chemical composition were not evident.

Initial *in vitro* analysis, which involved culturing rat calvarial cells on the various surfaces, showed that surface polishing did not significantly influence cell growth compared to standard micro-rough counterparts. Furthermore, viability on these surfaces was not found to be significantly different from standard micro-rough samples, indicating that overall, surface polishing does not affect the cytocompatibility of cpTi, TAN or Ti15Mo. However, paste polished TAN was found to be the exception. Specifically, viability was significantly reduced on this surface compared to standard micro-rough TAN. While cell growth was not significantly affected on paste polished TAN, it was observed that initial cell attachment for this surface was lower compared to standard micro-rough TAN. Fluorescent labelling of the cytoskeletal components actin, tubulin and vinculin revealed that cell morphology was differentially influenced by the various surface morphologies. Generally, polished surfaces advocated a more well spread, elongated phenotype compared to the cuboidal phenotype noted for cells cultured on micro-rough surfaces. Paste polished TAN and standard micro-rough TAN samples also showed some degree of cytoskeletal disruption attributable to the inherent presence of beta-phase particles on their surface. Subsequent analysis of genotype, using real time PCR technology, revealed that for cpTi, TAN and Ti15Mo samples, surface polishing essentially provokes its influence in different manners at initial stages of differentiation and consequently then similarly at the later stages of terminal differentiation, and that the magnitude of this effect is material dependent..

Subsequently, we applied surface polishing technology to two clinically relevant internal fixation systems, namely locking compression plates (LCP) and screws, and intramedullary nails (IM), to assess if surface polishing holds potential for reducing implant removal related morbidity. In our LCP model electropolished, paste polished and standard TAN cortical screws were evaluated in combination with electropolished, paste polished and standard cpTi plates, respectively, with stainless steel screws and plates included as a control system. Samples were implanted in a bilateral non-fracture sheep tibia model for 6, 12 and 18 months. At each timepoint, removal torque and percentage of bone contact were quantified for each screw type. Results indicate that both polishing techniques significantly reduce the torque removal required for cortical screws, compared to standard micro-rough cortical screws. Histomorphometric analyses indicated that polished constructs showed a trend for reduced bone contact, however, this was only found to be significantly different for paste polished screws. In our second *in vivo* model, IM nails fabricated from standard micro-rough TAN and paste polished TAN were implanted in a bilateral, non-fracture sheep model for 12 months. Control animals were implanted with Ss IM nails and standard micro-rough TAN IM nails in the contralateral tibia. Results indicate that surface polishing of TAN IM nails, significantly reduces the pull out force required for extraction, compared to standard micro-rough TAN IM nails and therefore, this surface modification may be used to improve IM technology for reducing removal related complications.

Combined, these results indicate that surface polishing holds great potential for reducing the occurrence of implant removal related morbidity. We believe that this technology will be used to improve approaches to fracture fixation, especially within the paediatric population, where removal procedures are commonplace.

List of contents:

Acknowledgements:

I am reminded of the old Irish saying 'Is fada an bothár nach mbíonn casadh ann,' or in other words, 'it is a long road that has no turning'. Never was a proverb so aptly used when I consider what it has taken to get to this point! However, as with every work of this kind, its completion relies not only on the person that has undertaken it but family, friends and colleagues who have offered support of some kind or another for the duration. I know I haven't always made it easy!

To my Mum, Dad and sister, who, let's face it, have little interest in knowing what I do (no, Mum, I am still not doing forensic science!) but as always offer their unwavering love and support, and remind me that stubbornness can be a positive trait☺. You lot drive me crazy, but mean the absolute world to me. I especially would like to thank my Mum for her advice, and sacrifices to help get me here. A special thanks to Declan. There are no words to let you know how grateful I am for your support.

I would like to say a huge thank you to all people in Cardiff University, and the AO Research Institute, Davos that have helped me along the way. So many of you have offered help and advice, it does not seem right to name you as I am bound to forget someone. A special thanks to all that helped from the experimental surgery, histology, and mechanical testing group, as well as Pamela and Christoph for their technical help and Karsten for his invaluable help with statistical analyses. But to those I have not named, and you know who you are, thank you.

Finally, I would like to thank my two supervisors Geoff Richards, and Charlie Archer. Your guidance over the years has been invaluable. Thank you so much for the wonderful opportunities you have given me. Thank you for always having confidence I would finally get to the end....even if I didn't always believe you ☺

To, my nanny Sheila – this is for you.

Abstracts & papers:

List of abstracts accepted for oral or poster presentation related to this PhD study.

Vos, DI; Hayes, JS; Hahn, J; Pearce, SG; Richards, RG *An evaluation of surface polishing of TAN intramedullary nails for ease of removal in an animal model.* 24th Orthopaedic Trauma Association, Denver, Colorado, USA, 2008. number 34 OTA-2008 (Poster)

Hayes, JS; Archer, CW; Richards, RG. *Control of osteoblast genotype with surface microtopography.* European cells & Materials, Davos, Switzerland, 2008. Vol 16: Supplement 02. pp22 (Oral)

Hayes, J.S; Seidenglanz, U; Pearce, SG; Archer, CW; Richards, RG. *Surface polishing positively influences ease of fracture fixation plate & screw removal, & the surgical time required for extraction.* European cells & Materials, Davos, Switzerland, 2008. Vol 16: Supplement 02. pp57 (Poster)

Hayes, JS Vos, DI; Hahn, J; Pearce, SG; Richards, RG. *Surface polishing eases intramedullary nail removal – a novel in vivo study.* European cells & Materials, Davos, Switzerland, 2008. Vol 16: Supplement 02. pp58 (Poster)

Hayes, JS; Archer, CW; Richards, RG *An in vitro evaluation for understanding the role of surface microtopography in controlling tissue integration.* 8th World Biomaterials Congress, Amsterdam, Netherlands, 2008. Vol: 8, P-Thu-H-508 (Poster)

Hayes, JS; Vos, DI; Hahn, J; Pearce, SG; Richards, RG. *Surface polishing of TAN intramedullary nails eases removal – an in vivo study.* Swiss Bone and Mineral Society, Davos, Switzerland, 2008. (Oral)

Hayes, JS; Vos, DI; Hahn, J; Pearce, SG; Richards, RG. *Effect of surface polishing of TAN intra-medullary nails upon bone tissue adhesion and ease of nail removal – an in vivo study.* 54th Orthopaedic Research Society Conference, San Francisco, USA, 2008. Vol: 33, paper number 1044 (Poster)

Hayes, JS; Archer, CW; Richards, RG. *The Potential of Surface Polishing for Elective Internal Fixator Retrieval.* 21st European Society of Biomaterials, Brighton, UK, 2007. presentation number SFM109 (Oral)

Hayes, JS; Archer, CW; Richards, RG. *Implant osseointegration: in vitro analysis of titanium microtopography.* European Cells and Materials, Davos, Switzerland, 2007. Vol 14: Supplement 01. pp20 (Oral)

Hayes, JS; Archer, CW; Richards, RG. *In vitro effect of surface polishing for reducing bony-overgrowth.* 13th Swiss Society for Biomaterials, Neuchâtel, Switzerland, 2007. Transactions in ECM journal: Vol. 13. Suppl. 3, pp 9 (Oral)

Hayes, JS; Archer, CW; Richards, RG. *In vitro effects of surface polishing on osteoblast behaviour – potential for reducing extraosseous formation for implant retrieval.* 13th Swiss Bone and Mineral Society, Zurich, Switzerland, 2007. (Oral)

Hayes, JS; Archer, CW; Richards, RG. *Reducing Bone Encasement of Metal Implants for Elective Removal.* 53rd Orthopaedic Research Society Conference, San Diego, USA, 2007. Vol: 32, paper number 1630 (Poster)

Hayes JS, Archer CW, Richards RG: Controlling hard tissue integration at the bone-implant interface. AO BAB Symposium, Lausanne 2006

Hayes, JS; Archer, CW; Richards, RG. *Controlling hard tissue integration at the bone-implant interface.* 20th European Society of Biomaterials, Nantes, France, 2006. (Poster)

Hayes, JS; Archer, CW; Richards, RG. *The effect of surface topogrpahy in controlling tissue integration.* 52nd Orthopaedic Research Society Conference, Chicago, USA, 2006. Vol: 31, paper number 0861 (Poster)

Hayes, JS; Archer, CW; Richards, RG. *The effect of surface topography of metals used in internal fracture fixation on osteoblast-like cells.* 19th European Society of Biomaterials, Sorrento, Italy, 2005. (Oral)

List of papers submitted related to this PhD study.

Surface polishing positively influences ease of fracture fixation plate & screw removal, & the surgical time required for extraction. JS Hayes, U. Seidenglanz, SG Pearce, CW Archer, RG Richards. Submitted to J.Bone & Joint Surg (Am)

An in vivo evaluation of surface polishing of TAN intramedullary nails for ease of removal. JS Hayes; DI Vos; SG Pearce; RG Richards. Submitted to J.Orthop. Res.

The role of surface microtopography in the modulation of osteoblast phenotype. JS Hayes; IM Khan; CW Archer; RG Richards. Submitted to Eur Cell and Mat.

Index of figures & tables:

Chapter 1: General introduction

Chapter 2: Surface characterisation

Chapter 3: Cell growth kinetics, viability, morphology & cytoskeletal organisation

Chapter 4: Analysis of genotype

Chapter 5: Efficacy of surface polishing for locked plate constructs screw removal – an *in vivo* evaluation.

Chapter 6: Efficacy of surface polishing for intramedullary nail removal– an *in vivo* evaluation.

Abbreviations:

ADP	Adenosine diphosphate
AFM	Atomic force microscopy
ALP	Alkaline phosphatase
ANOVA	Analysis of variance
BGP	Beta-glycerophosphate
BSE	Backscattered electrons
BSP	Bone sialoprotein
CA	Contact angle
Cbfa-1	Core binding factor alpha-1
cDNA	Complementary DNA
COL1	Type I Collagen
CO_2	Carbon dioxide
cpTi	Commercially pure titanium
DAPI	4,6-diamidino-2-phenylindole
ddH_2O	Double distilled water
DEPC	Diethyl pyrocarbonate
DMEM	Dulbecco's modified eagles medium
DNA	Deoxyribonucleic acid
ECM	Extracellular matrix
EDTA	Ethylenediaminetetraacetic acid
FA	Focal adhesion
FCS	Foetal calf serum
FESEM	Field emission scanning electron microscopy
FGF	Fibroblast growth factor
GOI	Gene of interest
LCP	Locking compression plate
LISS	Less invasive stabilization system
IM	Intramedullary
mRNA	messenger RNA
ME	Titanium-15%Molybdenum electropolished
MP	Titanium-15%Molybdenum paste polished
MRI	Magnetic resonance imaging
MS	Titanium-15%Molybdenum standard micro-rough
MSC	Mesenchymal stem cells
NE	Titanium-6%Aluminum-7%Niobium electropolished
NP	Titanium-6%Aluminum-7%Niobium paste polished
NS	Titanium-6%Aluminum-7%Niobium standard micro-rough
OCN	Osteocalcin
Osx	Osterix
PBS	Phosphate buffered saline
PCR	Polymerase chain reaction
PDGF	Platelet derived growth factor
PIPES	Piperazine-NN'-bis-2-ethane sulphonic acid
Ra	Roughness average
RC	Rat calvarial
r.p.m	revolutions per minute
RNA	Ribonucleic acid
SE	Secondary electrons
SEM	Scanning electron microscopy
Ss	Stainless steel
TAN	Titanium-6%Aluminum-7%Niobium
TBSS	Tyrode buffered salt solution
TCP	Tissue culture plastic
TE	Commercially pure titanium electropolished
Ti15Mo	Titanium-15%Molybdenum
TGFβ	Transforming growth factor β
TP	Commercially pure titanium paste polished
TS	Commercially pure titanium standard micro-rough
TXA2	Thromboxane A2
VEGF	vascular endotheleial growth factor
qPCR	quantitative PCR

The Clinical Problem

Normally, complete osseointegration of an internal fixation device is required to provide long-term stability and restorative function to the wound site (Puleo & Nanci, 1999). In adults, rarely are these devices the subject of revised surgery in terms of implant extraction except in the case of complications related to the presence of the device (reviewed by Peterson, 2005). However, the growing skeleton of a paediatric patient presents a different series of considerations. Obvious unwanted complications such as hindrance of bone modelling/ remodelling in this class of patients is irrefutable considering the longer remaining lifespan of children. Thus, the concept of asymptomatic elective removal has become common practice (for more details see section on hardware removal). Regardless of the actual cause for removal, be it symptomatic or asymptomatic, the procedure of extracting the device due to extraosseous formation, particularly on plates (Figure 1.1 a & b) and screw heads (Figure 1.2 b), is problematic and accounts for approximately 10% of all complications encountered in paediatric patients (Alzahrani *et al.*, 2003). This figure realistically represents thousands of children worldwide (Peterson, 2005) annually and thus, warrants due attention.

The complete integration of a device into the surrounding bone can make the implant both difficult and dangerous to remove (Peterson, 2005; Langkamer & Ackroyd, 1990). Based on this potential complication, some paediatric surgeons feel that the retention of the fixation device poses fewer potential complications than its removal (Kahle, 1994). The superior bonding properties of titanium with bone further complicate the matter (Steinemann, 1999). Essentially bone grows over the device, completely integrating the plate and screw heads into the surrounding hard tissue (Appendix A; CD from Dr. Christoph Summer, Kantonspital, Chur, showing difficulties of implant removal). Therefore prior to device removal, surplus bone overgrowth requires careful removal. This removal can however complicate surgery since risks of excessive surgical time, blood loss, re-fracture, nerve involvement and infection all become areas of concern (Swiontkowski, 1983). Even if this extraosseous formation is successfully removed, the surgeon must then tackle the task of screw removal. Since bone has been shown not only to grow over the implant but also up through the plate-screw holes, this presents an additional area of potential failure. Screws become embedded between the device and the new bone (Figure 1.2 a). It is highly common for the screw head to actually break upon retrieval as the bonding is extremely strong. Although the incomplete removal of a device is deemed a

surgical failure, it is postulated that once the extraosseous portion is removed, very few if any further complications are encountered in the retrieval (Schmalzried *et. al.*, 1991). Therefore, if the implant is to be removed, bone overgrowth is undesirable. Thus, reducing this bony overgrowth at implant specific sites via the simple approach of surface topography manipulation, in this case polishing, may potentially reduce the rate of complication endured during device retrieval.

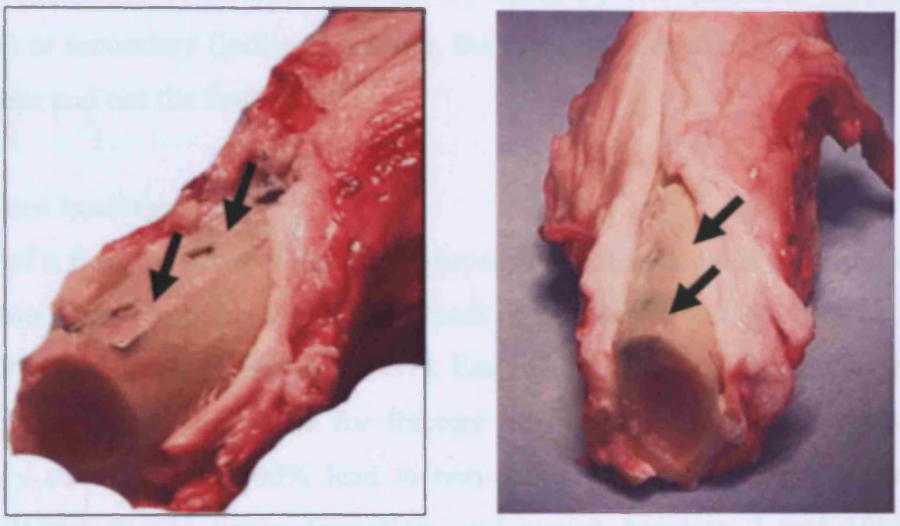

Figure 1.1 Plate fixation in a critical size defect model after 2 years implantation. Note the bony overgrowth over the device (black arrows) and its complete integration into the surrounding bone. This highlights the difficulty encountered by surgeons for implant retrieval (photos courtesy of AO Research Institute).

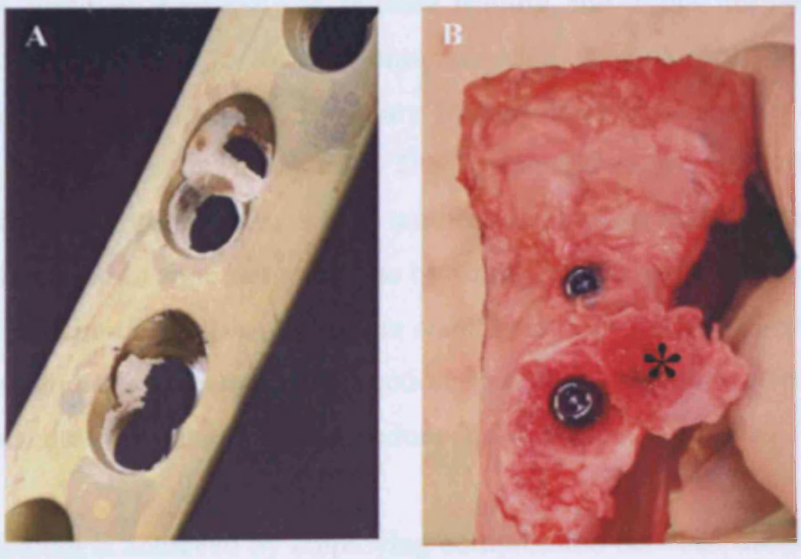

Figure 1.2. (A) Bone in-growth into plate holes. This in-growth results in locking screws becoming difficult to remove and can essentially lead to stripping of the screw heads as the metal-bone interface strength being stronger than the initial force required for removal. Consequently, (B) depicts the excess bone overgrowth (*) that required removal prior to implant retrieval. This procedure increases surgical time and exposes the patient to additional risks (photos courtesy of AO Research Institute).

Fracture healing:

The natural process of fracture healing in bone differs somewhat from other wound healing responses in that no scar tissue per se is formed. Indeed, stabilisation of the fracture site is normally achieved through callus formation, produced by osteoblasts and chondroblasts. The fracture site undergoes a variety of anabolic and catabolic events, some of which are shared with wound healing responses in soft tissues, to ultimately restore function to the injured site. The process of fracture healing can occur by two principal modes namely primary (direct) or secondary (indirect) healing, the main difference being the formation of callus in the latter and not the former.

Primary fracture healing:

Direct healing of a fracture occurs through the process of osteonal bone remodelling (Rahn *et al.*, 1971), thus a low strain healing environment is a necessity and can only be achieved through absolute stability (Ito & Perren, 2007). Essentially this method of fixation aims to provide a mechanically neutral niche for fracture healing. Perren (1979) postulated that interfragmentary strains above 100% lead to non-union whereas strains between 10 and 100% sustain initial fibrous tissue formation, and strains between 2 and 10% lead to cartilage formation and an endochondral ossification formation. However, strains under 2% would lead to direct bone formation and primary fracture healing.. Essentially the mechanism of primary healing is the same homeostatic method that exists for normal physiological bone turnover. Generally in fracture healing, the tissues formed stiffen the fracture gap, which in turn lead to lower strains, allowing formation of the next stiffest tissue until bone is formed. However, in primary fracture healing, the strain of the repair tissue is does not stimulate callus formation. Thus compared to secondary healing with callus formation, it is a slower process which requires an implant that maintains absolute stability over a long period of time but must also be strong enough to defend against fatigue during this time. The prime objective of absolute stability is not to induce direct healing but to restore and maintain perfect anatomical reduction. In essence, therefore, direct healing is an unavoidable consequence of using this procedure (Ito & Perren, 2007).

Primary fracture healing is achieved by employing compression between the fragment ends which exceed tractional forces. In addition to this, friction produced by the compressive forces of the fragments aids in resisting lateral shear and torsional forces. So long as there is no destruction of bone within this contact area and, in addition, the interfragmentary strain

is kept lower than 2% (allows for the existence of bone), bone will be capable of forming at the site (Rahn *et al.*, 1971; Perren & Rahn, 1980; Rahn, 2002). This interfragmentary gap is initially filled by loose connective tissue which is invaded by blood vessels during the first two weeks. This granulation tissue eventually gives way to lamellar bone that in the early stage of healing has become deposited at the fragments ends and then has slowly filled the gap. However, this primarily formed bone (formed without fibrocartilage) across the fracture gap is still a mechanically inferior union. Original integrity will eventually be restored via intracortical remodelling essentially resulting in a direct bony bridging of mature bone between fragment ends (Rahn *et al.*, 1971; Rahn, 2002; Ito & Perren, 2007). For this to occur, osteons within the fragment ends traverse the bone filled gap and enter the opposing fragment. Alternatively, osteons originating in the filled gap enter one of the fracture fragments. Mineralisation of the gap starts early in the first week but remodelling of the gap does not normally occur before the third week. A positive effect of absolute stability is that the blood vessels can traverse the fracture site easier which allows for vascularisation of the fracture site to be restored in a timely fashion.

Secondary fracture healing:

In contrast to primary bone healing, secondary or indirect bone healing occurs under relative stability and involves a process of repair which includes both intramembraneous and endochondral ossification, and thus is akin to that of embryological bone development (Tortora & Grabowski, 2000). In contrast to absolute stability, relative stabilisation allows for controlled micro-motion to occur. Nevertheless, large extremes in relative stability can be detrimental to callus formation. For instance, callus will fail to form if there is no movement applied to the fracture site, while too much movement will result in an unstable fracture and will subsequently delay healing (Perren & Rahn, 1980; Hayda *et. al.*, 1998). It has been shown extensively that controlled interfragmentary motion accelerates fracture healing (Goodship & Kenright., 1985; Kenwright *et. al.*, 1991; Kershaw *et al.*, 1993). However, excessive or uncontrolled loading and motion of a fracture will negatively influence fracture healing and may even cause failure (Buckwalter, 1996). In fact, an adverse reaction of rigid immobilisation of a fractured bone is that resorption may eventually exceed bone formation and while decreased activity may not readily produce any detectable changes in bone volume, shape and strength, the negative effects materialise as radiological changes including decreased cancellous bone density, loss of trabeculae and increased cortical bone porosity.

In fact Uhthoff & Jaworski (1978) have shown that without weight bearing after 12 weeks, bone mass diminishes to less than half of its normal value. On the other hand, persistent augmentation in cyclic loading can have the opposite affect by bone formation exceeding removal subsequently causing dramatic increases in bone density, volume and strength.

Some studies exist to highlight this to the extreme. For instance, Sedillot found that removal of the tibial diaphysis in a dog model actually resulted in the fibula increasing in size so much so it compensated for loss of the tibia (Buckwalter, 1996). Subsequently, Goodship and colleagues (1979) showed that subsequent to ulnar diaphysis resection in a pig model, the compressive strain of the radius was increased to almost 2.5 times its normal value leading to a rapid augmentation in the diameter of this bone. In fact, within 3 months, the cross-sectional area of bone of the radius was a similar value for the radius and ulna combined while the compressive strain had returned to almost the normal value.

The mechanical properties of the callus change as it matures becoming stiffer thus reducing the interfragmentary movement to the extent that bone can be maintained and formed via hard callus formation. The mechanobiology behind secondary fracture healing is extremely interesting and highlights nature's way of overcoming an anatomically traumatic situation. For instance, the amount of strain tolerated by a tissue varies greatly. Normal functioning bone has a tolerance of 2% deformation before fracture while granulation tissue can tolerate up to 100% deformation (Perren & Rahn, 1980). Although compact bone is the only tissue throughout the healing process that can fulfil all the requirements for adequate strength and stiffness, it cannot be initially formed because of the considerable elongation properties required (Rahn, 2002). Ergo, nature only produces tissues which can exist under specific mechanical conditions. This tissue is then replaced when the mechanical properties of the site change eventually resulting in a fracture gap with a deformation requirement less than 2%, thus supporting the formation of lamellar bone, and changes in tissue formation within the fracture site are always functioning to decrease the deformability of the site while increasing stiffness and strength (Rahn, 2002). To help describe these events, secondary fracture healing response can be subdivided into 4 principal events which do not necessarily occur independently of one another. These are inflammation, soft callus formation, hard callus formation and finally bone remodelling.

Inflammation

Upon fracture, blood vessels such as those found in the periosteum, osteons and medullary cavity in the vicinity of the injured site rupture. This results in the formation of an avascular cavity which fills with blood and forms what is known as a fracture haematoma between the fragment ends which normally forms 6-8 hours after injury (McKibbin, 1978; Figure 1.3 A). Since the blood supply is compromised in the injured site, a hypoxic state is created, and cells in this area die (Probst & Speigel, 1997). Thus, the fracture haematoma serves as a focus for the influx of cells that are required for repair and subsequent remodelling. The blood clot, which consists of a fibrin meshwork where blood derived cells are interspersed, fills the injured site and thus provides a temporary protection from external hazards as well as serving as a provisional matrix for repair cells to attach and migrate. However, the blood coagulum as a tissue has mechanical properties which are negligible in respect to fracture mechanics (Rahn, 2002). Disruption of vascular endothelium initiates a cascade of events which ultimately results in the activation and subsequent aggregation of the platelets which are essential for blood coagulation. The latter originate in the bone marrow via the fragmentation of larger cells known as megakaryocytes. Upon adherence to a surface the platelets contract, resulting in a process known as degranulation. This involves the release of intracellular contents such as potent platelet activators such as adenosine diphosphate (ADP) and thromboxane A2 (TXA2), which in turn recruit additional platelets to the wound site (Probst & Speigel, 1997).

Activated platelets also secrete a myriad of growth factors such as platelet-derived growth factor (PDGF) and transforming growth factor β (TGFβ). The latter factors possess chemotactic activity, thus serving as migratory signals for repair cells such as osteoblasts, fibroblasts, monocytes, neutrophils and leukocytes (Deuel *et al.*, 1982; Postlethwaite *et al.*, 1987). During any wound healing response, the presence of monocytes in the bone marrow increases as to meet the new demand for repair, a process by which monocytes differentiate into their active cell form known as the macrophage. The role of the macrophage is that of both a complex and critical one, and alone they secrete various substances essential for the healing process, such as PDGF, TGFβ, chemoattractants and proteolytic enzymes, as well as phagocytosing cellular debris. Their importance in this process is evident from a study where subcutaneous administration of hydrocortisone resulted in the almost complete eradication of macrophages, as well as the delayed appearance of fibroblasts to the injured site and as a result the rate of proliferation of the latter was significantly slower compared to

controls and the wounds themselves appeared 'immature' with regards to fibrosis and debridement (Leibovich & Ross, 1975).

The second line of defence following initial trauma to the tissue involves cells circulating in the bloodstream. In response to an increase in adhesion receptors on endothelial cells which occurs once the integrity of a blood vessel is breached, there is an increase in adhesion receptors for neutrophils also. Therefore, neutrophils adhere weakly to the endothelium and migrate along it towards the site of injury. Upon reaching a junction between endothelial cells that is flexible, the neutrophils project a pseudopod between the cell junctions and squeeze themselves through. This process allows for the neutrophils to migrate through the tissue to the injury site and subsequently phagocytose foreign entities and/or cellular debris (Simpson & Ross, 1972; Albelda *et al.*, 1994).

Soft callus formation

Eventually pain and swelling decrease and formation of the soft or fibrous callus (Figure 1.3 B) ensues and corresponds to approximately the same time that the fragment ends no longer are capable of moving freely (2-3 weeks post fracture). Angulations may still occur, however, but the stability provided by the soft callus is enough to prevent shortening. The infiltration of new blood capillaries into the fracture haematoma helps organise it into granulation tissue. The latter, which results from rapid fibroblast cell division, eventually replaces the fracture haematoma, and serves as a framework for the migration of epithelial cells into the wound site. In addition, granulation tissue secretes fluid into the site to prevent bacteria influx. For approximately three weeks, a myriad of cells condition the granulation tissue, or soft callus (also know as the procallus or fibrous callus), eventually forming connective tissue comprising collagen fibres which increases the callus stiffness before forming a fibrocartilaginous callus (Rahn *et al.*, 1971; Rahn, 2002), a mass of repair tissue that bridges the fractured ends of bones. The fibrocartilaginous component of the fracture site is a multi-purpose structure that resists compression and, in some instances, tension also. Specifically, fibroblasts synthesise and deposit extracellular matrix (ECM) components, while bone marrow stem cells differentiate into chondroblasts in areas of avascular healthy bone tissue and commence in the formation of fibrocartilage. Moreover, phagocytes such as macrophages continue in their quest to remove cellular debris, and, importantly, induce the process of angiogenesis through their secretion of specific growth

factors (such as VEGF and FGF). This process allows for restoration of blood supply to the hypoxic cavity region (Tortora & Grabowski, 2000).

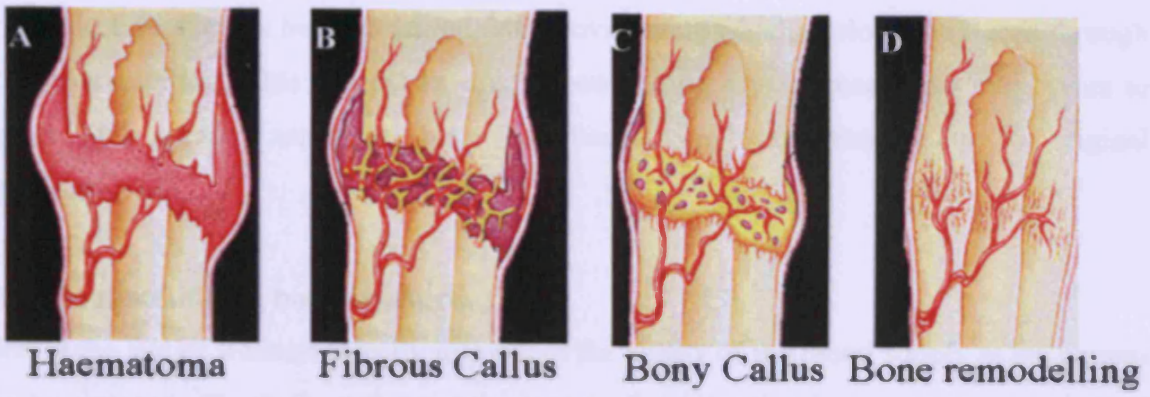

Figure 1.3. Diagrammatic representation of the principle events of fracture healing. (a) Upon fracture, blood vessels in the injured site rupture, resulting in the formation of an avascular cavity which fills with blood and forms a fracture haematoma, normally 6-8 hours after injury. (b) Granulation tissue, which occurs as a result of rapid cell division of fibroblasts, is conditioned by various cells to form the fibrous or soft callus which eventually forms a fibrocartilaginous callus, a mass of repair tissue that bridges the fractured ends of bones. (c) Fibrocartilage is replaced with spongy bone over a period of 3-4 months. Cartilage matrix hypertrophies and undergoes subsequent mineralisation and vascular buds concomitantly invade the area. Osteoblasts lay down bone matrix on the mineralised cartilage, thus producing bone trabeculae. (d) Osteoclasts resorb calcified cartilage and residual immature woven bone while osteoblasts remodel the callus area by producing mature lamellar bone.

Hard callus formation

The final phase involves reduction and remodelling of the wound site and occurs over a much longer time period in which a bony callus is formed (Figure 1.3 C) and subsequent bone remodelling of the callus takes place. Within the repair callus, some regions of the cartilage matrix undergo mineralisation and as the chondrocytes become enlarged and essentially hypertrophy and vascular buds concomitantly invade the area. In fibrocartilage, the mineralisation progresses from the fracture fragment ends towards the centre of the fracture gap, thus reducing deformation within reach of the 2% required for lamellar bone formation. Cells that migrate into this milieu subsequently resorb the central portion of the cartilage, thus forming a marrow cavity. Furthermore, osteoblasts which have originated from osteoprogenitor cells that have migrated into the cavity lay down bone matrix on the mineralised cartilage thus producing bone trabeculae. The latter proceed to join living and necrotic portions of the original fractured bone fragments. Once this process is complete (approximately 3-4 months) the fibrocartilage is replaced with spongy bone (Tortora & Grabowski, 2000; Figure 1.3 C).

Remodelling

It is the role of the chondroclasts and osteoclasts to then resorb the calcified cartilage and any remaining immature woven bone, while osteoblasts undergo the task of producing mature lamellar bone, thus remodelling the callus (Figure 1.3 D). This stage commences once the fracture site has become united with woven bone which is slowly replaced through osteonal remodelling. This process is continuous, taking several months or even years to complete and persists until the bone has been completely restored to its original morphology.

Vascularisation of long bone fractures:

Motion at the site of fracture directly influences the ability of the blood supply at the injured site to be restored effectively and a certain degree of stabilisation is required for the desired vascular responses to occur. In fact the extent of stabilisation greatly shapes the type and rate of healing while variations in bloody supply also affect this outcome. Thus, both stabilisation and vascularisation are required for effective bone healing to occur (Wilson, 2002). However, while the existing components of the normal blood supply become enhanced post-fracture, the normal ability of bone vasculature to react to injury is restricted. Therefore, an additional external supply originating in the adjacent soft tissues develops. This supplementary vasculature supply is preferably referred to as extraosseous (Rhinelander, 1974) contrary to its pseudonym of periosteal. In fact, the latter is an inaccurate description since this supply is not derived from the periosteal arterioles. The extraosseous blood supply commences development immediately subsequent to fracture/injury, however, it is a transitory supply and as the normal mechanism of blood supply are restored and eventually become capable of sustaining bone once again, this auxiliary supply becomes abated (Wilson, 2002). The main undertaking of the extraosseous vasculature is to supply the soft callus as well as re-vascularising bone that has been deprived of the medullary circulation because of injury. In doing so, it becomes merged with the periosteal arterioles in the regions in which they are present.

In terms of the blood supply to healing bone, three types of osseous callus exist (Figure 1.4). The periosteal callus is situated outermost and is originally supplied by the extraosseous vasculature contribution; however, as healing steadily progresses more of its supply comes from the medulla. In contrast, the medullary callus is confined to the medullary cavity and receives its bloody supply from the medullary arterial supply alone.

Between the opposing ends of cortex at the injured site, the intercortical callus forms and it is this structure upon which cortical bone is restructured. If the medullary arterial supply survives the initial injury, then it is this that supplies the intercortical callus. However, if this supply is interrupted during fracture then vascularity is provided by the extraosseous supply derived from the surrounding soft tissues. As is the case for the periosteal callus, once the medullary blood supply is repaired the influence of the extraosseous blood supply will become redundant (Wilson, 2002).

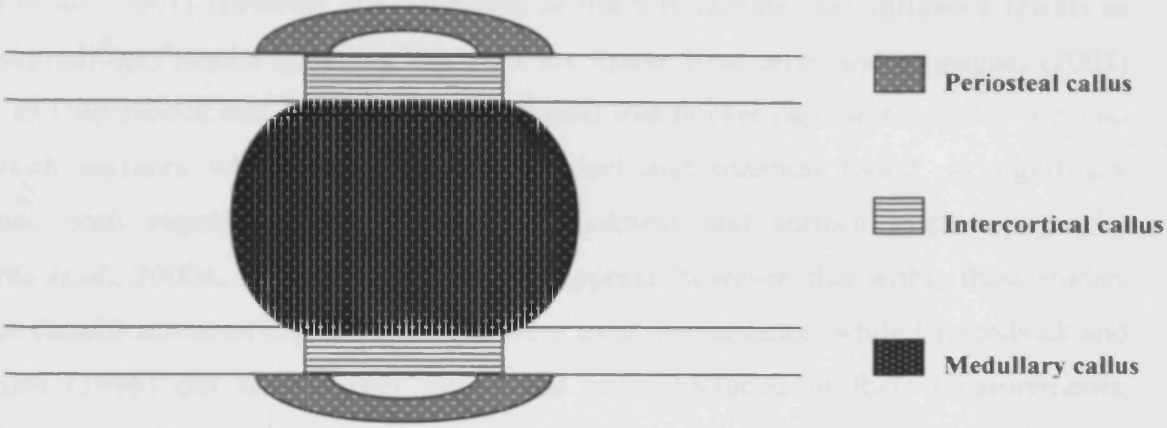

Figure 1.4. Diagrammatic representation of the three types of osseous callus encountered at the site of bone repair. Adpated from Bone in Clinical orthopaedics, Wilson, 2002.

Wound healing around implants:

The introduction of implant devices into the wound site normally occurs through invasive surgical practice which essentially triggers a wound healing response via cell and tissue trauma. The foreign body reaction commences as normal wound healing, where the accumulation of exudates at the site of trauma, infiltration of inflammatory cells to debride the area, and the formation of granulation tissue, all occur as anticipated. However, the continual presence of the biomaterial impedes full healing. Rather than the resorption and tissue reconstruction that occurs in wound healing, the foreign body reaction is characterized by the formation of 'foreign body giant cells', encapsulation of the device and, in a worse case scenario, chronic inflammation and potential necessity to remove the device. In contrast to normal wound healing, where macrophages can deal sufficiently with cellular debris *et cetera.*; in a foreign body response, the implant is far too large to be sufficiently digested, resulting in a frustrated state of phagocytosis (Dee *et al.*, 2002).

Subsequently, to circumvent this problem, macrophages fuse to form multinucleated 'foreign body giant cells', and adjacent activated leukocytes release enzymes and free

radicals capable of degradation (Zhao *et al.*, 1992). Nevertheless, the engulfment of large fixation devices by considerably smaller cells is just not possible although macrophages and, indeed, giant cells have been shown to persist at the tissue-implant interface for the duration of implant residence (Dee *et. al.*, 2002).

The normal host response is to attempt to wall-off the implant by engulfing the object with a dense fibrous tissue capsule (Morehead & Holt, 1994; Anderson *et al.*, 2004). Smooth surfaces appear to induce a thicker fibrous capsule compared to micro-textured surfaces (Boyan *et. al.*, 2001) However, the definition of the soft capsule may influence results as some contradictory results regarding this topic are found. Rosengren and colleagues (2002) as well as Ungersbock and colleagues (1996) found that thicker capsule formation is found on smooth surfaces whereas Richards using steel and titanium found no significant difference with regards to fibrous capsule thickness and surface micro-topography (Richards *et al.*, 2000a, Welton *et. al.*, 2007). It appears, however, that within these studies different classifications of capsule thickness were used. For instance, while Ungersbock and colleagues (1996) did not actually define the areas included in their measurements, Rosengren and colleagues (2002) categorise for their measurements the distance between the implant and the muscle boundary as the soft tissue capsule. Conversely, Welton and colleagues (2007) only measured capsule thickness as an area covered by densely orientated fibrous tissue adjacent to the implant and did not include the loose connective tissue located beneath since they based their analysis on the observation of Brunet and colleagues (1986) that there exist two zones within the capsule (superficial compact zone and looser deep zone).

Macrophages and giant cells have been reported to be present in increased numbers on micro-textured surfaces compared to smooth ones (Dee *et al.*, 2002). Although purely speculation, this reduced number of macrophages on smooth surfaces could indicate a concession in attempting to phagocytose these surfaces. Although fibrous encapsulation efficiently cordons off the implant from the surrounding delicately balanced biological niche, there are many complications that threaten not only the success of the fixation, but the health of the patient that arise from such a process. For instance, the release of therapeutic drugs may be impaired, or completely inhibited from the device if it is sealed/contained within the capsule.

Furthermore, in articulating prostheses rather than plates, mechanical function may be negatively affected. The problem is exacerbated when infection threatens. Since the interior of the capsule is completely isolated from its surroundings, micro-organisms such as bacteria find asylum within the capsules boundaries (Ungersbock *et al.*, 1994). Here, they are safe to thrive free from a comprehensive immunological response. Furthermore, since anti-bacterial reagents cannot penetrate the capsule easily, the quantity of antibiotic delivery is negligible to combat the now highly infectious milieu. Thus, when a bad infection occurs and antibiotic treatment fails to contain it, the only safe approach is to remove the device.

Fracture fixation

Bone is a dynamic tissue which functions to support articulation, protect organs as well as facilitating locomotion and mechanical function. Although known to be a hard, strong tissue, bone under single or multiple over-load becomes prone to fracture, resulting in a loss of bone continuity and ultimately pain and failure of function. The goals of fracture treatment are the anatomic realignment of bone fragments, stabilisation of the injured site, and finally restoration of form and function. It is not, however, the purpose of internal fixation to permanently replace a broken bone but to provide a temporary support to permit rehabilitation (Ito and Perren, 2007). Although mainly a mechanical process, bone fracturing also provokes a distinct biological response resulting eventually in restoration of the bone structure (see section on Fracture healing). For any researcher interested in the field of internal fixation it is also imperative to have an insight into the contributing factors of material choice for this application, as well as an understanding of the materials themselves. This section tackles these aspects.

Internal Fixation:

For internal fixation, metal currently remains the material of choice since it provides strength for bone fragment support, good ductility for pre-surgical contouring and has been shown extensively to be bio-passive (Boyan *et. al.*, 2001; Perren *et. al.*, 2001; Richards & Perren, 2007). Internal fixators today normally are fabricated of stainless steel, commercially pure titanium (cpTi) or titanium alloys (see sections below) however other alternative sources are available such as ceramics and polymers which are applicable for specific applications (Eschbach, 2000; Gogolewski, 2000; Marti, 2000). Whereas in previous years, external fixation was the treatment of choice observations of decreased mobility, bone, ligament and tendon degeneration and/or compromised function at the immobilised site as well as the high occurrence of pin tract infection necessitated new approaches.

Open fractures also represent a major challenge for the treating surgeon and, despite improvement in operative techniques and antibiotic therapy, septic complications still occur in severe open fracture forms up to 50%, compared to approximately 1.5% for closed fractures (EARSS, 2002). This is deleterious for the patient as well as a major economic factor for the treating hospital (Neubauer *et. al.*, 2006).

Nevertheless, improvements in sterile surgery practice have permitted surgeons to work openly with bone enabling them to implant materials directly into the body, allowing for a more focused approach of treatment.

Although spontaneous fracture healing can successfully bridge the fracture gap (if less than a critical size defect) via callus formation, the disadvantages of this process include the anatomical malalignment that may occur resulting in loss of function at the injured site. Additional complications such as improper or stunted healing are also a consideration. Thus, conservative or non-operative fracture fixation was achieved in most instances via the application of traction for bone reduction and anatomical alignment by manual reduction with fixation via plaster cast subsequent to manual reduction. Although bone union was almost always achieved, the immobility of the injured limb tended to compromise mobility of adjacent articulations (Ito and Perren, 2007). As a result of the immobilisation, surrounding soft tissues were prone to atrophy and reflex dystrophy (painful loss of bone) was commonly experienced (Ito and Perren, 2007).

Open fracture treatment which involves surgical intervention aims at re-establishing stability of the fractured bone as well as restoring anatomical form and function. Osteosynthesis (surgical fixation of bone fractures) involves the operating surgeon working openly with the fracture site. The main objective by doing so, is that the surgeon can then use direct or indirect application of traction etc. to the injured site with stable internal fixation. It averts the long term disadvantages experienced with conservative treatment, outlined above, as it permits the mobility of the articulating structures and function of the limb to recover early on in the treatment process. Open fracture treatment does not, however, function as a permanent support. Thus as soon as bone healing has occurred, the devices may be removed if required. However this topic will be discussed in further detail in the section dedicated to hardware removal issues.

Implant systems for internal fixation:

Bone screws

A screw can be an invaluable tool for internal fixation as it can be applied in many instances such as intrafragmentary compression (lag screw), fixation of plates and nails (plate screw), for direct fixation to the bone,(locking head screw) or alternatively it may be used in external fixation (Table 1.1). Lag screws are normally applied to obtain absolute

stability which is achieved as the head of the screw becomes pushed against the cortex creating a preload while the opposite end of the screw engages the inner cortex. This ultimately compresses the fracture thus preventing fragment separation. Contrastingly, locking head screws form a mechanical couple with the plate and, thus, do not depend on compression between the two components as the head of the screw has a thread that reciprocates with the hole thread of the bone plate producing an angular constancy. As the plate is not pushed against the bone, load transfer occurs via the screws to the plate as opposed to preload thus providing relative stability (Messmer *et. al.*, 2007). .

The majority of screws used in internal fixation share many design features such as a central core which provides strength, the thread that engages the bone and transfers rotational motion into linear movement, a specific tip (smooth, conical for insertion into tapped drill hole; self-tapping which produces a channel for the thread and self-tapping/self-drilling which produces a hole and channel for the thread), a screw head which connects to either bone or to a bone plate and finally a recess for screwdriver attachment. Two basic dimension varieties of bone screws are currently available, namely cortical and cancellous (Figure 1.5). Cancellous bone screws have a larger diameter and a deeper thread compared to their cortical counterparts (6.5mm and 4.0mm compared to cortical screws 4.5mm and 3.5mm for large and small fracture fragments, respectively). However, newly fabricated locking head screws (Figure 1.6), such as those fabricated for the less invasive stabilisation system (LISS), are also available. These are identified by their larger core diameter and relatively shallow thread with blunt edges, which are now also used for cancellous bone, since pull out force depends on final diameter, and not on thread depth. Compared to conventional screws, these features result in increased strength as well as a larger interface being achieved between bone and the screw. Finally, these screws also have a threaded screw head which allows for precise insertion.

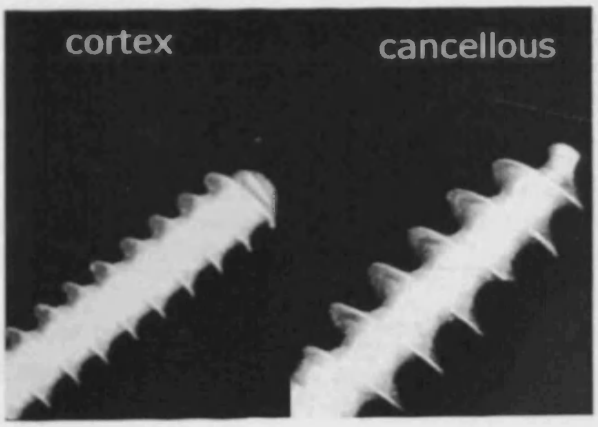

Figure 1.5. Cortical and cancellous bone screws. Note the larger diameter and a deeper thread of the cancellous screw compared to its cortical counterpart. Images reproduced with kind permission of the AO Foundation from AO principles of fracture management, 2nd Edition.

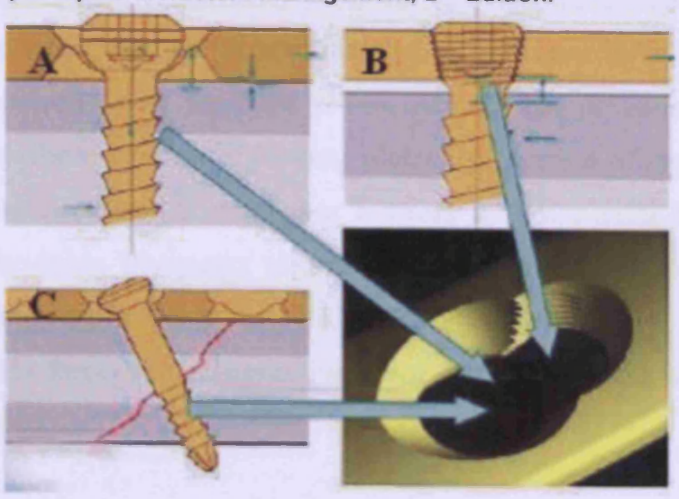

Figure 1.6. Conventional & locking head screws. (A) Design & force components of a conventional screw as used for Dynamic Compression Plate (DCP) & Limited Contact - Dynamic Compression Plate (LC-DCP). The mechanism of the screw involves producing friction between the underside of the plate and the bone surface due to compression of the interface. (B) Locking head screw used in LCP & Less Invasive stabilisation System (LISS). The screw provides fixation based on the fact that the screw head is locked in a position perpendicular to the body of the plate which is not pressed against the bone, thus functioning more like an internal 'external' fixator than plates. (C) The locking plate system allows for the incorporation of the "bridge plating" technique and lends itself well to minimally invasive insertion. This system merges locking screw technology with conventional plating techniques. It creates a fixed-angle construct in osteopenic or multi-fragmented bone and does not rely on plate-bone compression for stability. Adapted from Messmer *et. al.*, 2007 AO principles of fracture management, 2nd Edition.

Function		**Clinical Example**
Name	***Mechanism***	
Plate screw	Preload & friction is applied to create force between the plate & bone	Forearm LC-DCP
Lag screw	Glide hole allows compression between bone fragments	Fixation of medial malleolus fracture
Position screw	Holds anatomical parts in correct relation to each without compression	Articular fracture with defect of distal humerus
Locking head screw	Never used alone, always with a plate with the exception of when applied as position screw. Threads in screw head allow mechanical coupling to a reciprocal thread in plate and provide angular stability	LCP/LISS in osteoporotic bone
Interlocking screw	Couples an intramedullary nail to the bone to maintain length, alignment & rotation	Locked femoral/tibial intramedullary nail
Push-pull screw	Temporary point of fixation used to reduce fracture by distraction &/or compression	Use of articulated compression device
Reduction screw	Conventional screw used through a plate to pull fracture fragments towards the plate. The screw may be removed/exchanged once alignment is achieved	Minimally invasive percutaneous Osteosynthesis(MIPO) technique to reduce multifragmentary fracture onto a LCP

Table 1.1 Type and functions of bone screws. Adapted from Messmer *et. al.*, 2007 AO principles of fracture management, 2nd Edition.

Bone plates

The application of bone plates is normally practical to avoid undesirable excessive callus formation that may be brought on by micromotion which is a clear indication of an unstable fixation. Five key functions exist for bone plates, namely compression onto the bone to produce stability (with the exception of locking plates), protection of lag screw fixation by hindering bending and rotational forces, as a buttress to resist axial load, by providing relative stability by bridging fragments allowing for anatomical alignment, correction of bone length and rotation and finally by being attached to the tension side of the fracture and thus transferring tensile force into compressive force at the cortex adjacent to the implant (Lorich & Gardner, 2007).

Operating surgeons decide how the plate will be applied, thus deciding what function it will play. The dynamic compression plate (DCP) was originally introduced in 1969. However, observations of interrupted cortical blood perfusion leading to cortical necrosis (Akeson *et. al.*, 1976; Perren *et. al.*, 1988) beneath the plate resulting from the plate 'footprint' (area subjected to plate-bone contact) and subsequent porotic changes led to the development of the limited contact dynamic compression plate (LC-DCP) by Perren in 1990. As its name indicates, this plate greatly reduced plate-bone contact compared to the DCP (Figure 1.7). Although a significant reduction (Perren, 1991) of vascular disruption was reported for the LC-DCP system since its design involved only certain areas of the plate being in contact with the bone, it was still necessary to have relatively tight contact between the plate and bone to generate stability in order for it to fulfil its function.

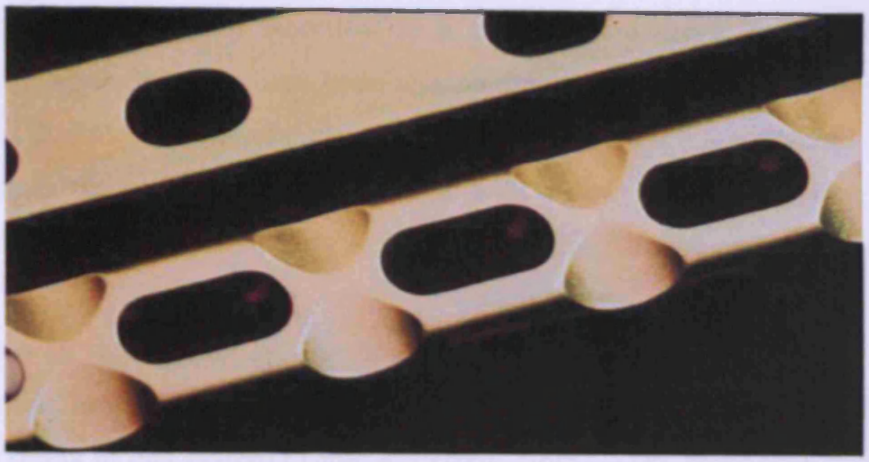

Figure 1.7. Dynamic Compression Plate (DCP; top) and Limited Contact Dynamic Compression Plate (LC-DCP; bottom). Several changes in design inspired from the DCP problems reporting hindrance of cortical perfusion beneath the plate – a direct result of the plate 'footprint' have led to the fabrication of the improved LC-DCP system. In the LC-DCP design the area of plate-bone contact (footprint) is greatly reduced thus improving cortical perfusion. As a result bone resorption is also reduced in this model. Images reproduced with kind permission of the AO Foundation from AO principles of fracture management, 2nd Edition.

With plating, most of the iatrogenic disruption to bone has been traced to the regions of direct bone-implant contact and is believed to result directly from periosteal blood supply disruption (Perren *et. al.*, 1988). This finding was the main motivation behind the large investment in the development of new generation internal fixation systems that effectively reduce the extent of contact of the plate with bone consequently avoiding temporary porosis as a result of disrupted periosteal vascularity. This allows an improved process of healing through the maintenance of local blood supply via reduced points of contact (further decreasing the risk and spread of infection). In order to eradicate any complications that may arise due to bone-plate contact a new approach locking plate was pioneered by Tepic (1995) with the development of PC-Fix system which allowed fixation by shear forces between the screw and bone rather than frictional forces generated between the bone and plate as with conventional plating methods (Tepic & Perren, 1995). Although no longer in production as it was replaced with a combination modification, the design and implication of this system reinvented the way plates were subsequently designed and thus warrants due attention. Two main reasons were the motivation behind the PC-Fix design, namely, to reduce the incident of infection, and to maintain vitality of the cortical blood supply for optimal healing to occur (Tepic & Perren, 1995). Mechanically, the PC-Fix is comparable to conventional plating techniques with the added advantages of decreased disruption of the periosteal vascular supply through its 'point contact' with underlying bone (Figure 1.8), thus reducing bone necrosis, the infection rate (Eijer *et al.*, 2001) and improving healing time (Tepic *et. al.*, 1997).

Moreover, the change from a bicortical to a monocortical screw design was employed whenever sufficiently thick cortical bone was available. This change was implicated after the realisation that most of the vascular damage resulting from internal fixation was due to bicortical screws transversing both cortices as well as the medullary cavity, producing a large extent of bone necrosis and early remodelling leading to temporary porosis.

Locked screws as used in the PC-Fix system do not need support from the distal cortex hence the use of monocortical screws was applicable because of the conical self-locking nature of the screw in this system (Tepic & Perren, 1995). Also, since only minimal force is required between the bone and the plate for insertion of the screws in this system, which is resisted at the points of contact of the plate, it avoids any significant damage to the periosteal blood supply. In contrast to conventional plating techniques, the PC-Fix system allows for neutral application to be achieved and eliminates any unnecessary stresses incurred by the bone during application (Tepic & Perren, 1995). Additionally, the undercuts employed in the design to prohibit vascular disruption also ensure the strength of the plate is uniform (Tepic & Perren, 1995) and, in fact, is superior to that of conventional plating in large bones (Miclau *et. al.*, 1995).

In addition to the PC-Fix, another of these new internal fixation systems includes the 'less invasive stabilisation system' (LISS; Figure 1.8). In contrast to the locking compression plate (LCP), the LISS and other specific use plates contain round thread holes to accommodate a single screw compared to the combination holes offered by the LCP (described below). These plates act primarily as internal fixators and only provide bridging between bone fragments. Bridge plating occurs when maximum blood supply is required for the fracture site, as the plate is only fixed to the two principle bone fragments. One drawback of the PC-Fix system is that it has restricted application in metaphyseal and epiphyseal regions. However, the development of the LISS was instigated precisely for these regions. As a result, its shape is contoured to specific areas of the bone so different implants are used depending on whether it is the right or left side that is affected. Another benefit of these systems is that no further contouring is required, as the plate does not necessarily need to be in direct contact with the bone thus vascular disruption of the periosteum is averted.

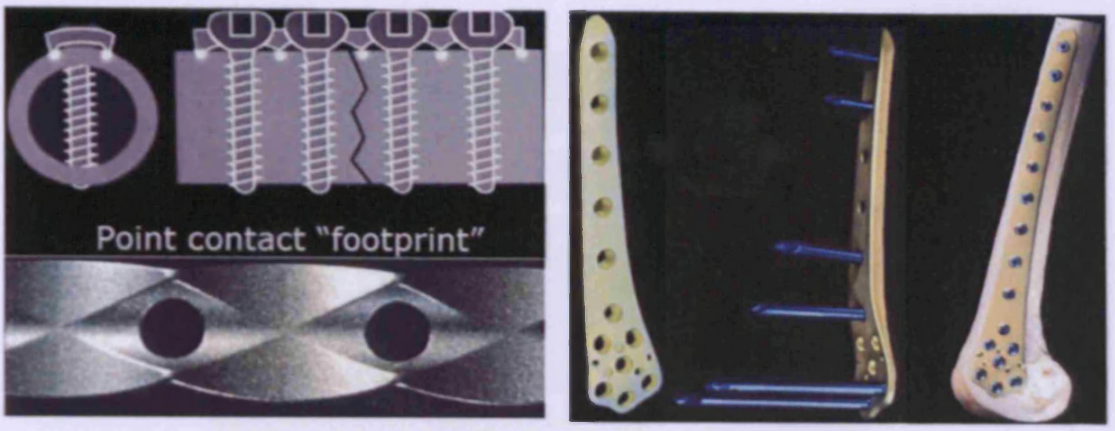

Figure 1.8. The PC-Fix (Left) functions like a fixator, that is, the fracture fragments are stabilised using a splint fixed to the bone by monocortical, angularly locked screws that are designed not to exert pressure between the splint and the bone. Thus, minimising implant-to-bone contact and consequently avoiding vascular damage to the osseous blood supply. The concept of the LISS (Right) comprises a contoured plate to which the screws interlock. A combined guide/aiming handle (not shown) allows the insertion of the plate and subsequent percutaneous placement of the screws with minimal incisions. Stability comes from the angular stability of the plate-screw interface and not from friction between plate and bone. Due to the locked screws and anatomical design, this system also remains some distance from the bone thus minimising periosteum damage and bone necrosis. Images reproduced with kind permission of the AO Foundation from AO principles of fracture management, 2nd Edition.

The locking compression plate (LCP) was developed in response to increasing requests from orthopaedic surgeons for the availability of a system that could offer a synergy between a threaded and a conventional screw hole allowing for the greatest possible flexibility for the treatment of fractures (Frigg, 2003). The operating surgeon thus has the scope of deciding which variation of the system would be applicable for treatment depending on type of fracture and quality of the bone since the system can be applied in either a conventional technique (compression), bridging method (internal fixator) or a combination of both (Wagner, 2003). The versatility achieved with this system provides surgeons with a previously unattainable method of treating complex fractures without compromising treatment which is achieved through the inclusion of a combination hole (Figure 1.9). Specifically, the possibility of applying multiple angle screw fixation in areas such as the metaphyseal region enables the treatment of fractures that would otherwise be untreatable with previous existing devices (Wagner, 2003). Furthermore, the potential of fretting is also lessened without compromising the strength or stability of the construct. Another advantage of the LCP system is that no compression is actually necessary unless required, thus preserving vascularity of the fracture site and, therefore, facilitating stable healing. The design of this system also means that very little, if any, intraoperative contouring of the plate is required since stability is not reliant on bone-implant compression.

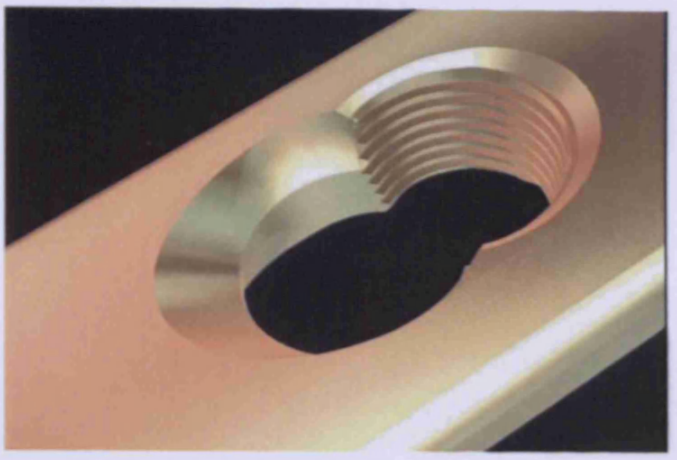

Figure 1.9. The LCP combination locking hole – this design allows for conventional as well as locking head screws to be placed within the same implant. Images reproduced with kind permission of the AO Foundation from AO principles of fracture management, 2nd Edition.

Intramedullary nailing

The gold standard treatment for long bone shaft fractures is generally accepted as being intramedullary (IM) nailing (Figure 1.10). Reaming may be carried out of the medullary cavity to enhance the mechanical properties of bone-implant interface as devices with larger diameters can be applied. Nonetheless, the actual reaming process can cause some unwanted biological responses such as heating of the adjacent tissues and augmentation in intramedullary pressure leading to bone necrosis (Krettek, 2007). Although reaming essentially interrupts cortical blood supply, animal experiments have shown this to be reversible within 8-12 weeks however this may be implicated in high infection rates (Schemitsch *et. al.*, 1994). Therefore, the application of reamed intramedullary nailing is usually avoided in open fractures. However, others suggest that, clinically, reaming does not increase infection rates (Ochsner, 2008). Fixation with reamed nailing systems in closed tibial fractures has also been shown to result in shorter union time without any further postoperative complications being observed compared to unreamed systems (Larsen *et. al.*, 2004).

Figure 1.10 Intramedullary nailing system which functions to secure fragments with deliberately placed screws locked into the device within the medullary canal. Image adapted with kind permission of the AO Foundation.

Systemic changes are also a consideration, especially for polytrauma patients with injuries sustained to the chest. IM nailing may inadvertently cause pulmonary complications as shown previously (Pape *et. al.*, 1996) by increasing pulmonary pressure. The incident of pulmonary embolism after tibial fractures has been reported to be approximately 19%, compared to 78% for femur fractures (Heim *et al.*, 1995). The lower occurrence within the tibia is believed to be attributed to the less extensive venous drainage system found in the latter compared to the femur. In recent years, a device known as the Reamer Irrigator-Aspirator (RIA) has been developed by SYNTHES to, as its name suggests, provide irrigation and aspiration during reaming to help prevent the occurrence of embolism from reaming by reducing the intramedullary pressure. Although unreamed intramedullary nailing also does not eliminate these risks, it does significantly reduce the chances of them occurring (Hildebrand *et. al.*, 2005).

IM nailing can be carried out without reaming but a distinct disadvantage is the necessity of additional external fixation. Moreover, since the devices could not be locked distally or proximally due to their small diameter, longitudinal and rotational instability occurs. For instance, the IM pressure for nailing without reaming is significantly lower to that with reaming (40-70mm Hg compared to 420-1510 mmHg respectively). There is also less heat production in adjacent tissues as well as less disruption to the cortical blood supply (Schemitsch *et. al.*, 1994). Possibly one of the advantages accounting for the lower infection rate reported for non-reamed nailing systems is attributable to the decrease in both the bone necrosis and damage to the vascular supply observed.

Hollow intramedullary nailing has also been shown to induce higher infections rates (59%) compared to solid nails (27%) in rabbits, most likely attributable to the increased dead space available for bacterial habitation (Melcher *et. al.*, 1994; 1996). In a study by Horn and colleagues (2005) the infection rates of hollow, cannulated and solid nails in rabbits were studied and found that while hollow and cannulated nails had similar infection rates (65% and 61% respectively) solid nails had significantly higher resistance with almost a two fold lower infection rate (23%).

It is postulated that the dead space within the tubular nail is the most likely culprit for the difference in infection rates observed. Hupel and colleagues (1998) have also shown in a dog model that had undergone tibial segmental osteotomy that loosely fitting IM nails did not affect the cortical perfusion as negatively as tightly bound nails. In addition the former permitted revascularisation as early as 11 weeks post operatively. Therefore, in severe tibial fractures with compromised vascular supply, there is a good indication for the application of intramedullary nailing without reaming.

Overall, the method of choice for femoral and closed tibial fractures tends to be reamed IM nailing. However, when polytrauma is a concern, early total care is usually substituted with damage control surgery as the latter has been shown to decrease the acute inflammatory response and infection rate compared to the former (Pape *et. al.*, 2002; Scalea *et. al.*, 2000). In open fractures, the choice becomes somewhat controversial. For instance, Gustilo type I and II open fractures (Type I has clean wound of less than 1cm with little/no contamination with a simple fracture such as spiral; type II involves a skin laceration longer than 1cm and the adjacent soft tissue has minor (or no) signs of contusion, with moderate to sever fracture instability) IM is the method of choice. However this is not the case for Gustilo type III fractures where extensive soft tissue damage and compromised vascularity occur. For this fracture type, instability is marked and the fracture itself complex thus treatment with IM nailing may increase infection susceptibility. Support for this notion has been provided in recent animal studies. For instance, IM nailing results in a higher infection rate in rabbits, especially if reaming has been carried out (Melcher *et. al.*, 1995). However, results from animal studies may not sufficiently reflect the actual clinical situation, as it is suggested that reaming potentially eliminates bone necrosis, dead bone sequestering and IM abscess formation (Ochsner, 2008).

Implant requirements:

The choice of material depends primarily on the requisite function to be accomplished and also on the manner of which the implant will be applied. Materials applied for internal fixation must fulfil a variety of fundamental mechanical requirements, many of which are contradictory in terms some of which are examined in this section. As it stands, of the potential biomaterials available, only metal can provide the stiffness and strength required as well as ductility, and importantly, biopassivity. The stiffness of a material is described as the relationship between applied load and subsequent deformation (Richards & Perren, 2007), in other words a material's ability to resist deformation.

In terms of bone fixation and ultimately bone healing, material stiffness is significant as it functions to avert buckling at the site of injury as well as reducing fracture mobility for repair tissue formation to occur appropriately. As mentioned, the ductility of a material determines the degree to which a device can be deformed, or contoured. This parameter also allows the surgeon some forewarning of implant failure during application. As commericially pure titanium (cpTi) has a lower ductility compared to stainless steel (Ss), the former provides less warning thus can be a cause of handling issues for the operating surgeon. The strength of a device, namely the level of load that can be tolerated by the implant prior to rupture is also a consideration as it is required to maintain reduction and stability of the fractured site. Although titanium has a 10% decrease in strength when compared to Ss this can be overcome by increasing the implant thickness slightly. Even more important is a materials resistance to fatigue brought on by repetitive load. Although Ss has a better resistance to static load compared to cpTi, it is the latter that proves superior under cyclic loading conditions (Perren *et. al.*, 2001).

Metals used in Orthopaedics:

Stainless steel

Since its discovery in 1904 by Leon Guillet (Disegi & Eschbach, 2000) and then its use in surgical applications as early as 1926 when the 18% chromium, 8% nickel and 2% molybdenum was patented by Strauss because of increased corrosion resistance, stainless steel (Ss) in orthopaedic surgery has been widely used. To date, Ss is still one of the most frequently used materials, especially in the USA for internal fixation treatment due to its proven combination of mechanical strength, ductility, cost effectiveness and biopassivity.

Stainless steel is classed as an austenitic material, that is it contains enough Nickel, Chromium and Manganese to retain austenite at atmospheric conditions. Despite its positive effect on corrosion resistance, Cr has an undesirable effect on austenite stability. The nominal nickel content in orthopaedic grade implants is actually higher than that found in commercial quality Ss and is the primary determinant of maintaining the austenitic nonmagnetic microstructure characteristic of Ss and tends to minimise the formation of a secondary phase such as delta ferrite (Disegi, 1998a). The inclusion of delta ferrite visible at 100 times magnification is unacceptable for implant quality Ss as it reduces the corrosion resistant properties of the surface as well as being ferromagnetic, thus increasing the magnetic permeability of Ss. This magnetic permeability can be an issue for patients that may be subjected to magnetic resonance imaging (MRI) procedures as the implant may potentially create tissue heating effects or undergo migration.

The increased resistance to corrosion of Ss is a result of chromium ions forming an oxide layer at the surface of the alloy, and is often referred to as the passive film. Although only a few nanometres thick, the passive film prevents further diffusion of oxygen into the base material and thus prevents corrosion. If this film is inadvertently disturbed or removed, this can lead to fretting corrosion which is an acceleration of the normal corrosion rate. This can potentially be dangerous since the particles that have been released can accumulate via the lymphatic system (Case *et. al.*, 1994). Even the 316L stainless steels can potentially corrode under certain circumstances, for instance, in a highly stressed and oxygen depleted region such as contact beneath screws or fracture plates. Thus Ss is suitable primarily only in temporary implant devices, such as fracture plates, screws and hip nails. However a combination of low nickel containing Ss and conventional Ss have been shown to produce less fretting compared to pure combinations (Eschbach *et. al.*, 2000).

Titanium

Commercially pure titanium

The introduction of unalloyed titanium, or commercially pure titanium (cpTi) into orthopaedic applications came as early as the 1940's (Bothe *et. al.*, 1940). Additionally, the introduction of dynamic compression plates, and screws fabricated of cpTi by the AO in 1965, helped prove the suitability of this material for bone fixation. Because of cpTi's superior strength, corrosion resistance, acceptance by bone and soft tissue, superiority over Ss under cyclic loading and excellent biopassivity, cpTi has in recent years, emerged in Europe as the forerunner in internal fixation devices. Additionally, cpTi implants are not ferromagnetic and, therefore, issues regarding safety for MRI are negated. Furthermore, they have the advantage that approximately 40% less image destruction occurs in their surrounding area compared to Ss devices (Pohler, 2000). Collectively, these attributes have made cpTi and its alloys an increasingly attractive option for use in medical applications. Additionally the density of unalloyed titanium is approximately 57% that of 316L stainless steel. This decrease in density equates to a weight reduction of approximately 50% when materials of similar volumes are compared. This attribute obviously allows for more comfort when implanted into the patient especially when considering large implant devices and small plates with limited space for example under tendons in distal radius fractures. In contrast to Ss, cpTi implants are not ferromagnetic and as a result artefact issues are negated. Moreover approximately 40% less magnetic resonance image interference is experienced with cpTi devices compared to Stainless steel (Ss; Pohler, 2000) due to cpTi's lower magnetic susceptibility, giving cpTi implants a distinct advantage over Ss.

Unalloyed pure titanium comprises four subdivisions dependent on the oxygen content of the material; grade 1 containing the lowest and grade 4 the highest. The strength of cpTi increases proportionally with the increasing oxygen content. A distinguishing characteristic of cpTi is its hexagonal close-packed crystal structure, known as the alpha phase, which was first reported by Branemark in 1977. Pioneering studies investigated the underlying biological processes involved in the ability of unalloyed titanium to adhere to bone and subsequently termed the phenomenon 'osseointegration'. The alpha phase of titanium is normally stabilized with the addition of small quantities of carbon and nitrogen. This phase is stable up to 882°C and transforms into the cubic face centred structure, more commonly referred to as the beta phase, above this temperature.

One disadvantage of cpTi microstructure is that it produces a less forgiving material than Ss, that is, it is less ductile and, therefore, cannot undergo the same range of deformation. However, cpTi and its alloys have an elastic modulus similar to that of bone thus local stress concentrations on bone are reduced with use of these materials (110GPa for cpTi compared to 200 GPa for Ss). Unalloyed titanium also contains a residual measure of iron. Here, iron functions to increase the solubility level of hydrogen, which must be kept low in titanium compositions to prevent embrittlement, which can decrease ductility (Pohler, 2000). In addition, the iron content contributes markedly to the corrosion resistance properties of the metal (Disegi, 1998b).

Another advantage of titanium is its ability to readily form a naturally occurring oxidised layer on its surface which provides additional protection against contaminants. Therefore, even when subjected to deformation damage during surgery, the oxide layer will spontaneously re-form as long as oxygen is present and will protect the material. This layer normally ranges between 5 to 6 nm thick but by treating the materials in a process know as anodizing, it can be increased in thickness. This layer readily repassivates if the film becomes abraded making titanium a highly corrosion resistant material. The importance of this oxide layer is not a new concept (Hay & Moreno, 1979; Baier *et. al.*, 1984; Jansen *et. al.*, 1989). However, more recently, a study by Eisenbarth and colleagues (2002) revealed interestingly that the oxide layer was capable of protecting cells from toxic alloying elements and ultimately it is the oxide layer that produces a cellular response and not that of the bulk material composite (Eisenbarth *et. al.*, 2002). Previously, Vinall and colleagues (1995) showed that thermal and electrochemical anodisation of cpTi surfaces did not have any deleterious effect on fibroblast cell viability or cytocompatibility *in vitro*. Moreover, there appears to be an absence of allergic reaction to this material attributed to the absence of appreciable quantities of Cr, Co and Ni, a distinct advantage over Ss. In fact, titanium dioxide is often used as a basis for many cosmetics because of the lack of allergic response experienced. As previously mentioned, cpTi or its alloys are preferred for Ni sensitive patients as it essentially circumnavigates the issues occurring due to sensitisation.

Other studies have also revealed that where infection is a risk, the use of cpTi implants is favoured over Ss. Hauke and colleagues (1997) tested the effect of intramedullary nail material (stainless steel versus cpTi) and showed that titanium had a higher infection resistance (59%) compared to steel (82%).However, this model included bulk implant

materials whereas, clinically, an implant system comprises a myriad of components such as nails, screws and plates. Thus the potential for fretting between elements is an important variable that was not tested by Hauke and colleagues. In contrast a study by Arens and colleagues (1996) designed a study exactly for the purpose of investigating the effect of implant material under conditions of possible fretting which included at least two components of a stabilising implant system. Dynamic compression plates made of Ss and cpTi were examined and the results left no doubt of the resistance superiority of cpTi to local infection over Ss with the resistance observed to be 35% and 75%, respectively (Arens *et. al.*, 1996). Recently, our group has shown that for locked implants (LCP) where minimal periosteal damage occurs, no difference in infection susceptibility was detected between Ss and cpTi. However, a point to bear in mind is that the *in vivo* rabbit model included in the latter study did not include a fracture, nor was there major trauma to the adjacent soft tissues.

Titanium Alloys

Titanium-6%aluminum-7%niobium

One issue that does surround the use of unalloyed titanium is its apparent weakness when used in considerable high load bearing regions. This concern has been circumfused by the fabrication of titanium alloys. For many years Ti-6Al-4V (titanium-6% aluminum-4% vanadium) has been the alloy of choice for prostheses. However, in the past 25 years, or so, TAN (Titanium-6% aluminum-7% niobium) has come to the forefront. The obvious major difference between the alloys is the replacement of vanadium with niobium. Studies carried out at the AO Research Institute, Switzerland have shown that although the biocompatibility of titanium-6%aluminum-4%vanadium was akin to that of vanadium free materials, there was, however, an undesirable biological response caused by its inclusion (Perren *et. al.*, 1986). Furthermore, Rogers and colleagues (1997) showed that wear debris generated by Ti-6Al-4V incited the augmentation of inflammatory response factors such as PGE2 and IL-1 compared to TAN and cpTi.

Compositionally, the microstructure of TAN is similar to that of Ti-6Al-4V, consisting of a dual phase alpha and beta (high temperature form of titanium comprising a cubic structure) configuration. This dual phase microstructure provides improved implant strength compared to cpTi but decreased tensile strength and ductility. Consequently, titanium alloys such as TAN are not used for cerclage wire as the insufficient ductility does not permit

malleability of the wire. Titanium alloys tend not to be used for areas that require a great deal of device contouring and manipulation due to the micro-cracking that can occur (Disegi, 2000). In contrast, the high strength and low modulus of elasticity (desirable to reduce stress shielding) of titanium alloys are ideal for implants demanding high resistance to stress loading, but, these characteristics make this material notoriously difficult to machine (see chapter 2 discussion).

Reservations regarding the presence of elements such as vanadium in long-term implants arose when it was revealed that they could be toxic (Gerber *et. al.*, 1980). Consequently, these concerns led to the development of other implant alloys such as TAN, which has been in use since 1985. Interestingly, X-ray photoelectron spectrometry (XPS) analysis has revealed that an oxide film consisting of TiO_2, Al_2O_3, and NbO_5 occurs on the surface of TAN (Maeusli, 1986). The insolubility of this stable oxide layer on titanium alloys is primarily responsible for the excellent biopassivity reported for these materials, and brings to light the significant point that the assorted oxide film demonstrated by TAN is chemically more stable compared to the oxide layer formed on cpTi (Maeusli, 1986).

Titanium molybdenum

An advanced class of metals known as the beta titanium alloys have in recent years come to the forefront. A specific heat treatment (of approximately 800°C) provides a stabilised beta microstructure, which makes this group of alloys unique. Superior properties such as lower modulus of elasticity (30% and 60% lower than cpTi and Ss, respectively), improved corrosion resistance, enhanced ductility and better resistance to notch sensitivity (Disegi, 2003) compared to alpha and beta alloys have propelled this class of alloys into the spot light. One particular beta alloy, titanium molybdenum (Ti15Mo) has emerged recently in implant applications. This system was originally conceived for the chemical industry to provide a titanium alloy with superior corrosive resistance. Thermal handling difficulties and microstructure instability have prevented prevalent use within the aerospace industry and alloy modifications with zirconium and aluminium failed to rectify the problem as the unique properties of the base alloy were lost. However, as an implant material, Ti15Mo has shown to evoke a biological response akin to that of cpTi, and as a result has been in use clinically since 1998 (Disegi, 2003).

The molybdenum component of the alloy is a stabilising element to retain 100% beta phase, a minimum content of 10% molybdenum is necessary, but normally ranges from 14%-16%. It is believed that beta titanium alloys devices would not provoke an allergic reaction *in vivo* due to their outstanding thermodynamically stable oxides of MoO_2 and MoO_3 (Disegi, 2003; Hierholzer & Hierholzer, 1992), and as a testament to this fact, Ti15Mo plates have been used in the treatment of hand fractures for over 10 years, without incident. As a general rule, beta titanium alloys tend to be more susceptible to picking-up hydrogen than alpha titanium (cpTi) or alpha-beta alloys (TAN). This potential problem is evaded by the fact that beta alloys such as Ti15Mo tend to have a higher forbearance to hydrogen embrittlement effects. Furthermore, several processes, such as applying surface protective coatings, exist by which the hydrogen intake is minimised during fabrication to further avoid contamination.

Ti15Mo, and other beta phase titanium alloys generally have low magnetic susceptibility, allowing for patients with these materials to be imaged with MRI routinely and without incident. Also, as they do not contain appreciable amounts of ferromagnetic iron within their composition, these alloys tend to produce very low quantities of artefacts during imaging, comparable to that obtained for cpTi. Furthermore, Khan and colleagues (1996) have shown that for a range of biomaterials, both cpTi and Ti15Mo were observed to have a level of corrosion resistance superior to the alpha and beta phase alloys, TAV and TAN. Studies by Zardiackas and colleagues (1996) have also indicated that both cpTi and Ti15Mo could be used in a multi-component implant system as galvanic corrosion would not be expected. In previous studies, the ductility of Ti15Mo has been shown to exceed that of cpTi and TAN as well as a higher resistance to stress cracking corrosion (failure of metals and alloys under combined force of corrosion and stress; Bogan *et. al.*, 2001).

The biological response to Ti15Mo has also produced promising results. Published data have failed to show sensitisation to Molybdenum for 705 patients that were patch tested and, thus, it is not considered a sensitisation agent and should not evoke an allergic response (Hierholzer & Hierholzer, 1992). Moreover, in a long term implant study in dog femurs to assess the degree of osseointegration for Ti15Mo compared to cpTi over a 2 year period revealed that both materials were biologically comparable. Additionally, soft tissue in contact with the material showed no adverse tissue reaction (Olmstead & Pohler, 1990; Welton, 2007).

The general requirements of an implant material for internal fixation still postulate that the metal should offer high stiffness and strength, good ductility, and be well tolerated biologically. These are quite demanding requirements especially since many are conflicting. However, the materials described in this chapter are used successfully within clinics for internal fixation applications worldwide. Continuing advancement in the field of biomaterials will not only refine our existing knowledge and success with these materials but may also potentially reveal new and exciting alternatives for use in orthopaedic applications.

Hardware removal:

The ubiquitous use and resulting success of biomaterials in medical applications is undeniable. Nevertheless, when referred to in the context of medical applications, it is generally accepted as referring to long-term implantation. However, this may not always be the case. For instance, elective removal of implantable devices in a paediatric niche has for many years been an event of common practice (Schmalzried *et al.*, 1991). Thus, the desired outcomes for the performance of these devices alter somewhat to long-term and permanent applications in an attempt to restore function to the affected site.

In the case of paediatric fixation devices, the lack of consensus regarding the issue of elective removal of internal fixation devices has resulted not only in decreased research focus, but also in the lack of comprehensive discussion and guidance for residents (Kahle, 1994; Peterson, 2005; Loder & Feinberg 2006; Busam *et al.*, 2006). Therefore, the decision of whether to remove or not to remove has largely been left to the discretion of the operating surgeon, and the rationale for such a decision based mainly on their individual good or bad past experiences and their respective surgical ability (Melo *et al.*, 2006). Moreover, the deficiency of tangible data regarding metal devices that have been left in patients and that have remained asymptomatic, only leads to further throw doubt and indecision on the matter. Additionally, the reasoning behind elective device removal is also debated; where many clinicians only support removal for patients requiring to return to high risk activities such as sports, others advise the removal of all metal devices based on potential bacteriological, immunological, oncological and metabolic risks associated with long term metal retention (see Peterson, 2005 for review).

Almost all hardware removal procedures in adults are a result of a complication. In contrast, for paediatric patients, the accepted protocol was removal of the device once its purpose had been spent (Schmalzried *et al.*, 1991). This approach was however, re-addressed and, since then, as a result of improvements in biomaterial fabrication and design and the manufacture of devices specifically to remain *in situ*. This development deterred somewhat from focused interest in reaching a consensus on elective device removal so to date. The value of elective hardware removal remains unproven since clinical data and articles regarding the risks associated with implant retention versus that of removal is meagre (Highland & LaMont, 1985; Labowsky *et al.*, 1990; Kahle, 1994; Peterson, 2005; Busam *et al.*, 2006). The case for and against elective hardware removal in paediatric and adolescent

patients is a multi-faceted problem. On the one hand, metal devices are largely removed in these patients in response to complications, or as a preventative measure to avoid potential complications such as infection, pain, migration of the implant, device failure and bone atrophy. On the other hand, the vast majority of these complications could be circumvented via elective device removal. In reality, the actual process of removing an internal fixation device can also be a source of potential complications, the most common being incomplete device removal and post-operative infection.

Reasoning for elective hardware removal:

Many complications surround the use of metal fixation devices but are normally alleviated upon extraction, and therefore, in essence, can be used as grounds for electively removing these devices. Common ailments experienced by patients include pain upon implantation of the device, irritation of adjacent soft tissues, and acute aseptic inflammation (also known as metallosis). In certain applications, tendons in contact with implants may result in irritation of these tissues by the implant. The formation of restrictive adhesions and subsequent limited motion is one of the most challenging areas of hand surgery. Specifically the tendon sheath, if irritated, produces a severe inflammatory response (Khan *et al.*, 2000). For example, dorsal plating of distal radius fractures with titanium plates has resulted in clinically observed tenosynovitis and tendon rupture. In areas such as this, that require ease of movement of anatomical structures over the implant, stainless steel devices are favoured (Sinicropi *et. al.*, 2005). Specifically, the latter study of distal radius implants in a dog model highlighted the incompatibility of titanium implants for this application since only 43% of free tendon gliding was reported, compared to 75% for titanium alloys and 100% for stainless steel. Additionally, a severe peri-tendinous inflammatory reaction was reported in 57% of the cp.Ti group compared to 63% for titanium alloys and 0% for stainless steel devices (Sinicropi *et. al.*, 2005). In addition to inflammation and loss of motion i.e. reduction in palmar flexion in hand/wrist fixation, device protrusion can be unsightly as well as causing pain to the patient. Alternatively, the device may encroach into the joint space resulting in pain, loss of motion and fracture instability and clearly require immediate attention.

In severe cases, an implant may migrate, which results in instability of the fracture site. Worryingly, with regards to wires and pins, this complication is common and has been fatal in some cases. Devices implanted originally in the humerus, mandible and shoulder have been reported to migrate to areas such as the mediastinum, spinal cord and jugular foramen, respectively (Seipel *et al.*, 2001). Clearly from the point of patient safety, this is irrefragable evidence for elective removal of these devices.

Infection, be it early or late, superficial or deep, is practically difficult to treat comprehensively unless the cause, which often is the device, is removed. This complication can arise at any given time and is not restricted to the early events that occur upon implantation. Highland and Lamont (1985) report the occurrence of deep late infection in six paediatric patients that had undergone internal fixation of the proximal femur (from a group of 63). The study reports the incidence of infection from 7 to 24-months after a period of recovery. Treatment included wound debridement, intravenous antibiotic administration and removal of the fixation device. As a result, the authors concluded that removal of metal implants in children should be implemented as standard procedure to decrease the occurrence of deep late infections.

In a case study cited by Peterson (2005), an eighteen-year-old male treated with open reduction suffered osteomyelitis some fifty years on after initial treatment. However, it is postulated that this be associated with a recent haematogenous infection rather than the organism remaining quiescent for those years. Nevertheless, the persistence of bacteria intracellularly has been reported (Vaudaux & Lew, 2007; Broekhuizen *et al.*, 2008). Intracellular residence may, therefore, provide a sanctuary for pathogenic bacteria by protecting them from host defence mechanisms and antibiotic treatment. In another study, eight infections were reported between a 7 and 24-month period from 152 patients (Schmalzried *et. al.*, 1991). Although the incidence of infection may appear low, the inability to treat this complication, and its occurrence at any given time if the device is retained, raises another point to be considered for elective removal once the desired treatment outcome has been achieved. In fact, orthopaedic device related infections are notoriously difficult to treat and several studies have reported the varying effect of antibiotics in treating pyogenic (pus producing) infections (Lew & Waldvogel, 2004).

Thus, in many instances, antibiotics are given prophylactically however the cost of continued treatment for a patient with an infected device can be staggering. In addition, the efficacies of standard continued prophylactic antibiotic treatments are waning, habitually resulting in need for device removal to provide a cure (review see Vaudaux & Lew, 2006). Thus, advocates of device removal postulate that complications such as infection and the subsequent time and cost it takes to treat are better avoided by extracting the implant.

Some patients have the unfortunate response of hypersensitivity to the metal device, the principal culprits being chromium, cobalt and nickel. Although other elements have also been reported to induce this response. A recent retrospective study reported elevated levels of metal ion concentrations in serum and hair of titanium, vanadium and aluminium in patients with titanium alloy fixation devices. Results showed that almost 35% (16 patients) demonstrated abnormal serum metal ion concentrations. In addition, approximately 24% (11 patients) showed elevated ion concentrations in hair (Kasai *et al.*, 2003). The worrying aspect of these elevated ion concentrations is that they may have negative biological effects on other organs and their presence has previously been reported in urine, lungs, liver, spleen, pancreas and the kidneys. With the exception of titanium many of these elements are involved in biological processes but their elevated levels may eventually give rise to adverse reactions.

The concept of stress shielding of the implant on the underlying bone was initially believed to ultimately result in bone atrophy, and was thought to occur when strength is transferred away from the bone onto the implant. Specifically, there appears to be an enlarging of the IM cavity, coupled with cortical bone loss via endosteal resorption (Akeson *et al.*, 1976). The chances of cortical indention are increased in larger plates and are suggested to prejudice the bone to re-fracture. In one case study a young boy that had treatment to a fractured left femur suffered from a re-fracture of the femur whilst running, 6 years after initial treatment. It was reported that the plate had become completely engulfed by bone which caused an apparent cortical indention in the lateral aspect of the bone.

However, the term 'stress protection' in terms of bone plate fixation, has become archaic since the theory of disturbed vascularity has come to light. For instance, Perren and colleagues (1988) originally suggested that the early bone atrophy documented after the first six months of fixation was due to hindered cortical perfusion rather than stress

shielding. Their hypothesis was that the initial increase in bone porosity was a result of the host attempting to eliminate necrotic bone and ultimately remodel the site. Studies demonstrating the ability of fixation devices to hamper perfusion are many. Rhinelander (1965) noted that beneath the tightly adhered portion of a bone plate implanted in a 3-week canine osteotomy model, vascularisation was absent. Contrastingly, beneath a portion of the plate that had been inadvertently loosened, blood vessels had penetrated the site and cortical vascularity was clear. It appeared to the author that devascularisation was a result of interrupted blood flow at the periosteal surface thus inhibiting any further influx from the medulla (Rhinelander, 1965). In another study, Gunst and colleagues (1979) administered intravital disulfine blue 15 minutes prior to euthanasia of the sheep. Their results also demonstrate a clear lack of cortical perfusion under the plates that had direct contact with the underlying bone, but were not observed in plates with limited contact (Figure 1.11). These findings were later supported in a study where railed and contact plates were used in a dog model (Uhthoff *et al.*, 1994).

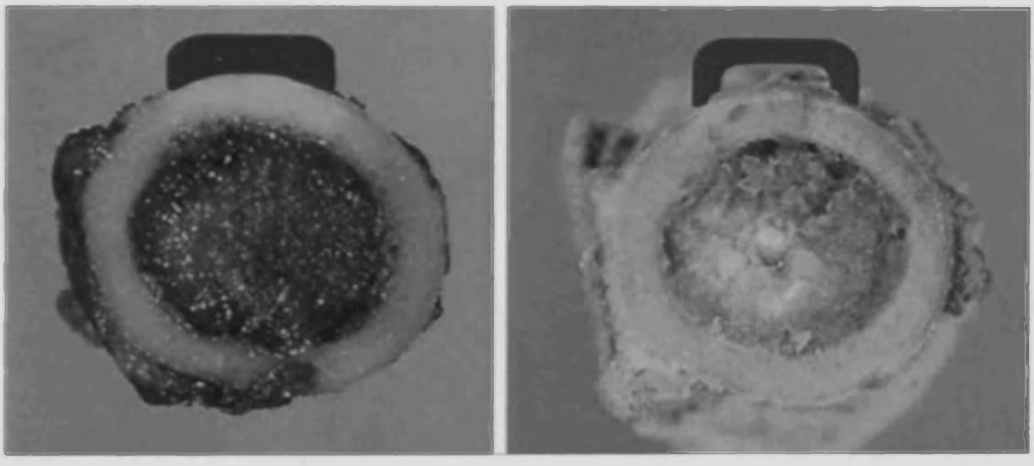

Figure 1.11. Decreased cortical perfusion is more pronounced with increased bone–plate contact with contact plates (left) versus railed plates (right) as demonstrated with intravital disulfine administration. Taken from Uhthoff *et al.*, 2006.

Based on the Perren theory, it would seem to imply that the porosis is a temporary event, which is reversed upon completion in remodelling the necrotic area. However, a later study by Uhthoff and colleagues (1994) addressed this issue and found no evidence to support this notion (Uhthoff *et al.*, 1994). They did, nevertheless, show in other studies that the immobilisation of canine limbs with plaster casts led to cortical thinning and widening of the medullary canal (Uhthoff *et al.*, 1978; Jaworski *et al.*, 1980). Furthermore, if the initial hypothesis put forth by Perren and colleagues was true, then surely, the increased porosity would be found at the area of necrosis. Recently, Tepic (2008) showed that for PC-Fix

plates, the area of porosity was as postulated increased in the vicinity of necrotic tissue. However, it has also been demonstrated previously that bone porosity is in fact increased more in the endosteal part of the cortex rather than the periosteal part where necrosis is most evident (Akeson *et al.*, 1976; Uhthoff *et al*, 2004). Despite the ambiguity surrounding this issue, these observations and clinical outcomes have resulted in the routine removal of many of these internal fracture repair devices, and are supported by the Arbeitsgemeinschaft für Osteosynthese fragen (AO) Foundation for many metal fixation devices.

In paediatric patients, the risk of premature physeal closure is increased when an implant transverses a physis, thus removal of the device is strongly advocated in the case of patients who have significant growth potential, unless the growth cessation is desired (Peterson, 2005). Togrul and colleagues (2005) reported that approximately 8% of premature epiphyseal closures in their retrospective study of 102 paediatric patients were all due to pins crossing the epiphysis (Togrul *et. al.*, 2005). Unfortunately, the occurrence of premature unwanted physeal closure, due to the presence of a fixation device, is high. For instance, Chen and colleagues (2002) observe a 41% occurrence of premature closure of physis while Bagatur & Zorer (2002) report its presence in 65% of the patients studied in their retrospective study. Others have reported success in avoiding this closure with the use of alternative devices such as dynamic screw fixation (Kumm *et. al.*, 2001) and standard cannulated screw fixation (Guzzanti *et. al.*, 2004). Both papers report these alternative techniques provided epiphyseal stability and maintained the capacity for physeal recovery and growth following treatment. However, until such point that these results can be widely verified, many surgeons still opt for device removal to prevent disturbance of normal growth in paediatric patients.

Other factors such as return to sports, carcinogenicity and peri-implant fracture/re-fracture are also relevant concerns to be taken into account. However, in terms of carcinogenicity and peri-implant fracture/re-fracture, the literature indicates that their association with metal implants appears to be negligible and thus, do not warrant routine removal. Nevertheless, some of those reported hold reason for revision.

For instance, Keel and colleagues (2001) report that sarcomas related to fixation devices tend to be high grade and behaved aggressively and frequently metastasized. In the 12 cases they reviewed, 10 were found in bone (the other 2 were found in adjacent soft tissues) and follow up was permitted in only eight. Of these, seven died between 2 and 30 months after diagnosis. Only one patient successfully won their battle for life.

In the case of patients wishing to return to sports, there seems to be a lack of consensus here too. Some believe that devices that restrict joint or muscle action should be removed prior to the patient returning to sport, be it contact or non-contact (Labosky *et al.*, 1990). In contrast, Evans and Evans report that 87% (13 out of 15) professional rugby players returned to full training with retained fixation devices (Evans & Evans, 1997).

Although this is not a comprehensive review on the reasoning behind elective hardware removal, one would hope that the rationale for such is abundantly clear. That being said, there are other factors that must be considered before the full and unchallenged implication of routine removal, and some of these are addressed in the following section

Reasoning against elective hardware removal:

Many surgeons, engineers and researchers alike fail to find sufficient relevant clinical or experimental evidence to convince them to adopt an attitude that routine elective hardware removal is the best option in the end treatment of fixation. Although few reasons exist for this failure, those that do, are just as valid and compelling.

From a purely economic view point, elective removal can be costly and time consuming. Hospitalisation, anaesthesia, imaging, antibiotics therapy and operating equipment, are all points that should be considered. Cost to patient earning is rarely considered but is equally valid.

Although the carcinogenicity risk associated with retained devices in animal models has been well documented, there appears to be few cases of implant-associated tumours in humans. Thus, advocates of implant retention suggest that this risk is impossible to quantify accurately, and does not warrant the application of routine removal based on its occurrence. A recent retrospective study of more than 116,000 patients, reported no correlation between implant retention and increased cancer risk when compared to the general population

(Signorello *et. al.*, 2001). They did, however, report an increase in prostate cancer and melanoma of those patients that had implants retained, but no increase was noted for bone or other connective tissue-related cancers.

It is maintained that conclusions regarding the carcinogenic potential of implants in patients is particularly difficult to make since variable factors such as the quantity of wear debris produced, and patient age may be possible contributory factors (Heath *et al.*, 1971). The question remains whether malignancy is correlated to the presence of long term implants, or, if it is in fact, caused by them. Katzer and colleagues (2003) reported that neither chromium cobalt molybdenum nor titanium aluminium wear particles produced toxic or mutagenic effects, whereas Doran and co-workers (1998) document significant increases in cell transformation for soluble forms of the same materials and appeared to relate directly to toxicity. Furthermore, macrophages have been previously shown *in vitro* to phagocytose laboratory produced debris from steel, cpTi, and Ti15Mo, in a dose dependent manner (Wilson, 1999). In addition, steel particles have also been reported to inhibit cell proliferation as well as disrupting cell membrane integrity.

These observations were also seen when the particles were not in direct contact with the cells. Steel particles are reported to be approximately 0.5 μm in size (ap Gwynn & Wilson, 2001), and thus, are easily dispersed throughout the body. In fact, wear debris generated from steel has also been noted in organs remote from the implantation site (Case *et. al.*, 1994). In contrast, particles generated from cpTi are approximately 10 μm in size (ap Gwynn & Wilson, 2001) and have been reported to be found in tissue adjacent to the implanted site giving the harmless discolouration of the tissue. Overall, since this facet of implantology is largely unproven many believe that the occurrence of malignancy due to metal fixation is nominal and therefore the risks associated with implant retrieval far out-weigh those of retention with regards to carcinogenicity.

Complications associated with the surgical aspect of device retrieval are a principal basis for hardware retention for many surgeons. Inherent risks such as iatrogenic impairment and complications with anaesthesia are considerations for any surgical procedure. In addition, the actual procedure of implant retrieval can add to the already serious pre-existing concerns. For instance, re-fracture, nerve damage, excessive blood loss, infection, and difficulty in removing the device e.g. stripping of the screw head or even breakage at the

screw neck (Figure 1.12) are all potential obstacles that must be reviewed carefully for one to carry out a successful retrieval.

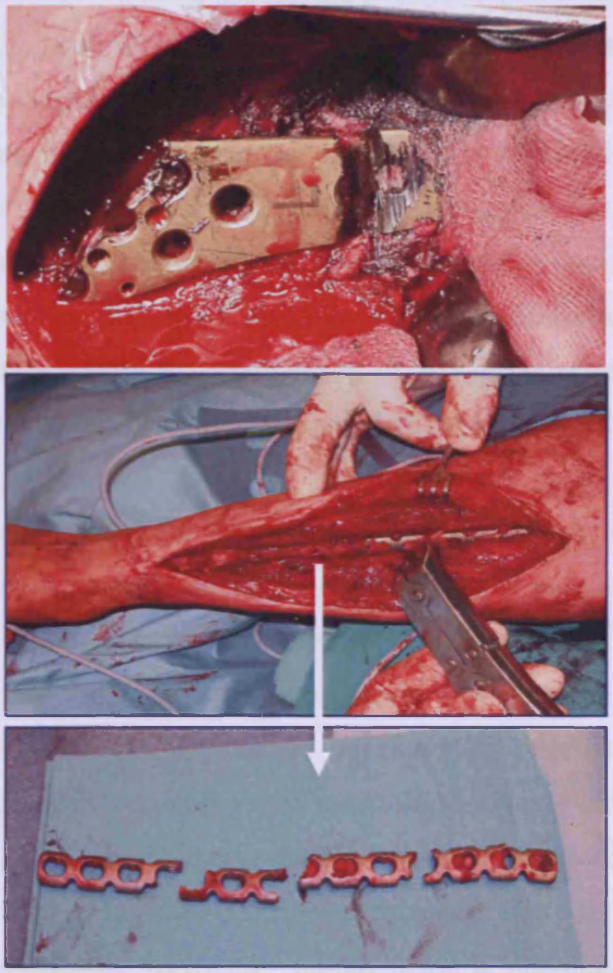

Figure 1.12. Difficulty in device removal. Implant breakage can occur for several reasons, the main culprits being extraosseous formation and loss of implant integrity. With kind permission of E. Saura, AO Foundation (top image), and N. Schwarz Klagenfurt, Austria (middle and bottom image).

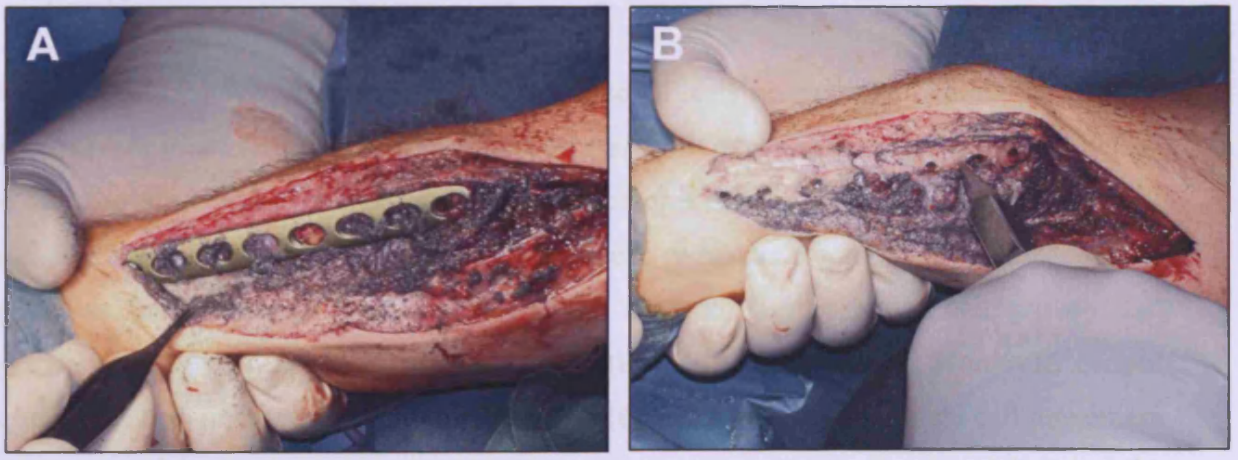

Figure 1.13. Difficulty in implant removal can result in excessive blood loss and/or debris contamination (A). Furthermore, once the plate is finally removed, the surgeon is often then faced with the added complication of attempting to remove broken screws (B). Photos used courtesy of N. Schwarz Klagenfurt, Austria.

The Cell-Surface Relationship

In a Presidential address to the American Biomaterials Society, Prof. Buddy Ratner meaningfully noted that current biomaterials have been developed as a result of trial and error optimization rather than specific design (Ratner, 1993). However, as acknowledged by Brunette (2001) to design materials that elicit specific responses from tissues is a complex proposition. The main reason for this is that the vast majority of the biological principles controlling cell interaction with implants remain largely ambiguous. For instance, the early eighties saw the introduction of the inhibition of epithelial down growth onto implants via contact inhibition (Brunette *et. al.*, 1983). Even in a well studied phenomenon such as contact guidance, elucidating controlling mechanisms of cell response remains challenging thus largely limiting these approaches to *in vitro* studies (Chehroudi *et. al.*, 1992).

Thus in terms of tissue engineering the 'tissue' part has slipped out of focus somewhat while the engineering part, or more accurately the production of new materials, comes to the forefront. Some studies have attempted to assign precedence to the tissue response in the tissue-implant interaction when fabricating materials; however, these are limited and infrequent. Moreover, the inclusions of features postulated to improve osseointegration, such as the incorporation of surface depressions mirroring osteocyte dimensions (Schulte, 1984), have limited *in vivo* evidential support mainly because a great deal of speculation is included with regards to cell behaviour. Therefore, projected outcomes are probabilistic rather than precise. Consequently, focus has shifted towards manipulating cell-material interactions from the implant side of the equation. Accordingly, despite the seemingly insurmountable task ahead, many imperative details regarding cell behaviour to materials have emerged.

Several studies have elucidated the importance of cell shape in a variety of cellular processes such as cell growth, differentiation and gene expression, all processes shown to be affected directly by the surface characteristics of a device. Interestingly, the effects of surface roughness appear to be cell type dependent. Whereas macrophages and osteoblasts appear to prefer rougher surfaces, fibroblasts tend to display better cell growth and spreading on smooth surfaces, ie. rugophobic (Rich & Harris, 1981). Moreover, certain surfaces such as titanium can induce hyptotaxis (Carter, 1967), a directional cell movement which is a result of adhesive gradients on the substrate. Thus if adhesive forces between the implant and the cells are stronger than the cell-cell cohesive force, it is reasonable to

postulate that cells would migrate onto the implant more readily. A role in cell distribution may also be attributed somewhat to hyptotaxis. This role can be highlighted by the reaction of osteoblast cells to titanium surfaces in long term culture where cells spontaneously detach from the substrate in a matrix and cell rich multi-layered tissue-like construct. Consequently, few cells actually remain on the substrate, and it is suggested that the migration of the cells from the titanium surface to the matrix may be mediated by hyptotaxis. Cooper and colleagues (1993) have also shown a tendency for titanium to compete with collagen (in this case a collagen gel) for osteoblastic binding. Interestingly, osteoblasts were found to bind to the collagen gels five to ten times more frequently compared to titanium. So the question arises – what is more desirable, direct cell-material attachment or matrix-material attachment? As with many facets of science, the questions often come more readily than the answers. As Brunette (2001) notes for long term fixation, direct matrix-material attachment may be more desirable to mediate cell interactions with the device. However, this point has never really been expanded upon but may hold the key for further vital revelations in the cell-material interaction saga.

The Role of Surface Chemistry

The topography and chemistry of a device are believed to directly affect cell response. It is of no great stretch of the imagination to see why the chemical composition of titanium has attracted interest. The excellent biopassivity, corrosion resistance and repassivation ability of titanium and its alloys are a direct consequence of the chemical stability and integrity of the oxide film. Further, importance has been assigned to the oxide layer since essentially it is this that interacts with proteins and cells upon implantation and persists at the interface for the life of the fixation (Eisenbarth *et. al.*, 2002). In fact, the sensitivity of cells to the chemical composition of a device is to the extent that even different grades of titanium are detected at a cell level (Ahmad *et. al.*, 1999). However, a point to note is despite identical preparation, the samples did acquire different surface morphologies; therefore, the effect of microtopography cannot be underestimated. Some studies suggest that by increasing the thickness of the oxide layer, then bony in-growth can be proportionally increased (Hazan *et. al.*, 1993) whereas others acknowledge the beneficial effects of the oxide layer but do not report major differences in fibroblast cell response based on oxide thickness alterations (Vinall *et. al.*, 1995). Recent studies have investigated the effect of both topography and chemical modification on bone formation (Larsson *et al.*, 1994, 1996, 1997) and have suggested that the degree of bone contact and bone formation around implants placed in rabbit cortical bone are directly affected by oxide thickness and surface topography

(Larsson *et al.*, 1994). Specifically, polishing of the surfaces resulted in less bone contact compared to machined devices. Since both samples had comparable oxide thickness (4-5nm) it would appear, in this case, that surface microtopography governed tissue responses. Characterisation data provided by the authors suggest that the surface roughness between samples was similar (approximately 30-40nm), however surface morphology differed. However, thicker oxide layers (21nm and 180nm) also appeared to enhance initial bone formation of the surrounding tissue. Nevertheless, it could be postulated that the effect of the oxide layer can be detected to some degree by individual cells but that this response is not oxide thickness dependent. Thus, the tissue response may potentially be the same for an oxide layer of 5nm or 50nm. Larsson and co-workers effectively support this notion as they conclude that a reduction in surface roughness appears to directly affect the rate of bone formation (Larsson *et al.*, 1994; 1996). However, they also postulate that this effect on initial bone formation is transient. After one year they did not find any evidence that the reduction in surface roughness (samples ranged from 2.9nm to 40.8nm) had any influence on the amount of bone (Larsson *et. al.*, 1997). Whether the comparable quality of bone was similar was not alluded to. To throw further indecision on the matter, Tzur and colleagues (1998), found that surface modification via heat treatment resulted in a significantly higher torque removal of treated stainless steel transcortical screws compared to untreated, thus suggesting an increase in fixation strength. However, without the inclusion of surface characterisation data by the authors, interpretation of these results becomes more difficult.

The importance of surface chemistry is demonstrated with greatest efficacy when considering protein adsorption. Cells bind to titanium and its alloys through a series of adhesive molecules such as vitronectin and fibronectin (Degasne *et. al.*, 1999). Thus, alterations in surface chemistry will effectively influence protein adsorption and conformation, and ultimately initial cell attachment. Yang and co-workers (2003) found that increased cell attachment was directly proportional to the amount of preadsorbed protein. However, this mechanism was also protein-type dependent. In this study, both fibronectin and albumin were assessed and it was reported that the concentration of adsorbed fibronectin onto the titanium surfaces was higher compared to albumin. Considering the hydrophilic nature of cpTi, and the fact that albumin is known to display improved binding to hydrophobic surfaces, this finding seems logical. Time also appeared to be a factor as the positive effect of preadsorbed fibronectin was observed to be highest after 15 minutes, however, after 180 minutes this effect on cell attachment was negated (Yang *et. al.*, 2003).

This outcome seems logical since the rapid adsorption of proteins onto devices is considered to be one of the first events to occur upon implantation (Meyer *et. al.*, 1988) an effect that is suggested to then diminish as the effect of topography comes to the fore. However, this system works in synergy rather than exclusively. Interestingly Howlett and colleagues (1994) found that vitronectin was essential for osteoblast cell attachment onto cpTi, stainless steel, alumina and polyethlyene-terephthalate (PET). However, this outcome was fibronectin independent a result which contradicts others identifying fibronectin as the principal component (Horbett & Schway, 1988). One must keep in mind, however, that this effect may also be cell type and/or species dependent (Howlett *et al.*, 1994 used human bone derived cells where Horbett *et al.*, 1988 used a mouse cell line). Furthermore, it is suggested by Howlett and co-workers that perhaps fibronectin (in this model) plays a role in cell adhesion rather than initial attachment and that vitronectin is a more effective competitor compared to other serum proteins for surface binding. Nevertheless, the 90 minute time point included by the authors may have clouded the outcome slightly. For instance, Meyer and colleagues (1988) showed that protein and lipid adsorption was already detectable after 5 minutes implantation, the earliest time point studied.

The role of surface microtopography *in vitro*

Although chemical modification of titanium is under close scrutiny at present, the focus still weighs heavily on investigating the role of surface microtopography on device performance and many studies have pin-pointed this feature as the major determining factor for fixation success. For instance, osteoblast attachment to titanium appears to be influenced directly by surface roughness (Bowers *et. al.*, 1992). This effect has also been found true for many other cell processes. Several studies have identified the effect of microtopography on cell proliferation. Martin and co-workers (1995) showed that osteoblast-like cells had decreased proliferation on rougher titanium surfaces (R_{max} up to 39.8μm) compared to control tissue culture plastic (no measurement given). Specifically, tritiated thymidine incorporation was inversely correlated to surface roughness. Postiglione and colleagues (2003) found during their investigations a similar relationship of surface topography of different titanium surfaces (smooth, sandblasted and plasma sprayed) on proliferation. Specifically they show that DNA synthesis is significantly lower on sandblasted and plasma sprayed samples compared to the smooth surface of tissue culture plastic (no surface roughness data included). A similar trend was observed by the authors with regards to cell number, that is, the sandblasted and plasma sprayed samples had a significantly lower cell number compared to the plastic control. The authors suggest that, as opposed to cell

apoptosis/necrosis being induced on the sandblasted and plasma sprayed surfaces that this effect was in fact due to lower cell numbers being present on these surfaces.

Advocating this finding is the observation that surfaces with many micro-discontinuities support osteoblast differentiation pertaining to alkaline phosphatase (ALP) activity (Martin *et al.*, 1995), gene expression (Masaki *et al.*, 2005; Schneider *et al.*, 2003) and mineralization (Boyan *et al.*, 2002). Thus a general consensus has emerged postulating that while surfaces lacking microtopography support a proliferative cell state, surfaces with micro-discontinuities support osteoblast phenotypic expression. For instance, core binding factor-1 and osterix, both factors implicated in the early fate determination of pre-osteoblasts (and in the case of cbfa1 regulator of genes associated with osteoblast differentiation and mineralization such as osteocalcin, osteopontin and collagen type I), were observed to be significantly increased on grit blasted cpTi surfaces. Alkaline phosphatase (ALP), another marker of early osteoblast differentiation is also found to be increased on surfaces with micro-discontinuities (Masaki *et al.*, 2005). Indeed, the effect is so great that the differentiation of preosteoblasts can effectively be influenced by surface microtopography (Schneider *et al.*, 2004).

The question, therefore, arises – how does the microtopography of a surface influence cell phenotype? One hypothesis is that cells are examples of a tensegrity model, or tensional integrity (Ingber, 1993) thus, are a dynamic network of filaments that are capable of dissipating signals both locally and globally by alterations in cell shape via its cytoskeleton. Therefore, the mechanism proposes that a surface with many micro-discontinuities would effectively alter the shape of a cell to a degree that would directly influence its mechanical and genetic activity. Indeed, it has been shown previously that osteoblasts assume distinct morphologies subject to the micro-architectural characteristics of the surface on which they are cultured. Brunette (1988) has highlighted the importance of surface microtopography on osteoblast morphology. It seems that once the peak to peak distance is lower than the length of the cell body then osteoblasts assume their characteristic cuboidal morphology. Conversely, osteoblasts cultured on substrates lacking micro-architectural features tend to adopt a more flattened appearance akin to that of a fibroblast and this alteration in cell shape appears to correlate with the physiological behaviour reported for osteoblasts, as advocated by Ingber (1993). Presenting additional support for this theory of tensegrity, is evidence that has emerged indicating that smoother surfaces support this 'fibroblast-like'

phenotype. Smooth surfaces essentially show lower cytokine, growth factor production, ALP activity and osteocalcin levels. In conjunction with these decreases there is a marked increase in the rate of proliferation over micro-rough surfaces as mentioned previously.

The effect on a genetic transcriptional and translational level is further supported by data accrued for the influence of microtopography on local cytokine and growth factor production involved in modulating the healing response. Boyan and colleagues (2003b for review) have extensively shown that local factors such as transforming growth factor beta-1 (TGF1) and prostaglandin E2 (PGE2) display a surface roughness dependent response. Specifically, they have shown in recent years that PGE2 increases proportionally with surface roughness. Although it has been elucidated as a necessary factor for osteoclastic activity at high levels (Raisz, 1984), interestingly it appears that PGE2 is actually required at low levels for osteoblastic activity (Raisz *et al.*, 1993). Therefore, the increase of this factor on rough surfaces would seem to be a negative outcome. This outcome does not seem to be the case, however, since the elevated levels of PGE2 reported for osteoblasts cultured on rough surfaces seem to be necessary for enhanced osteogenesis. For instance, hindrance of prostaglandin production by the non-steroidal anti-inflammatory drug, indomethacin, impedes the increase in osteoblastic phenotypic expression reported for these samples by blocking the normal expression of markers idiosyncratic of a differentiated osteoblast (Sisk *et al.*, 2001). In a later study, the group also reports the role of cyclooxygenase-1 and 2 in the surface-dependent response observed as inhibitors specific to only one form of the enzyme fail to hinder the prostaglandin-dependent effects (Boyan *et al.*, 2001).

Kieswetter and co-workers (1996) also identified the relationship between surface micro-roughness and TGFβ1 levels reporting a three to five times higher activity on coarse sandblasted and titanium plasma sprayed surfaces respectively, compared to tissue culture plastic. In a similar trend to PGE2 production, TGFβ1 is also found at low levels on smooth surfaces whereas a marked increase is reported for micro-rough substrates. This growth factor has been shown to be pivotal to bone formation for many reasons, some of which include its ability to stimulate mesenchymal stem cell (MSC) proliferation, matrix production, and the down regulation of osteoclast activity. Combined, the data accrued from these studies would suggest that osteoblasts cultured on titanium surfaces with rough micro-topographies appear to advocate a more optimal healing 'niche' with regards to cytokine and growth factor production compared to smooth substrates. However, it must be borne in

mind that plastic and metal are very different materials, thus, the value of including tissue culture plastic as a control surface can be misleading and potentially can lead for false positive or negative results.

Schneider and colleagues (2003) showed recently that mineralization is positively influenced by surface roughness. In their study, they compared osteoblast mineralization after 72 hours on both grooved and roughened (sandblasted) cpTi samples. However, while SEM images revealed a distinct morphology for the samples, no other characterization data was provided. Results indicate that a significant 50% increase in mineralization for rough over grooved surfaces was noted. Importantly, there did not appear to be a significant difference in rate of proliferation of the cultures, nor was there a marked difference in cell number for osteoblasts cultured on rough versus grooved titanium surfaces. Using epoxy coated resin replicas of mechanically polished (Ra=0.06μm), acid etched (Ra=0.58μm), coarsely blasted (Ra=5.09μm) and coarsely blasted/acid etched (Ra=4.33μm) samples, Wieland and colleagues (2005), showed that neonatal rat osteoblasts produced significantly bigger and more frequently occurring bone-like nodules on the coarsely blasted/acid etched substrates than any other substrate examined. These authors suggested that the ability of this substrate to support osteoblast differentiation or maturation earlier thus allowing maturation of the nodules prior to the end-point.

The role of surface microtopography *in vivo*

Recent short- and long-term *in vivo* studies using implant devices with varying surface topographies have shown that the mechanisms involved in this 'niche' are possibly more ill-defined than the *in vitro* situation and, in some cases, conflicting results are reported. For instance, Hayakawa and co-workers (2000) observed a difference in bone response to grit blasted and smooth substrates in rabbit cortical bone. However, this difference was not reported for the same samples when investigated in a trabecular bone model. Conversely, Pearce and colleagues (2008b) have shown that standard micro-rough cpTi and TAN had higher torque removal in both a trabecular and cortical sheep bone model compared to polished samples of the same materials over a period of 6, 12 and 18 weeks. Interestingly, this study also made evident a distinct difference in peak torque removal for both bone types. For the trabecular model, there was a peak increase in torque removal for all samples at 12 weeks which decreased by week 18. However, in all cases the removal torque for standard micro-rough samples was highest. In contrast, the cortical bone model showed a

time dependent decrease in torques removal over the full time course from 6-18 weeks. Again at all points the torque removal was highest for standard micro-rough samples despite of this general decrease in torque. The authors suggest that these differences may be a result of disparity in the remodeling rate of both bone types. In addition histomorphometric data showed a clear trend for the reduction in percentage bone contact for polished implants at 6 and 12 weeks in both the rib and tibia. At 18 weeks this trend was most apparent with stainless steel and polished cpTi in both bone types. Upon closer investigation, the authors also observed a soft-tissue interface at the Stainless steel implant surface and attribute this to the lower torque removal attained for these samples (Pearce *et. al.*, 2008b).

Bone quality and quantity is another important issue that gives rise to many debates for *in vivo* studies. Wennerberg and colleagues (1997) studied the effect of surface roughness of titanium implants (machined-0.96μm; 2 blasted-1.16 and1.94μm) on bone response, in rabbits after 1 year post-implantation. Using both torque removal and bone-implant contact to evaluate this response the authors reported that despite the blasted samples having higher torque removal and bone-implant contact, it was the machined samples that had the highest quantity of surrounding bone. One point that wasn't alluded to by this study, however, was the actual quality of the bone formed. Therefore, even if less bone was formed around the blasted samples, the quality of the bone may have been superior to that found adjacent machined samples. Furthermore an important point that should be considered prior to, and in critique of animal studies is the fact that variations in animal models as well as other factors (i.e. topography, material used) will directly influence the outcome. Therefore, results between studies are difficult to compare and the merit of their outcome should be duly considered. Pearce and colleagues (2008a) have covered this subject in detail and the reader is directed to their review for comprehensive reading. Briefly, the authors reveal that although used in the majority of animal studies (Neyt *et al.*, 1998), both the macro and micro-structure of rabbit bone differs greatly to that of humans. Based on these differences, the obvious concern of healing comparisons between rabbit and human become highlighted. Specifically, the anatomy of the bone with regards to size and shape as well as histological bone structure and, also loading, due to the differences in stance between the two species, is often overlooked. More importantly the actual process of bone remodelling in rabbits is much faster making results difficult to extrapolate to the human situation.

Other studies have failed to distinguish any effect of surface topography on the bone response. For example, Vercaigne and co-workers (1998a) examined the bone response to titanium alloyed samples with varying degrees of surface roughness (4.7-37.9μm) in goat cortical bone after 3 months insertion. Contradictory to previously cited studies, a statistical difference was not found for bone-implant contact for any of the devices nor did there exist a difference in torque removal for the samples tested (Vercaigne *et al.*, 1998a). Even more controversial were the findings that after 3 months, the authors failed to differentiate between bone responses for the distinct samples of varying surface roughness nor was there a distinguishable correlation between device topography and the quantity of bone contact to the implant (Vercaigne *et al.*, 1998b). Interestingly, bone composition, metabolic rate and remodelling have been shown to be similar between goats and humans (Pearce *et al.*, 2008a). However, it must be noted that morphologically, even the 'smoothest' surface included in this study had a huge degree of micro-discontinuities and therefore it is possible that between the ranges of roughnesses examined a similar response was evoked. This is discussed shortly.

Further, Kawahara and colleagues (2006) failed to find any significant confirmation of topographic dependency on bone formation in beagles around cpTi implants (Ra 0.4-1.9μm) when subjected to masticatory loading. However, an important consideration, as with any study which investigates roughness related cellular responses, is correct extrapolation between studies especially when such variance is present. For instance, if we just take the former study as an example, Vercaigne and colleagues (1998 a & b) failed to find a correlation between bone contact and surface roughness. However, the 'smoothest' surface in their study was 4.7μm which in most studies is considered micro-rough. Therefore a roughness related response may have been experienced by even the control 'smooth' surface making any differences between surfaces perhaps minimal. Moreover, the actual ability of an individual cell to detect a micro-rough or micro-smooth surface is directly influenced by the actual degree of roughness. For instance, if a surface is 'too' rough i.e. average roughness of the surface is greater than that of a cell, then the possibility arises that cells will react to that surface as if it was smooth. However as is the case with many studies the importance of surface characterisation is paramount especially since it is the features of the surface that will effectively evoke a biological response. Unfortunately however this importance is often overlooked with many studies employing one or two methods of characterisation apparently sufficing. As will be described in chapter two, this

analysis strategy is often a misconception, and one that can be costly when drawing conclusions from studies.

In the study by Vercaigne (1998a) the authors also indicate that the surgical procedure may have added to the negative effect seen. For instance, the shape of the implants used in this study did not allow for standard drill holes to be made thus resulting in a wider than normal gap being created. Previously it has been shown that increased gap size and reduced fit can have a negative influence on the integration of an implant (Cameron *et. al.*, 1973). Furthermore electron dispersive spectroscopy measurements revealed the presence of Al_2O_3 on the surface of the grit-blasted surfaces studied. Gross and Strunz (1985) have previously shown that the Al_2O_3 remained from the blasting procedure can have a negative effect on bone response essentially inhibiting the final mineralisation of bone. Then again Wennerberg and colleagues (1996) in contrast to the pre-mentioned studies could not demonstrate any negative effect of Al_2O_3 blasting procedure on the bone response.

The obvious question is why is there such variation in the conclusions drawn by these and other studies? Differences in the species used, surgical site, surgical fit, the surgery itself and subsequent parameters of analysis, device fabrication, and varying degrees of surface roughness are some of the principle areas from where variation between studies may stem. Definitions are certainly required as to what constitutes a 'rough' or 'smooth' surface (millimetres, micrometres, nanometres). For instance, Boyan states that if the average roughness of a surface is greater than the size of an individual osteoblast, then essentially this surface may been seen as smooth since the distance between peaks is too great as to be detected. This observation is fundamentally the same point that was made much earlier by Brunette who as mentioned previously reported that if the peak to peak distance is lower than the length of the cell body then osteoblasts assume their characteristic cuboidal morphology but if larger a well spread fibroblast-like morphology is assumed. Additionally, Richards (2008) has identified a spectrum of roughness between 0.2-2μm which is believed to provoke the optimal differences in cell behaviour for smooth versus rough samples. Despite this information many studies still included samples with average roughness of approximately 5μm and designate their 'smooth' surface to be less than 0.6μm (Boyan *et al.*, 2003a & b; Lossdörfer *et al.*, 2004). Clearly, this requires a degree of standardisation for studies to be comparable. Although alone these points do not completely resolve the discrepancies found for conclusions drawn from these and many other studies, it does pose

important questions for future *in vitro* and *in vivo* work essentially bringing our approach to material design and fabrication, albeit indirectly, towards a more empirical methodology.

Experimental Aim:

The overall aim of this study is to investigate the effect of two variations of surface polishing (Electro- and paste polishing) of three commercially available internal fixation materials (cpTi; TAN; Ti15Mo) on primary rat calvarial osteoblast cell response as a model of *in vitro* screening for osseointegration. After validation *in vitro*, the study aims to assess the influence of surface polishing on screw removal from locking compression plates and intramedullary nail removal in a bilateral non-fracture model using female Swiss alpine sheep from an orthopaedic research flock so that age, weight and health status are known as to create a standard model. The motivation behind this study arises from the complications reported during hardware removal due to bony overgrowth on the device. We postulate that by reducing the surface micro-discontinuities on site specific areas of the implant known to be prone to extraosseous formation via the novel, simple approach of surface polishing, ,that potentially the complications associated with this clinical problem can be circumnavigated.

Chapter 2: Surface characterisation.

Abstract

The notion that the morphological features of a surface can evoke distinct biological response *in vitro* and *in vivo* is not a novel one. Therefore, comprehensive characterisation of a surface is of paramount importance for any study of this kind, as it provides information regarding the surface properties that may inadvertently determine the success of a device for fracture fixation applications. Consequently this chapter focuses on the characterisation of clinically used orthopaedic materials with standard commercially available and experimental surface finishes. Specifically we investigated commercially pure titanium, Titanium-6%Aluminium-7%Niobium and Titanium-15%Molybdenum in their 'standard' micro-rough form as well as experimental electropolished and paste polished version of each material type. Stainless steel in its commercially available electropolished form was included as a control substrate to represent the orthopaedic 'gold standard' smooth surface. Scanning electron microscopy, atomic force microscopy, non-contact white light profilometry, contact angle measurements, and X-ray photoelectron spectroscopy revealed marked differences in surface roughness and morphology of polished samples compared to micro-rough counterparts without marked changes to their surface chemical composition.

Chapter 2: Surface characterisation

Advances in material fabrication methods and design over the years have resulted in significantly improved biomaterials such that practically all traditional areas of medicine employ them in the areas of treatment of diseased or traumatized organs. Thus the safe and efficacious interaction of any biomaterial with a host environment is of critical scientific and clinical importance. Furthermore, since effectively it is the outermost layers of the biomaterial that exert the biological response, it comes as no great surprise that characterisation of the material surface is paramount. Consequently one of the primary goals of biomaterial research is to devise optimal surfaces with the view to eliciting desired interfacial responses.

Characterisation of the surface properties of a device is, therefore, essential to relate important surface features with certain biological responses. Thus, by thoroughly characterising a material one can make tentative steps to discriminate specific mechanisms by which the host environment translates surface topographical features into a tissue response. Many facets of a surface may contribute to protein (Yang *et. al.*, 2003) and cell interactions (Boyan *et. al.*, 2003) upon implantation. Surface energy (Möller *et. al.*, 1994), surface chemistry (Curtis *et. al.*, 1983) and topography (Richards, 1996; Brunette & Chehroudi, 1999) are broadly the areas considered most important in the initial assessment of a material. Therefore for a comprehensive understanding of the surface features of a biomaterial several avenues must be examined since no one technique is available to provide an eclectic representation. However with the use of several techniques of surface characterisation available one can compile ample data to elucidate important surface features of a device.

It has been shown extensively that the micro-architectural features of a surface significantly influence cell behaviour upon contact (Brunette, 1986; Groessner-Schreiber & Tuan, 1992; Richards, 1996; Schneider *et. al.*, 2004; Masaki *et. al.*, 2005; Meredith *et. al.*, 2007a) and can potentially affect the *in vivo* and even clinical outcome (Buser *et. al.*, 1991; Pearce *et. al.*, 2008b). It has been shown comprehensively that manipulation of microtopography amongst other features can alter a cells response to its environment (Martin *et. al.*, 1995) resulting in an influx of research in this area.

Essentially, there are two common approaches of surface modification, namely chemical and topographical. The effects of surface chemistry upon cell/protein attachment occur within seconds to minutes upon implantation of a device. As mentioned previously, a study by Meyer and colleagues (1988) showed that protein and lipid adsorption occurred upon surfaces studied within 5 minutes. However this was the earliest time point studied but in an *in vivo* situation one would speculate that specific proteins are adsorbed onto materials instantaneously upon contact. Importantly adhesion and ultimately the wound response can be directly influenced by a surface's ability to adsorb molecules. Howlett and co-workers (1994) eloquently showed the dependence of vitronectin for the attachment of bone-derived cells onto stainless steel, titanium, alumina and polyethlyene-terephthalate. Their study also showed that fibronectin did not appear to be required for initial cell attachment but as the authors postulate may play a more prominent role in cell adhesion. In contrast, fibronectin has been shown to be necessary for mesenchymal cell (MSC) attachment (Yang *et. al.*, 2003) whereas laminin is required for epithelial attachment (Terranova *et. al.*, 1986). These studies highlight the complex relationship that exists between the biomaterial and initial protein/cell attachment. Thus, the inclusion of assessing the surface wettability profiles of a material is a fundamental consideration since ultimately the hydrophobicity /philicity of a surface will also determine whether protein/cell attachment is enhanced or inhibited.

A substantial research effort has been carried out in modifying surface chemistry to enhance bone bonding *in vivo*. Many approaches include the alteration of the surface of titanium with the addition of growth factors (Lind *et. al.*, 1995), calcium phosphate (Jansen *et. al.*, 2000), protein coatings (Yang *et. al.*, 2003) and peptides (El-Ghannam *et. al.*, 2004; Ferris *et. al.*, 1999). However issues regarding bonding and integrity of these chemical modifications have meant that significant and promising effects *in vitro* have been difficult to translate to the *in vivo* situation.

Extensive study of the surface of titanium over the years has highlighted the many parameters that influence material performance. On a macro-scale (mm) effects observed are mainly mechanical as demonstrated by the nature of screw heads. However the main issue with macro-topographical features is that the actual surface is smooth relative to cells and tissues, resulting in a fibrous tissue interface (Klokkevold *et. al.*, 1997). Thus much focus has been lent to assessing the modifications of surfaces on a micrometer level and it is this parameter that is the main focus of this study on osteoblast cell response.

It is postulated that at this level the microtopography of a surface can be sensed by individual cells thus opening the possibility of eliciting topographical dependent specific cell responses. It is suggested that the surface topography is potentially the strongest cue of surface features to influence a host response to a biomaterial (Thomas & Cook, 1985; Richards, 1996; Meredith *et. al.*, 2007a). In fact, a myriad of studies have been dedicated to investigating this poignant question (Martin *et. al.*, 1995; Cooper, 2000; Lossdorfer *et. al.*, 2004). Thus the importance in determining and evaluating topographical characteristics precisely should be a major consideration for any study.

Therefore this chapter is dedicated to surface morphological analysis using several widely accepted methods which collectively allow us to form a comprehensive but not definitive profile of the surfaces. Specifically we focused on topographical and chemical characteristics and surface wettability.

Chapter 2: Materials and Methods

Contact angle

Samples used in this chapter for all characterisation in this chapter are fabricated to 13mm discs. Contact angle measurements were made using the Sessil drop method with the Drop Shape Analysis System (Contact Angle Measuring Instrument G10 and DSA 10 Control Unit, KRÜSS GmbH) and analysed using the Drop Shape Analysis 1.50 software (KRÜSS GmbH). Samples were placed in a preheated chamber with an external water source to sustain a constant relative humidity (20°C). Using the computer controlled system, a 20µl droplet of distilled water was dispensed onto the sample and quantified exactly 1 minute after dispensed using the analysis software. Two separate measurements were taken for each sample and this process was repeated on a further 2 samples, thus totalling six measurements for each sample type.

Material	*Symbol*	*KKS Grinding*	*Vibratory Grinding (ceramic Tumbling)*	*Electro-polished*	*Blasted*	*Anodised by SYNTHES (colour)*	*Acid Etching (Pickled)*	*Gamma Sterilised*
cp titanium	TE	×	✓	Steiger SA	×	Gold	×	✓
	TP	✓	✓	×	×		✓	✓
	TS	×	✓	×	INOX[1]		✓	✓
Ti-6%Al-7%Ni	NE	×	✓	Steiger SA	×	Green	×	✓
	NP	✓	✓	×	×		✓	✓
	NS	×	✓	×	Wet		✓	✓
Ti-15%Mo	ME	×	✓	Steiger SA	×	Blue	×	✓
	MP	✓	✓	×	×		✓	✓
	MS	×	✓	×	Wet		✓	✓
Stainless steel	Ss	×	✓	✓	×	×	×	✓

Table 2.1. Summary of the production process of the 13mm sample materials used in this study. [1]INOX stainless steel balls. TE - electropolished cpTi; TP- paste polished cpTi; TS-standard cpTi; NE – electropolished TAN; NP – paste polished TAN; NS – standard TAN; ME - electropolished Ti15Mo; MP – paste polished Ti15Mo; MS - standard Ti15Mo; Ss – stainless steel

X-ray photoelectron spectroscopy

XPS measurements were carried out by Dr. V. Frauchiger of the Robert Mathys Foundation, Bettlach, Switzerland. Prior to surface analysis, the samples were ultrasonically treated for 20 minutes with alkaline 3% Deconex 12PA followed by rinsing with dionised water and subsequently cleaned with ethanol for 10 minutes. Samples were once again ultrasonically treated for 20 minutes in ultra-pure water and subsequently rinsed with methanol in order to remove debris and potential contaminants from the packaging material. The samples were allowed to air dry and were subsequently wrapped in aluminium foil. One additional sample was analyzed without cleaning, as a control. The samples were

mounted on aluminium sample plates by using double sided electrically insulating sticky tape which is vacuum compatible. All spectra were recorded on a Kratos Axis Nova (Kratos Analytical, UK) using monochromatic AlKα radiation (1486.69 eV) produced at an anode power of 225 W (15kV, 15 mA), an electron take-off angle of 90° relative to the surface plane and an electron analyser pass energy of 80 eV. During analysis, the base pressure remained below 10^{-8} torr. For quantification, survey scans with a step width of 0.5 eV were performed on two spots of 300 x 700 μm^2 per sample. Data was evaluated with CasaXPS 2.3.10 (CasaXPS Ltd, UK) using relative sensitivity factors supplied with the instrument.

Non-contact white light profilometry

Quantitative measurements for three separate discs of each sample were taken using a non-contact white light FRT MicroProf® (Standard) with CWL 300μm sensor profilometer (Fries Research & Technology, Germany). A roughness average (Ra – arithmetic mean of the roughness height expressed in micrometers) was measured from a 0.5x0.5mm scan area with a point density of 1000 points/line. Two separate measurements were taken for each sample, resulting in a total of six measurements per sample.

Scanning electron microscopy

The morphology of the sample surfaces was studied using a Hitachi S4700 field emission Scanning Electron Microscope (FESEM) fitted with an Autrata yttrium aluminium garnet (YAG) backscattered electron (BSE) scintillator type detector. The images were taken in both secondary electron (SE) and backscattered electron (BSE) mode, with an accelerating voltage of 5kV, an emission current of 40μA, a working distance of 12mm and a positive tilt of 30°.

Atomic force microscopy

Atomic force microscopy (AFM) was carried out using a Thermo Microscopes Explorer AFM, in conjunction with a Veeco MLCT-EXMT-A, non conductive silicon nitride AFM probe in contact mode. A scan range of 50 μm was analysed at a rate of 100μm/sec with a resolution of 500 data points/line. Data were collected in both forward and reverse mode to confirm reproducibility. Measurement data were processed using SPMLab software (Thermo Microscopes). Two measurements from three separate discs were taken resulting in a total of 6 measurements per sample and were preformed by Dr. D.M. Devine from the Athlone Institute of Technology, Ireland.

Chapter 2: Results

Contact angle

Results show (Table 2.2) that all polished variants (with the exception of NP) have lower contact angles compared to their positive control counterparts within each specific material group. However, this trend was not surface roughness related overall. As expected, these results do show that all samples studied are hydrophilic and polishing of the surfaces does not appear to alter the hydrophilicity of the surfaces to any significant extent. The negative control (Ss) presented the lowest contact angle whereas NP had the highest. The remaining samples range between 68-78°.

	TS	TE	TP	NS	NE	NP	MS	ME	MP	Ss
C.A (°)	74	70	69	75	68	83	78	68	72	49
(±)	2.05	3.12	1.78	2.01	0.89	2.85	3.53	3.85	2.73	5.01

Table 2.2 Contact angle (CA) measurements for all substrates. Polishing of the samples does not appear to alter the hydrophilicity of the samples to any significant extent. All substrates are below 90 degrees therefore are deemed wettable. The table represents the mean contact angle of 6 measurements of each sample, including standard deviations.

X-ray photoelectron spectroscopy

The measured elemental composition of the sample surfaces is given in Table 2.3 below in atomic concentration. Appendix B shows the typical XPS survey for all control and experimental samples. As expected, the spectra for the cpTi and both titanium alloys are dominated by Ti and O due to the naturally occurring titanium oxide layer. The strong C signal has previously been shown to be present on high surface areas oxide films that have undergone atmospheric exposure and storage. On all surfaces, contamination is detected mainly in the form of N, Na and P. For TAN samples in addition to the dominant Ti and O intensities, the alloying elements are also present (Al and Nb). With the exception of Ti15Mo samples and NS, Ca contamination is also detected on the surfaces most likely a result of contamination from handling. Analysis of the surface chemistry using XPS showed that neither electro- nor paste polishing followed by subsequent anodisation affected the final surface chemical properties from the positive controls (TS, NS, MS). Analysis of the negative control (Ss) demonstrates the diversity of elements required for alloying of this sample.

	Ti 2p	O 1s	Al 2p	Nb 3d	C1s	Ca2p	N1s	NaKLL	P2p
TS	17.6	50.1			27.3	0.1	0.5	1.4	3.2
TE	16.3	46.9			32.7	0.2	0.9	0.4	2.6
TP	17.5	48.7			30.4	0.1	0.8	0.4	1.7
NS	17.2	50.9	2.1	0.2	26.0		0.9	0.5	2.0
NE	17.1	49.2	1.4	0.2	28.2	0.3	1.1	0.3	2.3
NP	16.5	49.0	2.4	0.1	27.6	0.1	1.1	0.6	2.5
MS	14.3	43.7			38.3		1.3	0.4	2.0
ME	17.3	52.3			26.4		0.4	1.2	2.4
MP		45.3			35.7		0.5	0.6	2.5

	C 1s	Cr 2p	Fe 2p	Mo 3d	N 1s	Na 1s	Ni 2p	O 1s	P 2p	Si 2p
Ss	28.0	7.3	2.3	0.4	1.9	2.6	0.4	49.5	2.1	5.5

Table 2.3 XPS results for all substrates delineating the atomic concentration (%) of elements found. Polishing of the surfaces followed by anodisation does not appear to alter the chemical properties of the surface compared to the positive controls which are also anodised. Data represents the mean atomic concentration of 3 measurements of each sample.

Non contact white light profilometry

Polishing of the substrates appears to reduce the mean average roughness dramatically compared to positive controls (TS; NS; MS) as illustrated in Figure 2.1. The polished samples range between 0.2 and 0.4μm with the exception of TE which falls closer to the negative control (Ss) with an average roughness of 0.146 and 0.127μm, respectively. This slight increase over stainless steel is postulated to be due in part to sample processing and distinct material composition. Of the positive controls, TS presents the roughest surface with this evaluation method. At this point it must be noted that a large variability between sample batches was found. The reader is directed to Appendix D for further clarification.

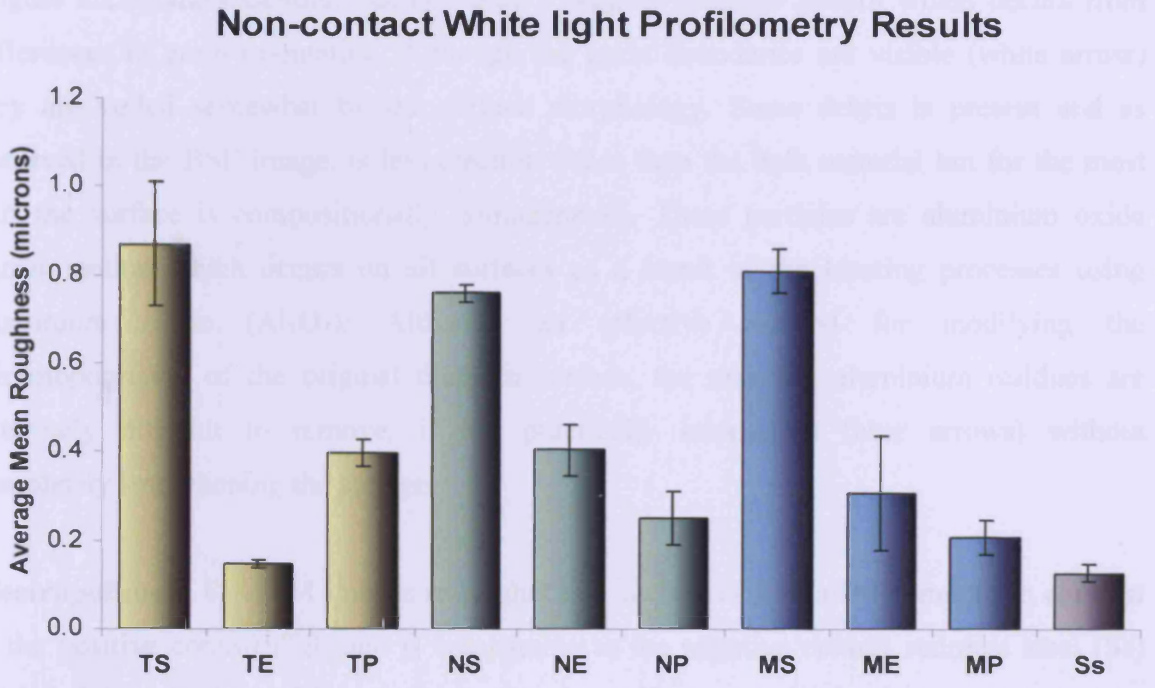

	TS	TE	TP	NS	NE	NP	MS	ME	MP	Ss
Mean Ra (μm)	0.869	0.146	0.397	0.758	0.404	0.249	0.809	0.305	0.208	0.127
Standard Deviation (μm)	±0.14	±0.01	±0.03	±0.02	±0.06	±0.06	±0.05	±0.13	±0.04	±0.02

Figure 2.1. Non contact white light profilometry results. The graph represents the mean average roughness of 6 measurements of each sample, including standard deviations. The table above is the same data but in numerical form to give the reader an overall impression of the data. Both variations of polishing dramatically reduce the mean average roughness of the surfaces compared to the micro-rough standard positive controls (TS, NS, MS), with TE (Electropolished cpTi) producing the surface most similar to the Stainless steel (Ss) negative control.

Scanning electron microscopy

Commercially pure titanium:

Standard micro-rough: This surface is clearly much rougher when compared to both polished variants. Variations in height of the grain boundaries throughout are clearly visible (Figure 2.2A) and essentially demonstrate a jagged, irregular pattern which occurs from differences in grain orientation. Although the grain boundaries are visible (white arrow) they are veiled somewhat by the surface morphology. Some debris is present and as observed in the BSE image, is less electron dense than the bulk material but for the most part the surface is compositionally homogeneous. These particles are aluminium oxide contamination which occurs on all surfaces as a result of the blasting processes using aluminium oxide (Al_2O_3). Although an effective method for modifying the microtopography of the original titanium surface, the resulting aluminium residues are extremely difficult to remove, if not practically impossible (blue arrows) without completely smoothening the surface.

Electropolished: SE SEM images show that this surface is particularly smooth in contrast to the positive control (TS) and is comparable to the negative control stainless steel (Ss) (Figure 2.5A). In fact, surface polishing has exposed more of the grain boundaries of the surface as demonstrated in Figure 2.2B (example highlighted by white arrow) compared to those on the TS surface (white arrow Figure 2.2A). Small micro-pits can also be observed on this surface but as shown in the BSE image, none of these features appear to deviate from the bulk composition of the material suggesting that they do not differ in density. Some Al_2O_3 particles left from processing are visible.

Paste polished: Paste polishing of the cpTi surface has left many obvious features in the surface (Figure 2.2C), however, compared to the positive control polishing has had a clear effect of smoothing the surface and obscuring the grain boundaries. Many large divots remain after the preparation process and some debris can also be observed. BSE imaging shows some areas of lesser electron density but, for the large part, the bulk composition is consistent throughout. It also highlights the difference in topography between the relatively smooth background surface and the divots. Grain boundaries are less defined than the TE sample and processing remnants are visible as 'drag marks' but do not appear to differ in composition to the material. Very few Al_2O_3 particles left from processing can be seen.

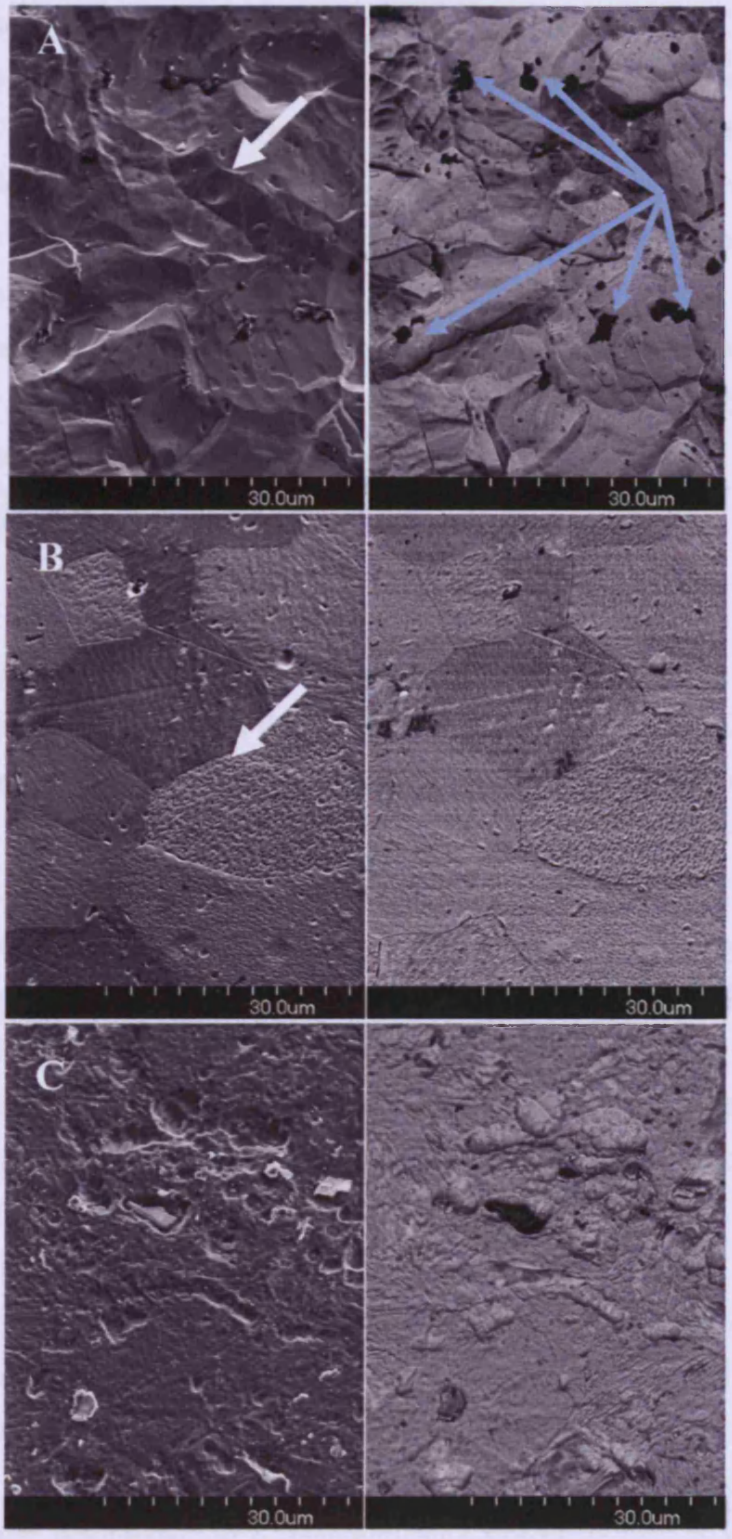

Figure 2.2 SEM images of the commercially pure titanium surfaces in SE (left image) and BSE mode (right image). (A) Standard micro-rough; (B) Electropolished; (C) Paste polished. Variations in height of the grain boundaries on the TS surface (A; white arrow) produce a jagged, irregular pattern which results from differences in grain orientation. BSE mode (A right image) highlights the Al_2O_3 particle contamination which occurs on all surfaces as a result of the blasting processes (blue arrows). In contrast Electropolishing (B) has clearly reduced the micro-topography of cpTi and consequently, the grain boundaries become more evident (white arrow). While paste polishing (C) has successfully reduced the microtopography the grain boundaries are not visible.

Titanium-6%Aluminium-7%Niobium:

Standard micro-rough: A wavy or undulating surface is observed with this material variant (Figure 2.3A). Large variations are seen between the peaks and valleys of the surface, cumulating in the peaks adopting rough, sharp edges (black arrow Figure 2.3A). Embedded in the surface are small particles that are seen to be lighter because they are a higher density material that with the aid of BSE imaging can be seen to differ in their composition to the rest of the material. The fragments protrude from the underlying surface which essentially adopts a rougher 'micro-spiked' (Meredith *et al.*, 2005; Meredith, 2006) topography because of them. These appear to be irregularly shaped and spaced along the surface.

Electropolished: The rolling pattern of the positive control surface (NS; standard micro-rough TAN) is observed here also but to a much lesser extent (Figure 2.3B) as the electropolishing process has reduced that roughness of the undulating surface noted for NS. A diverse density is seen between the base material and the embedded metal particles as described above. Topographically, these particles do not appear to protrude to the extent observed for the micro-rough TAN (NS), which is a result of the polishing essentially softening the sharp edges observed for NS (black arrow Figure 2.3B). However, compared to the negative control (Ss), this surface displays enhanced microtopography. In BSE mode, some small black specks (white arrow Figure 2.3B) also exist but are only present sporadically. These black specks are aluminium oxide (Al_2O_3) as mentioned which are deposited on all the surfaces of cpTi, TAN, Ti15Mo and Ss during processing. Although polishing reduces their presence, it does not eliminate them.

Paste polished: Although the base surface itself is relatively smooth, clearer evidence of the protruding particles embedded within the surface (Figure 2.3C) are evident compared to the electropolished sample. Again BSE imaging conveys that these features are heterogeneous to the remainder of the material. In contrast to its polished counterpart and the standard surface, this method of surface polishing appears to have completely removed the rolling or wavy feature described previously.

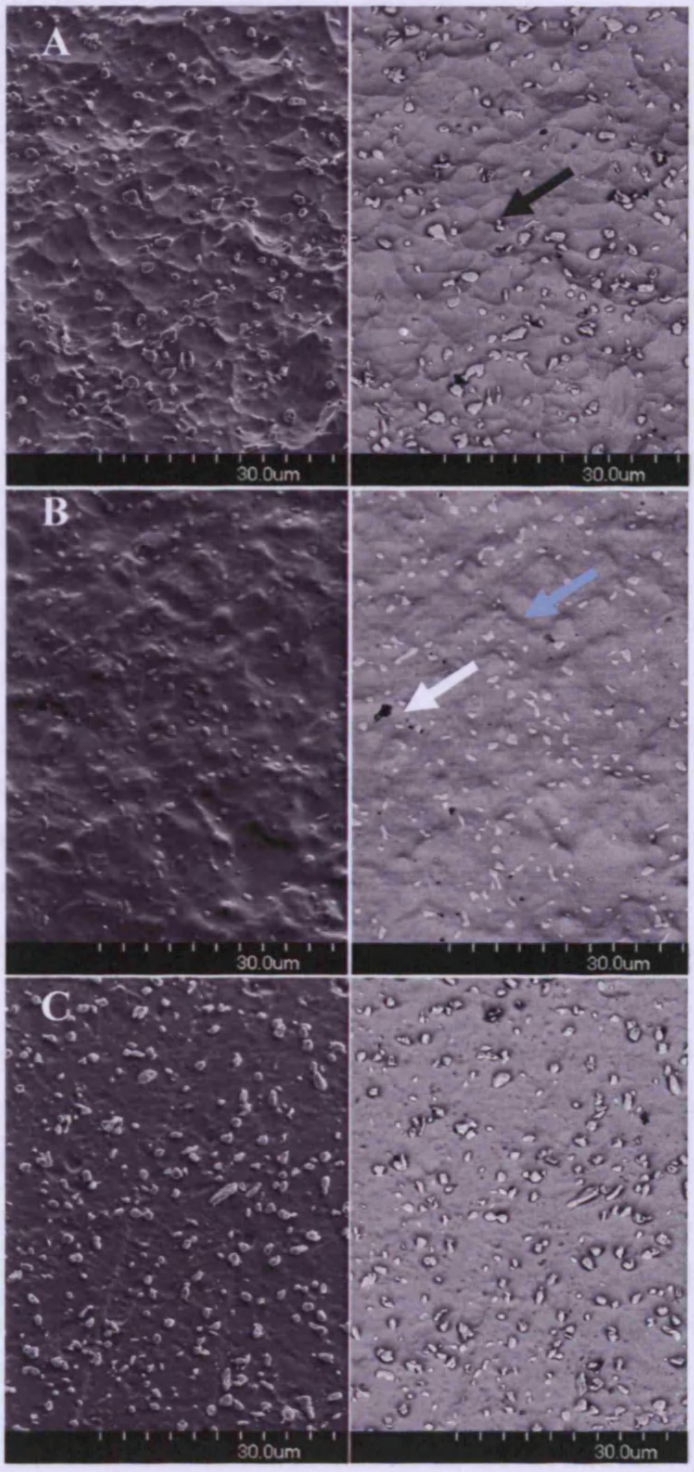

Figure 2.3 SEM images of the titanium-6%aluminum-7%niobium surfaces SE (left image) and BSE mode (right image). (A) Standard micro-rough; (B) Electropolished; (C) Paste polished. The characteristic β phase niobium-rich inclusions are clearly visible in the micro-spiked formation of the NS surface (A) as previously described (Meredith *et al.*, 2005; Meredith, 2006) in addition to the sharp roughened edges of the peaks (black arrow). In BSE mode the difference in composition is more evident. Electropolishing (B) clearly reduces the microtopography of the surface and although the niobium rich particles are still evident, (more clearly in BSE mode, white arrow highlights Al_2O_3 contamination) they have become less protruding due to the polishing. In addition, the sharpened peaks are softened by the polishing process (blue arrow) Paste polishing (C) again successfully reduces the microtopography of the surface. The niobium rich inclusions are more evident here compared to electropolishing highlighting the difficulty encountered with mechanically polishing these hard structures.

Titanium Molybdenum:

Standard micro-rough: SE imaging presents an extremely irregular undulating surface which results in large variations in topography (Figure 2.4A). Within the large valleys, further topographical features can be detected which in BSE mode become more evident. Micro-cracks outlining the grain boundaries (white arrow) of the surface can also been seen on this surface. However compared to paste polishing, they appear deeper and wider. BSE imaging also shows that this surface is highly homogeneous. Black spots/lines present appear to depict irregularities in the surface such as the micro-cracks mentioned previously and some debris in the form of Al_2O_3 particles from surface production embedded within the surface.

Electropolished: Using SE mode it appears that electropolishing titanium molybdenum results in a dramatic smoothening of the surface (Figure 2.4B) which is smoother than MS. Although smooth, the surface appears somewhat undulating. For the majority this seems to be a homogeneous surface with the exception of a reduced number of Al_2O_3 black spots detected in BSE mode, compared to MS. Again, electropolishing dramatically reduces the extent of surface micro-discontinuities compared to positive control (MS), and reflects a surface more akin to the negative control (Ss).

Paste polished: In contrast, paste polishing removes large undulations seen with MS. However this is obscured largely by an almost basket weave pattern resulting from surface preparation which appears to be irregularly spaced and randomly positioned (Figure 2.4C). Some deep surface micro-cracks are also evident in both SE and BSE mode defining the grain boundaries of the surface. Using BSE imaging it is shown that these are less electron dense than the bulk material but for the most part the surface is compositionally homogeneous. Furthermore BSE mode demonstrates remnants of Al_2O_3 from processing (white arrow in C). Paste polishing of the surface again reduces the extent of surface micro-discontinuities observed compared to MS. Although displaying a more micro-rough surface relative to the negative control, paste polishing of the surface still is effective in producing a smoother surface relative to the standard MS.

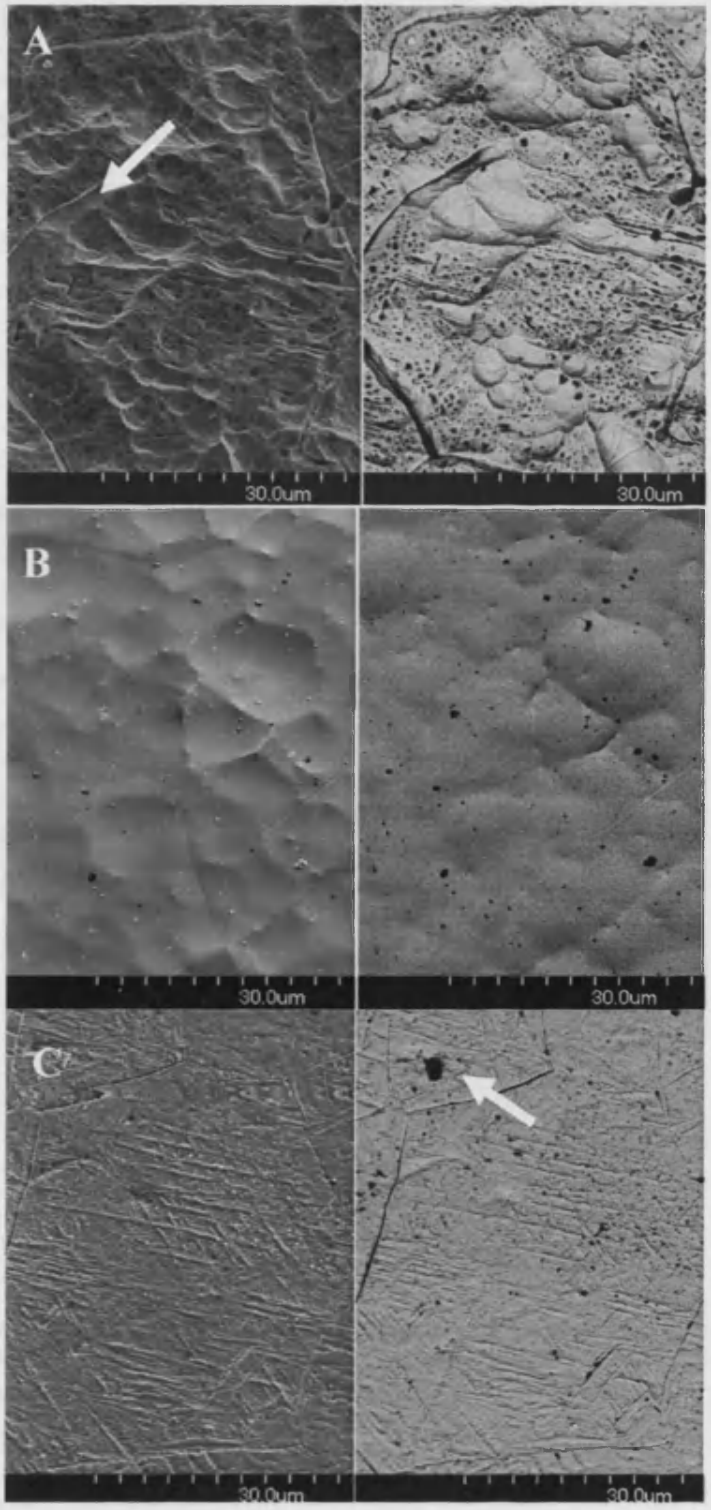

Figure 2.4 SEM images of the titanium-15%Molybdenum surfaces in SE mode (left image) and BSE mode (right image). (A) Standard micro-rough; (B) Electropolished; (C) Paste polished. SE imaging of MS (A) highlights the extremely irregular undulating surface with evident grain boundaries (white arrow) and intricate microtopography. Electropolishing (B) completely eradicates the microtopography seen in A to produce a smooth surface. Paste polishing again reduces the microtopography of Ti15Mo significantly producing a smooth basket weave pattern. In BSE mode the remnants of Al_2O_3 from processing are visible (white arrow)

Stainless steel: In SE mode, this surface appears very smooth and almost flawless. However some small scratches from processing do appear irregularly along the surface and some small particles are visible. A very slight difference can be observed in SE mode between the elements of the surface, namely due to the fact that approximately 5% of the electrons produced are BSE, thus SE images will always contain some small amount of BSE information (Richards *et. al.*, 1997). These differences in composition become more apparent in BSE mode where the surface resembles a marble-like pattern (Figure 2.5A). BSE electrons are produced as a result of changes in the direction of the incident beam electrons when coming in close contact to the electromagnetic field of a nucleus within the bulk of the material. There is little energy loss and the electrons re-emerge from the specimen as BSE. Variations in height within the specimen provide variation in the number of BSE produced which forms the image contrast. Sporadic less electron dense areas can be observed in the form of black spots in BSE mode. These appear to be a blend of particles which remain after processing and small pits within the surface.

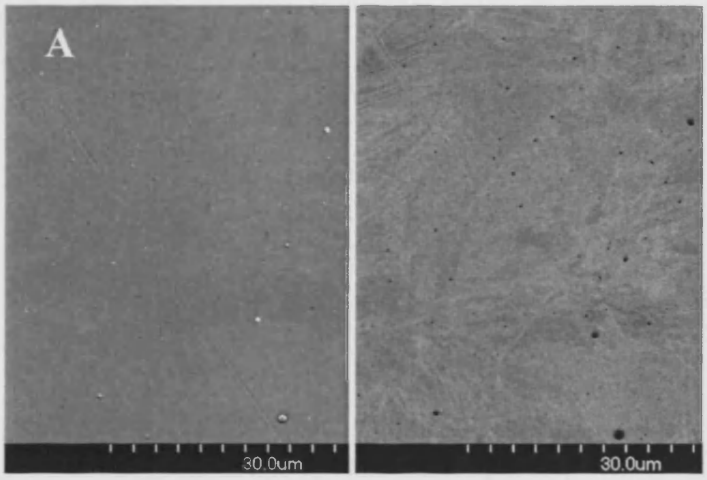

Figure 2.5 SEM images of the Stainless steel surface in SE (left image) and BSE mode (right image) showing an extremely smooth surface with very few micro-discontinuities. Minor remnants of Al_2O_3 particles and the polished grains of steel are visible.

Atomic force microscopy

Commercially pure titanium: The jagged irregular pattern seen with SEM for TS is confirmed here with this 3D AFM image (Figure 2.6A). Some of the grain boundaries along the surface are visible and in addition some small machining marks are visible along the sides of some of the jagged regions. The smooth surface recorded with WLP and SEM for TE is further confirmed with AFM measurements (Figure 2.6B). The grain boundaries (white arrow) of the surface are clearly visible based upon height differences, whereas with SEM the grains are differentiated by their differences in orientation. The base material of TP also appears smooth. However in addition to the divots witnessed in SEM imaging with AFM, there also appears to be some irregular increases in topography which may account for the higher average roughness documented with WLP (Figure 2.6C). Although the y-axis indicates that both TP and TS have similar sample heights this is in fact artefact (see Appendix B). Due to the sensitivity of the software the highest point on the surface defines this axis even though for the large part this may be a one off phenomenon. Two-D imaging in Appendix B clarifies this point.

(A) Standard micro-rough titanium

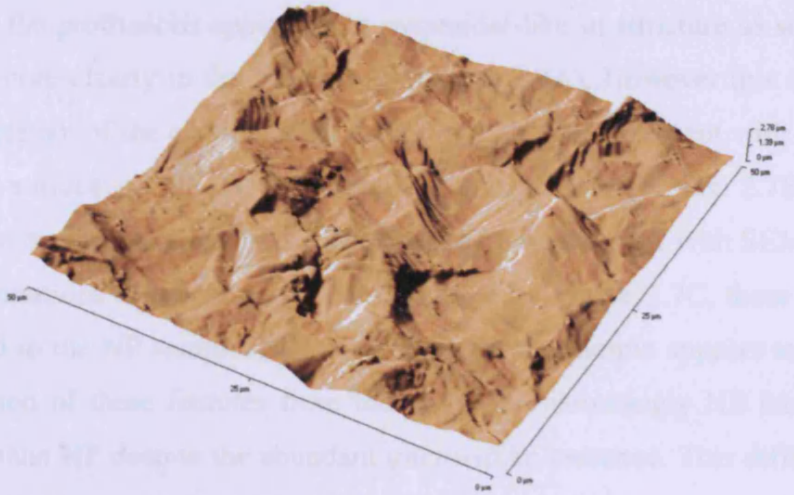

(B) Electropolished titanium

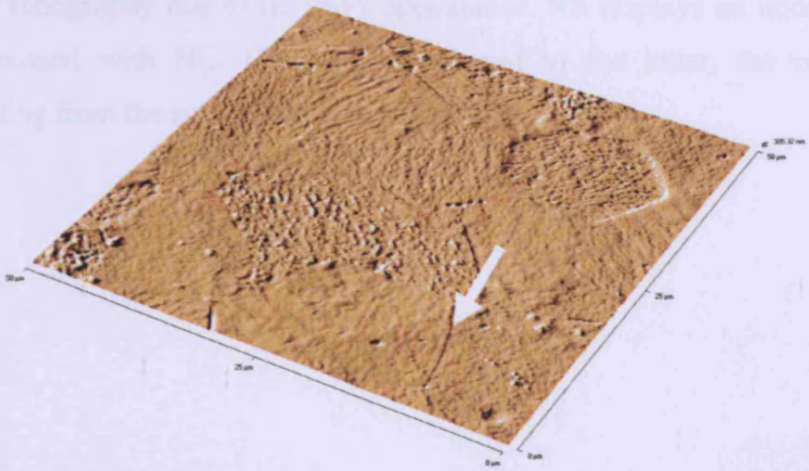

(C) Paste polished titanium

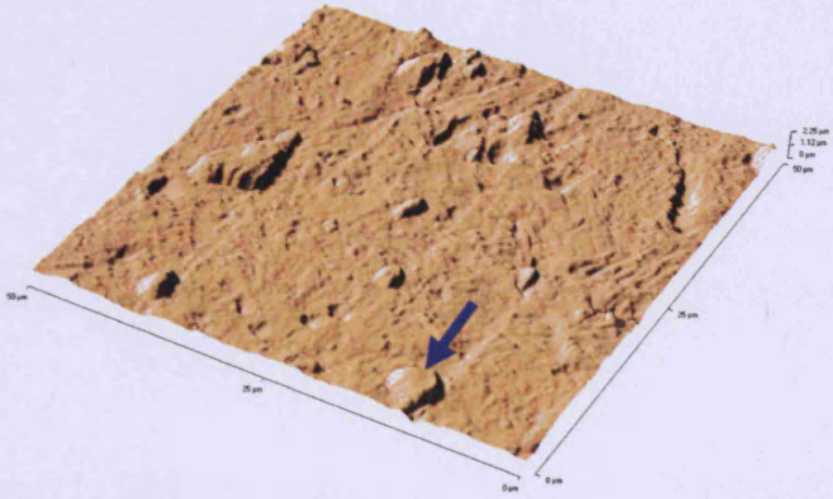

Figure 2.6. AFM of cp.Ti samples. Polishing of the surface (B & C) significantly reduces the micro-roughness of the cpTi surface compared to the positive control (A). Electropolishing (B) essentially removes the jagged surface pattern seen for the positive control to the extent that the grain boundaries are exposed (white arrow). Although paste polishing (C) appears to produce a relatively smooth surface, some microtopography remains (blue arrow for example) accounting for the higher Ra obtained with WLP.

Titanium-6%Aluminium-7%Niobium: Described as micro-spiked in appearance under SEM, here the protrusions appear more pyramidal-like in structure as seen in both the NP and again more clearly in the NS sample (Figure 2.7A). However this appearance is most likely an artefact of the cantilever tip from the AFM. In agreement with SEM imaging, the undulating surface of NE is also observed using AFM (Figure 2.7B). Metal particles identified to be compositionally distinct from the base material with SEM were visible here by small variations in height. As is demonstrated by Figure 2.7C, these particles are more pronounced in the NP sample. Electropolishing of the sample appears to remove or reduce the projection of these features from the surface. Interestingly NE has a higher average roughness than NP despite the abundant micro-spike presence. This difference may be due to the base/background material of NP being relatively smooth whereas NE clearly has more of varying topography due to its wavy appearance. NS displays an undulating base material as witnessed with NE. However in contrast to the latter, the micro-spiked structures projecting from the surface are clearly apparent.

(A) Standard micro-rough TAN

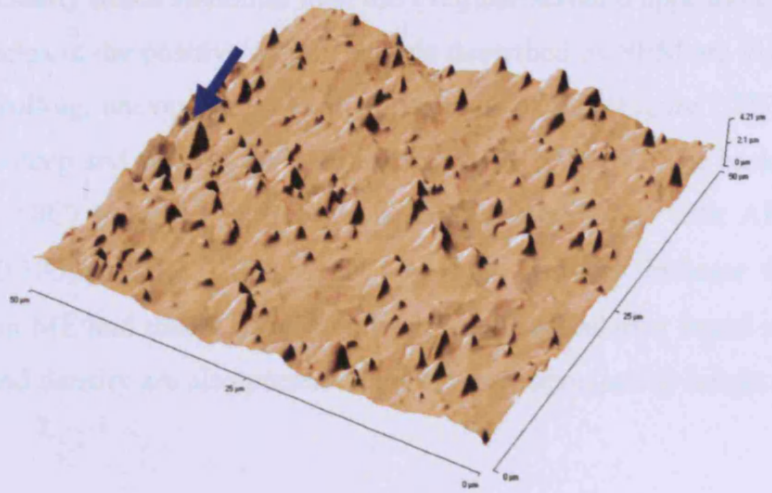

(B)Electropolished TAN

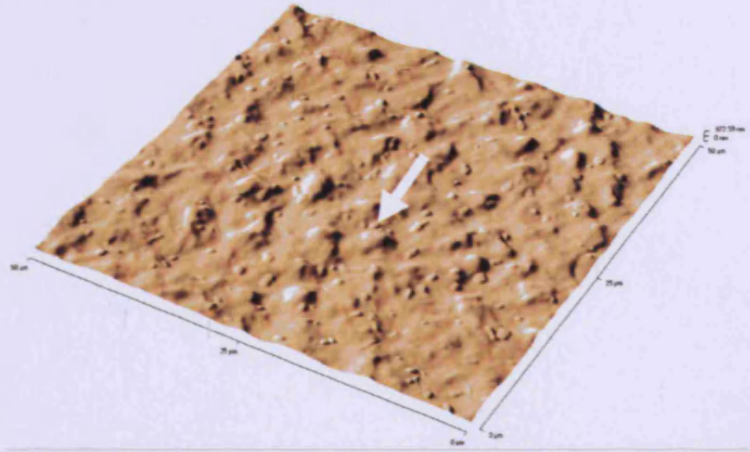

(C) Paste polished TAN

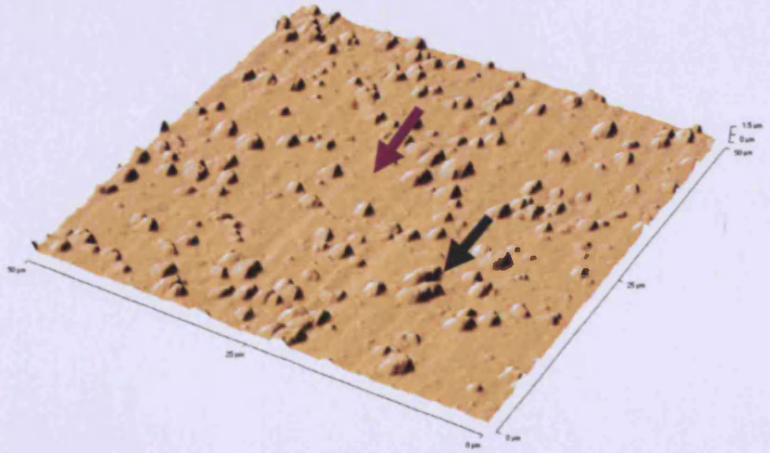

Figure 2.7. AFM of TAN samples. Protruding micro-spiked structures appearing pyramidal (Blue arrow) observed in the positive control (A), are eliminated by electropolishing (B). The remnants of these structures are observed embedded within the material (White arrow). In contrast paste polishing (C) appears to produce a smooth base material (Purple arrow) but fails to remove the protrusions although it does appear to have extensively reduced them (Black arrow) compared to the positive control.

Titanium Molybdenum: Compared to the positive control (Figure 2.8A) both polished variants are clearly much smoother than the irregular serrated appearance seen for MS. The grain boundaries in the positive control sample described by SEM are visibly present (white arrow). The rolling, uneven, yet smooth appearance of ME (Figure 2.8B) is confirmed with the relatively deep and shallow undulations are clearly evident. The basket-weave facade of MP (Figure 2.8C) observed with SEM is further established with AFM. Mean average roughness (0.305μm ME; 0.208μm MP) of both surfaces indicate that MP is in fact smoother than ME and that is advocated here. Grain boundaries found with SEM based on orientation and density are also presented here, based upon subtle height differences, for the MP sample.

(A) Standard micro-rough Titanium Molybdenum

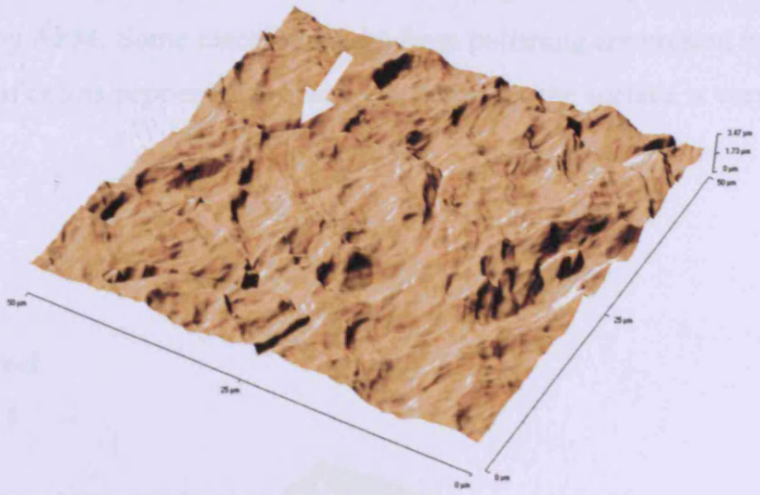

(B) Electropolished Titanium Molybdenum

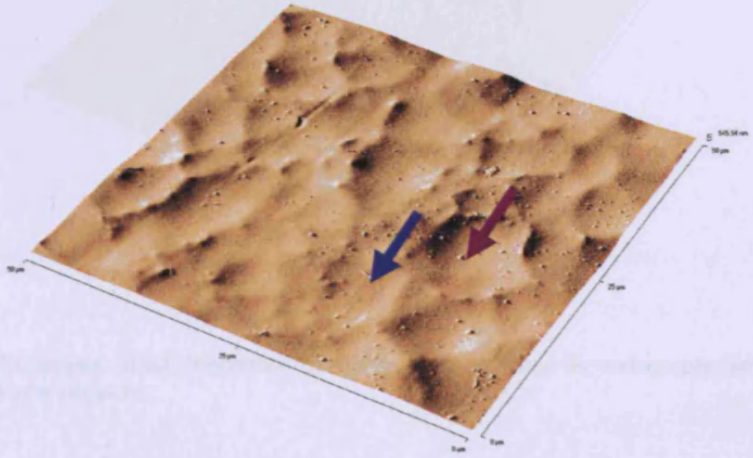

(C) Paste polished Titanium Molybdenum

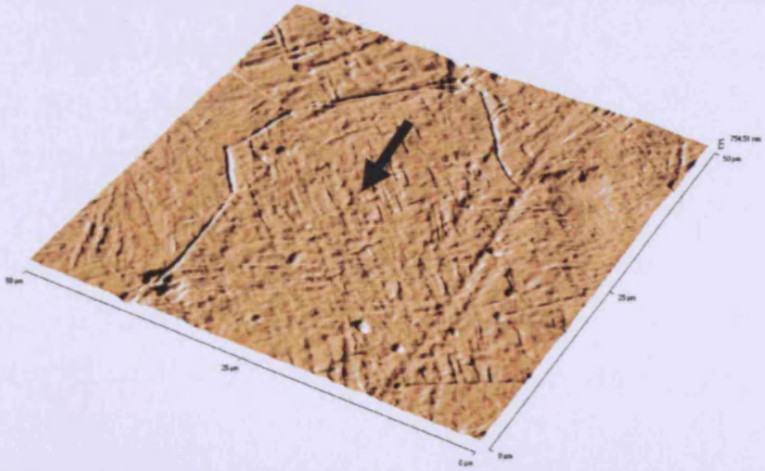

Figure 2.8. AFM for Ti15Mo samples. Both polishing variants reduce the surface microtopography of the positive control (A). Electropolishing (B) produces a smooth surface with an undulating surface containing relatively shallow (blue arrow) and deep (purple arrow) pits. In contrast, paste polishing (C) produces a smooth surface containing a basket-weave pattern (black arrow).

Stainless steel: The Ss surface is extremely smooth (Figure 2.9A) as supported by WPL, SEM and here by AFM. Some machine marks from polishing are present intermittently and small particles of debris pepper the surface, but generally the surface is very smooth.

(A) Stainless steel

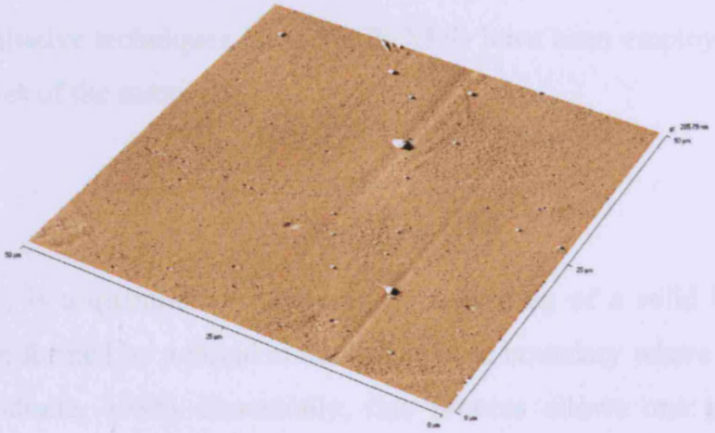

Figure 2.9. AFM for Stainless steel (negative control). This surface is extremely smooth with few machine marks and debris present.

Chapter 2: Discussion

In the rapidly developing field of biomaterials, characterisation of the surface features of any given device is becoming more and more important. Not only does it provide essential information regarding the surface properties of a device but this knowledge also allows researchers an insight into the specific mechanisms that may affect cell behaviour, by essentially understanding the factors that influence it. A myriad of techniques are available to characterise the surface, both chemically and topographically and while each approach provides specific information with regards to the surface, when combined, an overall but not definitive profile of the surface features can be gained. In this study, an assortment of both qualitative (SEM & AFM; in this instance although can also be used for quantitative analysis) and quantitative techniques (CA; WLP; XPS) have been employed to investigate the surface properties of the samples.

Contact Angle

Contact angle (CA) is a quantitative measure of the wetting of a solid by a liquid. It is defined as the angle formed by a liquid at the three phase boundary where a liquid, gas and solid intersect (Andrade, 1985). Essentially, this process allows one to determine the surface energy of a particular material, or more specifically, to determine if a surface is hydrophilic or hydrophobic. Despite the relative ease of use and low cost of this approach, controversy has surrounded its use for biomaterial applications since alterations in surface micro-features have been shown to enhance a surface wetting or repelling ability, essentially intensifying an already hydrophilic/hydrophobic surface (Martines *et al.*, 2005). Furthermore, Abdelsalam and colleagues (2005) have also shown that enhancement in surface hydrophobicity can also be achieved via defined surface changes on a nanometric scale for samples that normally are considered hydrophilic. With regards to the samples assessed in this study by these means, while no correlation was found for CA and roughness (Ra) as previously shown (Meredith *et. al.*, 2005) there was, however, a trend within each material group. Considering the distinctions in the manufacturing of titanium, dissimilarity between results for CA is not uncommon and can be found to be reported anywhere from 30 to almost 90 degrees for standard roughened titanium (Walivaara *et al.*, 1994; Taborelli *et al.*, 1997).

All surface treatments for cpTi samples produced similar CA results with the positive control presenting the highest CA at approximately 74°. Since all samples undergo anodisation after polishing, a chemical process which enhances the oxide layer of the material (Disegi, 1997), the chemical properties of the sample remained unchanged between control and experimental surfaces (confirmed with XPS). Hence the slightly higher CA obtained for TS is most likely a result of the increased surface area, in accordance with the Cassie-Baxter theory which postulates that for roughened samples, air becomes trapped beneath the asperities, or surface micro-features. Consequently, the water droplet as used in this case to study CA, sits on a composite surface made of air and solid. This would appear to fit, since by reducing the micro-topographical features of TS with electro- and paste polishing, the surfaces became slightly more hydrophilic. Similar results are found for Ti15Mo samples, with ME (68°) and MP (72°) presenting a slight increase in the hydrophilicity of the surfaces compared to MS (78°) attributed to the reduction in surface micro-topography.

For TAN derived materials, as is the case for cpTi and Ti15Mo samples, electro-polishing (NE, 68°) increases the hydrophilicity of the surface compared to NS positive control (75°). However, paste polishing of this material appears to increase the hydrophobicity (83°) of the surface which is not in accordance with the trend observed for other samples. As mentioned, the Cassie-Baxter theory hypothesises that the micro-topographical features of a surface may enhance its hydrophobicity when measured via CA. This effect is dependent on instead of the normal solid-liquid interface; a solid-air interface being achieved (Martines *et. al.*, 2005; Abdelsalam *et al.*, 2005). Here, although NS has a higher Ra as determined by WLP, SEM reveals an interesting point which may contribute to the increased hydrophobicity of the paste polished sample. Although purely theoretical, it may be worth considering that the previously defined niobium rich inclusions (Meredith *et al.*, 2005) have a role to play. It is clear that although NS has a higher Ra and with SEM visually is a rougher surface, that the niobium rich inclusions of NP are spaced in close proximity to one another. Although essentially a smoother surface, the inclusions give the impression of a rough surface for CA measurements, in essence creating micro-columns and increasing the surface area, as the closely packed inclusions retain a less spread droplet with small pockets of air trapped beneath. This notion is, of course purely speculative.

Another, more likely possibility is attributed to the complex oxide layer of TAN (Textor *et. al.*, 2001). Essentially these differences in the surface composition may affect the isoelectric point (IEP) of the surface and could, therefore, alter the hydrophilic/hydrophobic properties of the surface. In fact, recent work by Sittig and colleagues has provided evidence in support of this notion. Their studies show that while the stabilising elements of TAN, aluminium (Al) and niobium (Nb) are present in the oxide layer of the material as their most steady oxidised form of Al_2O_3 and Nb_2O_5 (Disegi, 1993), their actual distribution throughout the film is structure dependent. More specifically, Al is enriched within the α phase of the micro-structure, while Nb is found associated with the β phase (Sittig *et al.*, 1999b; Disegi, 1993). Furthermore, the concentrations of Al and Nb within the surface oxide layer were also shown to be strongly reliant on the pre-treatment process used. In the case of TAN, the authors report that augmented dissolution of the α phase that occurs with pickling (acid treatment normally involving nitric an hydrofluoric acid used to de-scale the surface) inherently enriching the presence of the β phase, which would as a result increase the level of Nb detected within the surface layers (Sittig *et al.*, 1999a). These local differences in oxide film composition, resulting from different modes of manufacturing, directly affect the surface charge of a sample associated with the distinct IEP of Al_2O_3 (approximately 8) and Nb_2O_5 (approximately 4.5) compared to cpTi (ranges between 5-7) (Sittig *et al.*, 1999b) thus producing differences in surface charge of a given surface depending on this prior treatment. This difference can directly influence the adsorption of proteins and furthermore affect their conformation on the surface, thus impacting the cell-material interaction (Sunny & Sharma, 1991).

X-ray photoelectron spectroscopy

X-ray photoelectron spectroscopy (XPS) is considered particularly useful for titanium surfaces since the information relayed comes from the 2-10nm region (Vörös et. al., 2001) and with regards to titanium this would encompasses the oxide layer, attributable to enhanced biopassivity of titanium (Ratner, 2001). However, the oxide layer of titanium has a high tendency to react with both organic (i.e. Carbon) and inorganic (i.e. Calcium, Sulphur, Sodium & Silicon) contaminants (Textor *et al.*, 2001). Furthermore, although their presence is clearly undesirable (Nichols *et al.*, 1997; Meleti *et al.*, 2000; Lohmann *et al.*, 2002a; Kasai *et al.*, 2003), ambiguity still exists with regards the extent of the negative effect of surface contaminants on the biological performance of a device when present in small quantities.

Neither polishing method appears to have any effect on reducing these contaminants. Nevertheless, considering the extremely small detectable levels of these, and the lack of transition metals detected, the biological performance of the samples should not be affected to any detrimental extent. Gamma sterilisation of samples, as is the case with the samples studied here, is known to increase the C surface concentration but not to the extent that it affects the surface composition (Wieland, 1999). Nonetheless, the differences are deemed relatively insignificant in view of the high standard deviations that occur for titanium oxide layers (Sittig *et al.*, 1999a).

Many studies have highlighted the importance of surface chemistry in the cell-material interaction (Meyer *et al.*, 1988; Howlett *et al.*, 1994; Yang *et al.*, 2003), thus XPS was carried out to investigate the affect, if any, polishing had on the chemical properties of the surfaces. However, as all samples undergo anodisation subsequent to their respective treatments, it appears that the chemistry of the surface does not differ for polished surfaces compared to their respective positive controls. Recent studies by Meredith and colleagues (2007a&b) have shown that surface micro-topography is a principle determinant in affecting fibroblast cellular behaviour on titanium and TAN surfaces. More recently, they also studied the effect of surface chemistry of NS with regards to fibroblast cellular performance since in their earlier study indicated that NS but not NE decreased fibroblast cell growth, number, morphology and cytoskeletal arrangement (Meredith *et al.*, 2005, 2007a). Thus, the authors continued their investigation of this effect by evaporating gold and titanium on the surface of NS allowing for different surface chemistries to be studied on surfaces of similar micro-topography. Interestingly, similar results were found for both studies indicating that, in fact, micro-topography was the main determinant of fibroblast cell interaction with these materials. Specifically, the authors report that on coated NS fibroblast cell proliferation, morphology and cytoskeletal structure was negatively affected when related to the control surfaces of coated TS and Ss where the same parameters remained unchanged compared to their uncoated counterparts (Meredith *et al.*, 2007b).

White light non-contact profilometry

Also known as white light interferometry, the principle of white light profilometry is based on the detection of a coherence peak which is created by two interfering, polychromatic shafts of light (Olzak *et al.*, 2001). This technique has come to the forefront of surface characterisation in recent years, as it is a non-contact measurement capable of achieving high resolution (approximately 50nm), and excellent reproducibility (Wyant & Schmit, 1997). In this study, the mean arithmetic average (Ra) of the surfaces was employed to assess the effect of surface polishing on surface roughness. As expected, polished surfaces were much smoother than their standard counterparts, and compare positively to the 'gold standard' orthopaedic smooth material represented by the negative control of Ss. For cpTi samples, electropolishing of the surface appears to produce a surface comparable to Ss with Ra's of 0.146 and 0.127μm, respectively; while, paste polishing, although still reducing the average roughness of the surface, produces a mean Ra of nearly 0.4μm. As mentioned previously, issues regarding surface reproducibility of the 13mm samples were common, and this is explored further in Appendix D.

Conversely, paste polishing of TAN and Ti15Mo samples appears to produce a smoother surface than electropolishing. The actual process of polishing would essentially have a role to play. For instance, the effectiveness of electropolishing would be dependent the electrical conductivity of the constituent metals. The electrical conductivity of the metals used were 377×10^3, 234×10^3, 187×10^3, and 69.3×10^3 for aluminium, titanium, molybdenum and niobium, respectively (Barbalace, 1995). When these values are taken into account, it goes some way to explaining the variations in the efficacy of the electropolishing process on the different surfaces. The relatively high conductivity of titanium would lead itself to be susceptible to electro-polishing which has been clearly shown by its low Ra and smooth surface features observed with SEM and AFM. Compared to cpTi, molybdenum has a lower conductivity which indicates that Ti15Mo would not be as susceptible to polishing by electrical means, a finding which is corroborated again here by AFM, SEM and WLP. For NS and NP samples niobium appears to have phase separated into niobium rich 'micro-spiked' structures on the surface of TAN as previously described (Meredith, 2006). As niobium is the least conductive material used this would be in line with the finding for WLP which showed that TAN had the roughest surface compared to the electro-polished samples. Since the aluminium component of TAN is alpha phase associated, ergo has superior alloying with titanium (Sittig *et al.*, 1999a) it, therefore, exists within the bulk of the metal

and is not seen to phase separate, hence the existence of the pyramidal peaks protruding from the material. On the contrary, paste polishing is a mechanical abrasive polishing technique, thus the hardness of the constituents will be a determinant in the efficacy of the treatment. The hardness of the elements on the Vickers scale are 167, 970, 1320 and 1530 MN/m^2, for aluminium, titanium, niobium and molybdenum, respectively (Barbalace, 1995). The alloy of molybdenum and titanium would have a hardness therefore, greater than titanium alone since this property is known to increase when a material is alloyed. Hence, a high degree of abrasion is possible when paste polishing Ti15Mo due possibly to the higher frictional force generated between the material and the mechanical processing. This concept would imply that the resistance of Ti15Mo to these abrasive forces yields the basket weave effect seen in SEM and AFM and led to a flatter surface compared to cpTi or TAN.

When the AFM image of TAN after paste polishing is examined, it was found that the niobium rich micro-spiked structures were decreased in size. Niobium is a relatively hard material (1320 MN/m^2), and as the structures formed by the suspected phase separation of the material protruded from the surface, it is reasonable to assume that it was these structures that carried the brunt of this abrasive polishing technique. It is, therefore, not unexpected, in view of the hardness of the material that these structures were not completely removed, but rather, the extent of the protrusion lessened. Of the paste polished samples, it was found that cpTi was the roughest surface after polishing. Titanium has a hardness of 970 MN/m^2, which is lower than molybdenum and niobium, and it is speculated that due to abrasive nature of the paste polishing process, large portions of material were removed randomly across the surface giving relatively high Ra values as observed with WLP. Another possible explanation for these observed surface deviations could be that the hardness of cpTi is not uniform throughout the surface thus polishing would have then occurred mainly in the softer regions of the surface, allowing the harder areas to remain, as highlighted with AFM and SEM imaging. Overall though, it appears that both variations of polishing successfully reduce the micro-roughness of the standard samples within range of the negative control.

Scanning electron microscopy

What is commonly believed to be the initial work describing the concept of SEM was cited more than 70 years ago by Knoll (1935). Pioneering research in this area, headed principally by Charles Oatley from the late 40s, has made the SEM an invaluable electron optical instrument for biomaterials research; while the AFM is a three-dimensional imaging technique that allows for remarkable topographical contrast of direct height measurements and unobscured examination of surface features (Binnig *et. al*, 1986; Grainger & Healy, 1999). Both are used in this instance for qualitative analysis to examine surface morphology of the samples after polishing. SEM analysis in both SE and BSE mode provided information regarding the surface features of the samples as well as advocating some previous observations made with use of quantitative methods. For cpTi, SEM supported the fact that TS is indeed a rougher surface than the polished variants (TE and TP). The characteristic roughening of the TS surface via acid etching in association with grain boundary orientation is also evident for the surface using this technique and appears to be characteristic of the surface identified for TS (Sittig *et al.*, 1999a; Pohler, 2000). As previously mentioned, electropolishing of the cpTi surface dramatically reduces the Ra of the cpTi surface and this is supported further by SEM. Furthermore, the extent of the success of electropolishing of cpTi is demonstrated clearly with SEM imaging. The process has non-selectively reduced the micro-roughness of the surface and the surface has become so smooth that the grain boundaries are clearly visible. Paste polishing of cpTi is also a successful method for reducing the micro-roughness of this material, however, when SEM images of TE and TP are compared, it is clear that electropolishing produces a more consistent surface. This is again advocated by WLP with TE producing a smaller Ra compared to TP. As with SEM, AFM further showed the grain boundaries noted previously for TE whereas the TP surface, although also relatively smooth compared to TS, has areas of obvious micro-mounds, most likely attributable to the higher Ra observed with WLP.

As indicated throughout, the dual $\alpha+\beta$ micro-structure of TAN becomes apparent with SEM and AFM analysis. With SEM the large surface area of NS is clear and supports observations made previously of alluding to a micro-rough surface, and is again characteristic of the known orthopaedic grade material (Sittig *et al.*, 1999b; Disegi, 2000; Meredith *et al.*, 2005). Furthermore, small particles are clearly visible on the surface in micro-spike formation which as previously explained is a direct result of the discriminating dissolution of the α phase, consequently enriching the niobium rich β phase in the form of

the inclusions witnessed (Meredith *et al.*, 2005; Sittig *et al.*, 1999b). Furthermore, BSE imaging shows that the latter differ in elemental composition compared to the bulk material. These are known to be niobium rich associated β phase particles and have, in recent studies, been shown to be detrimental to fibroblastic cell growth, adhesion as well as disrupting fibroblast cytoskeletal arrangement (Meredith *et al.*, 2005 & 2007a,b).

The non-selective electropolishing technique successfully reduces the micro-roughness seen with NS. Although the niobium rich β phase inclusions are still evident, more so in BSE mode due to the depth from which the BSE emerge, they have become less protruding because of electropolishing and therefore results in an undulating surface micro-topography. Paste polishing of the TAN surface produces interesting results. Both SEM and AFM analysis show NP being technically a 'rougher' surface than NE, however, quantitative data from WLP measurements seem to contradict this observation. In fact, compared to NE, the NP surface has almost half the Ra (0.404 and 0.249μm, respectively). A reason for this difference may be that although NP has clearly more apparent niobium rich β phase inclusions present on its surface, the actual base material of titanium is relatively smooth. In contrast, electropolishing has reduced the extent of the niobium rich β phase protrusions, producing a wavy surface, hence contributing to the higher Ra. In context however, paste polishing, as with electropolishing of TAN, successfully reduces the micro-topography of the surface to produce a smoother surface.

The notion of waviness of the TAN electro-polished surface contributing to the higher Ra compared to its paste-polished counterpart is supported here again for Ti15Mo samples. Both electro- and paste polishing of Ti15Mo again successfully reduce the micro-roughness reported for the MS sample, and appear to produce relatively similar Ra's (approximately 0.3 for ME and 0.2μm for MP). Nevertheless, their surface micro-features from the differing polishing processes vary dramatically. The electro-polished Ti15Mo sample produces a wavy surface while MP has an almost 'basket-weave' texture to it which may be of a size to affect cell behaviour. It must be considered that the basket weave appearance of MP from an individual cell level may directly influence cell behaviour whereas this pattern is not present on the ME surface so, therefore, the cell may recognise it as a smooth surface. This observation supports the notion that many methods of surface characterisation are required to provide an accurate profile of the surface in question (Dee *et. al.*, 2002).

Atomic force microscopy

Further analysis of the surface characteristics of the samples with AFM support and enhance the information accrued from SEM assessment. While SEM clearly shows differences in grain orientation and density (Richards *et al.*, 2000b), the sensitivity of AFM to height differences provides a new dimension to the topographical information accrued. Both SEM and AFM show that the negative control of Ss is clearly smooth as expected with only small debris producing any notable micro-topography on its surface. AFM also shows that few marks exist from machining of the surface. As mentioned previously, AFM supports many of the visual observations made with SEM, with additional information being provided from the z-axis. For cpTi the roughened grain oriented surface of TS is clearly visible while electro-polishing removes almost all micro-topographical features resulting in the grain boundaries been clearly exposed. The micro-mounds mentioned as contributing to the higher Ra observed for TP are also clearly apparent with AFM. With regards to the Ti15Mo samples, the effect of surface polishing is made further apparent. Both techniques produced smoother surfaces compared to the positive control but individually have clearly different surface micro-features.

AFM analysis of TAN samples produced more detail regarding the duplex structure. Whereas with SEM the niobium rich β phase inclusions appear rounded, or 'flagstone-like' with AFM they are clearly more pyramidal, advocating the need for several methods of surface characterisation to be included in any study to provide accurate data with regards to the surface topography. However, this appearance is believed to be artefacts from the AFM tip. Gadegaard (2006) reviews this issue and describes how the geometry of the tip can essentially determine the shape of the sample profile recorded. With SEM, the electrons are much smaller hence do not produce these artefacts giving a more 'closer' representation of the surface. This observation is in line with observations made by Meredith and colleagues (2007b) who originally described the niobium rich inclusion as micro-spiked (Meredith, 2006). The same group also elucidated that the negative effect observed on NS on fibroblast behaviour was a direct result of the spiked micro-structure seen on NS (Meredith *et. al.*, 2007b). The authors then assessed whether the affects observed where a direct result of this micro-topography or if chemical influences were involved. To this end, the authors created polycaprolactone surfaces coated with titanium, and they revealed that the same negative cellular effect was observed, hence implicating the surface micro-topography in inducing these effects. It will be interesting to investigate if the same cytoskeletal and, therefore,

growth and proliferative defects are observed when a different cell type, as here with osteoblasts, will have a similar response to the micro-topography of NS.

Additionally, AFM reveals that NP also has this micro-spiked structure observed on NS, but too a much lesser extent, most likely a result of these structures being subjected to the majority of the mechanical process. Perhaps enhancing polishing time may efficiently reduce these further thus, enhancing the potential smoothness of the surface. Furthermore, while NS has a rugged surface in addition to the inclusions, NP, as described with SEM previously, has a relatively smooth base topography. In contrast, AFM assessment of NE shows its 'bumpy' wavy surface with the non-selective polishing of the niobium rich β-phase inclusions to the extent they appear embedded within the surface.

Chapter Summary

In summary, both qualitative and quantitative surface characterisation techniques have shown that both electro- and paste polishing are effective methods of reducing the surface micro-roughness associated with standard micro-rough materials of varying types. Both processes are distinct in the means by which they reduce the micro-features of the surface, both are effective in doing so be it electrochemically or physically. However, certain processes more effectively treated certain materials more appropriately in reducing the micro-topography, electro-polishing was more effective for cpTi, while paste polishing was more influential for TAN and Ti15Mo samples. In addition, both polishing variants produced highly different topographies after treatment both visually and with regards to roughness, or indeed relative smoothness. Furthermore, surface polishing maintains a hydrophilic surface independent of material studied within a similar range to its positive control counterpart, but does not affect the surface chemistry as all samples are anodised prior to sterilisation and subsequent experimentation. A major consideration however, is the standardisation of these surface preparations for commercial clinical use as both polishing methods have varied during development (See Appendix D for details\examples regarding surface variability), for this work. Finally, this chapter has clearly shown the absolute necessity of combining several methods of characterisation for accurate extrapolation of any given surface profile as roughness measurements alone do not sufficiently reflect the morphologically features of a surface.

Chapter 3: Cell growth kinetics, viability and morphology.

Abstract.

The cell-material interaction is a finely balanced relationship that can be influenced by subtle changes in micro-topography. Altering surface micro-topography can have ramifications on a wide variety of cellular responses *in vitro*, such as its cytocompatibility and if negatively affected could be deleterious for implantation. Therefore within this chapter we have focused on confirming the cytocompatibility of polished samples and show that cell growth and viability remain unaffected or are improved on polished samples, compared to micro-rough counterparts. Morphologically, we also show using fluorescent labelling of the cytoskeletal components actin, tubulin and vinculin that surface polishing had a marked affect on cell spreading and adhesion compared to micro-rough samples. Specifically, the typical cuboidal morphology noted for cells cultured on micro-rough surfaces is generally negated on polished samples adopting instead an elongated well spread flattened morphology, akin to that observed for Ss. Interestingly we confirm that osteoblasts like fibroblasts (Meredith *et al.*, 2007a&b) appear to circumnavigate beta-phase particles associated with the TAN surface. Unlike fibroblasts, however, this cytoskeletal 'interruption' does not appear to be detrimental as osteoblasts continue to proliferate and remain viable on these surfaces. The affect of NP on cellular reaction is noteworthy as this surface appeared to reduce cell growth compared to NS, although this difference was not found to be significant. NP did display a significantly lower number of viable cells compared to NS. However it was observed that initial cell attachment for NP was lower compared to NE and NS samples. These observations may be important for delineating tissue responses to this surface during subsequent *in vitro* and *in vivo* studies.

Chapter 3: Cell growth kinetics, viability, & morphology.

Cytocompatibility:

Consideration of any biomaterial in short or long term applications for internal fixation must first be deemed biocompatible. Undoubtedly *in vitro* screening models are extremely useful for investigating functions of specific cell type in relation to a particular device; however, such an approach provides limited perspective of the complex milieu of the physiological niche. Hence the need for ratification of these results *in vivo* as to elucidate the dynamic events that mediate and control cell/tissue interactions to a biomaterial. However validation *in vitro* of the cytocompatibility of a device is a prerequisite prior to implantation *in vivo*. While the cyto- and biopassivity of cpTi and its alloys are widely accepted, any surface modification which may potentially affect this parameter must be investigated. In theory, surface polishing should not negatively influence any of the elements that render cpTi and its alloys attractive for biomaterial applications, as essentially, the material properties remain the same, with exception of the surface micro-roughness. Regardless this possibility must be tested.

Previous studies have already highlighted the influence of surface micro-topography on a wide range of factors that would directly contribute to the cytocompatibility of a device. For instance, Meredith and colleagues (2005) reported that commercially available standard micro-rough TAN selectively inhibited fibroblast proliferation. Subsequently it was elucidated that the niobium rich particles associated with the beta phase of the TAN surface produced significantly lower focal adhesion sites compared to Ss and standard cpTi. However when this surface was polished the negative effects on proliferation and focal adhesion structure were negated (Meredith *et al.*, 2005). In contrast standard TAN does not appear to negatively influence osteoblast attachment and proliferation in this manner, even in its standard micro-rough form. The effect of altering surface micro-topography has also been shown to be beneficial for selective cell adhesion (Brunette *et al.*, 1986; Boateng *et al.*, 2003). Differences in surface microtopography have also been implicated in controlling proliferation, with several studies indicating that micro-rough surfaces have reduced proliferative capacity compared to smooth surfaces (Lincks *et al.*, 1998; Schmidt *et al.*, 2001; Boyan *et. al.*, 2002; Postiglione *et. al.*, 2003).

However with this reduced proliferative capacity emerges a more differentiated osteoblast phenotype on the micro-rough surfaces as indicated with ALP activity (Lincks *et al,* 1998; Boyan *et al.*, 2002; Postiglione *et. al.*, 2003). Moreover it is suggested that the process of

matrix mineralisation is dependent on surface micro-roughness (Boyan *et al.*, 2002). This roughness dependent response is also seen for extracellular matrix (ECM) components with surface of varying roughness' displaying varied synthesis of collagen type I, vitronectin, and fibronectin (Howlett *et al.*, 1994; Postiglione *et. al.*, 2003). Other studies have even reported that different integrin receptors are expressed by osteoblasts cultured on rough versus smooth surfaces (Gronowicz & McCarthy, 1996; Postiglione *et. al.*, 2003; Wang *et al.*, 2006).

Sensitivity of cell shape to topography:

In terms of biomaterials, surface microtopography can greatly affect cell shape and function. Much information on this matter has come from Donald Brunette's group, which have spent several years investigating the effect of surface features on cell shape and subsequent behaviour, and have published extensively on the observation cells can be influenced by topographic guidance. For instance, in the early and late eighties much of their focus was spent assessing the response of fibroblast and epithelial cells to grooved substratum of varying dimensions. In early studies Brunette (1986) showed that epithelial cell aggregates where clearly orientated on all the grooved substrata examined (0.5 to 16μm) however the orientation was most guided on samples with the smallest repeated spacing (30μm). Previously they had used this finding to address the problem of epithelial down-growth onto implanted dental devices that breech the epithelium and found that by merely applying the appropriate topography to a titanium coated surface, that epithelial down-growth onto percutaneous devices can be inhibited *in vivo*.

Specifically Chehroudi and colleagues (1990) showed that relative to a smooth surface down-growth of epithelium can be inhibited on percutaneous dental implants which comprised grooves orientated horizontally to the long axis of the device. In contrast, vertical grooves enhanced tissue down-growth. Similarly they showed that fibroblasts also exhibited directed migration and orientation on a variety of substrata with grooved dimensions, but differences in epithelial and fibroblast cell response on the grooved substrata were observed. For instance, although both cell types on the grooved surfaces display signs of controlled migration in contrast to epithelial cells where locomotion remained unchanged, fibroblasts exhibited a surface dependent response with regards to the speed in which they migrate. Specifically, when cultured on grooved surfaces, fibroblasts proceeded at approximately double the velocity compared to fibroblasts cultured on smooth surfaces (Damji *et al.*, 1996).

More recently, Meredith and colleagues (2007a) have directly implicated the role of surface topography in influencing fibroblast cytoskeletal organisation and subsequent cell shape. Previous to this the authors had identified the negative affect of TAN surface micro-topography in influencing numerous cellular functions (Meredith *et. al.,* 2005) and, therefore, their more recent study aimed at elucidating this outcome. Specifically, they revealed the prominent influence of surface microtopography on cell shape and cytoskeletal arrangement with standard TAN as well as gold-coated and titanium-coated TAN have significantly reduced cell growth compared to the stainless steel and cpTi counterparts (also studies in their standard form and gold- and titanium-coated). While Ss advocated a well spread fibroblast morphology in all its forms with an unaffected cytoskeletal arrangement, cpTi presented a topography dependent cell alignment with no negative affect observed to the cytoskeleton and highly prominent filopodia (Meredith *et al.,* 2007b).

Contrastingly, fibroblasts cultured on TAN (standard, gold- and titanium-coated) presented an elongated or unspread morphology with filopodia observed to attempt to probe the surface and TAN associated niobium rich inclusions. Interestingly the authors describe a distinct disruption for all TAN variants of the microtubular network closely associated to the areas of niobium rich inclusions (Meredith *et al.*, 2007b). Thus implying the characteristic micro-spiked surface morphology of TAN is the principal contributing factor in restricting fibroblastic cell spreading and adhesion. Further to this Biggs and colleagues (2007 a & b) have found that while disordered nano-pit topographies increased osteoblast cellular adhesion and presented well developed cytoskeletal elements, nano-pits comprising highly ordered symmetry had a less spread morphology and perturbed formation of the cytoskeleton (Biggs *et al.,* 2007a). The authors postulate that this affect is brought on by the disruption of adhesion formation (Biggs *et al.,* 2007b) caused by the pit symmetry and order. Together these data highlights the prominent role of surface topography (nano and micro) has on cytoskeletal organisation and cell shape on subsequent fibroblast and osteoblast adhesion and growth.

Chapter 3: Materials & methods:

Surface Characterisation:

Quantitative measurements for five separate 13mm samples of each test substrate (the increase in sample size was due to sample variability experienced prior to this point) were taken using a non-contact white light FRT MicroProf® (Standard) with CWL 300μm sensor profilometer (Fries Research & Technology, Germany). A roughness average (Ra – arithmetic mean of the roughness height expressed in micrometers) was measured from a 0.5x0.5 mm scan area with a point density of 500 points/line. Two separate measurements were taken for each sample, resulting in a total of ten measurements per sample. Contact angle measurements were made using the Sessil drop method with the Drop Shape Analysis System (Contact Angle Measuring Instrument G10 and DSA 10 Control Unit, KRÜSS GmbH) and analysed using the Drop Shape Analysis 1.50 software (KRÜSS GmbH). Samples were placed in a preheated chamber (20°C) with an external water source to sustain a constant relative humidity. Using the computer controlled system, a 10μl droplet of distilled water was dispensed onto the sample and quantified exactly 1 minute after dispensed using the analysis software. Two separate measurements were taken for each sample and this process was repeated on a further 2 samples, thus totalling six measurements for each sample type. The morphology of the sample surfaces was studied using a Hitachi S4700 field emission Scanning Electron Microscope (FESEM) fitted with an Autrata yttrium aluminium garnet (YAG) backscattered electron (BSE) scintillator type detector. The images were taken in secondary electron (SE) mode, with an accelerating voltage of 5kV, an emission current of 40μA, a working distance of 10mm and a positive tilt of 30°.

Cell growth kinetics:

Rat calvarial (RC) cells were seeded at a density of 10,000 cells/disc/well in 24 well plates (Corning, UK) for 1, 2, 4, 6, 8, 10, 14 and 21 days (See appendix E for information regarding isolation and culturing of these cells). The cells were initially cultured in 400μl of DMEM containing 10% foetal calf serum (FCS), 50μg/ml of ascorbic acid, 1% penicillin-streptomycin, 10nM dexamethasone, and 5mM β-glycerophosphate (DMEM+5mMBGP) for the desired time. Tissue culture plastic (TCP) was included as an '*in vitro* control surface' however it must be noted that for analysis we generally focus on comparing material of similar type to one another i.e. polished cpTi to standard cpTi as differences in surface chemistry, and hydrophobicity etc between the materials themselves and TCP are wholly distinct. Plates were incubated at 37°C with an atmosphere of 5% CO_2 and 95% humidity. A

total of six samples were included. Cell number was quantified at 1, 2, 4, 6, 8, 10, 14 and 21 days after seeding. At each time point, the media was aspirated from the wells and the samples were subsequently washed three times with 500µl of 0.1M phosphate buffered saline (PBS) solution (Sigma, UK). After rinsing, 500µl of 0.1M PBS containing 300U/ml of collagenase type I (Worthington, USA) and trypsin-EDTA (Gibco, UK) were added to each well. Culture plates were incubated at 37°C with an atmosphere of 5% CO_2 and 95% humidity for approximately 5 minutes. After this time had elapsed, 500µl of DMEM+5mMBGP was added to each well to strop the reaction. A 50µl aliquot of each sample was transferred to a haemocytometer and the number of cells in 4 squares were counted and averaged. Subsequently the number of cells per 1ml was calculated. This calculation was done twice per sample. Results are expressed as an average of 6 measurements (3 samples, with 2 counts completed per sample).

Cell viability (Quantitative):

The viability of RC cells was assessed using the 'CellTiter' blue (Promega, USA) method. Briefly, this assay allows for the number of viable cells/per sample to be estimated by using the indicator dye resazurin to measure the metabolic activity of the cells. Viable cells reduce the resazurin into resorufin which fluoresces while non-viable cells have limited metabolic capacity and therefore cannot reduce the dye, hence cannot generate a fluorescent signal. Cell viability was quantified at 1, 2, 4, 6, 8, 10, 14 and 21 days after seeding by adding 500µl of DMEM+5mMBGP containing a 5% solution of CellTiter blue to each well subsequent to washing with 0.1M of PBS. Three no cell control wells were included. Culture plates were covered in aluminium foil, and incubated for 4 hours at 37°C with an atmosphere of 5% CO_2 and 95% humidity. After incubation a 150µl aliquot of each sample and media with dye alone, were transferred to a 96 well white plate. Samples were plated in duplicate. Sample fluorescent values were measured (excitation/emission ~550 nm/~595 nm) using a HTS 7000 Bio Assay Reader (Perkin Elmer). Results were calculated by averaging the fluorescent values of the samples and subtracting the average fluorescent values for wells containing media without cells.

Immunolabelling of cytoskeletal components actin, vinculin and tubulin:

Note – All volumes are 500µl unless otherwise stated.

RC cells were seeded at a density of 1000 cells/disc/well in 24 well plates (Corning, UK) for 24 hours. The cells were initially cultured in 400µl of DMEM+5mMBGP for the desired time. Plates were incubated at 37°C with an atmosphere of 5% CO_2 and 95% humidity. Two samples of each test substrate were included for qualitative analysis. After a 24 hours incubation period, samples were washed three times for 1 minute per wash with 0.1M Piperazine-NN'-bis-2-ethane sulphonic acid (PIPES), pH7.4 after which time they were permeabilised for 2 minutes with 0.1% Triton-X in 0.1M PIPES. For 1 minute subsequent to this samples were fixed using 0.5% glutaraldehyde. Samples were washed 3 times for 2 minutes with 0.1M PIPES. To block from non-specific labelling, 1:20 dilution of goat serum in 0.1M PBS, was added to the wells for 30 minutes. Primary antibodies were added to each well at a final volume of 1:800 mouse monoclonal anti-vinculin (V9131; Sigma, UK) or 1:200 mouse anti-β tubulin (T4026; Sigma, UK) with 1:50 Rhodamine conjugated phalloidin (R415; Molecular probes, UK) suspended in a 1:20 dilution of goat serum in 0.1M PIPES, and were kept overnight at 2-8°C wrapped in aluminum foil. Subsequently, samples were washed twice for 5 minutes with 0.1M PIPES after which time, the secondary antibody (Alexaflour 488, goat anti-mouse IgG, Molecular probes, UK, final dilution of 10µg/ml) was added for 45 minutes at room temperature protected from light. Finally, samples were washed 3 times for 2 minutes each with 0.1M PIPES. Approximately 10µl of Prolong anti-fade reagent with DAPI (4,6-diamidino-2-phenylindole; Molecular probes, UK) was added to the samples which were then enclosed with a glass cover-slip. Samples were stored in the dark at 2-8°C until required for image analysis.

Cell viability:

Due to the perceived insensitivity of the CellTiter blue (Promega) method at the 1 and 2 day time points, cell viability for cells cultured on the various samples, was also assessed at these time points qualitatively using a two-colour fluorescence cell viability test that is based on the simultaneous determination of live and dead cells. Live cells are distinguished by the presence of ubiquitous intracellular esterase activity, determined by the enzymatic conversion of the virtually non-fluorescent cell-permeant calcein-AM, to the highly fluorescent calcein. Calcein is well retained within live cells, producing an intense uniform green fluorescence in live cells

(excitation/emission ~495 nm/~515 nm). Ethidium homodimer-1 enters cells with damaged membranes and undergoes a 40-fold enhancement of fluorescence upon binding to nucleic acids, thereby producing a bright red fluorescence in dead cells (excitation/emission ~495nm/635 nm). RC cells were seeded at a density of 10,000 cells per sample (in duplicate) for 1 and 2 days. At each time point samples were washed extensively with 0.1M PBS, and 500µl of 0.1M PBS containing calcein-AM (1µl/ml of PBS) and Ethidium homodimer-1 (1µl/ml of PBS) were added to each well. Samples were covered in aluminium foil, and incubated for 20 minutes at 37°C with an atmosphere of 5% CO_2 and 95% humidity. Subsequently the solution was removed and 500µl of 0.1M PBS was added to each well, to prevent the sample drying out. Samples were immediately imaged using an Axioplan microscope.

Quantification of unattached cells:

Within the course of these experiments, the observation was made that for some samples initial attachment of cells was reduced for some surfaces. Thus this was assessed by investigating the percentage of unattached cells after a predetermined time from a known initial seeding density. RC cells were seeded at a density of 10,000 cells/disc/well in 24 well plates (Corning, UK) for 1 and 2 days. Plates were incubated at 37°C with an atmosphere of 5% CO_2 and 95% humidity. After 1 and 2 days media was removed from respective samples and transferred to 1.5ml tubes (Eppendorf, AG). A 50µl aliquot of each sample was transferred to a haemocytometer (1/10mm deep, 1/400 mm^2) and the number of cells in 4 squares were counted and averaged. Subsequently, the number of cells per 400µl was calculated. This calculation was repeated for each sample, resulting in a total of 6 measurements per sample type.

Statistical analysis:

Statistical evaluations were made using SPSS for Windows version 14.0 (SPSS Inc, Chicago, IL). Normality and homogeneity were tested using Shapiro-Wilk test of normality and Levene's test for equality of variances, respectively. Since the data did not meet the assumption of a Gaussian distribution, non-parametric Kruskall Wallis analyses were performed for cell number and cell viability data. Where applicable Mann-U Whitney tests were applied for individual comparisons and p-values were Bonferroni-corrected for multiple comparisons.

Chapter 3: Results:

Surface characterisation:

Analysis of the mean surface roughness of the samples, indicate that both methods of polishing effectively reduce the micro-roughness associated with commercially available micro-rough cpTi, TAN and Ti15Mo (figure 3.1). The polished samples range between 0.18 and 0.48μm with the exception of NE which falls closer to the negative control (Ss) with an average roughness of 0.18 and 0.12μm, respectively. In contrast, with this evaluation method, electropolishing appears to produce the most variability with respect to the average roughness of the surfaces, with Ra's ranging from 0.18μm for NE, to almost 0.5μm, for TE and ME. In contrast, paste polishing appeared to produce similar Ra's of approximately 0.3μm for all materials studied.

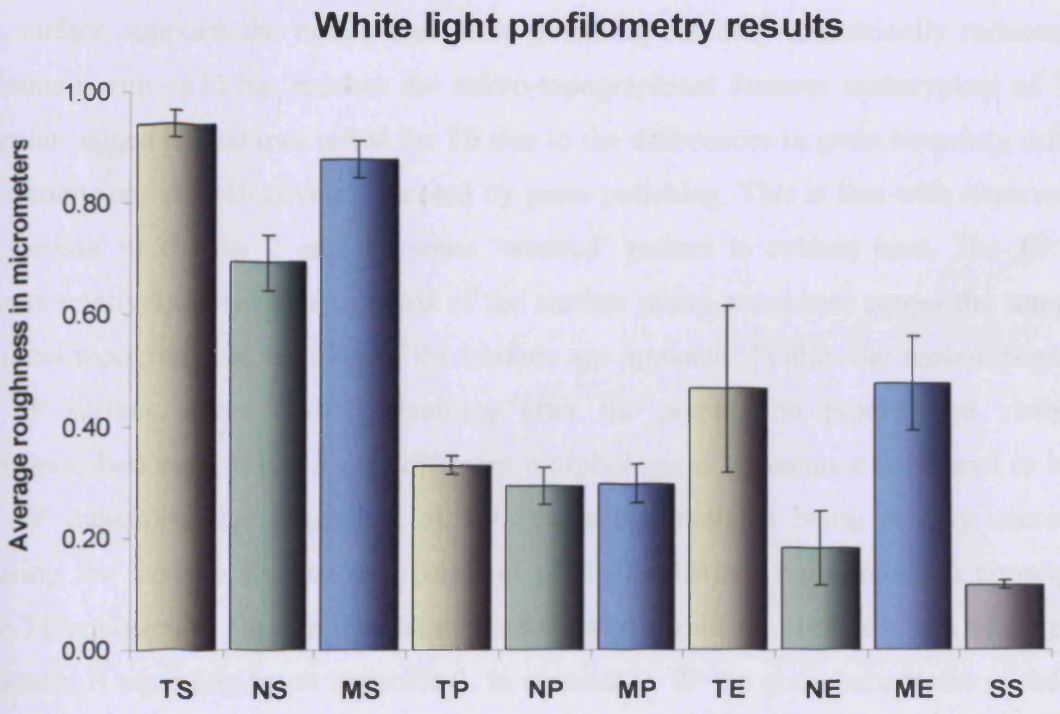

	TS	NS	MS	TP	NP	MP	TE	NE	ME	Ss
Mean Ra (μm)	0.94	0.69	0.88	0.33	0.29	0.30	0.47	0.18	0.48	0.12
Standard Deviation (μm)	±0.02	±0.05	±0.03	±0.02	±0.03	±0.03	±0.15	±0.07	±0.08	±0.01

Figure 3.1. White light profilometry results. Both electro- and paste polishing successfully reduce the mean average roughness associated with the commercially available micro-rough standard counterparts. Paste polishing appears to produce the most reproducible, and consistent reduction in Ra, with TP, NP and MP presenting Ra's of approximately 0.3μm, while electropolishing produces Ra's ranging from 0.18μm for NE to almost 0.5μm for TE and ME.

Contact angle results indicate that for the samples used in this portion of the study, that

	TS	NS	MS	TP	NP	MP	TE	NE	ME	SS
CA (°)	79	90	88	67	71	74	65	69	61	76
(°)	2.26	0.57	0.07	2.05	4.60	4.53	1.34	1.91	2.12	4.74

surface polishing increases the surface hydrophilicity compared to standard counterparts of the same material (Figure 3.2).

Figure 3.2. Contact angle measurements for the samples used in this portion of the study. Surface polishing appears to increase the hydrophilicity of the sample, compared to standard micro-rough samples within the same material group.

The micro-rough surface of cpTi is clearly evident in figure 3.3 and supports the observation from white light profilometry that this surface has a micro-rough morphology. The differences in grain boundary orientation and height are visible (figure 3.3, black arrow) and some nano-topographical detail is evident across the surface. SEM analysis of the TP (figure 3.3) surface supports the notion that paste polishing not only dramatically reduces the Ra associated with cpTi but reduces the micro-topographical features archetypical of TS. The irregular jagged appearance noted for TS due to the differences in grain boundary orientation and dimensions are effectively obscured by paste polishing. This is line with observations of this surface in chapter 2 and the same 'weaved' pattern is evident here. The TP surface appears relatively consistent in terms of the surface micro-roughness across the sample, and the nano-topographical features of the surface are apparent. Within the nano-topography of the TP surface, some divots remaining after the preparation process are visible. The electropolished surface has a very different morphological appearance compared to both TS, and TP indicating that regardless of both polishing methods being equally successful at reducing the surface Ra that each method produces distinct morphological consequences. Here TE appeared to have an undulating surface with variations in dimensions of the pits (See Appendix H regarding batch variability). In contrast to TP the grain boundaries of the surface are visible (figure 3.3, white arrow). The SEM analysis helps elucidate the higher Ra observed for TE, observed with white light profilometry. The undulating surface of TE would attribute to the higher Ra observed; however the dimensions of the pits appear sufficiently large enough not to disrupt the continuity of the surface. This conclusion is supported by observations for the TE in chapter 4.

SEM analysis of the NS surface revealed the previously characterised undulating surface noted for this sample in chapter 2. However contrasting to the micro-spiked appearance produced by the beta-phase particles of NS surface in chapter 2 the beta phase particles of this surface (blue arrow, figure 3.3) appear more 'strip-like'. Paste polishing successfully reduced the micro-roughness associated with standard micro-rough TAN as indicated with white light profilometry results; however the reasons behind the extent of the lesser degree of successful polishing compared to NE becomes more apparent with SEM analysis. Specifically the mechanically abrasive force of the paste polishing technique appears to exert its effect principally on the beta-phase of this material. Accordingly the beta phase structures adopt a fractured appearance with the beta phase appearing splintered (green arrow, figure 3.3). Conversely the efficacy of electropolishing at reducing the prominence of these particles is clearly evident in figure 3.3. The bulk material of NE displays a smooth, slightly wavy surface while the beta-phase particles appear to have become embedded within the material, rather than protruding out from it as observed for NS (purple arrow, figure 3.3).

SEM analysis reveals MS surface as an extremely irregular undulating surface with large variations in the dimensions and depth of the topography. Grain boundaries are clear and sometimes are demarcated by surface micro-cracks on their edges (figure 3.3, red arrow), surrounding them. Paste polishing appears successful at reducing these micro-topographical features noted for MS. As a result, a smooth surface deficient in the irregular jagged morphology of MS is produced with some processing marks evident across the surface. Data accrued from white light profilometry indicate that electropolishing does not reduce the Ra of the surface as successfully as MP. However, SEM imaging reveals some of the reasons behind this observation. As outlined in figure 3.3, ME has a surface morphology akin to that of TE, that is, the surfaces have extensive undulations (figure 3.3, yellow arrow) which would of course directly contribute to increasing the Ra. However upon inspection with SEM, it becomes clear that ME is in fact a very smooth surface and like TE the dimensions of the undulations appear large enough as appear smooth on a cellular level.

This point is highlighted by the morphology of the Ss surface which also has an undulating surface within this batch of samples (Appendix D and H for clarification regarding inter-batch variability) but a lower Ra compared to TE and ME. This may in part be attributable to the depth of the undulations which with the aid of SEM appear shallower compared to those observed for TE and ME. Interestingly the Ss surface morphology differs dramatically to that observed in chapter 2 despite the identical Ra's. While the Ss surface in chapter 2 was completely smooth with practically no discontinuities, here the Ss surface has a wavy appearance.

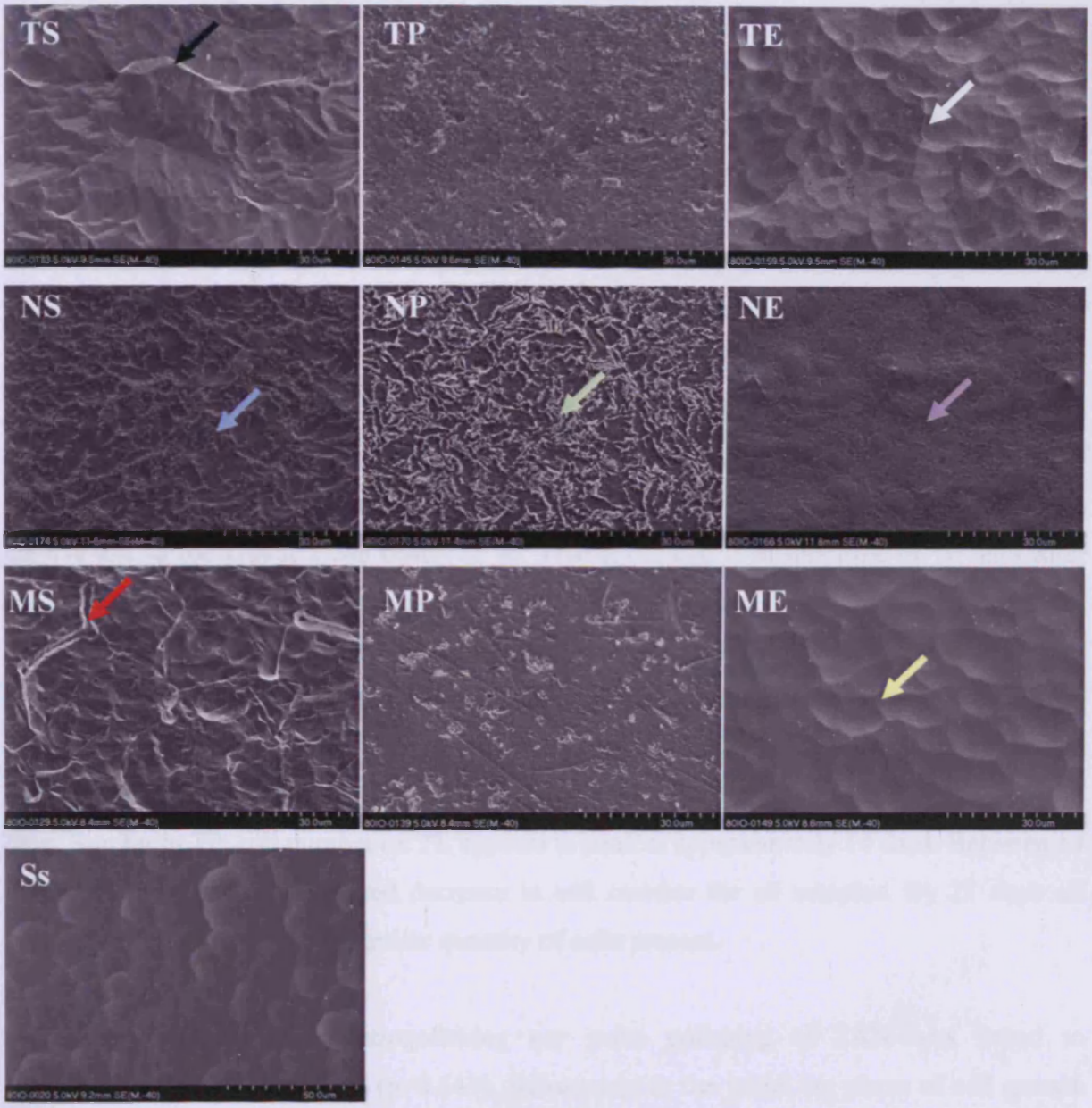

Figure 3.3. SEM images of the various surfaces used for *in vitro* testing. All three micro-rough samples (TS, NS, MS) display the archetypal surface morphologies as described in chapter 2. TS has an irregular jagged surface, with differences in grain boundary height and orientation evident (black arrow). NS displays the typical prominence of beta-phase particles, albeit, in a more strip-like manner (blue arrow). MS has and extremely irregular undulating surface with large variations in the dimensions and depth of the topography. Grain boundaries are visible and evidence of micro-cracks along some of the grain boundaries is evident (red arrow). For TP the grain boundaries of TS have become obscured, producing a very smooth surface. For NP, the beta-phase particles are selectively targeted, producing a splintered appearance (green arrow). MP has a smooth surface, with some processing marks evident. Electropolishing appeared to produce a highly undulating surface for both TE and ME, which is postulated to contribute to the higher Ra noted for these samples. Both surfaces have pits of varying depth and dimensions present on their surface (yellow arrow), and for TE, the grain boundaries are visible (white arrow). For NE, the efficacy of electropolishing at reducing the prominence of these particles is clearly evident. The bulk material of NE displays a smooth, slightly wavy surface, while the beta-phase particles appear to have become embedded within the material, rather than protruding out from it, as observed for NS (purple arrow). Ss also has an undulating surface, but a lower Ra compared to TE and ME. This may in part be attributable to the depth of the undulations, which with the aid of SEM appear shallower compared to those observed for TE, and ME.

Cell number:

Surface polishing of cpTi was not found to significantly alter cell number compared to TS, Ss or TCP ($p=0.874$). All surfaces induce an initial lag phase between initial seeding and day 2. For cpTi samples subsequent to this lag phase there was a phase of exponential growth between 2 and 6 days which occurs at a similar rate for TS, TE, and TP and was also comparable to the amount of cells present for Ss and TCP at these times (figure 3.4A). Between 6 and 8 days, there appeared to be a suspended rate of proliferation for TS and TP while cell number for TE increases. The latter reflects the trend in growth observed for Ss while results collected for cells cultured on TP and TS samples reflect more closely that observed for TCP. However after this perceived deferment in growth, most likely a result of contact inhibition, there appears to be another phase of high proliferation on TS which was comparable to the kinetic trend observed for TCP and Ss. It is at this time of 10 days after initial seeding that cell number appeared to peak for TS, Ss and TCP. This increase in cell number was also observed for TP at 10 days but to a much lesser extent than that observed for Ss, TCP and TS. Also the peak in cell number for TP does not occur until almost 4 days after TS, specifically at 14 compared to 10 days, respectively. Cells cultured on TE continued in their exponential growth phase albeit to a lessened ascent than observed between 2 and 6 days. Similar to TP, cell number on TE appears to peak at approximately 14 days. Between 14 and 21 days there was a marked decrease in cell number for all samples. By 21 days all samples appeared to display a similar quantity of cells present.

Similar to cpTi, neither electropolishing nor paste polishing of TAN was found to significantly affect cell number ($p=0.643$). Subsequent to the initial lag phase of cell growth on TAN samples between 0 and 2 days, a phase of exponential growth was observed for all samples (figure 3.4B). This phase continued until 6 days post-seeding, and appears to occur to a similar level for cells cultured on all TAN samples, with the exception of NP. While NE and NS cell numbers increased at a rate akin to that observed for Ss and TCP, NP appeared to induce a slower initiation of proliferative activity, relative to other samples. However, by 6 days, cell numbers on NP was similar compared to all other samples. Between 6 and 8 days a plateau in cell number was reached for NS and TCP samples. However similar to Ss during 6-8 days, cell number on NE and NP continued to increase. Between 8-10 days cell numbers on NE, NS, Ss and TCP appeared re-engaged in a phase of exponential growth which was observed to peak after 10 days in culture. However cell number on NP after 10 days culturing was considerably lower compared to other samples. Nevertheless by 14 days there was a decrease in cell number for NE, NS, Ss and TCP. Consequently, as cell number is still

increasing slowly on NP samples, by 14 days cell number on NP is akin to that recorded for other surfaces. Cell numbers continue to decline for all samples at 21 days, including NP, resulting in similar cell numbers being recorded for all samples at this time.

Cell number for Ti15Mo samples (figure 3.4C) showed the same lag phase noted for other samples between 0 and 2 days. However while an exponential phase of proliferation occurred for ME, MP and MS, it was to a lesser extent than that recorded for Ss and TCP. For TCP this phase appeared to plateau for 2 days after which time another growth phase was observed until 10 days when a peak in cell number was noted. In contrast, cell numbers on Ss appeared to continue increasing until day 10 to a similar level to TCP. In contrast, cell number on ME appeared to reach a plateau stage between 6-8 days. Furthermore with the exception of 21 days cell number for ME samples were never shown to be at a similar level to Ss or TCP. In contrast, cell number on MS samples appeared to increase steadily until 14 days after which time a peak in cell number was noted, which was followed by a slight decrease in cell number by 21 days. Similar to ME samples the rate of increase over time was less than that of Ss and TCP. Cell number on MP samples appeared to increase at a rate similar to that noted for ME and MS until 10 days by which time MP samples showed a higher number of cells present. This increase continues in parallel fashion to MS albeit at a higher rate until 14 days, when a peak in cell number for MP samples was recorded which was followed by a slight decrease in cell number at 21 days. Overall, however, it did not appear that ME or MP significantly influenced cell number ($p=0.06$).

A

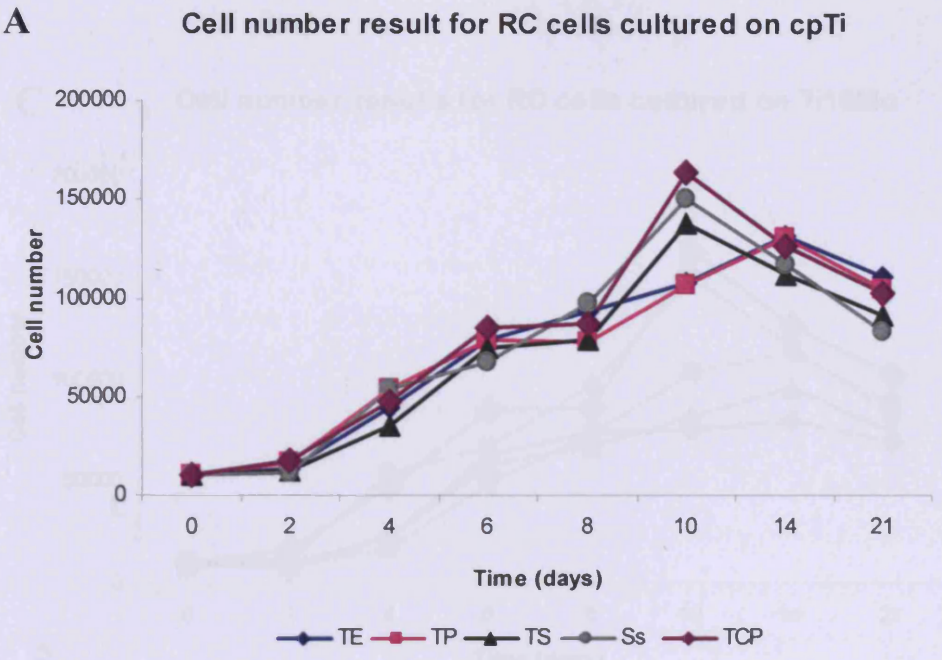
Cell number result for RC cells cultured on cpTi
200000
150000
100000
50000
0
Cell number
0
2
4
6
8
10
14
21
Time (days)
TE
TP
TS
Ss
TCP

B

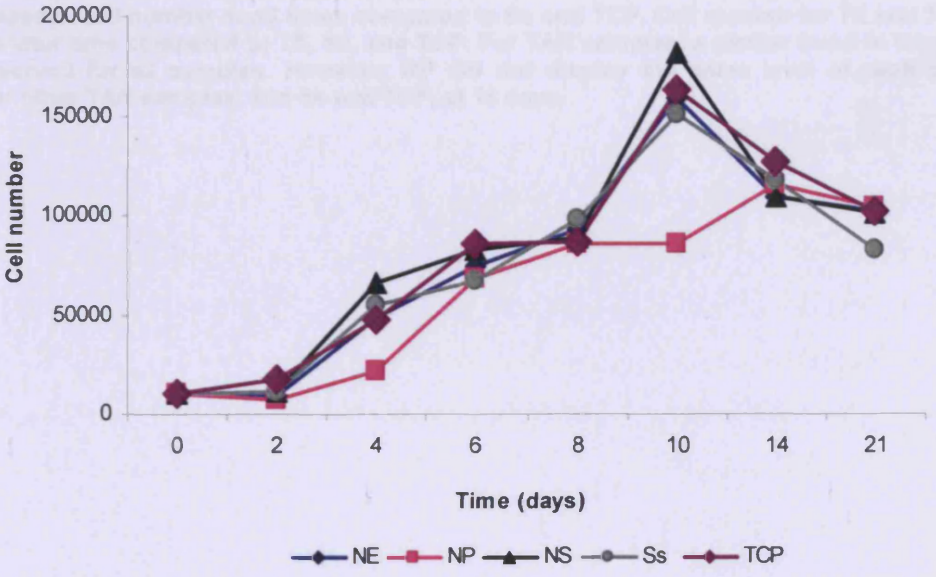
Cell number results for RC cells cultured on TAN
200000
150000
100000
50000
0
Cell number
0
2
4
6
8
10
14
21
Time (days)
NE
NP
NS
Ss
TCP

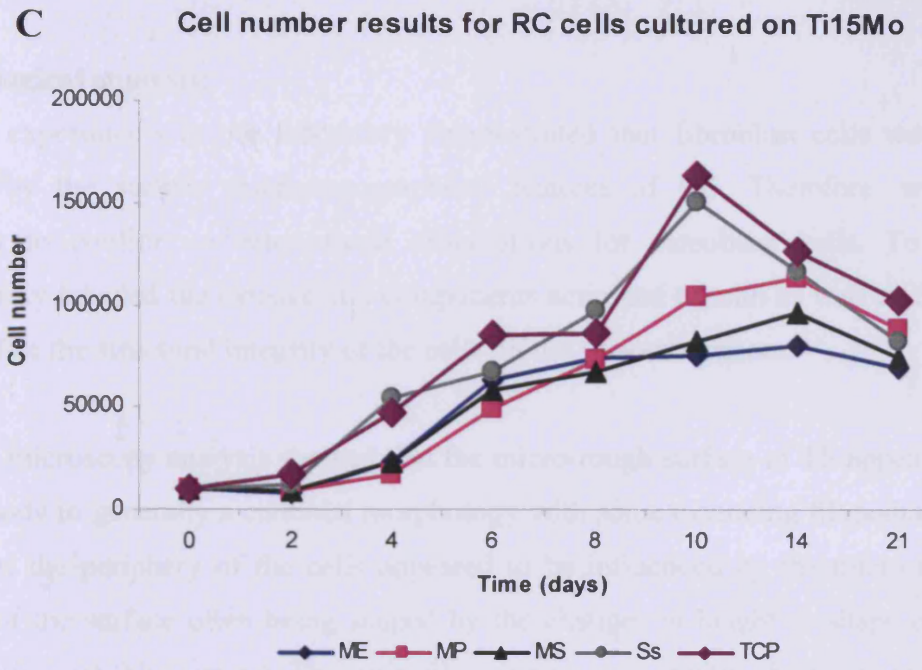

Figure 3.4. Cell number quantification of RC cells cultured on cpTi (A), TAN (B), and Ti15Mo (C) for 2, 4, 6, 8, 10, 14 and 21 days. Surface polishing was not found to significantly affect cell number for cpTi ($p=0.874$), TAN ($p=0.643$) or Ti15Mo ($p=0.06$) samples. An initial lag phase was observed for all samples between 0 and 2 days, which generally, was followed by a phase of exponential growth to a similar extent observed for Ss, and TCP. The exception to this was observed for Ti15Mo samples, which had a lower rate of increase in cell number at all times compared to Ss and TCP. Cell number for TE and TP appeared to peak at a later time compared to TS, Ss, and TCP. For TAN samples, a similar trend in increase of cell number observed for all samples. However, NP did not display the same level of peak cell number observed for other TAN samples, and Ss and TCP, at 14 days.

Morphological analysis:

Previous experiments in our laboratory demonstrated that fibroblast cells were negatively affected by the surface micro-topographical features of NS. Therefore, we deemed it necessary to confirm or rebut these observations for osteoblast cells. To do this we fluorescently labelled the cytoskeletal components actin and tubulin as well as the nucleus to aid visualise the structural integrity of the cells on the various surfaces.

Confocal microscopy analysis showed that the micro-rough surface of TS appeared to restrict the cell body to generally a cuboidal morphology with some extending filopodia (Figure 3.5). Moreover, the periphery of the cells appeared to be influenced by the micro-topographical features of the surface often being shaped by the changes in height or shape of the surface (Figure 3.5, inset; blue arrow). The actin filaments were generally observed closer to the cell periphery and appeared to be moulded by the surface features. The tubulin network appeared to radiate throughout the cell extending into the filopodia at the cells extremities. It was also noted that a condensation of tubulin was observed surrounding the nuclei of the cells. RC cells on TE surfaces, however, generally had a very different morphology. Cells on TE samples adopted a more 'fibroblast-like' triangular shape with three large lamellapodia typical of fibroblast cells. Cells on TE appeared better spread than cells on TS and had an elongated cell body. Also, cells on TE appeared unhindered by the small alterations in micro-topography unlike TS (Figure 3.5 inset; yellow arrow). Similar to Ss and TCP, cells cultured on TE samples also displayed a concentration of the tubulin network through the middle of the cell adjacent to the nucleus. This behaviour was also noted for TP samples which similar to TE samples, also had an elongated triangular morphology and appeared flattened compared to cells cultured on TS. Again for TP surface the dynamic action of the actin filaments was evident as it was observed that along the periphery they contributed to the arched appearance noted (Figure 3.5; purple arrow) perhaps resulting from interaction with surface micro-topography.

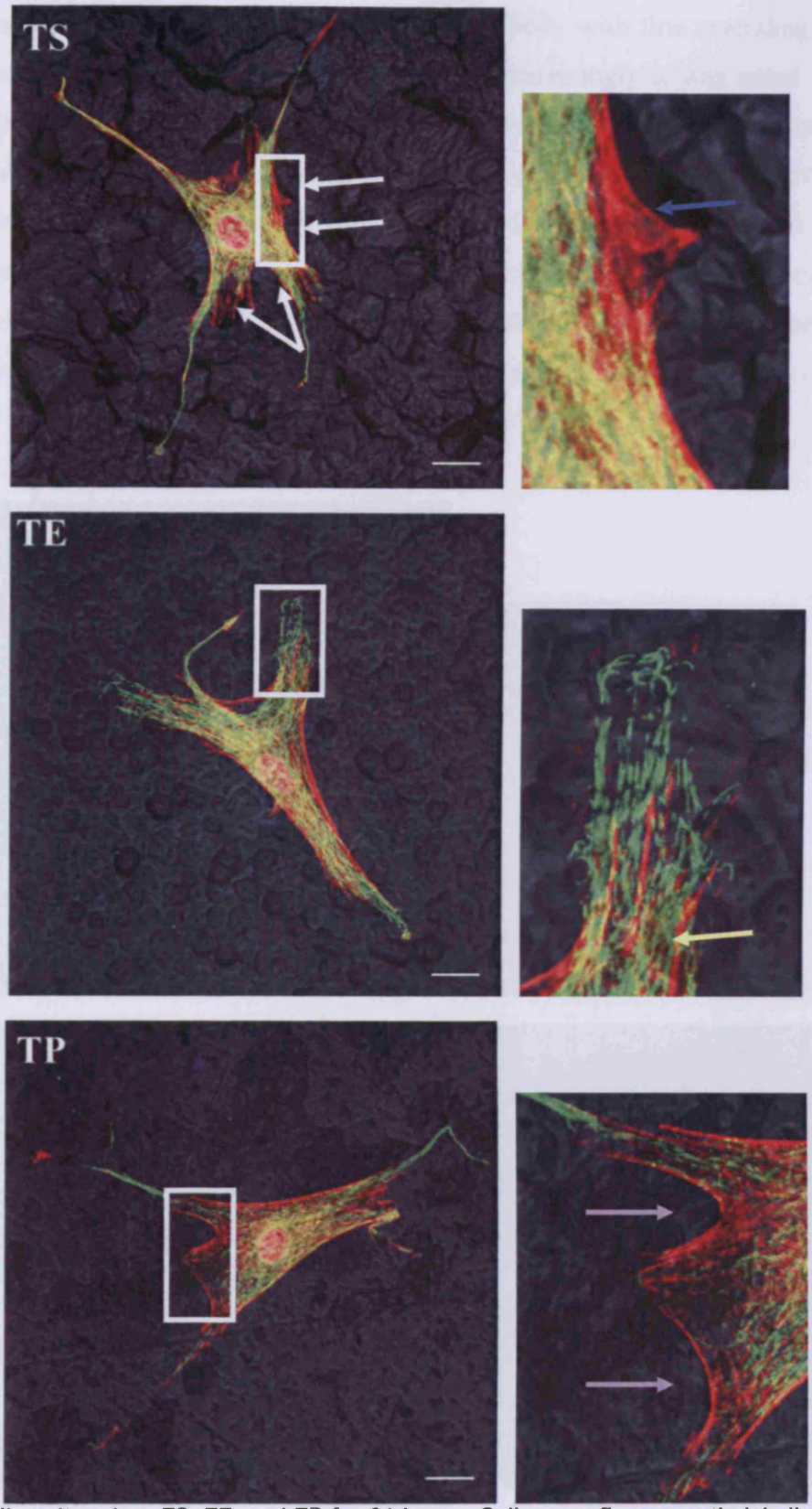

Figure 3.5. RC cells cultured on TS, TE, and TP for 24 hours. Cells were fluorescently labelled for actin (red) and tubulin (green). Cell nuclei were labelled using DAPI (pink/purple). The surface micro-discontinuities of TS induced a cuboidal cell body morphology. The actin filaments at the cell periphery appeared to be manipulated by the surface interaction (white & blue arrows). Cells cultured on TE and TP displayed an elongated, spindle shaped morphology more akin to that observed for Ss and TCP samples. Similarly, a concentration of tubulin network was noted radiating through the centre of the cell, encompassing the nucleus. Cells cultured on TE and TP did not appear to be restricted by small changes in the surface morphology (yellow and purple arrows). Scale bar=20μm.

Cells cultured on NS generally displayed a cuboidal cell body with fine extending filopodia due to interactions with the surface micro-topography. Interestingly it was noted that what appeared to be beta-phase particles breached the tubulin and actin cytoskeleton throughout the cell body (figure 3.6; white arrows). When investigated it was noted that specifically the tubulin network appeared to circumnavigate these particles and many of the filopodia appeared to attempt to do this also (figure 3.6; blue arrows). Using the Axioplan software we were able to delineate that features of the surface and confirm that the beta phase particles were responsible for this breaching of the tubulin network (figure 3.6; blue arrows on surface without cell).

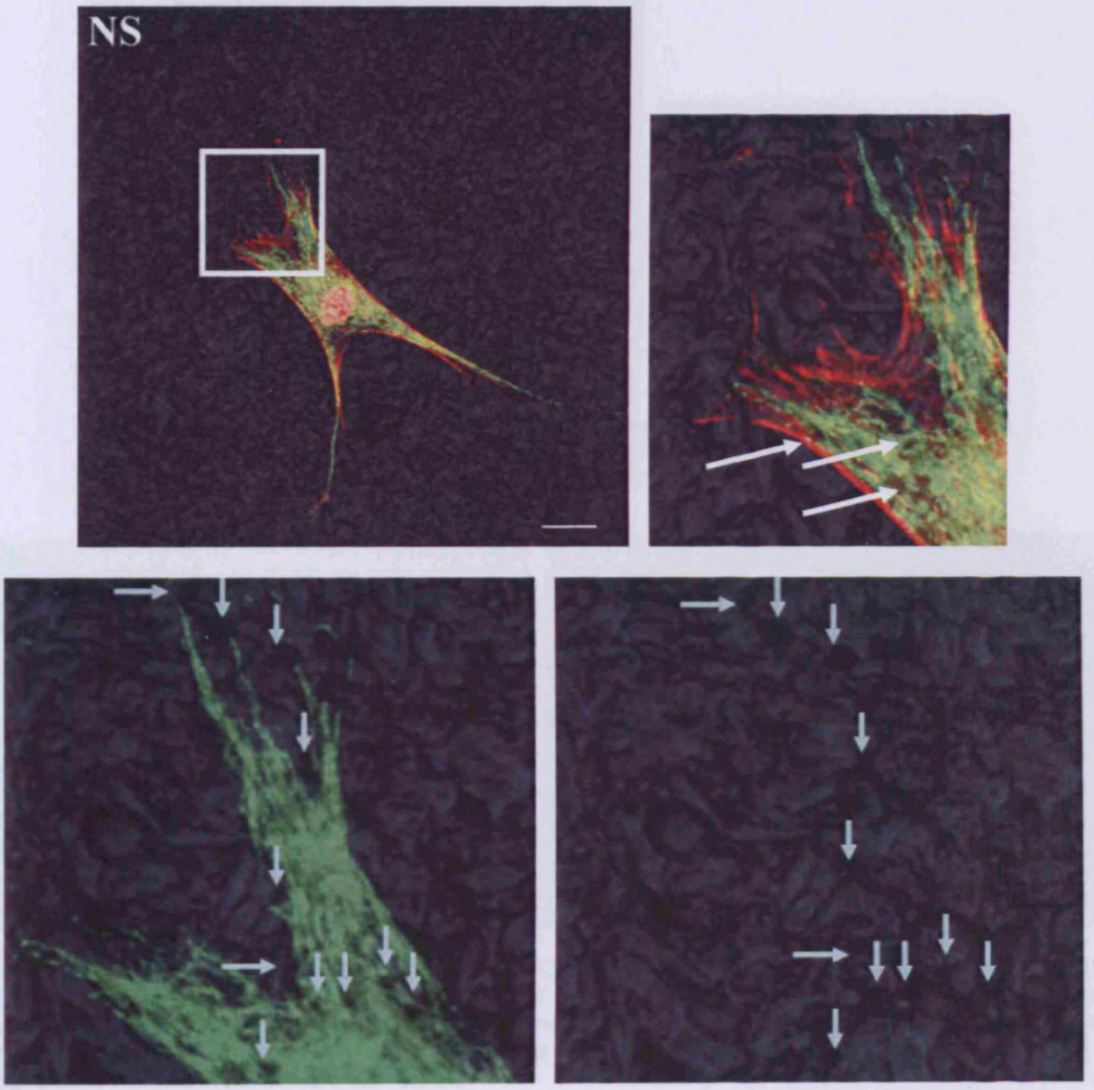

Figure 3.6. RC cells cultured on NS for 24 hours. Cells were fluorescently labelled for actin (red) and tubulin (green). The surface micro-discontinuities of NS induced a cuboidal cell body morphology. Cell nuclei were labelled using DAPI (pink/purple). The protruding beta-phase particles appeared to breach the actin and tubulin network (white arrows). When further investigated, it was seen that the tubulin network attempted in places to circumnavigate these particles, which was also observed for filopodia (blue arrows). Scale bar=20μm.

Electropolishing of the TAN surface dramatically reduced the prominence of the beta-phase particles. This allowed for a higher degree of cell spreading to occur and consequently a more fibroblast-like triangular shape with the 3 large lamellapodia described previously were generally noted. Cells on NE adopted a well spread elongated morphology akin of that noted for Ss. Even so it appeared that some nano-topographical variations in the surface could still be 'sensed' by cells cultured on NE (figure 3.7; black arrows, white arrows) however, the smoothened beta-phase particles did not appear to exert the same disruption of the tubulin network as noted for NS.

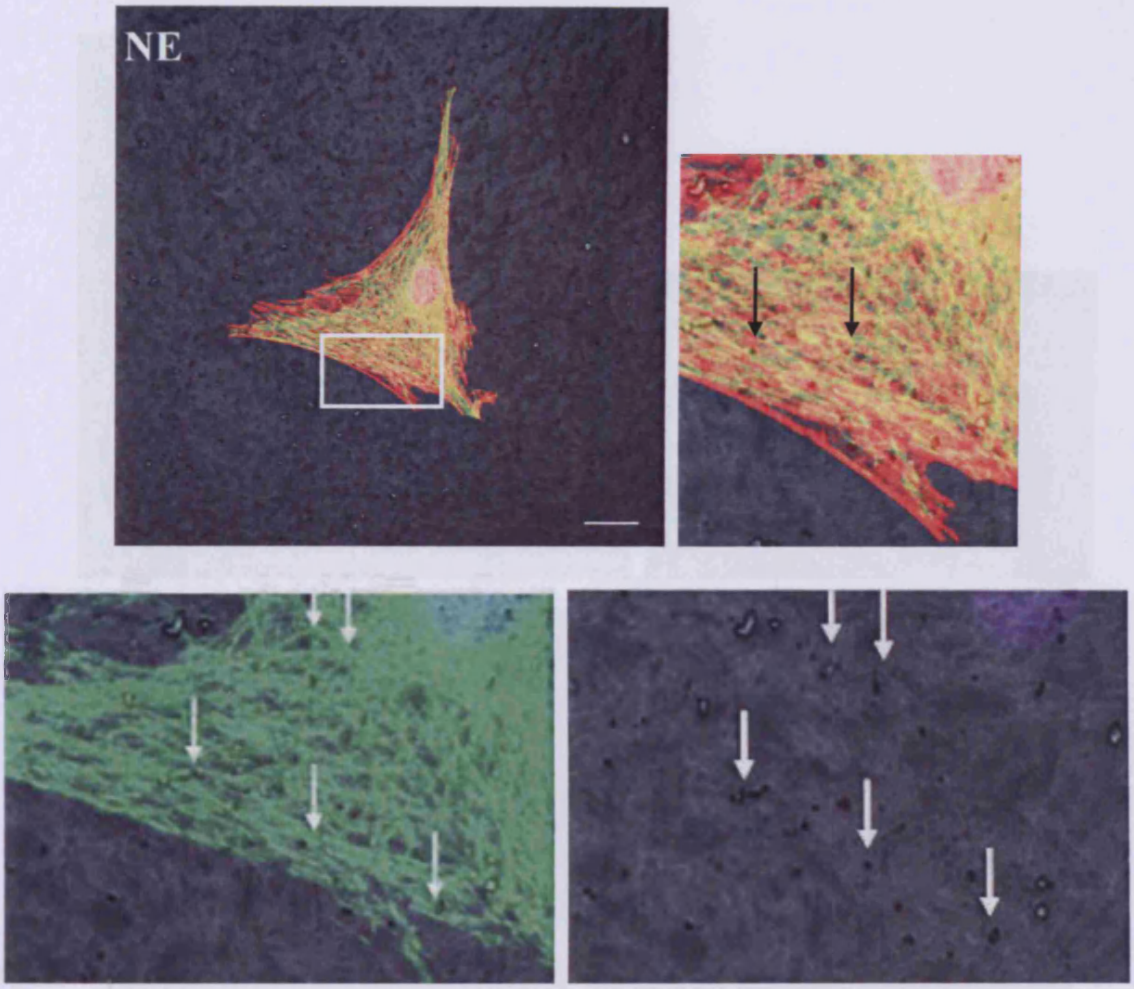

Figure 3.7. RC cells cultured on NE for 24 hours. Cells were fluorescently labelled for actin (red) and tubulin (green). The reduction in the prominence of the beta-phase particles allowed for a well spread elongated morphology. Moreover, further analysis revealed that RC cells cultured on NE did not appear to 'sense' the remnants of the particles. However, some nano-topographical variations on the surfaces were sensed (black, white arrows). Scale bar=20μm.

Similar to NS samples the beta phase particles of NP appeared to restrict cell spreading although a fibroblast-like elongated shape was evident. The morphology of the cells on NP appeared to be determined by the surface features. In fact in some areas it was observed that the cell attempted to circumnavigate the particles rather than attempt to cross over them while the particles also appeared to disrupt areas of the cytoskeleton (figure 3.8; white arrows). This interpretation was confirmed by separating the components of the cytoskeleton to reveal the underlying topography which was responsible for the breaches noted (figure 3.8; yellow arrows).

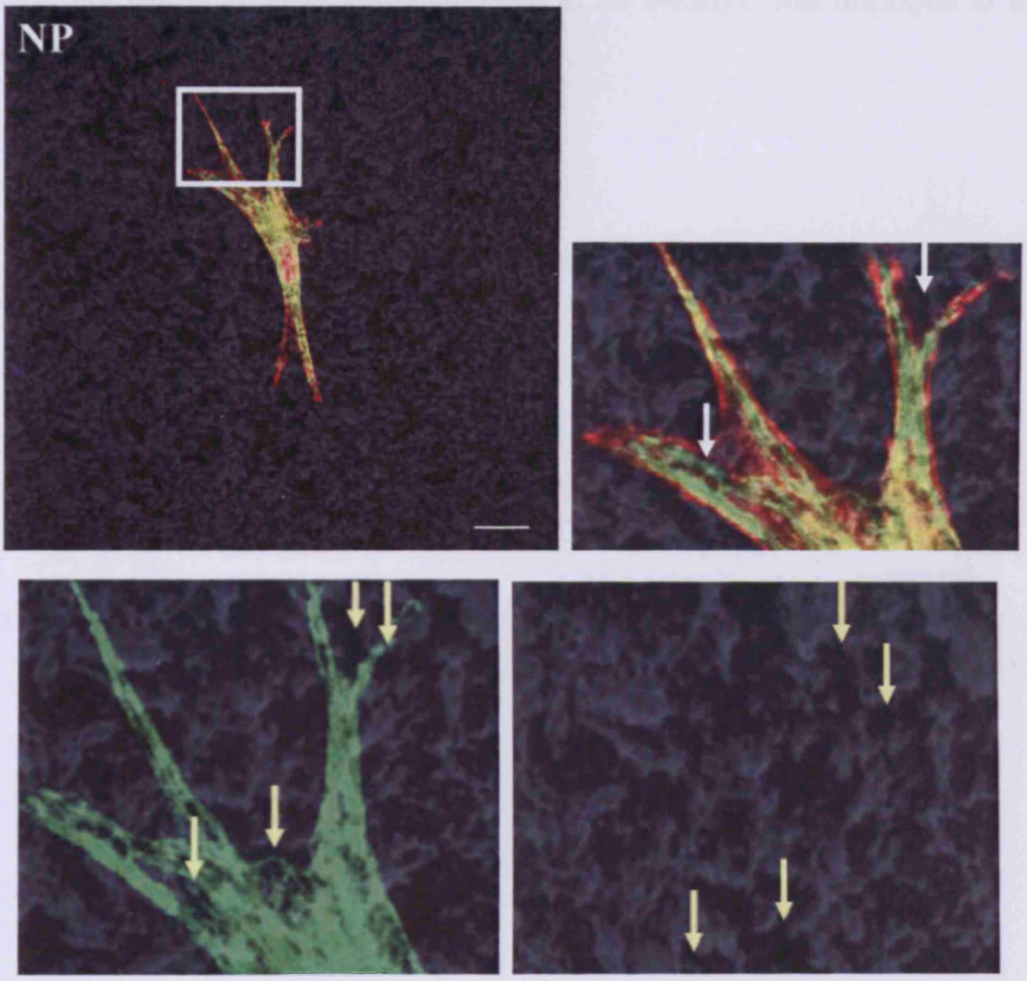

Figure 3.8. RC cells cultured on NP for 24 hours. Cells were fluorescently labelled for actin (red) and tubulin (green). The morphology of the cells on NP appeared to be restricted by the surface features, in particular the beta phase particles. In fact, in some areas it was observed that the cell attempted to circumnavigate the protrusions, rather than attempt to cross over them, while the particles also appeared to disrupt areas of the cytoskeleton (figure 3.8; white arrows). This was confirmed by separating the components of the cytoskeleton to reveal the underlying topography which was responsible for the breaches noted (figure 3.8; yellow arrows). Scale bar=20μm

Similar to TS and NS the micro-roughness of the MS surface appeared to restrict cell spreading compared to polished samples. Differences in surface micro-topographical features appeared to direct cell attachment and morphology (figure 3.9; purple arrows). In contrast, ME appeared to induce an elongated morphology and while surface micro-topographical features appeared to be generally imperceptible to the cells (figure 3.10; yellow arrows) there was evidence that cell morphology was directed by them to a small degree (figure 3.10; blue arrows). The reduction in surface micro-roughness of MP allowed for increased cell spreading and a flattened elongated morphology with a triangular fibroblast-like morphology (figure 3.10) akin to that noted for Ss and TCP. The differences in micro-topography of the MP surface were not perceived to be distinguishable as no evidence was displayed to show a micro-topographical directed morphology.

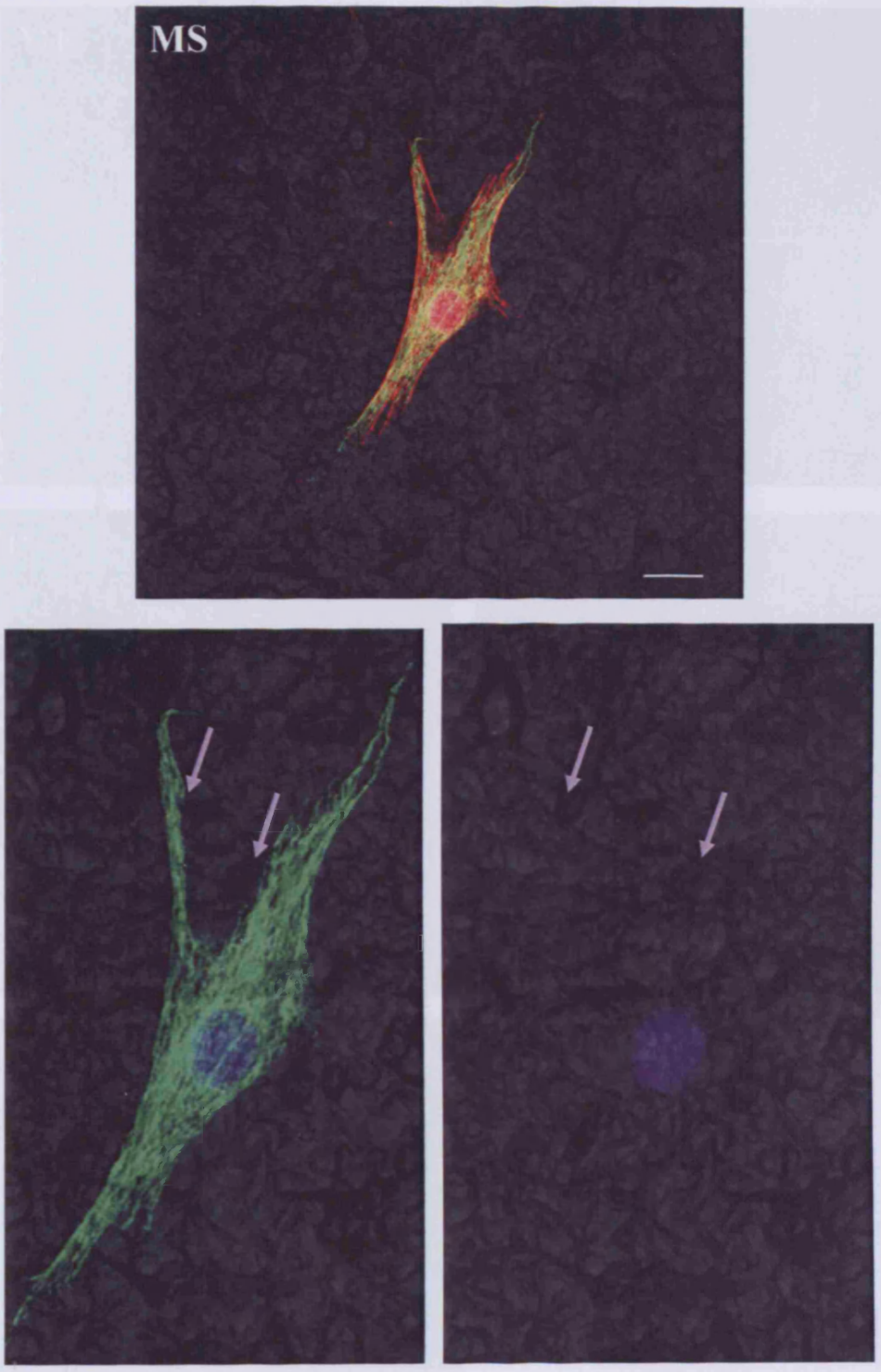

Figure 3.9. RC cells cultured on MS for 24 hours. Cells were fluorescently labelled for actin (red) and tubulin (green). Differences in surface micro-topographical features appeared to direct cell attachment and morphology (purple arrows).

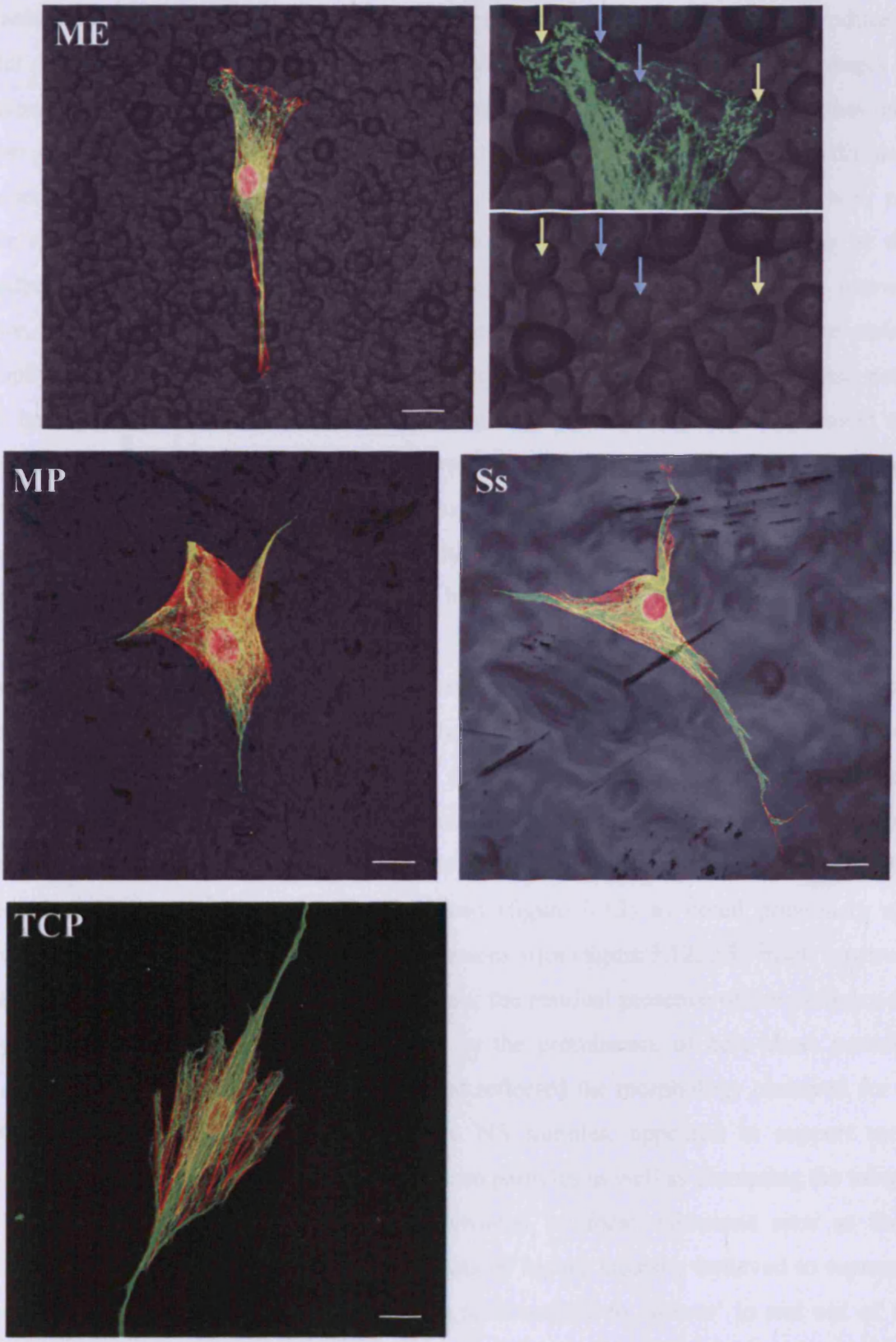

Figure 3.10. RC cells cultured on ME, MP, Ss and TCP for 24 hours. Cells were fluorescently labelled for actin (red) and tubulin (green). ME appeared to induce an elongated morphology, and while surface micro-topographical features appeared to be generally imperceptible to the cells (yellow arrows), there was evidence that cell morphology was directed by them to a small degree (blue arrows). The reduction in surface micro-roughness of MP allowed for increased cell spreading, and a flattened, elongated morphology akin to that noted for Ss and TCP. The differences in micro-topography of the MP surface were not perceived to be distinguishable, as no evidence was displayed to show a micro-topographical directed morphology. Scale bar=20μm.

The interaction of the RC cells with the micro-roughness of the TS surface again produced a cuboidal morphology. As was noted for the tubulin cytoskeletal network changes in dimensions of the micro-topography shaped the periphery of the cell. Here we noted that focal adhesion sites are also influenced by the changes in micro-roughness of TS. Focal adhesions (FA) sites were frequently noted on the edges of a micro-discontinuity. Moreover, one possible reason for the less spread appearance compared to polished samples may be that focal adhesion sites were restricted by micro-topography (figure 3.11; TS, white arrows), therefore, rather than spreading the cell 'sits' on the surface. As noted previously the surface topography of TE had very little influence on restricting cell spreading and was also noted here to have little effect on focal adhesion placement (figure 3.11; TE, white arrows) and these structures were regularly noted to transverse the small variations in topography. While the tubulin and actin networks did not appear to hindered by the small variations in micro-topography the focal adhesions sites of cells cultured on TP appeared to be sensitive to small changes on a nano-metric level (figure 3.11; TP, blue and white arrows).

We noted previously that surface features believed to be beta-phase particles disrupted the tubulin network for cells cultured on NS. When examining the focal adhesion sites we observed that these same particles appear to direct focal adhesion placement and these generally avoided the structures previously shown to be beta-phase particles (figure 3.12; NS, blue arrows). However, this was not observed for all sites labelled positive for vinculin. Cells cultured on NE in contrast appeared well spread (figure 3.12) as noted previously and appeared to have a higher frequency of focal adhesions sites (figure 3.12; NE, inset) however, this was not confirmed quantitatively. Furthermore, the residual presence of the particles did not appear to restrict adhesion. This reduction in the prominence of beta-phase particles allowed cells on NE to become highly spread and reflected the morphology observed for Ss and TCP (figure 3.14). NP samples similar to NS samples, appeared to support more restricted spreading of the cells. Also, the beta-phase particles as well as disrupting the tubulin network as noted previously appeared to be avoided by focal adhesions sites as these structures were often found circumnavigating areas of higher intensity believed to represent bet-phase particles. In fact many focal adhesion sites seemed to 'weave' in and out of the particles in an attempt to avoid the latter (figure 3.12; NP, yellow arrows).

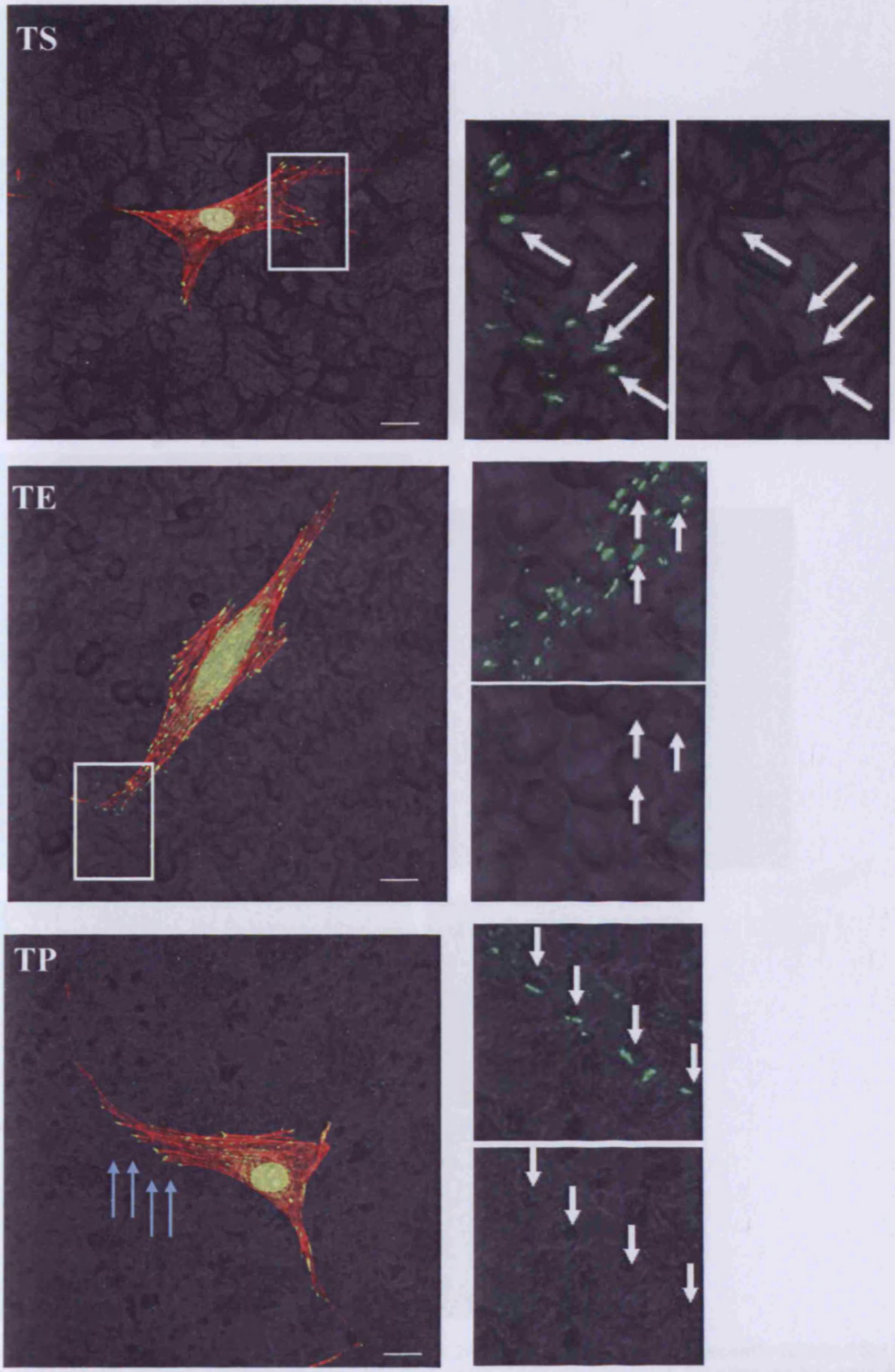

Figure 3.11. RC cells cultured on TS, TE, and TP for 24 hours. Cells were fluorescently labelled for actin (red) and vinculin (green). Cell nuclei were labelled using DAPI (pink/purple). FA sites on TS surfaces appeared regulated by variations in topography (TS; white arrows), and appeared frequently on peaks of the surface. In contrast, TE had very little influence on FA placement, and transverse variations topography. For cell cultured on TP, focal adhesions sites appeared sensitive to small changes on a nano-metric level. Scale bar=20μm.

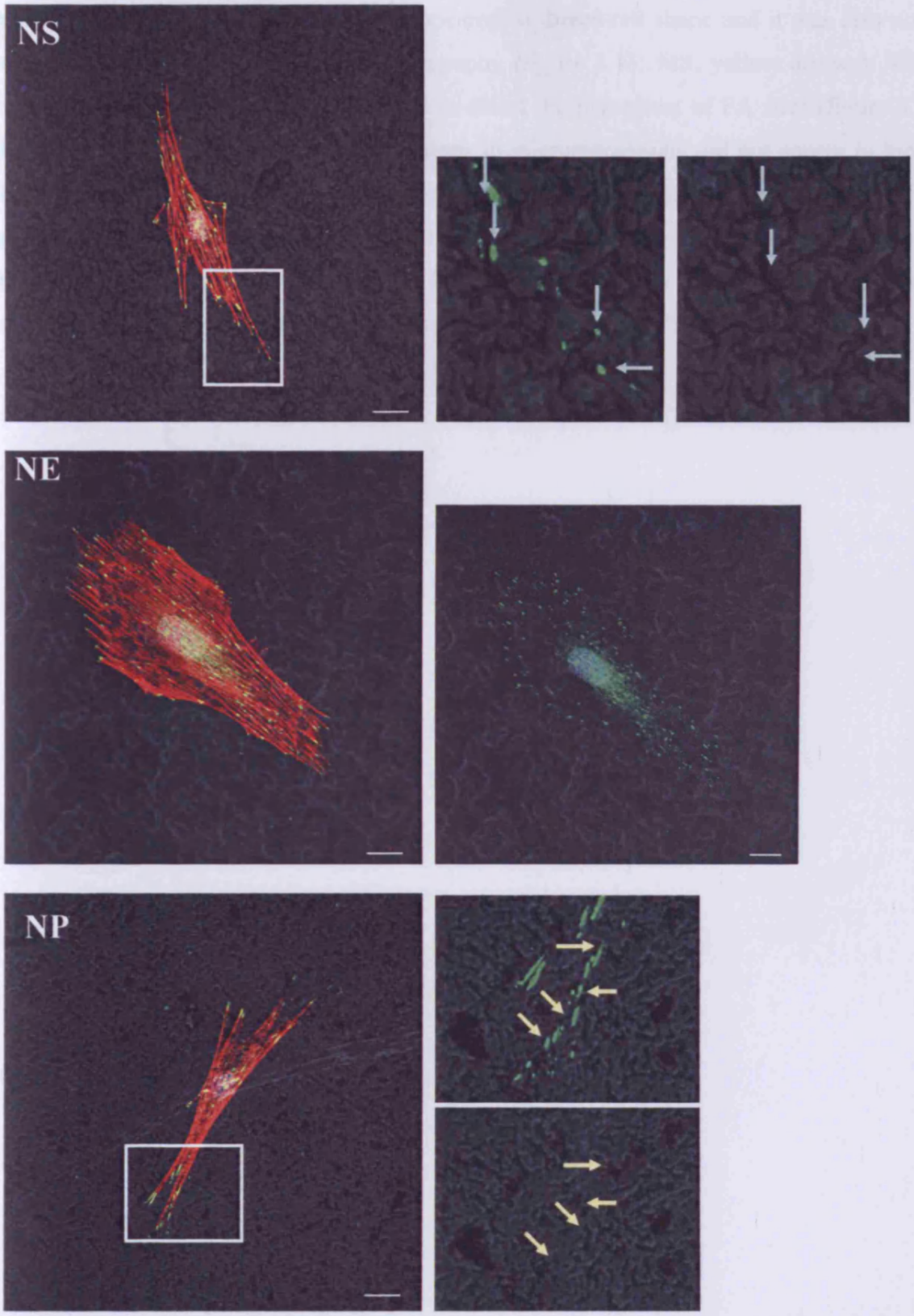

Figure 3.12. RC cells cultured on NS, NE, and NP for 24 hours. Cells were fluorescently labelled for actin (red) and vinculin (green). Cell nuclei were labelled using DAPI (pink/purple). FA sites on NS were found to generally avoid beta-phase particles (blue arrows), however this was not observed for all sites labelled positively for vinculin. In contrast, cells on NE appeared well spread and had a higher frequency of FA sites, although, this was not quantified. The remnants of beta phase particles on NE did not appear to interfere with FA sites. FA sites on NP were found circumnavigating areas of higher intensity, believed to represent beta-phase particles. In fact, many FA sites seemed to 'weave' in and out of the particles in an attempt to avoid the latter (yellow arrows). Scale bar=20μm.

The micro-roughness of the MS surface appeared to direct cell shape and it was also noted that FA sites conformed to the micro-topography (figure 3.13; MS, yellow arrows). While larger variations in topography were found to direct the placement of FA sites (figure 3.13; ME, blue arrow), generally the small variations in microtopography did not appear to hinder cell spreading and therefore FA sites were often noted on the small 'hills' of the surface (figure 3.13; ME, white arrow). Similarly the surface morphology of MP did not influence spreading and FA sites were readily able to form across the surface (figure 3.13, MP) and as a result cells adopted an appearance akin to that observed for Ss and TCP (figure 3.14).

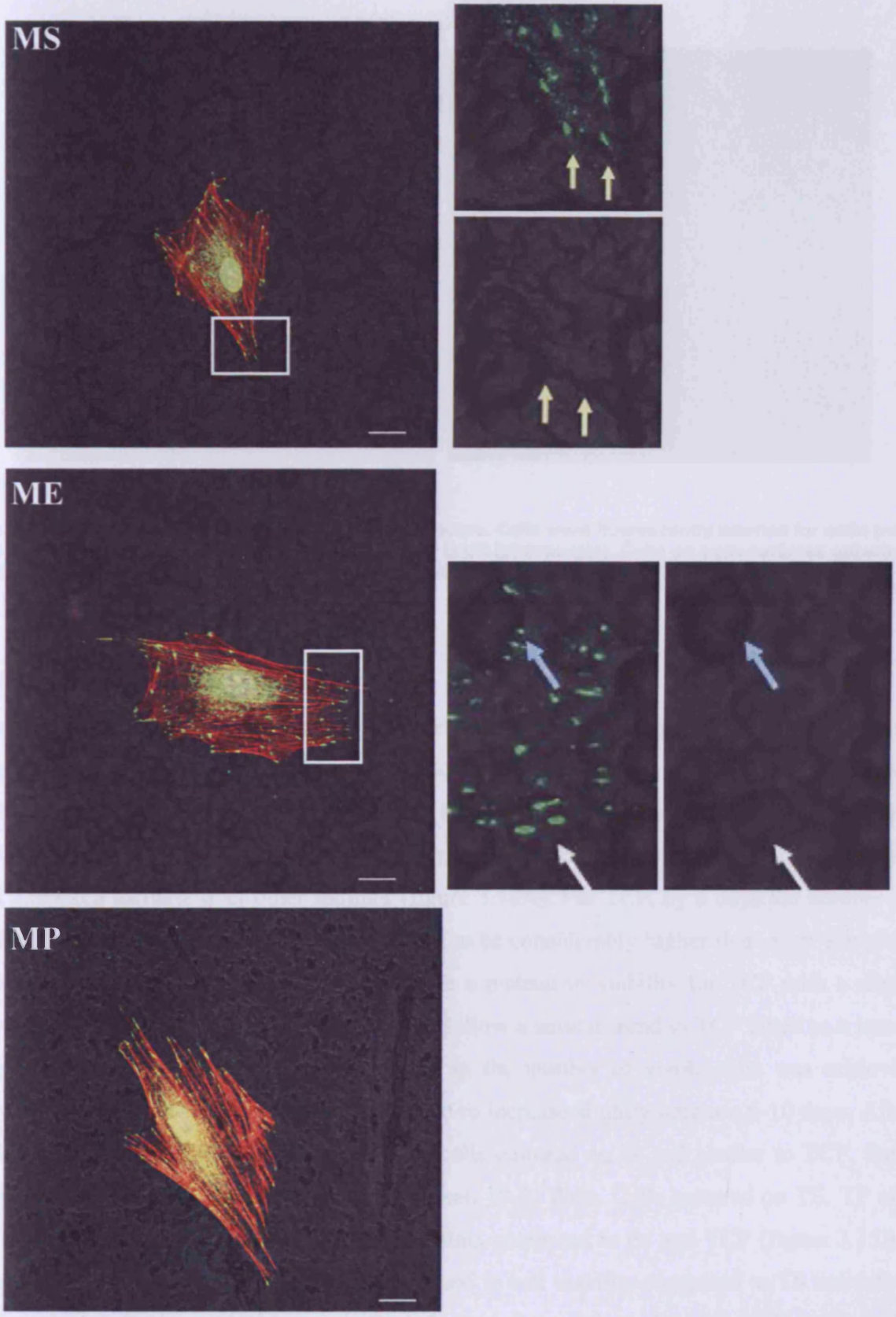

Figure 3.13. RC cells cultured on MS, ME, and MP for 24 hours. Cells were fluorescently labelled for actin (red) and vinculin (green). Cell nuclei were labelled using DAPI (pink/purple). FA sites on MS conformed to the micro-topographical features of the surface (yellow arrow). While larger variations in topography were found to direct FA sites (blue arrow), generally, the small variations in microtopography did not appear to hinder cell spreading. Similarly, the surface morphology of MP did not influence spreading and FA sites were readily able to form across the surface. Scale bar=20μm.

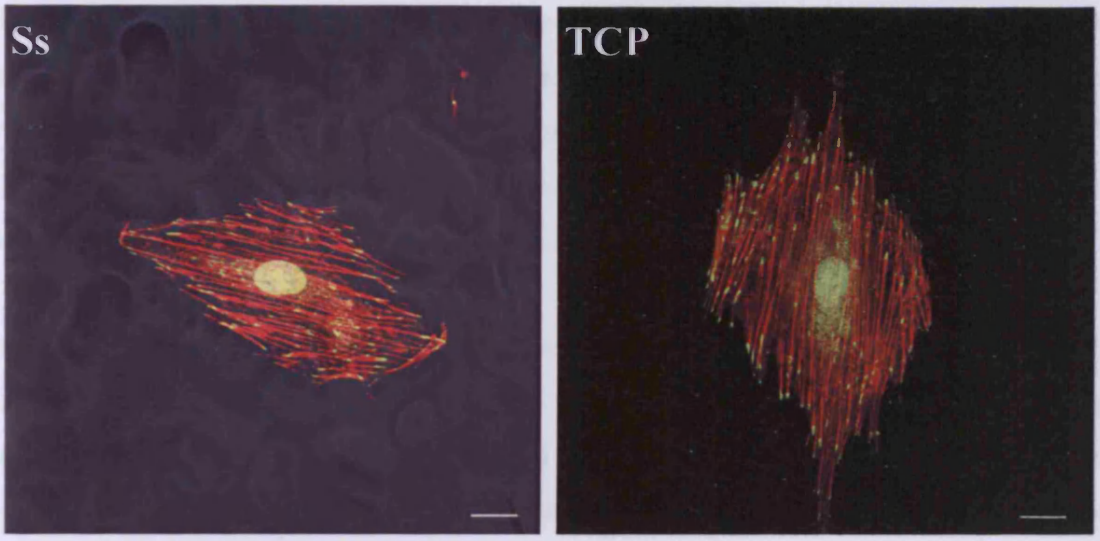

Figure 3.14. RC cells cultured on Ss and TCP for 24 hours. Cells were fluorescently labelled for actin (red) and vinculin (green). Cell nuclei were labelled using DAPI (pink/purple). Cells on both surfaces appeared well spread, and flattened with a high frequency of FA sites. Scale bar=20μm.

Cell viability:

Due to the perceived poor sensitivity of this method at 1 and 2 days quantitative data for these time points are not presented. However, to test viability at these earlier times qualitative viability staining has been included (figures 3.16-3.18). After 4 days culturing on the various cpTi samples cell viability appeared similar for all samples with the exception of TCP, which had a marked increase over other samples (figure 3.15A). For TCP, by 6 days the number of viable cells had increased and again was found to be considerably higher than other samples. However, from 8-21 days there appeared to be a plateau in viability for TCP with a slight decline noted from 10-21 days. Ss appeared to follow a similar trend to TCP albeit to a lesser degree. Again for Ss a considerable increase in the number of viable cells was achieved between 4-6 days which subsequently continued to increase slightly between 6-10 days. After this time, a plateau in viability was noted for cells cultured on Ss and similar to TCP, there was a slight decline in viability observed between 10-21 days. Cells cultured on TE, TP and TS had less fluorescent intensity at all time points compared to Ss and TCP (figure 3.15A). Nevertheless, TE and TP displayed a similar trend in cell viability compared to TS indicating that surface polishing did not negatively influence the number of viable cells present. In contrast to Ss and TCP, TE and TP did not display the initial marked increase in the number of viable cells between 4 and 6 days. Instead TE and TP follow a similar pattern to TS, displaying maintained viability over time. Statistically, it was found that neither polishing

method significantly affected cell viability compared to TS ($p=1.000$ for both comparisons). Furthermore, no significant difference in the number of viable cells was noted between polished variants ($p=1.000$). However, both Ss and TCP showed significantly higher number of viable cells compared to TE ($p=0.003$; $p<0.001$ respectively), TP ($p<0.001$ for both comparisons) and TS ($p=0.002$; $p<0.001$, respectively). However, cell viability on Ss was also found to be significantly lower compared to TCP ($p<0.001$).

After 4 days culturing both NE and NP displayed a similar maintenance of viability compared to Ss while viability for cells cultured on NS at this time were shown to be slightly higher (figure 3.15B). However surface polishing did not negatively affect viability as from 6 days viability of NE and NP samples reflected the trend observed for NS. Specifically there was a steady increase in the number of viable cells cultured NE and NP, akin to that of NS, from 2-10 days. Subsequently, all TAN samples reach a plateau in viability between 1-14 days which was followed by a slight increase between 14-21 days. By 21 days all TAN samples displayed a similar level of cell viability compared to Ss. Both Ss and TCP were found to have significantly higher number of viable cells compared to NE ($p=0.021$; $p<0.001$ respectively), and NP ($p=0.004$; $p<0.001$ respectively). However, the number of viable cells did not significantly differ for polished variants ($p=1.000$). Interestingly the number of viable cells on NP samples was found to be significantly lower compared to NS samples ($p<0.001$) however this was not observed or NE samples ($p=1.000$).

The number of viable cells cultured on MS appeared extremely low, even after 4 days of culture. Hence, qualitative cell viability staining and quantification of unattached cells was carried out after 1 and 2 days culturing to assess if the maintenance of viability (figure 3.18) or cell attachment (figure 3.19) was responsible for the reduction observed. However, regardless of which factor was contributing the lower number of viable cells observed for MS this effect was transient as by 6 days viability for MS was found to be similar compared to ME and MP, and this further increased between 6 and 8 days to exceed that observed for ME and MP samples (figure 3.15C). Furthermore, no significant differences in the number of viable cells were observed for ME ($p=1.000$) or MP ($p=1.000$) compared to MS. After 4 days culturing MP displayed an increased number of viable cells compared to ME, Ss and MS. However, this was not akin to that of TCP. The number of viable cells on ME samples was initially lower than MP, and reflected more the outcome for Ss at this time. However, between 4 and 6 days there was an increase in the number of viable cells for ME samples, which by 6 days was found to be similar to MP. For both ME and MP there was a slight increase in the

number of viable cells noted at 8 days and by 10 days viability on these surfaces was found to be similar to MS. From 10 to 21 days there is a slight increase in the number of viable cells for ME and MP which closely reflects the trend observed for MS and by 21 days, viability on the Ti15Mo samples is akin to that for Ss. As before, the number of viable cells on Ss and TCP samples was found to be significantly higher compared to ME ($p=0.021$; $p<0.001$ respectively) and MP ($p=0.046$; $p<0.001$ respectively) while MS had significantly lower number of viable cells compared to TCP ($p<0.001$), but not Ss ($p=0.087$). Furthermore, there was no significant different in the number of viable cells for either ME or MP samples ($p=1.000$).

A

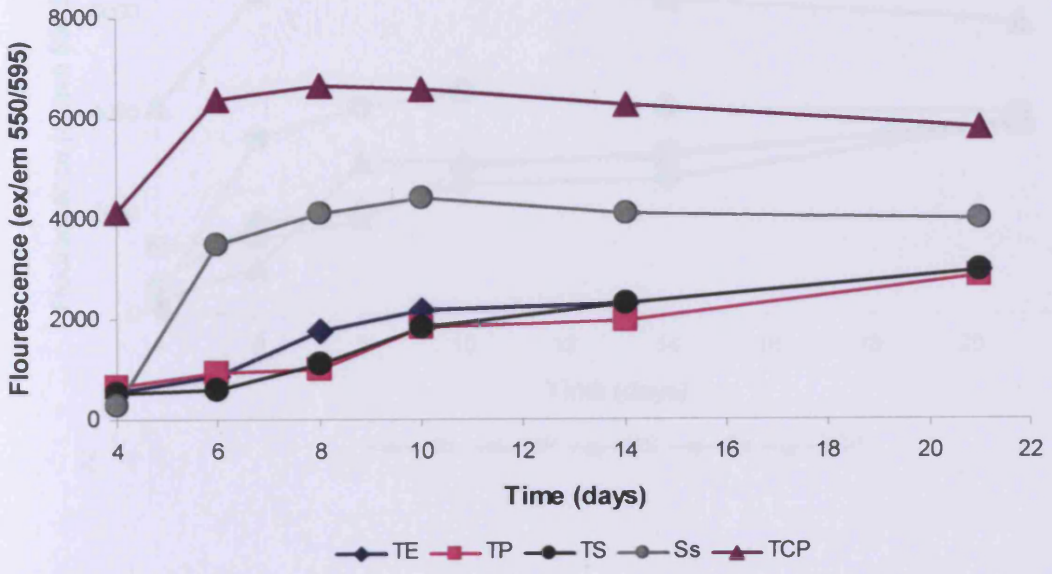
Cell viability results for RC cells cultured on cpTi
Flourescence (ex/em 550/595)
8000
6000
4000
2000
0
4
6
8
10
12
14
16
18
20
22
Time (days)
TE
TP
TS
Ss
TCP

B

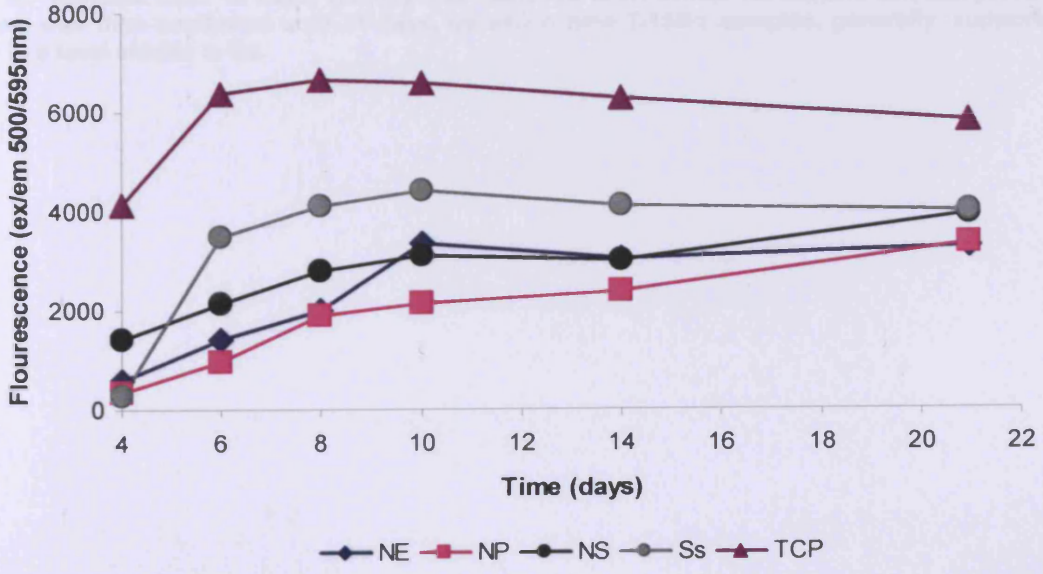
Cell viability results for RC cells cultured on TAN
Flourescence (ex/em 500/595nm)
8000
6000
4000
2000
0
4
6
8
10
12
14
16
18
20
22
Time (days)
NE
NP
NS
Ss
TCP

C

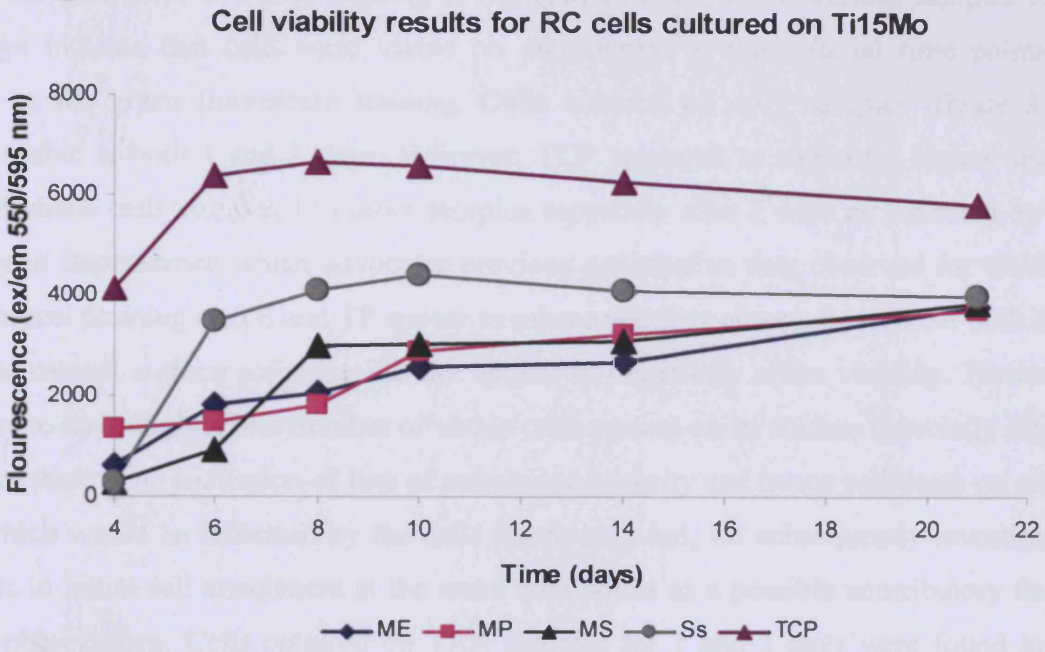

Figure 3.15. Cell viability of RC cells cultured on cpTi (A), TAN (B), and Ti15Mo (C). TCP consistently showed higher viability for all time points. While Ss generally had reduced number of viable cells compared to TCP, it remained higher than that observed for cpTi, TAN and Ti15Mo samples. However, by 21 days, all samples (with the exception of TCP) appeared to support a similar level of viability. Both TE and TP appeared to induce a similar trend in cell viability compared to TS, over time. NE and NP, however, appeared to have reduced number of viable cells compared to NS for 4-10 days. However, subsequently, all TAN samples displayed similar viability. The number of viable cells cultured on MS appeared extremely low, even after 4 days of culture. Hence, qualitative cell viability staining, and quantification of unattached cells was carried out after 1, 2 days culturing, to assess if reduced cell viability, or cell attachment was responsible for the reduction observed. However, the lower number of viable cells observed for MS was transient, as by 6 days, viability for MS was found to be similar compared to ME and MP, and this further increased between 6 and 8 days, to exceed that observed for ME and MP samples. After 10 days, viability was observed to be similar for ME and MP, compared to MS. This trend was then continued until 21 days, by which time Ti15Mo samples, generally, supported cell viability to a level similar to Ss.

Results from qualitative live/dead staining of RC cells cultured on the various samples for 1 and 2 days indicate that cells were viable on all samples at these initial time points as indicated by the green fluorescent staining. Cells cultured on cpTi samples (figure 3.16) appeared viable at both 1 and 2 days. However, TCP appeared to support a higher degree amount of viable cells compared to other samples especially after 2 days as indicated by the intense green fluorescence which advocates previous quantitative data observed for viability on this surface. Staining on TE and TP appear to mirror viability observed on Ss for both time points, and overall surface polishing did not appear to negatively affect viability. However, TS appears to have slightly less number of viable cells present on its surface especially after 2 days. Since there is no indication of loss of membrane integrity and hence cell death on either surface which would be indicated by the cells fluorescing red, we subsequently investigated differences in initial cell attachment at the same time points as a possible contributory factor for these observations. Cells cultured on TAN samples for 1 and 2 days were found to be viable (figure 3.17). No evidence of cell death was observed for these samples. Surface polishing did not appear to have any adverse affects on viability at these time points. The finding of perceived lower cell number as noted for TS was also observed for MS (figure 3.18). After 24 hours cells cultured on ME and MP appear to have more cells present compared to MS thus indicating that surface polishing enhances cell viability for this material, as indicated by the more intensely stained cells. After 48 hours MS still appears to have a lower number of cells present compared to ME and MP as well as other control surfaces. However, as with TS there is no indication of cell death on MS, as there was no red fluorescence (non-viable cells) detected.

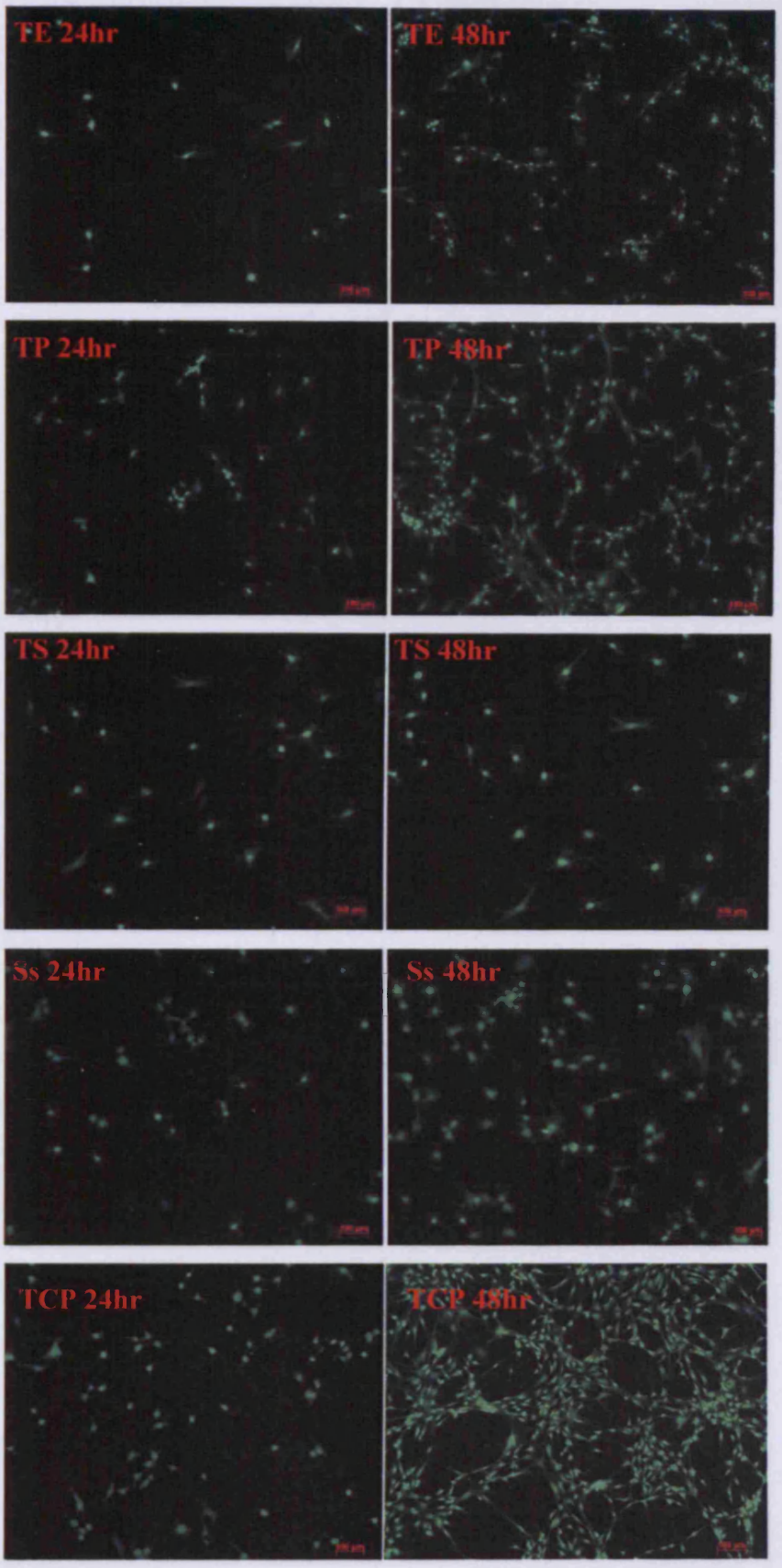

Figure 3.16. Qualitative cell viability for TE, TP, TS, Ss and TCP after 24 and 48 hours. Both TE and TP appear to support viability similar to Ss. While TS also has viable cells at both time points, there does not appear to be an increase at 48 hours, as shown for TE, TP, Ss and TCP. However, there is no indication that cell death (lack of red fluorescence) is responsible for this perceived lower viability. Staining on TCP advocates previous observations that this surface supports a higher degree of viability. Scale bar = 100μm.

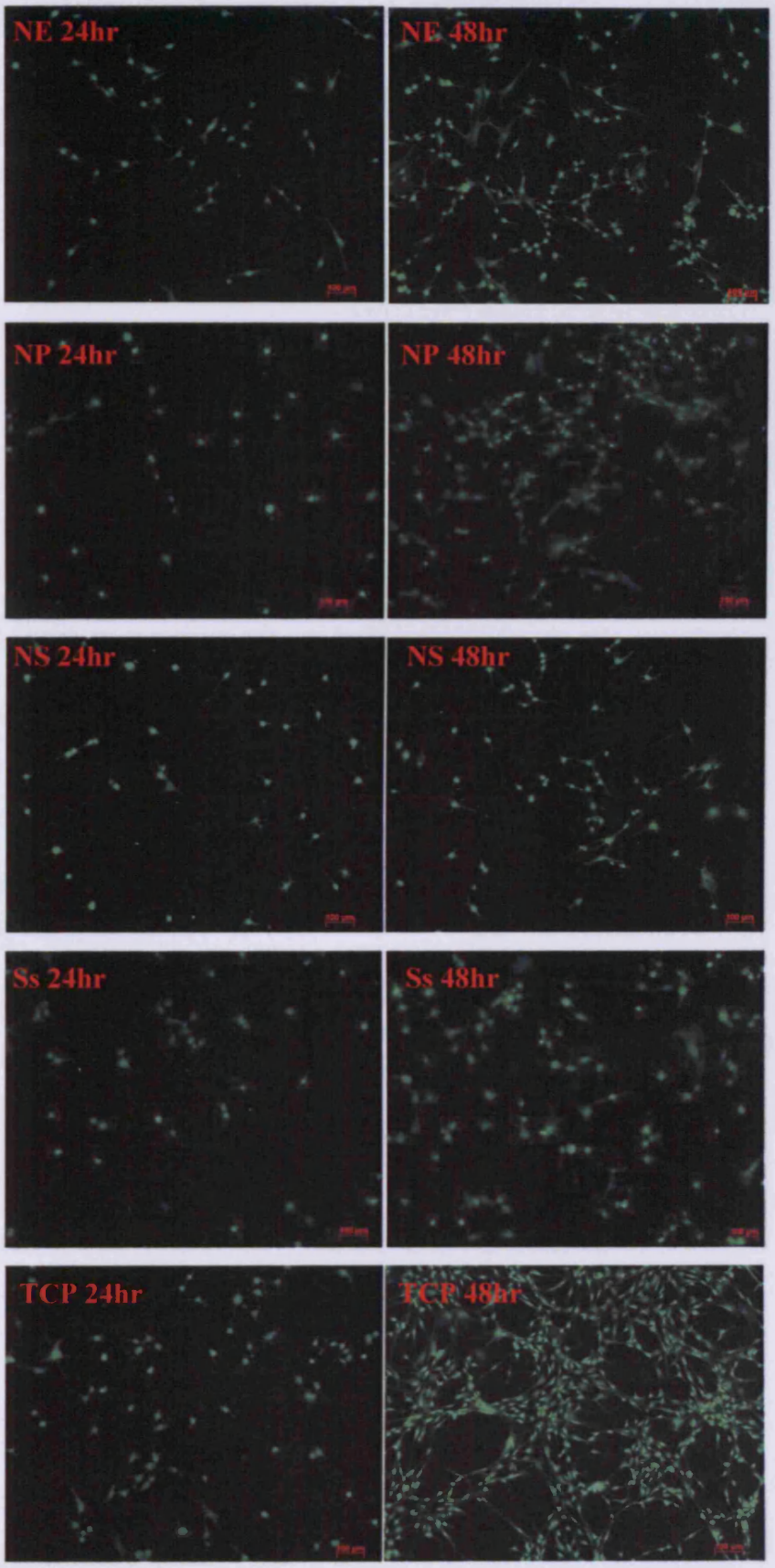

Figure 3.17. Qualitative cell viability for NE, NP, NS, Ss and TCP after 24 and 48 hours. Cells cultured on TAN samples for 1 and 2 days, were found to be viable. No evidence of cell death was observed for these samples. Scale bar = 100μm.

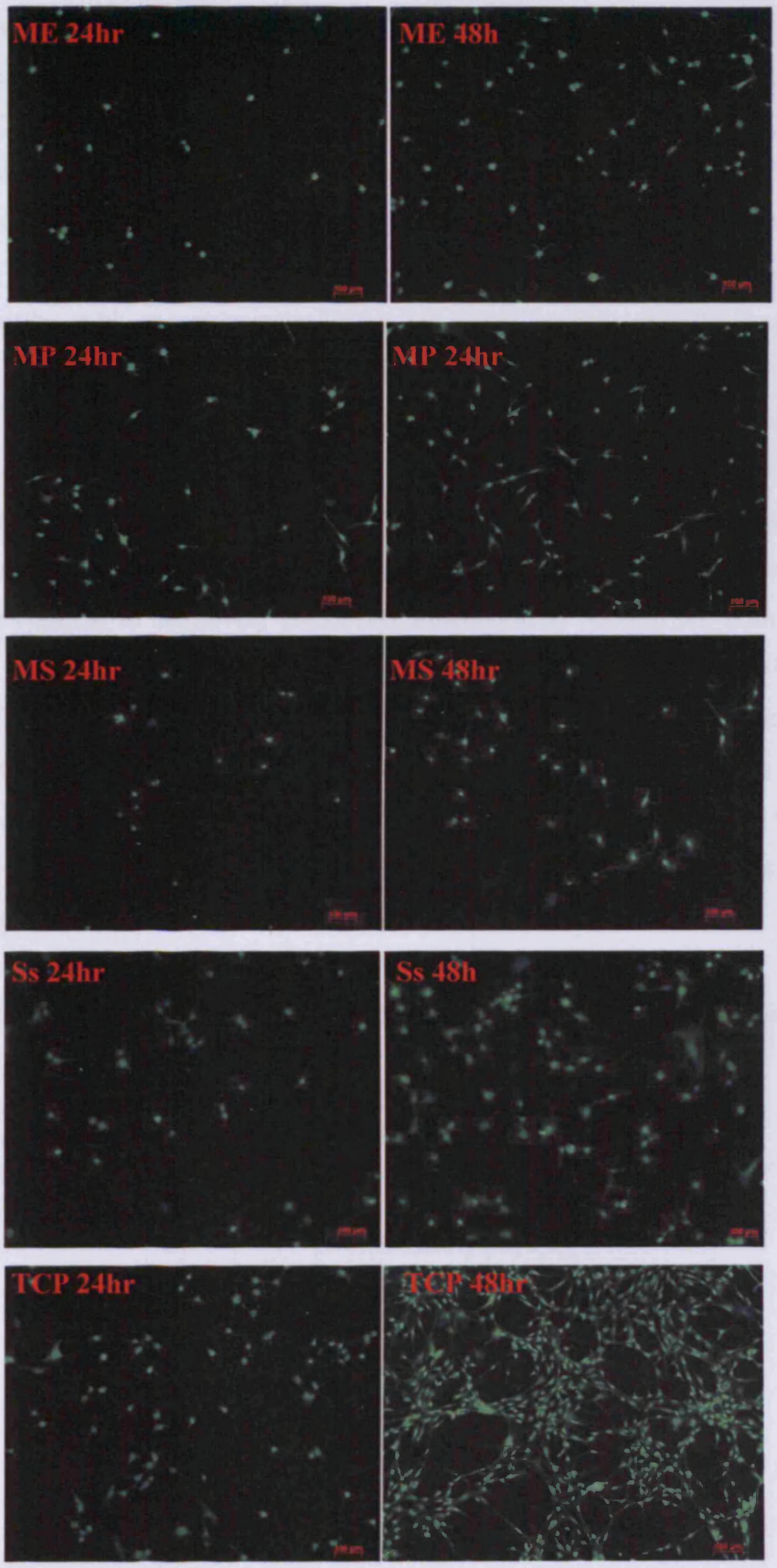

Figure 3.18. Qualitative cell viability for ME, MP, MS, Ss and TCP after 24 and 48 hours. MS samples support cell viability despite the lower number of cells observed. After 48 hours, MS still appears to have a lower number of cells present compared to ME, and MP, as well as other control surfaces. However, as with TS, there is no indication of cell death on MS, as there was no red fluorescence (non-viable cells), detected. Scale bar = 100μm.

Quantification of percentage of unattached cells:

Initial cell attachment appears to be increased on TE and TP compared to TS after 24 hours as both TE and TP had a lower percentage of cells unattached to the surface after this time. Thus surface polishing does not appear to negatively influence cell attachment on cpTi i*n vitro*. After 48 hours both TE and TP had approximately 15% of cells which remained unattached, compared to TS which had only 10% (figure 3.19). Ss and TCP have practically identical cell attachment profiles with approximately 30% of the total number of cells seeded remaining unattached to the surfaces after 24 hours. By 48 hours both Ss and TCP have a high percentage of cell attachment as approximately 7% of cells remain unattached for both surfaces. NS was found to reflect results accrued for Ss and TCP with only 27% of the initial seeding density remaining unattached after 24 hours (figure 3.19). By 48 hours attachment had further increased with only 7% of the cell population remaining unattached. Surface polishing didn't appear to negatively affect cell attachment as NE and NP both had a similar percentage of unattached cells remaining after 24 and 48 hours, compared to NS. Although NP did have slightly higher percentage at 24 and 48 hours compared to NE and NS. MS had the highest percentage of unattached cells after 24 and 48 hours compared to all other samples (figure 3.19). Electropolishing appeared to enhance initial attachment (ME) to within similar levels observed for other samples. Paste polishing (MP) did improve cell attachment within the first 24 hours of culturing, however, a higher percentage of unattached cells were recorded for MP compared to any other polished substrate. By 48 hours however the percentage of unattached cells for MP was akin to that noted for all other samples, independent of material type.

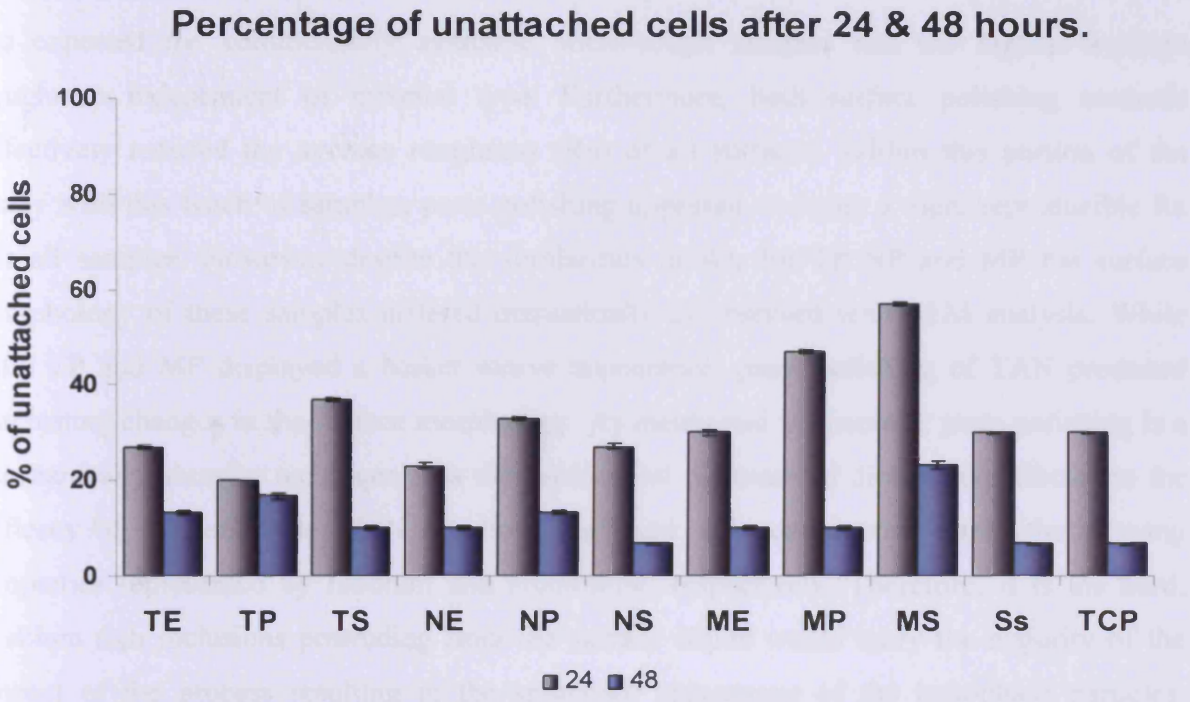

Figure 3.19. Percentage of unattached cells to the various surfaces studied, after 24 and 48 hours, ±S.E.M. Surface polishing does not negatively influence cell attachment, as for all material types, polishing either increased initial attachment, or had similar initial attachment compared to the standard micro-rough counterpart. MS had the highest percentage of unattached cells after 24, and 48 hours, compared to all other samples. Electropolishing appeared to enhance initial attachment (ME) to within similar levels observed for other samples. Paste polishing (MP) did improve cell attachment within the first 24 hours of culturing, however, a higher percentage of unattached cells were recorded for MP compared to any other polished substrate. By 48 hours, however, the percentage of unattached cells for MP was akin to that noted for all other samples, independent of material type.

Chapter 3: Discussion.

Surface characterisation:

As expected the commercially available micro-rough samples had the highest average roughness independent of material type. Furthermore, both surface polishing methods effectively reduced the average roughness (Ra) of all surfaces. Within this portion of the study with this batch of samples, paste polishing appeared to create a more reproducible Ra for all samples. However, despite the similarities in RA for TP NP and MP the surface morphology of these samples differed dramatically as observed with SEM analysis. While both TP and MP displayed a basket weave appearance, paste polishing of TAN produced interesting changes in the surface morphology. As mentioned in chapter 2 paste polishing is a mechanically abrasive technique thus the hardness of the material directly contributes to the efficacy of the technique. TAN has both hard and soft components within the alloying properties represented by niobium and aluminium, respectively. Therefore, it is the hard, niobium rich inclusions protruding from the surface which would carry the majority of the impact of the process resulting in the splintered appearance of the beta-phase particles. Electropolishing on the other hand appeared to produce more variability in the Ra of the surfaces. For TAN, electropolishing appeared extremely adept at reducing the micro-roughness associated with this material. In fact with SEM analysis the effectiveness of his method becomes more apparent as it was noted that electropolishing successfully reduced the prominence of the beta-phase particles. This resulted in a Ra for NE akin to that noted for the orthopaedic 'gold standard' smooth material, Ss. This is the opposite for observations made for NE and NP previously for a different sample batch. In chapter 2 we observed a lower Ra for NP samples compared to NE while SEM analysis revealed that in fact both surfaces, despite the differences in morphology, appeared similarly smooth. This difference is most likely a result of polishing optimisation by the vendor overtime as this was a different batch. This also highlights the need for extensive surface characterisation throughout a study as inter-batch variability may otherwise go unnoticed and therefore conclusions presented may be a misrepresentation. However, for TE and ME the efficacy of surface polishing did not appear to reduce the Ra of these samples to a similar level observed for NE. However, with SEM analysis it becomes clear that both TE and ME are very smooth surfaces. Both surfaces contain extensive waviness which would contribute directly to the higher Ra noted for these samples. This is advocated by observations for Ss. While the Ra for Ss is consistently low and comparable to the Ra recorded for Ss in the previous chapter which was shown to be an extremely smooth surface, the Ss within this portion of the study has a similar Ra, but the

morphology of the surface differs. While Ss in chapter 2 had a smooth surface void of micro-discontinuities, the Ss surface in this chapter had a distinct waviness as shown with SEM. This comparison aids in highlighting the necessity of multiple surface characterisation techniques.

Cytocompatibility:

Surface topographical changes have widely been shown to induce alterations in cell behaviour (Boyan *et al.*, 2002; Zinger *et al.*, 2005; Salido *et al.*, 2007; Schwartz *et al.*, 2007; Kubo *et al.*, 2008). Most studies use this parameter to effectively enhance osseointegration and the bone-implant interface as it has previously shown that the surface micro-topography is a major determinant for bone apposition on the device (Pearce *et al.*, 2008b). From *in vitro* studies we have learned that surface micro-roughness can reduce cell proliferation and thus support a more differentiated cell state (Martin *et al.*, 1995; Postiglione *et al.*, 2003). Furthermore, many have contributed this affect *in vitro* to changes in cell attachment (Schneider & Burridge, 1994; Anselme *et al.*, 2000; Boyan *et al.*, 2003b; Wang *et al.*, 2006) differentiation (Martin *et al.*, 1995), local factor response (Kieswetter *et al.*, 1996; Lohmann *et al.*, 2002b), and alterations in genotype (Schneider *et al.*, 2003; Masaki *et al.*, 2005; Arcelli *et al.*, 2007).

While the benefits of osseointegration are indisputable for long term implants such as spine cages and prostheses its occurrence on temporary internal fixation devices can be a hindrance for subsequent removal. While increasing the micro-roughness of a device can inherently increase osseointegration, albeit, within a specific spectrum of roughness, we believe that reducing the micro-roughness associated with clinically available orthopaedic materials that excessive bony overgrowth on these devices can be reduced for ease of removal. However, since we are altering one of the major components of the device it is important to investigate if the reduction in surface microtopography has any negative influence on its biocompatibility. However, before any device can be used *in vivo* the cytocompatibility must be elucidated.

Prior to testing we postulated that surface polishing would not negatively influence the cytocompatibility of these devices as essentially the properties of the material remain the same as prior to polishing. Furthermore, as we noted in chapter 2 the surface chemical composition of the respective surfaces remained similar due to anodisation subsequent to processing. Anodisation is an electrochemical surface modification treatment used to increase

the oxide thickness of commercially available fracture fixation devices. While cpTi and its alloys are capable of producing a naturally occurring oxide layer which normally ranges between approximately 2-5nm (Textor *et al.*, 2001) anodisation can increase this at a rate of 2-3nm per volt (Disegi, 1997). Essentially this process therefore improves the corrosion resistance of the device as it is the oxide layer, and its ability for repassivation, that is responsible for this protection. Thus without this layer any orthopaedic implant would be rendered incompatible within the physiological environment. Since in theory reducing the micro-roughness of a device should not alter the chemical components of an oxide film, and this is advocated with XPS in chapter 2, we suggested that surface polishing would not therefore negatively influence cytocompatibility. Results investigating cell growth and viability indicate that our hypothesis was correct, as neither electro- nor paste polishing of cpTi, TAN or Ti15Mo appeared to induce any significant differences for these parameters.

However, NP was found to be the exception to this observation as this surface supported lower numbers of cells compared to NS, but this difference was not found to be statistically significant. On the other hand the number of viable cells on NP was found to be significantly lower compared to NS. However, NP was also found to have the highest percentage of unattached cells after 24 and 48 hours so this may in part be attributable to the former observations. A possible explanation of this lower initial cell attachment is alluded to with cell morphology results which clearly show that the beta-phase particles noted to have a 'splintered' appearance with SEM, affect cell shape, adhesion and cytoskeletal organisation of the actin and tubulin network. Specifically we showed that these particles were responsible for interrupting the continuity of the tubulin network which resulted in these filaments attempting to circumnavigate their boundaries. Therefore, considering the dramatic affect this surface has on the cytoskeleton it is possible that cells initially find this surface more difficult to attach to. However it does seem that the initial lower rate of attachment is somewhat compensated for at later stages of culturing as no significant difference was observed for cell growth on NP compared to NS. The reduction in the viable number of cells noted for this surface may therefore be related to the cytoskeletal changes noted which have previously been shown to direct cellular behaviour (Forgacs, 1995; Chicurel *et al.*, 1998; Ingber, 2003a&b; Dalby *et al.*, 2008) and in particular the progression of cells through the cell cycle (Meredith *et al.*, 2007a) as well as the reduction in the quantity of cells attached at early stages of culturing. These observations are particularly noteworthy for delineating tissue responses to this surface during subsequent *in vitro* and *in vivo* studies.

The morphological assessment of RC cells on TAN samples is of particular interest as we have shown previously in our laboratory that NS can negatively influence fibroblast focal adhesion maturation and cell spreading, which is believed to be sufficient to hinder progression through the cell cycle thus negatively affecting fibroblast cell growth (Meredith *et al.*, 2005). With the addition of the data from this study investigating the influence of TAN on osteoblasts we have managed to show a cell-dependent response for NS. Meredith and colleagues (2005) showed that fibroblast cell growth was significantly lower on NS compared to NE surfaces, however for osteoblasts we have shown that cell growth is not significantly different between both surfaces. In addition cell viability is not affected for osteoblasts cultured on NS. In fact within this study we have found NS to support a high degree of cell attachment and differentiation. This is in line with *in vivo* observations that indicate that NS has an extremely high affinity for bone so much so, that less invasive stabilisation systems which include TAN locking plates and screws are practically impossible to remove because of enhanced bone over-growth over a relatively short period. It is unfortunate however that Meredith and colleagues did not have the opportunity to include NP samples in their study as it would be fascinating to see if fibroblasts show the same decreased viability and cytoskeletal changes as was noted for osteoblasts. Nevertheless, these results are especially interesting as it highlights the multifaceted influence of a specific surface micro-topography and can potentially provide possible solutions for areas of internal fixation where bone, but not soft tissue attachment is required.

For standard cpTi and Ti15Mo samples we have also shown that the cell shape is directly influenced by the variations in height and orientation of the surface. When these surface micro-discontinuities were removed with surface polishing cells cultured on these surfaces were no longer restricted by the micro-architectural features and therefore, generally adopted a more elongated well spread flattened morphology compared to the typical cuboidal morphology noted for cells cultured on TS and MS. Some sensitivity to micro-topography was noted for cells cultured on polished samples; however, these small variations in micro-topography did not appear to restrict cell spreading to the extent observed for TS and MS. It was noted however that focal adhesion sites of cells cultured on TP showed sensitivity on a nano-metric scale but this is not uncommon as osteoblasts in vitro have been shown to be sensitive to nano-topographical features as small as 10nm (Dalby *et al.*, 2006).

These differences in cell shape induced by the surface and the response of the cells to the differing surface morphologies may have direct ramifications on other systems due to the diverse functions of the cytoskeletal components. For instance, the cytoskeletal changes responsible for changes in cell shape will undoubtedly influence genotypic expression as cytoskeletal conformation and gene expression have been shown to be directly linked (Ingber, 2003a & b). Furthermore, microtubules have one end of their structure attached to the microtubular organising centre (centrosome) the site that initiates their formation, found beneath the nucleus. Microtubules grow outward from the centrosome to the periphery of the cell and help determine cell shape, intracellular transport of organelles and migration for chromosomes during cell division. Therefore, any disruption to the tubulin network such as that observed for NP, may inadvertently affect cell function.

The differences observed in the initial phases of attachment are likely due to conformational changes in protein attachment, or differences in the type and quantity of protein attachment. In fact previous studies have highlighted how subtle differences in micro-topography can affect not only the amount of a protein that interacts with a surface but also how a surface selectively adsorbs proteins and the effect this has on subsequent cellular behaviour. For instance, Yang and colleagues (2003) showed that pre-adsorbed proteins increased initial cell attachment compared to control cpTi surfaces. However, cell attachment was directly influenced by the type of protein adsorbed. Pre-adsorbed albumin did not significantly influence cell attachment, however, surfaces pre-adsorbed with fibronectin for 15 minutes significantly increased osteoblast cell attachment. This effect of fibronectin appeared time dependent as the authors note that cpTi samples pre-adsorbed with fibronectin for 3 hours did not influence cell attachment. Thus the concentration of fibronectin appears to also govern cell attachment (Yang *et al.*, 2003). A prior study delineated in more detail the effect of fibronectin on cell attachment (Howlett *et al.*, 1994). Specifically, Howlett and colleagues (1994) showed that vitronectin was indeed required for osteoblast attachment as removal of this protein resulted in an approximate 83% decrease in attachment while in fibronectin depleted cultures cell attachment was practically unaffected.

Perhaps the method of analysis contributed somewhat to this observations i.e. pre-adsorbed versus media depleted. The differences for these two studies may in part be attributable to the differing surfaces included, thus preferential attachment of a specific protein may be enhanced by a specific surface property such as chemistry, charge or micro-topography. This is highlighted by Gronowicz and McCarthy (1996) who showed that integrin-mediated adhesion was surface dependent. Therefore, future work focusing on changes in protein attachment would help elucidate these observations for differences in initial cell attachment for the samples included in this study.

The observation that a similar cell number occurs on all metal surfaces compared to TCP but that TCP has a higher degree of viability is perplexing. However, one possible explanation for this observation may lie in the methodology. For instance, viability testing relies largely on the ability of viable cells to reduce an indicator dye as a measure of their viability. Thus the metabolic capacity of the cells is essentially tested. Since none of the metal samples had non-viable cells present the possibility of these surfaces inducing increased cell death compared to TCP is not supported. Therefore, a possible explanation may lie in the fact that cells cultured on cpTi, TAN, Ti15Mo and to some extent Ss have a reduced metabolic rate compared to cells cultured on TCP. This theory is advocated by the observations of Bächle and colleagues (2005) who showed that osteoblast cells cultured on TCP have a significantly higher oxygen consumption rate compared to machined and titanium plasma sprayed cpTi plates with similar micro-topographies.

Chapter summary:

These studies have demonstrated that surface polishing of clinically available materials cpTi and Ti15Mo does not adversely affect the material cytocompatibility pertaining to attachment, growth and viability. It was also found that these conclusions were valid for NE samples; however, NP was found to have significantly lower number of viable cells compared to the standard micro-rough TAN surface. Morphologically, it was shown that polished samples regardless of material type allowed for a higher degree of cell spreading compared to standard micro-rough counterparts. Again NP proved the exception as cells on this surface appeared more restricted by the surface morphology. Interestingly for NS samples we confirmed the interruption of the cytoskeleton by beta-phase particles. However, unlike fibroblasts osteoblasts did appear hindered to the same extent by this breach, as growth occurred at a constant rate on NS samples and viability was maintained on these surfaces over an extended time period. In this study we also identified the effect of these particles even when their prominence was greatly reduced by electropolishing. Interestingly NP proved more problematic for osteoblasts than NS. This may in part be due to the difference in surface morphology, as beta-phase particles on NP had a more splintered appearance in the batch of samples used for these studies than NS and therefore, may prove more problematic for initial attachment which is advocated by the lower percentage of cells found attached to NP after 24 and 48 hours. However the disruption of the tubulin network can have ramifications on a wide variety of cellular processes and is most likely the causative factor for the adverse reactions of the cells on NP. Due to the synergistic nature of cytoskeletal organisation and gene expression it will be interesting to see in the subsequent chapter if this disruption of the cytoskeleton is sufficient to affect osteoblast differentiation molecularly, as examined using real time PCR technology.

Chapter 4: Analysis of genotype.

Abstract.

Osseointegration at the bone-implant interface requires activation of key regulatory pathways which influences osteoblastogenesis, promotion of osteoblastic differentiation and maturation and finally bone regeneration. Investigating changes in gene expression due to surface microtopography therefore provides information into the regulatory mechanisms behind bone formation at the bone-implant interface and help elucidate the effect of surface polishing on a cellular level for reducing bone over-growth. Therefore, this chapter focuses on investigating the effect of surface polishing on genotypic regulation of a variety of genes deemed essential for osteoblast recruitment, fate determination, matrix production and differentiation. Results indicate that for all material types surface polishing essentially provokes its influence at the later stages of terminal differentiation which is accompanied by decreases in early differentiation markers at specific points in a material dependent manner and that the magnitude of this effect is material dependent.

Chapter 4: Introduction

Real-time quantitative polymerase chain reaction (qPCR)

Rarely has any invention had such an affect on biological science so strongly in such a brief space of time as PCR. This technique allows for minute amounts of DNA to be replicated speedily and thereby amplified to such an extent that the DNA becomes easily detectable using conventional laboratory techniques. And since in theory a single DNA molecule should be sufficient for amplification this makes PCR one of the most sensitive biological techniques ever devised. Given these capabilities, ultimately PCR had a fundamental role in the age of genomics and thus there are few areas of genetic research today that do not depend on PCR. Only with the emergence of increasingly sensitive DNA chips has PCR faced any noteworthy competition. Nevertheless, even in this case it is often necessary to first copy or amplify the DNA of interest.

With regards to real-time qPCR, the accurate quantification of a starting template such as cDNA is achieved through measuring the fluorescence produced after each cycle with the amount of fluorescence being proportional to the quantity of PCR product. The amplification products can subsequently be detected by fluorescently labelled sequence-specific probes or alternatively using fluorescent dyes that bind double-stranded DNA, as was the case in this study. The point at which the fluorescence is calculated can either be at the end of the reaction (end-point qPCR) or while the amplification is still in progress (Real-time qPCR). As its name suggests endpoint qPCR analysis is carried out after the amplification has been completed. The final fluorescence is then used to back calculate the amount of template present prior to the reaction. However, inconsistent results due to the non-automated, low precision/sensitivity of end-point PCR have paved the way for the more sensitive and reproducible method of real-time qPCR. This approach allows for the fluorescence to be measured during the exponential phase of the amplification and thus circumvents limiting factors such as low resolution and semi-quantitative nature, often experienced with endpoint qPCR.

The role of surface microtopography in modulation of phenotype:

Gene regulation affords the cell control over structure and function and is the basis for cellular differentiation, morphogenesis and the versatility and adaptability of any organism. Osseointegration at the bone-implant interface requires activation of key regulatory pathways which influences osteoblastogenesis, promotion of osteoblastic differentiation and maturation and finally bone repair/regeneration. Investigating the effect of surface microtopography on changes in gene expression may provide information into the regulatory mechanisms behind bone formation at the bone-implant interface. Many genes have critical roles in osteogenesis and real time qPCR allows one to focus specifically on genes of interest. In terms of bony on-growth at the interface, the list is extensive. Nevertheless, the process of bone formation/remodelling has many definitive events and it is a sample of the genes involved in these stages that we have chosen to investigate. Specifically, we have chosen genes that have essential roles in osteoblast differentiation and matrix production and maturation (materials and methods section). This fundamentally allows an insight to the role of surface microtopography in controlling the genetic influence of osteoblast function and subsequent bone formation.

Recent studies have started to emerge using the sensitive method of gene expression quantification to help elucidate some of these micro-topographical induced changes. In particular, Schneider and colleagues (2003) have shown that a critical regulatory gene Core binding factor alpha 1 (Cbfa-1; also referred to as *Runx2*) involved in bone differentiation and downstream regulation of other key osteoblast genes required for the development of the mineralised phenotype, is differentially up-regulated for osteoblast cells cultured on roughened commercially pure titanium (cpTi) compared to those grown on smoothened grooved cpTi samples. In this study, the author also showed that bone sialoprotein II, a major phosphorlyated protein of bone, and believed to be directly involved in nucleation of hydroxyapatite at the mineralisation interface of bone, was also up-regulated on rough cpTi surfaces compared to smoothened groove surfaces (dimensions not specified by authors). However, the authors also present this latter result as being cell type specific as the increase was observed for the rapidly mineralising UMR-106-01 osteoblast cell line but not for the weaker mineralising primary rat calvarial cell cultures which were both included in the study. In a later study, Schneider and colleagues (2004) then showed that this influence can even extend to inducing preosteoblast cell differentiation into a mature osteoblast phenotype via micro-architectural features of an implant. Masaki and co-workers (2005) have also

implicated the surface microtopography as contributing to the regulation of osteoblast function via shaping the expression of bone related genes and transcription factors. Using human mesenchymal cells they show that Cbfa1 and osterix, two vital factors to osteoblast fate are up-regulated on grit-blasted and electrochemically etched surfaces compared to others studied. However, extrapolation of results can be difficult to say the least, firstly, because of the early time point studied and secondly, due to the distinct lack of characterization of the surfaces the authors investigated. At 72 hours, the time studied, many of the genes of interest determined by the authors would not have been up-regulated due to their known function in later stages of bone development. Furthermore, since no characterisation of the samples was carried out translating the results is practically impossible since it can be difficult to delineate the influence of the surface (see chapter two for insight into the importance of surface characterisation).

Brett and colleagues (2004) used a more general approach with regards to investigating genotypic expression on rough surfaces. Here, they employed microarray technology to study the expression profiles of alveolar bone cells cultured on three surfaces which they deemed smooth (Ra 0.3-0.42μm), moderately rough (Ra 4.12-4.24μm) and highly rough (Ra 6.16-6.66μm). With the use of microarray technology, which allows the user to identify up and down-regulated genes within their sample from a known gene database, the authors were capable of elucidating what they term as 'roughness' genes by comparing genes up/down-regulated on their rough surfaces compared to those up/down-regulated on their smooth surface. Again one has to be cautious of data interpretation, which is solely dependent on the investigator. In essence this is more a 'fishing expedition' in comparison to the focused approach of real time qPCR within the context of biomaterial studies, as outlined below. While, gene arrays are a valuable tool for elucidating gene profiles especially in terms of disease but in terms of biomaterials, their use can be limited considering the wide ranging variability in the micro-roughness, material type and chemistry of samples between studies. For instance, Brett and colleagues included 'smooth' surfaces in the range of 0.3-0.42μm, however our laboratory has identified a roughness spectrum which advocates a roughness average of 0.2μm or below as a smooth surface (Richards, 2008). Therefore, genes deemed 'roughness' genes by one study may not be present for other surfaces of lesser or greater roughness as well as the fact that data interpretation is a large factor in determining the role of a particular gene in any given context and is often unintentionally subjective.

This inter-study variability can be verified by a more recent study that also included DNA arrays. In this study, the authors used cpTi samples with Ra's of 0.77, 1.05, 1.93 and 2.74μm. After 24 hours Arcelli and colleagues (2008) report the up-regulation of 84 genes and a down-regulation of 95 genes. However, Brett and co-workers (2004) report an up-regulation of a total of 215 genes and a down-regulation of 269 for both rough surfaces after 24 hours. In addition, the sensitivity of both arrays differed dramatically. While the array used by Brett and co-workers encompassed 1156 genes, the microarray include by the Arcelli study included 19200 genes. Furthermore, many genes identified by the Brett study as being specifically up-regulated on their rough surfaces are not identified within the Arcelli study (or were not deemed important by the authors i.e. difference in data interpretation), and vice versa.

Therefore, while the influence of surface microtopography on osteoblast genotype is an important facet of cell biology to understand in context of understanding the cell-biomaterial interaction, it is equally important to understand the methods applicable to help us do so. In this chapter the gene expression profiles of rat calvarial osteoblasts are investigated over an extended time period of up to 21 days to allow a wider picture of the influence of surface microtopography on osteoblast genotype to emerge. To do so, we have used real time qPCR, a reliable and reproducible method, to study a variety of genes/transcription factors known for their pivotal role in osteoblast biology and function. Overall, in addition to morphological changes this will give an insight to the molecular mechanisms involved in controlling osseointegration at the bone-implant interface.

Chapter 4: Materials & methods:

Surface Characterisation:

Quantitative measurements for three separate 50mm sample were taken using a non-contact white light FRT MicroProf® (Standard) with CWL 300μm sensor profilometer (Fries Research & Technology, Germany). A roughness average (Ra – arithmetic mean of the roughness height expressed in micrometers) was measured from a 0.5x0.5 mm scan area with a point density of 500 points/line. Two separate measurements were taken for each sample, resulting in a total of six measurements per sample. The morphology of the sample surfaces was studied using a Hitachi S4700. The images were taken in secondary electron (SE) mode, with an accelerating voltage of 5kV, an emission current of 40μA, a working distance of 10mm and a positive tilt of 10°.

Cell culture:

RC cells were seeded onto 50mm the sample discs for all materials studied, at 100,000 cells/sample in 4ml of full DMEM+5mMBGP in 60x15mm petri-dishes (Corning, UK). The cells were incubated at 37°C with a 5% CO_2 atmosphere for 48 hours, 7, 14 and 21 days and the culture media was changed every 2.5 days. Four samples were included for each substrate. Any double distilled water used was pre-treated with 0.5ml/L of diethylpyrocarbonate (DEPC; Fluka) to ensure it was RNase-free.

RNA Isolation:

For RNA isolation, a combination of the traditional TRI-reagent method and RNeasy Mini-Kits (Qiagen, Gmbh) were used. This allowed for RNA to be precipitated from the samples directly and the homogenised sample was subsequently applied to the spin column where RNA binds to the silica-based membrane. Contaminants were then washed through the column allowing for high quality RNA (>200 bases) to be eluted in 30μl of RNA-free water. At specific time points, culture media was removed from the samples, and these were subsequently rinsed three times, with 0.1M PBS, pH 7.4. Then, 600μl of TRI-reagent (Sigma, UK) which contains the highly denaturing guanidine-thyiocyanate and phenol in a mono-phase solution, supplemented with 5μl of Polyacryl Carrier™(Molecular Research Center, USA), was added to the sample directly. This step ensures inactivation of RNases to allow for purification of intact RNA. After adding 300μl of 1-bromo-3-chloro-propane (Sigma, UK) and centrifuging at 12000g for 15 minutes at 4°C in an Eppendorf 5417R centrifuge (Eppendorf AG, Gmbh) the mixture separates into 3 phases: an aqueous phase containing the

RNA, the interphase containing DNA, and an organic phase, containing proteins. Approximately 300µl of the aqueous phase is removed and transferred to a new 1.5ml RNase free tube (Eppendorf AG, Gmbh). Then, 0.25 ml of 100% isopropanol (Fluka, CH) and 0.25 ml of a high salt precipitation solution (0.8 M sodium citrate and 1.2 M NaCl) (Molecular Research Center, USA) were added to the sample and mixed by inversion. Samples were stored at room temperature (20-22°C) for 10 minutes, and subsequently centrifuged for 8 minutes at 12000g at 4°C. Afterwards, 600µl of 75% ethanol was added directly to the sample. The sample was then applied to the column which was centrifuged for 15 seconds at 8000g. Once completed, 700µl of RW1 buffer contained within the Qiagen kit was applied to the column and again it was centrifuged for 15 seconds at 8000g. After discarding the flow through, 500µl of RPE wash buffer (contains ethanol) was applied to the column and the latter was centrifuged for 15 seconds at 8000g. Upon completion, the flow through was discarded and again, 500µl of RPE wash buffer was added to the column. The samples were left at room temperature for 2 minutes to allow the buffer to penetrate the membrane. After this time had elapsed, the column was centrifuged for 2 minutes at 8000g. To help prevent ethanol carryover, the column was then transferred to a new 2ml collection tube, and centrifuged for 1 minute at 8000g. Finally, the column was transferred to a 1.5ml collection tube and 30µl of RNA-free water was applied directly to the membrane. The column was centrifuged for 1 minute at 8000g. Eluted RNA is then transferred to RNase free 1.5ml tubes (Eppendorf AG, Gmbh). The purity of the RNA was assessed using 260/280 measurements using the Nanodrop system (Witec, Gmbh) and associated software. Samples were then stored at -80°C until required.

Reverse transcription:

All reagents were supplied by Applied Biosystems (USA) unless otherwise stated. For each reverse transcription reaction a Mastermix containing the following components were made, and then added to a 0.2ml reaction tube to make up a total reaction mix of 100µl (70µl of reagents and 30µl of RNase free water containing 2µg of RNA sample) per sample.

The following protocol encompasses the components required per 20µl reaction. Firstly, the non-enzymatic components of the solution were mixed. This included adding 2.0 µl of 10x TaqMan RT Buffer (PCR Buffer II), 4.4 µl of 25 mM Magnesium chloride, 4.0 µl of DeoxyNTPs mixture (2.5 mM each dNTP(dATP, dCTP, dGTP, dTTP)), and 1.0 µl of Random Hexamers (50 µM). Next, 0.5 µl of Multiscribe Reverse Transcriptase (50U/ µl) and

0.4 µl of the RNase inhibitor (20 U/µl) were added to the tube. Finally the solution was made up to 20µl by adding 7.7µl of RNase free water supplemented with RNA sample to the reaction tube. Samples underwent reverse transcription in a GeneAmp 5700 SDS instrument at 10 min at 25°C for primer incubation, 30 min at 48°C for reverse transcription, and 5 min at 95°C for reverse transcriptase inactivation. Samples were then stored at -20°C until required.

Real time quantitative polymerase chain reaction (qPCR):

Primers for the house keeping gene 18S as well as Osterix (osx), Cbfa1, alkaline phosphatase (ALP), Osteocalcin (OCN), and collagen type I (COLI) were purchased from PrimerDesign, UK (Table 4.1 and figure 4.1) were tested for efficiency using a diluted template from a positive control of RC cells cultured in a 75cm^2 flask until sub-confluent (Appendix F). Real time qPCR was carried out using the Precision Master Mix (PrimerDesign, UK) containing SYBR green. SYBR green is an intercalating dye that binds double stranded DNA and fluoresces proportionally to the amount of double stranded DNA present. A predetermined amount of 5µl of all experimental cDNA templates were transferred into a clear thermo-fast® 96 well detection plate (ABgene, UK) with a reaction mix containing 1µl of primer mix (PrimerDesign, UK; final concentration of 200nM); 10µl of 2x master mix of SYBR green (Primer Design, UK) and made up to a total of 20µl with double distilled water containing DEPC. The plate was then covered with a thermostable RNase-free cover-slip (Milian, CH), centrifuged for 30 seconds in a Rotanta 46 plate centrifuge (Hettich, CH), and transferred to an Applied Biosystems 7500 thermocycler, which permits analysis of melting temperature and threshold fluorescent values of the samples. The plate was then run at 95°C for 10 minutes (1 cycle) followed by 95°C for 30s; 60°C for 1 minute and 72°C for 1 minute for 40 cycles; the dissociation curve included incubation of the plate at 95°C for 15 seconds, 60°C for 1 minute and finally 95°C for 15 seconds and held at 20°C indefinitely. A no template control containing the same reagents minus the cDNA template was included for each plate as a negative control.

Data Analysis:

Analysis of real-time qPCR can be derived either by absolute or relative quantification. Absolute quantification employs a standard curve prepared from a dilution series of known concentrations of a control template. Normally this method of quantification is used when it is the goal of the experiment to elucidate exact levels of a target template from a sample. Although this method is accurate in determining absolute quantities of a target, measuring the relative concentration of a gene of interest in unknown samples to a control or calibrator sample can provide answers regarding gene expression accurately and reproducibly. This approach is known as relative quantification and with this method differences in threshold fluorescent values (Ct; the PCR cycle represents the point in which the fluorescence of the bound sample crosses the baseline threshold i.e. is deemed to be at a statistically significant level above the background signal) between unknown samples and the calibrator (which can be a time-point or untreated/control sample) can be determined. Essentially, allowing for changes (up/down-regulation) of unknown samples to be expressed relative to the expression of the calibrator. Here relative quantification was used to assess the fold change in gene expression over time on all the test materials which were calibrated to mRNA isolated from all materials after 48 hours culturing, to allow for sufficient attachment to occur.

Statistical analysis:

Statistical evaluations were made using SPSS for Windows version 14.0 (SPSS Inc, Chicago, IL). Normality tests were performed to confirm Gaussian distribution of the data prior to analysis. Three factor analyses of variance were performed on pooled data (see appendix G) for each of the 6 genes. The three factors included in the analysis were material, surface and time (in days). When variances were shown to be equal across the groups (Levene's homogeneity test) Bonferroni post-hoc tests were applied for individual comparisons. Games-Howell post hoc tests were applied when assumptions regarding homogeneity were not met. To delineate differences in expression at each time point, subsequent to normality and homogeneity tests, a Univariate ANOVA was performed. Bonferroni post-hoc tests were carried out to further elucidate significant differences between surface types at each time point on samples deemed significant by the Univariate ANOVA. Values of $p \leq 0.05$ were regarded as significant.

Gene of interest (GOI)	Sense primer	Anti-sense primer	Product size (base pairs)	Function (not exhaustive)
Osterix	GCAAGTTTGGTGGCTCCAG	GAAAGGTCAGTGTATGGCTTCT	82	Downstream of Cbfa1, required for ongoing osteoblast differentiation
Cbfa-1	CAGTCACGTCAGGCATGTC	GAGTGCTGCTGGTCTGGAA	120	Essential for osteoblast differentiation & skeletal formation. Regulates expression of bone ECM proteins that encode for COLI, BSP and OCN.
ALP	GCTCTGCCGTTGTTTCTCTATTC	AAAATAAGGTGCTTTGGGAATCTG	105	Reaction of released inorganic phosphate with calcium results in the formation of hydroxyapatite. Vital for osteoblast differentiation & subsequent mineralisation. Believed to hydrolyze pyrophosphate to maintain levels of this mineralisation inhibitor.
Osteocalcin	CAAAGCCCAGCGACTCTGAG	CTCCAAGTCCATTGTTGAGGTAG	102	Major constituent of non-collageneous protein component in bone, accounting for approx.10%. Accumulates in bone as a consequence of the strong affinity of the Gla residues to hydroxyapatite & binds calcium.
BSPII	AAGCAGAAGTGGATGAAAATGAG	GGCTTCTTCTCCGTTGTCTC	107	Major phosphorlyated protein of bone, believed to be directly involved in nucleation of hydroxyapatite at the mineralisation interface of bone
Collagen I	CAACAGACTGGCAACCTCAAG	CAAGCGTGCTGTAGGTGAATC	100	Makes up approx. 90% of bone matrix. Fibrils contain future sites of mineralisation.
18S	Not provided	Not provided		Endogenous control

Table 4.1. Summary of the different primers, and their respective function in osteoblast genotypic expression.

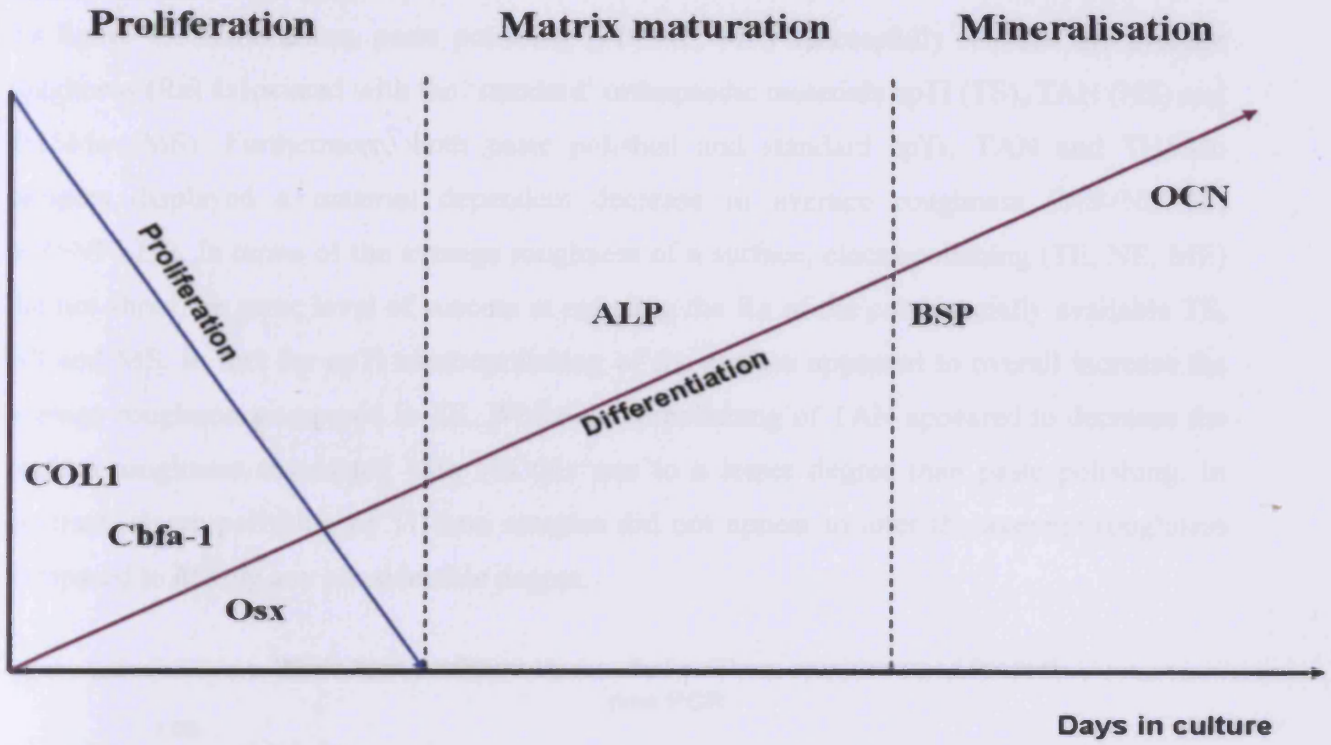

Figure 4.1. Schematic representation of the temporal expression of the 6 genes of interest included in this study. During an initial period of proliferation, and fundamental to the development of an osteoblast phenotype, collagen type I is actively expressed in association with formation of the extracellular matrix. This expression gradually declines, with collagen I being maintained at basal levels during subsequent stages of osteoblast differentiation. This increase in collagen I and its subsequent integrin-mediated matrix interaction activates the phosphorylation of Cbfa-1, a master regulatory gene for osteoblast commitment and differentiation (although there are other known pathways also responsible for activating Cbfa-1 transcription). The major influence of Cbfa-1 is its regulation of major bone matrix genes such as COL1, BSP and OCN through its ability to bind to the osteoblast specific promoter of these genes. Expression is transient as maintained Cbfa-1 can inhibit terminal differentiation. Osterix is downstream of Cbfa-1 and is essential for osteoblast differentiation, and is expressed transiently during initial differentiation. Post-proliferatively, the extracellular matrix undergoes a series of modifications in composition and organization that renders it competent for mineralisation. As progression into the mineralisation stage occurs, ALP increases, and this is considered one of the earliest phenotypic markers of the osteoblast lineage. However, in heavily mineralised cultured ALP mRNA levels decline. With the onset of mineralisation, bone-synthesized proteins such as bone sialoprotein and osteocalcin are induced to maximal levels, paralleling the accumulation of mineral. BSP expression precedes that of OCN, and is potent inducer of apatite nucleation and growth. On the other hand, OCN functionality studies suggest a role for this protein in delaying apatite nucleation, thus indicating that OCN negatively regulates mineralisation. (Adapted from Lian & Stein, 1992)

Chapter 4: Results

Surface characterisation:

As figure 4.2 summarises, paste polishing (TP, NP, MP) successfully reduced the average roughness (Ra) associated with the 'standard' orthopaedic materials cpTi (TS), TAN (NS) and Ti15Mo (MS). Furthermore, both paste polished and standard cpTi, TAN and Ti15Mo samples displayed a material dependent decrease in average roughness (MS>NS>TS; MP>NP>TP). In terms of the average roughness of a surface, electropolishing (TE, NE, ME) did not show the same level of success at reducing the Ra of the commercially available TS, NS and MS. In fact for cpTi electropolishing of the surface appeared to overall increase the average roughness compared to TS. While electropolishing of TAN appeared to decrease the surface roughness associated with NS this was to a lesser degree than paste polishing. In contrast, electropolishing of Ti15mo samples did not appear to alter the average roughness compared to MS by any considerable degree.

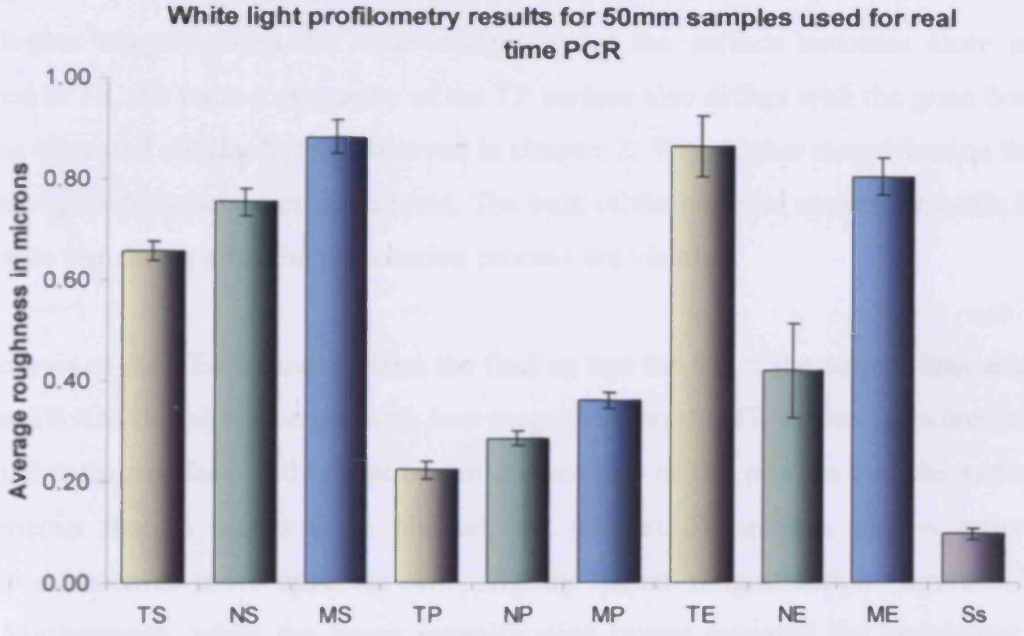

	TS	NS	MS	TP	NP	MP	TE	NE	ME	Ss
Mean Ra (μm)	0.66	0.75	0.88	0.22	0.29	0.36	0.87	0.42	0.81	0.10
Standard Deviation (μm)	±0.02	±0.05	±0.03	±0.02	±0.03	±0.03	±0.15	±0.07	±0.08	±0.01

Figure 4.2. White light profilometry results for the 50mm samples used for real-time PCR. Of both polishing methods, paste polishing appeared to be the most successful at reducing the average roughness of the standard materials. Electropolishing on the other hand was less successful in terms of reducing the Ra, and in the case of cpTi, the Ra for TE was higher than that of TS. Electropolishing of Ti15Mo did not appear to alter the Ra to any significant degree, and while NE had a lower Ra compared to NS, this was not to the same level as paste polishing.

Results from the SEM portion of the study advocated many of the observations made regarding the roughness of the materials studied. Additionally, SEM also elucidated some of the issues raised by the previous quantitative results. For instance, as highlighted by figure 4.3, SEM analysis of the TS surface advocates initial profilometry findings that this surface is micro-rough. As noted in chapter 2 the grain boundaries of the surface are clearly evident (white arrow, figure 4.3). The differences in the height of the grains and grain boundaries result in the jagged irregular appearance of the surface. With higher magnification the micro- and nano-topographical features of the surface are more apparent. The peaks in the surface are heterogeneous ranging in size, shape, micro/nano texture and orientation, which even at high magnification is clearly visible (blue arrows, figure 4.3). As noted with white light profilometry, paste polishing effectively reduced the micro-roughness associated with the standard commercially available cpTi surface. SEM analysis also supports this finding. As is clearly visible in figure 4.3 the irregular jagged appearance noted for TS is removed by paste polishing. The TP surface appears more homogenous in terms of the surface micro-roughness and at higher magnification the nano-topography of the surface becomes more apparent. Compared to TS, the nano-topography of the TP surface also differs with the grain boundaries becoming obscured similar to that observed in chapter 2. With higher magnification the extent of the paste polishing becomes more lucid. The bulk of the material appears smooth; however some divots remaining after the preparation process are visible.

SEM analysis of the TE surface clarifies the finding that the Ra of the surface was akin to that noted for TS. On initial inspection with low magnification the TE surface appeared to have a highly undulating surface with variations in dimensions of the pits. In fact the surface is so heterogeneous that in places these pits are not present (figure 4.3, yellow arrow). This observation becomes more apparent with slightly higher magnification (figure 4.3, green arrow). Furthermore, while the lower magnification image revealed the undulating surface that would attribute to the higher Ra observed for TE, the higher magnification images clearly show that this is a highly smooth surface with few micro-discontinuities upon the undulations. The dimensions of the pits appear sufficiently large enough not to disrupt the continuity of the surface. In fact overall it appears with high magnification, smoother than TP.

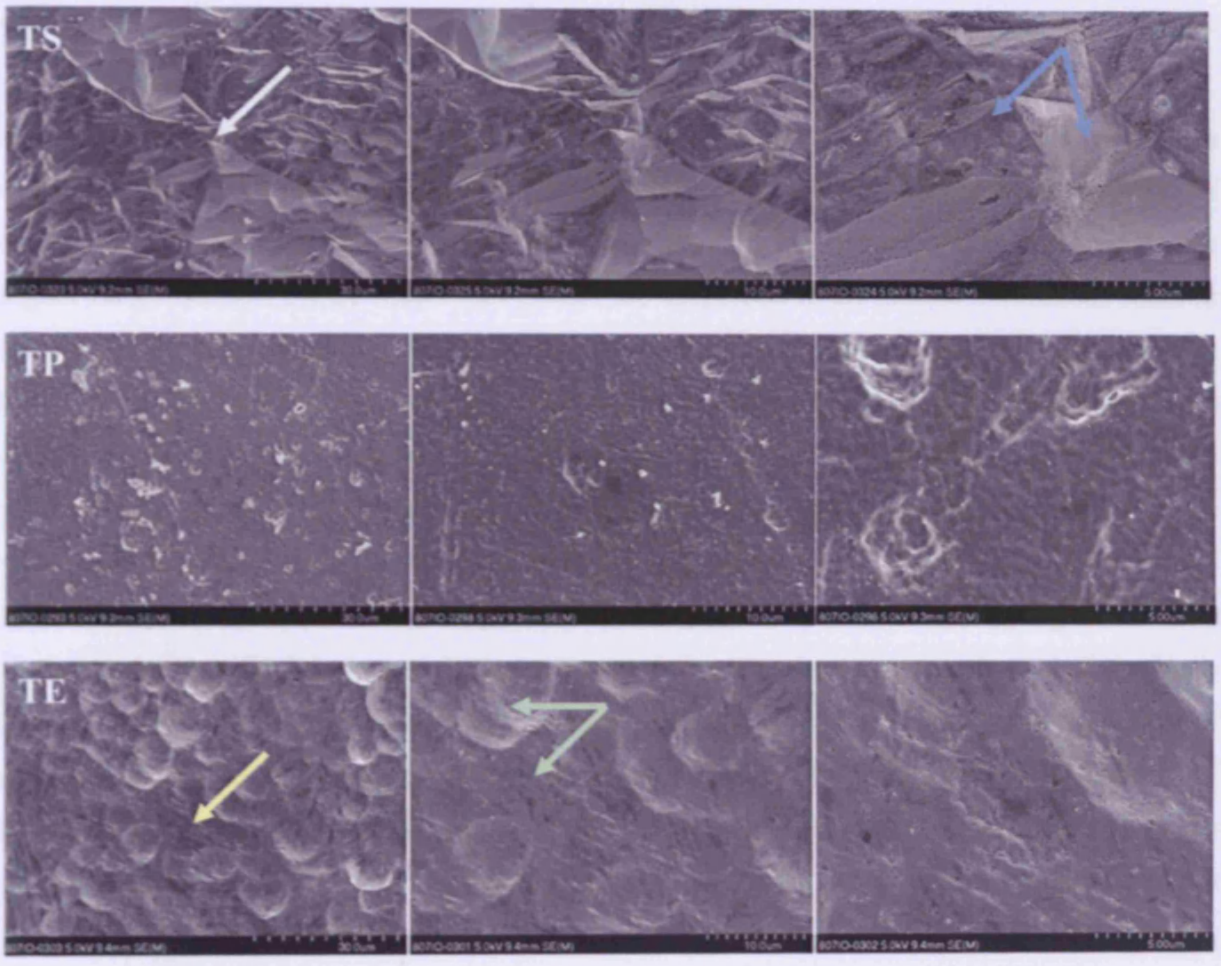

Figure 4.3. SEM images of the cpTi surfaces in SE mode for standard micro-rough (TS), paste polished (TP) and electropolished (TE) commercially pure titanium. Variations in height of the grain boundaries on the TS surface (white arrow) produce a jagged, irregular pattern which results from differences in grain orientation. Conversely, paste polishing clearly reduced the micro-topography associated with micro-rough TS, producing a weaved pattern with nano-topography evident. While the Ra of TE was noted to be akin to that of TS, SEM analysis shows that this surface has an undulating surface, with heterogeneous distribution. In some areas, the pits are not present (yellow arrow, green arrows). With higher magnification, the smoothness of the surfaces becomes more apparent.

SEM analysis of the NS surface revealed the typical undulating surface previously noted for this sample in chapter 2. However, different to the NS surface characterized in chapter 2, which had beta-phase particles adopting a micro-spiked appearance, the beta-phase particles of this surface (white arrow, figure 4.4) appear more 'strip-like', as previously outlined in chapter 3 and appear to run along the grain boundaries of the surface. As highlighted by the higher magnification image these beta-phases are dispersed in an almost continuous manner across the surface. While paste polishing to some degree reduced the micro-topography associated with standard micro-rough TAN the reasons behind the extent of the lesser degree of successful polishing compared to NE come to light with SEM analysis. Specifically, the mechanically abrasive force of the paste polishing technique appears to exert its force principally on the alpha-phase of this material. Consequently, these structures adopt a fractured appearance with the beta-phase appearing splintered (blue arrow, figure 4.4). In contrast, electropolishing appears to have successfully decreased the prominence of the beta-phase particles. The NE surface appears very similar to the NS surface with the exception of protruding particles and undulations which appear to follow the grains. The bulk material of NE appears smooth with a slight waviness irregularly dispersed, while the beta-phase particles appear to have become embedded within the material rather than protruding out from it as observed for NS (green arrow, figure 4.4).

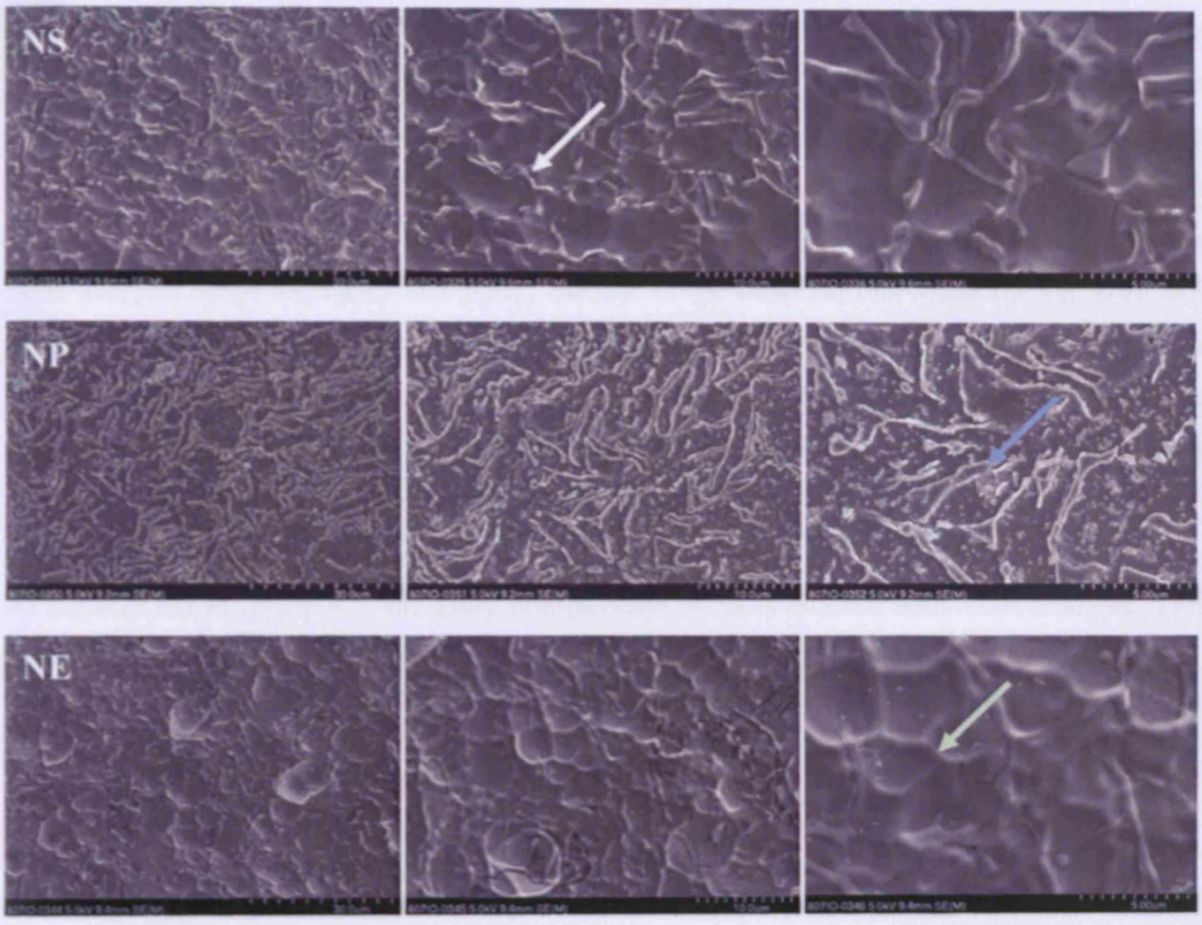

Figure 4.4. SEM images of the Titanium6%Aluminium7%Niobium surfaces in SE mode for standard micro-rough (NS), paste polished (NP) and electropolished (NE) TAN. The characteristic undulating surface of NS, with prominent beta-phase particles (white arrow) is clearly evident here. While paste polishing (NP) of TAN did reduce the Ra associated with this material, it was not shown to be as successful as electropolishing. Evidence to suggest why is found in the prominent appearance of splintered beta-phase particles (blue arrow). Conversely, electropolishing (NE) effectively reduces the surface micro-topographical features associated with this material. The technique is so effective, that the beta-phase particles appear embedded within the bulk material (green arrow).

SEM imaging of the MS surface presents an extremely irregular undulating surface with large variations in the dimensions and depth of the topography. With higher magnification, the micro-discontinuities appear frequent and of varying depth (figure 4.5, white arrows). In contrast paste polishing produced a smooth surface devoid of undulations. Findings from white light profilometry suggest that there is no difference in the Ra of MS and ME. Again SEM analysis helps to clarify this point. Similar to the observations made for TE, here ME has an irregular distributed waviness. The dimensions of the pits are non-uniform and appear to vary in depth also. However, similar to TE, upon higher magnification it is noted that these undulations are extremely smooth with virtually no micro-discontinuities and appear much wider compared to the pits observed for MS and more shallow (figure 4.5, green arrow).

As highlighted in figure 4.5, the alloy composition of Ss is evident with SEM analysis. This surface, as expected, is extremely smooth and practically no micro-discontinuities are visible.

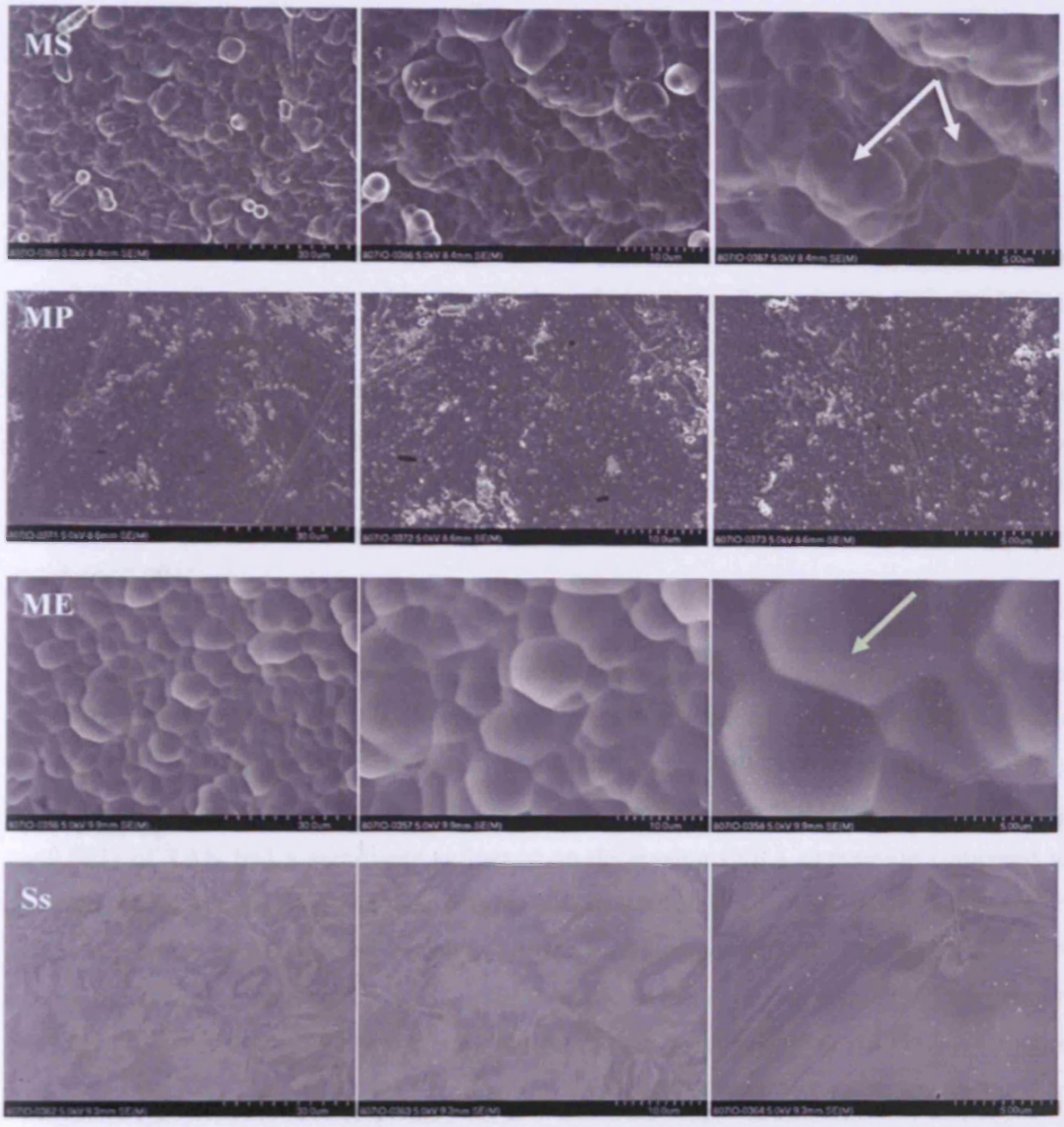

Figure 4.5. SEM images of the Titanium15%Molybdenum surfaces in SE mode for standard micro-rough (MS), paste polished (MP) and electropolished (ME) Ti15Mo, and stainless steel (Ss). The MS surface has an extremely irregular, undulating surface, with large variations in the dimensions and depth of the topography. Higher magnification reveals that the micro-discontinuities appear frequently across the surface and of vary in depth (white arrows). Paste polishing successfully reduces the micro-topography of the standard micro-rough surface, producing a smooth surface with a weaved pattern, devoid of undulations. While ME and MS were found to have similar Ra's, SEM analysis reveals that ME has an irregular distributed waviness. The dimensions of the pits are non-uniform and appear to vary in depth. With higher magnification it is noted that these undulations are extremely smooth, without micro-discontinuities, and appear much wider, and shallower, compared to the pits observed for MS (green arrow). The typical 'marble-like' appearance of Ss is evident. This surface is extremely smooth, and practically no micro-discontinuities being visible.

Analysis of genotype:

Influence of time, surface and material: Results from 3 factor ANOVA, Univariate ANOVA & post hoc tests.

Collagen I:

Three factor ANOVA evaluation of collagen I expression revealed that time ($p<0.001$), material ($p<0.001$) and surface ($p<0.001$) all had significant influences on expression. There was also a significant interaction between all three factors on collagen I expression ($p=0.001$). Subsequent post-hoc analysis revealed that for the factor 'material' cpTi was found to significantly decrease collagen I expression compared to TAN ($p<0.001$) and Ti15Mo ($p<0.001$) samples. In contrast, TAN and Ti15Mo samples appeared to evoke similar responses ($p=0.254$). Post-hoc analysis for the factor 'surface' showed that as a treatment, only paste polishing significantly influenced COL1 expression compared to standard micro-rough ($p<0.001$).

Results from the Univariate ANOVA suggest that cpTi surface finish was not a significant factor for COL1 expression ($p=0.073$) (Figure 4.6A). In contrast, Univariate ANOVA results for TAN revealed that surface finish was a significant factor for COL1 expression ($p<0.001$). Subsequent post-hoc analysis showed that both electropolishing ($p<0.001$) and paste polishing ($p<0.001$) of TAN had a significant influence on decreasing COL1 expression compared to standard micro-rough TAN samples (Figure 4.6B). Moreover, no significant difference in COL1 regulation was observed between polished variants ($p=1.000$). Univariate ANOVA results for Ti15Mo revealed that surface finish was a significant factor in COL1 expression ($p<0.001$). Subsequent post-hoc analysis indicated that paste polishing of Ti15Mo (Figure 4.6C) significantly decreases COL1 expression compared to standard micro-rough Ti15Mo ($p=0.001$) samples while electropolishing did not appear to significantly alter COL1 expression ($p=0.148$).

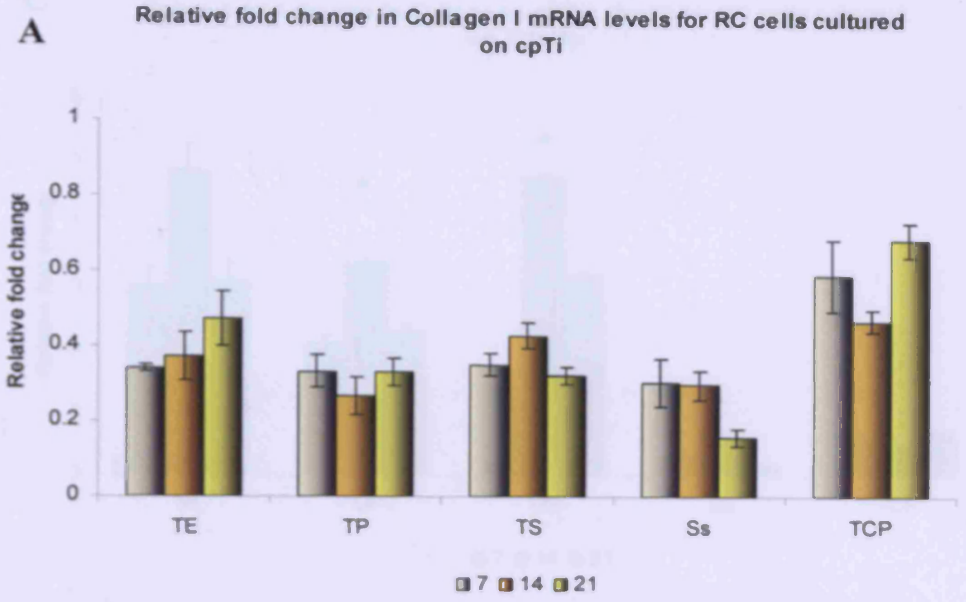

Figure 4.6A: Results from the Univariate ANOVA suggest that cpTi surface finish was not a significant factor for COL1 expression (p=0.073).

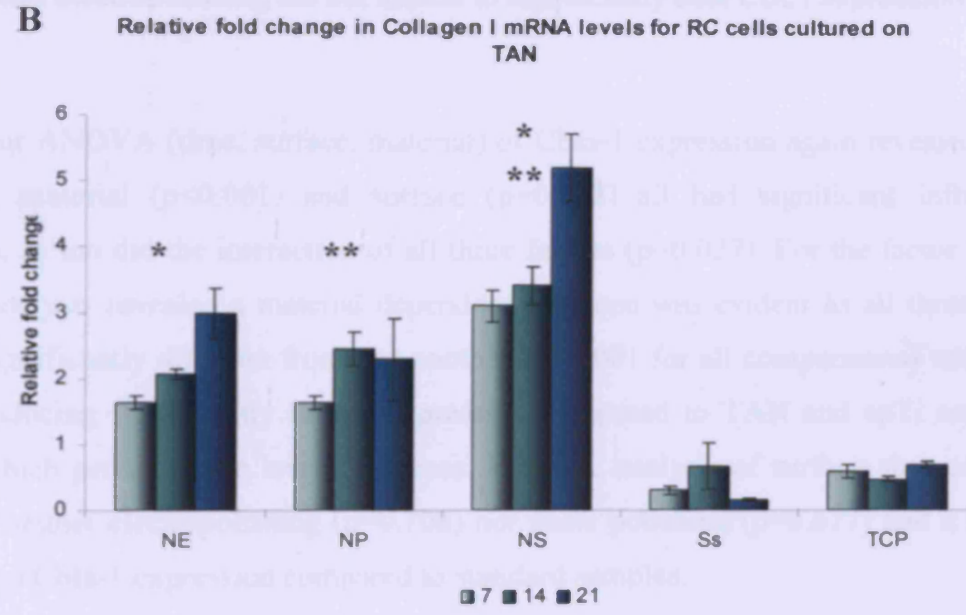

Figure 4.6B: Univariate ANOVA results for TAN revealed that surface finish was a significant factor for COL1 expression (p<0.001). Post-hoc results for TAN samples showed that electropolishing (*p<0.001) and paste polishing (p<0.001) significantly decreases COL1 expression compared to standard TAN.**

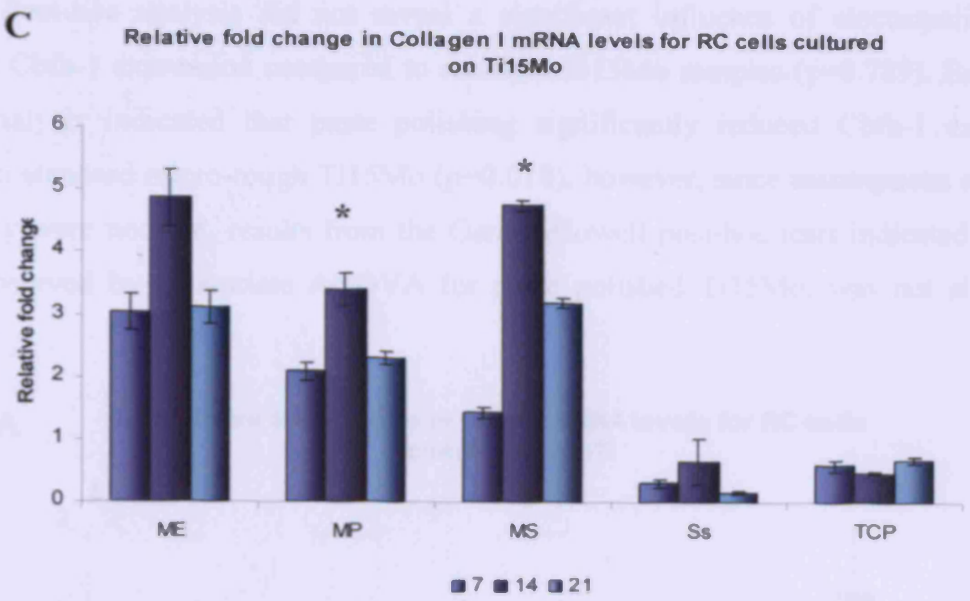

Figure 4.6C: Univariate ANOVA results for Ti15Mo revealed that surface finish was a significant factor in COL1 expression ($p<0.001$). Post-hoc results indicate that paste polishing Ti15Mo significantly decreases COL1 expression compared to standard micro-rough Ti15Mo (*$p<0.001$) samples while electropolishing did not appear to significantly alter COL1 expression ($p=0.148$).

Cbfa-1:

Three-factor ANOVA (time, surface, material) of Cbfa-1 expression again revealed that time ($p<0.001$), material ($p<0.001$) and surface ($p=0.032$) all had significant influences on expression, as too did the interaction of all three factors ($p=0.027$). For the factor 'material', post-hoc analysis revealed a material dependent response was evident as all three materials behaved significantly different from one another ($p<0.001$ for all comparisons) with Ti15Mo samples inducing significantly higher expression compared to TAN and cpTi samples, the latter of which produced the lowest increase. Post-hoc analysis of surface showed that as a treatment, neither electropolishing ($p=0.708$) nor paste polishing ($p=0.677$) had a significant influence on Cbfa-1 expression compared to standard samples.

Results from the Univariate ANOVA showed that for the factor 'surface' polishing significantly influenced Cbfa-1 expression ($p=0.015$) (figure 4.7A). Post-hoc analysis showed that Cbfa-1 mRNA expression did not significantly differ between TE ($p=0.763$) or TP ($p=0.142$) samples compared to TS. However, TP samples appeared to significantly decrease Cbfa-1 expression compared to TE samples ($p=0.010$). Univariate ANOVA results for the factor 'surface' indicate that surface finish of TAN did not significantly ($p=0.691$) affect Cbfa-1 expression (figure 4.7B). For Ti15Mo samples, results from Univariate ANOVA (figure 4.7C) suggest that surface finish of Ti15Mo significantly alters Cbfa-1 expression

(p=0.020). Post-hoc analysis did not reveal a significant influence of electropolishing of Ti15Mo on Cbfa-1 expression compared to standard Ti15Mo samples (p=0.789). Bonferroni post-hoc analysis indicated that paste polishing significantly reduced Cbfa-1 expression compared to standard micro-rough Ti15Mo (p=0.018), however, since assumptions regarding homogeneity were not met, results from the Games-Howell post-hoc tests indicated that this decrease observed by Univariate ANOVA for paste polished Ti15Mo, was not significant (p=0.211).

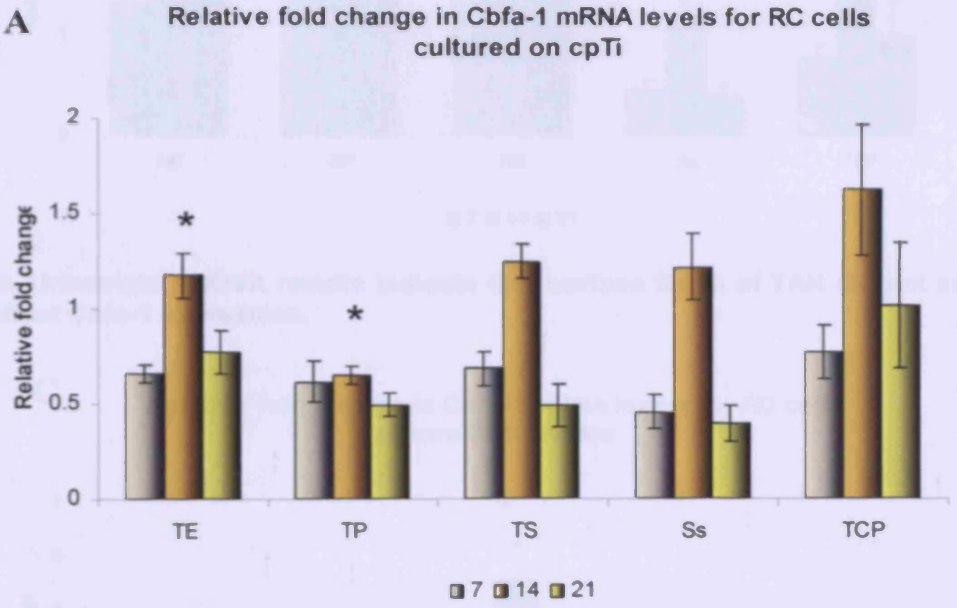

Figure 4.7A: Results from the Univariate ANOVA showed that for the factor 'surface' polishing significantly influenced Cbfa-1 expression (p=0.015). Post-hoc analysis showed that Cbfa-1 mRNA expression did not significantly differ between TE (p=0.763) or TP (p=0.142) samples compared to TS. However, TP samples appeared to significantly decrease Cbfa-1 expression compared to TE samples (*p=0.010).

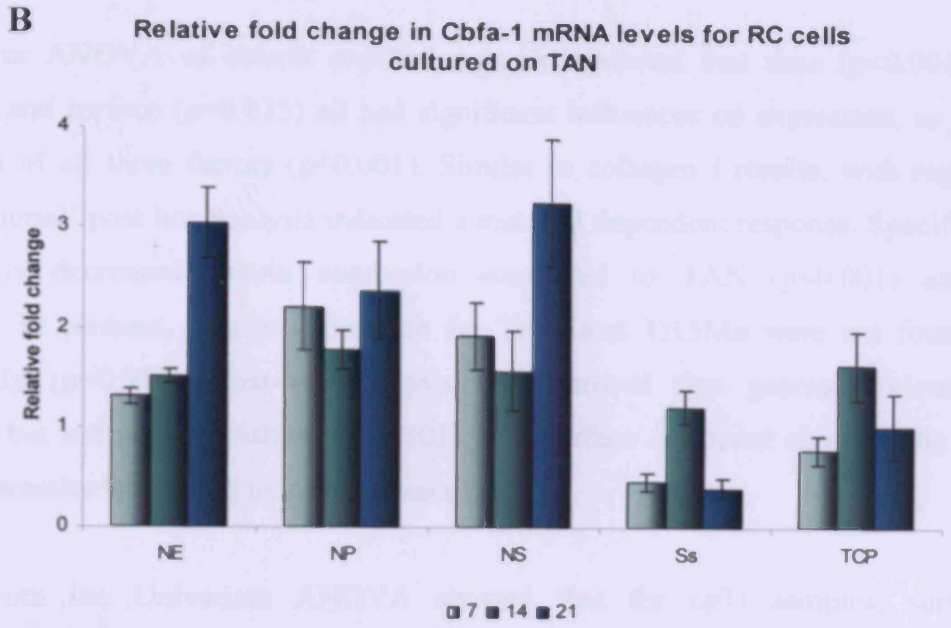

Figure 4.7B: Univariate ANOVA results indicate that surface finish of TAN did not significantly (p=0.691) affect Cbfa-1 expression.

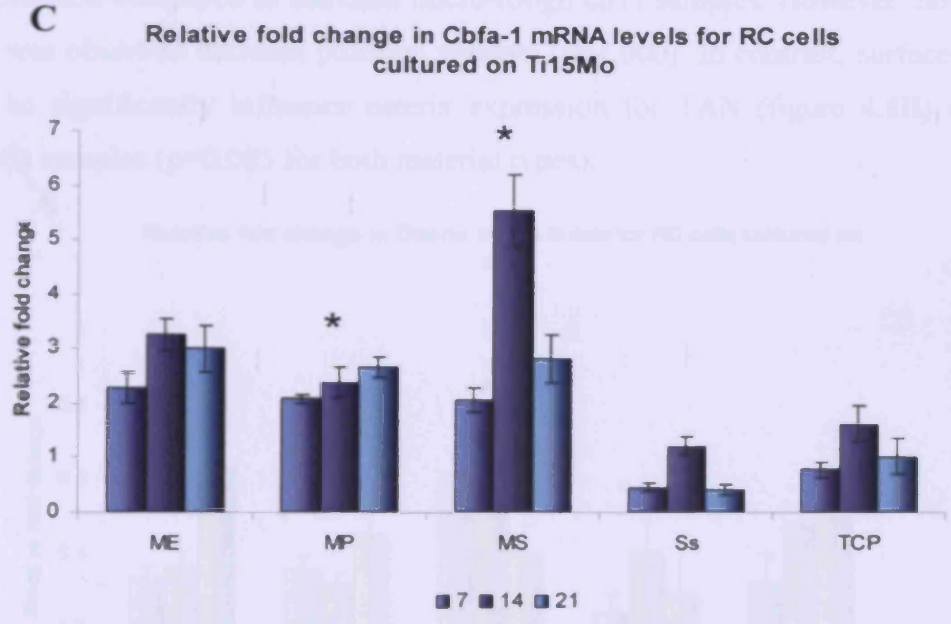

Figure 4.7C: Univariate ANOVA suggest that surface finish of Ti15Mo significantly altered Cbfa-1 expression (p=0.020). Post-hoc analysis did not reveal a significant influence of electropolishing of Ti15Mo on Cbfa-1 expression compared to standard Ti15Mo samples (p=0.789). Bonferroni post-hoc analysis indicated that paste polishing significantly reduced Cbfa-1 expression compared to standard micro-rough Ti15Mo (*p=0.018), however, since assumptions regarding homogeneity were not met, results from the Games-Howell post-hoc tests indicated that this decrease observed by Univariate ANOVA for paste polished Ti15Mo, was not significant (p=0.211).

Osterix:

Three-factor ANOVA of osterix expression again revealed that time ($p<0.001$), material ($p<0.001$) and surface ($p=0.035$) all had significant influences on expression, as too did the interaction of all three factors ($p=0.001$). Similar to collagen I results, with regards to the factor 'material' post hoc analysis indicated a material dependent response. Specifically, cpTi significantly decreased osterix expression compared to TAN ($p<0.001$) and Ti15Mo ($p<0.001$). In contrast, osterix expression for TAN and Ti15Mo were not found to differ significantly ($p=0.919$). Post-hoc analysis also showed that generally electropolishing ($p=0.030$) but not paste polishing ($p=0.101$) as a surface treatment significantly influenced osterix expression compared to standard samples.

Results from the Univariate ANOVA showed that for cpTi samples, surface finish significantly influenced osterix expression ($p=0.003$) (figure 4.8A). With post-hoc analysis it was revealed that both TE ($p=0.013$) and TP ($p=0.013$) samples had significantly different osterix expression compared to standard micro-rough cpTi samples. However, no significant difference was observed between polished variants ($p=1.000$). In contrast, surface finish was not found to significantly influence osterix expression for TAN (figure 4.8B) or Ti15Mo (figure 4.8C) samples ($p=0.085$ for both material types).

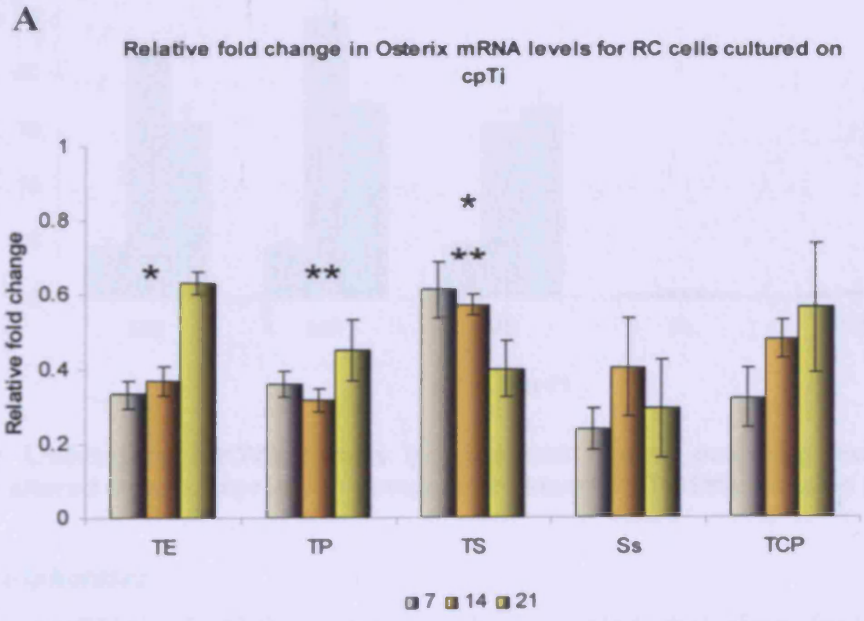

Figure 4.8A: Results from the Univariate ANOVA showed that for cpTi samples, surface finish significantly influenced osterix expression (p=0.003). Post-hoc analysis revealed that both TE (*p=0.013) and TP (p=0.013) samples had significantly different osterix expression compared to standard micro-rough cpTi samples. No significant difference was observed between polished variants (p=1.000).**

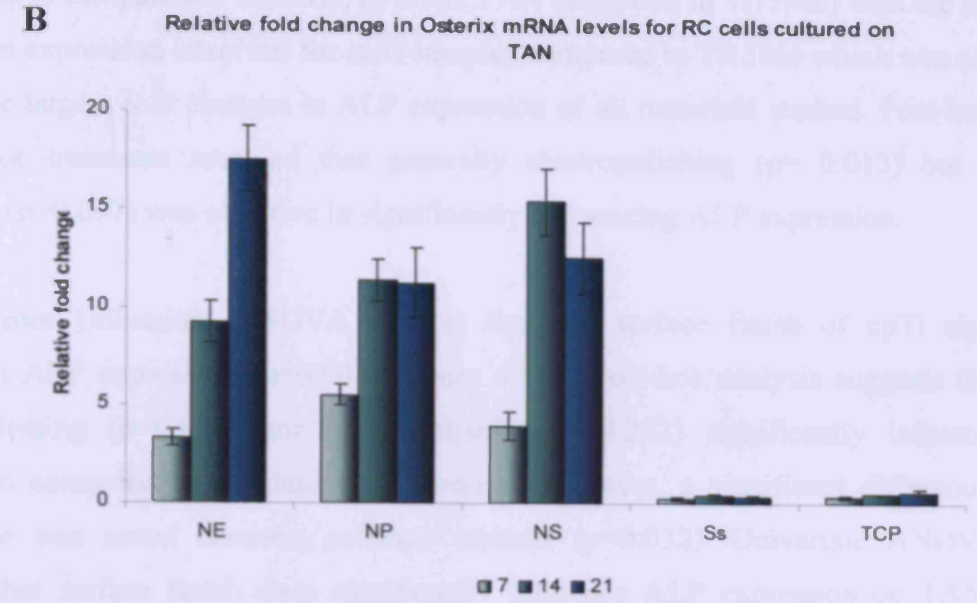

Figure 4.8B: Univariate ANOVA results indicate polishing of TAN does not significantly alter osterix expression compared to standard micro-rough TAN samples (p=0.085).

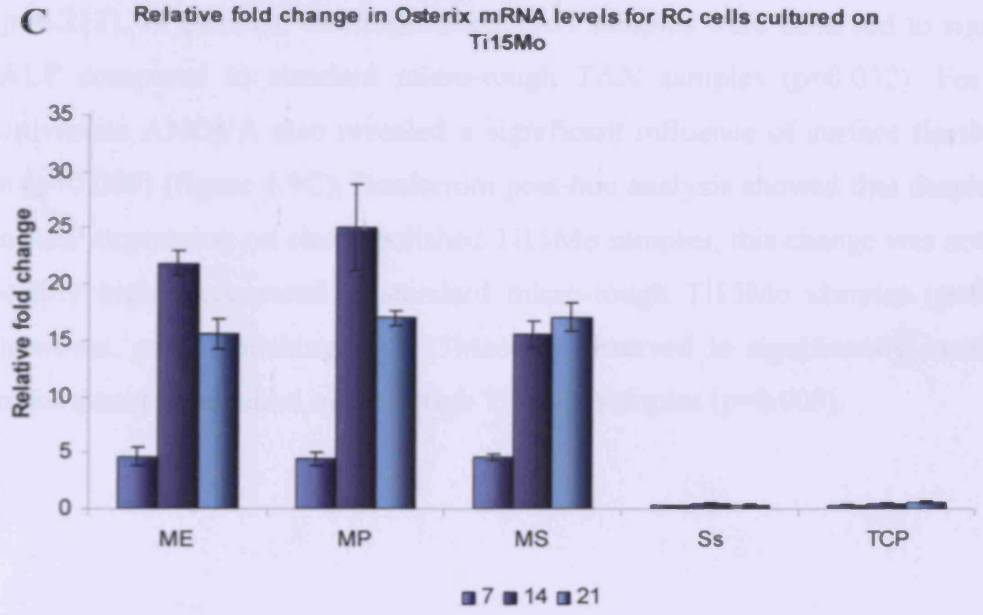

Figure 4.8C: Univariate ANOVA results indicate that neither polishing method of Ti15Mo significantly altered osterix expression compared to standard Ti15Mo samples (p=0.085).

Alkaline Phosphatase:

Three-factor ANOVA of ALP expression also revealed that time ($p<0.001$), material ($p<0.001$) and surface ($p=0.016$) all had significant influences on expression. However, there was no significant interaction of all three factors ($p=0.158$). Similar to post-hoc results for Cbfa-1 expression for the factor 'material', a material dependent response was evident, with all three materials significantly differing from one another ($p<0.001$ cpTi compared to TAN;

$p<0.001$ cpTi compared to Ti15Mo; $p=0.002$ TAN compared to Ti15Mo) with the lowest fold changes in expression observed for cpTi samples compared to Ti15Mo which was observed to induce the largest fold changes in ALP expression of all materials studied. Post-hoc analysis for surface treatment revealed that generally electropolishing ($p= 0.013$) but not paste polishing ($p=0.097$) was effective in significantly influencing ALP expression.

Results from Univariate ANOVA suggest that the surface finish of cpTi significantly influences ALP expression ($p=0.008$) (figure 4.9A). Post-hoc analysis suggests that neither electropolishing ($p=0.857$) nor paste polishing ($p=0.232$) significantly influenced ALP expression compared to standard cpTi controls. However, a significant difference in ALP expression was noted between polished variants ($p=0.032$). Univariate ANOVA results indicate that surface finish does significantly influence ALP expression on TAN samples ($p=0.032$) (figure 4.9B). Bonferroni post-hoc analysis showed that paste polishing was not found to significantly influence ALP expression compared to TAN standard micro-rough samples ($p=0.211$). In contrast, electropolished TAN samples were observed to significantly increase ALP compared to standard micro-rough TAN samples ($p=0.032$). For Ti15Mo samples Univariate ANOVA also revealed a significant influence of surface finish on ALP expression ($p=0.009$) (figure 4.9C). Bonferroni post-hoc analysis showed that despite a small increase in ALP expression on electropolished Ti15Mo samples, this change was not found to be significantly higher compared to standard micro-rough Ti15Mo samples ($p=0.936$). In contrast, however, paste polishing of Ti15Mo was observed to significantly increase ALP expression compared to standard micro-rough Ti15Mo samples ($p=0.009$).

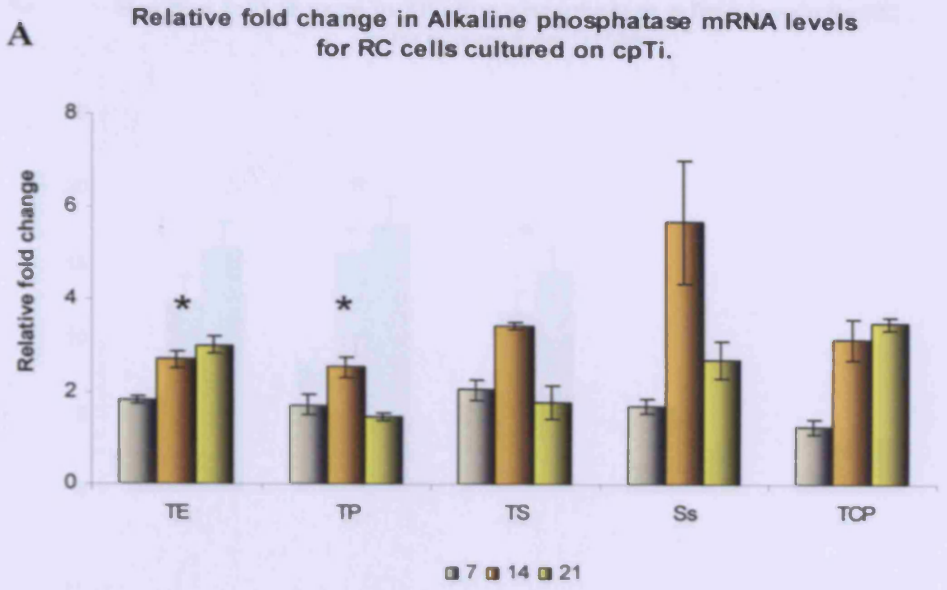

Figure 4.9A: Univariate ANOVA results suggest that the surface finish of cpTi significantly influences ALP expression (p=0.008). Post-hoc analysis indicates that neither electropolishing (p=0.857) nor paste polishing (p=0.232) significantly influenced ALP expression compared to standard cpTi controls. However, a significant difference in ALP expression was noted between polished variants (*p=0.032).

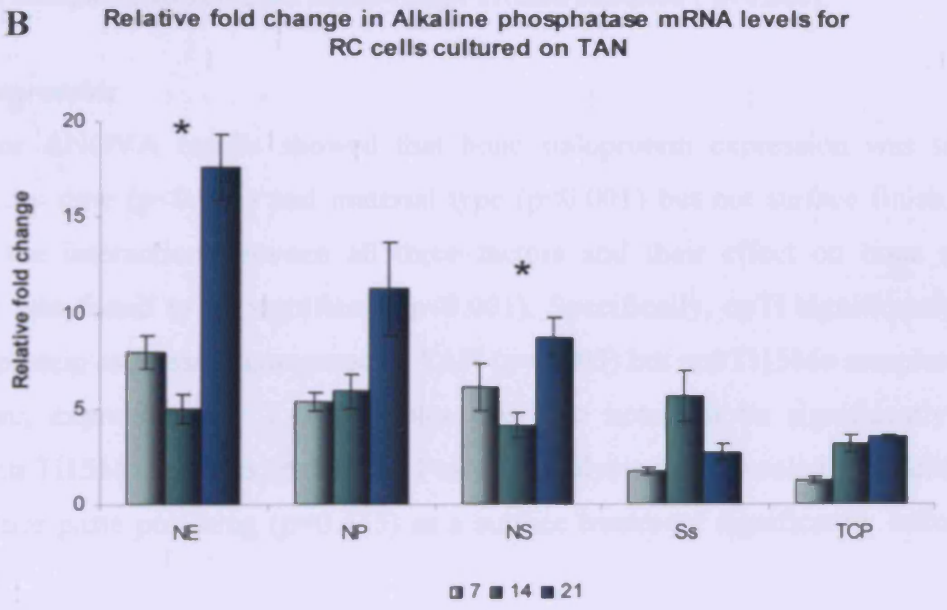

Figure 4.9B: Univariate ANOVA results indicate that surface finish does significantly influence ALP expression on TAN samples (p=0.032). Bonferroni post-hoc analysis showed that paste polishing was not found to significantly influence ALP expression compared to TAN standard micro-rough samples (p=0.211). In contrast, electropolished TAN samples were observed to significantly increase ALP compared to standard micro-rough TAN samples (*p=0.032).

C

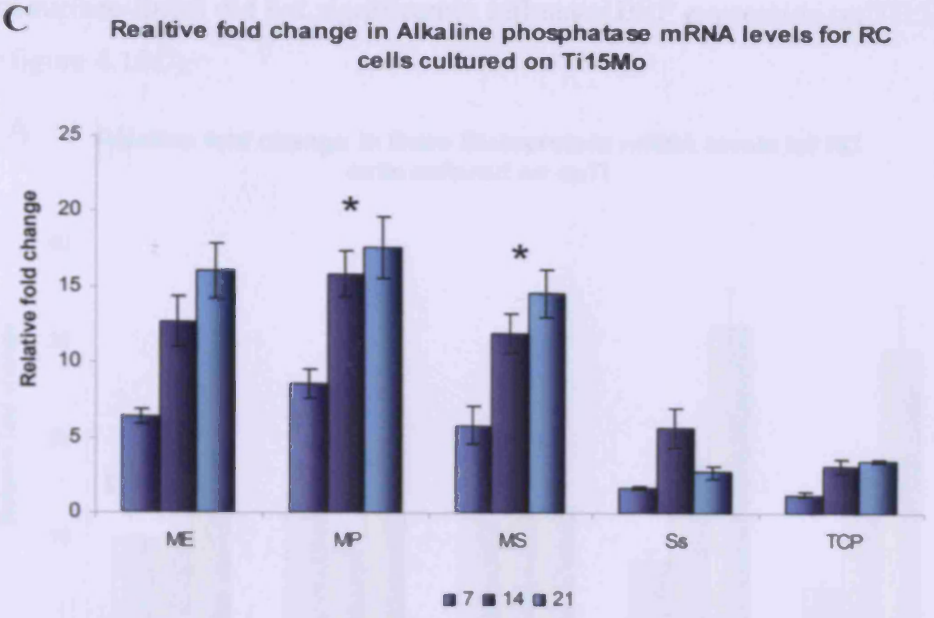

Figure 4.9C: Univariate ANOVA results revealed a significant influence of Ti15Mo surface finish on ALP expression (p=0.009). Bonferroni post-hoc analysis showed that despite a small increase in ALP expression on electropolished Ti15Mo samples, this change was not found to be significantly higher compared to standard micro-rough Ti15Mo samples (p=0.936). In contrast, however, paste polishing of Ti15Mo was observed to significantly increase ALP expression compared to standard micro-rough Ti15Mo samples (*p=0.009).

Bone Sialoprotein:

Three-factor ANOVA results showed that bone sialoprotein expression was significantly influenced by time ($p<0.001$) and material type ($p<0.001$) but not surface finish ($p=0.259$). However, the interaction between all three factors and their effect on bone sialoprotein expression was found to be significant ($p<0.001$). Specifically, cpTi significantly increased bone sialoprotein expression compared to TAN ($p=0.005$) but not Ti15Mo samples ($p=0.068$). Furthermore, expression for TAN samples was also noted to be significantly decreased compared to Ti15Mo samples ($p<0.001$). Post-hoc analysis also revealed that neither electro- ($p=1.000$) nor paste polishing ($p=0.435$) as a surface treatment significantly influenced BSP expression.

Results from Univariate ANOVA indicate that cpTi surface finish is not a significant factor in BSP expression ($p=0.555$) (figure 4.10A). In contrast, surface finish of TAN was found to be a significant factor for BSP expression ($p=0.001$) (figure 4.10B). However, Bonferroni post-hoc analysis indicates that BSP expression was not significantly influenced on electropolished ($p=0.104$) or paste polished ($p=0.126$) TAN samples compared to standard micro-rough TAN samples. BSP expression was found to be significantly reduced on paste polished samples compared to electropolished TAN samples ($p=0.001$). Finally, Univariate ANOVA results

indicate that surface finish did not significantly influence BSP expression on Ti15Mo samples (p=0.455) (figure 4.10C).

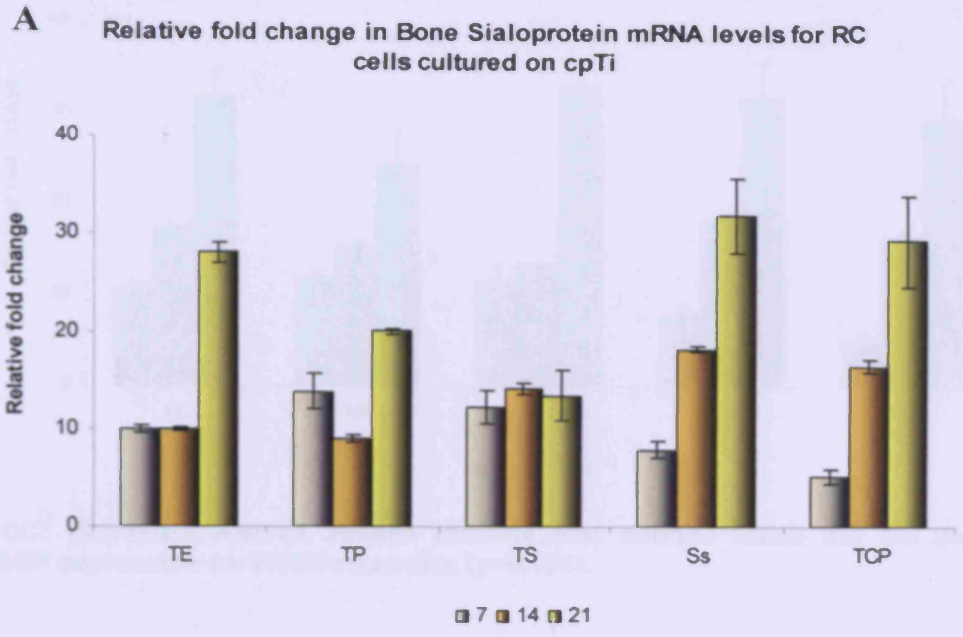

Figure 4.10A: Results from Univariate ANOVA suggest that cpTi surface finish is not a significant factor for BSP expression (p=0.555).

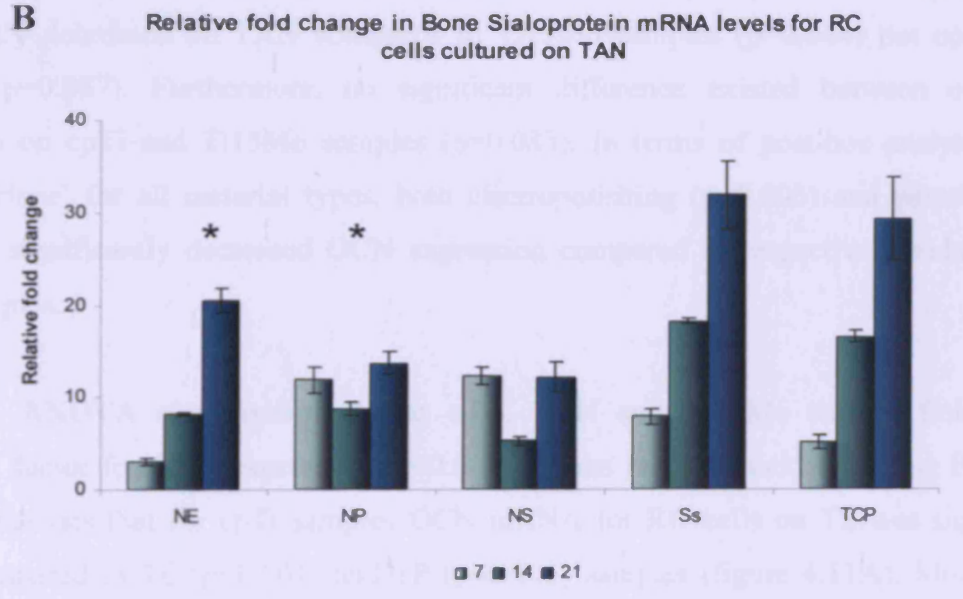

Figure 4.10B: Univariate ANOVA results show that surface finish was a significant factor in BSP expression (p=0.001). Bonferroni post-hoc analysis indicates that BSP expression was not significantly influenced on electropolished (p=0.104) or paste polished (p=0.126) samples compared to standard micro-rough TAN samples. There was a significant decrease in BSP expression on paste polished TAN compared to electropolished TAN (*p=0.001).

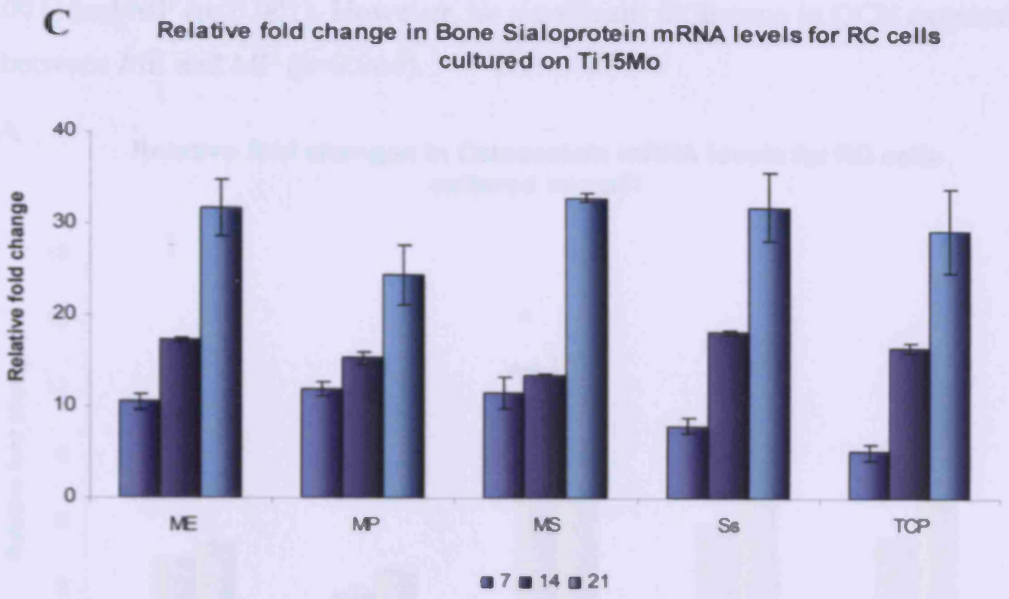

Figure 4.10C: Univariate ANOVA results indicate that surface finish did not significantly influence BSP expression on Ti15Mo samples (p=0.455).

Osteocalcin:

Finally, three-factor ANOVA showed that osteocalcin expression was significantly influenced by time ($p<0.001$) material type ($p<0.001$) and surface finish ($p<0.001$). OCN expression was significantly decreased on TAN compared to Ti15Mo samples ($p=0.044$) but not on cpTi samples ($p=0.987$). Furthermore, no significant difference existed between osteocalcin expression on cpTi and Ti15Mo samples ($p=0.083$). In terms of post-hoc analysis for the factor 'surface' for all material types, both electropolishing ($p=0.005$) and paste polishing ($p=0.004$) significantly decreased OCN expression compared to respective standard micro-rough samples.

Univariate ANOVA also confirmed that cpTi, TAN and Ti15Mo surface finish was a significant factor for OCN expression ($p<0.001$). It was further elucidated using Bonferroni post-hoc analysis that for cpTi samples OCN mRNA for RC cells on TS was significantly higher compared to TE ($p<0.001$) and TP ($p<0.001$) samples (figure 4.11A). Moreover, no significant difference in OCN regulation was observed between TE or TP samples ($p=0.053$). Similarly, it was shown for TAN samples (figure 4.11B), using post-hoc analysis that OCN expression was significantly increased for cells cultured on NS samples compared to NE ($p<0.001$) and NP ($p<0.001$). However, no significant difference was noted between polishing methods ($p=0.053$). Furthermore, post-hoc analysis of Ti15Mo data (figure 4.11C) indicated that OCN expression was significantly higher for cells cultured on MS samples compared to

ME ($p<0.001$) and MP ($p<0.001$). However, no significant difference in OCN expression was observed between ME and MP ($p=0.064$).

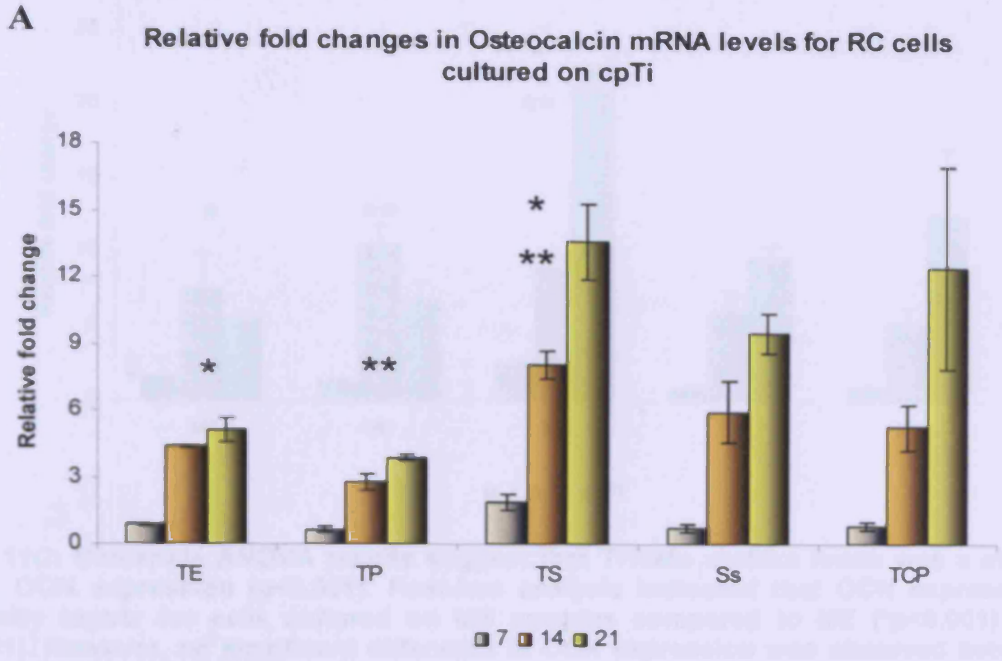

Figure 4.11A: Univariate ANOVA results suggest that cpTi surface finish was a significant factor in OCN expression ($p<0.001$). Post-hoc analysis showed that for cpTi samples OCN mRNA for RC cells on TS was significantly higher compared to TE (*$p<0.001$) and TP ($p<0.001$) samples. Moreover, no significant difference in OCN regulation was observed between TE or TP samples ($p=0.053$).**

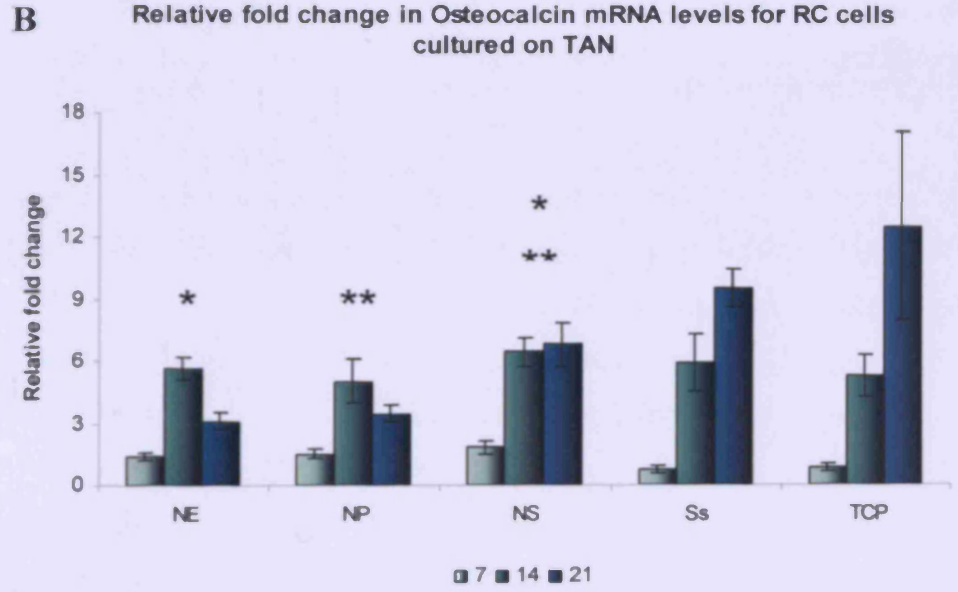

Figure 4.11B: Univariate ANOVA results suggest that TAN surface finish was a significant factor in OCN expression ($p<0.001$). Post-hoc analysis that OCN expression was significantly increased for cells cultured on NS samples compared to NE (*$p<0.001$) and NP ($p<0.001$). However, no significant difference was noted between polishing methods ($p=0.053$).**

C

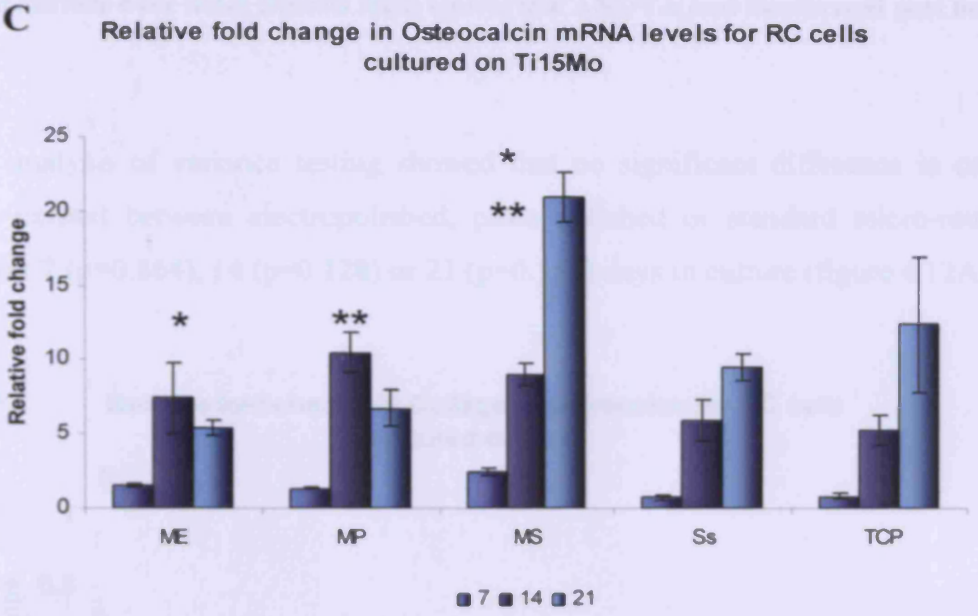

Figure 4.11C: Univariate ANOVA results suggest that Ti15Mo surface finish was a significant factor in OCN expression ($p<0.001$). Post-hoc analysis indicated that OCN expression was significantly higher for cells cultured on MS samples compared to ME (*$p<0.001$) and MP ($p<0.001$). However, no significant difference in OCN expression was observed between ME and MP ($p=0.064$).**

Influence of surface over time: Results from Univariate ANOVA and Bonferroni post hoc test

Collagen I:

Univariate analysis of variance testing showed that no significant difference in collagen I expression existed between electropolished, paste polished or standard micro-rough cpTi samples after 7 ($p=0.864$), 14 ($p=0.128$) or 21 ($p=0.168$) days in culture (figure 4.12A).

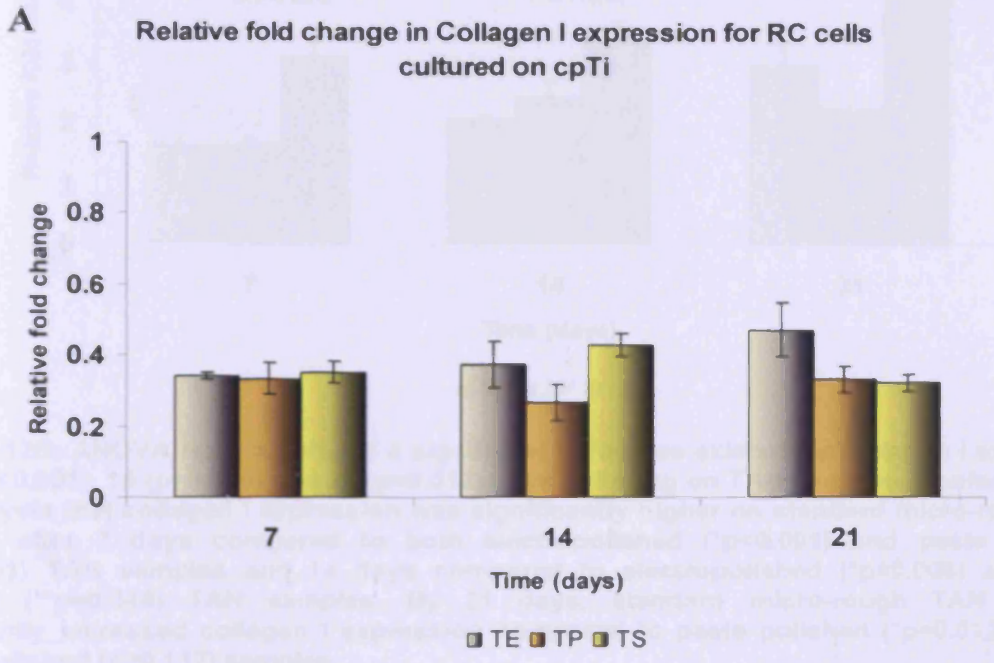

Figure 4.12A: ANOVA results indicate that neither surface polishing treatment had a significant influence on COL1 expression at any time point compared to standard micro-rough cpTi samples.

For TAN samples, Univariate analysis of variance testing showed that a significant difference existed for collagen I expression after 7 days culturing ($p<0.001$). Bonferroni post-hoc analysis showed that collagen I expression was significantly higher on standard micro-rough TAN samples after 7 days compared to both electropolished ($p<0.001$) and paste polished ($p<0.001$) TAN samples (figure 4.12B). Similarly, after 14 days culturing, collagen expression was found to be significantly influenced by surface type ($p=0.006$). Again, using the Bonferroni post hoc test, standard micro-rough TAN samples were observed to significantly increase collagen I expression compared to electropolished ($p=0.006$) and paste polished ($p=0.046$) TAN samples after 14 days culturing. Univariate analysis of variance testing also showed that a significant difference existed for collagen I expression after 21 days culturing ($p<0.012$) on TAN samples. However, unlike previous time points, standard micro-

rough TAN samples significantly increased collagen I expression compared to paste polished (p=0.012) but not electropolished (p=0.112) samples.

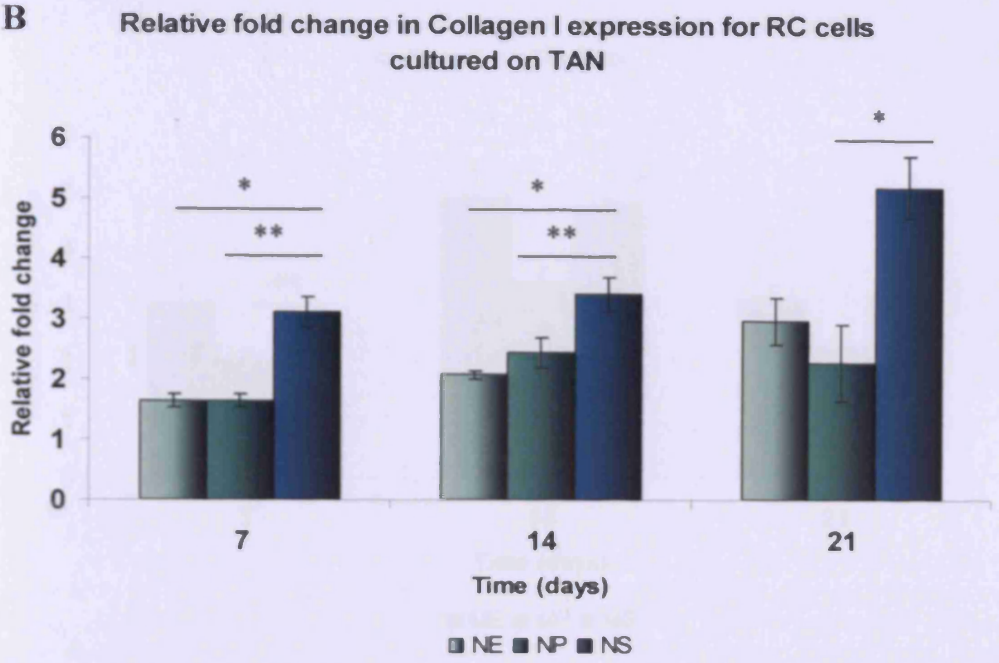

Figure 4.12B: ANOVA results showed a significant difference existed for collagen I expression after 7($p<0.001$), 14 ($p=0.006$) and 21 ($p=0.012$) days culturing on TAN samples. Bonferroni post hoc analysis that collagen I expression was significantly higher on standard micro-rough TAN samples after 7 days compared to both electropolished (*$p<0.001$) and paste polished ($p<0.001$) TAN samples and 14 days compared to electropolished (*$p=0.006$) and paste polished (**$p=0.046$) TAN samples. By 21 days, standard micro-rough TAN samples significantly increased collagen I expression compared to paste polished (*$p=0.012$) but not electropolished ($p=0.112$) samples.**

Univariate analysis of variance testing showed that a significant difference existed for collagen I expression after 7 days culturing on Ti15Mo samples ($p<0.001$). Bonferroni post hoc analysis showed that both electropolished ($p<0.001$) and paste polished ($p=0.036$) Ti15Mo samples had significantly higher collagen I expression compared to standard micro-rough Ti15Mo samples after 7 days (figure 4.12C). After 14 days culturing Univariate analysis of variance also delineated a significant affect ($p=0.010$) of surface type on collagen I expression. Specifically, after 14 days culturing, collagen expression for paste polished samples was significantly decreased compared to electropolished ($p=0.020$) and standard micro-rough ($p=0.024$) Ti15Mo samples. No significant difference in collagen I expression was observed between electropolished and standard micro-rough Ti15Mo samples after 14 days ($p=1.000$). After 21 days, Univariate analysis of variance testing revealed a significant influence of surface on collagen I expression ($p=0.004$). Bonferroni post hoc tests showed that again both electropolished ($p=0.012$) and standard micro-rough ($p=0.006$) Ti15Mo samples had significantly higher collagen I expression compared to paste polished samples. However,

no difference was observed between electropolished or standard micro-rough Ti15Mo samples at 21 days (p=1.000).

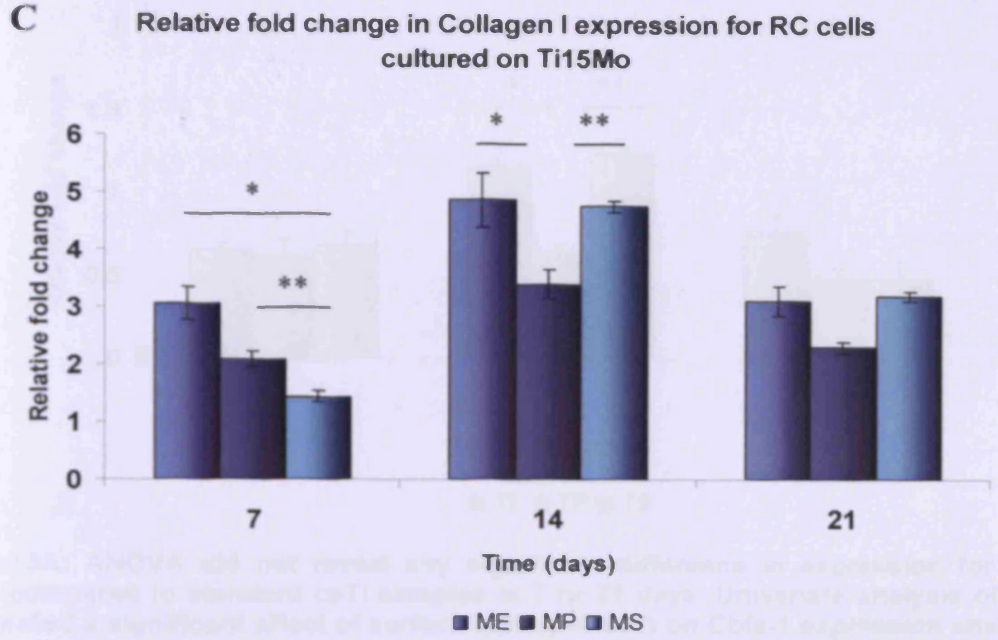

Figure 4.12C: ANOVA showed that a significant difference existed for collagen I expression after 7 (p<0.001) and 14 (p=0.010) days culturing on Ti15Mo samples. Bonferroni post hoc results indicate that both electropolished (*p<0.001) and paste polished (p=0.036) Ti15Mo samples had significantly higher collagen I expression compared to standard micro-rough Ti15Mo samples after 7 days. After 14 days, collagen expression for paste polished samples was significantly decreased compared to electropolished (*p=0.020) and standard micro-rough (**p=0.024) Ti15Mo samples. No difference was observed after 21 days culturing (p=1.000).**

Cbfa-1:

Univariate analysis of variance testing showed that no significant difference existed in Cbfa-1 expression for electropolished, paste polished or standard micro-rough cpTi samples after 7 (p=0.769) or 21 (p=0.181) days in culture (figure 4.13A). Univariate analysis of variance did delineated a significant affect of surface type (p=0.002) on Cbfa-1 expression after 14 days culturing. Bonferroni post hoc analysis showed that Cbfa-1 expression was significantly decreased on paste polished cpTi samples compared to both electropolished (p=0.006) and standard micro-rough (p=0.003) cpTi samples after 14 days.

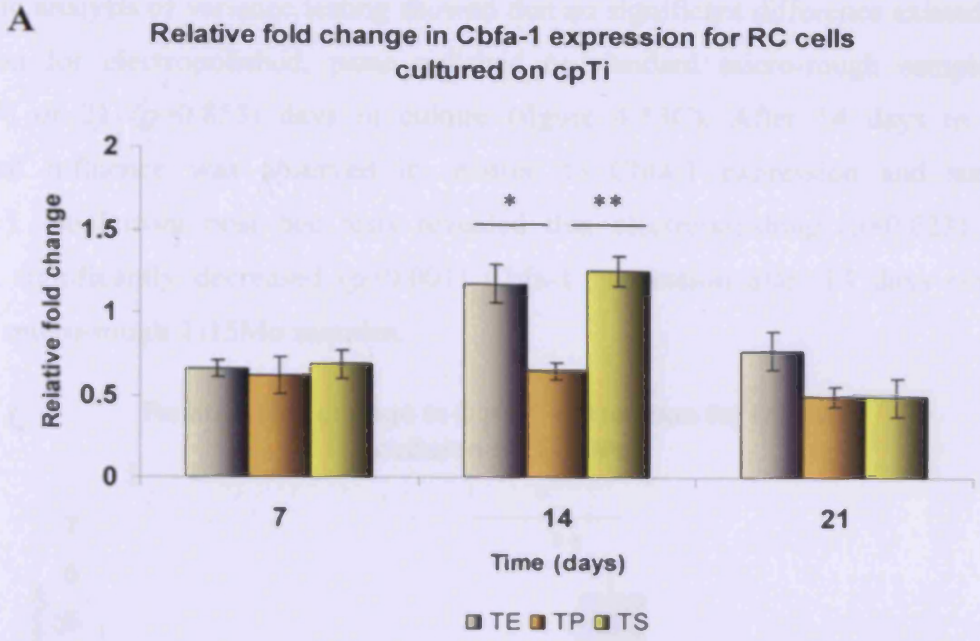

Figure 4.13A: ANOVA did not reveal any significant difference in expression for polished samples compared to standard cpTi samples at 7 or 21 days. Univariate analysis of variance did delineated a significant affect of surface type (p=0.002) on Cbfa-1 expression after 14 days culturing. Bonferroni post hoc analysis showed that Cbfa-1 expression was significantly decreased on paste polished cpTi samples compared to both electropolished (*p=0.006) and standard micro-rough (p=0.003) cpTi samples.**

Univariate analysis of variance testing showed that no significant difference in Cbfa-1 expression existed between electropolished, paste polished or standard micro-rough TAN samples after 7 (p=0.138), 14 (p=0.685) or 21 (p=0.411) days in culture (Figure 4.13B).

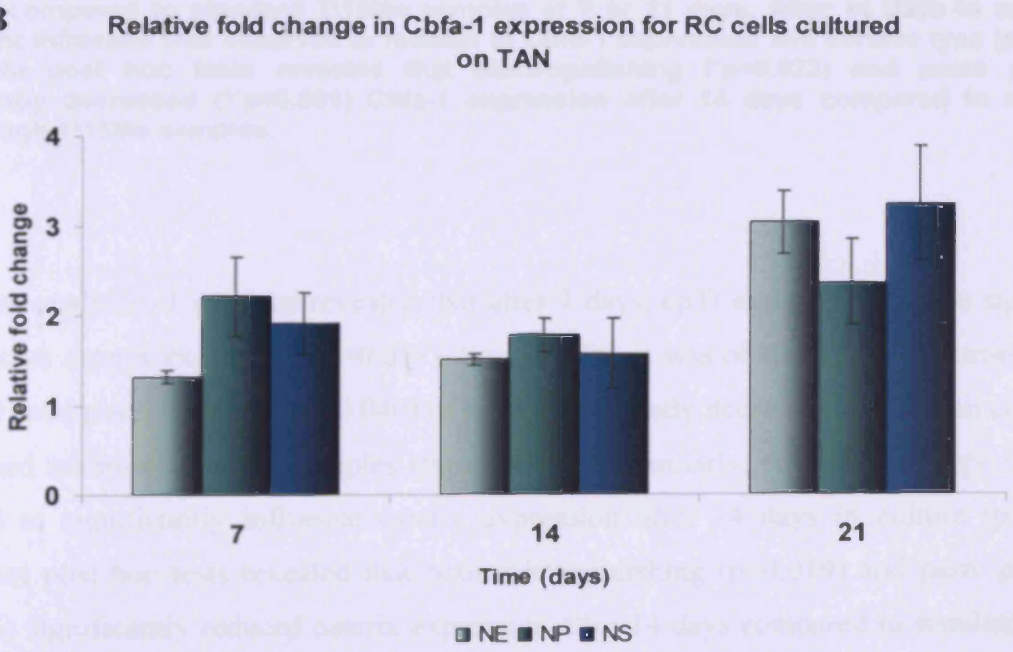

Figure 4.13B: ANOVA delineated no significant alteration in Cbfa-1 expression on TAN samples at 7, 14 or 21 days.

Univariate analysis of variance testing showed that no significant difference existed in Cbfa-1 expression for electropolished, paste polished or standard micro-rough samples after 7 (p=0.647) or 21 (p=0.853) days in culture (figure 4.13C). After 14 days in culture, a significant influence was observed in relation to Cbfa-1 expression and surface type (p=0.001). Bonferroni post hoc tests revealed that electropolishing (p=0.023) and paste polished significantly decreased (p=0.001) Cbfa-1 expression after 14 days compared to standard micro-rough Ti15Mo samples.

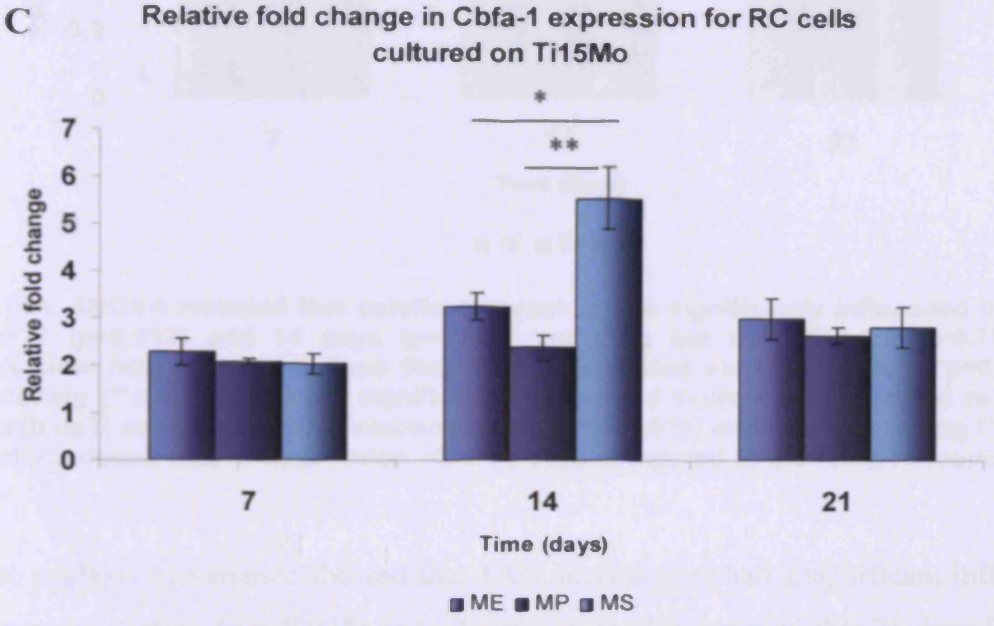

Figure 4.13C: ANOVA did not reveal any significant difference in expression for polished samples compared to standard Ti15Mo samples at 7 or 21 days. After 14 days in culture, a significant influence was observed in relation to Cbfa-1 expression and surface type (p=0.001). Bonferroni post hoc tests revealed that electropolishing (*p=0.023) and paste polished significantly decreased (p=0.001) Cbfa-1 expression after 14 days compared to standard micro-rough Ti15Mo samples.**

Osterix:

Univariate analysis of variance revealed that after 7 days, cpTi surface type had a significant influence on osterix expression (p=0.013). Specifically, it was observed that electropolishing (p=0.019) and paste polishing (p=0.040) of cpTi significantly decreased expression compared to standard micro-rough cpTi samples (figure 4.14A). Similarly, cpTi surface type was also observed to significantly influence osterix expression after 14 days in culture (p=0.004). Bonferroni post hoc tests revealed that both electropolishing (p=0.019) and paste polishing (p=0.006) significantly reduced osterix expression after 14 days compared to standard micro-rough cpTi samples. The influence of cpTi surface type on osterix expression was not observed by 21 days culturing (p=0.794).

A

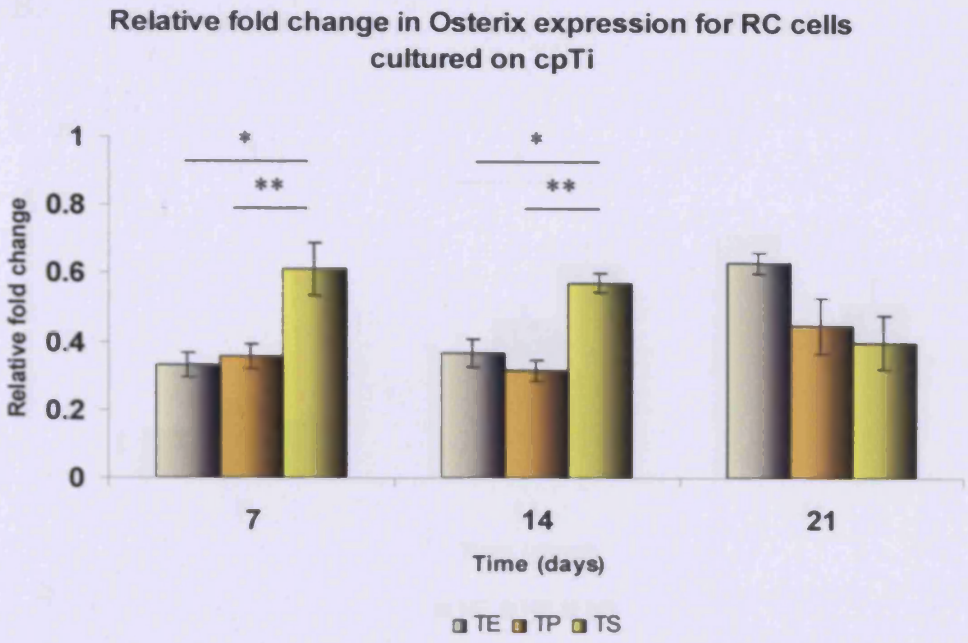

Figure 4.14A: ANOVA revealed that osterix expression was significantly influenced by surface type after 7 (p=0.013) and 14 days (p=0.004) culturing but not after 21 (p=0.794) days. Bonferroni post hoc analysis defined that after 7 days that electropolishing (*p=0.019) and paste polishing (p=0.040) of cpTi significantly decreased expression compared to standard micro-rough cpTi samples and that electropolishing (*p=0.019) and paste polishing (**p=0.006) significantly reduced osterix expression after 14 days compared to standard micro-rough cpTi samples.**

Univariate analysis of variance showed that TAN surface type had a significant influence on osterix expression after 7 (p=0.048) and 14 days (p=0.040) but not after 21 days (p=0.059) culturing (figure 4.14B). After 7 days, however, Bonferroni post hoc tests did not reveal any significant difference for osterix expression on electropolished (p=1.000) or paste polished (p=0.204) samples compared to standard micro-rough TAN samples. Similarly, after 14 days paste polishing was not observed to significantly affect osterix expression (p=0.340). However, electropolishing of TAN samples was observed after 14 days to significantly reduce osterix expression compared to standard micro-rough TAN samples (p=0.042).

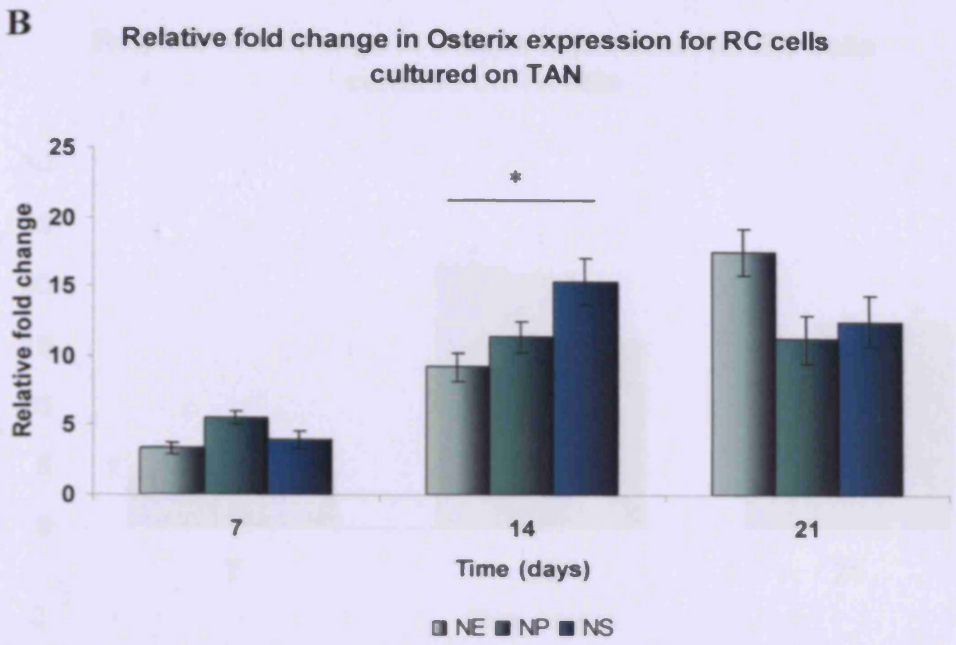

Figure 4.14B: ANOVA showed that TAN surface type had a significant influence on osterix expression after 7 (p=0.048) and 14 days (p=0.040) but not after 21 days (p=0.059) culturing. However, Bonferroni post hoc tests did not reveal any significant difference for osterix expression on electropolished (p=1.000) or paste polished (p=0.204) samples compared to standard micro-rough TAN samples. After 14 days paste polishing was not observed to significantly affect osterix expression (p=0.340). However, electropolishing of TAN samples was observed after 14 days to significantly reduce osterix expression compared to standard micro-rough TAN samples (*p=0.042).

Univariate analysis of variance showed that Ti15Mo surface type had a significant influence on osterix expression after 14 (p=0.042) and 21 days culturing (p=0.031) but not after 7 days (p=0.963). However, Bonferroni post-hoc tests were unable to delineate any significant differences between electropolished (p=0.160) or paste polished (p=0.052) Ti15Mo surfaces compared to standard micro-rough Ti15Mo at 14 days (figure 4.14C).

C Relative fold change in Osterix expression for RC cells cultured on Ti15Mo

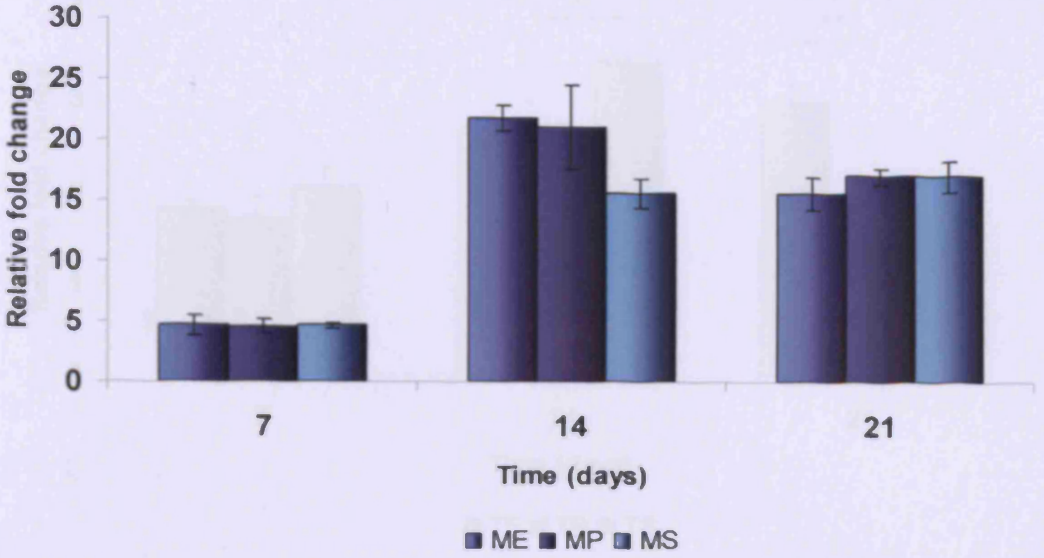

Figure 4.14C: ANOVA showed that Ti15Mo surface type had a significant influence on osterix expression after 14 (p=0.042) and 21 days culturing (p=0.031) but not after 7 days (p=0.963). However, Bonferroni post-hoc tests were unable to delineate any significant differences between electropolished or paste polished Ti15Mo surfaces compared to standard micro-rough Ti15Mo.

Alkaline phosphatase:

Univariate analysis of variance revealed that after 7 days culturing, cpTi surface type did not significantly influence ALP expression (p=0.476). However, cpTi surface type was found to significantly influence ALP expression after 14 (p=0.019) and 21 (p=0.007) days culturing (figure 4.15A). Bonferroni post-hoc tests showed that paste polishing of cpTi significantly reduces ALP expression compared to standard micro-rough cpTi after 14 days (p=0.029). After 14 days, no significant difference in expression was observed between electropolished or standard micro-rough cpTi samples (p=0.061). After 21 days, Bonferroni post-hoc tests revealed that electropolishing of cpTi significantly increases ALP expression compared to paste polished (p=0.009) and standard micro-rough samples (p=0.032). However, no difference was observed between paste polished cpTi and standard micro-rough cpTi samples after 21 days (p=1.000).

A

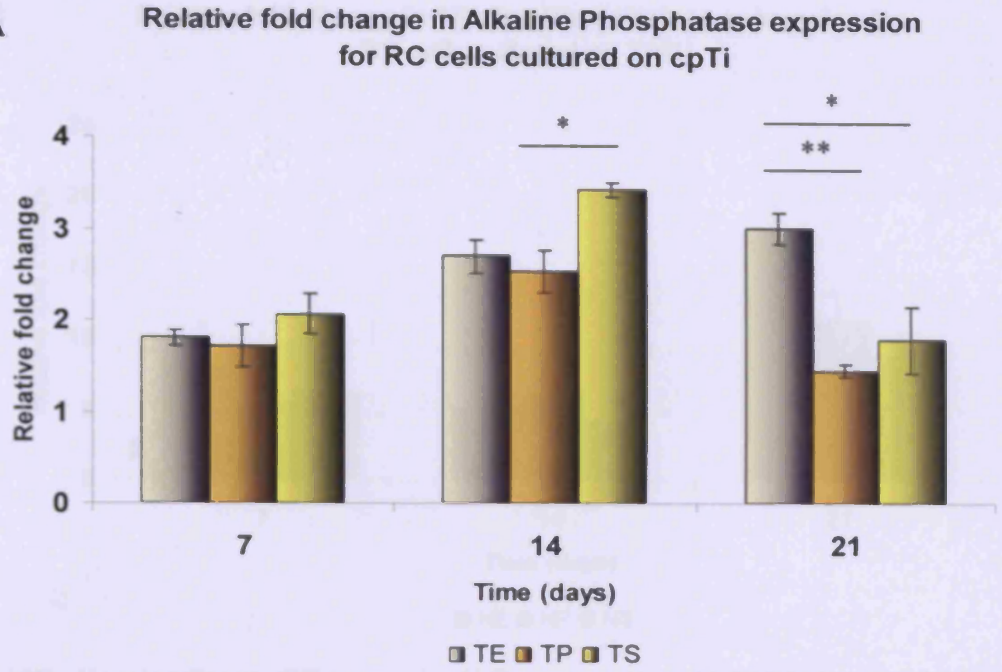

Figure 4.15A: ANOVA revealed that after 7 days culturing, cpTi surface type did not significantly influence ALP expression (p=0.476). However, cpTi surface type was found to significantly influence ALP expression after 14 (p=0.019) and 21 (p=0.007) days culturing. Bonferroni post-hoc tests showed that paste polishing of cpTi significantly reduces ALP expression compared to standard micro-rough cpTi after 14 days (*p=0.029) but no difference was noted compared to electropolished samples (p=0.061). Bonferroni post-hoc tests also revealed that electropolishing of cpTi significantly increases ALP expression compared to paste polished (p=0.009) and standard micro-rough samples (*p=0.032) after 21 days culturing.**

Univariate analysis of variance testing showed that no significant difference in ALP expression existed between electropolished, paste polished or standard micro-rough TAN samples after 7 (p=0.190), 14 (p=0.282) or 21 (p=0.123) days in culture (figure 4.15B).

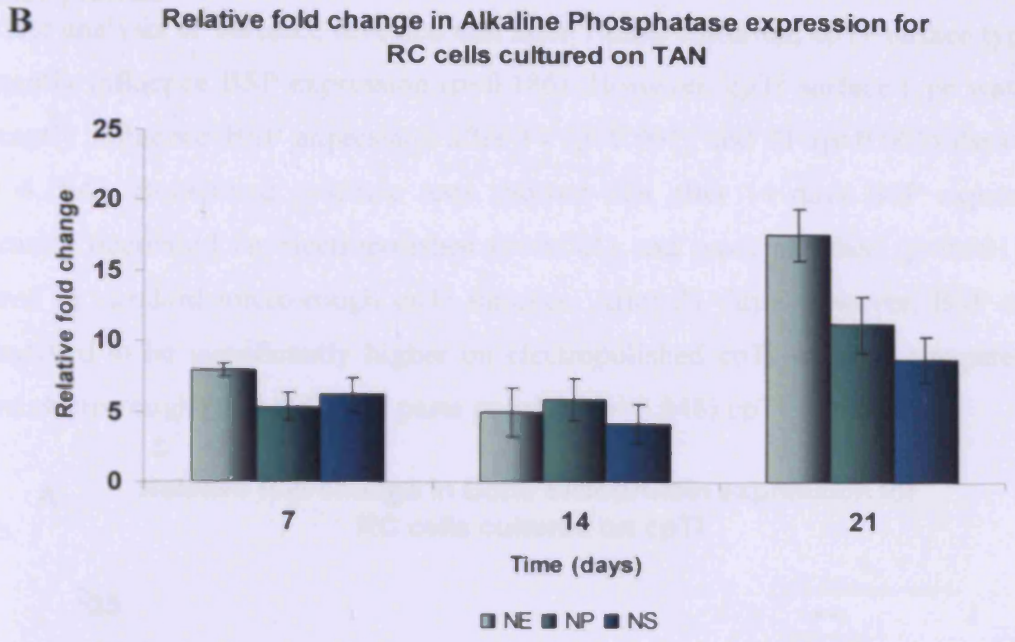

Figure 4.15B: No significant difference in ALP expression existed between electropolished, paste polished or standard micro-rough TAN samples after 7 (p=0.190), 14 (p=0.282) or 21 (p=0.123) days in culture.

Similarly, univariate analysis of variance testing showed that no significant difference in ALP expression existed between electropolished, paste polished or standard micro-rough Ti15Mo samples after 7 (p=0.0.73), 14 (p=0.172) or 21 (p=0.540) days in culture (figure 4.15C).

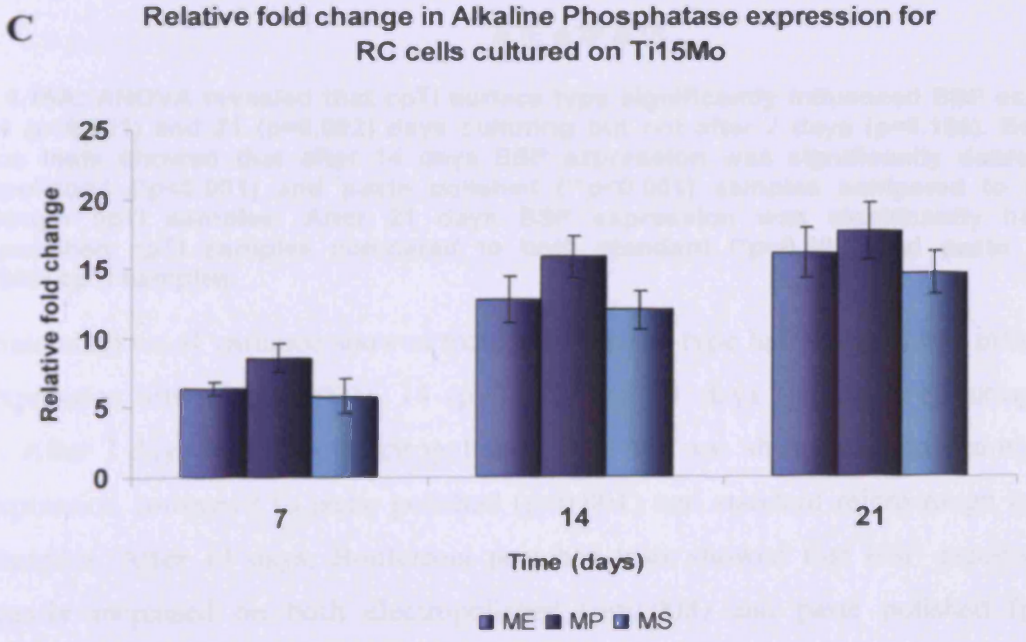

Figure 4.15C: No significant difference in ALP expression existed between electropolished, paste polished or standard micro-rough Ti15Mo samples after 7 (p=0.0.73), 14 (p=0.172) or 21 (p=0.540) days in culture.

Bone Sialoprotein:

Univariate analysis of variance revealed that after 7 days culturing, cpTi surface type did not significantly influence BSP expression ($p=0.186$). However, cpTi surface type was found to significantly influence BSP expression after 14 ($p<0.001$) and 21 ($p=0.002$) days culturing (figure 4.16A). Bonferroni post-hoc tests showed that after 14 days BSP expression was significantly decreased on electropolished ($p<0.001$) and paste polished ($p<0.001$) samples compared to standard micro-rough cpTi samples. After 21 days, however, BSP expression was observed to be significantly higher on electropolished cpTi samples compared to both standard micro-rough ($p=0.002$) and paste polished ($p=0.048$) cpTi samples.

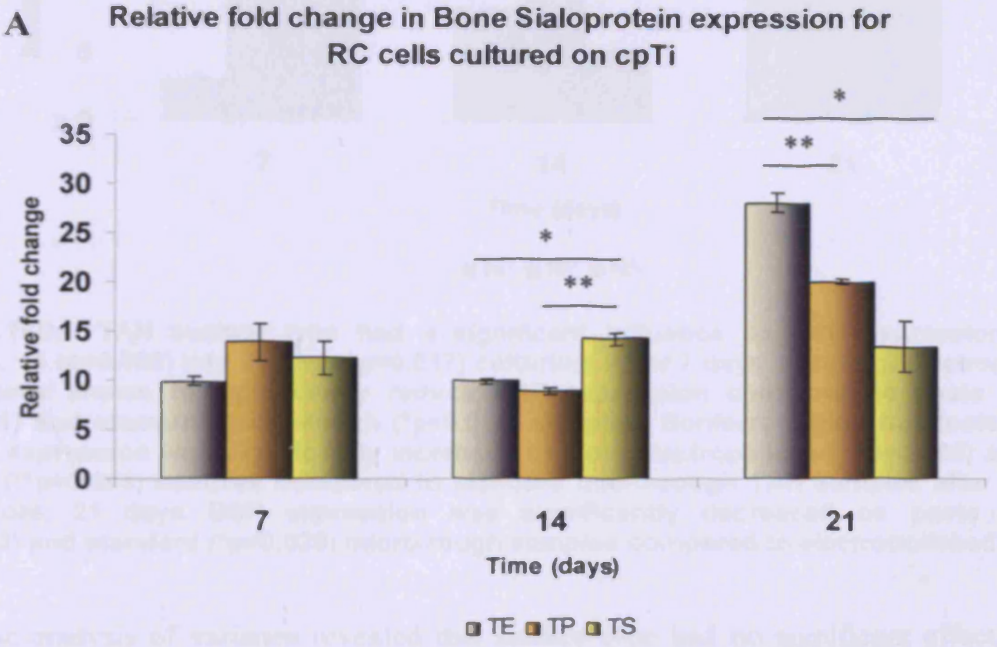

Figure 4.16A: ANOVA revealed that cpTi surface type significantly influenced BSP expression after 14 ($p<0.001$) and 21 ($p=0.002$) days culturing but not after 7 days ($p=0.186$). Bonferroni post-hoc tests showed that after 14 days BSP expression was significantly decreased on electropolished (*$p<0.001$) and paste polished ($p<0.001$) samples compared to standard micro-rough cpTi samples. After 21 days BSP expression was significantly higher on electropolished cpTi samples compared to both standard (*$p=0.002$) and paste polished (**$p=0.048$) cpTi samples.**

Univariate analysis of variance showed that TAN surface type had a significant influence on BSP expression after 7 ($p<0.001$), 14 ($p=0.002$) and 21 days ($p=0.017$) culturing (figure 4.16B). After 7 days culturing, electropolishing of TAN was shown to significantly reduce BSP expression compared to paste polished ($p<0.001$) and standard micro-rough ($p<0.001$) TAN samples. After 14 days, Bonferroni post hoc tests showed that BSP expression was significantly increased on both electropolished ($p=0.008$) and paste polished ($p=0.004$) samples compared to standard micro-rough TAN samples. By 21 days, BSP expression was

noted to be significantly decreased on paste polished (p=0.043) and standard (p=0.029) micro-rough TAN samples compared to electropolished TAN samples.

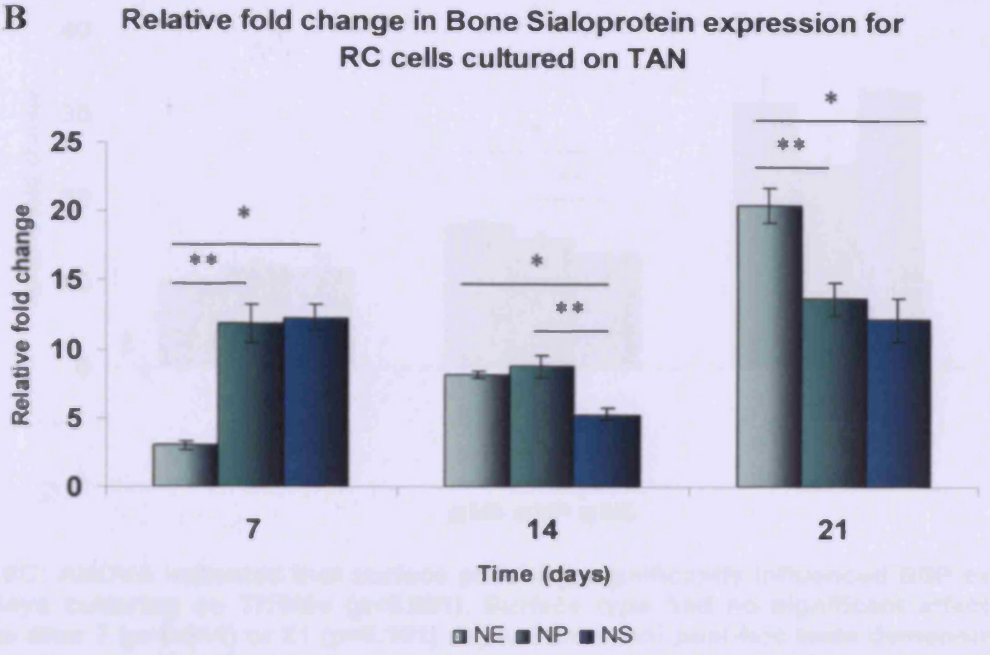

Figure 4.16B: TAN surface type had a significant influence on BSP expression after 7 ($p<0.001$), 14 ($p=0.002$) and 21 days ($p=0.017$) culturing. After 7 days culturing, electropolishing of TAN was shown to significantly reduce BSP expression compared to paste polished ($p<0.001$) and standard micro-rough (*$p<0.001$) samples. Bonferroni post hoc tests showed that BSP expression was significantly increased on both electropolished (*$p=0.008$) and paste polished (**$p=0.004$) samples compared to standard micro-rough TAN samples after 14 days. Furthermore, 21 days BSP expression was significantly decreased on paste polished (**$p=0.043$) and standard (*$p=0.029$) micro-rough samples compared to electropolished TAN.**

Univariate analysis of variance revealed that surface type had no significant affect on BSP expression after 7 ($p=0.644$) or 21 ($p=0.101$) days culturing on Ti15Mo samples (figure 4.16C). However, surface polishing was found to significantly influence BSP expression after 14 days culturing on Ti15Mo ($p<0.001$). Bonferroni post-hoc tests demonstrated that BSP expression was significantly increased on electropolished ($p<0.001$) and paste polished ($p=0.028$) Ti15Mo surfaces compared to standard micro-rough samples at 14 days. Moreover, electropolished Ti15Mo induced significantly higher BSP expression compared to paste polished ($p=0.029$) samples after 14 days culturing.

C

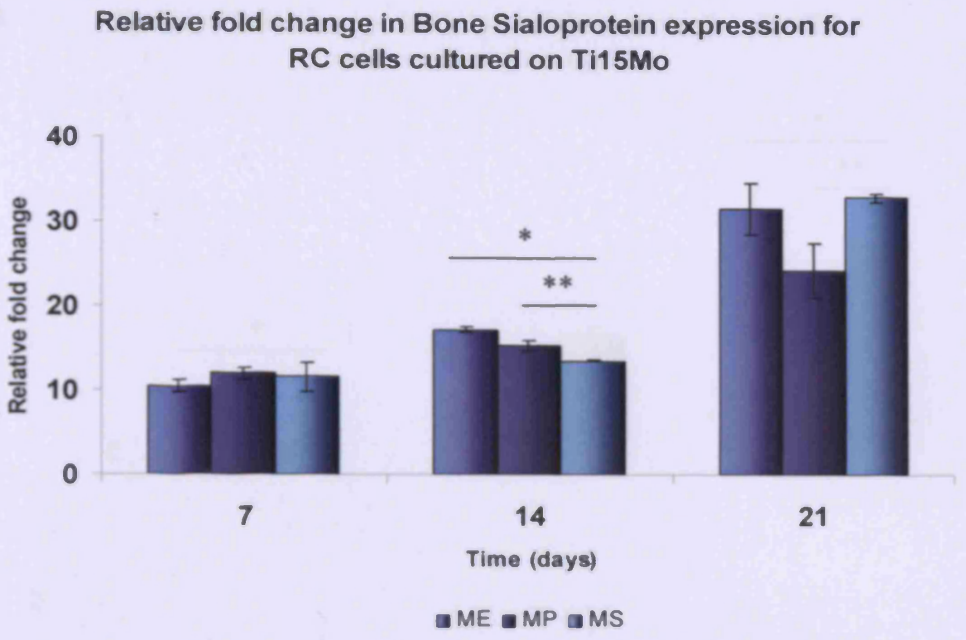

Figure 4.16C: ANOVA indicated that surface polishing significantly influenced BSP expression after 14 days culturing on Ti15Mo ($p<0.001$). Surface type had no significant affect on BSP expression after 7 ($p=0.644$) or 21 ($p=0.101$) days. Bonferroni post-hoc tests demonstrated that BSP expression was significantly increased on electropolished (*$p<0.001$) and paste polished ($p=0.028$) Ti15Mo surfaces compared to standard micro-rough samples after 14 days.**

Osteocalcin:

Univariate analysis of variance showed that cpTi surface type had a significant influence on OCN expression after 7 ($p=0.004$), 14 ($p<0.001$) and 21 days ($p<0.001$) culturing (figure 4.17A). Bonferroni post hoc tests revealed that after 7 days OCN expression was significantly reduced on electro- ($p=0.030$) and paste polished ($p=0.004$) cpTi samples compared to standard micro-rough cpTi. Similarly, after 14 days, both electro- ($p=0.004$) and paste polishing ($p<0.001$) significantly reduced OCN expression compared to standard micro-rough cpTi samples. Furthermore, OCN expression was significantly decreased on paste polished ($p=0.012$) samples compared to electropolished cpTi samples after 7 days. After 21 days, OCN expression was also significantly reduced on electro- ($p<0.001$) and paste polished ($p<0.001$) cpTi samples.

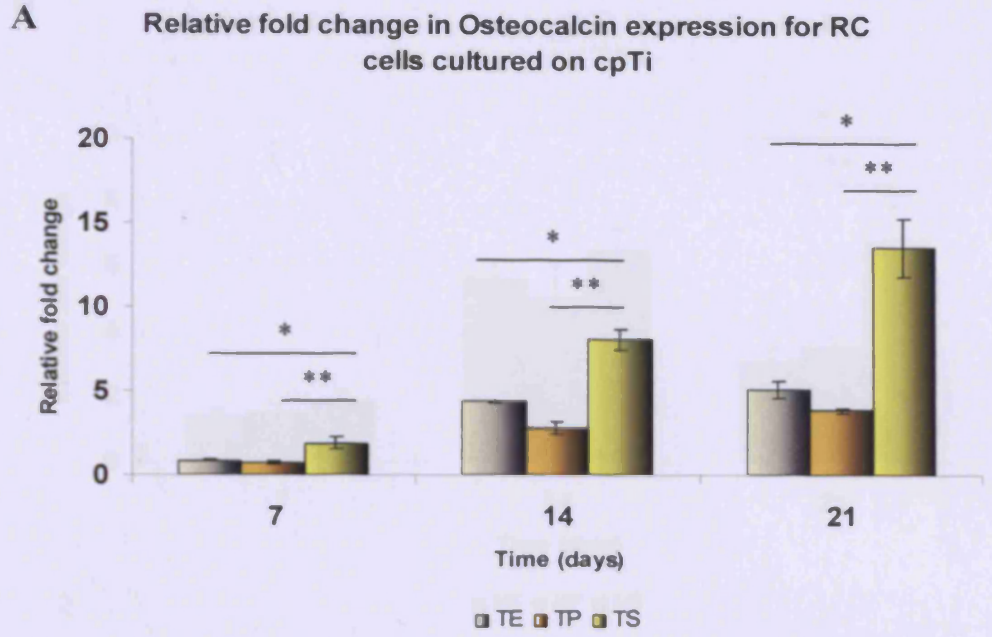

Figure 4.17A: ANOVA delineated that cpTi surface type had a significant influence on OCN expression after 7 (p=0.004), 14 (p<0.001) and 21 days (p<0.001) culturing. Bonferroni post hoc tests revealed that after 7 days OCN expression was significantly reduced on electro- (*p=0.030) and paste polished (p=0.004) cpTi samples compared to standard micro-rough cpTi. After 14 days, both electro- (*p=0.004) and paste polishing (**p<0.001) significantly reduced OCN expression compared to standard micro-rough cpTi samples. After 21 days, OCN expression was also significantly reduced on electro- (*p<0.001) and paste polished (**p<0.001) cpTi samples.**

Univariate analysis of variance revealed no significant affect of TAN surface type in OCN expression after 7 (p=0.554) or 14 (p=0.453) days culturing (figure 4.17B). However, TAN surface type was observed to have a significant influence on OCN expression after 21 days (p=0.004). Bonferroni post hoc tests demonstrated a significant reduction in OCN expression for electro- (p=0.006) and paste polished (p=0.017) samples compared to standard micro-rough TAN samples after 21 days.

B

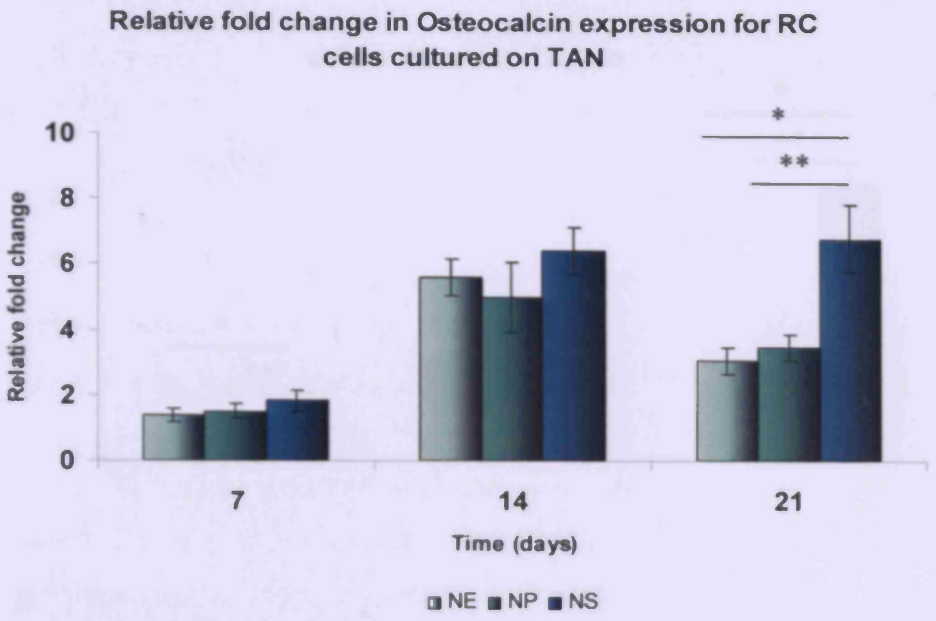

Figure 4.17B: ANOVA showed that TAN surface type was observed to have a significant influence on OCN expression after 21 days (p=0.004). Bonferroni post hoc tests demonstrated a significant reduction in OCN expression for electro- (*p=0.006) and paste polished (p=0.017) samples compared to standard micro-rough TAN samples after 21 days. No significant affect of TAN surface type in OCN expression after 7 (p=0.554) or 14 (p=0.453) days culturing.**

For Ti15Mo samples, univariate analysis of variance results suggest that surface type had a significant influence on OCN expression at 7 ($p=0.002$) and 21 ($p<0.001$) days but not 14 days ($p=0.277$). Specifically, Bonferroni post hoc tests demonstrated a significant reduction in OCN expression after 7 days for electro- ($p=0.016$) and paste polished ($p=0.002$) Ti15Mo samples compared to the standard micro-rough control (figure 4.17C). Similarly, at 21 days, a significant reduction in OCN expression on electro- ($p<0.001$) and paste polished ($p<0.001$) samples was noted compared to standard micro-rough Ti15Mo samples.

C

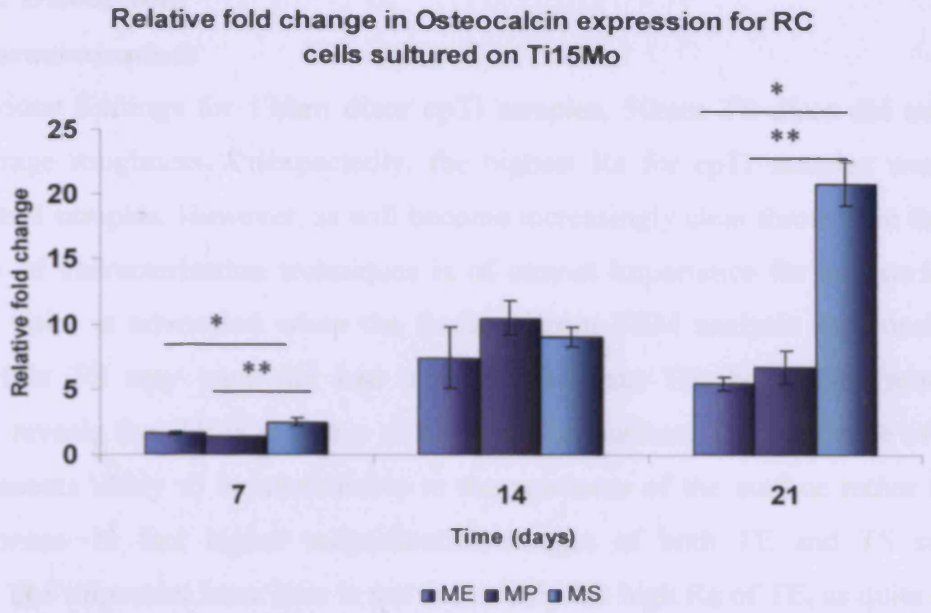

Figure 4.17C: ANOVA showed that Ti15Mo surface type had a significant influence on OCN expression at 7 (p=0.002) and 21 (p<0.001) days but not 14 days (p=0.277). Bonferroni post hoc tests demonstrated a significant reduction in OCN expression after 7 days for electro- (p=0.016) and paste polished (p=0.002) Ti15Mo samples compared to the standard micro-rough control a significant reduction in OCN expression on electro- (p<0.001) and paste polished (p<0.001) samples was noted compared to standard micro-rough Ti15Mo samples after 21 days.

Chapter 4: Discussion:

Surface characterisation:

Unlike previous findings for 13mm discs cpTi samples, 50mm TS discs did not have the highest average roughness. Unexpectedly, the highest Ra for cpTi samples was noted for electropolished samples. However, as will become increasingly clear throughout the inclusion of a variety of characterisation techniques is of utmost importance for any surface related study. This point is advocated when the findings from SEM analysis are considered. For instance, while TS may have not had a higher Ra than TE the surface morphological information reveals that TE is in fact a much smoother surface. The incidence of the higher Ra for TE seems likely to be attributable to the waviness of the surface rather than actual micro-roughness. In fact higher magnification images of both TE and TS support this conclusion. The important issue here is not necessarily the high Ra of TE, as quite clearly this is actually a smooth surface compared to the jagged irregularly orientated TS surface morphology, but that of the effect of the surface on a cell level. Based on this one could suggest that the morphology of the TE surface is sufficiently smooth not to induce a cellular response akin to TS. Although pits are evident throughout the TE surface, with higher magnification it becomes clear that these fall outside spectrum of micro-roughness that is required for the roughness-dependent response reported for TS. This will be expanded upon later within the discussion section, but suffice is to say that essentially cells will not react with micro-roughness that have larger dimensions than themselves (Richards, 2008), therefore if, as in this case, the pits present on TE are larger than the osteoblast itself then the osteoblast will react to the surface as smooth, since within this pit very few, if any micro-discontinuities are present.

On the other hand, paste polishing appears to successfully reduce the Ra associated with the commercially available TS surface as well as producing a surface a smooth surface with a nano-topographical weaved appearance. This finding may be noteworthy, as while the influence of nano-topography *in vivo* may be negligible its effect *in vitro* is well established (Dalby *et al.*, 2004, 2006; Biggs *et al.*, 2007 a & b). In our laboratory we have previously shown that culturing of primary human osteoblasts (HOB) on ordered nano-pits led to disruptive effects on adhesion formation; specifically they induce decreased adhesion formation and a reduction in adhesion length. In contrast, when a degree of controlled disorder was included in the form of near-square arrays, findings indicate that there was an increase in focal adhesion formation and size. The morphological conformation of the pits

also contributed to differences in cellular spreading. Specifically, ordered arrays negatively influenced HOB cell spreading and induced an elongated cellular phenotype indicative of increased motility, while near-square nanopit samples induced HOB spreading (Biggs *et al.*, 2007a). Thus, alterations in gene expression for cells cultured on TP or any similarly affected sample may be influenced not only by the reduction in micro-roughness but also by the micro- and nano-topographical features of the surface. In fact recently, Nguyen and colleagues (2007) demonstrated an up-regulation in genes involved in the cell cycle, DNA replication, cell proliferation, and signalling transduction pathways for nano-porous alumina membranes with pores of various sizes (200nm and 20nm).

With regards to TAN, in line with expectations, the commercially available micro-rough TAN surface had the highest mean average roughness (Ra) of all the TAN samples studied. This is supported by the SEM images which clearly show the characteristic undulating beta-phase micro-spiked morphology, previously outlined in chapter 2. Polishing of this TAN surface produces interesting results. Similar to observations made for NE and NP samples in chapter 2, paste polishing appears to reduce the Ra of the TAN surface more successfully than electropolishing. However, again similar to chapter 2, SEM analysis reveals NP as being 'rougher' surface morphologically than NE, while quantitative data from WLP measurements contradict this finding as was the case for both samples in chapter 2 also. Another similarity to previous findings is the fact that compared to NE; the NP surface has almost half the Ra (0.42 and 0.29μm, respectively). This discrepancy between quantitative WLP results and qualitative SEM analysis may be attributable to the observation that while the niobium rich β phase inclusions present on the surface NP are clearly more apparent than those of NE the actual base material of titanium is relatively void of discontinuities. On the contrary, electropolishing reduces the degree the niobium rich β phase project out from the surface hence producing a wavy surface, which as seen previously for other electropolished samples directly contributes to the increasing the perceived Ra.

With regards to MS, both WLP and SEM analysis support the conclusion that this surface has an extensive micro-roughness. The variations in depth and width of the undulations are most likely a result in the selective degradation of the softer titanium phase of the alloy giving the micro-rough appearance archetypal of commercially available MS. As was the case with cpTi and TAN, paste polishing Ti15Mo samples appears to produce a smoother surface than electropolishing. As mentioned previously in chapter 2, paste polishing is a mechanically

abrasive technique thus the hardness of the component elements of a material will directly contribute to the efficacy of a particular polishing treatment. As molybdenum is a harder material than titanium (described in chapter 2) effectively a higher degree of abrasion is possible when paste polishing Ti15Mo, as a higher frictional force is generated between the material and the mechanical processing. A similar nano-topographical appearance to TP is evident for the MP sample and again one has to consider the potential influence this will have on a cell, *in vitro*. On the other hand, as observed for the other electropolished samples, electropolishing of Ti15Mo does not reduce the Ra to any significant extent. However, similar to NP and TP, with SEM analysis the waviness of the surface becomes apparent. Similar to TE and NE, the actual dimensions of the pits contained within the surface are much larger and shallower compared to those of the standard counterpart. The occurrence of the waviness associated with the electropolished samples may be in part attributable to the efficacy of the polishing technique itself. For instance, the relatively high conductivity of titanium would lead itself to be more susceptible to electro-polishing than the lesser conductive material of T15Mo. This would contribute perhaps to the morphological differences observed for ME as titanium would be selectively removed at a higher rate than Ti15Mo. Another consideration is that the material itself may not be homogenous; hence areas of the samples may be less conductive than others, also producing the surface waviness described.

Analysis of genotype:

A myriad of studies investigating alterations in cellular behaviour patterns such as adhesion, morphology, DNA synthesis, integrin and extracellular matrix expression and enzyme activity have been carried out to elucidate the finer elements of the osteoblast response to materials used in fracture fixation. However, changes in molecular events such as gene expression that occur at the cellular level during bony integration are largely undetermined. Nevertheless, some previous studies have implicated the influence of surface micro-topography in preosteoblast lineage determination (Schneider *et al.*, 2004) and its affect as potentially enhancing osseointegration (Schneider *et al.*, 2003; Masaki *et al.*, 2005; Isa *et al.*, 2006; Guo *et al.*, 2007) and in particular the identification of perceived 'roughness response' genes which are postulated to be differentially expressed on surfaces of varying micro-roughness' (Brett *et al.*, 2004; Arcelli *et al.*, 2007). Thus, here we have employed real-time PCR technology to elucidate the influence of surface polishing on a molecular level, for potentially reducing excessive bony over-growth for clinically available internal fracture fixation devices destined for removal.

One of the main findings from these results suggest that surface polishing appears to target the events relating to terminal differentiation as OCN mRNA levels were markedly reduced for both electropolished and paste polished samples, regardless of material type. OCN is to date the only 'osteoblast specific' marker as it is synthesised, secreted and deposited by differentiated osteoblasts during mineralisation. Therefore, it is no great surprise that as a measure of osteoblast activity on metal samples, OCN provides a reliable method for evaluating the effect of micro-topography. Although the precise functions of OCN are still under investigation previous studies have suggested a role for this protein in bone mineralization. However, unlike BSP, the main action of OCN appears to be delay HA nucleation (Hunter *et al.*, 1996), suggesting a role for this protein in inhibiting mineralisation. Advocating this notion is the observation that mice lacking OCN displayed increased mineralisation (Ducy *et al.*, 1996). Since decreasing OCN allows mineralisation to occur, these results, regardless of the events involved in their occurrence, would suggest that terminal differentiation occurs at delayed rate on polished samples compared to micro-rough counterparts. This is an extremely important point as this may elucidate the mechanism by which surface polishing effectively reduces bone over-growth compared to standard devices of similar material. In subsequent sections, analysis will be presented per material type in an effort to delineate possible reasons behind the consistent decrease in OCN observed for polished samples.

Commercially pure titanium:

Polishing of cpTi was shown in this study to significantly reduce terminal differentiation compared to standard micro-rough cpTi. Specifically, both electropolished and paste polished cpTi samples were observed to have significant decreases in OCN expression at all time point's studied. Therefore, as mentioned previously, terminal differentiation on standard cpTi appears to occur at an accelerated rate compared to polished cpTi samples. Some indications as to why this may be occurring arise from data for the other genes of interest studied. For instance, for polished cpTi samples, early differentiation events and initiation of mineralisation appear affected compared to standard cpTi samples. This is supported by the significant decrease in osterix expression noted for polished samples after both 7 and 14 days culture periods. While regulation mechanisms are still relatively unknown, genetically modified mice lacking the zinc-finger transcription factor Osterix (osx) have revealed the importance of this factor for osteoblast differentiation. Specifically, osx-deficient mice display an absence of osteoblasts and consequently, defective bone formation (Nakashima *et*

al., 2002). However, Cbfa-1 is still expressed in osx-deficient mice indicating that this factor acts downstream of Cbfa-1. This may also partly explain why Cbfa-1 expression on polished cpTi samples appeared relatively unaffected while osterix was significantly decreased. However, given the influence of Cbfa-1 as a 'master' regulatory gene for controlling osteoblast commitment and differentiation through its ability to bind to the osteoblast specific element (OSE) promoter of major bone matrix genes such as COL1, BSP and OCN (Ducy *et al.*, 1997; Komori *et al.*, 1997; Otto *et al.*, 1997), it is noteworthy that its expression is not affected given the decrease in BSP and OCN. It is possible that other transcriptional regulators are responsible for this observation as Cbfa-1 is not the only transcriptional control element for expression of these genes. Additionally, different isoforms of Cbfa-1 may also potentially induce higher up-regulation of specific bone matrix genes compared to others. For instance, Harada and colleagues (1999) have previously shown that the stimulatory affect on COL1 mRNA is not markedly different for Cbfa-1 type I, II or III isoforms. In contrast, while all three isoforms induced expression of OCN, type II Cbfa-1 isoform more potently induced OCN expression. Since the interaction between $\alpha 2\beta 1$ integrin found on the osteoblast surface and COL1 activates the phosphorylation of Cbfa-1 (Xiao *et al.*, 1998) and is required for activation of Cbfa1 and induction of osteoblast-specific gene expression, this may also explain why no difference in COL1 expression was noted for cpTi samples. It may also be possible that through an alternative signalling mechanism independent of Cbfa-1 or through Cbfa-1 binding with a co-factor specific for OCN repression (Lamour *et al.*, 2007), OCN is decreased, therefore, terminal differentiation would occur at a later time on polished samples and therefore accounting for the genetic patterns observed for cpTi samples.

Further indications to support the notion that terminal differentiation is on-going on polished cpTi samples also comes from observations for ALP and BSP expression. Both genes have important roles in mineralisation initiation and apatite crystal growth and propagation, respectively. It has been proposed that the role of ALP in the bone matrix is to generate inorganic phosphate required for crystallisation of hydroxyapatite. However, recent studies have provided convincing evidence that a major function of tissue non-specific ALP in bone tissue involves hydrolyzing inorganic pyrophosphate to maintain a suitable concentration of this mineralization inhibitor, to ensure normal bone mineralization (Hessle *et al.*, 2002; Harmey *et al.*, 2004) The strongest evidence for the role of ALP in skeletal formation is presented in the disorder hypophosphatasia were there is a complete absence of cartilage and bone ossification due to a deficiency in tissue non-specific ALP (Whyte, 1994 for review)

resulting in rickets and osteomalacia. Biochemical analysis of this bone marker for cells cultured on various biomaterial surfaces have suggested that ALP activity is increased on micro-rough surfaces (Boyan *et al.*, 2001). This finding has also been advocated with mRNA data for similar surfaces (Masaki *et al.*, 2005). These findings appear to be in agreement to some extent with results for ALP expression for cpTi samples. Specifically, we showed that ALP expression is significantly decreased on polished cpTi samples after 14 days culturing. Therefore, given the information on this factor, these results would suggest that in correlation with data accrued for OCN expression, the process of mineralisation on polished samples is occurring at a slower rate compared to standard cpTi, which after 14 days is already producing increased levels of mineralisation inhibitor for progression into terminal differentiation. In contrast, polished samples have reduced levels of ALP indicating that there may be a reduction in the hydrolysis of pyrophosphate; hence mineralisation is permitted to continue. This supports observations that OCN is also reduced on polished samples.

Bone sialoprotein is one of the principal non-collageneous proteins found in bone and since it is highly expressed in mineralised tissues many studies have consequently focused on the potential function of this protein in the nucleation and growth of apatite crystals (Hunter & Goldberg, 1993). However, it has been shown that dependent on structure and concentration BSP has also the ability to inhibit apatite crystal formation (Stubbs *et al.*, 1997). Given that BSP functions in apatite nucleation and growth, the significant decrease observed in this gene on polished cpTi samples after 14 days culturing compared to standard cpTi, would also suggest that events directly related to mineralisation are occurring sooner on standard samples compared to polished cpTi. This finding for BSP expression is in disagreement with results accrued by Maskai and colleagues (2005) and Isa and co-workers (2006) for human palatal mesenchymal cells cultured on cpTi samples with average roughness' of approximately 1.2μm. However, in contrast to this study, both groups included relatively early time points for analysis (72 hour for Masaki *et al.*, 2005; 1, 3 and 7 days for Isa *et al.*, 2006) and since the action of this gene involves events related to initial mineralisation it is possible that the time involved for these studies was not sufficient enough to encompass induction of BSP activity.

Interestingly, events relating to mineralisation do not appear to be completely hindered by surface polishing as peaks in ALP and BSP are observed after 21 days culturing. Therefore, one can speculative that given the week delay compared to standard cpTi for peak increase of these factors, that OCN expression would also peak approximately one week later.

Titanium-6%Aluminium-7%Niobium:

Similar to cpTi samples, surface polishing of TAN was found to significantly reduce OCN expression. However, unlike cpTi samples, this decrease was most evident after 21 days culturing, indicating a material dependent response to some extent. In this case, surface chemistry is undoubtedly a major determining factor for the differing genetic responses observed.

The influence of surface chemistry for titanium and its alloys is largely attributable to the oxide layer. The composition, the stability and the thickness of this layer will directly affect initial attachment and conformation of proteins. It is these initial protein-metal interactions that are believed to prime the material for subsequent cell phenotypic and genotypic performance (Meyer *et. al.*, 1988; Degasne *et. al.*, 1999; Yang *et. al.*, 2003) and as a consequence the ensuing tissue response. In context of this study, the role of surface chemistry cannot be excluded as previous studies have highlighted the influence of the chemical composition of a surface in modulating which integrins and extracellular proteins are expressed by osteoblasts upon attachment to a substrate (Gronowicz & McCarthy, 1996). As mentioned previously, these integrin-material interactions are essential for the expression of bone matrix proteins which determine the osteoblast phenotype. More recent studies have also shown that different functional surface chemistries control not only initial protein adsorption and production but also the differentiation potential of human mesenchymal cells (Curran *et al.*, 2006).

The biological responses evoked by surface chemical differences are not exclusive to *in vitro* studies. For instance, heat-treatment of Ss and Ti-6%Al-4%V has been shown to alter the oxide thickness and chemical composition of these materials which when implanted into the femur of rats was observed to increase their potential for osseointegration (Hazan *et al.*, 1993). Larsson and colleagues (1996) also showed that both oxide thickness and surface topography had a synergistic influence on the rate of bone formation in rabbit cortical bone up to 6 weeks *in vivo*.

As previously mentioned, the $\alpha 2\beta 1$ integrin-COL1 interaction has been shown to have a major role in the control of osteoblast specific transcription and differentiation by initiating phosphorylation of Cbfa-1 (Xiao *et al.*, 1998). Like any matrix producing cell osteoblast

precursors must secrete a collageneous matrix before they will differentiate and subsequently they must be capable of monitoring the composition of the matrix it is producing, as well as adapting its composition in response to changes in the mechanical niche. Collagen type I is the most abundant protein in bone matrix. Evidence for the role of collagen I in osteoblast differentiation comes from studies in which collagen synthesis has been inhibited which results in complete hindrance of osteoblast differentiation (Quarles *et al.*, 1992). Furthermore, *in vivo*, animals deficient for vitamin C have severely reduced bone formation and osteoblast differentiation, as assessed by the reduction in expression of osteocalcin (OCN) and alkaline phosphatase (ALP) mRNA (Togari *et al.*, 1995; Mahmoodian *et al.*, 1996). Thus, the extracellular matrix (ECM) is an important regulator of the osteoblast differentiation pathway. For TAN polished samples it appears that these events are potentially influenced as at 7 and 14 days both polishing methods resulted in a significant reduction in COL1 expression compared to standard TAN samples. This decrease was also evident after 21 days although was found only to be significantly decreased on electropolished TAN samples. However, the significant reduction in COL1 mRNA for polished TAN samples did not appear to affect subsequent activation of Cbfa-1. This finding is interesting given that BSP and OCN expression are altered on polished samples, indicating that other regulatory elements may be involved. Support for this hypothesis also comes from results accrued for ALP and osterix expression. While ALP expression was clearly increased on polished samples compared to standard TAN after 21days culturing, these differences were not found to be significant, however this result implies that initiation of mineralisation may be occurring at a slower rate on polished TAN samples, hence the later introduction of ALP and subsequently the necessary reduction in OCN. Furthermore, osterix expression was also found to be significantly increased on polished TAN samples compared to standard TAN after 21 days culturing, supporting the notion that cells on polished samples are still undergoing early changes related to differentiation and initiation of mineralisation, by the stage terminal differentiation is induced in cells on standard samples. This may be in part due to slower ECM production and maturation which would reduce the quantity of fibrils available as future sites of mineralisation, and may also account for differentiation occurring at a later point on polished samples.

Titanium-15%Molybdenum:

Similar to cpTi and TAN samples, OCN expression was also significantly affected by surface polishing Ti15Mo. Specifically, at both 7 and 21 days a significant reduction in OCN expression was noted for both polished Ti15Mo variants compared to standard samples. This decrease in OCN expression on polished Ti15Mo samples may be in part explained by the significant reduction also observed in Cbfa-1 expression for these samples compared to standard Ti15Mo after 14 days culturing. As previously outlined, much of the influence of Cbfa-1 on bone formation relies on its ability to regulate the major bone matrix genes COL1, BSP and OCN through binding to the OSE promoter of these genes. However, despite the essential role of Cbfa-1 in osteoblast commitment more recent studies have shown that this gene is not vital for sustaining expression of the major bone matrix genes in mature osteoblasts (Marauyama *et. al.*, 2007). In fact, it appears that persistent expression of Cbfa-1 negatively influences osteoblast terminal differentiation as overexpression of Cbfa-1 in mice results in osteopenia de to a reduced number of mature osteoblasts (Liu *et al.*, 2001). The role of this gene also appears to extend into adulthood skeletal regeneration as recent studies have also elucidated the role of this gene in bone regeneration via similar transcriptional mechanisms involved during embryogenesis (Ferguson *et al.*, 1999; Tu *et al.*, 2007) and have displayed potential use of this gene for tissue engineering applications (Gordeladze *et. al.*, 2008; Sakai *et al.*, 2008).

However, COL1 expression was not decreased by polishing of Ti15Mo, in fact after 7 days both polished Ti15Mo samples had increased COL1 expression compared to standard Ti15Mo, indicating that regulation of Cbfa-1 may result from alternative genetic signalling mechanisms or from hormonal or growth factor control (Marie, 2008). Cbfa-1 binding with a co-factor specific for OCN repression may also be an alternative explanation (Lamour *et al.*, 2007). Alternatively phosphorylation of Cbfa-1 interaction with COL1 may be more efficient in downstream activation of master transcription factors such as cAMP regulatory element binding 2 (CREB2) for example, which has been shown to interact with Cbfa-1 to regulate the transcriptional activity of OCN.

Interestingly, BSP expression was observed to be significantly increased on both polished Ti15Mo samples compared to standard Ti15Mo after 14 days culturing, indicating that apatite crystal nucleation and growth are induced on these samples. This type of peak in BSP expression was not observed for standard Ti15Mo samples; however OCN expression is

increased on standard samples after 21 days which would seem to suggest that mineralisation has been completed on these samples. Therefore, it may be that the peak expression of BSP on standard TAN samples was just not encompassed by the time points studied, and in fact this peaked expression may have occurred prior to 14 or 21 days. Initiation of mineralisation does not seem affected since ALP expression was similar for all TAN samples over time. The increase in BSP for polished samples at 14 days may be an indication of on-going mineralisation as previously suggested, hence the reduced OCN expression observed for these samples after 21 days culturing compared to standard TAN samples.

General points of discussion:

An important consideration for the interpretation of these results is the suitability of the cell model and the maturation stage of the cell. The biological relevance of the rat calvarial osteoblast cell model has been tested extensively structurally (Nefussi *et al.*, 1989; 1991) and biochemically (Collin *et al.*, 1992). Additionally, the temporal genetic expression of these cells *in vitro* has been highly characterised (Lian & Stein, 1992) and suggested to be consistent with expression of cells at different stages of differentiation *in vivo* (Chen *et al.*, 1992) as well as during foetal calvarial development (Machwate *et al.*, 1995). However, despite the apparent appropriateness of this cell model for the investigation of sequential expression of the osteoblast phenotype, some considerations for data extrapolation exist.

For instance, the method of intramembranous ossification of rat calvarial cells differs greatly from that of endochondral ossification employed by long bones. For internal fracture fixation the vast majority of fracture sites would involve long bones hence would involve endochondral ossification. Therefore, the molecular mechanisms involved with bone regeneration undoubtedly differ to some extent. Moreover, cellular heterogeneity from isolation must also be considered. Evidence from rat calvarial cell bone nodule assays indicate that at least 2 populations of osteoprogenitors exist. One subpopulation of rat calvarial osteoblasts appears to have a default pathway that renders them capable of differentiation *in vitro* leading to a mature osteoblast phenotype. In contrast, the second subpopulation appears to be an inducible osteoprogenitor population. That is, under certain *in vitro* culturing conditions such as the addition of growth factors or steroids such as dexamethasone, they can be induced to undergo osteoblastic differentiation (Aubin, 1999).

Interestingly, intercellular heterogeneity in genetic profiles expressed by rat calvarial osteoblasts appears to exist and this heterogeneity appears to span the different stages of

differentiation. In fact when individual osteoblasts from 21 day foetal rat calvaria were studied only ALP and parathyroid hormone/parathyroid hormone receptor protein appeared to be ubiquitously expressed by all osteoblasts *in vivo*. However, other bone matrix related genes such as BSP, OCN, c-fos and msx-2 were differentially expressed at both mRNA and protein levels only in a subset of osteoblasts. This expression was further dependent on the maturational state of the bone and the age of the osteoblast, its microenvironment, as well as its location of origin (endocranium or ectocranium). Thus, indicating that histologically identical, differentiated, cuboidal matrix synthesising osteoblasts are molecularly heterogeneous.

It is also a possibility that the size of cells, shown in the previous chapter to range from 20-50μm+ with SEM, may negate many of the effects of surface micro-topography. This concept is supported by recent studies which have specifically focused on identifying the functional range of surface micro-topography that remains applicable for cell-material interactions. Dalby and colleagues (2004) have shown *in vitro* that surface features as small as 10nm are sensed. However, the applicability of this finding in an *in vivo* situation is questionable considering that many other factors would induce prominent responses. Richards (2008) suggests that an 'effective roughness spectrum' exists for cells; within which cells would optimally interact with internal fixation biomaterials. Based on previous work within our laboratory this spectrum has been identified to be within the range of approximately 0.2 μm to 2μm. Others have shown that cellular reactions to microtopography are negated by approximately 6 μm (Ansleme *et al.*, 2007) however, the efficacy of cellular stimulation at this point becomes subsidiary as the dimensions of the surface increase. While Richards (2008) acknowledges the fact that topographies below 0.2 μm will evoke certain biological responses *in vitro*, he limited the roughness spectrum at this point as cellular/tissue responses below this threshold have not been observed *in vivo*.

Another interesting outcome from this study is the superior osteoinductive nature of Ti15Mo as a material, even in comparison to other materials such as cpTi and TAN, known for the high affinity that bone has to them. In this study, we observed that for all genes of interest, Ti15Mo induced the highest fold change in expression. While surface polishing was shown to significantly reduce this affect, even polished Ti15Mo samples induced a high rate of up-regulation of the bone markers studied, relative to cpTi and TAN samples. Therefore, while this study revealed that Ti15Mo may not be the optimal material for temporary internal fixation devices, its potential use in other applications, such as fixation in osteoporotic bone,

where the issue of bone quality and quantity is an issue, has to be considered. Furthermore, for permanent fixation devices, where rapid osseointegration is required for structural integrity of the device is required, Ti15Mo appears to be a highly desirable material. However, the limited resources and subsequent cost of Ti15Mo may be considered potential limitations to the use of this material in wide-spread internal fixation.

Interestingly, despite the marked reduction on average roughness and surface micro-topographical features of the experimental surfaces, that all polished surfaces still responded differently compared to Ss. As will be shown in later chapters this effect is also translated *in vivo*. Again differences in the surface oxide thickness and composition could be responsible for these observations. It is well known that the thickness of Ss oxide layer is less than cpTi and its alloys and as a consequence does not undergo repassivation as readily as cpTi and its alloys, thus rendering Ss vulnerable to metal ion release (Disegi, 1998a). Considering the many known toxic elements such as iron, chromium, cobalt and nickel contained within the alloying elements of Ss, this is a distinct biological disadvantage. Thus, one must also be mindful of extrapolating *in vitro* results to an *in vivo* situation. For the most part Ss performs in a manner which theoretically would be a desirable response as far as reducing bony over-growth is concerned. However, in a clinical environment this material is considered inferior compared to cpTi and its alloys with regards to biocompatibility, modulus of elasticity, strength and imaging quality.

Chapter summary:

Investigating changes in genotypic expression of key regulators of the osteoblast phenotype due to alterations in surface microtopography provides valuable information into the regulatory mechanisms involved in bone regeneration, and osseointegration at the bone-implant interface. This information is especially important in delineating the influence of surface polishing for reducing excessive bony overgrowth for ease of removal of internal fixation devices. While the efficacy of surface polishing *in vivo* for easing removal of cortical screws and intramedullary nails will become apparent in subsequent chapters, the main focus of this chapter was elucidation of the cellular mechanisms behind this affect. We have shown using real-time PCR for investigating changes in mRNA levels of several essential factors involved in bone formation and regeneration that surface polishing does not negatively influence initial molecular events involved in recruitment, differentiation and initial mineralisation of osteoblasts and their matrix. Importantly, we have also identified the value of OCN as a sensitive, reliable and reproducible marker in osteoblast-biomaterial interactions, as indications of delayed terminal differentiation for cells on polished samples have been observed. For cpTi, TAN and Ti15Mo polished samples the affect of polishing appears to target terminal differentiation while TAN polished samples principally appear to influence upstream events involved in matrix production which are postulated to interfere with subsequent downstream signalling cascades. While previous studies of this kind have focused intently on defining potential enhancers of osseointegration, this is the first time that data has been presented regarding alterations on a cellular level for genetic control of phenotype for osteoblast cells cultured on polished samples directed at reducing bony overgrowth for ease of device removal. Results indicate that both micro-topography and material type/surface chemical composition directly influences the expression profiles of osteoblasts cultured on these smoothened surfaces. Thus, *in vitro* surface polishing has shown the potential for reducing excessive bony over-growth by acting on a molecular level to influence bone matrix genes directly involved in osteoblast phenotype and bone regeneration. The effect of surface polishing will now be validated *in vivo* in subsequent chapters, which assess the influence of surface polishing for reducing the removal torque required for clinically available cortical screws within a locked plate system and intramedullary nails, which are both commonly used devices in the application of internal fixation.

Chapter 5: Efficacy of surface polishing for locked plate constructs screw removal – an *in vivo* evaluation.

Abstract

Observations from our initial *in vitro* studies indicate that surface polishing may be a promising method for reducing bony over-growth. Of course ratification of this notion requires *in vivo* testing. Therefore, we have applied surface polishing technology to two clinically relevant internal fixation systems, namely locking compression plates and intramedullary nails, to assess if surface polishing holds potential for reducing implant removal related morbidity. Therefore, this chapter first focuses on the promise of surface polishing for removal of cortical screws from a locked compression plate system. Specifically, we investigated removal torque and percentage of bone contact for electropolished, paste polished and standard TAN cortical screws from electropolished, paste polished and standard cpTi plates, respectively, with stainless steel screws and plate included as a control system. Constructs were implanted in a bilateral non-fracture sheep tibiae model for 6, 12 and 18 months. Results indicate that both polishing techniques significantly reduce the torque removal required for cortical screws compared to standard micro-rough cortical screws. Furthermore, histomorphometric analyses indicate that polished constructs have reduced bone contact however this was only found to be significantly different for paste polished screws. Interestingly tissue removal from polished constructs was approximately 4 times less than micro-rough systems which is highly relevant for clinical implant removal applications for reducing the additional costs and patient risks associated with superfluous surgery when complications are encountered.

Chapter 5 - Introduction:

The success and efficacy of plate fixation in orthopaedic applications is indisputable. However, once the process of recovery has occurred the function of these devices becomes redundant. So the age old predicament of the orthopaedic trauma surgeon arises – removal or retention of the construct? For the large part unfavourable symptoms such as pain, irritation and infection effectively solve this impasse (Rallis *et al.*, 2006; Theodossy *et al.*, 2006; Bakathir *et al.*, 2008). Thus despite divulging the patient to the dangers associated with a second procedure such as anaesthesia, re-fracture and neurovascular damage, the clinical decision to extract the device can be vindicated. However, in asymptomatic patients answering this dilemma has become controversial to say the least mainly because explicit indications for removal in this class of patients remain ambiguous and the long-term effect of metal retention is not fully understood.

Indications do exist to suggest that device retention is not ideal. Studies over the years have shown that subsequent to fulfilling its function a device can negatively affect the host by evoking foreign body responses that can give rise to complications such as delayed infections (Emel *et al.*, 2007; Highland & LaMont, 1985), allergic reactions (Summer *et al.*, 2007), implant breakage (Sommer *et al.*, 2005), device migration (Seipel *et al.*, 2001) and hindrance of skeletal maturity and growth (Togrul *et al.*, 2005). For hand applications the irritation of free gliding tendons due to contact with the plate is also of concern. Furthermore, the negative influence of metal ions and salts on adjacent tissues and organs has been well documented (Case *et al.*, 1994; Sommer *et. al.*, 2005; Kasai *et al.*, 2003; Keegan *et al.*, 2007). Regardless of debatable indications or contraindications for removal in adults, device extraction in children can further cloud the matter (Schmalzried *et al.*, 1991; Kahle, 1994; Alzahrani *et al.*, 2003; Peterson, 2005; Busam *et al.*, 2006). One such study reported a complication rate as high as 42% in forearm plate removal in children. Specifically re-fracture has emerged as particular concern accounting for a great deal of the complications encountered (Chapman *et al.*, 1989: Rosson & Shearer, 1991; Kim *et al.*, 2005).

Nevertheless, the potential negative outcome of device retention in children urges most surgeons to advocate removal. For bone fixation plates such as the locking compression plate (LCP) and the less invasive stabilisation system (LISS), insight to the difficulty encountered by surgeons when attempting implant removal has emerged (Figure 5.1). Two recent studies have emerged that clearly identify the issue regarding excessive bone in/on-growth for plating

systems, specifically LISS which is fabricated from standard micro-rough TAN. Hamilton and colleagues (2004) report that after just two weeks postoperatively (the patient showed signs of pullout of the top screws) they encountered difficulty in removing two proximal screws from the LISS plate. Subsequently, a further two weeks later the patient suffered a fracture above the plate. The decision was made to remove the plate and insert a supracondylar nail; however, the screws within the plate could not be removed despite many attempts. Consequently, the whole construct was extracted as a unit via the lateral femoral condyle. Interestingly, even *ex vivo* attempts to remove the nails failed.

Due to the distinct lack of literature on this subject it is somewhat difficult to decide if this is the status quo situation although others have presented data to support this notion (Saura, 2005; Sommer, 2006-Appendix A). However, what is definitely noteworthy is that the authors suggest that this 'successful' removal occurred mainly due to the osteoporotic nature of the patient. One has to question the difficulty involved for any surgeon removing this device in children or otherwise healthy adult patients given their normal bone density and the short duration involved to cause these difficulties.

Georgiadis and colleagues (2004) also report difficulties when removing LISS constructs 12-24 months post-implantation from three young patients. Specifically, the authors report the frequent (17%) stripping of LISS screws and for all three patients the authors had to resort to cutting the LISS plate to successfully remove it. In fact in many instances the screw extraction device itself broke, mostly likely as a result of the strong bone-metal contact and metal-metal contact of the implant material. Although the authors indicate that the stripped screws and not bone on-growth was the culprit for the failures encountered. Unfortunately, the authors fail to elucidate why they thought the screws stripped therefore the role of bony on-growth between the screw threads and up through the screw holes can not be overruled, as will be highlighted here.

One important question to be asked if attempts are to be made to solve this clinical problem which is not only time consuming but raises large demands on resources is: What factor(s) contribute to the excessive presence of bone at these sites? One major determining factor that has been identified is the distinct role of implant surface microtopography (Meredith *et al.*, 2007a & b; Biggs *et al.*, 2007a&b; Biggs *et al.*, 2008; Pearce *et al.*, 2008b; Schlegel *et al.*, 2008). By controlling this parameter we have previously shown that tissue integration

including fibrous tissue (Richards *et al.*, 2000a), bone (Pearce *et al.*, 2008b; Hayes *et al.*, 2008a) and capsule formation (Richards *et al.*, 2000a; Welton, 2007) can be controlled. Specifically in terms of bone contact we have shown that reducing the surface microtopography of the implant can directly reduce not only the percentage of bone contact to the device, in this case cortical screws (Pearce *et al.*, 2008b) and intramedullary nails (Hayes *et al.*, 2008a) but effectively reduces the force required to remove the device. Therefore, here we address the clinical problem associated with device removal in this case with LCP constructs. Specifically, we investigated the influence of reducing implant surface microtopography via polishing on reducing bone contact to LCP constructs, as well as assessing the influence of surface polishing for reducing the force required for their removal.

Figure 5.1. Bony in-growth to the plate hole of a LCP after implantation within a sheep during experimental study. Picture courtesy of the AO Research Institute.

Chapter 5 - Materials & methods:

Implants were provided by SYNTHES®. A 4-hole locking compression plate (LCP) approximately 51mm in length and 3.5mm diameter with self-tapping locking head monocortical screws (12mm) were employed in this study. The materials used were electropolished stainless steel (Ss) plates with Ss locking head screws as a control system; a standard, micro-rough cpTi (TS) plate with standard, micro-rough TAN (NS) locking head screws as a control system for osseointegration; and two experimental systems consisting of paste polished cpTi (TP) plates with paste polished TAN (NP) locking head screws; and finally, electropolished cpTi (TE) plates with electropolished TAN (NE) locking head screws (Figure 5.2). All cpTi plates and TAN screws were anodised as the final finishing process with the exception of the TE plates with NE screws. Prior to implantation, all implants were packaged individually, and steam sterilised at 134°C, for 20 minutes.

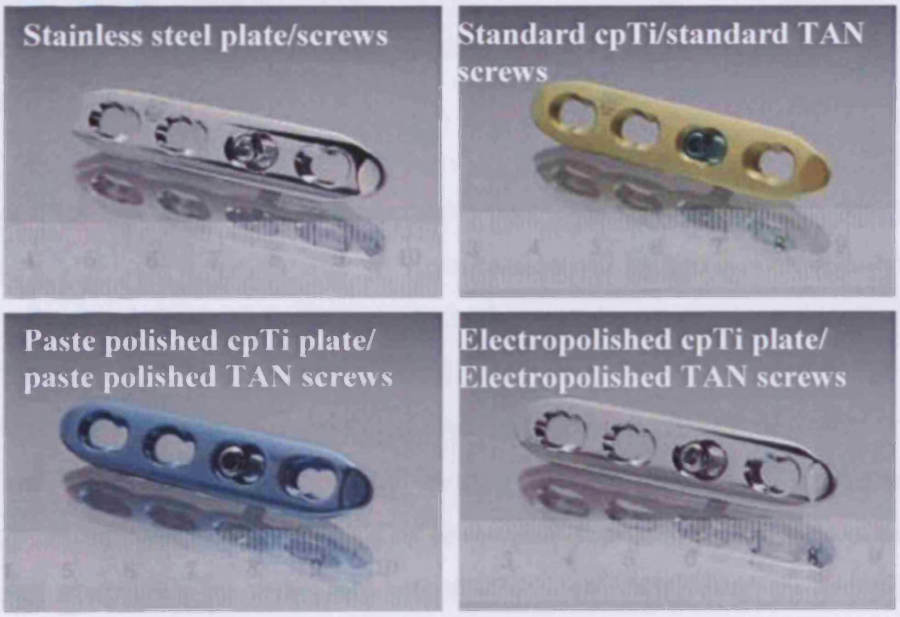

Figure 5.2. The locking compression plate (LCP) constructs used in this study. Listed on the images are the variations in materials and surface finishes used.

Surface characterisation:

The surface topography of each material was quantitatively measured with a non-contact white-light FRT MicroProf 200 Profilometer (Fries Research & Technology, Germany). Roughness average (Ra— arithmetic mean of the absolute values of all points of the profile) of three separate implants (2 measurements per implant) were measured from a 0.5x0.5 mm analysis area scan at a point density of 500 points/mm. Contact angle measurements for the LCP's were made using the Sessil drop method with the Drop Shape Analysis System (Contact Angle Measuring Instrument G10 and DSA 10 Control Unit, KRÜSS GmbH) and analysed using the Drop Shape Analysis 1.50 software (KRÜSS GmbH). Samples were placed in a preheated chamber (20°C) with an external water source to sustain a constant relative humidity. Using the computer controlled system a 20μl droplet of distilled water was dispensed onto the sample and quantified exactly 1 minute after dispensed using the analysis software. Contact angle was not preformed for the screws due to their small size and hence difficultly in collecting an accurate measurement. The morphology of the plate and screw surfaces was examined using a Hitachi S4700 FESEM. Images were taken in the secondary electron mode (SE) with an accelerating voltage of 5 kV, an emission current of 40μA and a working distance of 10-12 mm.

The chemical composition of the surfaces was assessed using X—ray photoelectron spectroscopy (XPS). XPS measurements were carried out by the Robert Mathys Foundation, Bettlach, Switzerland. Prior to surface analysis the samples were ultrasonically treated for 20 minutes with alkaline 3% Deconex 12PA (Borer Chemie, CH) followed by rinsing with deionised water and subsequently cleaned with ethanol for 10 minutes after which time the samples were once again ultrasonically treated for 20 minutes in ultra-pure water and subsequently rinsed with methanol in order to remove debris and potential contaminants from the packaging material. The samples were mounted on aluminium sample plates by using double sided electrically insulating sticky tape which is vacuum compatible. All spectra were recorded on a Kratos Axis Nova (Kratos Analytical, UK) using monochromatic AlKα radiation (1486.69 eV) produced at an anode power of 225 W (15kV, 15 mA), an electron take-off angle of 90° relative to the surface plane and an electron analyser pass energy of 80 eV. During analysis, the base pressure remained below 10^{-8} torr. For quantification, survey scans with a step width of 0.5 eV were performed on two spots of 300 x 700 μm^2 per sample. The spectra were acquired from 2 positions per sample. Data was evaluated with CasaXPS 2.3.10 (CasaXPS Ltd, UK) using relative sensitivity factors supplied with the instrument.

Surgical procedure:

Prior to its commencement, approval to perform this study was granted by both an internal institutional review board and the Cantonal Animal Ethics Committee (Graubünden #6/2006). Eighteen Swiss Alpine sheep were selected from a flock kept for orthopaedic research, such that size, shape, and age, were standardised as much as possible. A bilateral model was used consisting of two test constructs implanted on each tibia, (two plates, approximately 1 cm apart, were inserted in each tibia) and, therefore, each animal received each treatment implant. The location of implantation of the implants was randomised. Sheep were separated into 3 groups according to the timepoints for euthanasia; namely 6, 12 and 18 months after surgery.

Animals were anaesthetised (Diazepam (Valium ®) 0.3 mg/kg i.v. & Butorphanol (Morphasol®) 0.08 mg/kg i.v.; Thiopenthal (Penthotal®) 4-8 mg/kg i.v.; Isoflurane (approx 2% in oxygen: Oxygen flow rate was approx 0.5 L/min)), and placed in the appropriate lateral recumbency such that the operated limb was dependent (the animal was rotated into the opposite recumbency for operation of the second limb). Both tibiae were prepared for aseptic surgery. A skin incision approximately 12 cm was made over the medial aspect of the tibia and continued down to the bone. Care was taken to ensure that the periosteum remained *in situ* and was not damaged (Figure 5.3A). The implant insertion occurred in two stages. The first stage involved drilling the screw holes using a 2.7 mm drill bit with saline irrigation to prevent thermal necrosis, and placement of the plates and locking-head screws using a 1.5 Nm torque limiting screw driver. The most proximal and distal screws in each plate were inserted first (Figure 5.3B) followed by the two central screws (Figure 5.3C), to ensure central placement of the plate on the tibia (Figure 5.3D). The subcutaneous tissues were closed with absorbable sutures and the skin closed with stainless steel skin staples. A light adhesive bandage was placed over the medial aspect of each tibia to protect the wound from contamination during the recovery phase. This bandage remained for 5-7 days. Skin staples were removed 10-14 days post operatively. Each sheep was radiographed every 4 weeks for the duration of the study. The final radiographs were taken after euthanasia. Postoperative analgesia consisted of Caprofen (Rimadyl®; 4 mg/kg, i.m., q24h) for 5 days, and Buprenorphin (Temgesic®; 0.1 mg/kg, i.m., q8h) for 3 days. Sheep were euthanized at the appropriate timepoint (6, 12, 18 months post-operatively) with an overdose of Pentobarbital (Vetanarcol®). Subsequently, the soft tissues were harvested and major soft tissues removed. The tibiae containing the plates and screws were wrapped in saline soaked gauze to prevent dehydration. Tissues on and surrounding the plates were then carefully dissected to expose the

screw holes for torque measurements. For polished samples, this involved using a scalpel to remove the soft tissue adhering to the plate, and a K-wire to displace any tissue within the screw head, and plate hole. For standard samples, any soft tissue was also removed with a scalpel; however, bone had grown over the majority of the plate holes, and onto the plates, especially at the later time points, which required removal with a chisel after fixation within a vice

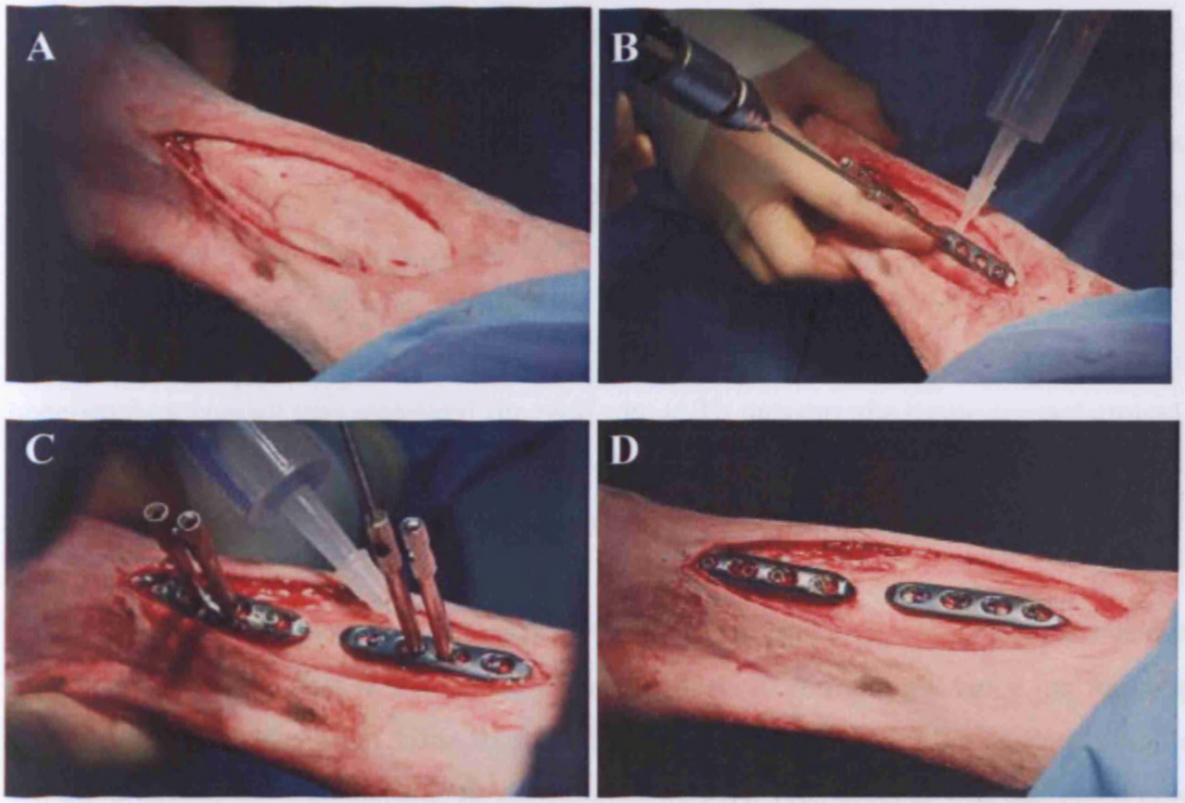

Figure 5.3 Plate and screw implantation. (A) A 12cm incision was made over the medial aspect of the tibia. (B) Screw holes were drilled with a 2.7mm drill bit with saline irrigation. The most proximal and distal screws in each plate were inserted first to ensure central placement. (C) The insertion of the central two screws were placed subsequently. (D) Shows the plates in place, approximately 1cm apart.

Torque measurements:

In surgery, after insertion of the screws to 1.5 Nm, the screws were immediately loosened with a torque measuring screw driver. This procedure aims to measure the frictional effect of the five surface topographies being investigated, before the additional effect of bone-on-growth. Measurement of removal torque force was also performed after 6, 12 and 18 months implantation, on three of the screws from each plate, using an instrumented screwdriver (Advanced Force Gauge, Mecmesin, United Kingdom). Tissue adhering to the screw head was removed to enable adequate screwdriver contact. The same operator was used to perform all of the torque removal tests.

Histological evaluation:

After euthanasia, and the removal of 3 of the locked screws (torque measurements), the plate containing the final screw was left *in situ*. Histomorphometric analyses were performed on the one intact screw from each plate to assess the amount of bone contact quantitatively. A segment of the plate was cut with the screw attached. The cut segments were fixed in 70% methanol for approximately 2 and half weeks. Subsequently dehydration of the samples was achieved by immersing the samples in increasing concentrations of ethanol (70%, 96%, and 100%) for 1 week per concentration. Samples were then placed in Xylol for 2 days prior to being embedded with methylmethacrylate (MMA). Sections were cut with an annular saw, ground (Exact Micro Grinding System, Gmbh), and polished to a thickness of approximately 100μm and stained with Giemsa and Eosin (Appendix H). Light microscopic images were taken using a Zeiss Axioplan microscope (Carl Zeiss, Göttingen, Germany). Using the computer software package AxioVision 3.1. (Carl Zeiss Vision GmbH, Germany), the direct bone-implant contact was measured for each screw. To measure the tissue contact around the screw, a line was drawn from the first screw thread to the last screw thread on the opposite side (yellow line, Figure 5.4) – this was thus deemed the region of interest.

Using the measurement option included in the software program, a curved line was drawn from the line of the first screw thread along the specific tissue type. Once the tissue type changed, for example, from bone to soft tissue, the line was discontinued and a new one started to denote the change (blue box, inset, Figure 5.4). This process was continued around the screw, until the line on the last screw thread was reached. Any area of the screw protruding into the medullary cavity was excluded from the quantitative analysis, but was included in the initial calculation of the total area of potential tissue contact on the screw (Figure 5.4, area denoted by red line). The normalised results were then expressed as a percentage of bone or soft tissue attachment to the screw.

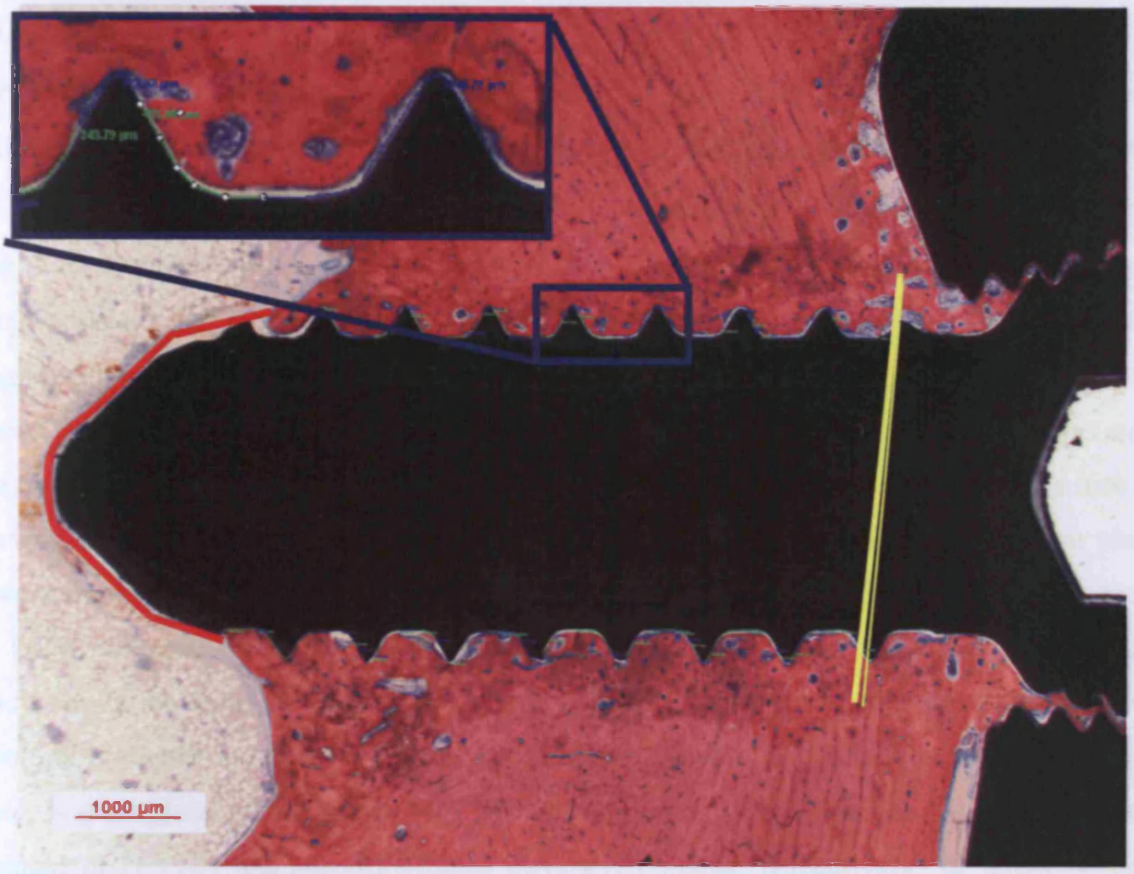

Figure 5.4. Representative image to show the process of histomorphometric analyses used in this study. Before measurement commenced, a line was drawn on the first and last screw threads (shown by yellow line). Subsequently, the bone and soft tissue contact to the screw was quantitatively measured by tracing their occurrence along the screw threads, within the region of interest (blue box inset showing the bone (green line) and soft tissue (blue line) contact). The area of the screw that penetrates the medullary canal, depicted by the red line, was calculated separately as it was not considered as soft tissue in the context of our calculations. Therefore, results are expressed as the percentage of bone, or soft tissue in contact with the screw.

Statistical analyses:

Statistical evaluations were made using SPSS for Windows Version 14.0 (SPSS Inc, Chicago, IL). Prior to analysis, normality and homogeneity were tested using Shapiro-Wilk test of normality and Levene's test for equality of variances, respectively. Maulchly's sphericity test was performed to validate the use of repeated measures ANOVA. The influence of the material as a within-subject factor, and time as a between-subject factor, upon removal torque, and percentage bone contact was analysed by repeated-measures ANOVA, using the Bonferroni post-hoc test for individual group comparisons.

Chapter 5 - Results:

Surface characterisation:

White light profilometry results (Figure 5.5) show that both paste polishing (Ra 0.22μm; NP) and electropolishing (Ra 0.52μm; NE) TAN screws produces a lower average surface roughness compared to the standard counterpart (Ra 1.04μm; NS) and compare positively to electropolished Ss screws (Ra 0.33μm). However, a high variation in average screw roughness was observed for all screw samples including the standard micro-rough TAN screws (NS) indicating that although surface polishing can essentially reduce the mean average roughness of the screw surface, the technique for the geometry and size of the locking screws used is not optimised. In contrast surface polishing of locking compression plates appears more reproducible with regards to surface micro-roughness. This is most likely due to the larger dimensions of the plates which afford themselves better to surface manipulation which is evident from the smaller deviations noted for the average surface roughness. Both polishing methods compare favourably to the 'gold standard' smooth orthopaedic surface of stainless steel plates (Ra 0.15μm) with average roughness' of 0.27μm and 0.18μm for paste polished cpTi (TP) and electropolished cpTi (TE) plates, respectively. In terms of cpTi locking compression plates, surface polishing is shown here to successfully and reproducibly reduce the mean average roughness consistent with clinically available standard micro-rough cpTi (TS) plates (Ra 0.79μm).

Results from contact angle measurements indicate that surface polishing does not alter the wettability of the LCP's to any considerable extent, as TS, TE and TP LCP's had contact angles of approximately 83° (Figure 5.6)

Analysis of the surface chemistry using XPS showed that neither electropolishing nor paste polishing (TE/NE; TP/NP) followed by subsequent anodisation affected the final surface chemical properties from the positive controls (TS, NS). As expected, the spectra for the cpTi plates and TAN screws are dominated by Ti and O due to the naturally occurring titanium oxide layer (Figure 5.7). The strong C signal has previously been shown to be present on high surface areas oxide films that have undergone atmospheric exposure and storage. Ca contamination is also detected on the surfaces most likely a result of contamination from handling. Other contaminants include N, Na and P. For TAN samples in addition to the dominant Ti and O intensities, the alloying elements are also present (Al and Nb). Analysis of (Ss) demonstrates the diversity of elements required for alloying of this sample.

SEM imaging supports the observations made with white light profilometry. The undulating surface associated with the micro-rough surface of TAN is clearly evident as are the niobium-rich inclusions associated with the beta-phase of this material (Figure 5.8A, white arrows). The micro-roughness associated with this material is clearly reduced with paste polishing (Figure 5.8B) as indicated by white light profilometry, and is advocated with SEM. Indeed, the characteristic beta phase particles are reduced so pertinently that they are not noticeably apparent. NE screws produced a higher average roughness compared to NP screws. However, SEM imaging shows that this is due to the waviness of the surface rather than perceived micro-roughness (Figure 5.8C). The Ss surface is extremely smooth (Figure 5.8D) which supports the initial observations of WLP.

As mentioned previously, the LCP's used in this study had more reproducible average roughness' compared to the locking screws used. Again SEM imaging advocates the conclusions drawn from WLP of these plates. Standard cpTi plates have the characteristic 'basket-weave' morphology associated with this material (Figure 5.9A). Grain boundaries are clearly evident as well as presenting varying orientations. Furthermore, the grains contain obvious nano-topographical features. WLP indicated that paste polishing and electropolishing of cpTi plates dramatically reduced the average surface roughness of this material. SEM imaging supports this conclusion as the paste polished cpTi plates had a very smooth appearance and minimal micro-topography, with the exception of processing marks (Figure 5.9B). Electropolishing of cpTi plates also appears to be highly successful at reducing the surface micro-topography associated with the cpTi plates and produces an extremely smooth almost flawless surface (Figure 5.9C) to the extent that TE plates reflect the success achieved with Ss electropolished plates (Figure 5.9D).

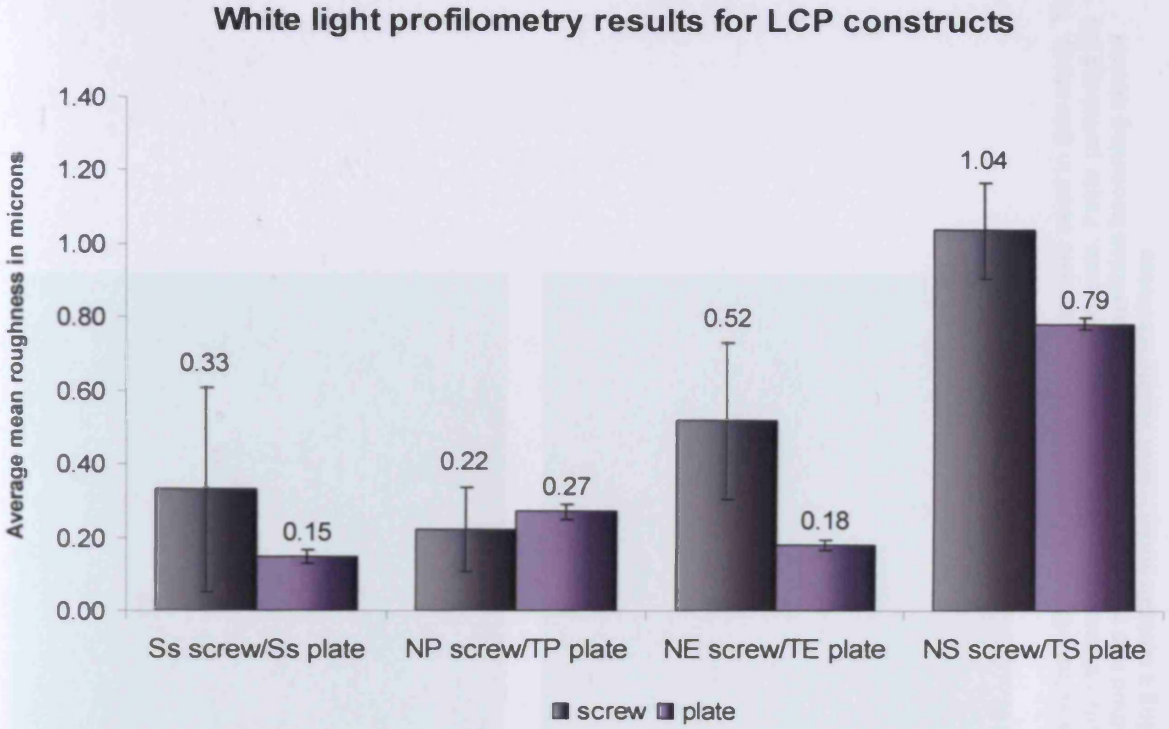

Figure 5.5. White light profilometry results for screws (grey) and plates (purple) from the LCP constructs included in this study. Polishing of the plates appears to produce more reproducible surface micro-topographies for all materials studied. In contrast, polishing of the cortical screws appears more difficult to optimise, most likely due to the smaller dimensions involved. Three randomly chosen screws and plates representing each material were used for WLP analysis. Two measurements from each implant were taken, resulting in a total of six measurements per implant.

	TS	TE	TP	Ss
C.A (°)	82	83	83	75
(±)	4.57	5.18	3.10	2.48

Figure 5.6. Contact angle (CA) measurements for all plate substrates. Polishing of the samples does not appear to alter the hydrophilicity of the samples to any considerable extent.

Plates	Ti 2p	O 1s	Al 2p	Nb 3d	C1s	Ca2p	N1s	NaKLL	P2p
TS	18.8	55.4	1.7	0.0	21.0	0.2	0.3	0.4	2.5
TP	15.5	48.8	0.0	0.0	31.2	0.2	0.6	0.3	2.2
TE	17.1	42.6	0.0	0.0	38.7	0.2	1.2	1.2	0.0
Screws									
NS	10.6	38.8	1.3	0.2	47.5	0.2	0.0	0.6	1.3
NP	12.2	42.8	1.7	0.3	40.7	0.2	0.3	0.6	1.7
NE	13.5	43.9	2.2	0.8	39.4	0.1	0.0	1.4	0.0

Figure 5.7. X-ray photoelectron spectroscopy results for the plates and screws used in this study. As noted previously fro 13mm samples, as anodisation is included as a final step during processing, no major differences in the chemical composition of the surfaces are noted.

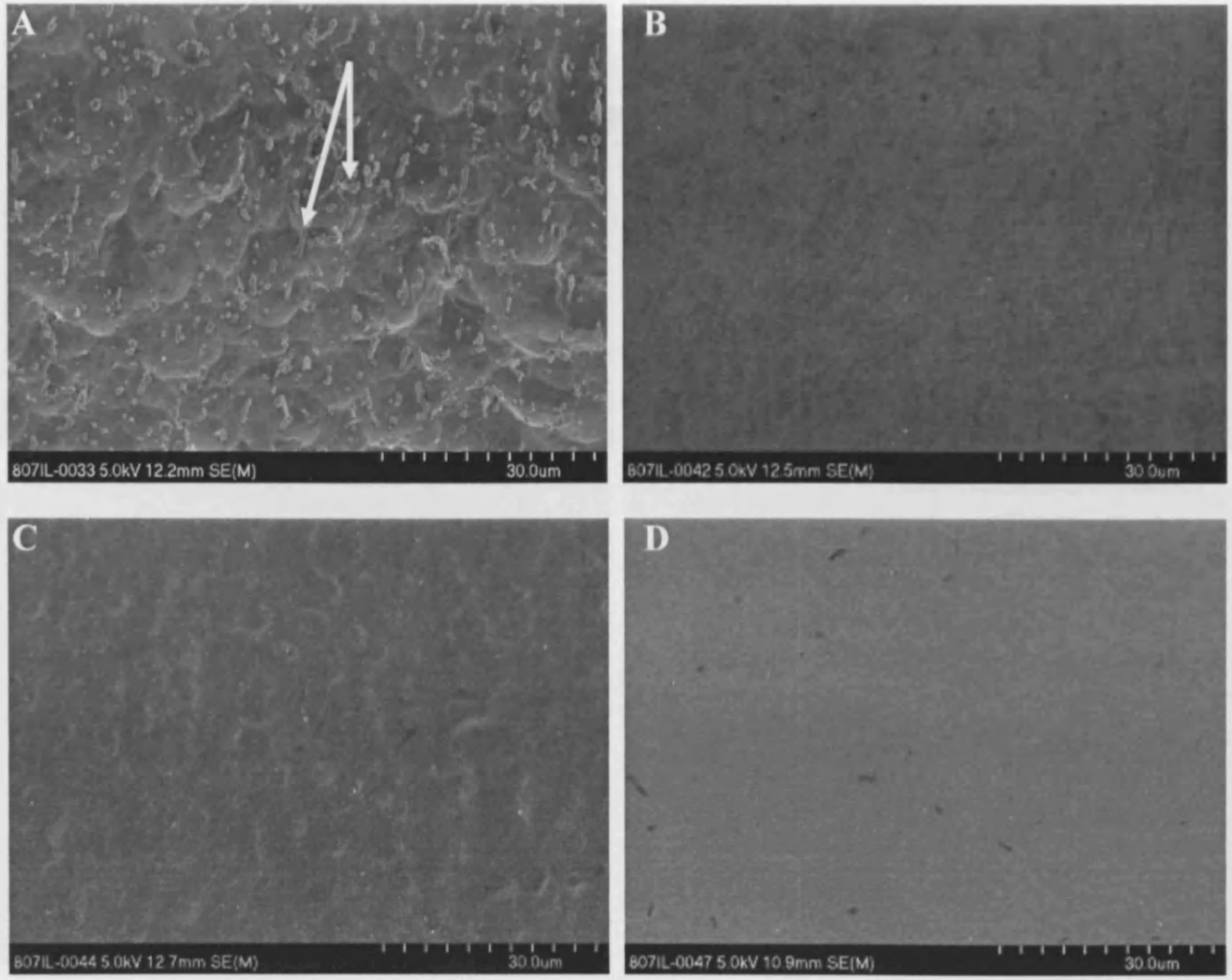

Figure 5.8. SEM images of standard TAN (A), paste polished TAN (B), electropolished TAN (C) and electropolished stainless (D) locking screws used in this study. The characteristic 'micro-spiked' appearance of NS (A; white arrows denoting beta-phase) is considerably influenced by both polishing techniques. Paste polishing (B) appears particularly suited for creating a smooth surface, void of waviness. The efficacy of this method has resulted in the beta phase particles becoming almost indistinguishable. Electropolishing (C) also successfully reduces the micro-roughness of NS, creating a smooth surface with visible waviness.

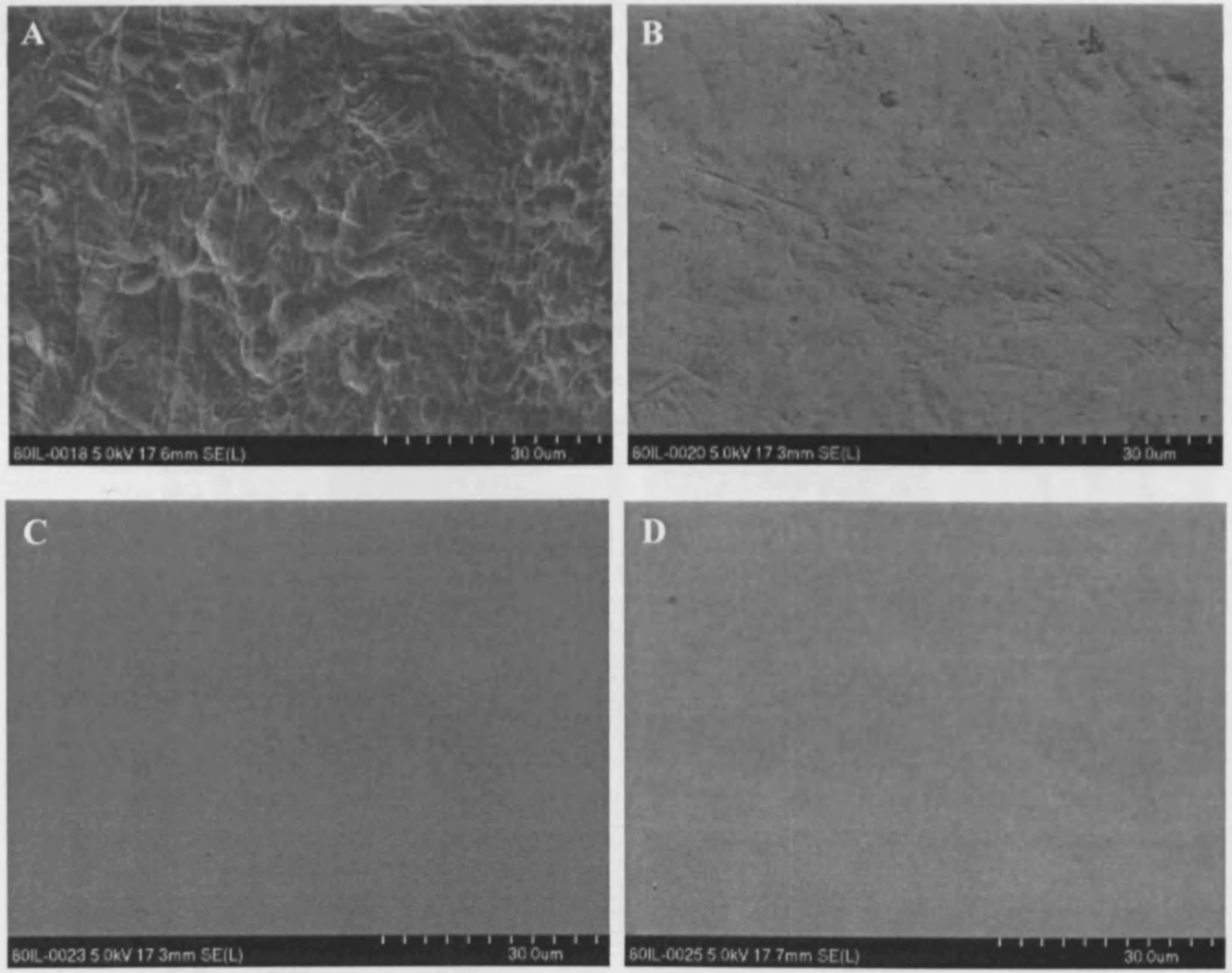

Figure 5.9. SEM images of standard cpTi (A), paste polished cpTi (B), electropolished cpTi (C) and electropolished stainless (D) locking compression plates used in this study. Both polishing techniques are highly successful at reducing the microtopography of the commercially available standard cpTi surface. Paste polishing leaves some mechanical abrasions but the overall surface is free from the micro-discontinuities evident for standard cpTi. Electropolishing of cpTi produces an extremely smooth surface, akin to that of Ss.

***Ex vivo* observations:**

After explanation and removal of adhering soft tissues, a clear difference in the tissue attachment between constructs was evident between micro-rough and polished LCP systems (Figure 5.10). Observations made for the NS screw/TS plate systems saw an increased amount of bone overgrowth on the plates and in-growth into the holes for the majority of the NS/TS systems (Figure 5.10A).In contrast, polished systems tended to retain soft tissue within these structures (Figure 5.10B, representative image). However, by 18 months bone was infrequently noted in some of the holes of the polished samples, however, this was easier to remove compared to micro-rough systems.

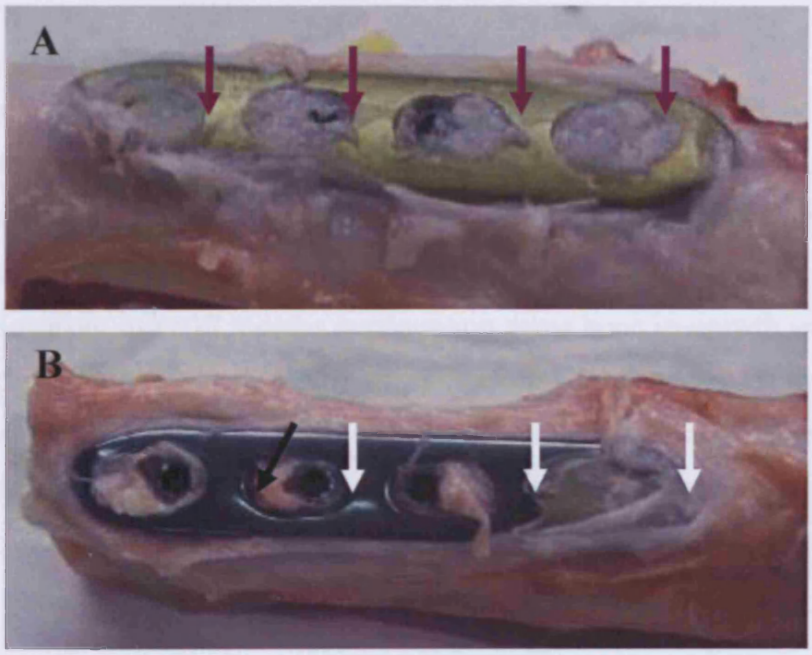

Figure 5.10. Tissue on-growth on standard (A) and polished (B) constructs after 18 months implantation. After removal of soft tissue, a clear difference in tissue contact was observed for (A) micro-rough and (B) polished systems. The presence of bone within the plate holes, and the screw head for micro-rough samples was frequent (A; purple arrows), while polished samples, in contrast, tended to have soft tissue within these structures (B; white arrows). However, after an extended implantation time such as 18 months, the presence of bone within the plate holes of polished samples was sometimes observed (B; black arrow), albeit, infrequently.

Figure 5.11 highlights the difficultly incurred for removal of bone from the standard micro-rough systems. After removal of adherent soft tissue the presence of bone within the plate holes was evident. At first we attempted to displace this hard tissue with a K-wire but proved unsuccessful. We also tried to dislocate the tissue by use of a scalpel. Further attempts to breach the bone to expose the screw head proved unsuccessful. As the screw heads generally remained unexposed at this point, samples would be transferred to a vice and the bone was subsequently removed using a hammer and chisel. This bone became increasingly difficult to remove, dramatically increasing the operating time of actually removing excess tissue for exposure of the screw holes for subsequent torque removal tests. This resulted in the operational time of tissue removal been dramatically increased to approximately 4 times that noted for polished samples (20 minutes compared to 5 minutes for polished samples).

Polished samples on the other hand proved considerably easier to remove tissue from (Figure 5.12). After removal of the adhering soft tissue with ease the presence of soft tissue within the plate holes and screw heads became evident. In contrast to micro-rough constructs, the tissue within the screw head was easily removed with a K-wire from the majority, if not all of the screw holes. However, after 18 months implantation some bone in-growth was noted in some of the polished plate holes, however, this was infrequent and did not pose the same difficulty for removal as micro-rough systems. The total operational time for polished systems to the point by which the screw heads were exposed adequately for removal torque experiments generally took less than 5 minutes. This is highlighted by figure 5.12G-I, which shows in 'real time' the ease of tissue removal from the polished screw holes.

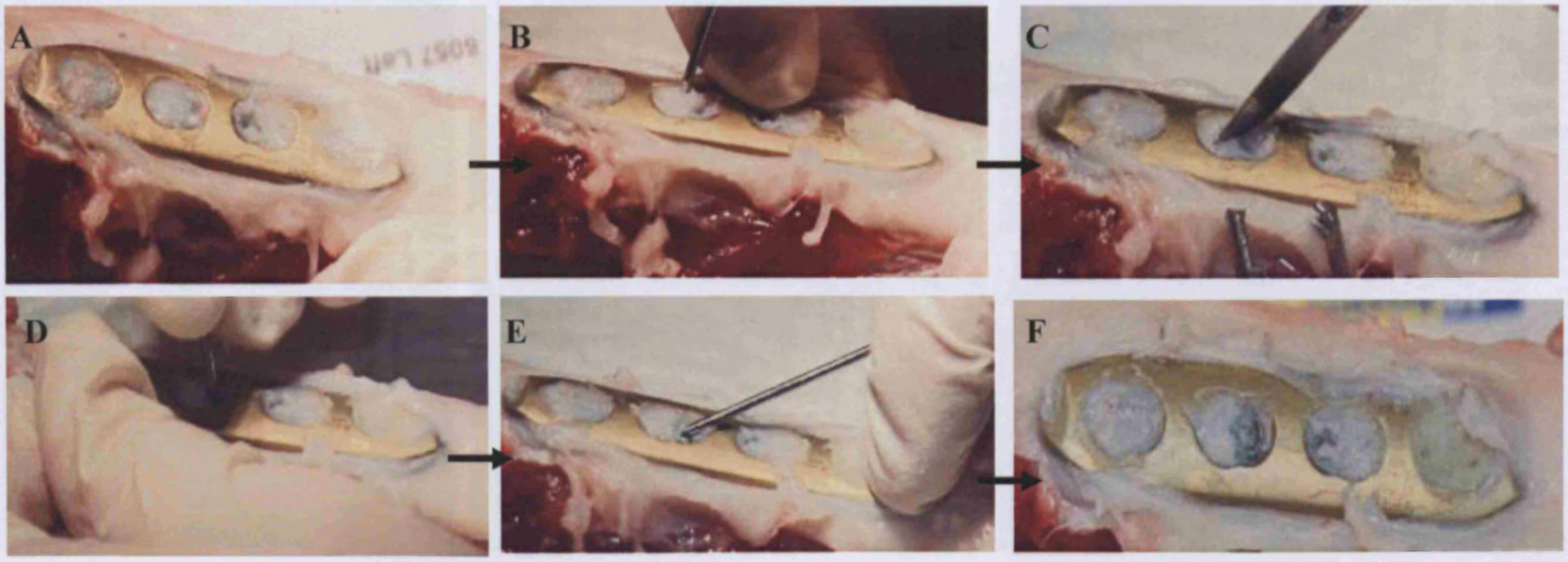

Figure 5.11. Attempted clearing of soft tissue and bone from the plate holes of the standard micro-rough cpTi LCP, containing the standard micro-rough TAN screws prior to torque removal tests. After removal of adherent soft tissue, the presence of bone within the plate holes is evident (A). At first, we attempted to displace this hard tissue with a K-wire, but proved unsuccessful (B). We also tried to dislocate the tissue by use of a scalpel (C). Further attempts to breach the bone to expose the screw head proved unsuccessful (D,E). As the screw heads generally remained unexposed at this point (F), samples would be transferred to a vice, and the bone was subsequently removed using a hammer and chisel. This resulted in the operational time of tissue removal been dramatically increased to approximately 4 times that noted for polished samples.

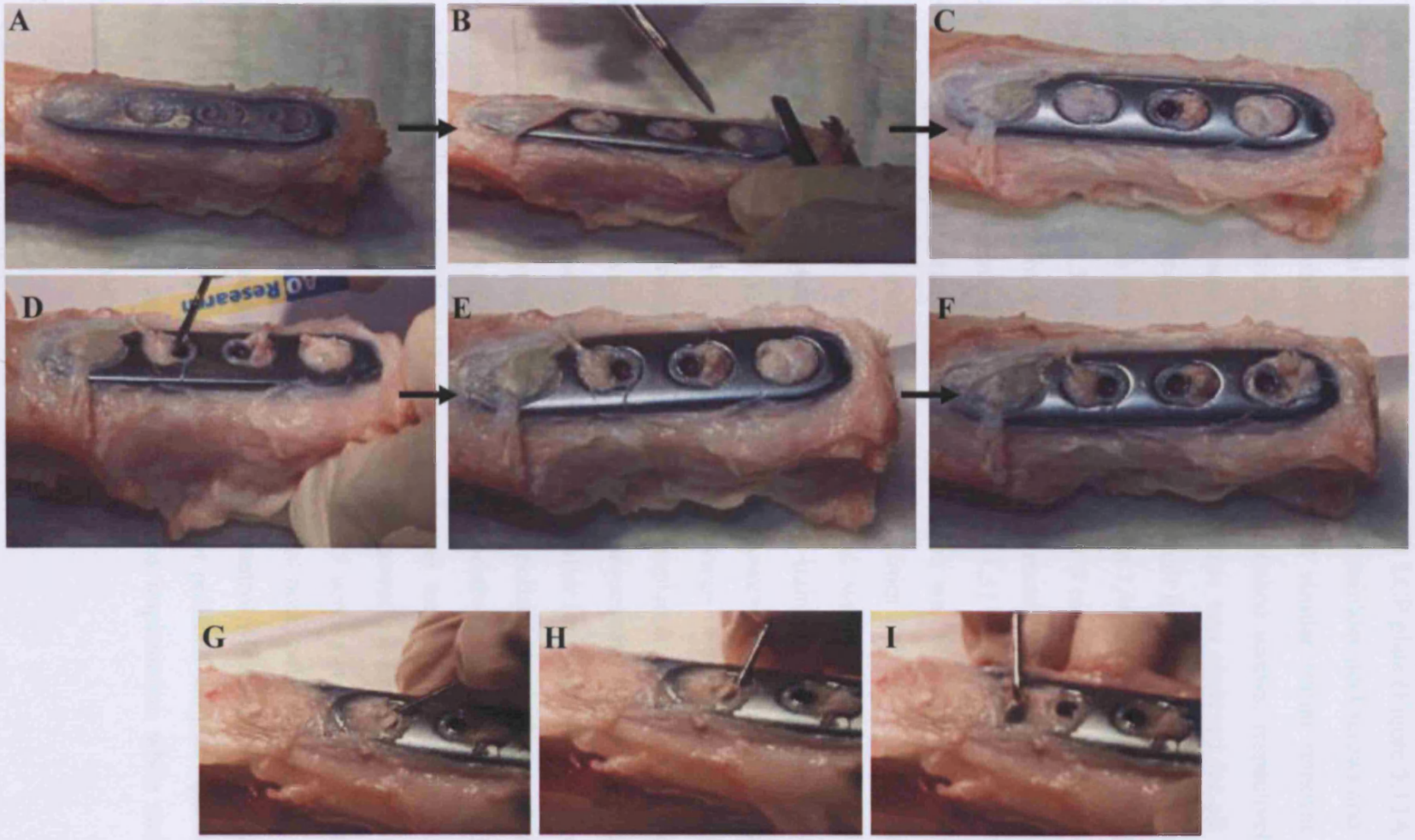

Figure 5.12. A thin layer of fibrous tissue was generally observed to be adhered to polished constructs (A). This layer was easily removed to expose the underlying samples without damage to the plates (B). Soft tissue was observed within the plate holes of the polished samples (C). This tissue was easily displaced by a K-wire (D-E) to expose the screw heads for subsequent removal torque analysis. After 18 months, bone was sometimes noted within the plate hole of some of the polished constructs, however, this was infrequent, and easily removed (F). The operational time for soft tissue removal was almost instantaneous (G-I), and resulted in a total operational time of approximately 5 minutes, to the point adequate access to the screw holes was achievable.

Torque measurements:

Immediately subsequent to insertion, removal torque measurements were taken of the each screw to determine the frictional force involved for each LCP plate (Figure 5.13A). All plates produced similar results within the range of 1.35Nm for stainless steel screws and 1.49 for NS screws. Both experimental polished screws produced similar initial removal torques of 1.57Nm and 1.51Nm for paste polished and electropolished screws, respectively. After 6 months implantation an increase in screw removal torque was observed for all screw/plate plates. After 6 months implantation (Figure 5.13B) a small increase of 0.05Nm was observed for stainless steel screw torque removal (from 1.35Nm to 1.40Nm). For paste polished screws a more marked increase of 0.59Nm was observed after 6 months implantation compared to initial insertion (from 1.57Nm to 2.16 Nm). After 6 months implantation, an increase of 0.79Nm was noted for electropolished screws (from 1.51 Nm to 2.22 Nm). The largest increase in torque removal after 6 months implantation was observed for standard micro-rough screws which produced a difference of 0.82Nm (from 1.49 Nm to 2.31 Nm). After 12 months implantation (Figure 5.13C) a similar trend was observed to the 6 months implantation standard>electropolished>paste polished>stainless steel with screw removal torques of 2.27, 1.98, 1.80 and 1.30Nm, respectively. However, compared to removal torques after 6 months implantation all screws showed an obvious decrease in torque removal 12 months post-implantation. Subsequent to 12 months implantation there was a decrease of 0.1Nm for stainless steel screws compared to removal torques after 6 months implantation. At this time, 1 screw stripped. The decrease noted was smaller for standard TAN screws, with a reduction of 0.04Nm in removal torque. Both paste polished and electropolished screws showed similar decreases of 0.36Nm and 0.24Nm, respectively. Nevertheless, subsequent to 18 months implantation (Figure 5.13D) screw removal torque had increased once again. Similar to each other time point stainless steel screws showed the lowest removal torque after 18 months implantation (1.51Nm) while standard TAN screws were observed to have the highest torque required for removal (3.26Nm). Again both polished variants had lower removal torque compared to the standard micro-rough control while remaining slightly higher than that of stainless steel. Interestingly, this increase for polished samples equated to similar torque removal measurements compiled after 6 months implantation while standard TAN screws showed a marked increase.

Over the complete implantation time, the torque required for removal of stainless steel screws did not appear to dramatically differ from that of the initial insertion torque (Figure 5.13). In contrast, torque removal for standard micro-rough TAN screws steadily increased with extended implantation time, therefore, seemingly becoming more difficult to remove with only a slight but not significant decrease in removal torque 12 months post-implantation. The difficulty observed in removing standard micro-rough TAN screws can also be highlighted by the fact that 1 screw stripped after 6 months implantation and 4 screws stripped over 4Nm after 18 months *in vivo* (Figure 5.14). Both polished variants showed similar results for screw torque removal over the total implantation time (Figure 5.14). Paste polished and electropolished screws at 6, 12 and 18 months were easier to remove compared to their standard micro-rough counterparts. At 6 and 12 months however, 1 paste polished TAN screw stripped. Akin to that of stainless steel and standard TAN, 12 months post-implantation showed a slight decrease for both polished variants for removal torque. Even at this time point however, polished screws were easier to remove than standard micro-rough samples (Figure 5.13). Statistically, surface polishing had a significant influence on the torque required for screw removal. Specifically, it was observed that NE screws ($p=0.001$), NP screws ($p=0.01$) and Ss screws ($p<0.001$) were significantly easier to remove compared to NS screws. Additionally, we found that Ss screws were significantly easier to remove compared to NE ($p=0.002$) and NP ($p<0.001$) screws. Moreover, no statistical correlation was observed regarding the time of implantation, and its effect on torque removal ($p=0.07$). Specifically, no significant difference was observed between 6 and 12 months ($p=0.567$), 6 and 18 months ($p=0.339$) or 12 and 18 months ($p=1.000$).

A

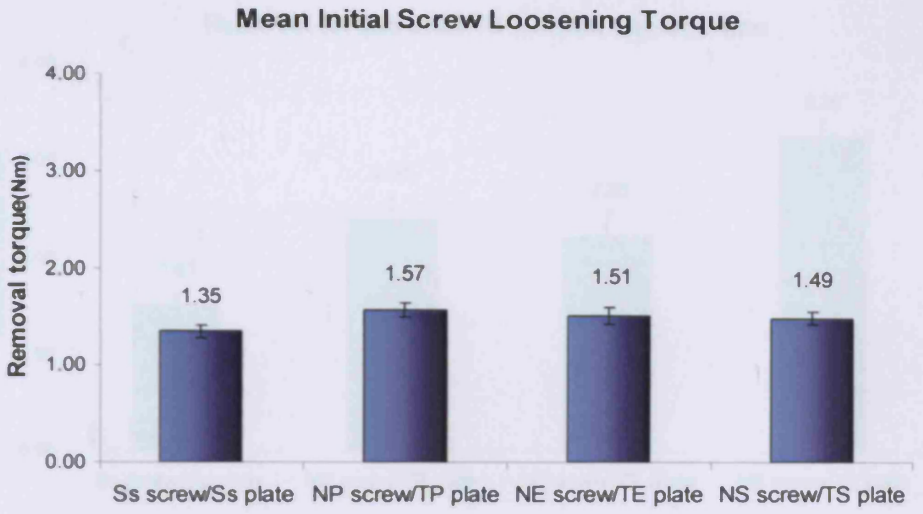
Mean Initial Screw Loosening Torque
Removal torque(Nm)
4.00
3.00
2.00
1.00
0.00
1.35
1.57
1.51
1.49
Ss screw/Ss plate
NP screw/TP plate
NE screw/TE plate
NS screw/TS plate

B

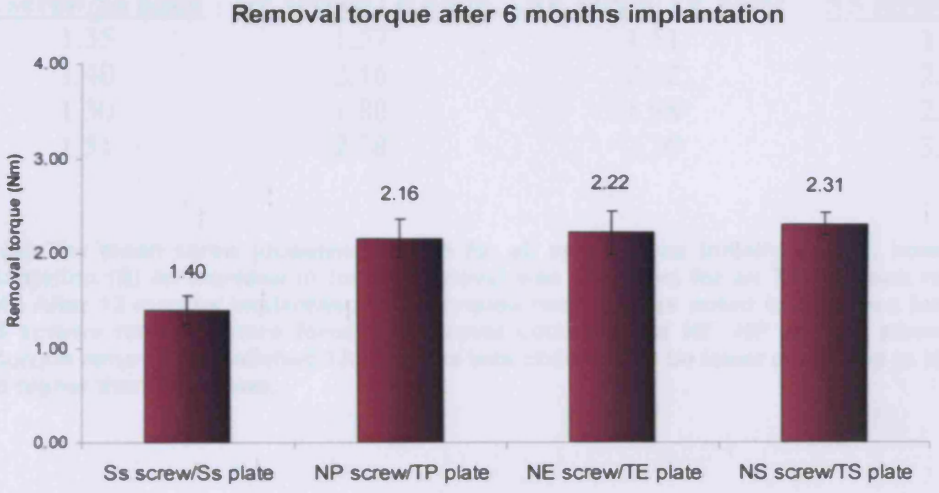
Removal torque after 6 months implantation
Removal torque (Nm)
4.00
3.00
2.00
1.00
0.00
1.40
2.16
2.22
2.31
Ss screw/Ss plate
NP screw/TP plate
NE screw/TE plate
NS screw/TS plate

C

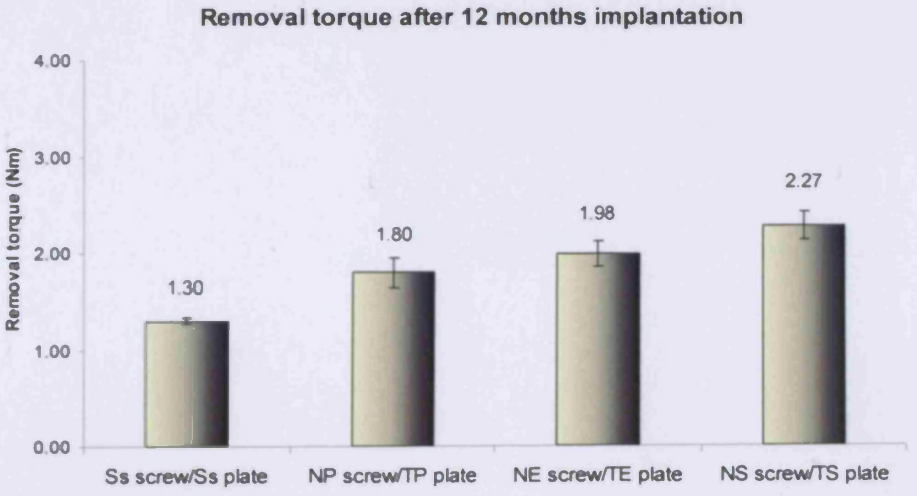
Removal torque after 12 months implantation
Removal torque (Nm)
4.00
3.00
2.00
1.00
0.00
1.30
1.80
1.98
2.27
Ss screw/Ss plate
NP screw/TP plate
NE screw/TE plate
NS screw/TS plate

D

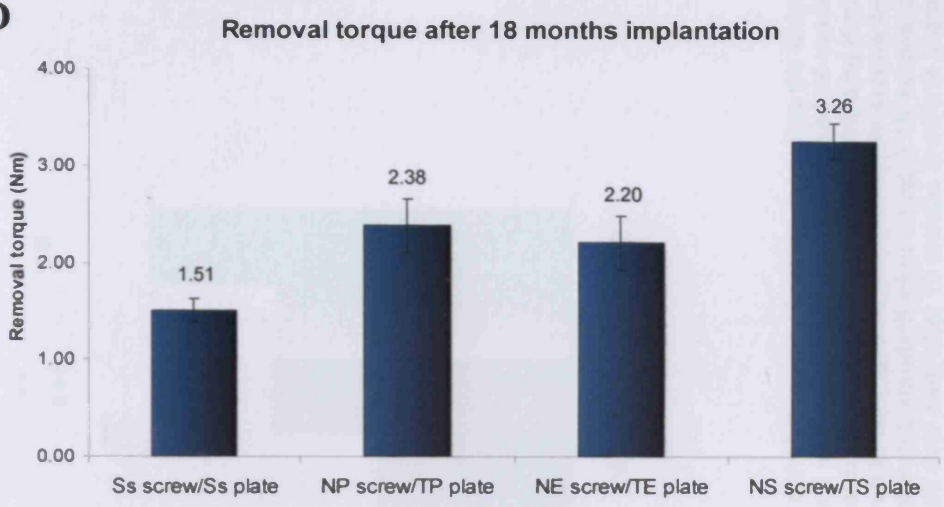

	Ss screw/Ss plate	NP screw/TP plate	NE screw/TE plate	NS screw/TS plate
Initial	1.35	1.57	1.51	1.49
6	1.40	2.16	2.22	2.31
12	1.30	1.80	1.98	2.27
18	1.51	2.38	2.20	3.26

Figure 5.13 (A) The mean screw loosening torque for all screws was initially similar, however after 6 months implantation (B) an increase in torque removal was observed for all TAN screws regardless of surface finish. After 12 months implantation (C), torques removal was noted to decrease for all screws, however, NS screws required more force for removal compared to NE, NP and Ss screws. After 18 months (D), torque removal for polished TAN screws was observed to be lower compared to NS screws, but remained higher than Ss screws.

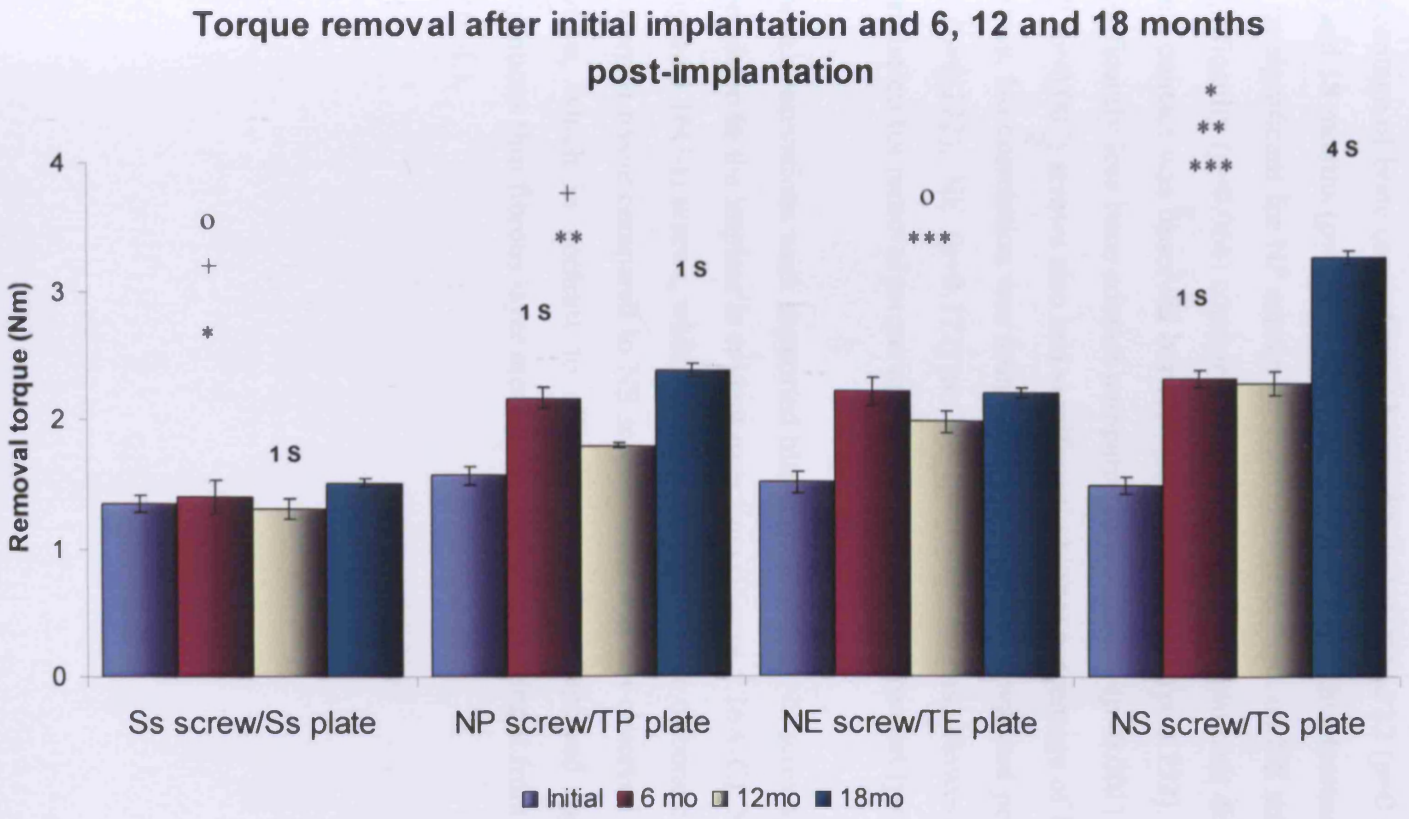

Figure 5.14. Screw removal torque after initial implantation, and 6, 12 and 18 months post-implantation. No statistical correlation was observed regarding the time of implantation, and its effect on torque removal (p=0.07). Specifically, no significant difference was observed between 6 and 12 months (p=0.567), 6 and 18 months (p=0.339) or 12 and 18 months (p=1.000). Stainless steel screws, regardless of implantation time, had similar removal torques, despite one screw stripping during testing of the 12 month samples (1 S – yellow bar). As expected, Ss screws were significantly easier to remove compared to NS (* p<0.001). Moreover, Ss screws were also significantly easier to remove compared to NE (^{o}p=0.002), and NP ($^{+}$p<0.001) screws. The difficulty observed in removing standard micro-rough TAN screws can also be highlighted by the fact that 1 screw stripped after 6 months implantation (1 S – pink bar) and 4 screws stripped over 4Nm after 18 months *in vivo* (4 S-green bar). NP (**p=0.001) and NE (***p=0.001) screws were significantly easier to remove compared to their NS screw counterparts. At 6 (1S-pink bar) and 12 months (1S – green bar), however, 1 paste polished TAN screw stripped. Similarly, a slight decrease after 12 months implantation was observed for both polished variants, as noted for stainless steel and standard TAN. Even at this time point, however, polished screws were easier to remove than standard micro-rough samples. Mean±SEM.

Histological evaluation:

Surface polishing appeared to decrease the percentage of bone contact compared to NS screws, independent of time (Figure 5.15). However, time was not determined to be a significant factor ($p=0.236$) regarding bone contact. No significant difference in the percentage of bone contact was observed between 6 and 12 ($p=0.567$), 6 and 18 ($p=0.339$), or 12 and 18 months ($p=1.000$) implantation time. While this decrease in bone contact was found to be significant for NP screws ($p<0.001$) bone contact on NE screws was not found to differ significantly ($p=0.066$) compared to NS screws. No significant difference in the percentage of bone contact was observed between polished variants ($p=0.752$). As expected, Ss screws had significantly less bone contact compared to NS screws ($p<0.001$) however, NE ($p<0.001$) and NP ($p=0.007$) screws also had significantly higher percentage of bone contact compared to Ss screws. No correlation was found between torque removal and percentage of bone contact for Ss ($p=0.272$), NE ($p=0.172$) or NP ($p=0.402$) screws. However, NS screws did show a correlation for removal torque and percentage of bone contact ($p=0.026$).

These observations were supported histologically. For NS screws, the high frequency of bone apposition to the implant is evident over time (Figure 5.16A-C). NE (Figure 5.16D-F) and NP (Figure 5.16G-I) screws, while displaying a high degree of bone contact, had a higher incident of fibrous tissue compared to NS screws. This was not observed however to be similar to Ss screws, which in contrast to all other samples displayed the persistent presence of a continuous thin fibrous layer around the screw, separating it from adjacent hard tissue (Figure 5.16J-L).

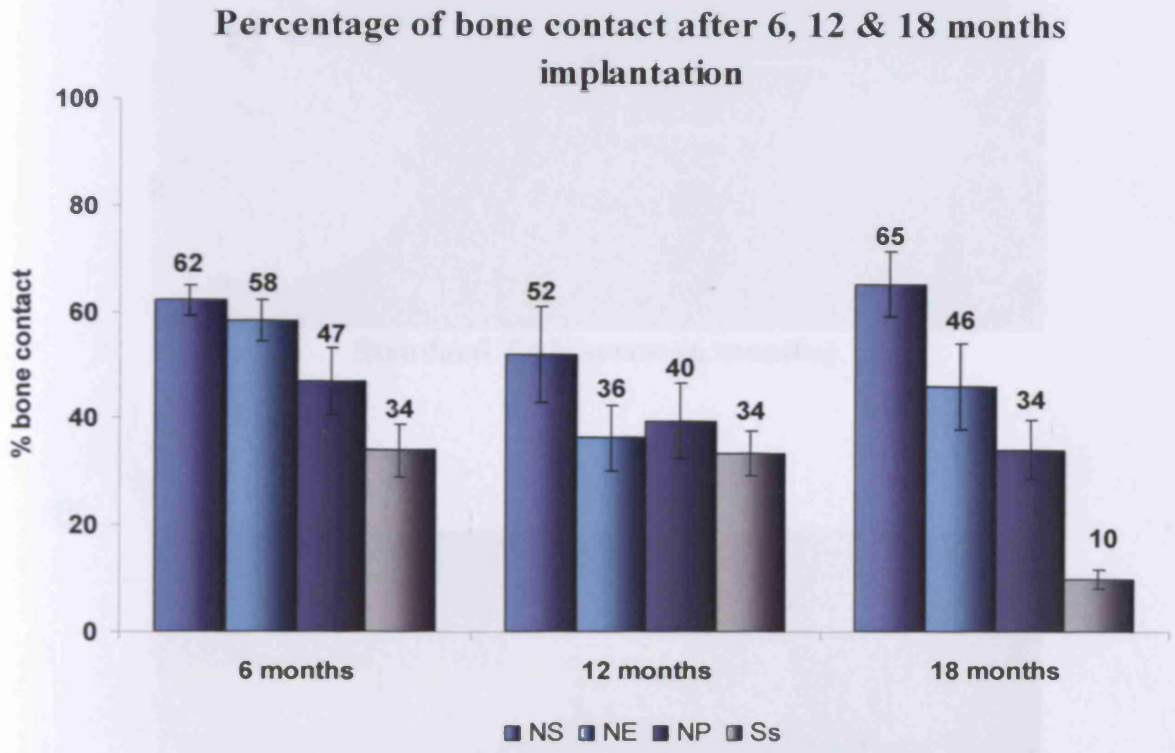

Figure 5.15 Percentage of bone contact for NE, NP, NS and Ss screws after 6, 12 and 18 months implantation, Mean ±S.E.M. Ss screws had significantly less bone contact compared to NS ($p<0.001$), NE ($p<0.001$) and NP ($p=0.007$) screws, NP screws had significantly less bone contact, than NS ($p<0.001$), but this was not observed for NE screws ($p=0.066$). Furthermore, no significant difference in bone contact was noted for polished TAN screws ($p=0.752$). No significant difference in the percentage of bone contact was observed between 6 and 12 ($p=0.567$), 6 and 18 ($p=0.339$), or 12 and 18 months ($p=1.000$) implantation time. No correlation was found between torque removal and percentage of bone contact for Ss ($p=0.272$), NE ($p=0.172$) or NP ($p=0.402$) screws. However, NS screws did show a correlation for removal torque and percentage of bone contact ($p=0.026$).

A

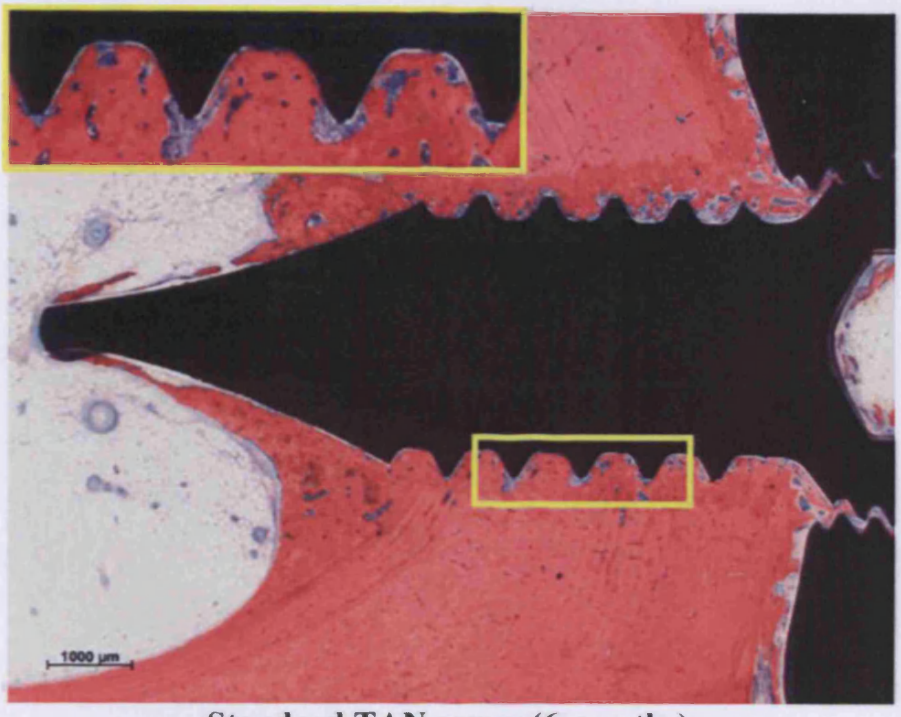

Standard TAN screw (6 months)

B

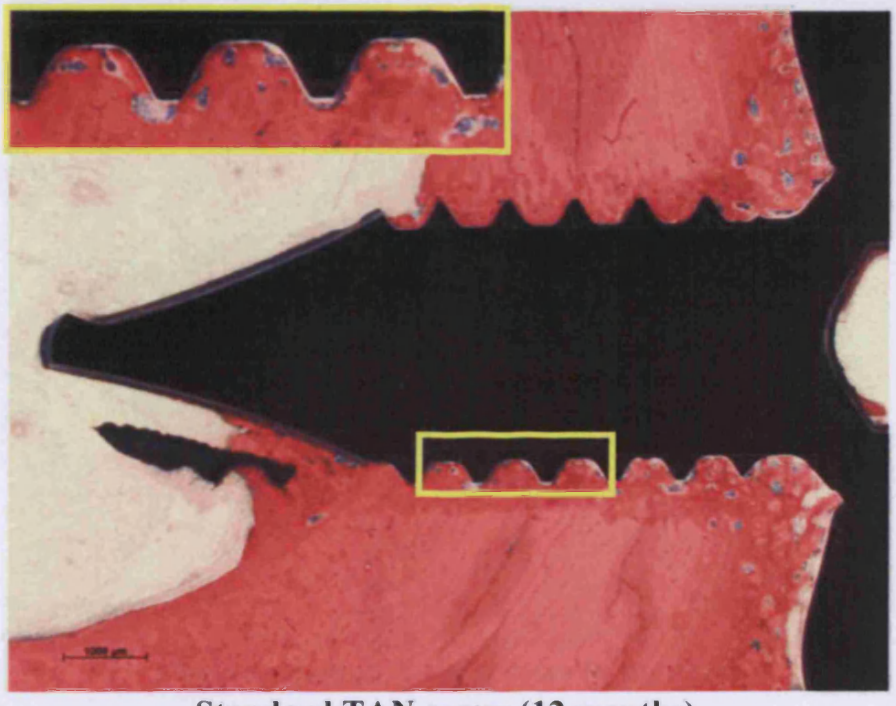

Standard TAN screw (12 months)

C

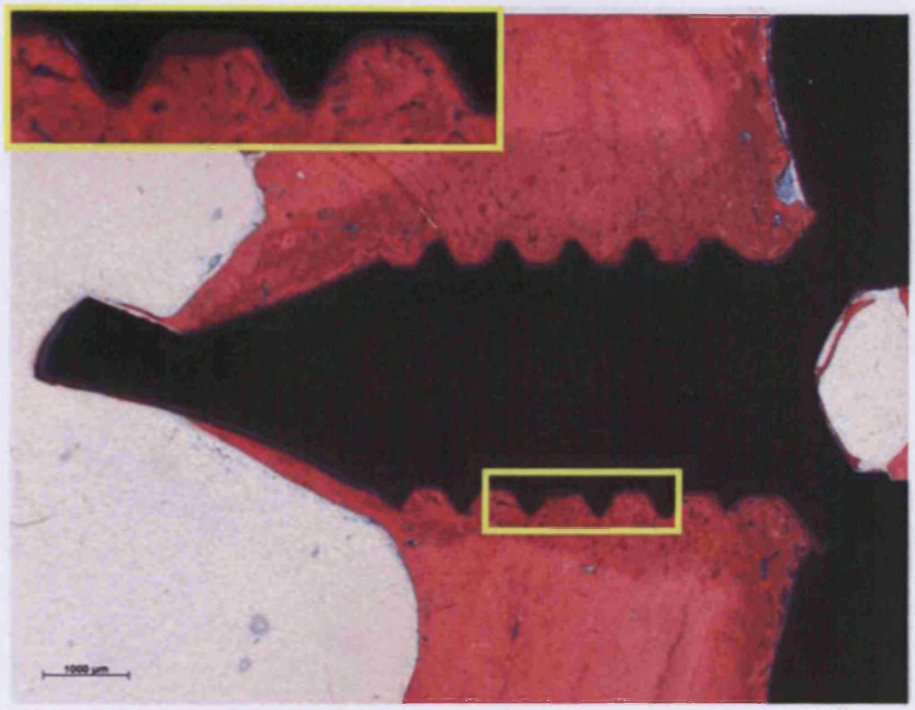

Standard TAN screw (18 months)

D

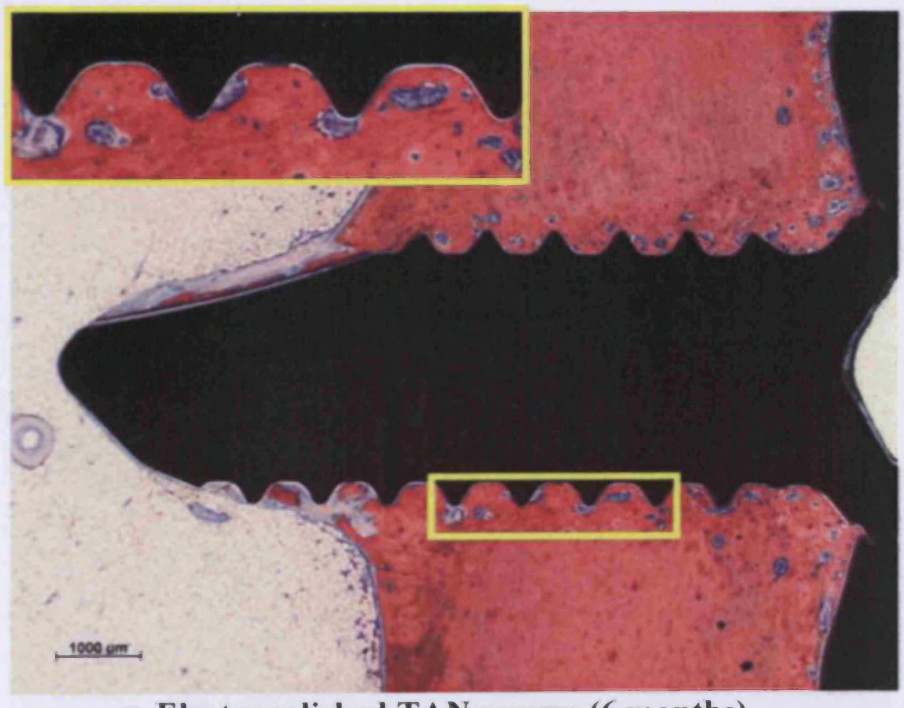

Electropolished TAN screws (6 months)

E

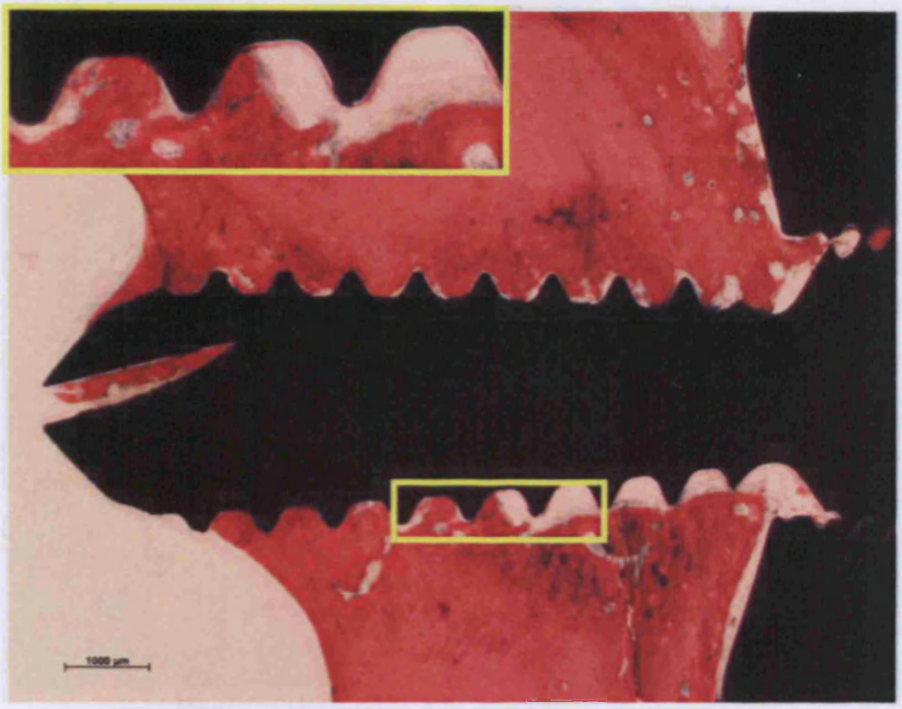

Electropolished TAN screws (12 months)

F

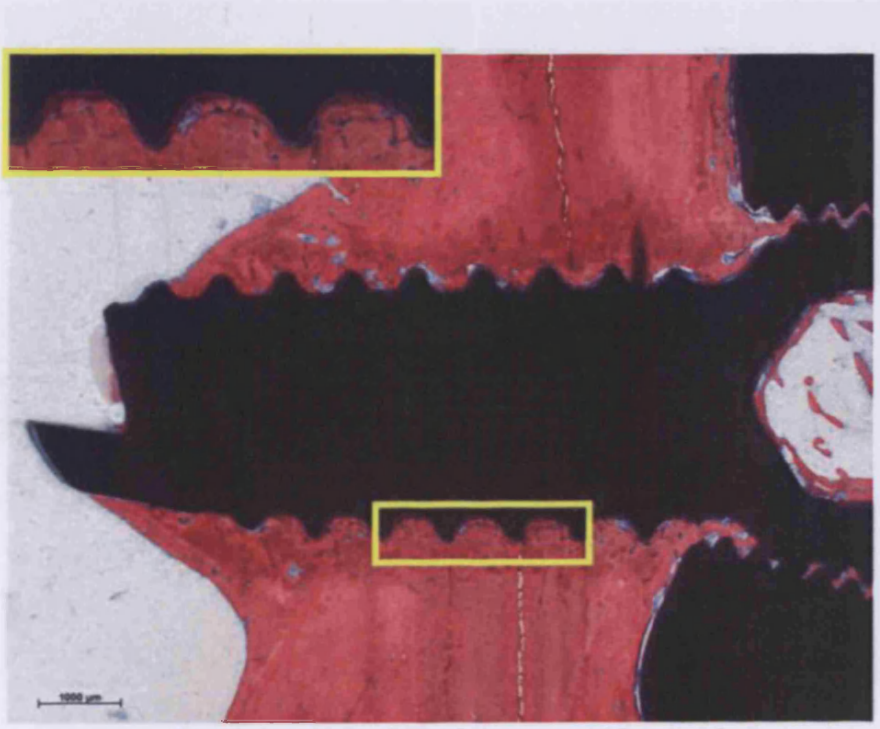

Electropolished TAN screw (18 months)

G

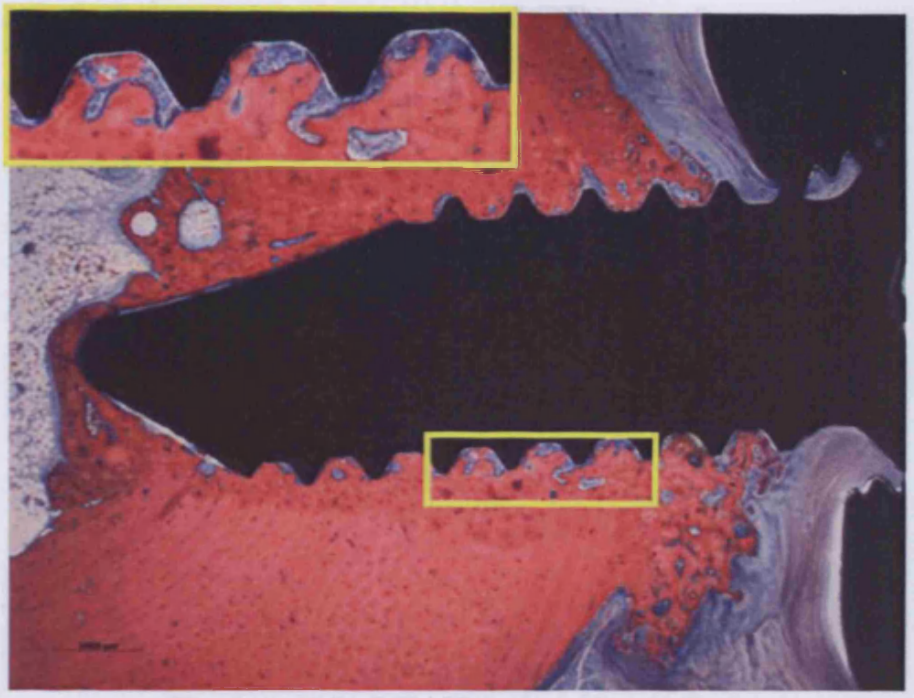

Paste polished TAN screw (6 months)

H

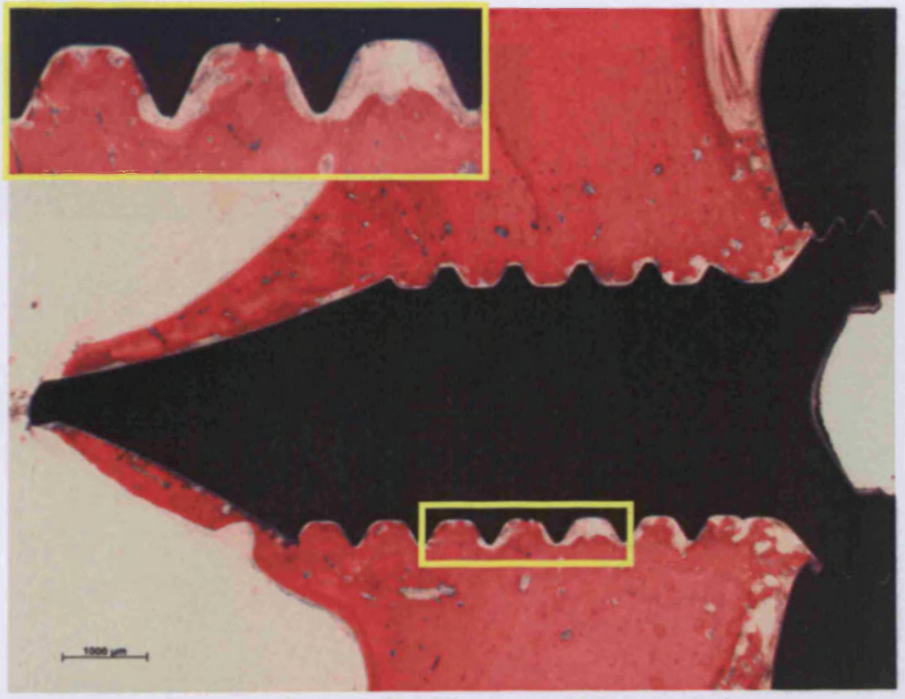

Paste polished TAN screw (12 months)

I

Paste polished TAN screw (18 months)

J

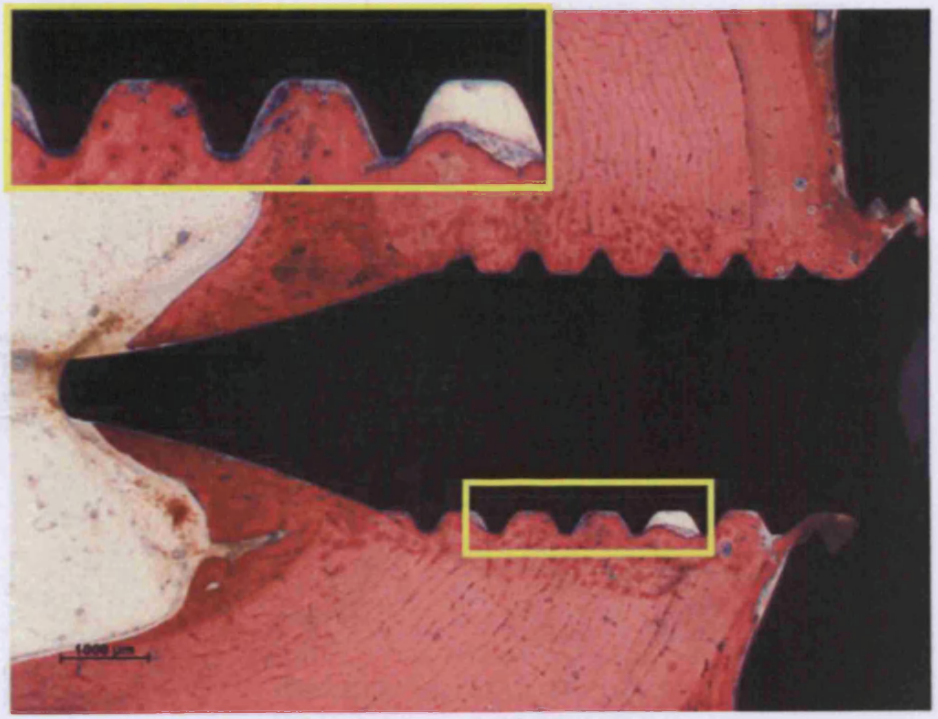

Stainless steel (6 months)

K

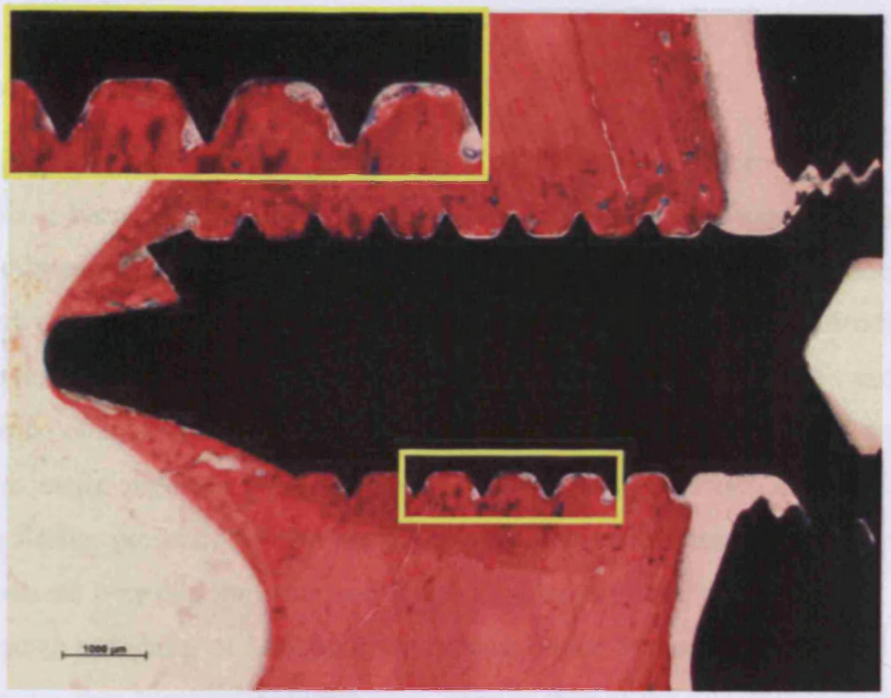

Stainless steel (12 months)

L

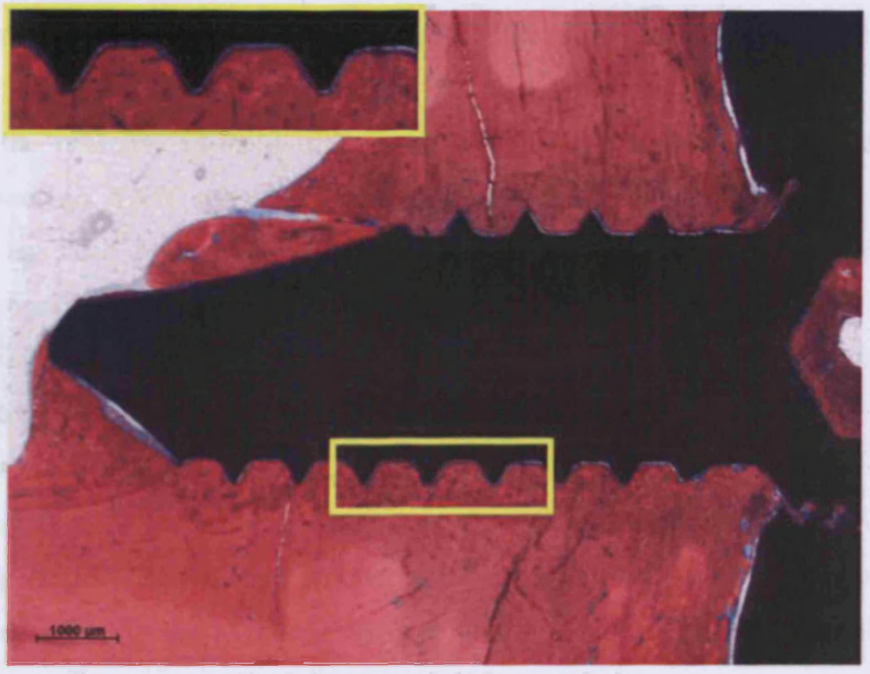

Stainless steel (18 months)

Figure 5.16. Representative histological sections of NS (A, B, C), NE (D,E,F), NP (G,H,I) and Ss (J,K,L) screws stained with Giemsa-Eosin to demonstrate soft tissue (blue) and bone (pink) attachment, after 6, 12 and 18 months implantation. Within each inset is a higher magnification image to show the tissue apposition to each screw. As expected, NS screws display a high frequency of bone apposition, while Ss screws had a continuous thin fibrous layer separating the screw from adjacent hard tissue. While NE and NP screws had soft tissue attachment, this was not seen to the same extent observed for Ss. However, neither NE nor NP had direct bone contact to the extent observed for NS screws.

Discussion:

Surface characterisation:

No major changes in the chemical composition of the surfaces were noted subsequent to polishing. This is because all surfaces undergo anodisation as a final step (with the exception of TE/NE combination). Furthermore, the hydrophilicity of the cpTi surfaces does not appear to be affected by surface polishing as both electro- and paste polishing produced similar contact angle results to the TS plate. Both standard micro-rough TAN screws and cpTi plates were found to be consistent with 13mm samples used for *in vitro* work in this study (chapter 2) and as previously reported (Meredith *et al.*, 2007a; Pearce *et al.*, 2008b). TAN screws displayed the similar presence of beta phase particles, while the basket-weave surface of cpTi was also consistent between implants and discs. Profilometry and SEM imaging showed that electro- and paste polishing of locking compression plates dramatically reduced the average surface roughness that is associated with cpTi, akin to that of the clinically smooth surface of Ss. However, TAN screws proved more difficult to produce an optimised surface smoothness with polishing. This may in part be due to the dimensions and geometry of the screws as Ss screws which normally within this study for discs, LCP's and intramedullary nails have a highly reproducible smooth surface, also had a high variability in average surface roughness.

Additionally the presence of hard niobium-rich inclusions associated with the beta phase particles present in TAN would further hinder optimal polishing of the screws. This phenomenon has also been reported previously for TAN cortical screws (Pearce *et al.*, 2008b). Electropolishing appears to be the least successful method for polishing TAN screws, most likely due to the low conductivity of the alloy, in particular niobium, as discussed in detail in chapter 2. For further optimisation perhaps increasing the polishing time would aid in fabricating a more reproducible smooth surface. Paste polishing of TAN screws appears to be a more optimal method for reducing the micro-topography associated with NS. Since paste polishing is a mechanical abrasive technique it would indicate that the dimensions of the screws lend themselves better to the mechanical polishing compared to electropolishing.

Since titanium and niobium are relatively hard materials a high degree of abrasion is possible when paste polishing TAN due to the high frictional force generated between the material and actual mechanical process. These results are in line with findings for 13mm samples used in the *in vitro* portion of the study. For TAN discs, paste polishing also produced a lower average roughness compared to electropolished samples, which also had a high variability.

In the following chapter it is also seen that paste polishing of intramedullary nails also results in a smooth reproducible surface comparable to the TAN screws used in this study, and the 13mm samples used for *in vitro* work. However, it should be noted that for the intramedullary nails used in the subsequent chapter the variability was much lower for paste polishing compared to the NP screws which had a greater variability, most likely due to the more intricate screw dimensions.

Screw removal and histological observations:

Due to the uncertainty surrounding the issue of device removal many studies have emerged that focus intently on the reasons for or against (Kahle, 1994; Peterson, 2005; Busam *et al.*, 2006) this procedure. One of the most quoted reasons for removal of bone plates and screws is infection (Manor *et al.*, 1999; Mosbah *et al.*, 2003; Bhatt *et. al.*, 2005; Rallis *et al.*, 2006; Theodossy *et al.*, 2006) while the decision to remove asymptomatic fixation devices is based mainly on the surgeon's experience and preference and has led to large variations in the rate of removal. For instance, Alzahrani and colleagues (2003) report a removal rate of 62% for uncomplicated healing in paediatric patients, while Bakathir and colleagues (2008) quote a removal rate of 53.4% within the same population. In craniomaxillofacial applications removal rates are reported from approximately 1% (Shoamanesh *et al.*, 2007) to as high as 93% for the mandible alone (Walsh & Somiya, 2007). Interestingly, information regarding typical complications encountered during extraction, which also would contribute to a consensus regarding removal, is distinctly lacking. Despite this deficiency in published evidence verbally time and time again it is conveyed that the most challenging prospect to face a surgeon once the decision is made to remove a fixation device, is the difficultly in actually doing so due to the excessive bone overgrowth onto the plate and screws (personal communication with Christoph Sommer, head of trauma, Chur Kantonal hospital). In recent years some scientific evidence has also emerged to support this notion (Hamiliton *et al.*, 2004; Georgiadis *et al.*, 2004). Schmalzried and colleagues (1991) report incomplete removal of devices in 7% of their cases, while Jago and Hindley (1998) report a complication rate of 14% with regards to difficulty in removing the device, and Alzahrani (2003) report difficulty in removing devices in all 304 of their cases, with 61% pin breakage rate.

Increased surgery time is an inadvertent complication of difficulty in removing a fixation device. Swiontkowski (1983) reported for 61% of the patients treated for slipped capital femoral epiphysis having increased blood loss and surgical time exceeding that of the original procedure. Ilchmann and Parsch (2006) report a doubling in the surgical time necessary for removal of cannulated titanium screws compared to insertion reportedly because the sockets proved to be too weak to overcome the necessary torque for loosening the screw from bone and applying the reverse-cutting-force necessary to extract the device. It can be speculated that the bone on-growth to the device while *in situ* contributed to this observation. Alzahrani and colleagues (2003) also report a significant increase in the surgical time in 22% of their paediatric patients that underwent device removal. The authors contributed the augmented surgery time to the abundant callus observed radiologically resulting from an extended implantation time of three years or more. Due to the lengthy implantation time the authors showed that this directly and significantly resulted in increased surgical time and blood loss for these patients (all approximately 16 years of age).

We have shown here that polishing of LCP's and screws can positively influence this outcome. It was noted upon *ex vivo* tissue removal from the constructs that tissue adhered to the polished constructs was markedly easier to remove compared to the micro-rough counterparts. Specifically, we noted that soft tissue was present more frequently on polished plates and within the screw head which was easily displaced with a scalpel and K-wire with a maximum removal time of approximately 5 minutes. In contrast, standard micro-rough plates and screws had hard tissue deposited on the plates and within the plate holes which, after attempting to remove for approximately 15-20 minutes, resulted in surface damage to the plates, the construct was placed into a vice (which obviously cannot be done in surgery and likely would result in increased stripping due to inadequate fit of the screwdriver due to the presence of tissue) and the bone removed after extensive chiselling. This observation is supported by our torque removal data which shows that with increasing implantation time there is a significantly greater force required to remove the screws made of micro-rough TAN. In fact this force is so great that stripping of the screws at 18 months occurred in 4 cases, compared to 1 for NP screws and none for NE or Ss screws. Furthermore, already after 6 and 12 month's implantation the quantity of bone in direct contact to the NS screws is greater than that to both polished variants which seem to support a higher contact of fibrous tissue comparable to Ss. This is an especially important result considering that device removal in Europe alone generally costs approximately €3000.

However, if a surgeon encounters difficulties when removing the device the associated cost of surgery inadvertently increases along with the potential risk to the patient. Therefore, polished samples also alleviate the economic burden of superfluous surgical time, as well as preventing excessive risks to the patients that are associated with unplanned surgical intervention.

The concept of surface polishing for reducing bony on-growth and torque removal of fixation screws is not novel, although has not been the driving force of many studies up until now. For instance, in an effort to predict if commercially available cpTi or Ss was best suited to evoke fewer retrieval problems in the treatment of slipped capital femoral epiphysis, Lee and colleagues (1996) advocated the potential of polished fixation devices over micro-rough cpTi screws, in which the latter were observed to have over 90% direct bone contact. An earlier study by Carlsson and colleagues (1988) advocating the use of standard micro-rough screws for enhanced adhesive strength *in vivo* also unknowingly highlighted the potential of surface polishing for reducing the force required for screw removal compared to commercially available standard implants. The authors report a significant reduction in the amount of removal torques required for electropolished cpTi screws compared micro-rough cpTi screws (average roughness' not included) after 6 weeks implantation within rabbit tibiae. Histologically, however, the authors did not find any difference in tissue contact between the implants.

Twenty years later in a similar study, Pearce and colleagues (2008b) examined the effect of polishing cpTi and the TAN on the removal torque and percentage bone-implant contact in cortical and cancellous bone of sheep after 6, 12 and 18 weeks. Similar to the Carlsson study the authors report that polishing had a significant effect on the removal torque with both types of polished implants demonstrating a significantly lower removal torque in both cortical and cancellous bone. Also similar to the previous mentioned study (Carlsson *et al.*, 1988), Pearce and co-workers (2008b) did not observe a significant difference in the percentage of bone contact to polished cpTi and TAN screws compared to their standard counterparts for cortical or cancellous bone. Interestingly, however, is the observation made by the authors with regards to difference histologically between Ss screws compared to TE and NE screws used. Namely, the authors report a thin fibro-cellular layer adjacent to the surface of the SS implants. This fibro-cellular layer was present along almost the entire length of each Ss screw but was not consistently apparent for TE or NE screws.

This is similar to the results found in this study for Ss screws. Here it was found that as well a significantly lower percentage of bone contact compared to the TAN screws, a thin fibrous shell was evident for the Ss screws independent of implantation time. This may in part contribute to the consistent low removal torque observed for Ss screws. Furthermore, Ss screws had the lowest percentage of bone contact of any of the screws studied. Thus, it can be postulated that even when bone does become directly appositional to Ss screws that the strength of this attachment is inferior to that of TAN.

As the TE cortical screws used by Pearce and co-workers (2008b) and the NP screws used in this study, had a lower average roughness than Ss within their respective investigations, the consistent presence of a soft tissue interface is most likely due to differences in surface chemistry between cpTi, TAN and steel. Supporting this is the observation that while there was a significant decrease in the percentage of bone contact for NP screws compared to NS screws, and bone contact was lower for NE screws compared to NS screws, both polished samples still had significantly higher percentage of bone contact compared to Ss screws. Thus, a material dependent response to bone exists to some extent which is supported by results presented by Pearce and colleagues (2008b), and is further advocated with results accrued for previous *in vitro* analysis (chapter 4) and for intramedullary nails (chapter 6).

Interestingly, NP screws had a significantly lower percentage of bone contact compared to NS screws while NE screws did not, although they did show a trend for lower bone contact. This is not a surprising observation however as clearly the morphology of the NP screws had a lower surface roughness than NE, and morphologically was very smooth. NE screws in contrast had a higher degree of surface waviness which undoubtedly contributed to the higher Ra noted for this sample, in addition to the higher variability in surface roughness. Even so, both polished samples showed a trend for reduced bone contact compared to NS screws and with further optimisation of electropolishing the small dimensions of the screws, a further reduction in percentage of bone contact would potentially be possible. However, for both polished screw types, no statistical correlation was found between the quantity of bone contact and torque removal. Therefore, it may also be possible that the strength of bone attachment to polished screws is less compared to NS screws and that this is also a contributing factor for the reduced removal torques noted for polished samples.

This is supported by the fact that polished screws had less stripping compared to micro-rough TAN screws. This is may in part be explained by *in vitro* observations in chapter 4, which indicated that polished samples had a slower rate of terminal differentiation compared to standard micro-rough samples. Therefore, it is possible that polished samples do not evoke the same accelerated remodelling rate observed for standard micro-rough samples.

Another area which may potentially benefit from screw polishing is the complication reported for re-fracture, especially through vacant screw holes subsequent to removal. This was one of the areas that sparked the most interest in a recent AO symposium dedicated to material removal (Salzburg, 2008). In fact attending surgeons reported a re-fracture rate of 13-35% for devices extracted from the femur. Kim and colleagues (2005) also report a re-fracture rate of approximately 7% after plate removal, while Rosson and colleagues (1991) report a re-fracture rate of approximately 8% for patients over 16 years of age, while those below this threshold did not present with any re-fractures after plate and screw removal. However, in an early study Hidaka & Gustilo (1984) report a re-fracture rate of approximately 20% which may be contributed to the 4.5mm screws used in this study compared to 3.5mm screws which have been observed to produced less occurrence of re-fracture (Chapman *et al.*, 1989). The process of screw removal produces micro-fractures in the wall of the bone that weaken the bone making it more susceptible to fracture. One can suggest that this may be in part due to the force required to remove the screw to the strong bone adherence to the implant. Here we have shown that this force can be significantly reduced for polished cpTi and TAN screws which may contribute to less surrounding tissue damage being caused upon removal. With a more optimised method of polishing the screws this force would likely be further reduced and less injury to adjacent tissues would be caused. A point to note however, is that the common dominating factor between the studies just mentioned with regards to re-fracture is the use of dynamic compression plating, which as mentioned previously hinders cortical perfusion adjacent to the plate, specifically in the periosteum, causing bone necrosis and weakening of the bone, which may also be a contributable aspect for the frequency of re-fracture.

Chapter summary:

While the success of plate fixation within orthopaedic trauma has revolutionised fracture fixation, difficulty to remove the implants is known to increase surgery time, intra-operative complications and surgical morbidity. Regardless of the potential risks associated with plate and screw removal, many surgeons still advocate its occurrence to avoid complications such as growth disturbances, metal ion/salt reaction, infection and irritation, to name a few. For bone fixation plates such as the LCP and LISS, excessive bony on-growth to the plates and in-growth within the screw holes has been identified as a major contributor to removal failure. Some studies suggest early removal once a fracture has healed in an attempt to circumvent this problem however, by the time fracture healing has occurred encasement of the implant by bone may have also occurred. Additionally, premature removal of an implant can jeopardise the healing of a fracture. In this study we addressed the problem of implant removal with regards to excessive bone over-growth by reducing the surface micro-topography, a known determinant of osseointegration, of clinically available LCP's, LISS and locking screws. Specifically, our findings indicate that surface polishing significantly reduces the force required for removal of TAN cortical screws compared to standard micro-rough counterparts. Furthermore, there was a trend for lower percentage of bone contact on the polished samples compared to micro-rough screws; however, this was always significantly higher than that observed for Ss screws. These findings support work from our laboratory (Pearce *et al.*, 2008). Therefore, collectively; these results indicate that surface polishing reduces the extraction torque required for removal, at least in part by supporting a lower percentage of bone contact compared to micro-rough screws. Moreover, the significant reduction in time required for tissue removal from polished devices, will directly reduce the surgical time associated with implant removal, thus improving not only the economic burden associated with surgical procedures, but also the surgical related complications with regards to the patient which are both principal deciding factors for implant removal. Consequently, we suggest that surface polishing is a promising technique for fixation devices destined for removal which would positively influence the prevalence of implant removal-related complications.

Chapter 6: Efficacy of surface polishing for intramedullary nail removal – an *in vivo* evaluation.

Abstract

To date, IM nails are fabricated for orthopaedic clinics from either TAN or Ss. Yet removal of standard TAN (NS) IM nails often produces more extraction related complications compared Ss IM nails of the same design. The difficulty in removing nails due to excess bone on-growth has not been described for steel which for clinical orthopaedics is supplied with a smooth surface. In contrast, TAN has a micro-rough surface containing a micro-spiked surface morphology due to the fact that the alloy is a mix of soft alpha and harder beta phases. Due to the superior mechanical properties and improved biocompatibility over Ss, TAN IM nails are the preferred choice for IM nailing technology. However, the high affinity of bone for TAN can prove highly problematic for removal applications. Therefore, we believe that TAN IM nails would be an ideal fixation system to benefit from surface polishing. We hypothesise that paste polishing TAN IM nails will reduce the pull-out force required compared to clinically available standard micro-rough TAN nails of the same design. To test this hypothesis we implanted 9.5mm human humeral nails in a bilateral non-fracture sheep tibiae model. Specifically, in 7 sheep we implanted standard micro-rough TAN IM nails in the tibia of a sheep, with an experimental paste polished TAN IM nail in the contralateral tibia. We also implanted Ss IM nails in another 7 sheep with a standard micro-rough TAN IM nail in the contralateral tibia. Total implantation time was 12 months, after which time pull-out tests were preformed on the IM nails (n=6 per group). Results indicate that surface polishing of TAN IM nails significantly reduces the pull out force required for extraction compared to standard micro-rough TAN IM nails and therefore, this surface modification may be used to improve IM technology for reducing removal related complications.

Chapter 6 - Introduction:

Intramedullary (IM) nailing is one of the greatest advances within trauma surgery in recent times. Today, IM nailing has become a widely established and accepted method in the treatment for fractures of the femur, tibia and humerus. However, controversy still surrounds this device such as the indications for its removal (Toms *et. al.*, 1996; Boerger *et. al.*, 1999; Gösling *et al.*, 2004; Karladani *et al.*, 2007; Morshed *et al.*, 2007) which are reviewed in chapter 1. Removal of an IM nail in symptomatic patients is primarily due to pain experienced by the patient or infection of the device and adjacent tissues (Husain *et al.*, 1996; Luhmann *et al.*, 2003; Flynn *et al.*, 2004; Hui *et al.*, 2007). Nevertheless, a large number of extractions still occur in asymptomatic patients especially paediatric patients, in order to prevent subsequent growth disturbances (Simanovsky *et al.*, 2006; Vierhout *et al.*, 2006; Gogi *et al.*, 2006; Mutimer *et al.*, 2007).

In the United Kingdom alone, approximately 13% of all active members of the British Orthopaedic Association (BOA) claimed to routinely carry out IM nail removal surgeries after uncomplicated healing (Zenios *et al.*, 2004). Interestingly, however, is that a patient being asymptomatic was listed in the same study as a contraindication by most surgeons for nail removal (Zenios *et al.*, 2004). Thus one can postulate that advocates of nail retention arise not because they wholly believe there are benefits for retaining the device rather that the risks associated with removal outweigh those surrounding nail retention. An additional complexity to the question of whether to remove or not to remove is the issue surrounding IM nail extraction in children. Within this subset of patients nail removal is often warranted to avoid growth complications such as limb shortening and related growth disturbances (Peterson, 2005; Simanovsky *et al.*, 2006; Gogi *et al.*, 2006; Vierhout *et al.*, 2006; Mutimer *et al.*, 2007). Indeed, approximately 53% of BOA surgeons claim to routinely remove IM nails in asymptomatic paediatric patients (Zenios *et al.*, 2004). Clearly the issue of nail removal in asymptomatic patients remains ambiguous, especially in light of there being a distinct lack of published consensus regarding the unequivocal indications for removal, as referred to in chapter 1. Nevertheless, the routine removal of IM nails occurs worldwide and is generally considered a low risk procedure.

Despite the low recorded number of complications related for this procedure, one issue that has arisen is the excessive bony on-growth on nails that cause intra-operative complications. In a retrospective study of five cases of IM nail removal complications associated with excessive bone on-growth were reported for all patients (Seligson *et al.*, 1997). In only two of these cases was nail removal achieved upon primary attempt however, both cases resulted in subsequent minimal fractures of the surrounding site due to difficult removals. For the remaining three cases, removal was incomplete upon the first extraction attempt. All three cases resulted in the nail being re-inserted and only one of these cases subsequently resulted in a second successful removal attempt (Seligson *et al.*, 1997). Therefore, difficulties associated with excessive bone on-growth are not only surgically related complications such as increased operative time, blood loss, patient trauma and possible re-fracture, but can also produce device related complications such as incomplete/failed removal, debris contamination, and implant/instrument failure (Husain *et al.*, 1996; Bombaci & Gorgec, 2003).

Whether it is the choice of the surgeon or the patient, fundamentally once fracture healing has occurred the function of an IM nail in spent. Therefore, no definitive scientific or clinical reason exists for retention of an IM nail. Hence, following healing removal of the nails is still considered by most a common and low risk procedure. However, removal of titanium-6%aluminium-7%niobium (TAN) IM nails often has complications, whereas electropolished stainless steel (Ss) IM nails of the same design are less often associated with removal problems (Im & Lee, 2003; Milia *et al.*, 2003; Woodruff *et al.*, 2003; Gösling *et al.*, 2005). Since nail design and geometry are similar between these two nail types, we believe the problem to be surface related.

Previous *in vitro* work by our laboratory (Baxter *et al.*, 2002; Meredith *et al.*, 2007a&b; Hayes *et al.*, 2007) and others (Boyan *et al.*, 2001; Schneider *et al.*, 2003) have highlighted the importance of surface microtopography in determining cell phenotype. Specifically we have shown that the surface of an implant can directly influence fibroblastic (soft tissue) and osteoblastic (hard tissue) behaviour (Baxter *et al.*, 2002; Biggs *et al.*, 2007a & b; Meredith *et al.*, 2007a & b; Hayes *et al.*, 2007). In terms of hard tissue response we have shown that smoother surfaces compared to the clinically available 'standard' micro-rough counterparts hold potential for reducing bony over-growth by essentially reducing osteoblast 'specific' genotypic expression via alterations in the cell shape and cytoskeletal organisation (Hayes *et*

al., 2008b). We have also observed this affect translated to a tissue level *in vivo,* where the importance of the surface characteristics of clinically used devices were found to directly control specific tissue outcomes (Welton, 2007; Schlegel *et al.*, 2008; Pearce *et al.*, 2008b).

With these points in mind, we believe that the removal difficulty reported for TAN IM nails is due to the excellent ability of this material to promote strong bone on-growth. Indeed the difficulties encountered during nail removal due to excessive bony on-growth have been reported (Seligson *et al.*, 1997) but few feasible solutions have been put forth and experimental data remains restricted to animals (Miettinen *et al.*, 1992) and human cadaveric samples (Roure *et al.*, 1999). We hypothesise that a smooth surface, created by polishing of standard micro-rough TAN nails will help to eliminate the nail removal problems associated with excessive bone-on-growth and will require lower pull out forces than the standard nails with rough TAN surfaces. Here we aim to compare the pull out forces required for the removal of standard TAN (NS), and Ss IM nails, and for the removal of NS and paste polished TAN (NP) IM nails, from a bilateral, non-fracture sheep tibia model after a 12 month implantation.

Chapter 6 - Materials & Methods:

Surface Characterisation:

Commercially available Synthes® 9.5mm Universal Humeral Nails (UHN) made of standard micro-rough TAN (NS) (ISO 5832/11) and shot-peened electropolished stainless steel (Ss) (ISO 5832/1) along with experimental paste-polished TAN (NP) were included in this study. Implant surface characterization of each nail type was assessed using a non-contact white light FRT MicroProf® profilometry (Fries Research & Technology, Germany) on 3 test samples which were not implanted. A roughness average (Ra – arithmetic mean of the roughness height expressed in micrometers) was measured from a 1x1mm scan area with a point density of 1000 points/line. Hydrophobicity was evaluated with static contact angle measurements using the Sessil drop method with the Drop Shape Analysis System (Contact Angle Measuring Instrument G10 and DSA 10 Control Unit, KRÜSS GmbH) and analysed using the Drop Shape Analysis 1.50 software (KRÜSS GmbH). Samples were placed in a preheated chamber (20°C) with an external water source to sustain a constant relative humidity. Using the computer controlled system, a 10µl droplet of distilled water was dispensed onto the sample and quantified exactly 1 minute after dispensed using the analysis software. Surface morphology of the nails was examined using a Hitachi S4100 field emission scanning electron microscope (FESEM). The images were taken in secondary (SE) and backscattered (BSE) electron mode with an accelerating voltage of 5 kV and a 40µA emission current.

The chemical composition of the surfaces was assessed using X—ray photoelectron spectroscopy (XPS). XPS measurements were carried out by the Robert Mathys Foundation, Bettlach, Switzerland. Prior to surface analysis, the samples were ultrasonically treated for 20 minutes with alkaline 3% Deconex 12PA (Borer Chemie, CH) followed by rinsing with deionised water and subsequently cleaned with ethanol for 10 minutes after which time the samples were once again ultrasonically treated for 20 minutes in ultra-pure water and subsequently rinsed with methanol in order to remove debris and potential contaminants from the packaging material. The samples were mounted on aluminium sample plates by using double sided electrically insulating sticky tape which is vacuum compatible. All spectra were recorded on a Kratos Axis Nova (Kratos Analytical, UK) using monochromatic AlKα radiation (1486.69 eV) produced at an anode power of 225 W (15kV, 15 mA), an electron

take-off angle of 90° relative to the surface plane and an electron analyser pass energy of 80 eV. During analysis, the base pressure remained below 10^{-8} torr. For quantification, survey scans with a step width of 0.5 eV were performed on two spots of 300 x 700 μm^2 per sample. The spectra were acquired from 2 positions per sample. Data was evaluated with CasaXPS 2.3.10 (CasaXPS Ltd, UK) using relative sensitivity factors supplied with the instrument.

Surgical procedure:

Approval to perform this study was granted by the Cantonal animal ethics committee (GR 5/2006). Fourteen adult female Swiss Alpine sheep were selected from a flock of 200 subsequent to radiological analysis being preformed on both tibiae to control length and diameter of the tibia to be large enough for the UHN. This allowed for a standard model to be created. The fourteen sheep were divided into two groups of 7 sheep. Using a bilateral, non-fracture model, seven sheep were implanted with an NS nail in the one tibia and an Ss nail in the contralateral tibia. The remaining 7 sheep were implanted with an NS nail in one tibia and a NP nail in the contralateral tibia. For surgery, a 5 cm incision was made on the medial aspect of the patella ligament of the stifle joint for both hind limbs. Subsequently, the joint was flexed approximately 90 degrees in order to gain access to the proximal tibia. Approximately half-way between the patellar tendon and the cranial edge of the medial femoral meniscus, a hole was drilled into the joint surface of the proximal tibia. The tibia was reamed in increments of 0.5 mm to a maximum diameter of 11 mm with a rigid reamer in order to create a more uniform amount of contact between the nail and tibial cortex. The tibia plateau was reamed to 12 mm to ease nail insertion. A human 9.5 mm diameter UHN (humeral nail) was inserted (with hammering) into the tibia through an extra-articular approach and a proximal locking bolt was inserted via a small incision through the skin and finally an endcap was placed at the proximal site of the nail.

Initially nails were locked proximally and distally in orthogonal planes using a 5.0 mm locking screw made from the same material and surface treatment as the nail. Locking was facilitated using a custom made aiming device attached via the threads in the proximal aspect of the nail that are used for attaching the insertion device and the endcap. However, due to the close fitting of the human nail in the reamed sheep intramedullary canal, two interlocking screws were later considered to be redundant to prevent migration of the nail. Therefore, in the interest of reducing surgical time for the sheep, and preventing fracture of the highly reamed bone, the use of the distal locking screw was discontinued after the first 5 sheep in the

NS versus Ss group and was not used in the NS versus NP group. Since it was a paired design, we believed the influence of discontinuing the distal screw would have the same effect upon both nails tested within the sheep.

The subcutaneous tissue was closed with an absorbable suture material and the skin was closed with stainless steel skin staples. The limbs were bandaged with cotton wool and an adhesive bandage was left in place for 5-7 days, or less if believed to be causing irritation to the animal. Post-operatively, analgesia consisted of Carprofen (4mg/kg subcutaneous, q24h for 3 days, Rimadyl®, Pfizer, USA) and Buprenorphine (0.01mg/kg subcutaneous, q12h for 3 days, Temgesic®). Immediately post-surgery and for the first week of the observation period all animals were housed in individual boxes in protection slings that allowed full weight bearing on the legs, but not reclining. No complications were encountered during, or subsequent to surgery. Each sheep was evaluated every 4 weeks clinically for the duration of the study and every 8 weeks radiographs were taken in two plains latero-medial and cranio-caudal to monitor the nail position, stability and any visible signs of bone on-growth. The nails were left in place for a total implantation time of 12 months. The animals were euthanized by means of an intravenous overdose of barbiturate (Pentobarbital, Vetanarcol® 60 mg/kg).

Mechanical testing:

After euthanasia, the tibiae were excised and adjacent soft tissues removed. The locking bolts and the end cap were removed from the nails of 6 sheep from each group. Subsequent pull-out tests were preformed on these nails using an electro-mechanical testing machine Instron 5866 (Instron inc., Norwood, US) with a 10kN load-cell and a custom made pull-out device (Figure 5.1). All nails were removed with a constant force (1mm/min). Load- and displacement-data was recorded with a sampling rate of 50Hz. Data were evaluated using Matlab® software (V6.5, Mathworks inc., Natick, US) with a custom made procedure. The one remaining nail from each group remained *in situ*, and, will be used for histomorphometric analyses (not reported here due the extensive time required to embed a whole tibia containing a IM nail of approximately 9 months).

Statistical analysis:

Statistical evaluation was performed using SPSS for Windows Version 14.0 (SPSS Inc, Chicago, Illinois, USA). The effect of polishing with a paired model (Ss versus NS; NP versus NS) was assessed using a non-parametric test (Wilcoxon signed ranks) for Ss versus NS samples, as assumptions regarding normal distribution were not met for SS samples (Shapiro-Wilk test). Furthermore, a paired t-test was performed for NP versus NS as assumptions regarding normality were met. For both comparisons, p-values less than 0.05 were deemed significant

Figure. 6.1 Testing Device, with adapter screwed into the endcap holder of the nail within the tibia before pull out was performed. A constant force of 1mm/min was applied.

Chapter 6 - Results:

Surface characterisation

Non contact profilometry revealed that the nails made of NS, Ss and NP used in this study had average surface roughness' (Ra's) of 0.97μm, 0.57μm and 0.21μm, respectively (Figure 6.2). Hence, surface polishing of the commercially available TAN IM nails successfully reduced the perceived roughness of the nail. In terms of Ra's, paste polishing of TAN IM nails produced a smoother surface than the archetypical orthopaedic grade, shot-peened smooth material, stainless steel, with Ra's of 0.21μm and 0.57 μm, respectively. In terms of surface wettability, compared to the control standard TAN surface (64.2±7.7), contact angle results (Figure 6.3) showed that paste polishing (64.1±2.9) of the NS IM nail did not markedly affect the surface hydrophilicity. No difference in the chemical composition of the surfaces was noted. As expected, the spectra for the TAN IM nails were dominated by Ti and O due to the naturally occurring titanium oxide layer (Figure 6.3). The alloying elements of Al and Nb were also present in small amounts. The strong C signal has previously been shown to be present on high surface areas oxide films that have undergone atmospheric exposure and storage (chapter 2). Ca contamination was also detected on the surfaces most likely a result of contamination from handling. Other contaminants included N, Na and P.

SEM analysis in both SE and BSE mode provided information regarding the surface features of the samples. For NS nails (Figure 6.4A) the undulating surface of this material was evident. Again, distinct variations were seen between the peaks and valleys of the surface, with the micro-spikes adopting a rough, sharp edged appearance. With the aid of BSE imaging the niobium rich particles embedded within the surface, as described in chapter 2, were evident and differed in their composition as they are denser, therefore produce more BSE, compared to the rest of the material (light green arrows, Figure 6.4A). Paste polishing clearly reduced the microtopography of the TAN surface (Figure 6.4B). In SE mode, the surface appeared smooth and free of niobium rich particles (not absent, just indistinguishable in SE mode), suggesting that the mechanical abrasiveness of this method works particularly well for TAN IM nails. Only in BSE mode did the smoothened niobium rich particles become evident (yellow arrows, Figure 6.4B) and even then, these are evidently embedded within the material and play only a minimal part in enhancing the surface roughness. Imaging of Ss again highlights the importance of using various techniques for characterising surfaces. While non contact profilometry assessed the surface as being relatively rough (Ra 0.57μm), SEM imaging demonstrates that the actual surface was extremely smooth, however, the waviness

encountered on areas of the surface, clarified in particular in BSE mode, would contribute to the higher Ra observed (Figure 6.4C).

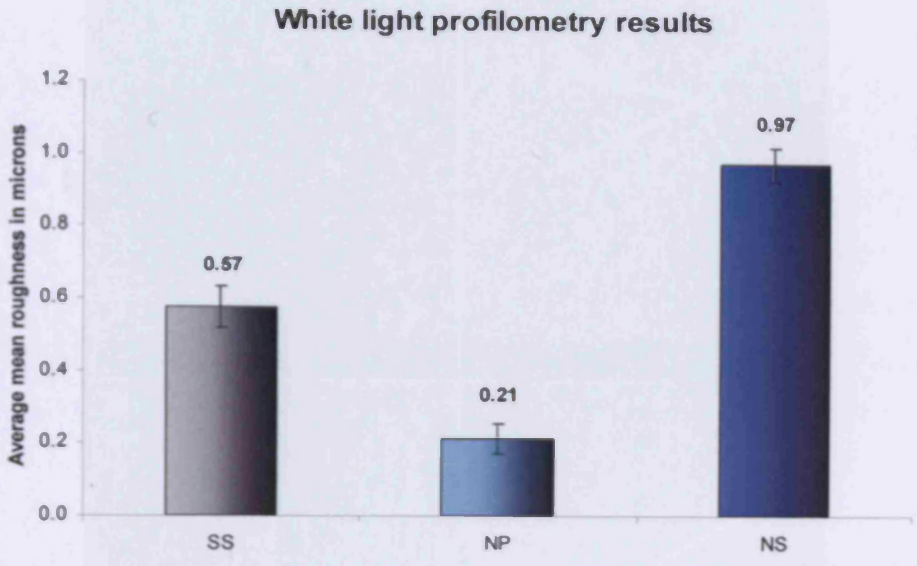

Figure 6.2. Non contact white light profilometry results. The graph represents the mean average roughness of 6 measurements of each sample, including standard deviations. Paste polishing (NP) dramatically reduces the mean average roughness of the TAN surface compared to the micro-rough standard positive control (NS).

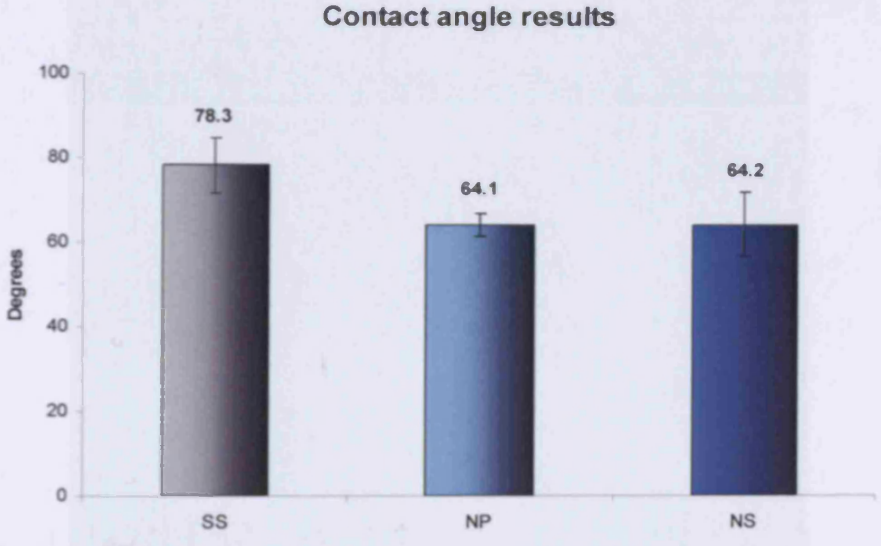

	Ti 2p	O 1s	Al 2p	Nb 3d	C1s	Ca2p	N1s	NaKLL	P2p
NS	13.3	41.7	2.9	0.7	39.0	0.1	0.2	0.0	1.7
NP	12.3	39.8	1.6	0.1	42.5	0.2	0.2	1.1	1.7

Figure 6.3. Contact angle (CA) measurements for all substrates. Polishing (NP) does not appear to alter the hydrophilicity of the samples to any significant extent compared to the clinically available TAN IM sample nail (NS). As all IM nails were anodised subsequent to processing, no major differences in the chemical composition of the surface was noted. Data represents mean of 6 measurements from each sample, including standard deviations.

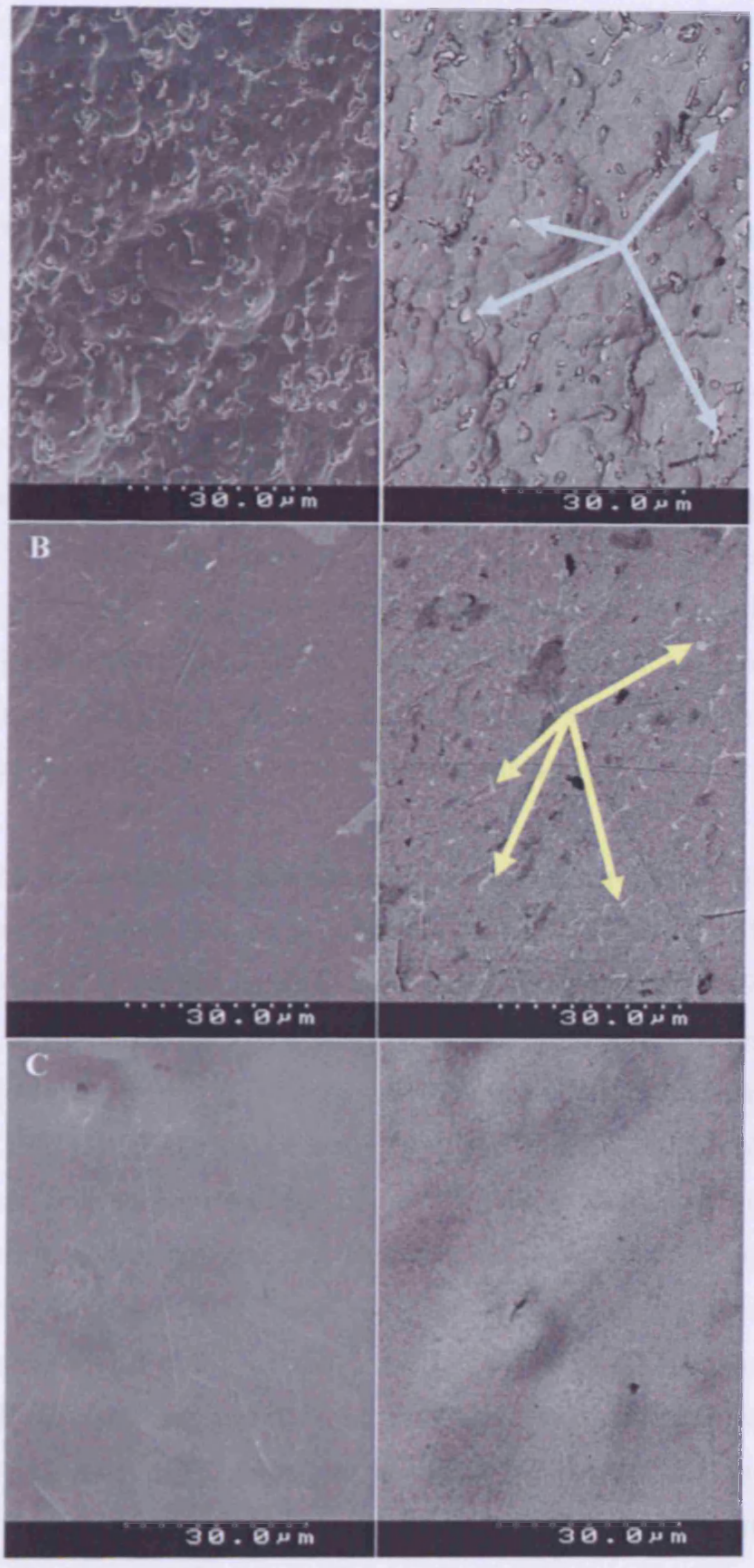

Figure 6.4. SEM images of the titanium-6%aluminum-7%niobium surfaces and stainless steel surface in SE (left image) and BSE mode (right image). (A) NS; (B) NP; (C) Ss. The characteristic β phase niobium-rich inclusions are clearly visible in the micro-spiked formation of the NS surface (A). In BSE mode the difference in composition of the niobium particles is more evident (blue arrows). Paste polishing (B) clearly reduces the microtopography of the surface. The niobium rich inclusions are not evident in SE mode. In BSE mode, the niobium rich inclusions are evident (yellow arrows).

Mechanical testing

Figures 6.5 and 6.6 demonstrate the differences in pull out force for NS versus Ss, and NS versus NP nails, for the 6 six sheep within each paired group i.e. the nail from the right and left tibia of the same sheep. Results from individual sheep from the NS and Ss groups show that for all sheep (Figure 6.5, sheep 1-6) a lower pull out force was recorded for Ss nails. For the first sheep the pull out force required for the NS nail was 23.39N, compared to only 8.48N for the Ss nail. The same trend was observed for sheep 2-6 with values of 3065.89N, 66.05N, 1013.23N, 2728.45N and 2062.54N being noted for the remaining NS nails, while Ss nails within the same sheep required significantly lower forces of 974.56N, 17.51N, 123.49N, 97.89N and 20.83N, respectively (Figure 6.5, sheep 1-6). Overall, mechanical pull-out tests of the Ss nails and NS nail from all sheep demonstrated that the Ss nails had a significantly lower ($p=0.028$) pullout force than the NS nails (Fig.6.7B). For two sheep in this group (sheep number 1 and 3) the pullout force was very low in both tibiae which was attributable to a wide medullary canal, which was observed radiologically.

Similarly, results of the mechanical pull out tests from the second group of sheep containing NS and NP IM nails showed that paste polishing reduces the pull out force required for extraction. For NS nails within this group pull out forces of 6027.116N, 489.328N, 3743.38N, 2207.922N, 2968.671N and 6027.116N were observed for sheep 1-6, respectively (Figure 6.6, sheep 1-6). However, for paste polished nails implanted within the same sheep, pull out forces were 40.32.997N, 355.865N, 3580.033N, 1011.086N, 3732.711N and 4032.997N, respectively (Figure 6.6, sheep 1-6). Again, for all sheep mechanical pullout tests of the experimental NP nails also demonstrated a markedly lower pullout force compared to the NS nail implanted in the same ($p=0.05$) (Fig.6.7B). However, within this group two exceptions were noted (sheep number 3 and 5). Firstly, one NP nail (Fig 6.8) was revealed to have a slightly higher pull out force compared to the contra-lateral tibia containing the NS IM nail (Figure 6.6, sheep 5). Additionally, during testing of the NP IM nail, due to the tight fit of the human nail to the sheep medullary canal, the bone broke. Secondly, pull out forces of NP and NS from a different sheep produced similar results for both nails (Figure 6.6, sheep 3). Radiological analysis, as well as analysis by eye after the pull out tests showed bony in-growth (Fig 6.9) of the lower hole of both the NP and NS nails, so that a cylinder of bone of equal volume had to be broken for both nails, accounting for the similar pull forces noted. Therefore, the results for the pullout test were a reflection of the force to break a cylinder of the bone in the hole for both nails, rather than on the force required to remove the nail.

The data from this sheep was excluded from the statistical analysis. Observations after removal of polished TAN nails showed no bone adhesion to the surfaces. Bone was not observed to grow directly onto the surfaces within the nail interlocking holes of the polished nails, and any tissue within the screw holes was easily displaced with a K wire (Fig. 6.10A). Contrastingly, within the interlocking holes of standard TAN nails bone on-growth onto the surface of the holes was evident (Fig. 6.10B). Furthermore, this hard tissue could not be displaced. Bone was also observed on the cutting flutes at the tip of the standard TAN locking bolts whereas for paste polished TAN locking bolts of the same design, bone tissue adhesion was not observed (Figure 6.10C).

Figure 6.5 Paired mechanical pull out results for Ss nails compared to NS.

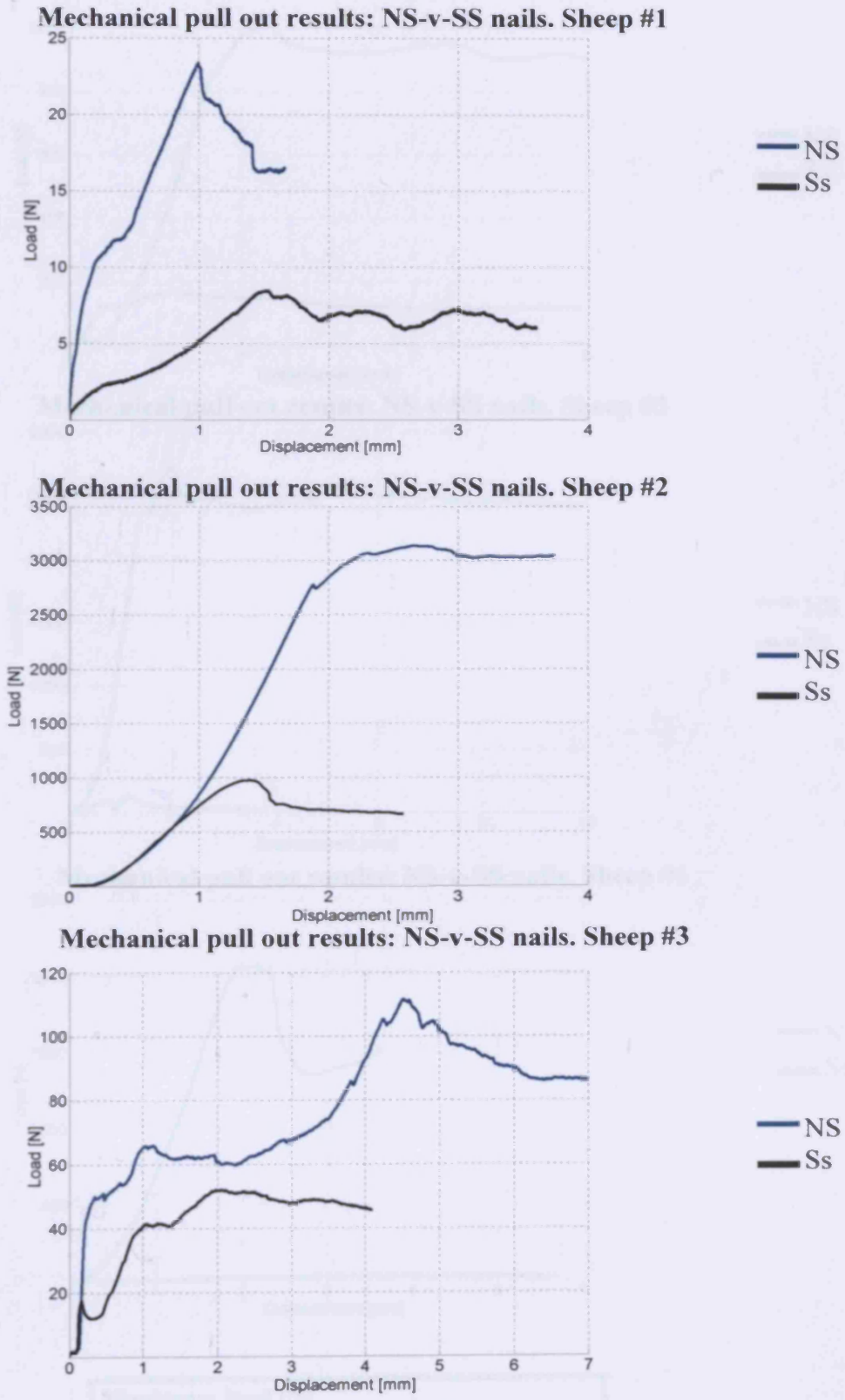

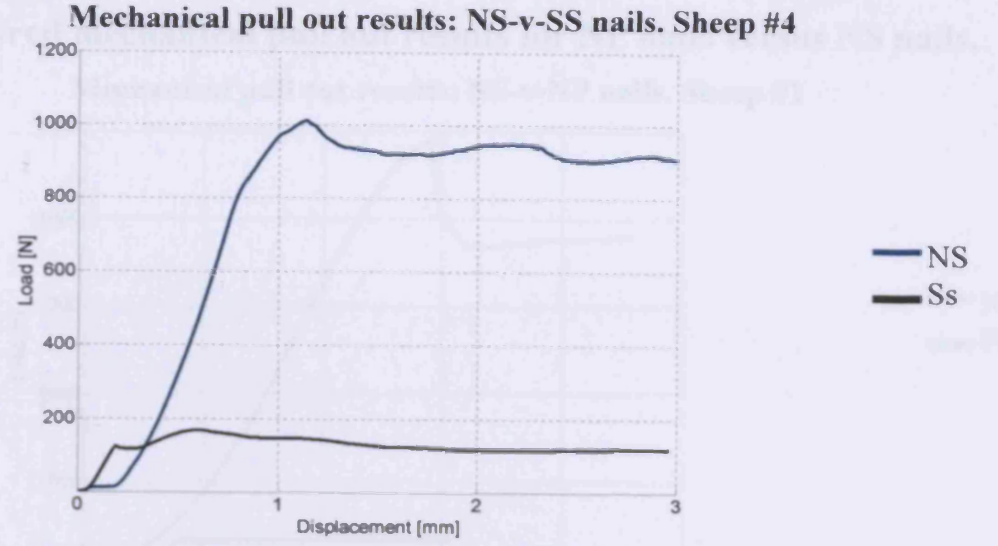

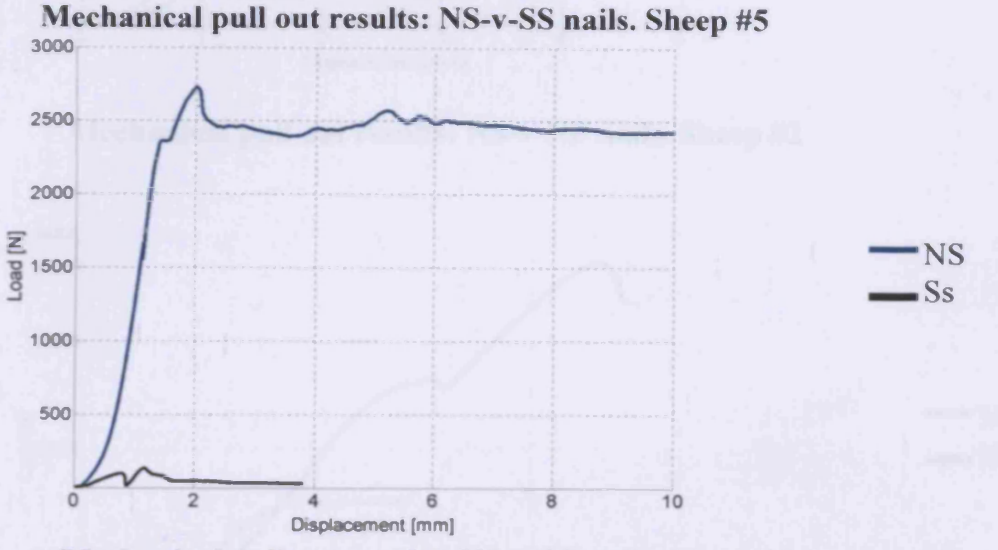

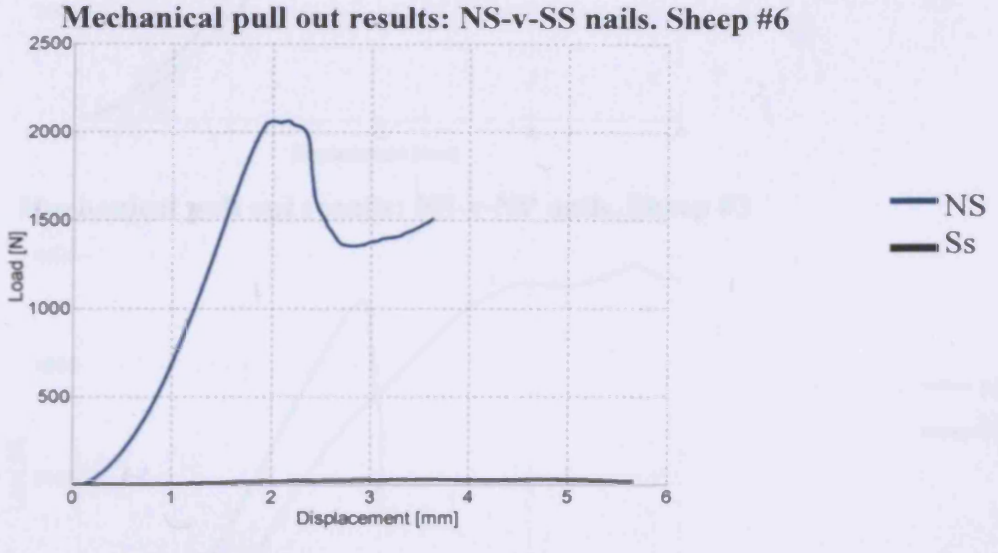

	Maximum load [N]					
	1	2	3	4	5	6
NS	23.39	3065.89	66.05	1013.23	2728.45	2062.54
Ss	8.48	974.56	17.51	123.49	97.89	20.83

Figure 6.5. Maximum load [N] required for stainless steel (Ss; black lines) and standard TAN (NS; green lines) IM nail displacement within the same sheep (1-6). Actual values displayed above for each sheep.

Figure 6.6 Paired mechanical pull out results for NP nails versus NS nails.

Mechanical pull out results: NS-v-NP nails. Sheep #1

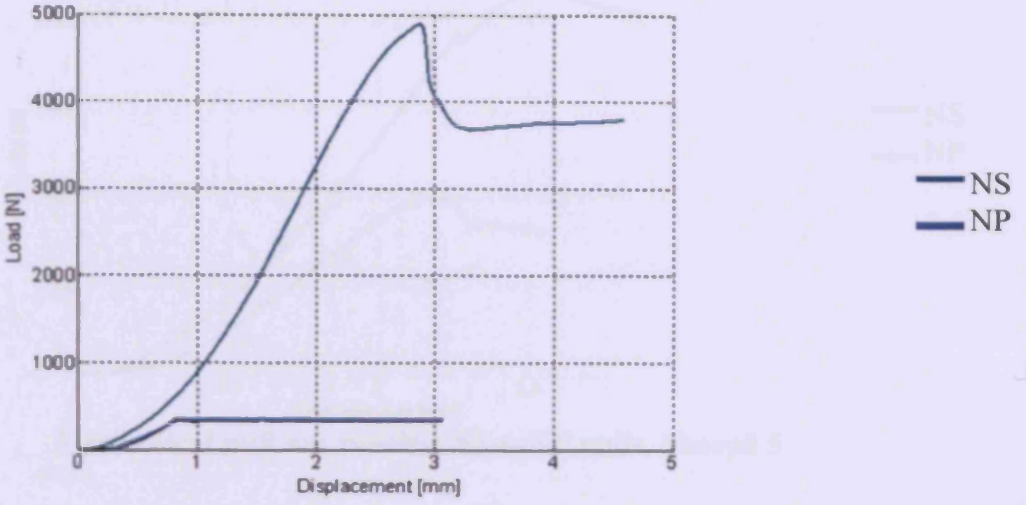

Mechanical pull out results: NS-v-NP nails. Sheep #2

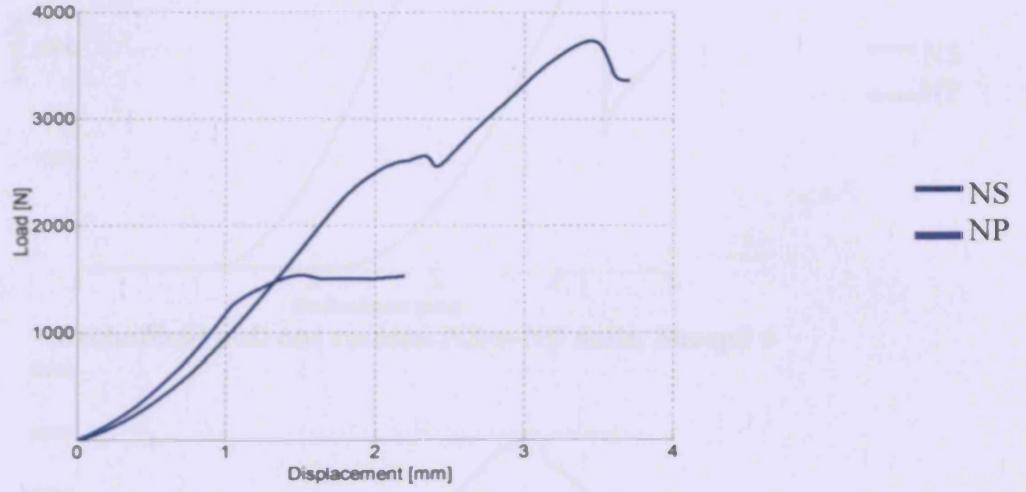

Mechanical pull out results: NS-v-NP nails. Sheep #3

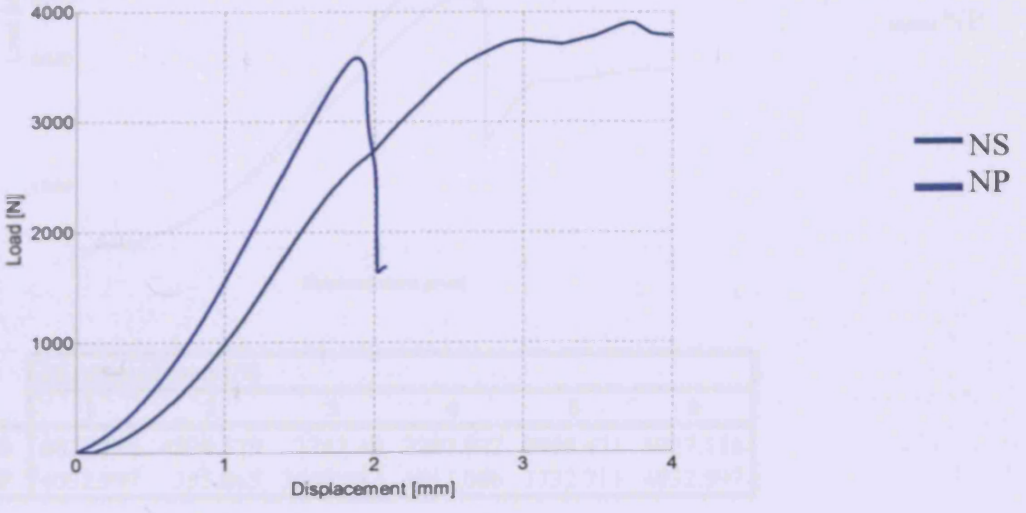

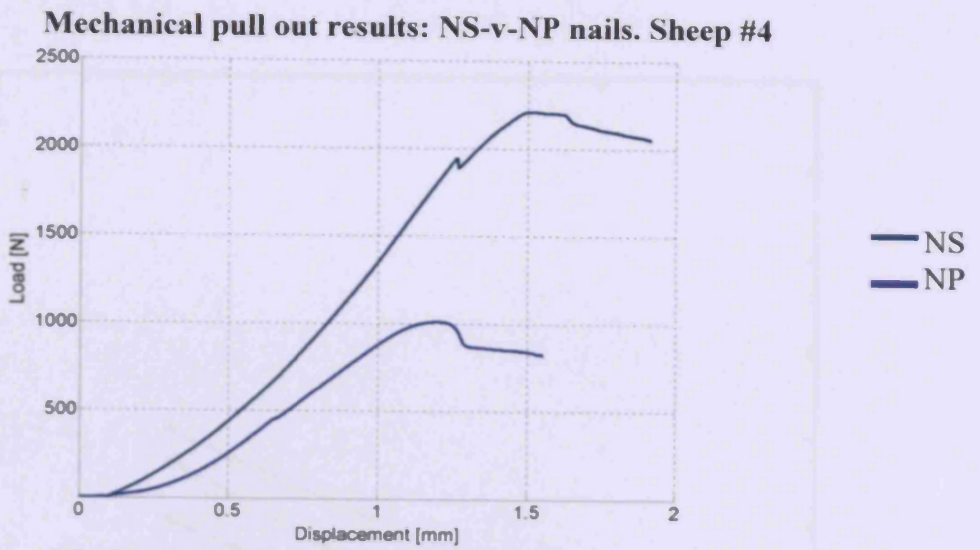

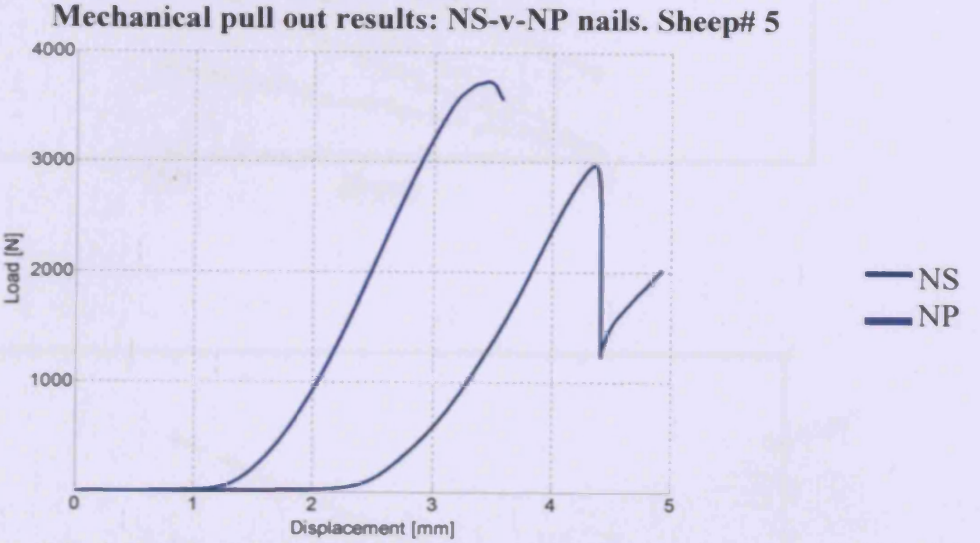

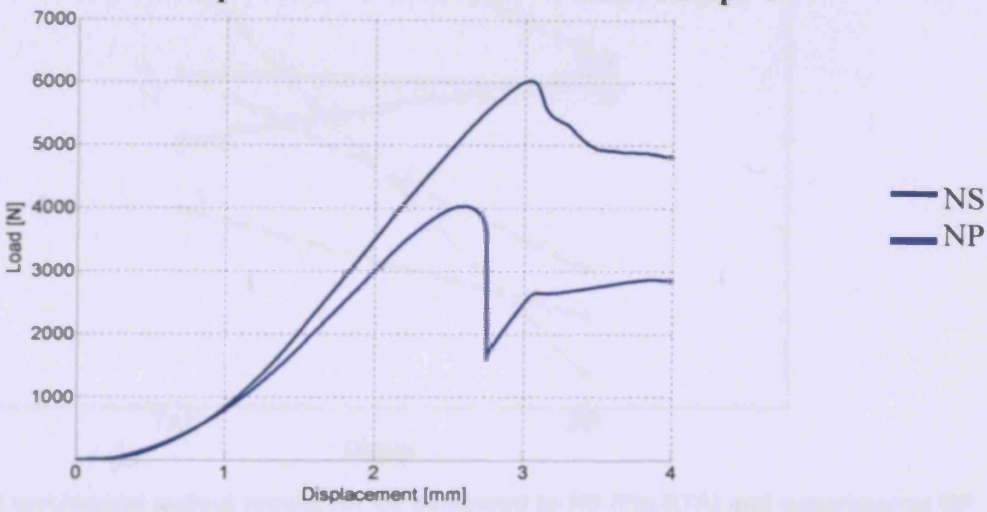

	Maximum load [N]					
	1	2	3	4	5	6
NS	6027.116	4894.328	3743.38	2207.922	2968.671	6027.116
NP	4032.997	355.865	3580.033	1011.086	3732.711	4032.997

ure 6.6. Maximum load [N] required for standard TAN (NS; green lines) and paste polished TAN (NP; blue es) IM nail displacement within the same sheep (1-6). Actual values displayed above for each sheep.

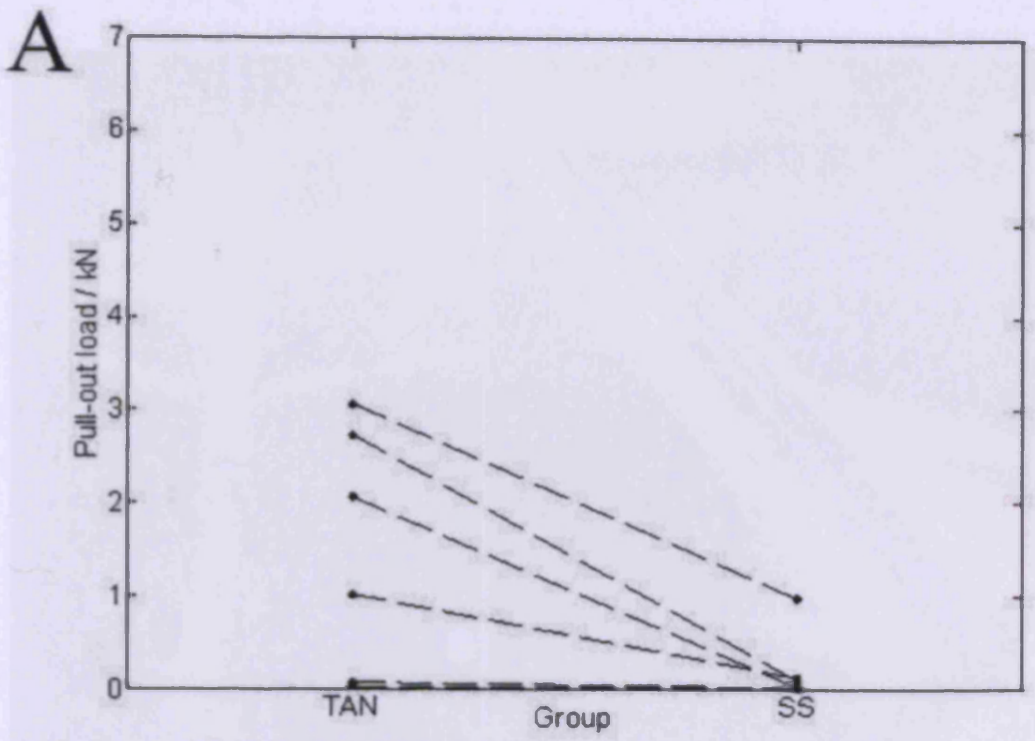

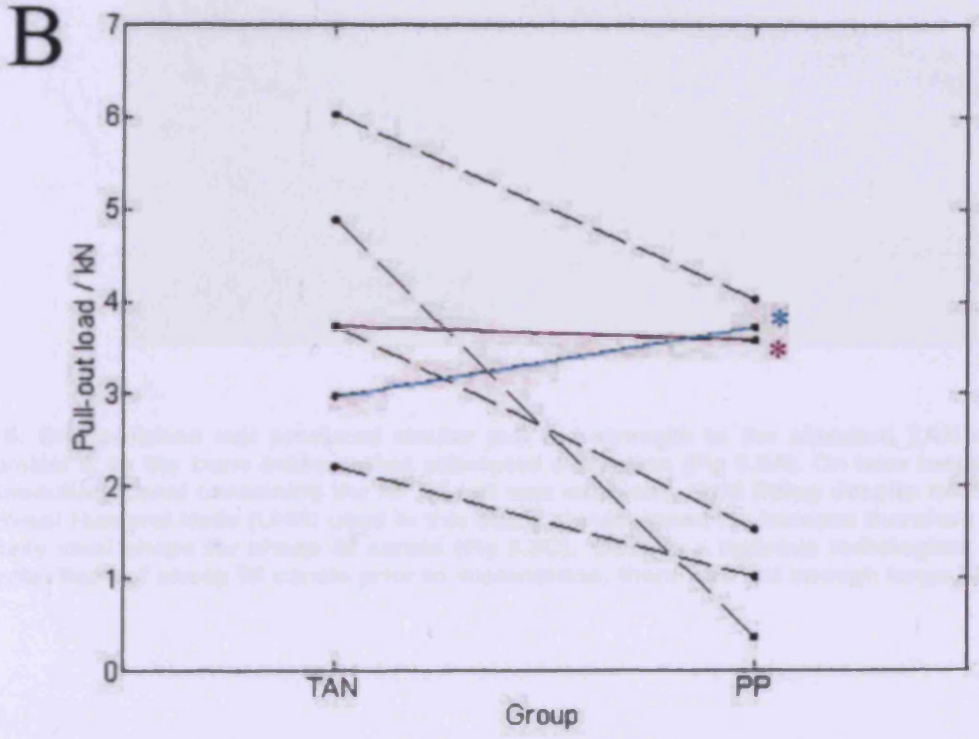

igure 6.7. Combined mechanical pullout results for Ss compared to NS (Fig.6.7A) and experimental NP ompared to NS nails (Fig.6.7B) within the same sheep. Results demonstrate that the surface icrotopography of IM nails has a significant effect upon the force required for their removal. Both Ss ails ($p=0.028$) and the polished TAN nails ($p=0.05$) were significantly easier to remove compared to andard micro-rough TAN nails implanted in the respective contralateral tibia of the same sheep. Two ceptions (blue and purple asterix, Fig 6.7B) were however, observed for the NP group.

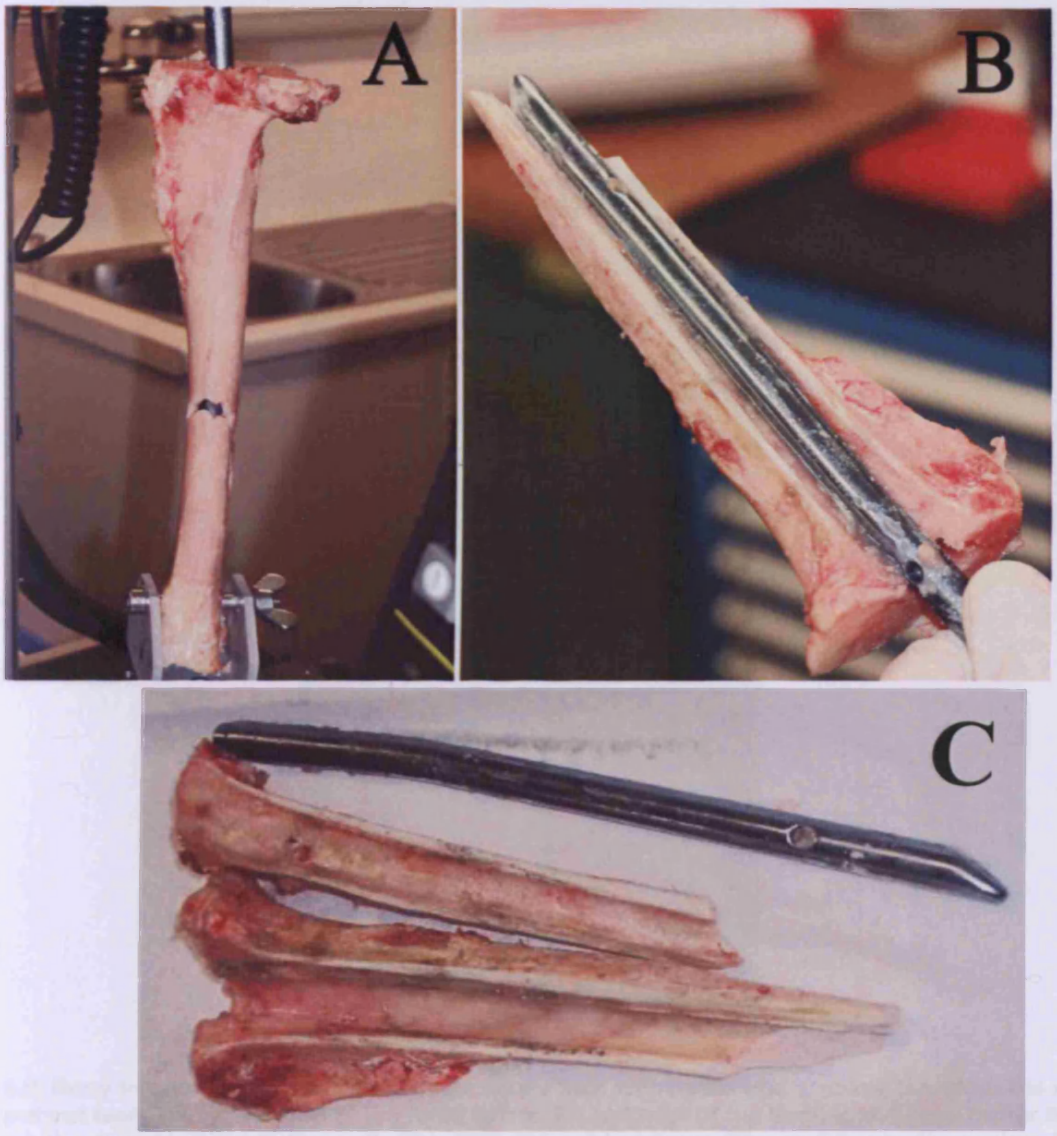

Figure 6.8. One polished nail produced similar pull out strength to the standard TAN nail (Figure 6.6, sheep number 5, as the bone broke during attempted extraction (Fig 6.8A). On later inspection we noted that the medullary canal containing the NP IM nail was extremely tight fitting despite reaming (Fig. 6.8B). The Universal Humeral Nails (UHN) used in this study are designed for humans therefore do not have an anatomically ideal shape for sheep IM canals (Fig 6.8C). Despite a rigorous radiological analysis of 200 experimental flock of sheep IM canals prior to implantation, there was not enough large IM canals for this study.

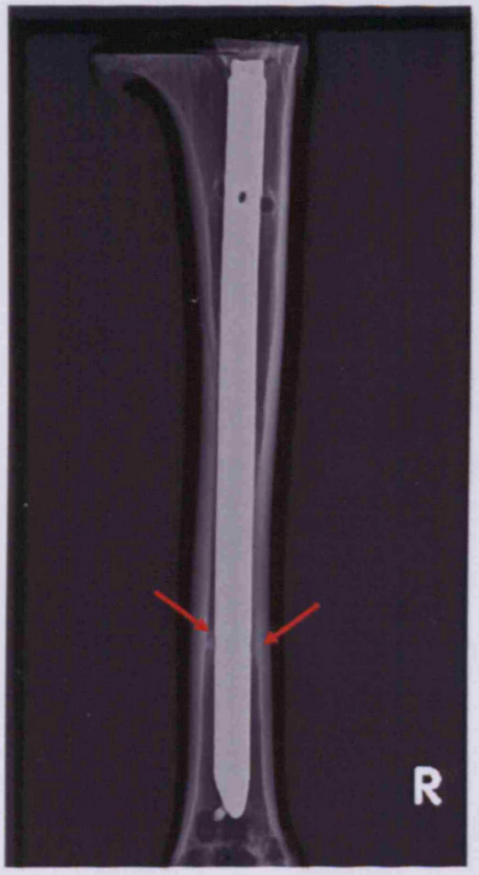

Figure 6.9. Bony in-growth into the empty distal screw hole was noted (red arrows), therefore the results for the pullout test was a reflection of the force to break a cylinder of the bone in the hole, rather than on the force required to remove the nail. The data from this sheep (Figure 6.6, sheep number 3) was excluded from the statistical analysis.

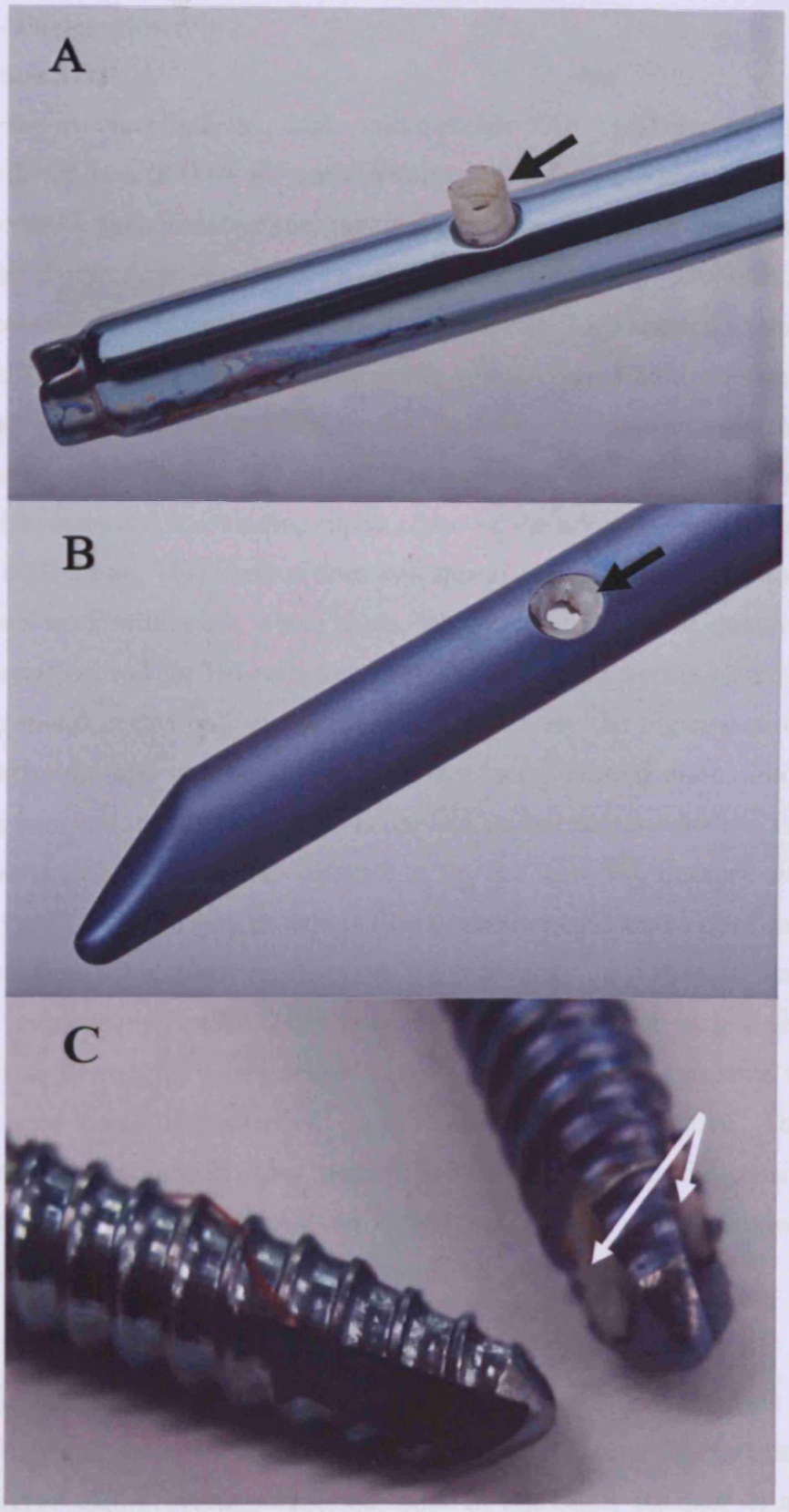

Figure 6.10. Observations after removal of polished TAN nails showed no bone adhesion to the surfaces. Bone was observed to grow directly within the nail interlocking holes of the polished nails, but was easily displaced with a K wire (Fig. 6.10A, black arrow). Contrastingly, within the interlocking holes of standard TAN nails, bone in-growth was also evident (Fig. 6.10B, black arrow). Furthermore, this hard tissue could not be displaced. Standard TAN proximal interlocking bolts also showed evidence of bone on-growth (white arrows, Fig. 6.10C), while no tissue adhesion was observed for paste polished TAN interlocking bolts (light blue screw).

Chapter 6 - Discussion:

Surface characterisation:

As expected, the commercially available micro-rough TAN (NS) surface had the highest mean average roughness (Ra) of all samples studied. This is supported by the SEM images which clearly show the characteristic undulating micro-spiked morphology discussed in chapter 2. The mechanical abrasiveness of the paste polishing technique appears to be extremely successful for IM nails as the Ra is dramatically lowered and as the SEM images reveal the surface becomes void of the majority micro-discontinuities associated with the standard surface of the material, to the point that the harder niobium rich inclusions have also been smoothened significantly. In fact, to the untrained eye with SE imaging they are indistinguishable from the surrounding alpha phase of the alloy. However, their presence is reinforced in BSE mode. This surface does not appear the same to the 13 and 50mm discs used for *in vitro* work within this whole study, which may partially be due to differences in source of material i.e. rod for IM nails versus sheet metal used for the 13mm discs, and the paste used i.e. wood versus nut, and highlights expressively the importance of consistency within manufacturing (this will be discussed further in the general discussion). Inconsistent manufacturing is one of the biggest threats to applied surface science studies. Essentially, this renders extrapolation between studies difficult to say the least. For instance, one cpTi screw from one study may compare well in terms of Ra to another cpTi screw from another study or even within the same study, however the surface morphology may differ so dramatically that the biological response may evoke differences. Furthermore, when testing a new implant the surface should be thoroughly characterised, even when stated that the same treatment was performed on previously characterised implants of the same material. Therefore, it is unacceptable to assume one particular material will morphologically be consistent between studies. Additionally, by delineating these differences a more eclectic knowledge can be gained from cell and/or tissue-material interactions.

Another major area of contention is inferior surface characterisation. This point can be supported by the results obtained here for Ss. Unexpectedly, the average roughness of Ss was noted to be higher than previously reported, both in this study (chapter 2) and elsewhere (Meredith *et al.*, 2006; 2007a&b; Pearce *et al.*, 2008b) however this is most likely a result of the Ss used in this study being shot-peened while this has not been the case for previous studies with discs, plates and screws.

However, clarification is given with the SEM images which show that in fact this is an extremely smooth surface and few undulations have inadvertently 'falsely' augmented the Ra. If this study was only to employ profilometry as the method of choice for surface characterisation, which has been unfortunately been the case elsewhere (Brett *et al.*, 2004; Schneider *et al.*, 2004), misrepresentation may have easily occurred in either a positive or negative manner (i.e. giving the surface a more or lessened height profile). Often little or no characterisation is employed at all (Walboomers *et al.*, 1998; Postliglione *et al.*, 2003) which again renders any conclusions questionable. Once again this strengthens the argument for extensive surface characterisation within any study. Without a complete characterisation of the surface being employed as standard approach time and time again studies will miss vital information regarding the biological response exerted by a material, as well as risking drawing ill-informed conclusions.

As mentioned in chapter 2, the contact angle of a material is defined as the angle formed by a liquid at the three phase boundary where a liquid, gas and solid intersect (Andrade, 1985). However, its use in the field of biomaterials is limited and is generally employed in a synergistic approach with other characterisation methods to obtain surface information. With regards to the samples included in this study made from rod TAN it appears that paste polishing of TAN IM nails does not affect surface hydrophilicity. This observation is in agreement with results obtained from the paste polished TAN 13mm discs made from TAN sheet metal used in the *in vitro* section of this work. For all three IM nails the contact angle results suggest they are within what is considered to be hydrophilic.

Nail removal:

To date, AO IM nails are fabricated for orthopaedic clinics from either TAN or Ss. Yet, removal of standard TAN (NS) IM nails often produces more extraction related complications compared Ss IM nails of the same design (Im & Lee, 2003; Milia *et al.*, 2003; Woodruff *et al.*, 2003; Gösling *et al.*, 2005). The difficulty in removing nails due to excess bone on-growth has not been described for steel which for clinical orthopaedics is supplied with a smooth surface (Disegi *et al.*, 1998a). In contrast, TAN has a micro-rough surface containing a micro-spiked surface morphology due to the fact that the alloy is a mix of soft alpha and harder beta phases (Sittig *et al.*, 1999a&b; also see chapter 2 discussion). Due to this surface morphology TAN has been shown to integrate extremely well with bone (Schmidt *et al.*, 2002). Therefore, we believe that by reducing the surface micro-roughness that is associated

with NS IM nails via surface polishing that TAN IM nails will be easier to extract due to a reduce capacity to support excessive bone on-growth. Other studies have noted the promise of this approach however there have been few and inconsistent results to confirm this concept (Albrektsson & Hansen, 1986; Carlsson *et al.*, 1988; Sun *et al.*, 1999). For instance, a histological study by Larsson and colleagues (1996) compared the bone response to machined and electropolished titanium screw implants in rabbit cortical bone. They included both anodised and un-anodised samples to also investigate the influence of oxide thickness. They showed that for anodised machined and electropolished titanium cortical screws (since our samples were anodized only these are relevant in this context) that less bone-metal contact was noted around electropolished screws 1-week postoperatively. However, subsequent to 3 weeks post-operatively the author's note that no difference in bone-metal contact was observed between machined and electropolished screws indicating a faster rate of bone formation adjacent to electropolished screws within this 2 week period. By 6 weeks post-implantation bone-metal contact appeared to be similar for both polished and machined screws. One must question however, the relevance of rabbit bone (Pearce *et al.*, 2008a) for reflecting the clinical bone healing situation. Also, the length of the study time only covers initial healing period and not particularly the later remodelling phases that would also contribute to bone on-growth, thus essentially the influence of polishing on this parameter was negated. Moreover, while histology provides information regarding the quantity of tissue attachment the actual strength or quality of tissue attachment was not assessed. This is supported by a recent study carried out in our laboratory which assessed the influence of surface polishing for reducing bone-implant contact and removal torque (Pearce *et al.*, 2008b) While the bone contact, determined histologically, was similar for polished and standard screws which is in line with observations made by Larsson and colleagues (1996) the mechanical force required to remove the screws was different. Specifically, significantly less force was required to remove polished screws. This essentially provides a clearer indication with regards to the strength of bone attachment for polished and standard screws, as histology alone cannot address this issue.

Despite the knowledge that surface microtopography can be a major determinant of bone osseointegration, this avenue in terms of IM nailing technology has not previously been explored as a potential resolution to issues involving device removal. In fact many studies suggest alternative methods for removal once conventional methods have failed (Alan *et al.*, 2007; Weinrauch & Blakemore, 2007) such as alternative surgical approaches or use of

surgical instruments in a different manner initially intended to aid removal; although this only addresses the issue once complications have been encountered. Instead, in this novel study we offer a simple and cost-effective method for reducing the problems associated with IM nail removal and resulting intra-operative complications due to excessive bony in-growth. Results from this study support the indication that the surface microtopography of the IM nails has a significant effect upon the force required for removal. As excepted the pull out forces required for removal of Ss IM nails was significantly lower than contra-lateral NS IM nails implanted within the same sheep. Interestingly, by reducing the surface microtopography of the clinically available standard TAN IM nails we also observed a significant reduction in the force required for nail removal. Of course one may postulate that Ss already offers a solution without the need for further developments. However, issues surrounding toxic metal ion release (Case *et al.*, 1994; Hanawa, 2004) mechanical inferiority under cyclic loading (Perren *et. al.*, 2001; Eschbach *et. al.*, 2001), imaging disadvantages (Pohler, 2000; Eschbach, 2003) and second-rate biocompatibility (Massone *et. al.*, 1991; Nichols & Puleo, 1997) compared to TAN, has resulted in its reserved potential within IM nailing technology.

Supporting this notion is the fact that there appears to be a material dependent outcome for extraction. Specifically, regardless of similar topographies Ss IM nails generally had lower extraction force needed for removal compared to NP TAN IM nails. This result may partially be attributable to the locking bolts which were included for all Ss nails but not all NP and NS nails. Essentially, this would prevent any major hard-tissue in-growth thus negating this effect on removal as observed with sheep number 3 (figure 6.6). However, the overriding contribution is likely to be a product of differences in the respective polished nails surface chemistry. A myriad of studies have emerged that highlight the importance of the surface chemistry and in particular the importance of the oxide layer of fixation materials. This topic has also been discussed in chapter 1 (The Role of Surface Chemistry). Specifically, the surface chemistry of a device has been implicated in the initial protein-metal interactions (Meyer *et. al.*, 1988; Degasne *et. al.*, 1999; Yang *et. al.*, 2003) and it is believed that this relationship primes the material for subsequent cell phenotypic and genotypic performance and as a consequence, the ensuing tissue response. Unfortunately, however, studies linking the initial protein attachment to tissue integration of an implant are noticeably lacking. However, one study which does emphasise this issue is that of Thomsen and colleagues (1997) whom investigated the influence of titanium, zirconium and gold implants on rabbit tibial bone response. The authors report that subsequent to 1 and 6 months post-operatively

bone-implant contact was similar for titanium and zirconium implants but significantly less for gold devices. The authors contribute these results to the stable oxide layers of titanium and zirconium compared to gold which due to its noble metal origins only produces an oxide layer under extreme conditions. Similarly here the difference in composition of the surface oxide layers of Ss and NP are undoubtedly a major contributable factor in the material dependent response observed for IM nail removal.

Essentially, the bio-passivity of an implant is attributable to the oxide layer. Many alloying elements tend to show favourable properties in terms of low charged species at physiological pH with the likes of titanium, aluminium and niobium being accepted by tissue as 'inert' materials, thus do not evoke adverse tissue reactions. However, other oxides have been reported to show either a tendency to evoke a foreign body reaction resulting in a tendency to produce a fibrous capsule or indeed an outright toxic response (such as chromium and cobalt found in stainless steel). Iron oxide, another of the major elements found in Ss, is known to induce encapsulation through its corrosion products and their solubility (Textor *et al.*, 2001) while contrastingly cpTi and its alloys are known to have a superior corrosion resistance compared to Ss (Disegi, 1997). Due to the clear differences in oxide thickness between Ss (approximately 2nm) and TAN (approximately 5nm) the former affords itself more readily to corrosion than the latter, especially since Ss takes a longer period to repassivate thus inadvertently allowing increased time over TAN for metal ion release (Hanawa, 2004). The release of ions into surrounding tissue has previously been shown to play a role in periprosthetic pathology by contributing to implant failure by impairing bone repair while allowing fibrous tissue formation following debris-induced osteolysis (Nichols & Puleo, 1997). Additionally, the alloying elements of these implants will produce different isoelectric points across the surface of the device which may influence the cellular response (Sunny & Sharma, 1991).

Therefore, one can speculate that the differences in surface oxide chemistry between Ss and NP would produce different ultrastructural tissue responses, hence in terms of NP, support a tighter bone contact while with Ss, an amphorous fibrous encapsulation would ensue. Essentially this would result in less resistance at extraction for Ss IM nails thus accounting for the lower extraction forces noted in this study. However, this would have to be compared by directly comparing Ss IM nails to NP IM nails within the same sheep model.

Differences in the ultrastructural morphology of bone at the different implant interfaces have been previously described. For example, Albrektsson and Hansson (1986) described the distinct tissue response differences observed between polycarbonate sputter coated with stainless steel or cpTi after 3 months implantation within rabbit tibial metaphyses. The authors report that Ss essentially evokes a local inflammatory response producing a thin layer of approximately 1-2 cellular layers thick which separated the bone from the metal. Furthermore, inflammatory cells were abundant as well as a wide proteoglycan coat lacking collagen filaments was evident. In contrast, titanium coated devices produced a proteoglycan layer of about 200-400 Å in diameter and organized collagen bundles appeared at a minimum distance of 1000-2000 Å from the metal surface. The authors also report that calcium deposits were occasionally observed within approximately 30-50 Å of the titanium oxide (Albrektsson & Hansson, 1986). More recently, Klinger and colleagues suggest that the improved bone bonding capabilities of titanium and titanium alloyed devices are due to their ability to induce accelerated degradation of a hyaluronan meshwork formed as part of the wound-healing response (Klinger *et al.*, 1998). It would seem that these factors in combination would directly contribute to the lower removal force required for Ss IM nails compared to NP IM nails noted in this study.

Chapter summary:

Intramedullary nail removal is carried out worldwide for a variety of reasons, be it symptomatic or asymptomatic. However, despite the regular occurrence of this procedure, no clinically feasible approach has been investigated to solve the economic and resource burden that is incurred when nail removal fails. Many previous attempts to rectify this complication have involved essentially only addressing the complication once it has happened, such as different methodologies for removal of broken or impaired devices once failure has occurred. While these studies perhaps enhance the surgical approach one can adopt they do not address the problem behind its incidence. We believe that device removal can be directly hindered by the implant itself, specifically, the surface micro-topography of the device. Here we have shown that the simple method of surface polishing, which is already used to produce clinically available Ss, can significantly reduce the removal force required for TAN IM nails. Since TAN IM nails are generally preferred over Ss nails due to their excellent biocompatibility and mechanical properties we believe these findings will greatly improve IM nail design for future long bone fractures. Moreover, since infection remains one of the major limiting factors to successful fixation, the effect of polishing on infection susceptibility is of paramount importance since essentially this is one factor that will decide if the application of this technology in clinics is feasible. To this end, our group have previously shown that electro-polishing TAN discs reduced *in vitro* bacterial adhesion in comparison with NS (Harris *et al.*, 2007). To test this further *in vivo*, female New Zealand White rabbits had LCP's implanted onto the medial tibial diaphysis and subsequent to fixation *Staplylococcus aureus* was added at the implantation site. After 28 days, the local infection rate was evaluated and the authors show that no significant difference existed between the rate of infection of clinically available standard micro-rough LCPs (TAN and cpTi) and experimental polished samples (paste polished TAN and cpTi) (Moriarty *et al.*, 2008). Thus, surface polishing should not increase the susceptibility of an implant to bacterial colonization. This theory is now being extended to test infection susceptibility of polished IM nails.

Chapter 7: General Discussion:

The aim of this study was to assess the potential of surface polishing as a simple method for addressing implant removal related morbidity due to excessive bony over-growth for clinically available materials. Since all the materials used in the study were deemed biocompatible, we first assessed *in vitro* if surface polishing would negatively affect cytocompatibility. We also attempt to elucidate using real time PCR technology if surface polishing exerted any influence on a molecular level to potentially reduce excessive bony over-growth. We then applied this technology to two commonly used internal fixation systems in bilateral non-fracture sheep models, to ratify *in vivo* our previous observations regarding the effect of reducing surface micro-topography for controlling tissue integration.

Surface characterisation:

The extensive characterisation carried out for every sub-study in each chapter throughout this study allowed us to come to the conclusion that surface polishing successfully reduced the average roughness and morphology of commercially available devices, without affecting the chemical composition, regardless of whether the implants were made from rod or sheet metal. A major outcome of this study was the realisation that the investigation of surface topography cannot be confined to just roughness height measurements. Surface morphology is also highly important and comprehensive assessment using a variety of methods is essential for accurate representation of a given surface. If we had opted just to rely on height measurements we would have found interpreting our *in vitro* and *in vivo* results more difficult and conclusions drawn would undoubtedly be erroneous in many cases. This point is especially supported by observations in chapter 4 that the Ra for TE and ME were similar to that noted for TS and MS. If we had only used profilometry as an indicator of surface micro-roughness we would have failed to identify the morphological reasoning behind the perceived high Ra. On more than one occasion through this study we have found that high average roughness does not necessarily equate to a micro-rough surface. One should understand the limitations of any given characterisation method and in this case, the waviness of the electropolished surfaces contributed to the higher Ra, while morphologically, they were all found to be smooth.

The importance of surface characterisation should not be underestimated and throughout this study that has become increasingly clear. In this study we included a large variety of qualitative and quantitative techniques to assess the surface morphology of the samples as well as potential chemical compositional changes. While industrial grade metal biomaterials are known to differ morphologically due to innate material property differences we have also shown that these surface properties are also affected differently by different polishing techniques, resulting in distinct morphologies. Thus, despite similar Ra's a surface's morphological appearance can differ dramatically and as a result may be responsible for evoking distinct biological responses. For instance, all micro-rough samples included in the *in vitro* portion of this study had similar average roughnesses; however, clearly with SEM analysis the difference in micro-topography became evident. TS displayed an irregular jagged surface resulting from differences in grain boundary height and orientation, while NS displayed the typical undulating surface interspersed with protruding beta-phase particles. MS on the other hand had extensive micro-topography and distinct grain boundaries.

While the starting Ra was similar for all standard micro-rough samples the morphological appearance of the surface differed dramatically and thus subsequent to polishing; distinct surface profiles were evident for each individual surface depending on the material and surface finishing technique. For instance, electropolishing of cpTi was particularly suited for reducing the surface micro-roughness of this material, so much so, that the grain boundaries of cpTi were exposed. However, while paste polishing was also generally well suited for reducing the micro-roughness of cpTi the surface morphology differed from that observed for TE. For instance, the grain boundaries of the material were not frequently observed as clear as TE, and the mechanically abrasive paste polishing technique tended to show a 'basket weaved' appearance. No material supports the notion that surface morphology, rather than surface height alone is important better than TAN. Throughout this study we have observed a higher Ra recorded for NE compared to NP. However, when observed using SEM it became clear the dramatic difference in surface morphology between the two. Firstly, electropolishing appears more adept at reducing the prominence of the beta-phase particles and this efficacy was found to improve throughout the study. Paste polishing of 13mm and 50mm TAN samples on the other hand consistently displayed prominent beta-phase particles protruding from the surface which were subsequently noted to affect cellular function.

Interestingly, however, NP screws and IM nails had extremely smooth surface finishes which may be a result of increased technique optimisation, but more likely is a result of the material source i.e. sheet versus rod or the paste used i.e. wood paste versus nut paste. Unfortunately, however, the details of polishing were not fully disclosed by the sample suppliers; therefore, these propositions cannot be confirmed. Nevertheless, it appears that sample shape also can influence the efficacy of surface polishing.

Sample variability.

A myriad of techniques are available to characterise a surface chemically and topographically, and while each approach provides specific information with regards to the surface when combined a comprehensive profile of the surface features can be gained. The importance of surface characterisation is highlighted within this study. We have found that a huge degree of sample variability existed between batches of samples, between 13mm and 50mm samples of the same materials, and between discs, screws, plates and nails. The extent of this variability is outlined in Appendix D and I. This variability obviously made comparison between *in vitro* tests difficult and in an attempt to address this we included extensive surface characterisation for each sub-study and chapter. Also, for any given experiment we only included samples from the same batch to try to limit the extent of variability we encountered.

A large contributing factor to this variability is down to manufacturing. Over the course of this study suppliers obviously continue to optimise their processing techniques which will undoubtedly produce differences in surface characteristics. For instance, in one of the first batch of NE samples (i.e. chapter 2) while the prominence of the beta-phase particles were greatly reduced, subsequent NE samples had a greater level of smoothness and the beta phase particles were often difficult to distinguish (i.e. chapter 3, 4, 5, 6). Two possibilities for this exist. Firstly, it is possible that the raw metal origin changes. This change could involve using different suppliers or changing from sheet metal to rod for example. Secondly, the processing could have been altered to include a longer polishing step which would have extended the exposure time of the beta-phase particles to processing. For paste polished samples changing the type of paste would greatly influence the surface morphology produces during processing.

Overall, it can be concluded that both electro- and paste polishing are suited methods for reducing the surface micro-topography associated with commercially available standard materials. Interestingly, however, we have also shown in this study that implant shape and dimensions can determine the suitability of the polishing technique. It appears that cortical and small locking screws hold the greatest challenge of all the devices studied for effective polishing since a greater variability was noted with regards to their Ra's and surface morphology. In contrast, IM nails lend themselves particularly well to paste polishing which produced a Ra akin to that normally reported for the orthopaedic smooth surface of Ss. Morphologically this surface was noted to be extremely smooth to the extent that the beta-phase particles which are characteristic of this surface were indistinguishable. Material type also proved a determining factor in the success of surface polishing. Therefore, depending on material and implant type, one polishing method may prove more suitably applied. However, if manufacturers were to opt for only one method, either electropolishing or paste polishing would prove successful, albeit, with further optimisation for certain fixation device applications.

The influence of surface polishing *in vitro*:

Previous *in vitro* studies from our laboratory (Baxter *et al.*, 2002; Meredith *et al.*, 2005; Welton, 2007; Pearce *et al.*, 2008b) and others (Anselme *et al.*, 2000; Boyan *et al.*, 2002) have implicated the role of surface micro-topography in influencing a wide variety of cellular mechanisms. Initially in this study we assessed *in vitro* to influence of surface polishing on cell growth, viability and morphology and subsequently we investigated the effect of polishing on controlling genotypic expression.

As expected, both electro- and paste polishing samples did not significantly alter cell growth compared to standard micro-rough counterparts, independent of material type. These findings are contradictory to previous reports of smooth surfaces which report of a higher osteoblastic proliferative rate compared to micro-rough samples. However, one fundamental difference between these studies and ours, besides cell source, is the spectrum of roughness investigated. This inter-study variation pertaining to what is perceived as 'smooth' and 'micro-rough' can be problematic for comparison of data. As outlined in chapter 4, previous work from our laboratory has identified a spectrum of roughness between 0.2-2μm which is believed to provoke the optimal differences in cell behaviour for smooth versus rough samples (Richards, 2008). However, many of the studies that have reported a decreased proliferative rate for

'micro-rough' samples have included samples with average roughness of approximately 5μm or above and deem a 'smooth' surface to be less than 0.6μm (Boyan *et al.*, 2003a; Boyan *et al.*, 2003b; Lossdörfer *et al.*, 2004). Yet recent studies have highlighted the loss of sensitivity to micro-topography approaching 6μm *in vitro* and within the spectrum of roughness we propose 0.6μm can be approaching micro-rough rather than smooth.

The biocompatibility of cpTi and its alloys has been widely determined and therefore, as expected all three standard samples were found to be cytocompatible. However, there were differences. For instance, more cells appeared to attach initially to the NS surface which on one hand was interesting due to observations made by Meredith and colleagues (2005) regarding hindered fibroblast growth on the same surface, while on the other hand, the proven biocompatibility of NS *in vivo* and reports of the high affinity of bone for TAN support our *in vitro* observations with primary osteoblasts (Hamilton *et al.*, 2004; Georgiadis *et al.*, 2004).

Interestingly, both polishing techniques appeared to improve initial attachment for cpTi and Ti15Mo as a lower percentage of unbound cells were observed for TE, TP, ME and MP. Furthermore, no significant differences in viability were noted for these samples compared to micro-rough counterparts. NP however produced interesting results as it was the only polished sample to have a higher percentage of unattached cells compared to its micro-rough counterpart. NP was also found to have lower cell growth compared to NE and NS, but this was not found to be significant. However, NP samples were found to have a significantly lower number of viable cells compared to NS but not NE samples. In light of the lower percentage of cells initially attached to NP, this may contribute to the latter finding.

Meredith and colleagues (2007a & b) have already elucidated the effect of beta-phase micro-topography on eliciting negative cellular effects for fibroblasts. Initially, Meredith and colleagues (2005) reported that NS hindered cell fibroblast cell growth and that this inhibitory effect was negated with polishing the NS surface. Subsequent studies elucidated the affect of the beta-phase particles of NS in reducing the mean length of focal adhesion sites for fibroblasts grown on the NS surface as well as disruption of the tubulin and actin cytoskeleton by beta-phase particles (Meredith *et al.*, 2007a&b) which lead them to propose that the impairment of focal adhesion numbers, maturation, and cell spreading was possibly sufficient on standard TAN to block cell cycle progress and eventually cell growth on the NS surface.

Furthermore, the authors showed that electropolishing of TAN removed this effect with the fibroblasts behaving the same on polished cpTi, TAN and Ss. Subsequently, using coated samples and polymer samples mimicking the micro-topography of NS, the authors equated the negative cellular influence to the micro-topography of beta-phase particles (Meredith *et al.*, 2007b).

We have shown in this study a similar outcome with electropolishing of TAN. Specifically, NP and NS are both surfaces with prominent beta-phase particles which were observed breaching the microtubular network. In contrast, NE samples which had a high reduction in the prominence of these particles were found to support a morphologically distinct cell shape and the disruptive cytoskeletal effect was less pronounced. Therefore, in agreement with Meredith and colleagues (2007b) it appears that micro-topogrpahy rather than chemistry (since XPS analysis indicated no compositional changes) induced these affects. The next logical step therefore, would be to confirm this micro-topographical influence pertaining to osteoblasts however others have already highlighted the differences in hard versus soft tissue specific response to differences in oxide chemistries, so this facet of the cell-material response should not be over-looked (Hazan *et al.*, 1993; Vinall *et al.* 1995).

The more definitive results regarding the potential of surface polishing for reducing bony over-growth come from gene expression analysis for osteoblast 'specific' factors. We showed that both material type and surface microtopography affected RC cell differentiation, matrix production and mineralisation in different manners. Since XPS analysis indicated that no alterations in chemical composition of the surface occurred due to anodisation the changes in genotype can be attributed directly to the morphological changes of the surface. Analysis of alterations in mRNA levels for a variety of osteoblast 'specific' genes, indicate that the influence of reducing surface micro-topography is governed on an mRNA level. Specifically, both surface morphology, and material type appeared to influence genotype. While the influence of surface micro-topography have been shown previously to regulate osteoblast genotype, this is the first time that data has been presented to support the notion that surface polishing exerts its affect on tissue integration by reducing matrix-material interactions, osteoblast differentiation and subsequent terminal differentiation.

The latter is an interesting finding as studies of this kind that have focused on accelerating osseointegration have generally implied that osseointegration may be controlled primarily at the initial phase of cell recruitment and cell fate determination (Masaki *et al.*, 2005; Schneider *et al.*, 2003). Here however, we have shown that while the influence of polishing also appears to influence these stages of differentiation, its influence is also exerted on downstream events such as ongoing osteoblast differentiation, matrix-material interactions and subsequently terminal differentiation. For cpTi samples osterix expression was significantly altered on polished samples. Both electro- and past polished cpTi samples showed distinctive osterix expression profiles compared to the micro-rough counterpart. Specifically, it appeared that polished samples had ongoing differentiation while standard micro-rough samples induced a more rapid differentiation. This ongoing differentiation and hence delayed maturation and progression into terminal differentiation on polished samples is supported by results observed for Bone sialoprotein after 14 days and OCN expression showing a significant decrease in expression on polished cpTi samples at all time points studied. TAN and Ti15Mo polished samples similarly appeared to exert their affect on terminal differentiation as assessed by OCN expression. This decrease in OCN expression on polished Ti15Mo samples may be in part explained by the significant reduction also observed in Cbfa-1 expression for these samples compared to standard Ti15Mo after 14 days culturing, given the major influence of Cbfa-1 in regulating bone matrix genes such as OCN. In contrast, TAN polished samples appeared to target matrix interaction which may be partly attributable to the changes in cytoskeletal organisation observed for these samples. Regardless, it appears that despite the differences that polishing of the various materials had in modulation of the diverse stages of differentiation, the outcome on terminal differentiation was similar as OCN expression on TAN polished samples was also found to be significantly reduced after 21 days culturing compared to standard controls. These findings appeared to be echoed by *in vivo* data that showed that bone contact for polished cortical and locked screws was markedly lower compared to standard micro-rough counterparts. Therefore, in light of our data and the data of others, we postulate that bone apposition *per se* is not negatively affected by surface polishing; rather it is accelerated by micro-rough surfaces and that polished devices prevent the long term strong bone adherence. Thus, the combination of the reduced strength of matrix adhesion to polished samples with slower rate of remodelling/apposition relative to standard micro-rough devices would directly influence the occurrence of bony over-growth.

It would also be interesting for future work to analyse quantitatively, the differences, if any, in cell shape and cytoskeletal arrangement i.e. frequency of focal adhesion sites, as was performed by Meredith *et al.*, 2007a &b with fibroblasts previously. While in this study we have qualitatively shown that while cytoskeletal disruption for osteoblasts by beta-phase particles does exist but not to the extent observed for fibroblasts, we have not addressed the possibility of changes in cell shape and differences in adhesion as contributing factors for changes observed in genotype. Also, contrasting to *in vitro* fibroblast proliferation studies by Meredith and colleagues (2005) we did not find a hindered cell growth for osteoblasts on the NS surface despite the similar observation of cytoskeletal disruption. Therefore, it would be of interest to investigate the cell cycle progression of both fibroblasts and osteoblasts on the NS surface to confirm propositions made by Meredith and colleagues that this was in fact reason for decreased fibroblast cell growth on NS, and how this differed to cell cycle progression of osteoblasts on the NS surface.

Interestingly, we have also shown that the material type has a role in genotype determination. Specifically, Ti15Mo appeared to induce the most dramatic differences in mRNA levels. As mentioned in chapter 4 this material dependent influence is most likely a result of the differences in chemistry of the oxide layer of the surfaces. This observation is advocated by previous studies which also showed some degree of material dependent response. For instance, Pearce and colleagues (2008b) showed that surface polishing of cortical cpTi and TAN screws reduced the force required for removal compared to standard micro-rough screws of similar material type. Notably, cpTi generally required less force for removal of the screws compared to TAN locked screws of similar surface finish. This result is also noted by other studies that highlight the affinity of bone for TAN. Furthermore, within our study we have shown that despite a lower Ra and extremely smooth surface, paste polished TAN nails required more pull out force for removal compared to Ss nails of the same design. This affect also appears to be cell dependent as Meredith and colleagues (2005) showed that the highest amount of changes in gene expression micro-array profiles for fibroblasts was observed for cpTi, rather than TAN.

Of course, as with any *in vitro* study, limitations do exist and conclusions drawn should be translated to the *in vivo* situation with due care. One of the main considerations of this study is the cell type. Initially, we decided upon use of primary rat calvarial cells because of their accessibility and ease of isolation as well as their biological relevance in terms of nodule

formation and well defined temporal genetic expression *in vitro*. We did originally investigate RC cells in conjunction with two commercially available osteoblast-like cell lines known as SaOs-2 and MG63, both cell lines resulting from human osteosarcoma clones. However, while established cell lines pose the advantage of being easy to culture as well as being phenotypically more stable with passages (which would therefore allow for reproducible results) some issues surrounding their use exist. For instance, established cell lines tend to reflect a specific stage of osteoblast differentiation or there suitability pertaining to an osteoblast phenotype may be questionable. For instance, The SaOs-2 cell line represents a well differentiated osteoblast cell exhibiting high ALP expression levels, cAMP (cyclic adenosine monophosphate) response to PTH (parathyroid hormone) stimulation in conjunction with the expression of osteonectin, BSP, and decorin (a proteoglycan expressed during osteoblast differentiation). However, these cells seemingly do not express osteocalcin at any stage in culture (Jaaskelainen *et. al.*, 1994).

In contrast, the MG-63 cell line exhibits less attributes of a mature osteoblast compared to SaOs-2. However, there is a level of uncertainty surrounding the osteoblastic character of the MG63 cell line since it has been shown that approximately 40% of the total collagen produced by these cells is in fact type III collagen (Jukkola *et. al.*, 1993). Additionally MG-63 cells have a very low ALP activity and do not readily express osteocalcin, although 1,25 dihydroxyvitamin D_3 has been shown to stimulate both these factors to a small extent (Franceschi & Young, 1990). Moreover, this cell line does not form a mineralized matrix *in vitro* even in the presence of dexamethasone. Furthermore, both these established cell lines display a wide range of variability compared to primary isolated human osteoblasts (Pautke *et al.*, 2004).

During the course of the study we did also compare qualitatively and quantitatively, rat calvarial cells to commercially available human osteoblasts and generally found little or no differences for the parameters tested. However, some of the main areas of dissimilarity were found to be cell morphology and the temporal staining of ALP which for RC cells, occurred earlier and more intensely than for commercial human osteoblast cells. This is most likely a result of differences in ossification and cell origin. Nevertheless, this highlights the fact that results may be cell-dependent as well as material or surface dependent.

Results from chapter 4 highlight the difficulty in extrapolating results relating to genetic expression as many conclusions are drawn based on the data available. Of course, this only involves the genes that are predetermined to be of special interest for that study. Inadvertently, therefore, much of the biological changes evoked by alterations in topography are neglected. Therefore, future studies attempting to elucidate the influence of surface polishing on a cellular level would benefit from investigating some of the other factors that may play a role in this effect. For instance, investigating integrin expression the surfaces would help validate if this contributed to the down-regulation of collagen I observed for polished TAN surfaces. Ideally, the amalgamation of real time PCR and gene array technology would prove a useful biological tool.

For instance, by producing an array that simultaneously examines samples for a wide variety of genes known to be directly related to bone regeneration (or another biological process of interest) would potentially provide valuable data regarding genetic control of tissue integration. Subsequently, with these data a more focused approach could be devised. It would also be interesting to investigate the role of surface polishing *in vitro* under motion and the effect this would have on genotype which would reflect the *in vivo* situation more closely. However, the first logical step would be to confirm that the changes in mRNA for the tested genes of interest reported in this study are translated to a protein level which would confirm observations, and aid in validating our conclusions.

The influence of surface polishing *in vivo*:

We and others have shown extensively that the role of surface micro-topography is a major determinant in the type and extent of tissue integration (Albrektsson & Hansen, 1986; Chehroudi *et al.*, 1997; Welton, 2007; Pearce *et al.*, 2008b; Schlegel *et al.*, 2008). While most *in vivo* studies focus intently on enhancing osseointegration for permanent fixation devices we have opted to address the clinical problem related to removal of these devices. Only recently, in an AO symposium aimed at material removal (Salzburg, April 2008) did 150 participants suggest that the removal of internal fixators can have complications rate of up to 40%. In Europe alone the costs associated with material removal can be approximately €3,000 which would obviously increase with the superfluous surgery time required when complications are encountered.

Furthermore, the risks to the patient associated with unplanned surgical complications, are clearly undesirable. Interestingly, many of the questions put forth by surgeons at the symposium were unanswered, indicating the lack of consensus between surgeons on this matter. A recent study by Hanson and colleagues (2008) has poignantly revealed the extent of division amongst surgeons regarding indications for device removal. For instance, 42% of surgeons (655 respondents) agreed that routine implant removal is necessary. While 48% of respondents believed that removal was riskier than leaving the implant *in situ*. Reasoning for removal was also found to produce an array of results with palpable/irritating devices ranking, pain and implant breakage ranking highest as indications for removal, while patient request was lowest.

In an effort to address this problem in this study we have investigated the influence of surface polishing for easing removal of internal fixation devices, specifically locked screws from a locked plate system and intramedullary nails, which are both systems commonly used in the treatment of long bone fractures. We have shown conclusively that in bilateral non-fracture sheep models that electropolishing and paste polishing of these commonly available clinical devices significantly reduced the extraction force required for both TAN locked screws and TAN IM nails. Furthermore, for LCP's the operational time for removal was found to be approximately 4 times less for cpTi polished plates compared to the standard cpTi plates used clinically to date. This is an especially important finding as the significant reduction in time required for tissue removal from polished devices will directly reduce the surgical time associated with implant removal, thus improving not only the economic burden associated with surgical procedures but also the surgical related complications with regards to the patient, which are both principal deciding factors for implant removal.

Biologically what affect does surface polishing have? Our *in vitro* analysis suggests that terminal osteoblast differentiation is delayed on polished samples which considering the significant reduction in bone contact found for polished screws may resolve somewhat the effect. However, the additional biological factors and mechanical stimulation *in vivo* would undoubtedly contribute also. From the material stand-point essentially two major contributions from the surface could potentially result in the reduced bone contact we found for polished locked screws, namely surface micro-topography and surface chemistry. Within this study we have seen that both factors have played a role in determining both a cellular and tissue response.

In terms of a tissue response we have shown for locked screws and IM nails that a reduction in surface micro-topography can significantly reduce the force required for removal. While data from chapter 5 indicated that this occurs in part due to a reduction in bone contact to polished screws we have also seen in chapters 5 and 6, that a material dependent response was evident. Specifically, for locked screws we noted that the different biopassivity of TAN compared to Ss induced a different tissue response to the surface, regardless of similar surface morphologies and micro-roughness.

For IM nails, despite the lack of histomorphometric data so far we also report that despite similarities in surface morphology and a reduction in Ra of paste polished TAN IM nails compared to Ss, the removal force for Ss IM nails was still lower. As mentioned in the respective chapters the surface oxide layer is undoubtedly a major reason for these observations. Moreover, ratification of this suggestion comes from histological evidence presented for locked screws in chapter 5 where consistently Ss screws had a thin continuous fibrous layer separating the material from the adjacent bone. In contrast, both electropolished and paste polished TAN screws had bone apposition, albeit, intermittently disrupted by the presence of soft tissue. This observation has also been noted by others for cortical screws in both cancellous and cortical bone (Pearce *et al.*, 2008b).

Biologically, the combination of surface micro-topography and chemistry would influence ease of removal at potentially several stages of fracture healing. One of the main areas surface micro-topography may play a role is wound retraction. For instance, during fracture healing the migration of osteogenic cells as a well as a variety of other cell populations involved in fracture healing will migrate to the fracture site via a fibrin meshwork that forms during clot formation. However, as mentioned in chapter 1, concomitant with cell migration is the retraction of the haematoma. Therefore, the ability of a biomaterial to retain fibrin attachment during this retraction phase is crucial in determining if migrating cells will reach the device. It is suggested that the complexity of a micro-rough surface provides a three dimensional topography so that fibrin remains sufficiently attached to the implant to withstand retraction, allowing for cell migration (Davies, 1998). Therefore, by reducing the surface microtopography of an implant it is reasonable to postulate that fibrin retraction may provide adequate force to detach the fibrin that is adherent to the smooth implant surface. Consequently, the initial recruitment and migration of cells (quantity) to the wound site could potentially be reduced.

Alternatively, or rather synergistically local factor production in response to differences in topography may also regulate bone formation at the implant-bone interface. For instance, the role of micro-topography in regulating osteogenesis through factors such as transforming growth factor-β have shown to be controlled *in vitro* in a surface dependent manner (Kieswetter *et al.*, 1996). Moreover, recently it has been shown that parathyroid hormone mRNA regulation can be affected by differences in surface micro-topography (Pham *et al.*, 2008). This hormone has also been implicated in the induction of osteocalcin (OCN; Jiang *et al.*, 2004) thus control of terminal differentiation and subsequent bone formation may also occur through alterations in the local niche. This is supported by our *in vitro* studies which indicated that the reduction in surface micro-topography resulting from surface polishing can potentially affect differentiation of osteoblast cells through genotypic regulation.

One factor that may be highlighted as a limitation of the *in vivo* studies is the inclusion of the non-fracture models. While the author appreciates the value of reproducing the *in vivo* physiological niche associated with a fracture model, the inclusion of a non-fracture model was chosen for several reasons. For instance, variations in healing such as non-union, mal-union and implant migration due to instability, were evaded. Additionally, the non-fracture models allowed for conclusions to be drawn specifically related to material-dependent responses rather than biological responses based on variations in healing. Also, in the nailing study since the medullary canal was extensively reamed essentially many of the same biological stimuli, similar to those found in fracture healing, were evoked. However, it may be of interest in the future to repeat some of the *in vivo* experiments under optimised conditions with the inclusion of a fracture model to assess if indeed the same conclusions are presented. The worth of this has to be debated however, as any *in vivo* study carries with it extensive costs and ethically the inclusion of more animals requires careful consideration. Importantly, however, within Switzerland ethical permission for a bilateral fracture model would not be supplied due to ethical implications to the animal as well has the increase in animal number which would be required to compensate for the loss of simultaneous comparisons within the same sheep. Moreover, even if under ethical indications a fracture model was permitted this ethically, could only be applied unilaterally to prevent excessive pain and suffering to the animal, therefore, extrapolation of results from different sheep for the different materials would be incomparable due to inherent differences in healing.

Moreover, in chapter 5 two plates per tibia were implanted in the bilateral model allowing for all test materials to be investigated without animal/biological variations. If a fracture model was ethically permitted in this case we would again have lost the ability to compare all materials simultaneously; as it is unlikely 4 fractures would have been permitted per animal. Therefore, to accommodate for the fracture model the number of animals included in the study would have rose exponentially to allow for the statistical power of the study to be relevant.Of course, as with any *in vivo* model the relevance of the animal model to the human situation is also questionable. Indeed, several differences between sheep bone and human bone exist, and one must be conscious of these differences before it can be said for certain that a particular surface modification will benefit human fracture fixation. For instance, sheep bone consists histologically of a primary bone structure (osteons less than 100μm diameter containing at least two central blood vessels and the absence of a cement line), while human bone is largely secondary bone.

Furthermore, a difference in bone density between sheep and human bone also exists however, bone remodelling between species is thought to be comparable (for review see Pearce *et al.*, 2008a). Despite these differences we are confident of the applicability of polished internal fixators for human clinical applications especially in light of the success of hand polished Ti15Mo plates used in hand surgery during recent years. Specifically, with the exception of just 2 cases due to initial misplacement of the plates (personnel communication J Jupiter & R.G. Richards) clinical data collated from 1800 patients with polished Ti15Mo plates have showed no tendon irritation, compromised stability, or adverse effects to fracture healing.

What about stainless steel?

Considering the aim of this work is to use surface polishing for reducing the surface micro-topography of clinically available materials to ease removal, the question may arise: Why not just use stainless steel (Ss)? Granted the surface micro-topography of this material is nearly ideal and reproducible. In addition, traditional Ss devices generally cost less than titanium and titanium alloy counterparts (although this is no longer true for complex implants such as LCP and expert tibia nails where the cost of the implant is the same for Ss, cpTi and TAN). So, why not use Ss in applications where removal is required?

As previously outlined in chapters 2 and 6, the bio-passivity of an implant is partly attributable to the oxide layer. It is this layer, often only a few nanometres in thickness, which is crucial to the application of metal devices *in vivo*. The major differences between the oxide layers of Ss and titanium and its alloys involve the actual thickness of the layer and the chemistry, both of which result in evoking distinct biological responses. This distinction is highlighted most poignantly by an early study by Albrektsson and Hansson (1986) which studied in much detail the ultrastructural differences evoked by Ss and cpTi screws in rabbit bone. Specifically, the authors report a continuous 1-2 cell thick layer separating the Ss device from bone while cpTi had direct anchorage to the bone. Furthermore, inflammatory cells were found adjacent to Ss devices and a proteoglycan coat void of collagen filaments was observed within the interface. However, in contrast, cpTi had a proteoglycan layer at the interface with collagen bundles in close proximity.

The authors also note that Ss devices were slightly unstable in the bone at time of sacrifice (Albrektsson & Hansson, 1986). The importance of this direct apposition of the proteoglycan layer on cpTi is believed to directly result in the accelerated osseointegration properties of this material due to the enhanced degradation of the hyaluronan network which is formed as a result of the wound healing response (Klinger *et al.*, 1998). In this study we have also shown that TAN produces a distinct tissue reaction compared to Ss. Specifically, for standard TAN locked screws we observed direct bone apposition to the implant with some small areas of soft tissue contact. This tissue reaction was also observed for electropolished and paste polished locked screws within LCPs. However, Ss screws produced a thin continuous fibrous layer which separated the device from hard tissue contact. We have also observed difference in tissue response for cpTi screws implanted in cortical and cancellous bone in a previous study (Pearce *et al.*, 2008b) using cortical screws alone, without plates.

While Ss is more ductile than cpTi and therefore can undergo more deformation, the Young's moduli of these samples differ dramatically. In fact Ss has a modulus of elasticity almost twice that of cpTi (200 GPA compared to 110GPA, respectively). Since the modulus of elasticity of bone is approximately 25GPA, one can see that Ss would cause problems for bone later on especially in children where the life span of the device needs to be longer to survive physiological environment (Perren *et al.*, 2001).

Fretting corrosion is an accelerated form of corrosion, occurring when the passive film of a device is abraded. Two major contributors to implant/fixation failure namely aseptic loosening and osteolysis are believed to result from the biological response that occurs to the released particles at the bone–implant interface and can be detrimental to implant success (Grose *et. al.*, 2006). This aspect is becoming an increasing concern given the dramatic increase in the number of young patients requiring orthopaedic intervention and as a result there is an increase in the life-span of a device *in vivo*. Therefore, this is clearly an unwanted outcome and directly influences the bio-passivity of a device. As mentioned previously, accumulation of metal particles have been identified in a vast array of organs such as the lymph nodes, liver and spleen. Nevertheless, due to the nano-scale of the particles the true extent of their dissemination has yet to be fully elucidated. Nevertheless, many constituents of orthopaedic implants have clearly emerged as potential hazards to a variety of systems such as the vascular, immune, excretory, reproductive, integumentary, and nervous systems. Specifically, components of Ss such as chromium, cobalt, iron and nickel, have been implicated as major contributors in the negative biological response evoked by metal particulates and salts.

Cobolt metal ions have been shown to be among the most cytotoxic with corrosion products such as CoO, Cr_2O_3 and $CrPO_4$ also shown to induce moderate cytotoxicity. Within the nucleus itself Cr has been implicated in DNA mutagenesis. Particularly, Ni, Cr and Co have been implicated in the inhibition of DNA repair and altered gene expression and have also been shown to produce reactive oxygen species, which have previously been shown to provoke oxidative damage to DNA, proteins and lipids and are thought to be significant in the development and/or progression of neurodegenerative disorders.

Furthermore, Cr has been found to be concentrated within epithelial cells of the proximal renal tubules and have been found to hinder renal function as well as causing necrosis of the tubules themselves. However, the effect of Cr on the excretory system is not limited to the kidneys as Cr has also been found to induce hepatocellular necrosis in response to high level Cr ingestion. On the other hand, Co has been implicated in the stimulation of cardiomyopathy while Ni has been shown to increase the mortality to cardiovascular disease.

Additional concerns regarding the influence of metal debris on the reproductive system has emerged. Specifically, it has been shown that chronic Cr exposure can result can decrease

sperm quantity and induce sperm abnormalities as well as reducing the number of follicles and ova produced in mice (Elbetieha & Al-Hamood, 1997). These negative effects are not restricted to the reproduction. In fact, developmental toxicology studies have identified an increase of Co and Cr in the cord blood of 10 pregnant women, all of whom had metal fixation devices and had become pregnant subsequently. The indication that orthopaedic metal ions/particles may be translocated from maternal to foetal circulation is a horrific notion as several metals including Cr, Co, Ni, that are found in Ss, may been identified as possible inducers of developmental toxicity. For instance, Cr exposure in male or female mice prior to or during gestation can directly influence the number of implantations and viable foetuses to result from conception. Furthermore, Cr and Ni have are also implicated in provoking teratogenic malformations.

Recently developed Ni-free Ss, not only provides superior mechanical properties compared to standard Ss but also offers the additional benefit of nearly completely omitting one of the most wide-spread skin allergens, Ni, from its bulk material. Current implant quality stainless steels include between 13 and 16 weight % nickel (Ni), however, testing shows that 10–20% of people have Ni sensitivity (Massone *et. al.*, 1991). Therefore, in recent years, new 'nickel-free' Ss have been fabricated in an effort to address this issue. In reality, no Ss is completely free of Ni so should more accurately referred to as low Ni containing (since they contain approximately 0.03% Ni). Consequently, if a patient has a known sensitivity to nickel then more often than not titanium implants are used where applicable to prevent additional aseptic or septic complications (Arens *et. al.*, 1996). Few studies exist that compare the cytocompatibility of low Ni containing devices to cpTi or conventional Ss devices. However, it has been shown that low Ni containing Ss can display a large variation in their corrosion behaviour (Reclaru *et al.*, 2006). However Montanaro and colleagues (2005) found that low Ni containing Ss did not increase mutagenic or genotoxic responses compared to conventional Ss. In a later study, the authors also report that low Ni containing Ss are cytocompatible pertaining to osteoblasts and fibroblasts (Montanaro *et al.*, 2006). However, as described previously MG63 cells do not optimally represent the osteoblasts phenotype so these results must be accepted tentatively until further ratification is produced.

Furthermore, allergic reactions to chromium are an additional risk thus immediately eliminating the possibility of low Ni Ss being a reasonable alternative to cpTi in these patients. Consequently, for Ss implants to remain viable in the biomaterial field this advance

of low Ni Ss fixation devices should provide all the advantages of current orthopaedic grade Ss as well as efficaciously reducing the Ni allergen issue. For the most part these parameters are met. For instance, the low Ni containing alternatives also have superior dynamic strength and mechanical properties as well as further corrosion resistance. The improved attributes are a result of their high chromium, molybdenum and nitrogen content (for review see Disegi & Eschbach, 2000). Importantly, nitrogen replaces nickel in these implants and is a particularly effective stabilizing agent preventing the formation of secondary magnetic phases, in addition to contributing to the enhanced corrosion resistance and strength reported.
However, a concern regarding the possibility that the high nitrogen content may be responsible for nitride precipitation at grain boundaries which is thought to facilitate inter-granular fracture is a concern with regards to implant stability (Eschbach *et. al.*, 2001). In addition, the manganese content is increased to allow for nitrogen solubility. Nevertheless, fatigue tests carried out under physiological conditions have shown that low Ni Ss plates were observed to have a lower resistance to cyclic loading compared to cpTi and 316L Ss plates (Eschbach *et. al.*, 2001). Moreover, the increased strength of low Ni containing Ss means a reduction in its machinability.

Although low Ni containing Ss contain typically less than 0.1% residual Ni content, the biological effect on a Ni sensitive patient has not been fully elucidated. In the guinea pig maximisation testing, it appears that Ni concentrations below this threshold are unlikely to induce allergic sensitisation (Allenby & Goodwin, 1983; Emmett *et al.*, 1988; Eedy *et al.*, 1991). However, the issue of cost effectiveness is another concern since the cost of low Ni containing Ss implants is as much as cpTi so the latter would generally be chosen due to numerous additional reasons (chapter 1) leaving a question mark over the successful application of low Ni containing Ss. Therefore, cost and machinability of these implants will be influential in the widespread use of these materials in bone surgery.

Magnetic resonance imaging (MRI) has become an important diagnostic tool in orthopaedics as well as many other facets of medicine as the information it can provide with regards visualisation of structures and pathological entities is superior to that of conventional radiography and computed tomography. However, the effect of the magnetic field on implanted metal devices has raised the issue of patient safety especially as migration and dislodgement of the devices have been reported for some implants (Shellock & Crues, 2004

for review). In addition to these problems, image interruption can be markedly affected due to the creation of magnetic susceptibility artefacts.

In a review by Eschbach (2003) the author reports the major differences that exist between the magnetic properties of stainless steel and cpTi and its alloys with the lowest susceptibility being observed for cpTi, TAN and Ti15Mo. Stainless steel reportedly produces artefact susceptibility ten times higher than that of cpTi however; these materials are not necessarily deemed ferromagnetic since it still meets the requirements of comprising a single phase austenitic microstructure without detectable traces of delta ferrite being present.
Furthermore, newly emerging low nickel containing Ss also have a strongly stabilised austenitic microstructure thus lowering their susceptibility compared to conventional stainless steel (Eschbach, 2003).

A difficulty in the application of MRI is that when attempting to visualise the area adjacent to the device there can be focal signal loss also known as a black spot at the site of implantation which occurs due to distortion of the magnetic field by the metal. The sizes of these artefacts are proportional to the magnetic susceptibility as well as the mass of the implant. Thus, materials with susceptibility close as possible to that of human tissue produce the least image distortion. As the human body contains mostly water, a device should have as close a magnetic susceptibility to water as possible for the least amount of artefacts to occur. Water has a magnetic susceptibility of 12.9710^{-6} at ambient temperature whereas cpTi TAN and Ti15Mo are approximately 232.10^{-6}, 217.10^{-6} and 250.10^{-6}, respectively compared to 2200.10^{-6} for Ss and 1720.10^{-6} for low nickel containing Ss. This clarifies the fact that cpTi and titanium alloyed implants produce less artefacts compared to Ss devices.

Other future studies:
As mentioned previously, the importance of cell-dependent response to a surface is an area requiring clarification. Therefore, it would be interesting to investigate how surface polishing affects preferential cell attachment. For instance, does polishing when applied to a co-culture system allow for preferential attachment of one particular cell type, and does this differ to micro-rough surfaces? Leading on from this, as previously mentioned, investigating the changes in the type of protein attachment and conformation would provide more valuable information into the mechanism of surface polishing on cell-material interactions. This could

be further improved by extending *in vitro* investigations to include studying cytokine release resulting from changes in micro-topography,

The biological efficacy of surface polishing for reducing the force required for locked screws in combination with plates and intramedullary nail removal are clearly established. Therefore, in terms of *in vitro* analysis exploring this concept further would seem somewhat redundant. However, *in vitro* analysis concerning the cell-material interactions and the ensuing biological responses are always of great interest for elucidating the biological mechanisms responsible for the differing tissue reactions observed. We have already highlighted the cellular specificity regarding biological responses evoked by certain biomaterials, thus it would be interesting to explore this further. Work *in vitro* in this study and previously in our laboratory has revealed NS as a favourable surface for advocating an osteoblast phenotype but for fibroblasts this surface can be detrimental. Therefore, it would be off great clinical interest to elucidate the 'why' behind these two differing responses to the same surface. One strong possibility is the method of attachment of the cells. While fibroblasts optimally like to spread on a surface and form very close contact with the underlying surface, so much so, that it has been shown that parts of the cell are left behind upon migration (Richards *et al.*, 1995; Qu *et al.*, 1996) osteoblasts prefer to maintain a cuboidal morphology and 'sit' on the surface rather than becoming flattened onto it.

Therefore, perhaps the beta-phase particles don't have the opportunity to interfere with osteoblast adhesion as they do for fibroblasts. Another possible avenue to explore regarding this issue is protein attachment. It is very possible that the chemical composition of a surface would preferentially adsorb more of a specific protein and as seen previously this can influence subsequent cellular attachment. It would be interesting to investigate whether this is true for NS and if differences in protein attachment and subsequent integrin expression contribute to the preferential attachment of osteoblasts on the NS surface compared to fibroblasts.

Study conclusions:

Scanning electron microscopy, atomic force microscopy, non-contact white light profilometry, contact angle measurements and X-ray photoelectron spectroscopy revealed marked differences in surface roughness and morphology of polished samples, without marked changes to their surface chemical composition. However, one major outcome of this study was the necessity for on-going sample characterisation each time a new batch is produced. We have shown that due to the different natures of polishing i.e. electrochemical versus mechanically abrasive, that distinct surface morphologies are produced regardless of similar starting material and that this morphology is surface dependent.

Biologically, surface polishing techniques appear to hold great potential for reducing removal related complications as *in vivo* we have comprehensively shown that for clinically applicable internal fracture fixation systems polishing consistently reduces the extraction force required for removal. However, as only NP and not NE screws were found to have significantly less bone contact compared to NS we can not say definitively that this is the major attributable factor for reduced removal forces. Also, no statistical correlation was found between polishing and removal force. More likely, the actual strength of bone attachment is reduced for polished samples due to the omission of micro-roughness.

Indications from *in vitro* studies suggest that the effect of surface polishing is partly due to alterations in gene expression and that depending on material type, this can act at an early stage of differentiation or during terminal differentiation.

Overall, it is hoped that the outcomes of this study will be used to improve internal fixation technology to include surface polishing of devices for ease of implant removal. This will potentially alleviate the high percentage of implant removal related morbidity especially for a paediatric population where due to the continuing skeletal growth implant removal is commonplace. In the spirit of the AO 50th year anniversary this work will hopefully contribute to the mantra of 'transforming surgery-changing lives'.

Chapter 8 - References:

Abdelsalam,M.E.; Bartlett,P.N.; Kelf,T.; Baumberg,J. (2005). Wetting of regularly structured gold surfaces. *Langmuir.* 21: 1753-1757

Ahmad,M.; Gawronski,D.; Blum,J.; Goldberg,J.; Gronowicz,G.(1999). Differential response of human osteoblast-like cells to commercially pure (cp) titanium grades 1 and 4. J *Biomed Mater Res.* 1999 Jul;46(1):121-31.

Akeson,W.H.; Woo,S.L.; Rutherford,L.; Coutts,R.D.; Gonsalves,M.; Amiel,D. (1976). The effects of rigidity of internal fixation plates on long bone remodeling. A biomechanical and quantitative histological study. *Acta. Orthop Scand.* 47: 241-249.

Alan RK, Baig R, Voss FR. (2007) Exchange femoral nailing: a new technique for removal of a broken nail. *Am J Orthop.* 36:500-502

Albelda,S.M.; Smith,C.W.; Ward,P.A. (1994). Adhesion molecules and inflammatory injury. *FASEB J.* 8: 504-512

Albrektsson, T; Hansson, HA. (1986). An ultrastructural characterisation of the interface between bone and sputtered titanium or steel surfaces. *Biomaterials* 7: 201-205

Allenby, CF & Goodwin, BFJ. (1983). Influence of detergent washing powders on minimal eliciting patch test concentrations of nickel and chromium. *Contact Dermitis* 9: 491-499.

Aubin, JE. Osteogenic cell differentiation. In: Bone Engineering (Ed: JE Davies).EM squared Inc. Canada (1999). Ch:3 pp19-30.

Alzahrani AG; Behairy, YM; Alhossan, MH; Arab, FS; Alammari, AA. (2003). Removal of internal fixation devices in pediatric patients. *Saudi Med J* 24: 254-255

Anderson, JM; Cook, G; Costerton, B; Hanson, SR; Hensten-Petterson, A; Jacobsen, N; Johnson, RJ; Mitchell, RN; Pasmore, M; Schoen, FJ; Shirtliff, M; Stoodley, P. (2004). Host reactions to biomaterial and their evaluation. In Biomaterials Science: An introduction to materials in medicine (eds Ratner, BD; Hoffman, AS; Schoen, FJ; Lemons, JE). Amsterdam: Elsevier Academic Press.

Andrade, J. D. (1985). Chapter 7: The Contact Angle and Interface Energetics. In Surface and Interfacial Aspects of Biomedical Polymers: Surface Chemistry and Physics, vol. 1 (ed. J. D. Andrade). New York and London: Plenum Press.

Anselme,K.; Bigerelle,M.; Noel,B.; Dufresne,E.; Judas,D.; Iost,A.; Hardouin,P.(2000). Qualitative and quantitative study of human osteoblast adhesion on materials with various surface roughnesses. *J.Biomed.Mater.Res.* 49(2): 155-166

Arcelli, D; Palmieri, A; Pezzetti, F; Brunelli, G; Zollino, I; Carinci, F. (2007). Genetic effects of titanium surface on osteoblasts: A meta-analysis. J Oral Sci 49: 299-309.

Arens, St; Schlegel, U; Printzen, G; Ziegler, W.J; Perren, S.M; Hansis, M (1996). Influence of materials for fixation implants on local infection. An experimental study of steel versus titanium DC-plates in rabbits. *J. Bone Joint Surg.* 78: 647-651

Bächle,M; Mahi, MA; Kohal, RJ. (2005). On-line analysis of CAL72 cells on two different titanium surfaces in a perfusion bioreactor. *Dental materials* 21:633-640.

Bakathir AA, Margasahayam MV, Al-Ismaily ML (2008). Removal of bone plates in patients with maxillofacial trauma: a retrospective study. *Oral Surg Oral Med Oral Pathol Oral Radiol Endod.* 105(5):e32-7.

Baier,R.E.; Meyer,A.E.; Natiella,J.R.; Natiella,R.R.; Carter,J.M.(1984) Surface properties determine bioadhesive outcomes: methods and results. *J. Biomed. Mater. Res* 18: 337-355

Bagatur A.E; Zorer G (2002). Complications associated with surgically treated hip fractures in children. *J Pediatr Orthop B.*11:219-228

Barbalace,K.L.(1995).Periodic table of elements.
http://environmentalchemistry.com/yogi/periodic/Al.html [accessed 15/03/2007]

Baxter LC, Frauchiger V, Textor M, ap Gwynn I, Richards RG. (2002) Fibroblast and osteoblast adhesion and morphology on calcium phosphate surfaces. *Eur Cell Mater.* 30;4:1-17.

Bhatt V, Chhabra P, Dover MS. (2005). Removal of miniplates in maxillofacial surgery: a follow-up study. *J Oral Maxillofac Surg.* 63(6):756-60.

Biggs,M.J.; Richards,R.G.; Gadegaard,N.; Wilkinson,C.D.; Dalby,M.J.(2007a). The effects of nanoscale pits on primary human osteoblast adhesion formation and cellular spreading. *J.Mater.Sci.Mater.Med.* 18(2): 399-404.

Biggs,M.J.; Richards,R.G.; Gadegaard,N.; Wilkinson,C.D.; Dalby,M.J. (2007b). Regulation of implant surface cell adhesion: characterization and quantification of S-phase primary osteoblast adhesions on biomimetic nanoscale substrates. *J.Orthop.Res.* 25(2): 273-282.

Binnig G, Quate CF, Gerber C (1986). Atomic force microscope. *Phys Rev Lett.* 3;56(9):930-933

Boateng,S.Y.; Hartman,T.J.; Ahluwalia,N.; Vidula,H.; Desai,T.A.; Russell,B.(2003). Inhibition of fibroblast proliferation in cardiac myocyte cultures by surface microtopography. Am.J.Physiol Cell Physiol. 285(1): C171-C182

Boerger TO, Patel G, Murphy JP. (1999).Is routine removal of intramedullary nails justified? *Injury* 30:79-81.

Bogan, J; Zardiackas, L; Disegi, J. (2001). Stress corrosion cracking resistance of titanium implant materials. 27th Annual meeting society for biomaterials. April 24-29 pp438

Bombaci, H; Gorgec, M. (2003).Difficulty in removal of a femoral intramedullary nail: the geometry of the distal end of the nail. *Yonsei Med J* 44(3): 1083-1086

Bothe, R.T; Beaton, L.E; Davenport, H.A (1940). Reaction to bone to multiple metallic implants. *Surg., Gynecology and Obstetrics* 71: 598-602

Bowers,K.T.; Keller,J.C.; Randolph,B.A.; Wick,D.G.; Michaels,C.M.(1992). Optimization of surface micromorphology for enhanced osteoblast responses in vitro. Int.J.Oral Maxillofac.Implants. 7(3): 302-310

Boyan BD; Dean, DD; Lohmann, CH; Cochran, DL; Sylvia, VL; Schwartz, Z. (2001). The titanium-bone interface in vitro: The role of the surface in promoting osseointegration. In: Titanium in Medicine (Ed: Brunette, DM; Tengvall, P; Textor, M; Thomsen, P). Springer.Ch17 pp561-586

Boyan,B.D.; Bonewald,L.F.; Paschalis,E.P.; Lohmann,C.H.; Rosser,J.; Cochran,D.L.; Dean,D.D.; Schwartz,Z.; Boskey,A.L. (2002). Osteoblast-mediated mineral deposition in culture is dependent on surface microtopography. *Calcif Tissue Int.* 71(6):519-29.

Brett, PM; Harle, J; Salih, V; Mihoc, R; O Boyan,B.D.; Bonewald,L.F.; Paschalis,E.P.; Lohmann,C.H.; Rosser,J.; Cochran,D.L.; Dean,D.D.; Schwartz,Z.; Boskey,A.L. (2003a) Osteoblast-mediated mineral deposition in culture is dependent on surface microtopography. Calcif.Tissue Int. 71: 519-529

Boyan,B.D.; Lossdorfer,S.; Wang,L.; Zhao,G.; Lohmann,C.H.; Cochran,D.L.; Schwartz,Z. (2003b). Osteoblasts generate an osteogenic microenvironment when grown on surfaces with rough microtopographies. Eur.Cell Mater. 6:22-27

Isen, I; Jones, FH; Tonetti, M. (2004). Roughness response genes in osteoblasts. *Bone* 35:124-133

Broekhuizen CA, de Boer L, Schipper K, Jones CD, Quadir S, Vandenbroucke-Grauls CM, Zaat SA. (2008). Staphylococcus epidermidis is cleared from biomaterial implants but persists in peri-implant tissue in mice despite rifampicin/vancomycin treatment.*J Biomed Mater Res A*.85(2):498-505.

Brunet, J.A; Sarkar, K; Uhthoff, H.K (1986). Ultrastructure of the fibrous tissue surrounding internal fixation devices. *Clin. Orthop. Relat. Res.*208: 84-94

Brunette,D.M.; Kenner,G.S.; Gould,T.R. (1983). Grooved titanium surfaces orient growth and migration of cells from human gingival explants. *J Dent Res.* 62:1045-8.

Brunette,D.M. (1986). Spreading and orientation of epithelial cells on grooved substrata. Exp.Cell Res. 167:203-217

Brunette DM, Chehroudi B.(1999). The effects of the surface topography of micromachined titanium substrata on cell behaviour in vitro and in vivo. J Biomech Eng.121(1):49-57.

Brunette,D.M. (2001). Principles of cell behaviour on titanium surfaces and their application to implanted devices. In: Titanium in Medicine (Ed: Brunette, DM; Tengvall, P; Textor, M; Thomsen, P). Springer. Ch15. pp486-512.

Buckwalter, J.A. (1996). Effects of early motion on healing of muscloskeletal tissues. Hand Clinics 12: 13-24

Busam, ML; Esther, RJ; Obremskey, WT. (2006). Hardware removal: Indications and expectations. *J Am Acad Orthop Surg* 14: 113-120

Buser D,Schenk RK,Steinemann S, Fiorellini JP,Fox CH,Stich H.(1991). Influence of surface characteristics on bone integration of titanium implants. A histomorphometric study in miniature pigs. J Biomed Mater Res.25:889-902

Cameron HU, Pilliar RM, Macnab I. (1973) The effect of movement on the bonding of porous metal to bone. *J Biomed Mat Res* 7: 301-311.

Carlsson L, Röstlund T, Albrektsson B, Albrektsson T. (1988). Removal torques for polished and rough titanium implants. *Int J Oral Maxillofac Implants*. 3(1):21-4

Carter,S.B. (1967). Haptotaxis and the mechanism of cell motility. *Nature*.213:256-60.

Case,C.P.; Langkamer,V.G.; James,C.; Palmer,M.R.; Kemp,A.J.; Heap,P.F.; Solomon,L. (1994) Widespread dissemination of metal debris from implants. *J Bone and Joint Surg Br;* 76(5):701–712.

Chapman MW, Gordon JE, Zissimos AG. (1989). Compression-plate fixation of acute fractures of the diaphyses of the radius and ulna. *J Bone Joint Surg Am.* 71(2):159-69.

Chehroudi,B.; Gould,T.R.; Brunette,D.M. (1990). Titanium-coated micromachined grooves of different dimensions affect epithelial and connective-tissue cells differently in vivo. J.Biomed.Mater.Res. 24(9): 1203-1219.

Chehroudi,B.; Gould,T.R.; Brunette,D.M. (1992). The role of connective tissue in inhibiting epithelial downgrowth on titanium-coated percutaneous implants. *J Biomed Mater Res.*26:493-515

Chehroudi B, McDonnell D, Brunette DM.(1997). The effects of micromachined surfaces on formation of bonelike tissue on subcutaneous implants as assessed by radiography and computer image processing. *J Biomed Mater Res.* 5;34(3):279-90.

Chen J, Shapiro HS, Sodek J. (1992). Development expression of bone sialoprotein mRNA in rat mineralized connective tissues. *J Bone Miner Res.* 7(8):987-97.

Chen C.E; Ko J.Y; Wang C.J. (2002). Premature closure of the physeal plate after treatment of a slipped capital femoral epiphysis. *Chang Gung Med J.*25:811-818.

Chicurel, ME; Singer, RH; Meyer, CJ; Ingber, DE. (1998). Integrin binding and mechanical tension induce movement of mRNA and ribosomes to focal adhesion. *Nature* 392: 730-733

Collin P, Nefussi JR, Wetterwald A, Nicolas V, Boy-Lefevre ML, Fleisch H, Forest N. (1992). Expression of collagen, osteocalcin, and bone alkaline phosphatase in a mineralizing rat osteoblastic cell culture. *Calcif Tissue Int.* 50(2):175-83

Cooper,L.F.; Handelman,B.; McCormack,S.M.; Guckes,A.D. (1993). Binding of murine osteoblastic cells to titanium disks and collagen I gels: implications for alternative interpretations of osseointegration. *Int J Oral Maxillofac Implants*. 8:264-72.

Cooper,L.F.(2000) A role for surface topography in creating and maintaining bone at titanium endosseous implants. J Prosthet Dent. 84(5):522-34

Curran JM, Chen R, Hunt JA. (2006). The guidance of human mesenchymal stem cell differentiation in vitro by controlled modifications to the cell substrate. *Biomaterials.* 27(27):4783-93

Curtis AS, Forrester JV, McInnes C, Lawrie F. (1983). Adhesion of cells to polystyrene surfaces. J Cell Biol.97:1500-6.

Dalby, MJ; Berry, CC; Riehle, MO; Sutherland, DS; Agheli, H; Curtis, ASG. (2004). Attempted endocytosis of nano-environment produced by colloidal lithography by human fibroblasts. *Exp Cell Res.* 295: 387-394.

Dalby, MJ; McCloy, D; Robertson, M; Agheli, H; Sutherland, D; Affrossman, S; Oreffo, ROC. (2006). Osteoprogenitor response to semi-ordered and random nano-topogrpahies. *Biomaterials* 27: 2980-2987.

Dalby MJ, Andar A, Nag A, Affrossman S, Tare R, McFarlane S, Oreffo RO. (2008) Genomic expression of mesenchymal stem cells to altered nanoscale topographies. *J R Soc Interface.* Feb 12. [Epub ahead of print]

Davies, JE. (1998). Mechanisms of endosseous integration. *Int J Prosthodontics.* 11(5): 391-400

Dee, KC; Puleo., DA; Bizios, R. (2002). Wound healing around implants in Adults In An introduction to tissue-biomaterial interaction. Ch 7 pp138-142. Wiley-Liss

Degasne,I.; Basle,M.F.; Demais,V.; Hure,G.; Lesourd,M.; Grolleau,B.; Mercier,L.; Chappard,D.(1999). Effects of roughness, fibronectin and vitronectin on attachment, spreading, and proliferation of human osteoblast-like cells (SaOs-2) on titanium surfaces. *Calcif Tissue Int.* 64(6):499-507.

Deuel,T.F.; Senior,R.M.; Huang,J.S.; Griffin,G.L. (1982). Chemotaxis of monocytes and neutrophils to platelet-derived growth factor. *J Clin Invest* 69: 1046-1049

Disegi, J.A. (1993). AO ASIF Titanium-6%Aluminum-7%Niobium Implant material.

Disegi, JA. (1997). Anodizing treatments for titanium implants. IEEEE 97:129-132

Disegi, J. (1998a). AO ASIF Wrought 18% Chromium-14% Nickel-2.5% Molybdenum Stainless steel implant material. AO ASIF technical Comission pamphlet, 1st Ed.

Disegi, J. (1998b). AO ASIF unalloyed titanium implant material. AO ASIF technical Comission pamphlet, 4th Ed.

Disegi,J.A. (2000). Titanium alloys for fracture fixation implants. Injury 31 Suppl4: 14-17

Disegi, J. (2003). AO ASIF. Wrought Titanium-15% Molybdenum Implant material AO ASIF technical Comission pamphlet, 1st Ed.

Disegi, J & Eschbach, L (2000). Stainless steel in bone surgery. *Injury, Int. J.* Care Injured 31: SD2-6

Doran, A; Law, FC; Allen, MJ; Rushton, N (1998). Neoplastic transformation of cells by soluble but not particulate forms of metals used in orthopaedic implants. *Biomaterials* 19: 751-759.

Ducy P, Desbois C, Boyce B, Pinero G, Story B, Dunstan C, Smith E, Bonadio J, Goldstein S, Gundberg C, Bradley A, Karsenty G. (1996). Increased bone formation in osteocalcin-deficient mice. *Nature.* 1;382(6590):448-52.

Ducy P, Zhang R, Geoffroy V, Ridall AL, Karsenty G. (1997). Osf2/Cbfa1: a transcriptional activator of osteoblast differentiation. *Cell.* 30;89(5):747-54

Eedy, DJ; Burrows, D; McMaster, D. (1991). The nickel content of certain metallic patch test materials and its relevance in nickel sensitive subjects. *Contact Dermatitis* 24: 11-15

Eijer, H; Hauke, C; Arens, S; Printzen, G; Schegel, U; Perren, S.M. (2001). PC-Fix and local infeaction resistance – Influence of implant design on postoperative infection development, clinical and experimental results. *Injury* 32: 38-43

Eisenbarth,E.; Velten,D.; Schenk-Meuser,K.; Linez,P.; Biehl,V.; Duschner,H.; Breme,J.; Hildebrand,H. (2002). Interactions between cells and titanium surfaces. *Biomol Eng.* 19(2-6):243-9.

El Ghannam,A.R.; Ducheyne,P.; Risbud,M.; Adams,C.S.; Shapiro,I.M.; Castner,D.; Golledge,S.; Composto,R.J. (2004). Model surfaces engineered with nanoscale roughness and RGD tripeptides promote osteoblast activity. J Biomed Mater Res A. 2004 Mar 15;68(4):615-27.

Elbetieha A, Al-Hamood MH. (1997) Long-term exposure of male and female mice to trivalent and hexavalent chromium compounds: effect on fertility. *Toxicol*;116:39-47.

Emel E, Karagöz Güzey F, Güzey D, Seyithanoğlu H, Sel B, Alataş I. (2007). Delayed infection 6 years after spinal instrumentation: a case report. *Turk Neurosurg.* 17(2):116-20.

Eschbach, L. (2000). Nonresorable polymers in bone surgery. *Injury* 31: 22-27

Emmett EA; Risby, TH; Jiang, L; Ng SK; Feinman, S.(1988). Allergic contact dermatitis to nickel: Bioavailability from consumer products and provocation threshold. *J Am Acad Dermatol* 19:314-322

Eschbach, L; Marti, A; Gasser, B (2000). Fretting corrosion testing of internal fixation plates and screws. In: Materials for medical engineering (Ed. Stallforth et al.) Euromat Vol. 2. Wiley.

Eschbach, L; Bigolin, G; Hirsiger, W; Gasser, B. (2001) Low-Nickel steel for small bone fragment fixation plates and screws. MAEG meeting, Lausanne Feb 2001.

Eschbach, L. (2003). 10 Frequently asked questions about magnetic resonance imaging in patients with metal implants. AO ASIF Materials Expert Group.

European Antimicrobial Resistance Surveillance System Annual Report (EARSS). 2002

Evans, NA & Evans, RO. (1997). Playing with metal: Fracture implants and contact sport. *Br J Sports Med* 31: 319-321

Ferguson C, Alpern E, Miclau T, Helms JA.(1999). Does adult fracture repair recapitulate embryonic skeletal formation? Mech Dev. 87(1-2):57-66.

Ferris,D.M.; Moodie,G.D.; Dimond,P.M.; Gioranni,C.W.; Ehrlich,M.G.; Valentini,R.F.(1999). RGD-coated titanium implants stimulate increased bone formation in vivo. Biomaterials.23-24:2323-31

Franceschi RT & Young J. (1990). Regulation of alkaline phosphatase by 1,25-dihydroxyvitamin D3 and ascorbic acid in bone-derived cells. *J Bone Miner Res.* 5:1157-1167.

Forgacs, G. (1995). On the possible role of cytoskeletal filamentous networks in intracellular signalling: an approach based on percolation. *J Cell Sci.* 108: 2131-2143

Frigg, R. (2003). Development of the LCP. *Injury* 34: 31-42

Gagegaard, N. (2007). Atomic force microscopy in biology: technology and techniques. *Biotechnic & Histochemistry.* 81: 87-97.

Georgiadis GM, Gove NK, Smith AD, Rodway IP. (2004) Removal of the Less Invasive Stabilisation System. *J Orthop Trauma;*18:562–564

Gerber, H & Perren, SM (1980). Evaluation of tissue compatibility of in vitro cultures of embryonic bone. Evaluation of Biomaterials (GD Winter; JL Leray; K deGroot (Eds)) 307-314

Gogi N, Khan SA, Varshney MK. (2006) Limb length discrepancy following titanium elastic nailing in paediatric femoral shaft fractures. *Acta Orthop Belg.* 72(2):154-8

Gogolewski, S (2000). Bioresorable polymers in trauma and surgery. *Injury* 31: 28-32

Goodship, A.E; Kenwright, J (1985). The influence of induced micromovement upon healing of experimental tibial fractures. J Bone Joint Surg 67: 650-655

Goodship, A.E; Lanyon, L.E; McFie, H. (1979). Functional adaption of bone to increased stress. *J Bone Joint Surg* 61: 539-546

Gordeladze JO, Noël D, Bony C, Apparailly F, Louis-Plence P, Jorgensen C. (2008). Transient down-regulation of cbfa1/Runx2 by RNA interference in murine C3H10T1/2 mesenchymal stromal cells delays in vitro and in vivo osteogenesis, but does not overtly affect chondrogenesis. *Exp Cell Res.* 15;314(7):1495-506.

Gösling T, Hufner T, Hankemeier S, Zelle BA, Muller-Heine A, Krettek C. (2004) Femoral nail removal should be restricted in asymptomatic patients. *Clin Orthop Relat Res.* 423:222-6.

Gottlieb, S; Leventhal, GS (1951). Titanium, a metal for surgery. *J Bone Joint Surg.* 33: 473-474

Grainger, D. W. and Healy, K. E. (1999). Biomaterial Surface Analysis. In Hanbook of Biomaterial Evaluation - Scientific, Technical, and Clinical Testing of Implant Materials, (ed. A. von Recum): Taylor & Francis.

Groessner-Schreiber, B & Tuan, R.S. (1992). Enhanced extracellular matrix production and mineralisation by osteoblasts cultured on titanium surfaces *in vitro. J. Cell Sci.* 101: 209-217

Gronowicz,G.; McCarthy,M.B. (1996). Response of human osteoblasts to implant materials: integrin-mediated adhesion. J.Orthop.Res. 14(6): 878-887

Grose A, González Della Valle A, Bullough P, Lyman S, Tomek I, Pellicci P.(2006). High failure rate of a modern, proximally roughened, cemented stem for total hip arthroplasty. *Int Orthop.* 30(4):243-7.

Gross,U.; Strunz,V. (1985). The interface of various glasses and glass ceramics with a bony implantation bed. *J.Biomed.Mater.Res.* 19(3): 251-271

Gunst M.A; Suter C; Rahn B.A. (1979) Bone perfusion after plate osteosynthesis: a study of the intact rabbit tibia with disulfin blue vital staining. *Helv Chir Acta;*46:171–175

Guo, J; Padilla, RJ; Wallace, A; DeKoK, IJ; Cooper, LF. (2007). The effect of hydrofluoric acid treatment of TiO2 grit blasted titanium implants on adherent osteoblast gene expression in vitro and in vivo. *Biomaterials.* 28 (36):5418-5425.

Guzzanti V; Falciglia F; Stanitski C.L (2004). Slipped capital femoral epiphysis in skeletally immature patients. *J Bone Joint Surg Br.* 86:731-736

ap Gwynn I, Wilson C (2001) Characterizing fretting particles by analysis of SEM images. *Eur Cell Mater;* 1:1–11.

Hanawa,T. Metal ion release from metal implants. (2004) *Material science & engineering.* 24: 745-752

Hanson, B; van der Werken, C; Stengel, D. (2008). Surgeon's beliefs and perceptions about removal of orthopaedic implants. *BMC Muscolskeletal disorders* 9:73

Hamilton P, Doig S, Williamson O (2004). Technical difficulty of metal removal after LISS plating. *Injury, Int. J. Care Injured* 35, 626-628.

Harada, H; Tagashira, S; Fujiwara, M; Ogawa, S; Katsumata, T; Yamaguchi, A; Komori, T; Nakatsuka, M. (1999). Cbfa1 isoforms exert functional differences in osteoblast differentiation. *J Biol Chem.* 274(11): 6972-6978

Harmey D, Hessle L, Narisawa S, Johnson KA, Terkeltaub R, Millán JL.(2004). Concerted regulation of inorganic pyrophosphate and osteopontin by akp2, enpp1, and ank: an integrated model of the pathogenesis of mineralization disorders. *Am J Pathol.* 164(4):1199-209.

Harris LG, Meredith DO, Eschbach L, Richards RG. (2007) Staphylococcus aureus adhesion to standard micro-rough and electropolished implant materials. *J Mater Sci Mater Med.* 18(6):1151-6.

Hay, D.I & Moreno, E.C. (1979). Differential adsorption and chemical affinities of proteins for apatitic surfaces. *J. Dent. Res.* 58: 930-942

Hayakawa T, Yoshinari M, Nemoto K, Wolke JG, Jansen JA. (2000). Effect of surface roughness and calcium phosphate coating on the implant/bone response. *Clin Oral Implants Res.* 11(4):296-304.

Hayda, R.A; Brighton, C.T; Esterhai, J.L. (1998). Pathophysiology of delayed healing. *Clin Orthop Relat Res.* 355: 31-40

Hayes JS, Archer, CW, Richards RG. (2007) Reducing bone encasement of metal implants for elective removal. Trans. 53rd ORS (San Diego), 1630.

Hayes, JS; Vos, DI: Hahn, J; Pearce, SG; Richards, RG. (2008a). An *in vivo* evaluation of surface polishing of TAN intramedullary nails for ease of removal. (Submitted to JBJS).

Hayes, JS; Archer, CW; Richards, RG. (2008b). Control of osteoblast genotype with surface microtopography. Oral presentation, June 16th at ECM IX: Muscolskeletal trauma Davos, CH.

Hauke, C; Schlegel, U; Melcher, G.A. (1997). Local infection in relation to different implant materials. An experimental study using stainless steel and titanium solid, unlocked intramedullary nails in rabbits. *Orthop Trans.* 21: 835-836

Hazan,R.; Brener,R.; Oron,U.(1993). Bone growth to metal implants is regulated by their surface chemical properties. *Biomaterials.* 14(8):570-4.

Heath,J.C.; Freeman,M.A.; Swanson,S.A.(1971). Carcinogenic properties of wear particles from prostheses made in cobalt-chromium alloy. *Lancet.* 1: 564-566

Hessle L, Johnson KA, Anderson HC, Narisawa S, Sali A, Goding JW, Terkeltaub R, Millan JL (2002). Tissue-nonspecific alkaline phosphatase and plasma cell membrane glycoprotein-1 are central antagonistic regulators of bone mineralization. *Proc Natl Acad Sci.* 9;99(14):9445-9.

Hidaka S, Gustilo RB. (1984). Refracture of bones of the forearm after plate removal. *J Bone Joint Surg Am.* 66(8):1241-3.

Highland, TR & LaMont, RL. (1985). Deep, late infections associated with internal fixation in children. *J Pediatr Orthop* 5: 59-64

Hildebrand F, Giannoudis P, van Griensven M, Chawda M, Probst C, Harms O, Harwood P, Otto K, Fehr M, Krettek C, Pape HC. (2005). Secondary effects of femoral instrumentation on pulmonary physiology in a standardised sheep model: what is the effect of lung contusion and reaming? *Injury*. 36(4):544-55.

Heim,D; Regazzoni,P; Tsakiris,D.A; Aebi,T; Schlegel,U; Marbet,G.A; Perren,S.M. (1995). Intramedullary nailing and pulmonary embolism: does unreamed nailing prevent embolization? An in vivo study in rabbits. *J. Trauma* 38: 899-906

Hierholzer, S & Hierholzer, G (1992). Internal fixation and metal allergy – Clinical investigations, immunology and histology of the implant tissue interface. NY: Thieme.

Horbett,T.A.; Schway,M.B.(1988). Correlations between mouse 3T3 cell spreading and serum fibronectin adsorption on glass and hydroxyethylmethacrylate-ethylmethacrylate copolymers. *J Biomed Mater Res.*22(9):763-93

Horn, J; Schlegel, U; Krettek, C; Ito, K. (2005). Infection resistance of unreamed solid, hollow slotted and cannulated intramedullary nails: an in vivo experimental comparison. *J Orthop. Res.* 23: 810-815

Howlett,C.R.; Evans,M.D.; Walsh,W.R.; Johnson,G.; Steele,J.G.(1994). Mechanism of initial attachment of cells derived from human bone to commonly used prosthetic materials during cell culture. Biomaterials. 15: 213-222

Hui C, Jorgensen I, Buckley R, Fick G. (2007) Incidence of intramedullary nail removal after femoral shaft fracture healing. *Can J Surg.* 50(1):13-8.

Hupel T.M; Aksenov, S.A; Schemitsch E.H. (1998). Cortical bone blood flow in loose and tight fitting locked unreamed intramedullary nailing: a canine segmental tibia fracture model. *J Orthop Trauma.* 12(2):127-35

Hunter, GK; Goldberg, HA. (1993). Nucleation of hydroxyapatite by bone sialoprotein. Proc. Natl. Acad. Sci. 90:8562-8565.

Hunter, GK; Hauschka , PV; Poole, AR; Rosenberg, AR; Goldberg, HA. (1996). Nucleation and inhibition of hydroxyapatite formation by mineralized tissue proteins. *Biochem. J.* 317: 59-64

Husain A, Pollak AN, Moehring HD, Olson SA, Chapman MW. (1996) Removal of intramedullary nails from the femur: a review of 45 cases. *J Orthop Trauma.* 10(8):560-2.

Ilchmann T, Parsch K.(2006). Complications at screw removal in slipped capital femoral epiphysis treated by cannulated titanium screws. *Arch Orthop Trauma Surg.* 126(6):359-63.

Im GI, Lee KB. (2003) Difficulties in removing ACE tibial intramedullary nail. *Int Orthop* 27:355-8.

Ingber, DE (1993). Cellular tensegrity: defining new rules of biological design that govern the cytoskeleton. *J Cell Sci* 104:613-627

Ingber, DE. Tensegrity I. (2003a). Cell structure and hierarchical systems biology. J Cell Sci 116: 1157-1173

Ingber, DE. Tensegrity II. (2003b). How structureal networks influence cellular information processing networks. J Cell Sci 116: 1397-1408.

Isa ZM, Schneider GB, Zaharias R, Seabold D, Stanford CM. (2006). Effects of fluoride-modified titanium surfaces on osteoblast proliferation and gene expression. *Int J Oral Maxillofac Implants.* 21(2):203-11.

Ito, K. & Perren, S.M. (2007). Biology and biomechanics in bone healing. In: AO Principles of fracture management 2nd Ed. (Ed: Rüedi, T.P; Buckley, R.E; Moran, C.G) Thieme. Ch. 1 pp 9-32

Jaaskelainen, T; Pirskanen, A; Ryhanen S; Palvimo JJ; Deluca HF; Maenpaa PH. (1994). Functional interference between AP-1 and the vitamin D receptor on osteocalcin gene expression in human osteosarcoma cells. *Eur J Biochem* 224:11-20.

Jago, RD; Hindley, CJ. (1998). The removal of metalwork in children. *Injury*, 29(6): 439-441.

Jansen,J.A.; van der Waerden,J.P.; de Groot,K. (1989). Effect of surface treatments on attachment and growth of epithelial cells. *Biomaterials* 10: 604-607

Jansen, J; Vercaigne, S; Hulshoff, A; Corten, F; ter Brugge, P; Naert, I (2000). Bone regenerative implant surfaces: the effect of surface roughness and Ca-P coatings. In: Davies JE (ed) Bone Engineering. Em^2, Torronto, pp 345-357.

Jaworski ZFG, Liskova-Kiar M, Uhthoff HK. (1980). Regional disuse osteoporosis and factors influencing its reversal. In: Uhthoff HK. editor. Current concepts of internal fixation of fractures. Berlin; Springer:. p. 17–26.

Jiang D, Franceschi RT, Boules H, Xiao G. (2004). Parathyroid hormone induction of the osteocalcin gene. Requirement for an osteoblast-specific element 1 sequence in the promoter and involvement of multiple-signaling pathways. *J Biol Chem.* 279(7):5329-37.

Jukkola A; Risteli L; Melkko J; Risteli J. (1993). Procollagen synthesis and extracellular matrix deposition in MG-63 osteosarcoma cells. *J Bone Miner Res.*8:651-657.

Kahle, WK. (1994). The case against routine metal removal. J Pediatr Orthop 14:229-237

Karladani AH, Ericsson PA, Granhed H, Karlsson L, Nyberg P. (2007). Tibial intramedullary nails - should they be removed? A retrospective study of 71 patients. *Acta Orthop.* 78(5):668-71.

Kasai, Y; Iida, R; Uchida, A. (2003). Metal concentrations in the serum and hair of patients with titanium alloy spinal implants. *Spine* 15: 1320-1326

Katzer, A; Hockertz, S; Buchhorn, GH; Loehr, JF. (2003). In vitro toxicity and mutagenicity of CoCrMo and Ti6Al wear particles. *Toxicology* 190: 145-154

Kawahara,H.; Aoki,H.; Koike,H.; Soeda,Y.; Kawahara,D.; Matsuda,S. (2006). No evidence to indicate topographic dependency on bone formation around cp titanium implants under masticatory loading. *J.Mater.Sci.Mater.Med.*17(8): 727-734

Keel, SB; Jaffe, KA; Petur Nielsen, J; Rosenberg, AE. (2001). Orthopaedic implant related sarcoma: a study of 12 cases. Mod Pathol 14: 969-977

Keegan, GM; Learmonth, ID; Case, CP. (2007). Orthopaedic metals and their potential toxicity in the arthroplasty patient. *J Bone J Surg.* 89(5): 567-573.

Kenwright, J; Richardson, J.B; Cunningham, JL; White, S.H; Goodship, A.E; Adams, M.A; Magnussen, P.A; Newman, J.H. (1991). Axial movement and tibial fractures: A controlled randomised trial of treatment. *J Bone Joint Surg.* 73: 654-659

Kershaw, C.J; Cunningham, J.L; Kenright, J. (1993). Tibial external fixation, weight bearing and fracture movement. *Clin. Orthop.* 293: 28-36

Khan, M.A; Williams, R.L; Williams, D.F (1996). In vitro corrosion and wear of titanium alloys in the biological environment. *Biomaterials* 17: 2117-2126

Khan, U; Kakar, S; Akali, A; Bentley, G; McGrouther, D.A. (2000). Modulation of the formation of adhesions during healing of injured tendons. *J Bone Joint Surg Br.* 82: 1054-1058

Kieswetter,K.; Schwartz,Z.; Hummert,T.W.; Cochran,D.L.; Simpson,J.; Dean,D.D.; Boyan,B.D. (1996). Surface roughness modulates the local production of growth factors and cytokines by osteoblast-like MG-63 cells. J.Biomed.Mater.Res. 32(1): 55-63

Kim, WY; Zenios, M; Kumar, A; Abdulkadir, U. (2005). The removal of forearm plates in children. *Injury, Int. J. Care Injured* 36, 1427—1430

Klinger MM, Rahemtulla F, Prince CW, Lucas LC, Lemons JE. (1998).Proteoglycans at the bone-implant interface. *Crit Rev Oral Biol Med.* 9(4):449-63.

Klokkevold,P.R.; Nishimura,R.D.; Adachi,M.; Caputo,A. (1997). Osseointegration enhanced by chemical etching of the titanium surface. A torque removal study in the rabbit. Clin Oral Implants Res. (6):442-7.

Knoll M (1935): Aufladepotentiel und Sekundäremission elektronenbestrahlter Körper. Z tech. Phys. 16, 467-475

Komori T, Yagi H, Nomura S, Yamaguchi A, Sasaki K, Deguchi K, Shimizu Y, Bronson RT, Gao YH, Inada M, Sato M, Okamoto R, Kitamura Y, Yoshiki S, Kishimoto T. (1997). Targeted disruption of Cbfa1 results in a complete lack of bone formation owing to maturational arrest of osteoblasts. Cell. 30;89(5):755-64.

Krettek, C. (2007). Intramedullary nailing. In: In: AO Principles of fracture management 2nd Ed. (Ed: Rüedi, T.P; Buckley, R.E; Moran, C.G) Thieme. Ch. 3 pp 257-283

Kubo K, Att W, Yamada M, Ohmi K, Tsukimura N, Suzuki T, Maeda H, Ogawa T. (2008). Microtopography of titanium suppresses osteoblastic differentiation but enhances chondroblastic differentiation of rat femoral periosteum-derived cells. J Biomed Mater Res A. [Epub ahead of print]

Kumm DA, Lee SH, Hackenbroch MH, Rutt J (2001). Slipped capital femoral epiphysis: A retrospective study of dynamic screw fixation. *Clin Orthop Relat Res.* 384:198-207

Lamour V, Detry C, Sanchez C, Henrotin Y, Castronovo V, Bellahcène A. (2007). Runx2- and histone deacetylase 3-mediated repression is relieved in differentiating human osteoblast cells to allow high bone sialoprotein expression. *J Biol Chem.* 14;282(50):36240-9.

Labowsky, DA; Cermak, MB; Waggy, CA. (1990) Forearm fractures: to remove or not to remove. *J Hand Surg* [Am]. 15: 294-301

Langkamer, VG & Ackroyd, CE (1990). Removal of forearm fractures: A review of the complications. *J Bone Joint Surg Br.* 72: 601-604

Larsen, L.B; Madsen, J.E; Hoiness, P.R; Ovre, S. (2004). Should insertion of intramedullary nails for tibial fractures be with or without reaming? A prospective, randomized study with 3.8 years' follow-up. *J. Orthop. Trauma.* 18: 144-149

Larsson,C.; Thomsen,P.; Lausmaa,J.; Rodahl,M.; Kasemo,B.; Ericson,L.E.(1994). Bone response to surface modified titanium implants: studies on electropolished implants with different oxide thicknesses and morphology. *Biomaterials.* 15(13):1062-74.

Larsson,C.; Thomsen,P.; Aronsson,B.O.; Rodahl,M.; Lausmaa,J.; Kasemo,B.; Ericson,L.E. (1996). Bone response to surface-modified titanium implants: studies on the early tissue response to machined and electropolished implants with different oxide thicknesses. *Biomaterials.* 17(6):605-16.

Larsson,C.; Emanuelsson,L.; Thomsen,P.; Ericson,L.E.; Aronsson,B.O.; Kasemo,B.; Lausmaa,J. (1997). Bone response to surface modified titanium implants - studies on the tissue response after 1 year to machined and electropolished implants with different oxide thicknesses. *J Mater Sci Mater Med.*8(12):721-9.

Lee TK, Haynes RJ, Longo JA, Chu JR. (1996). Pin removal in slipped capital femoral epiphysis: the unsuitability of titanium devices. *J Pediatr Orthop.* 16(1):49-52.

Leibovich SJ & Ross R. The role of the macrophage in wound repair. *Am J Pathol.* 78: 71-100

Lew, D.P & Waldvogel, F.A. (2004). Osteomyelitis. *Lancet* 364: 369-379

Lian, JB; Stein, GS. (1992). Concepts of osteoblast growth and differentiation: basis for modulation of bone cell development and tissue formation. *Critical reviews in Oral biology and medicine* 3(3): 269-305.

Lincks,J.; Boyan,B.D.; Blanchard,C.R.; Lohmann,C.H.; Liu,Y.; Cochran,D.L.; Dean,D.D.; Schwartz,Z. (1998). Response of MG63 osteoblast-like cells to titanium and titanium alloy is dependent on surface roughness and composition. Biomaterials 19(23): 2219-2232

Lind,M.; Deleuran,B.; Thestrup-Pedersen,K.; Soballe,K.; Eriksen,E.F.; Bunger,C.(1995). Chemotaxis of human osteoblasts. Effects of osteotropic growth factors. APMIS. 1995 Feb;103(2):140-6

Liu W, Toyosawa S, Furuichi T, Kanatani N, Yoshida C, Liu Y, Himeno M, Narai S, Yamaguchi A, Komori T (2001). Overexpression of Cbfa1 in osteoblasts inhibits osteoblast maturation and causes osteopenia with multiple fractures. *J Cell Biol.* 155(1):157-66

Loder, RT & Feinberg, JR. (2006). Orthopaedic implants in children: Survey results regarding routine removal by the pediatric and nonpediatric specialists. *J Pediatr Orthop* 25: 510-519.

Lohmann,C.H.; Dean,D.D.; Koster,G.; Casasola,D.; Buchhorn,G.H.; Fink,U.; Schwartz,Z.; Boyan,B.D. (2002a). Ceramic and PMMA particles differentially affect osteoblast phenotype. Biomaterials. 23: 1855-1863

Lohmann,C.H.; Tandy,E.M.; Sylvia,V.L.; Heil-Vocke,A.K.; Cochran,D.L.; Dean,D.D.; Boyan,B.D.; Schwartz,Z. (2002b). Response of normal female human osteoblasts (NHOst) to 17beta-estradiol is modulated by implant surface morphology. J.Biomed.Mater.Res. 62(2): 204-213

Lorich, DG & Gardner, MJ (2007). Plates. In: AO Principles of fracture management 2nd Ed. (Ed: Rüedi, T.P; Buckley, R.E; Moran, C.G) Thieme. Ch. 3 pp 227-248

Lossdorfer,S.; Schwartz,Z.; Wang,L.; Lohmann,C.H.; Turner,J.D.; Wieland,M.; Cochran,D.L.; Boyan,B.D. (2004). Microrough implant surface topographies increase osteogenesis by reducing osteoclast formation and activity. J Biomed Mater Res A. 70(3):361-9

Luhmann SJ, Schootman M, Schoenecker PL, Dobbs MB, Gordon JE. (2003) Complications of titanium elastic nails for pediatric femoral shaft fractures. J Pediatr Orthop. 23(4):443-447.

Machwate M, Jullienne A, Moukhtar M, Marie PJ. (1995). Temporal variation of c-Fos proto-oncogene expression during osteoblast differentiation and osteogenesis in developing rat bone. *J Cell Biochem.* 57(1):62-70

Maeusli, P (1986). Surface characterisation of titanium and titanium alloys. Biological and biomechanical performance of biomaterials. Elsevier science publishers. Amsterdam. 63-68

Mahmoodian, F; Gosiewska, A; Peterkofsky, B. (1996). Regulation and properties of bone alkaline phosphatase during vitamin C deficiency in guinea pigs. *Arch Biochem Biophys.* 336(1):86-96.

Manor, Y; Chaushu, G; Taicher, S. (1999). Risk factors contributing to symptomatic plate removal in orthognathic surgery patients. *J Oral Maxillofac surg.* 57:679-682.

Maruyama Z, Yoshida CA, Furuichi T, Amizuka N, Ito M, Fukuyama R, Miyazaki T, Kitaura H, Nakamura K, Fujita T, Kanatani N, Morishi T, Yamana K, Liu W, Kawaguchi H, Nakamura K, Komori T. (2007). Runx2 determines bone maturity and turnover rate in postnatal bone development and is involved in bone loss in estrogen deficiency. *Dev Dyn.* 236(7):1876-90.

Marti, A. (2000). Inert bioceramics (Al_2O_3, ZrO_2) for medical applications. *Injury.* 31: 33-36

Martin JY; Schwartz, Z; Hummert, TW; Schraub, DM; Simpson, J; Lankford Jr. J; Dean, DD; Cochran, DL; Boyan, BD (1995). Effect of titanium surface roughness on proliferation, differentiation and protein synthesis of human osteoblast-like cells (MG-63) J Biomed Mater Res 29: 389-401

Martines,E.; Seunarine,K.; Morgan,H.; Gadegaard,N.; Wilkinson,C.D.; Riehle,M.O.(2005). Superhydrophobicity and superhydrophilicity of regular nanopatterns. Nano Letters. 5: 2097-2103

Masaki,C.; Schneider,G.B.; Zaharias,R.; Seabold,D.; Stanford,C. (2005). Effects of implant surface microtopography on osteoblast gene expression. *Clin Oral Implants Res.* 16(6):650-6.

Massone L, Anonide A, Borghi S, Isola V. (1991). Positive patch test reactions to nickel, cobalt, and potassium dichromate in a series of 576 patients. *Cutis*. 47:119-122.

McKibbin, B. (1978). The biology and fracture healing in long bones. *J Bone Joint Surg Br.* 60:150-162

Melcher, G.A; Claudi, B; Schelegel, U; Perren, S.M; Printzen G, Munzinger J. (1994). Influence of type of medullary nail on the development of local infection. An experimental study of solid and slotted nails in rabbits. *J Bone Joint Surg Br.* 76:955-9

Melcher G.A, Metzdorf A, Schlegel U, Ziegler W.J, Perren S.M, Printzen G. (1995). Influence of reaming versus nonreaming in intramedullary nailing on local infection rate: experimental investigation in rabbits. *J Trauma*. 39:1123-1128.

Melcher, G.A; Hauke, C; Metzdorf, A Perren SM, Printzen G, Schlegel U, Ziegler WJ. (1996). Infection after intramedullary nailing: An experimental investigation on rabbits. *Injury* 27: 23-26

Meleti,Z.; Shapiro,I.M.; Adams,C.S. (2000) Inorganic phosphate induces apoptosis of osteoblast-like cells in culture. Bone 27: 359-366

Meredith,D.O.; Eschbach,L.; Wood,M.A.; Riehle,M.O.; Curtis,A.S.; Richards,R.G. (2005). Human fibroblast reactions to standard and electropolished titanium and Ti-6Al-7Nb, and electropolished stainless steel. J Biomed. Mater. Res A. 75: 541-555.

Meredith, D.O. (2006). Biocompatibility of orthopaedic metal implants: The influence of surface chemistry and topography. Thesis from AO Research Institute Davos, CH. Chapter 2. Metals & Surfaces pp19-41.

Meredith,D.O.; Riehle,M.O.; Curtis,A.S.; Richards,R.G. (2007a). Microtopography of metal surfaces influence fibroblast growth by modifying cell shape, cytoskeleton & adhesion. *J.Orthop.Res.*25(11): 1523-1533

Meredith,D.O.; Riehle,M.O.; Curtis,A.S.; Richards,R.G. (2007b). Is surface chemical composition important for orthopaedic implant materials? *J. Mater Sci. Mater. Med* 18: 405-413

Melo, MD; Shafie, H; Obeid, G. (2006). Implant survival rates for oral and maxillofacial surgery residents: A retrospective clinical review with analysis of resident level of training on implant survival, *J Oral Maxillofac Surg.* 64: 1185-1189.

Messmer, P; Perren, S.M; Schum, N (2007). Screws. In: AO Principles of fracture management 2nd Ed. (Ed: Rüedi, T.P; Buckley, R.E; Moran, C.G) Thieme. Ch. 3 pp 213-225

Meyer,A.E.; Baier,R.E.; Natiella,J.R.; Meenaghan,M.A.(1988) Investigation of tissue/implant interactions during the first two hours of implantation. J Oral Implantol. 14:363-79

Miclau, T; Remiger,A; Tepic,S; Lindsey,R; McIff,T. (1995) A mechanical comparison of the dynamic compression plate, limited contact-dynamic compression plate, and point contact fixator. J Orthop Trauma 9: 17-22

Milia MJ, Vincent AB, Bosse MJ. (2003) Retrograde removal of an incarcerated solid titanium femoral nail after subtrochanteric fracture. *J Orthop Trauma* 17:521-4.

Miettinen H, Mäkelä A, Rokkanen P, Törmälä P, Vainio J. (1992) Fixation of diaphyseal femoral osteotomy with self-reinforced biodegradable intramedullary implants: an experimental study on growing dogs. *Clin Mater.* 9(1):31-6.

Möller, K; Meyer, U; Szulczewski, DH; Heide H; Priessnitz, B; Jones, DB (1994). The influence of zeta potential and interfacial tension on osteoblast-like cells. Eurpean Cells & Materials. 4: 263-268

Montanaro L, Cervellati M, Campoccia D, Prati C, Breschi L, Arciola CR.(2005). No genotoxicity of a new nickel-free stainless steel. Int J Artif Organs. 28(1):58-65.

Montanaro L, Cervellati M, Campoccia D, Arciola CR.(2006). Promising in vitro performances of a new nickel-free stainless steel. J Mater Sci Mater Med. 2006 Mar;17(3):267-75

Morehead, JM & Holt, GR. (1994). Soft tissue response to synthetic biomaterials. *Otolaryngol Clin North Am.* 27: 195-201

Moriarty, T.F; Debefve, L; Boure, L; Richards, R.G. (2008). Influence of material and micro-topogrpahy on the development of local infection *in vivo*; experimental investigation in rabbits. Submitted to the Journal of Orthopaedic Research.

Morshed S, Humphrey M, Corrales LA, Millett M, Hoffinger SA. (2007) Retention of flexible intramedullary nails following treatment of pediatric femur fractures. *Arch Orthop Trauma Surg.* 127(7):509-14

Mosbah MR, Oloyede D, Koppel DA, Moos KF, Stenhouse D. (2003). Miniplate removal in trauma and orthognathic surgery--a retrospective study. *Int J Oral Maxillofac Surg.* 32(2):148-51.

Mutimer J, Hammett RD, Eldridge JD.(2007) Assessing leg length discrepancy following elastic stable intramedullary nailing for paediatric femoral diaphyseal fractures. *Arch Orthop Trauma Surg.* 127(5):325-30.

Nakashima K, Zhou X, Kunkel G, Zhang Z, Deng JM, Behringer RR, de Crombrugghe B.(2002). The novel zinc finger-containing transcription factor osterix is required for osteoblast differentiation and bone formation. *Cell.* 11;108(1):17-29.

Neubauer,T.; Bayer,G.S.; Wagner,M. (2006). Open fractures and infection. Acta Chir *Orthop Traumatol Cech.* 73:301-12

Nefussi JR, Pouchelet M, Collin P, Sautier JM, Develay G, Forest N. (1989). Microcinematographic and autoradiographic kinetic studies of bone cell differentiation in vitro: matrix formation and mineralization. *Bone.* 10(5):345-52.

Nefussi JR, Sautier JM, Nicolas V, Forest N.(1991). How osteoblasts become osteocytes: a decreasing matrix forming process. J Biol Buccale. 1991 Mar;19(1):75-82.

Neyt JG, Buckwalter JA, Carroll NC (1998) Use of animal models in musculoskeletal research. Iowa Orthop J. 18:118-23

Nichols,K.G.; Puleo,D.A. (1997) Effect of metal ions on the formation and function of osteoclastic cells in vitro. J. Biomed. Mater Res. 35: 265-271.

Nguyen KT, Shukla KP, Moctezuma M, Tang L.(2007) Cellular and molecular responses of smooth muscle cells to surface nanotopography. J Nanosci Nanotechnol. 7(8):2823-32.

Ochsner, PE. (2008). Intramedullary reaming in chronic (posttraumatic) osteomyelitis of long bones. Presentation: 03.06.2008 at AO Trustees meeting, Davos Switzerland.

Olmstead, M & Pohler, O (1990). Report on long term compatibility testing of new titanium alloys. AO research grant 1987/1988 Stratec medical, Jan 1990.

Olzak, AG; Schmit, J; Heaton, MG. (2001). Interferometry: technology and Applications. Veeco Intruments library (www.vecco.com/library/appnotes{accessed 17/10/2006})

Otto F, Thornell AP, Crompton T, Denzel A, Gilmour KC, Rosewell IR, Stamp GW, Beddington RS, Mundlos S, Olsen BR, Selby PB, Owen MJ. (1997). Cbfa1, a candidate gene for cleidocranial dysplasia syndrome, is essential for osteoblast differentiation and bone development. Cell. 30;89(5):765-71.

Pape, H.C; Krettek, C; Maschek, H; Regel G; Tscherne H. (1996). Fatal pulmonary embolization after reaming of the femoral medullary cavity in sclerosing osteomyelitis: a case report. *J Orthop Trauma.* 10:429-32

Pape H.C, Giannoudis P, Krettek C. (2002). The timing of fracture treatment in polytrauma patients: relevance of damage control orthopedic surgery. *Am J Surg.* 183:622-629.

Pautke C, Schieker M, Tischer T, Kolk A, Neth P, Mutschler W, Milz S. (2004). Characterization of osteosarcoma cell lines MG-63, Saos-2 and U-2 OS in comparison to human osteoblasts. Anticancer Res. 24(6):3743-3748.

Pearce AI, Richards RG, Milz S, Schneider E, Pearce SG (2008a). Animal models for implant biomaterial research in bone: a review. *Eur Cell Mater.* 13:1-10.

Pearce AI, Pearce SG, Schwieger K, Milz S, Schneider E, Archer CW, Richards RG. (2008b). Effect of surface topography on removal of cortical bone screws in a novel sheep model. *J Orthop Res.* [Epub ahead of print].

Perren, SM. (1979). Physical and biological aspects of fracture healing with special reference to internal fixation. Clin Orthop 138:175-196

Perren, SM & Rahn, BA. (1980), Biomechanics of fracture healing. *Can J Surg* 23(3): 228-232

Perren, S.M; Geret, V;Tepic, M; Rahn (1986). Quantitative evaluation of biocompatibility of vandium free titanium alloys. In: Biological and biomechanical performance of biomaterials (eds Christel, P; Meunier, A; Lee, AJC) Elsevier Science Publishers

Perren, SM; Cordey, J; Rahn, BA; Gautier, E; Schneider, E. (1988). Early temporary porosis of bone induced by internal fixation implants. A reaction to necrosis, not stress protection? *Clin Orthop Rel Res.* 232: 139-151

Perren, S.M. (1991). The concept of biological plating using the limited contact-dynamic compression plate (LC-DCP). Scientific background, design and application. *Injury* 25: 1-41.

Perren, S.M; Pohler, O; Schneider, E. (2001). Titanium as an implant material for osteosynthesis applications. In: Titanium in Medicine (Ed: Brunette, DM; Tengvall, P; Textor, M; Thomsen, P). Springer. Ch23. pp771-823.

Perren, S.M & Richards, R.G. (2007). Implants and materials in fracture fixation. In: AO Principles of fracture management 2nd Ed. (Ed: Rüedi, T.P; Buckley, R.E; Moran, C.G) Thieme. Ch. 1 pp 33-44.

Peterson, HA. (2005). Metallic implant removal in children. J Pediatr Orthop. 25: 107-115

Peterson, L (1947). Fixation of Bones by plates and screws. *Journal of bone and joint surgery.* 29: 335-347

Pham QP, Kurtis Kasper F, Scott Baggett L, Raphael RM, Jansen JA, Mikos AG.(2008). The influence of an in vitro generated bone-like extracellular matrix on osteoblastic gene expression of marrow stromal cells. *Biomaterials.* 29(18):2729-39.

Pohler, O.E.M (2000). Unalloyed titanium for implants in bone surgery. *Injury* 31: 7-13

Postlethwaite,A.E.; Keski-Oja,J.; Moses,H.L.; Kang,A.H. (1987). Stimulation of the chemotactic migration of human fibroblasts by transforming growth factor beta. *J Exp Med* 165: 251-256

Postiglione,L.; Di Domenico,G.; Ramaglia,L.; Montagnani,S.; Salzano,S.; Di Meglio,F.; Sbordone,L.; Vitale,M.; Rossi,G. (2003). Behavior of SaOS-2 cells cultured on different titanium surfaces. *J.Dent.Res.*82:692-696.

Probst, A. & Speigel, HA (1997). Cellular mechanisms of bone repair. *J Invest. Surg.* 10: 77-86

Puleo, DA & Nanci, A (1999). Understanding the controlling the bone-implant interface. *Biomaterials* 20: 2311-2321

Qu, J; Chehroudi, B; Brunette, DM. (1996). The use of micromachined surfaces to investigate the cell behavioural factors essential to osseonintegration. *Oral Dis* 2:102-115

Quarles LD, Yohay DA, Lever LW, Caton R, Wenstrup RJ.(1992). Distinct proliferative and differentiated stages of murine MC3T3-E1 cells in culture: an in vitro model of osteoblast development. *J Bone Miner Res.* 7(6):683-92.

Rahn, B.A; Gallinaro, P; Baltensperger, A; Perren, S.M. (1971) Primary bone healing. An experiemtnal study in the rabbit. *J Bone Surg Am.* 53: 783-786

Rahn, B.A. (2002). Bone healing: histological and physiological concepts. In: Bone in clinical orthopaedics 2nd Edition (Ed: Summer-Smith, G.). Thieme NY. Ch: 2 pp 23-105

Raisz,L.G (1984) Studies on bone formation and resorption in vitro. *Horm.Res* 20(1):22-27

Raisz,L.G.; Pilbeam,C.C.; Fall,P.M.(1993). Prostaglandins: mechanisms of action and regulation of production in bone. Osteoporos.Int. 3(1): 136-140

Rallis, G; Mourouzis, C; Papakosta, V; Papanastasiou, G; Zachariades, N. (2006). Reasons for miniplate removal following maxillofacial trauma: A 4 year study. *J Cranio-Maxillo Surg.*34:435-439.

Ratner, BD. (1993). New ideas in biomaterials science--a path to engineered biomaterials. J *Biomed Mater Res.*(7):837-50

Ratner, B.D (2001). A perspective on Titanium biocompatibility. Titanium in Medicine (Ed: Brunette, DM; Tengvall, P; Textor, M; Thomsen, P). Springer.Ch1 pp1-12

Reclaru, L; Ziegenhagen, R; Eschler, PY; Blatter, A; Lemaître, J. (2006). Comparative corrosion study of 'Ni-free' austenitic stainless steels in view of medical applications. *Acta Biomaterialia 2* 433–444

Rhinelander, F.W. (1965). Some aspects of the microcirculation of healing bone. *Clin Orthop.* 40:12

Rhinelander, F.W. (1974). Tibial blood supply in relation to fracture healing. Clin. Orthop. 105: 34-81

Rich,A.; Harris,A.K. (1981). Anomalous preferences of cultured macrophages for hydrophobic and roughened substrata. *J Cell Sci.* 50:1-7.

Richards, RG; apGwynn, I; Bundy, KJ; Rahn, BA. (1995). Micro-jet impingement followed by scanning electron microscopy as a qualitative technique to compare cellular adhesion to various biomaterials. *Cell Biol Int.* 19:1015-1024

Richards, R.G. (1996). The effect of surface roughness on fibroblast adhesion *in vitro*. *Injury* Suppl 3: 38-43

Richards, R.G; Persson, A; Gasser, B; Wieling, R. (2000a). Influence of surface microtopography on formation of capsules: An in vivo study of stainless steel implants in rabbits. 10th Annual conference European Orhtopaedic Research Society., Wiesbaden, October 13th-15th. Transactions volume10: 0-136

Richards RG, Wieland M, Textor M (2000b). Advantages of stereo imaging of metallic surfaces with low voltage backscattered electrons in a field emission scanning electron microscope. *J Microsc.* 199 (2):115-23.

Richards, RG & Perren, SM. (2007). Implants and materials in fracture fixation. In: AO principles of fracture management 2nd edition (Ed: Rüedi, TP; Buckley, RE; Moran, CG). Thieme, Ch1 pp33-44

Richards, RG. (2008). The Relevance of Implant Surfaces in Hand Fracture Fixation In: Osteosynthesis in the Hand: Current Concepts. FESSH Instructional Course 2008. Basel, Karger,, pp 20–30

Rogers, S.D; Howie, D.WW; Graves, S.E; Pearcy, M.J; Haynes, D.R (1997). In vitro human monocytes response to wear particles of titanium alloy containing vanadium or niobium. *J. Bone Joint Surg.* 79: 311-315

Rosengren, A; Wallman, L; Danielsen, N; Laurell, T; Bjursten, L.M. (2002). Tissue reactions evoked by porous and plane surfaces made out of silicon and titanium. *IEEE Trans Biomed Eng.* 49: 392-399

Rosson, JW; Shearer, JR. (1991). Refracture after removal of plates from the forearm. *J Bone J Surg.* 73(3): 415-417.

Roure P, Ip WY, Lu W, Chow SP, Gogolewski S.(1999) Intramedullary fixation by resorbable rods in a comminuted phalangeal fracture model. A biomechanical study. *J Hand Surg* [Br]. 24(4):476-81.

Sakai S, Tamura M, Mishima H, Kojima H, Uemura T. (2008). Bone regeneration induced by adenoviral vectors carrying til-1/Cbfa1 genes implanted with biodegradable porous materials in animal models of osteonecrosis of the femoral head. *J Tissue Eng Regen Med.* 2(2-3):164-7

Salido M, Vilches JI, Gutiérrez JL, Vilches J. (2007) Actin cytoskeletal organization in human osteoblasts grown on different dental titanium implant surfaces. *Histol Histopathol.* 22(12):1355-64

Saura, E. (2005). We put it in, do we have to remove it? Oral presentation at 82nd masters course, Davos, Switzerland. December 7th.

Scalea T.M, Boswell S.A, Scott J.D, Mitchell K.A, Kramer M.E, Pollak A.N. (2000). External fixation as a bridge to intramedullary nailing for patients with multiple injuries and with femur fractures: damage control orthopedics. *J Trauma.* 48:613-623

Schemitsch E.H, Kowalski M.J, Swiontkowski M.F, Senft D (1994). Cortical bone blood flow in reamed and unreamed locked intramedullary nailing: a fractured tibia model in sheep. *J Orthop Trauma.* 8:373-382.

Schlegel, P; Hayes, J.S.; Frauchiger, V. M.; Wieling, R; Textor, M; Richards, R.G.(2008). An *in vivo* evaluation of the biocompatibility of anodic plasma chemical treatment with calcium phosphate of titanium. Submitted to *J. Orthop, Res.* (submitted)

Schneider, G; Burridge, K. (1994). Formation of focal adhesions by osteoblasts adhering to different substrata. *Exp Cell Res* 214(1): 264-269

Schneider,G.B.; Perinpanayagam,H.; Clegg,M.; Zaharias,R.; Seabold,D.; Keller,J.; Stanford,C. (2003). Implant surface roughness affects osteoblast gene expression. *J Dent Res.* 82:372-6.

Schneider GB, Zaharias R, Seabold D, Keller J, Stanford C. (2004). Differentiation of preosteoblasts is affected by implant surface microtopographies. *J Biomed Mater Res A.* 69: 462-8

Schmalzreid, TP; Grogan, TJ; Neumeier, PA; Dorey, FJ. (1991). Metal removal in a Pediatric population: Benign procedure or necessary evil? *J Pediatr Orthop.* 11: 72-76.

Schmidt,C.; Ignatius,A.A.; Claes,L.E. (2001). Proliferation and differentiation parameters of human osteoblasts on titanium and steel surfaces. J.Biomed.Mater.Res. 54(2): 209-215.

Schmidt C, Kaspar D, Sarkar MR, Claes LE, Ignatius AA. (2002). A scanning electron microscopy study of human osteoblast morphology on five orthopedic metals. *J Biomed Mater Res.* 63(3):252-61.

Schulte, W. (1984). The intra-osseous AL_2O_3 (Frialit) Tubingen implant. Developmental status after eight years. *Quintessence Int.* 1: 9-26.

Schwartz Fo HO, Novaes AB Jr, de Castro LM, Rosa AL, de Oliveira PT. (2007). In vitro osteogenesis on a microstructured titanium surface with additional submicron-scale topography. Clin Oral Implants Res. 18(3):333-44.

Seipel, R.C; Schmeling, G.J; Daley, R. (2001). Migration of a K-wire from the distal radius to the heart. *Am J Orthop* 30: 147-151

Seligson D, Howard PA, Martin R. (1997) Difficulty in removal of certain intramedullary nails. *Clin Orthop Relat Res* 340:202-6.

Shellock, F.G & Crues, J.V. (2004).MR Procedures: Biologic effects, safety, patient care. *Radiology* 232: 635-652.

Shoamanesh A, Pang NK, Oestreicher JH. (2007). Complications of orbital implants: a review of 542 patients who have undergone orbital implantation and 275 subsequent PEG placements. *Orbit.*26(3):173-82

Signorello,L.B.; Ye,W.; Fryzek,J.P.; Lipworth,L.; Fraumeni,J.F.,Jr.; Blot,W.J.; McLaughlin,J.K.; Nyren,O.(2001). Nationwide study of cancer risk among hip replacement patients in Sweden. *J Natl Cancer Inst* 93: 1405-1410

Simanovsky N, Tair MA, Simanovsky N, Porat S. (2006) Removal of flexible titanium nails in children. *J Pediatr Orthop.* 26(2):188-92.

Simpson,D.M.; Ross,R. (1972). The neutrophilic leukocyte in wound repair a study with antineutrophil serum. *J Clin Invest.* 51:2009-2023

Sinicropi, S.M; Su, B.W; Raia, F.J; Parisien, M; Strauch, R.J; Rosenwasser, M.P. (2005). The effects of implant composition on extensor tenosynovitis in a canine distal radius fracture model. *J Hand Surg [Am].* 30: 300-307

Sisk,M.A.; Lohmann,C.H.; Cochran,D.L.; Sylvia,V.L.; Simpson,J.P.; Dean,D.D.; Boyan,B.D.; Schwartz,Z. (2001). Inhibition of cyclooxygenase by indomethacin modulates osteoblast response to titanium surface roughness in a time-dependent manner. *Clin.Oral Implants.Res.* 12(1): 52-61

Sittig,C.; Textor,M.; Spencer,N.D.; Wieland,M.; Vallotton,P.H.(1999a). Surface characterization of implant materials c.p. Ti, Ti-6Al-7Nb and Ti-6Al-4V with different pretreatments. J Mater. Sci. Mater. Med. 10: 35-46

Sittig,C.; Hahner,G.; Marti,A.; Textor,M.; Spencer,N.D.; Hauert,R.(1999b). The implant material, Ti6Al7Nb: surface microstructure, composition and properties. J Mater. Sci. Mater Med. 10: 191-198

Sommer B, Felix R, Sprecher C, Leunig M, Ganz R, Hofstetter W.(2005). Wear particles and surface topographies are modulators of osteoclastogenesis in vitro. *J Biomed Mater Res A.*72(1):67-76.

Sommer, C. (2006). Implant removal after ORIF distal tibia shaft with LC-DCP 4.5 (elsewhere). CD included as appendix A. November 12th 2006.

Steinemann SG. (1999) Compatibility of titanium in soft and hard tissue – The ultimate in osseointegration. *Proc. Euromat 99.*

Stubbs, JT; Mintz, KP; Eanes, ED; Torchia, DA; Fisher, LW. (1997). Characterisation of native and recombinant bone sialoprotein: delineation of the mineral binding and cell adhesion domains and structureal analysis of the RGD domain. *J Bone Min Res.* 12(8): 1210-1222

Summer B, Fink U, Zeller R, Rueff F, Maier S, Roider G, Thomas P. (2007). Patch test reactivity to a cobalt-chromium-molybdenum alloy and stainless steel in metal-allergic patients in correlation to the metal ion release. *Contact Dermatitis*. 57(1):35-9.

Sun C, Huang G, Christensen FB, Dalstra M, Overgaard S, Bunger C.(1999) Mechanical and histological analysis of bone-pedicle screw interface *in vivo*: titanium versus stainless steel. *Chin Med J (Engl)* 112(5):456-460

Sunny,M.C.; Sharma,C.P. (1991). Titanium-protein interaction: changes with oxide layer thickness. J. Biomater. Appl. 6: 89-98

Swiontkowski MF. (1983). Slipped capital femoral epiphysis: Complications related to internal fixation. *Orthopedics* 6: 705-712.

Taborelli,M.; Jobin,M.; Francois,P.; Vaudaux,P.; Tonetti,M.; Szmukler-Moncler,S.; Simpson,J.P.; Descouts,P. (1997). Influence of surface treatments developed for oral implants on the physical and biological properties of titanium. (I) Surface characterization. Clin. Oral Implants Res. 8: 208-216

Tepic, S & Perren, S.M. (1995). The biomechanics of the PC-Fix internal fixator. *Injury* 26: 5-10

Tepic,S; Remiger,A.R; Morikawa,K; Predieri,M; Perren,S.M. (1997). Strength recovery in fractured sheep tibia treated with a plate or an internal fixator: an experimental study with a two-year follow-up. J Orthop Trauma. 11: 14-21

Tepic, S (2008). Locking Screw Implants in Internal Fixation. Presentation: 15.06.2008 at European cells and Materials IX congress: Muscloskeletal trauma: 50 years of AO research.

Terranova,V.P.; Aumailley,M.; Sultan,L.H.; Martin,G.R.; Kleinman,H.K. (1986). Regulation of cell attachment and cell number by fibronectin and laminin. J Cell Physiol. 127:473-9

Textor, M; Sittig, C; Frauchiger, V; Tosatti, S; Brunette, D.M. (2001). Properties and biological significance of natural oxide films on titanium and its alloys In: Titanium in Medicine (Ed: Brunette, DM; Tengvall, P; Textor, M; Thomsen, P). Springer.Ch7 pp171-230

Theodossy T, Jackson O, Petrie A, Lloyd T. (2006). Risk factors contributing to symptomatic plate removal following sagittal split osteotomy. Int J Oral Maxillofac Surg. 35(7):598-601.

Thomas,K.A.; Cook,S.D. (1985). An evaluation of variables influencing implant fixation by direct bone apposition. J Biomed Mater Res. 19(8):875-901.

Tograi, A; Arai, M; Nakagawa, S; Banno, A; Aoki, M; Matsumoto, S. (1995). Alteration of bone status with ascorbic acid deficiency in ODS (Osteogenic Disorder Shionogi) rats. *Jpn J Pharmacol.* 68: 255-261.

Togrul, E; Bayram, H; Gulsen, M; Kalaci, A; Ozbarlas, S. (2005). Fractures of the femoral neck in children: long-term follow up in 62 hip fractures. *Injury* 36: 123-130

Toms AD, Morgan-Jones RL, Spencer-Jones R. (1996) Intramedullary femoral nailing: removing the nail improves subjective outcome. *J Orthop Trauma.* 10(8):560-2.

Thomsen P, Larsson C, Ericson LE, Sennerby L, Lausmaa J, Kasemo B. (1997). Structure of the interface between rabbit cortical bone and implants of gold, zirconium and titanium. *J Mater Sci Mater Med.* 8(11):653-65.

Tortora, GJ & Grabowski, SJ. (2000). Fracture and repair of bone In Principles of anatomy and physiology (9th Ed.). Chapter 6 pp172-175.Wiley & sons Inc.

Tu Q, Valverde P, Li S, Zhang J, Yang P, Chen J.(2007). Osterix overexpression in mesenchymal stem cells stimulates healing of critical-sized defects in murine calvarial bone. *Tissue Eng.* 13(10):2431-40

Tzur,I.; Goodship,A.E.; Steinman,A.; Maltz,L.; Oron,U. (1998). Enhancement of bone apposition to stainless steel cortical screws by surface modification using heat treatment: an experimental study. *J Orthop Trauma.* 12(7):504-9

Ungersbock, A; Pohler, O; Perren, SM. (1994). Evaluation of the soft tissue interface at titanium implants with different surface treatments: experimental study on rabbits. *Biomed Mat Eng.*4: 317-325

Ungersbock, A; Pohler, O.E; Perren, S.M. (1996). Evaluation of soft tissue reactions at the interface of titanium limited contact- dynamic compression plate implants with different surface treatments.: an experimental sheep study. *Biomaterials* 17: 797-806

Uhthoff,H.K & Jaworski, Z.F. (1978). Bone loss in response to long-term immobilisation. J *Bone Joint Surg.* 60: 420-429

Uhthoff,H.K; Boisvert,D; Finnegan,M. (1994). Cortical porosis under plates. Reaction to unloading or to necrosis? J Bone Joint Surg Am. 76: 1507-1512

Uhthoff,H.K; Poitras,P; Backman,D.S. (2006). Internal plate fixation of fractures: short history and recent developments. *J Orthop Sci.* 11:118-126

van Frank Haasnoot, E; Munch, T.W; Matter, P (1995). Radiological sequences of healing in internal plates and splints of different contact surface to bone. (DCP, LC-DCP and PC-Fix).*Injury* 26: 28-36

Vaudaux, P & Lew, D.P. (2006). Tolerence of staphylococci to bactericidal antibiotics. *Injury* 37: 15-19

Vaudaux, P & Lew, D.P. (2007). Tolerence of staphylococci to bactericidal antibiotics. *Folia Traumatologica Lovaniensia.* Pp 16-20

Vercaigne,S.; Wolke,J.G.; Naert,I.; Jansen,J.A. (1998a). Histomorphometrical and mechanical evaluation of titanium plasma-spray-coated implants placed in the cortical bone of goats. *J.Biomed.Mater.Res* 41(1): 41-48

Vercaigne,S.; Wolke,J.G.; Naert,I.; Jansen,J.A. (1998b). The effect of titanium plasma-sprayed implants on trabecular bone healing in the goat. *Biomaterials* 19(11-12): 1093-1099

Vierhout BP, Sleeboom C, Aronson DC, Van Walsum AD, Zijp G, Heij HA. (2006). Long-term outcome of elastic stable intramedullary fixation (ESIF) of femoral fractures in children. *Eur J Pediatr Surg.* 16(6):432-7.

Vinall, RL;Gasser, B, Richards, RG. (1995). Investigation of cell compatibility of titanium test surfaces to fibroblasts. Injury. 26: Suppl 1: 21-27

Vörös, J; Wieland, M; Ruiz-Taylor, L; Textor, M; Brunette, DM. Characterisation of Titanium Surfaces. In: Titanium in Medicine (Ed. Brunette, DM; Tenggvall, P; Textor, M; Thomson, P). Springer 2001 Ch.5: pp87-144.

Wagner, M. (2003). General principles for the clinical use of the LCP. *Injury* 34: 31-42

Walboomers XF, Croes HJ, Ginsel LA, Jansen JA.(1998). Growth behavior of fibroblasts on microgrooved polystyrene. *Biomaterials.* 19(20):1861-8.

Walivaara,B.; Aronsson,B.O.; Rodahl,M.; Lausmaa,J.; Tengvall,P. (1994). Titanium with different oxides: in vitro studies of protein adsorption and contact activation. Biomaterials 15: 827-834

Wang L, Zhao G, Olivares-Navarrete R, Bell BF, Wieland M, Cochran DL, Schwartz Z, Boyan BD. (2006). Integrin beta1 silencing in osteoblasts alters substrate-dependent responses to 1,25-dihydroxy vitamin D3. Biomaterials. 27(20):3716-25

Weinrauch PC & Blakemore M. (2007). Extraction of intramedullary nails by proximal stacked wire technique. *J Orthop Trauma.* 21:663-664.

Welton, JL. (2007).Masters thesis: In vivo evaluation of defined polished surfaces to prevent soft tissue adhesion. AO Research Institute, Davos, CH.

Wennerberg A, Albrektsson T, Johansson C, Andersson B. (1996). Experimental study of turned and grit-blasted screw-shaped implants with special emphasis on effects of blasting material and surface topography. *Biomaterials* 17(1):15-22

Wennerberg A, Ektessabi A, Albrektsson T, Johansson C, Andersson B. (1997). A 1-year follow-up of implants of differing surface roughness placed in rabbit bone. Int J Oral Maxillofac Implants. 12(4):486-94.

Whyte MP. (1994). Hypophosphatasia and the role of alkaline phosphatase in skeletal mineralization. *Endocr Rev.* 15(4):439-61.

Wieland M (1999). Experimental determination and quantitative evaluation of the surface composition and topography of medical implant surfaces and their influence on osteoblastic cell surface interactions. PhD Thesis 13247, ETH, Zurich, CH.

Wieland M, Textor M, Chehroudi B, Brunette DM.(2005). Synergistic interaction of topographic features in the production of bone-like nodules on Ti surfaces by rat osteoblasts. *Biomaterials.* 26(10):1119-30

Wilson, CMG. (1999). In vitro biocompatibility evaluation and morphological description of fretting wear debris from orthopaedic implant materials. PhD thesis: Institute of biological sciences, University of Wales, Aberystwyth (UK).

Wilson, J.W. (2002). Blood supply to developing, mature and healing bone. In: Bone in clinical orthopaedics 2nd Edition (Ed: Summer-Smith, G.). Thieme NY. Ch: 2 pp 23-105

Woodruff MJ, Hanson JR, Shaw DL. (2003) Intramedullary tibial nails: a novel approach to removal when the standard method is not possible. *Injury* 34:789-90.

Wyant, JC & Schmit, J. (1997). Large Field of view, high spatial resolution surface measurements. In Proc. Of the 7th Int Conference on metrology and properties of engineering surfaces pp 294-301. Chalmers University of Technology, Göteborg, Sweden. Taken from Veeco Intruments library (www.vecco.com/library/appnotes{accessed 17/10/2006}).

Xiao, G; Wang, D; Benson, D; Karesenty, G; Franceschi, RT. (1998). The role of the α2-integrin in osteoblast specific gene expression and activation of the Osf2 transcription factor. The J Biol Chem 273(49): 32988-32994

Yang Y, Cavin R, Ong JL (2003). Protein adsorption on titanium surfaces and their effect on osteoblast attachment. J Biomed Mater Res A.67:344-9

Zardiakas, L.D; Mitchell, D.W; Disegi, J.A (1996). Characterisation of ti-15Mo beta titanium alloy for orthopaedic implant applications. In: medical applications of titanium and its alloys: The material and biological issues. (Eds. Brown, S.A, Lemons, J.E). pp60-75

Zenios M, Malik MHA, Al-Mesri, AR, Vhadra R, Khan SA.(2004) Current intramedullary nail insertion and removal practice in the UK. *Eur J Orthop Surg Traumatol.* 14: 19-22.

Zhao, QH; Anderson, JM; Hiltner, A; Loden, GA; Payet, CR. (1992). Theoroetical analysis on cell size distribution and kinetics of foreign body giant cell formation in vivo on polyurethane elastomers. *J Biomed Mater Res* 26: 1019-1038

Zinger O, Zhao G, Schwartz Z, Simpson J, Wieland M, Landolt D, Boyan B. (2005). Differential regulation of osteoblasts by substrate microstructural features. Biomaterials. 6(14):1837-4

Appendix B – X-ray photoelectron spectroscopy

The typical XPS survey for control and experimental samples. For cpTi, TAN and Ti15Mo samples, Ti and O are dominant as expected, with the additional presence of aluminium and niobium on TAN samples. On all surfaces, contamination is found in the form of Nitrogen, Sodium and Phosphor with the additional presence of Ca on all Ti15Mo and standard micro-rough TAN samples. Survey results for stainless steel show the diversity of the alloy where Nickel, Iron, Chromium, Oxygen and Molybdenum are evident.

Commercially pure titanium

(i) Standard micro-rough

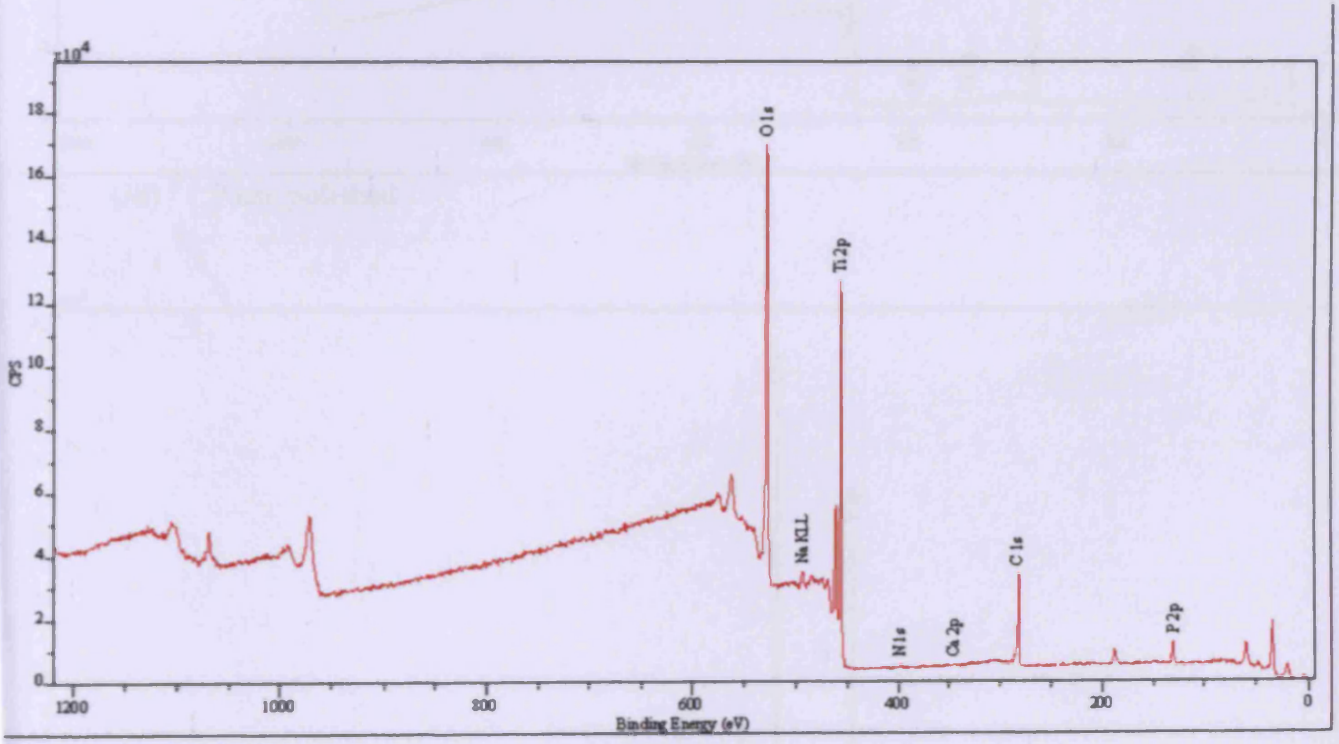

(ii) Electropolished

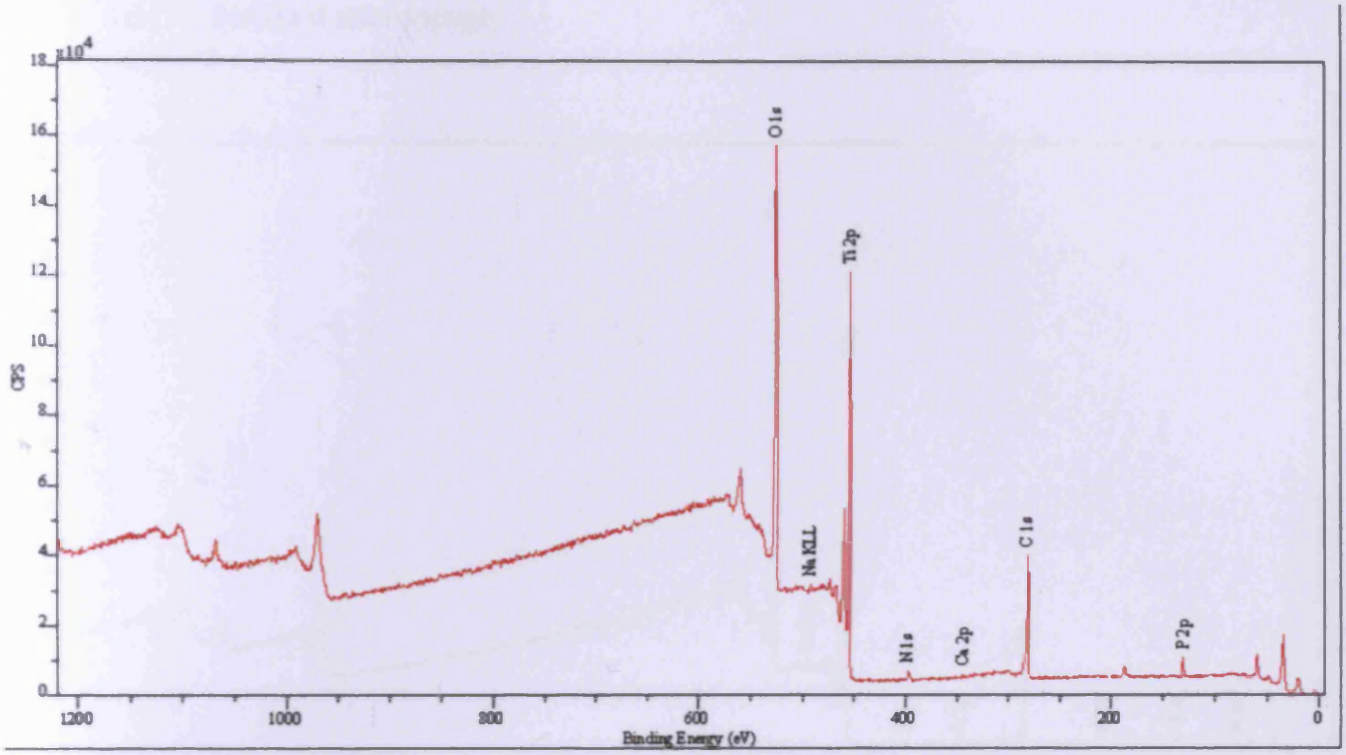

(iii) Paste polished

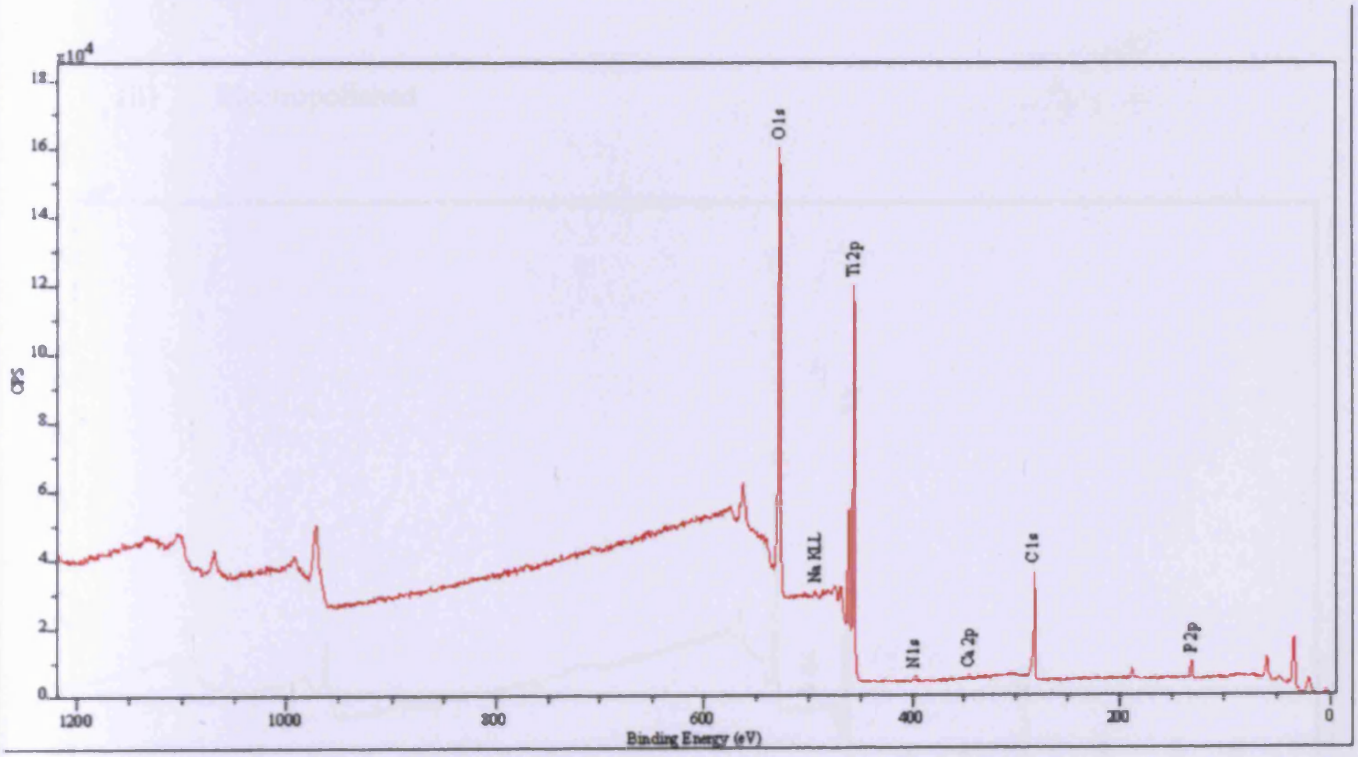

Titanium-6%Aluminum-7%Niobium

(i) Standard micro-rough

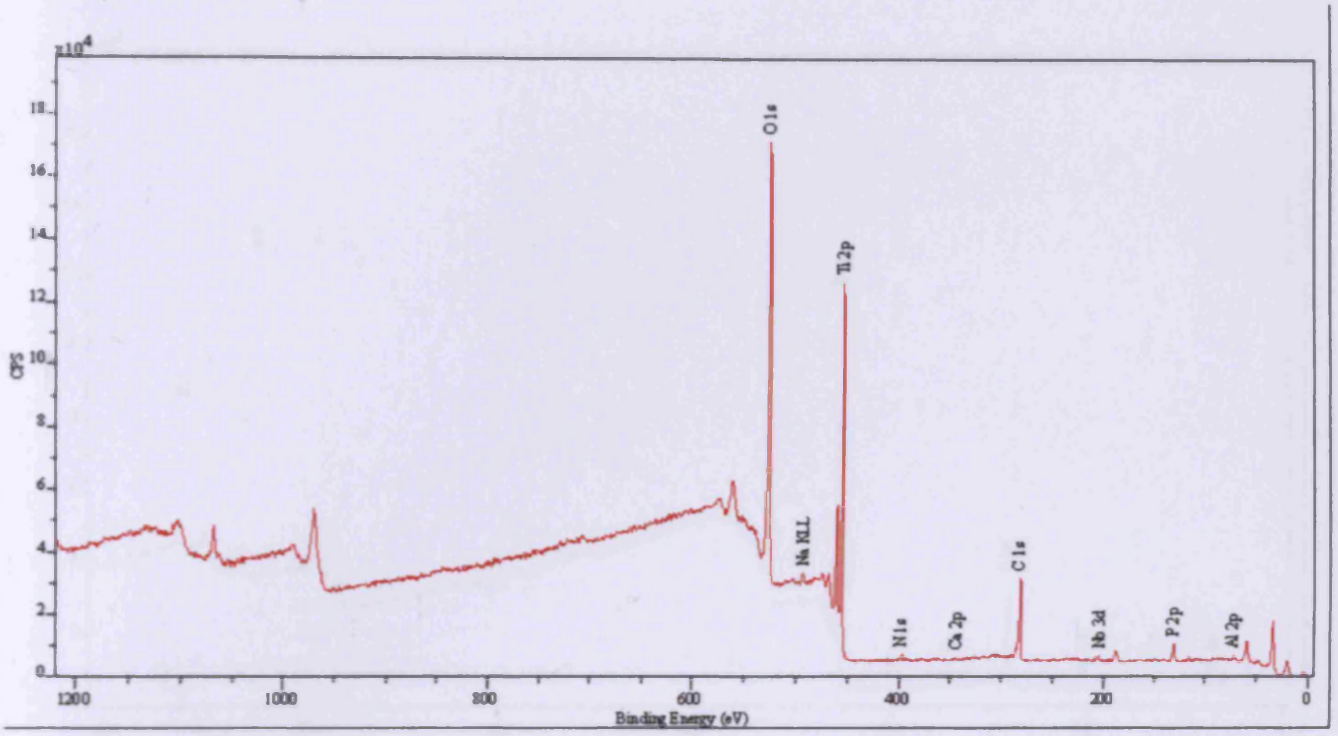

(ii) Electropolished

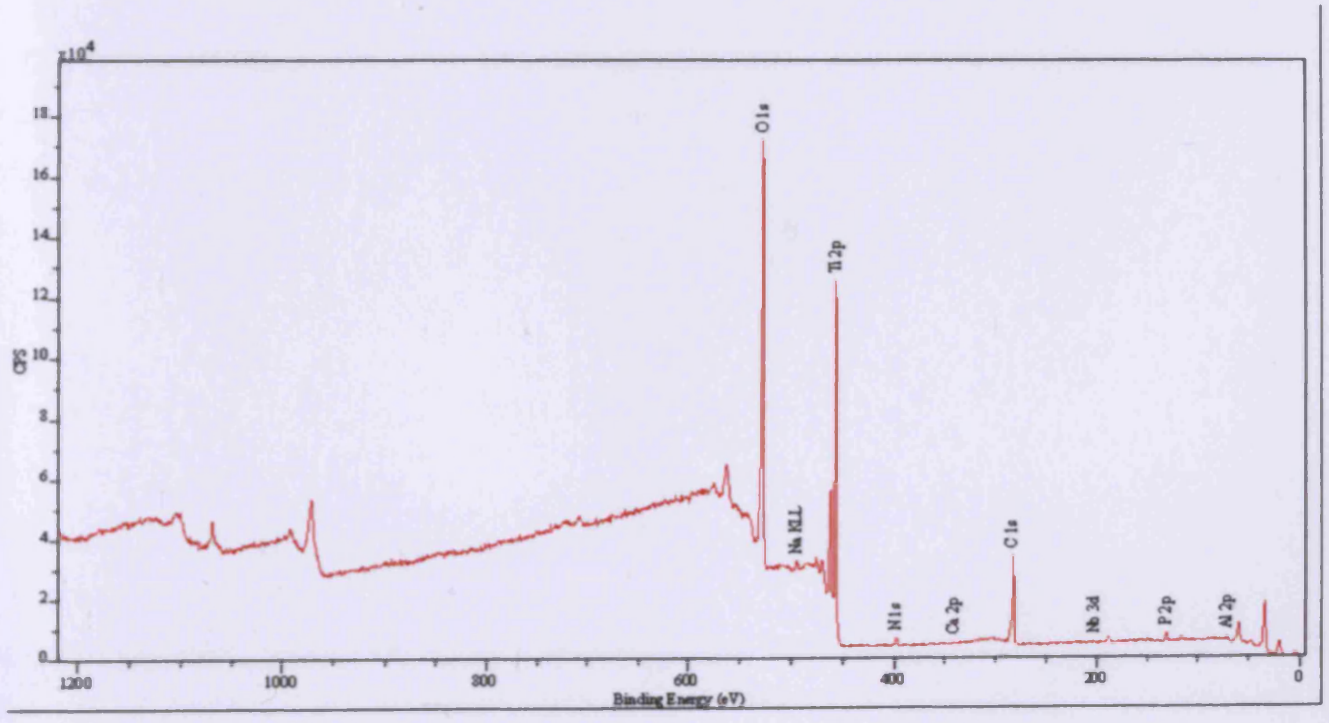

(iii) Paste polished

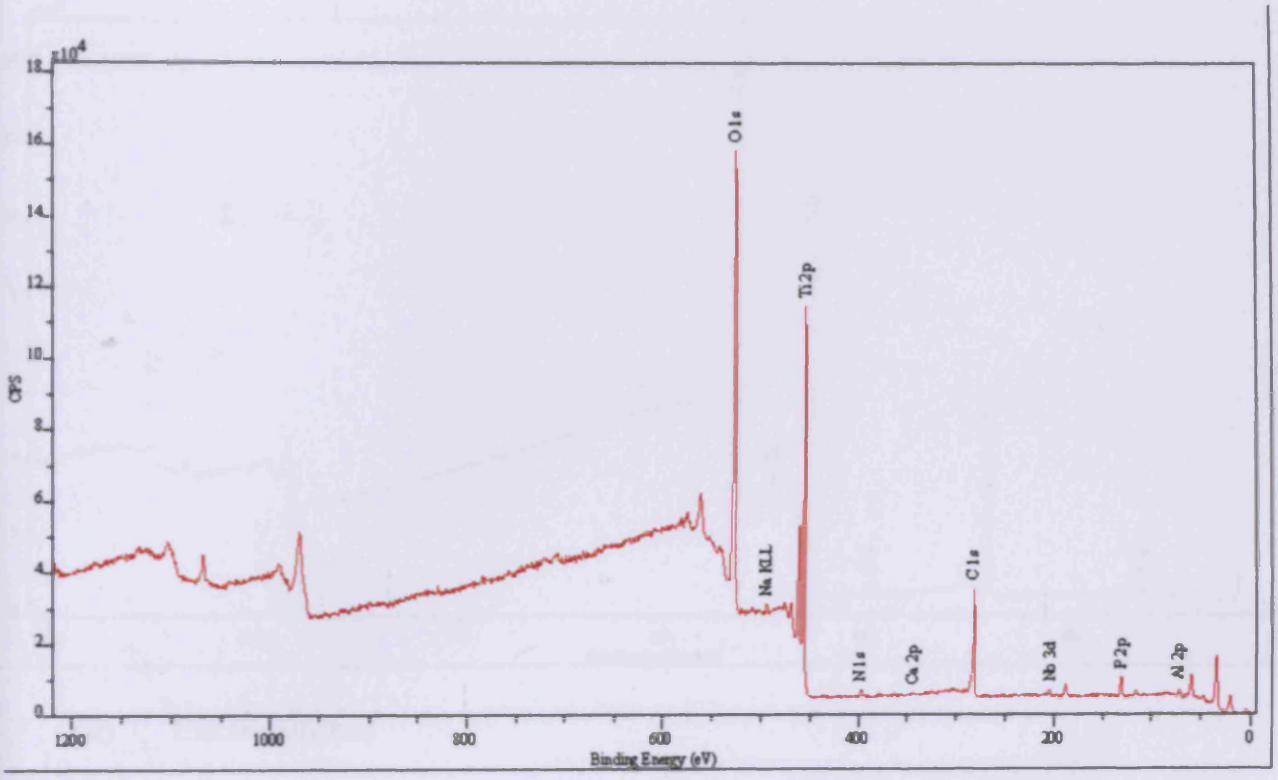

Titanium-15%Molybdenum

(i) Standard micro-rough

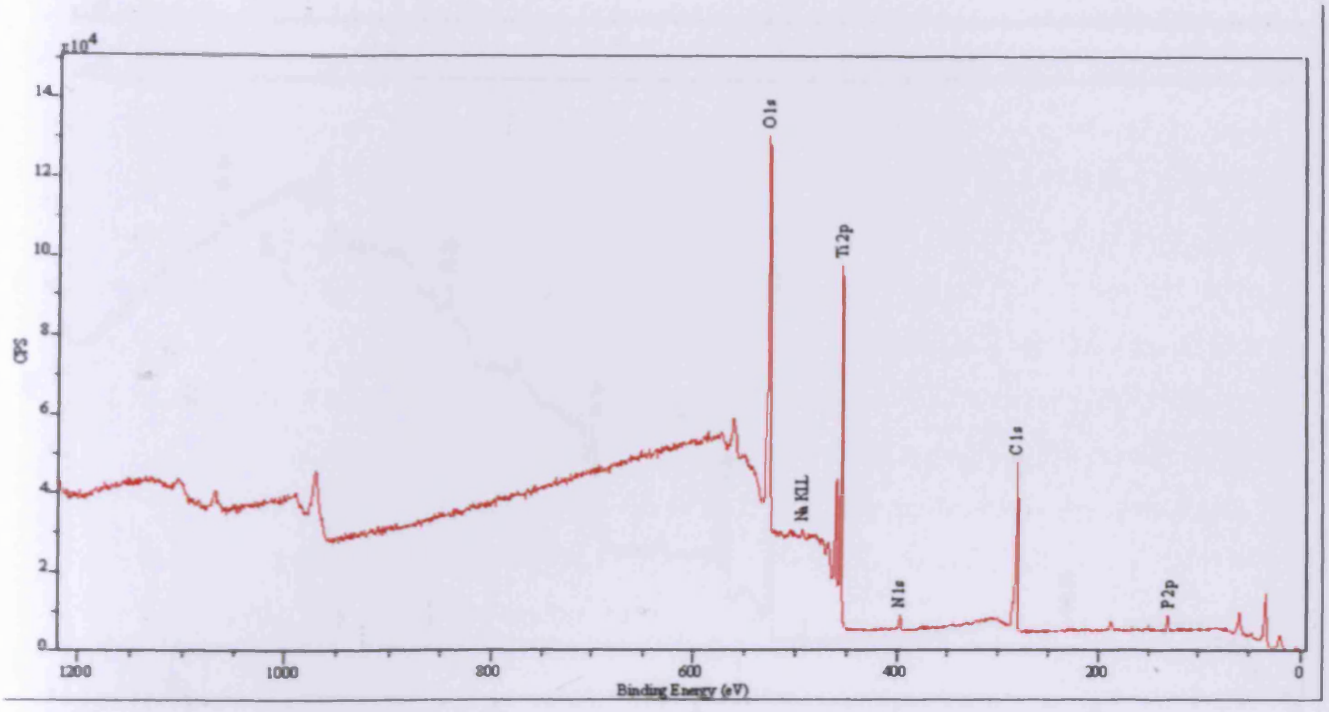

(ii) Electropolished

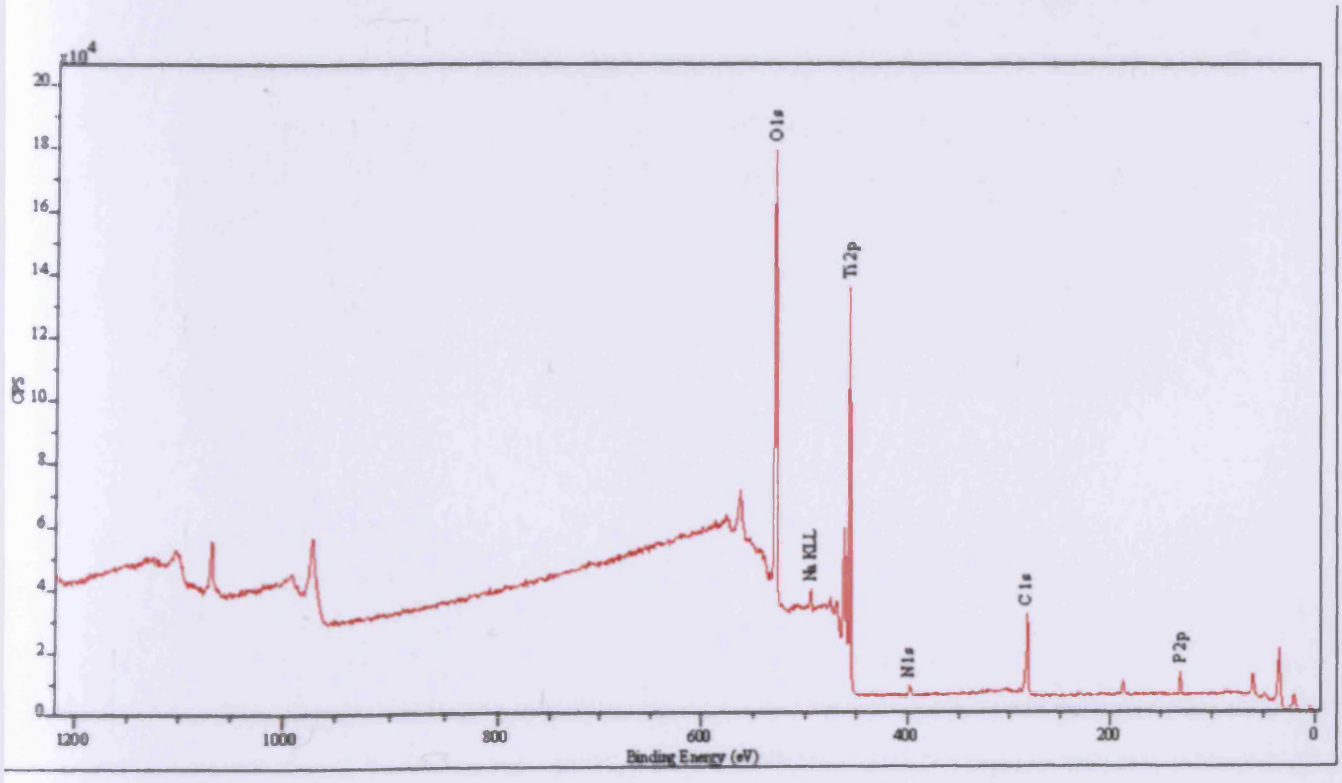

(iii) Paste polished

Stainless Steel

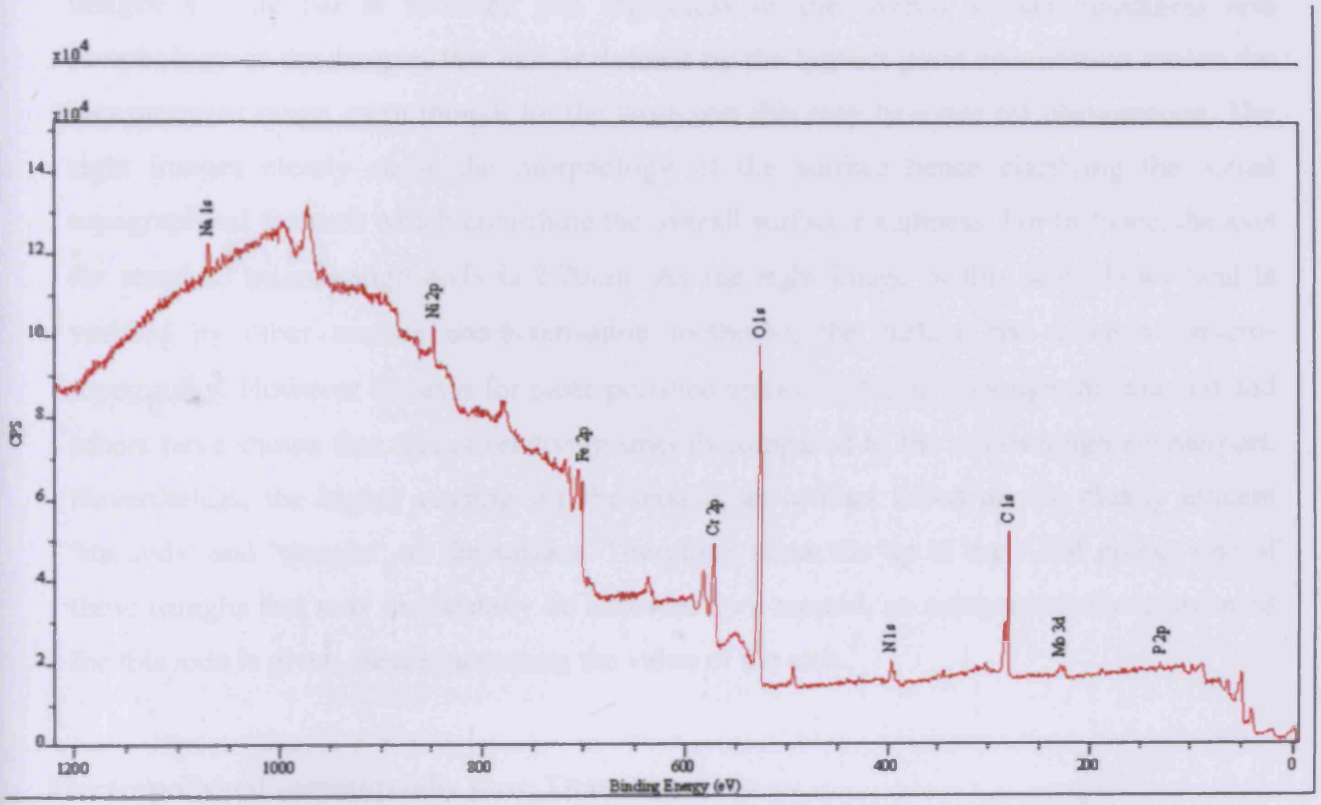

Appendix C – Atomic Force Microscopy

Two-Dimensional AFM imaging of control and experimental surfaces. Note that for the left images a scale bar is included and regardless of the overall surface roughness and morphology of the sample, this axis is defined by the highest point encountered within the measurement range, even though for the large part this may be a one off phenomenon. The right images clearly show the morphology of the surface hence clarifying the actual topographical features which contribute the overall surface roughness. For instance, the axis for standard micro-rough cpTi is 2.70μm. As the right image of this scan shows (and is verified by other surface characterisation methods), the surface has extensive micro-topography. However the axis for paste polished cpTi is 2.25μm, although this method and others have shown that this is relatively smooth compared to the micro-rough counterpart. Nevertheless, the higher reading for the axis is an artifact based on the clearly evident 'mounds' and 'troughs' on the surface. Therefore, when the tip of the AFM probes one of these troughs that may incidentally be followed by a mound, an unrepresentative roughness for this axis is given, hence increasing the value of the axis.

Electropolished commercially pure Titanium,

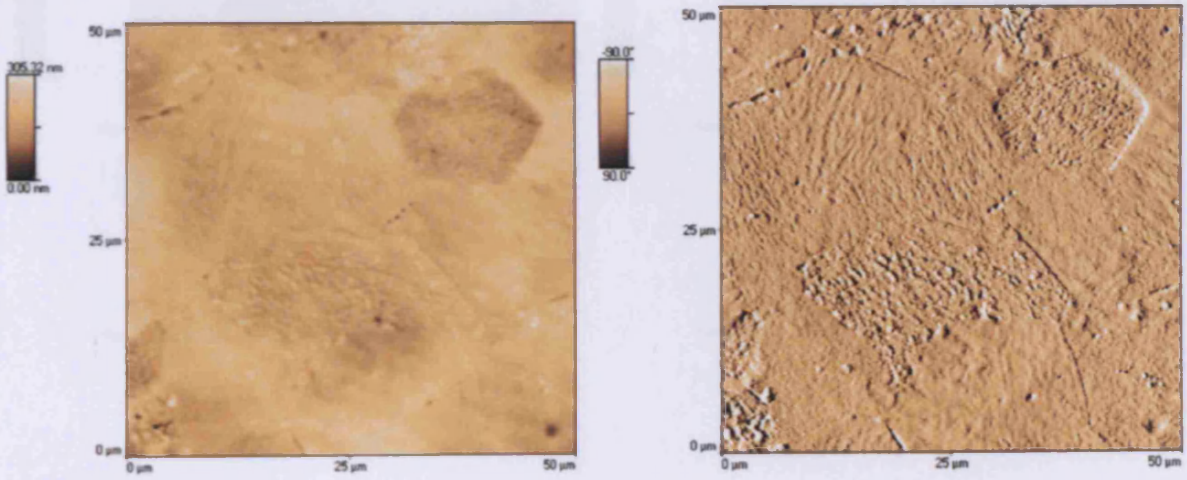

Paste polished commercially pure Titanium

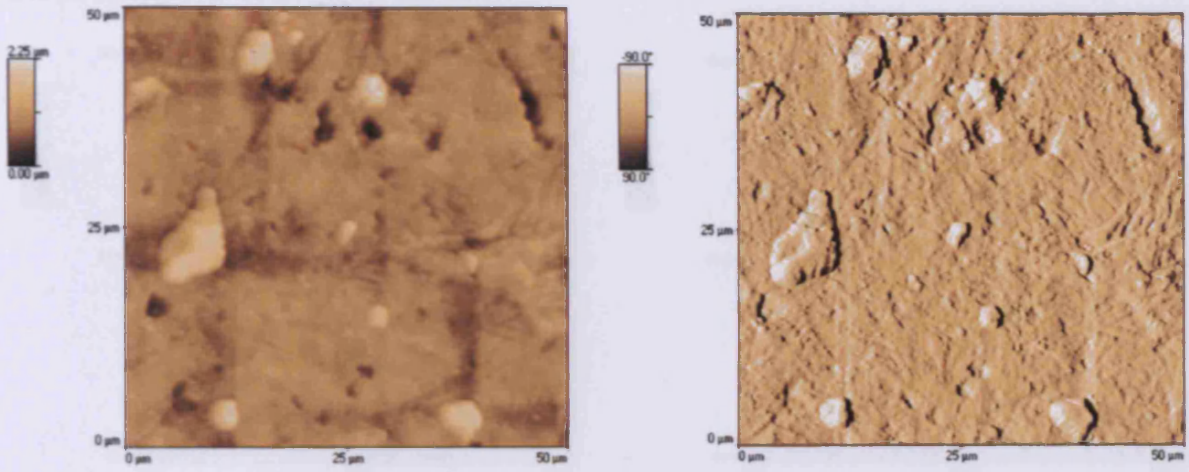

Standard Micro-rough commercially pure Titanium

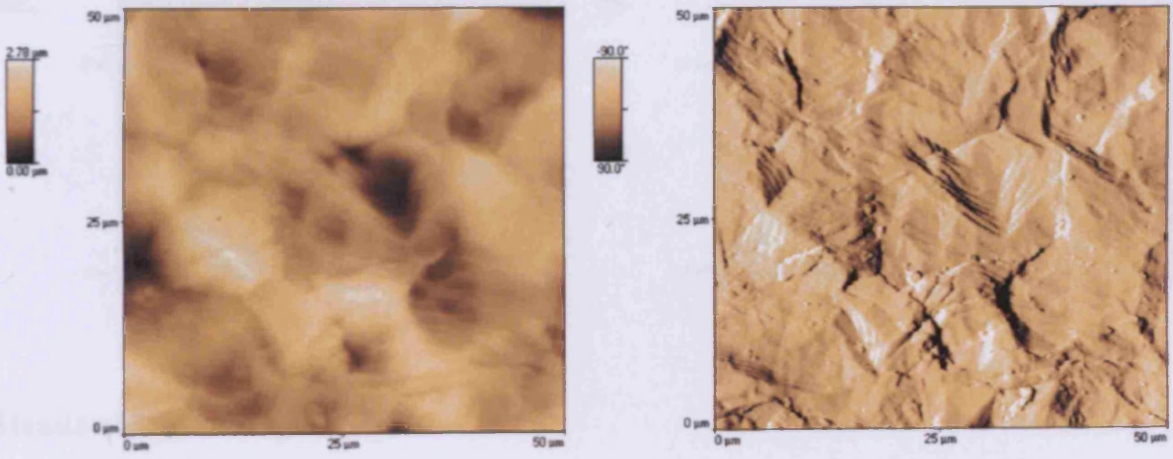

Electropolished TAN

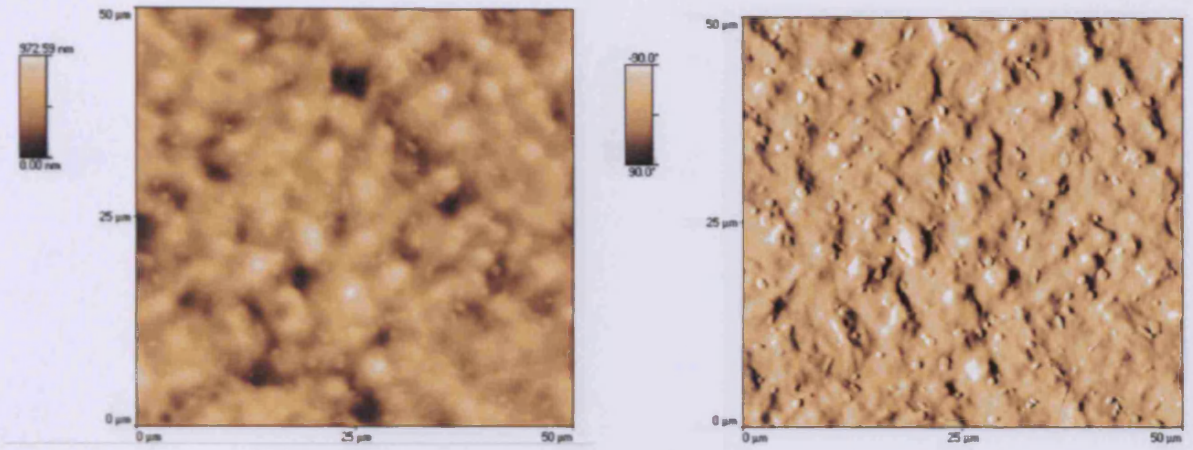

Paste Polished TAN

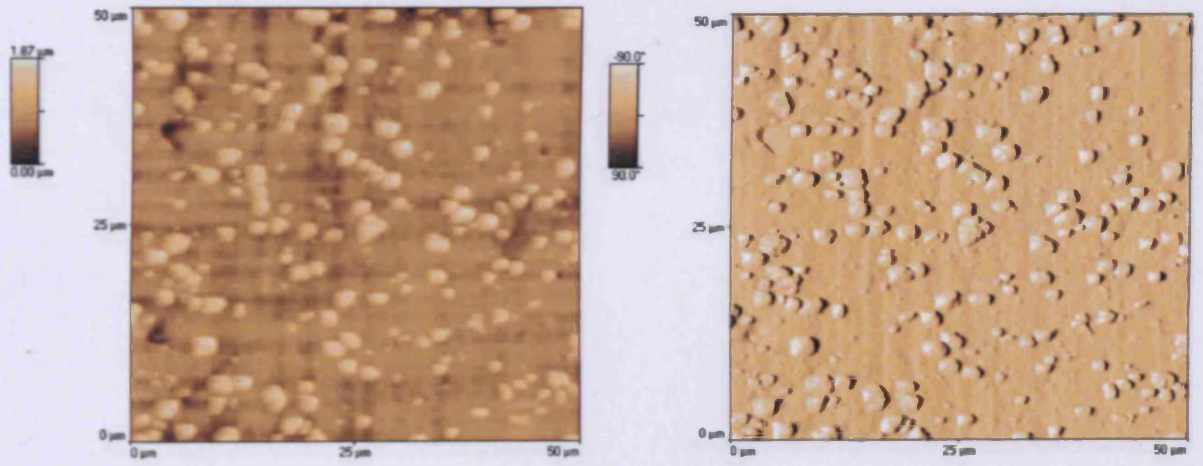

Standard Micro-rough TAN

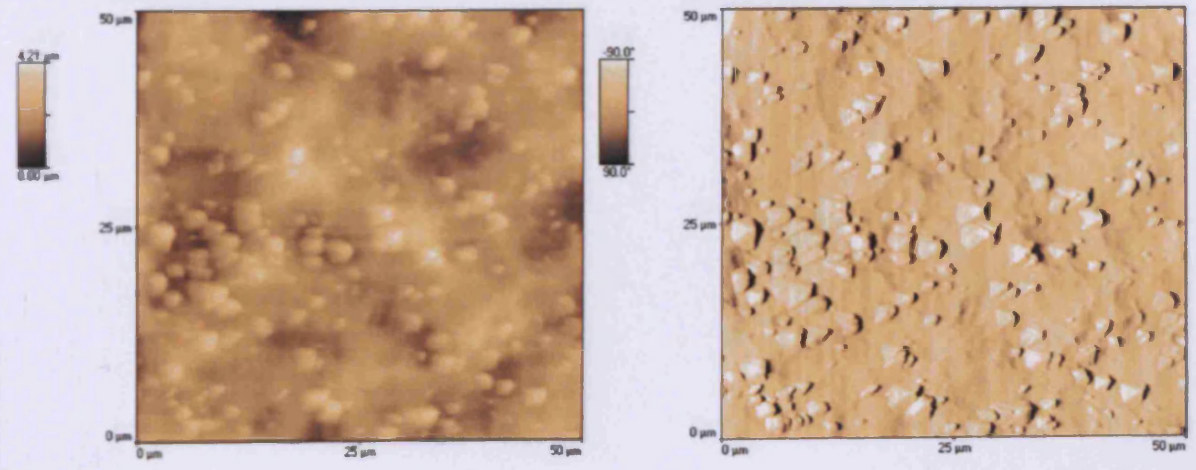

Electropolished Titanium Molybdenum

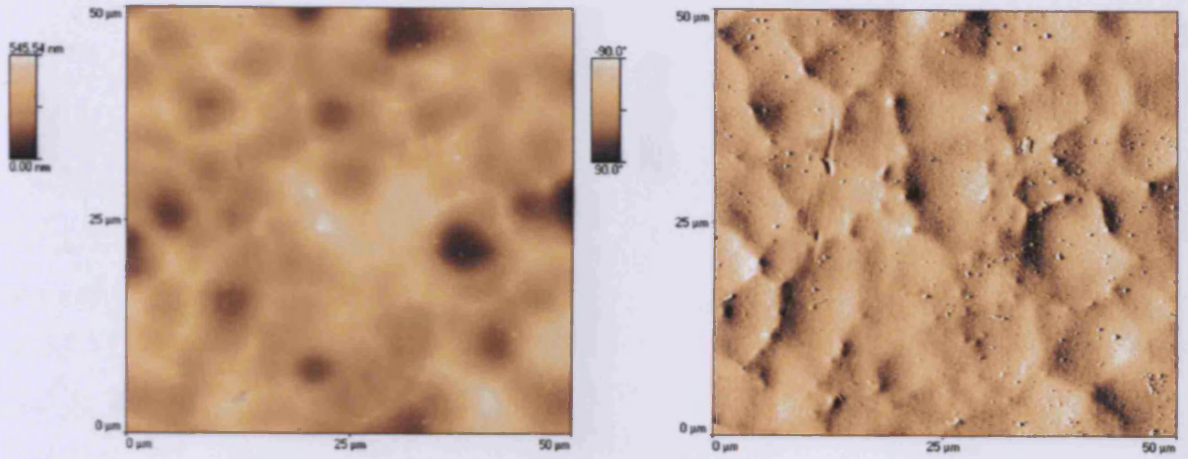

Paste polished Titanium Molybdenum

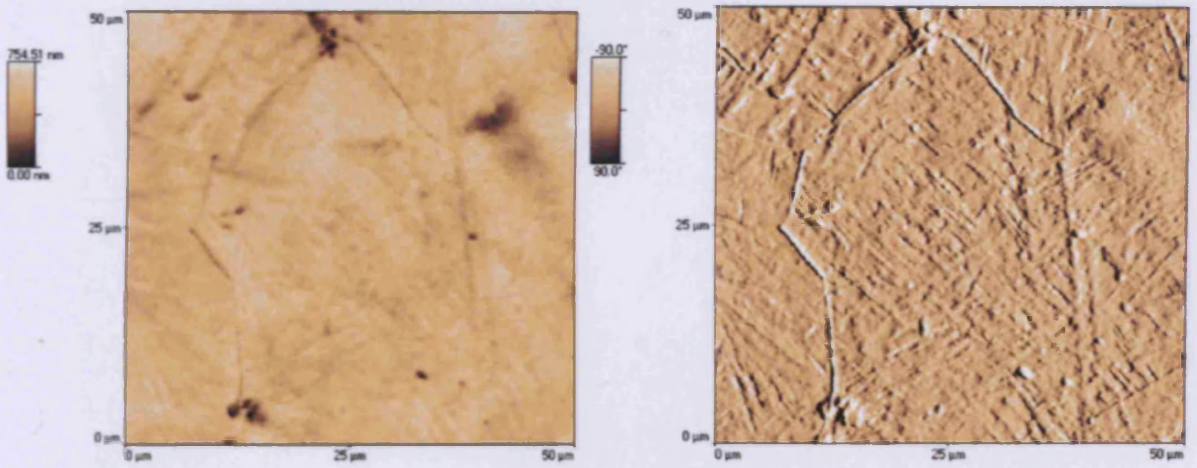

Standard micro-rough Titanium Molybdenum

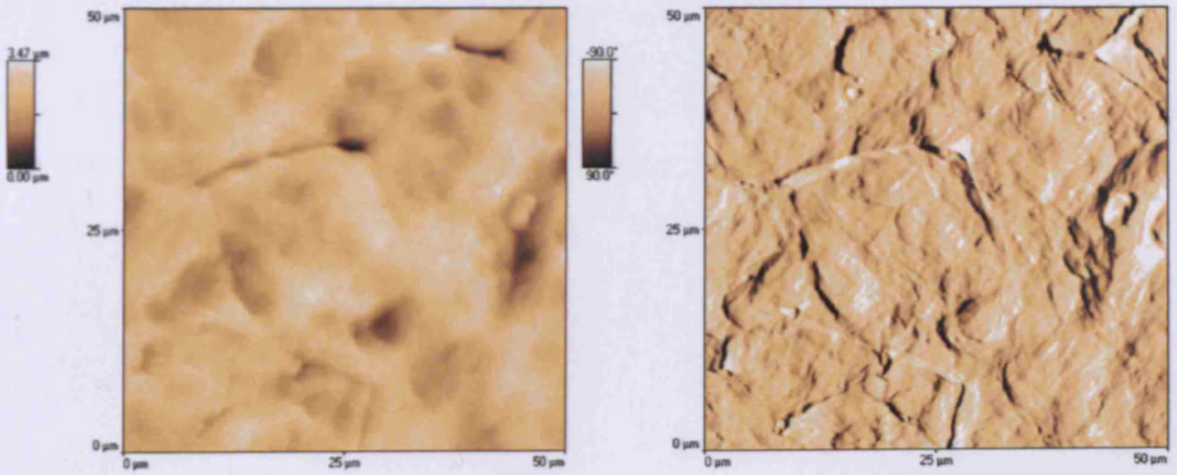

Stainless steel

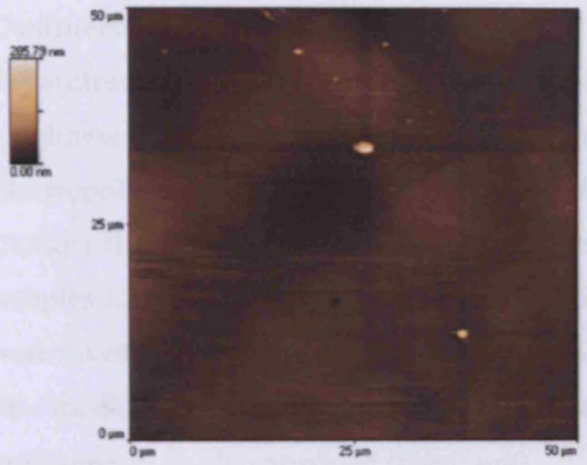

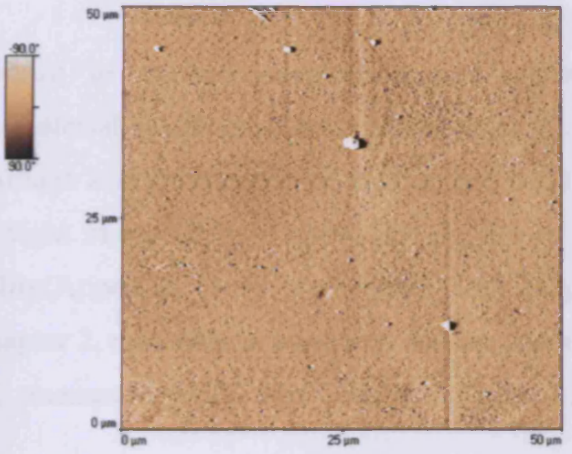

Appendix D: Variability of the 13mm samples used for surface characterisation

Commercially pure titanium:

Regardless of surface finish, results pertaining to surface morphology and average roughness were generally reproducible for this material. (A,B) Standard micro-rough; (C,D) Electropolished; (E,F) Paste polished. The left image is representative of the original samples (A,C,E) first supplied for the study, while the right image (B,D,F) shows the second set of samples to demonstrate the inter-batch variability(Appendix G for more detail). All images were taken under the same SEM conditions (Chapter 2, materials & methods) and are taken in SE mode. The average surface roughness, measured with non contact white light profilometry, is also provided (inset; μm).

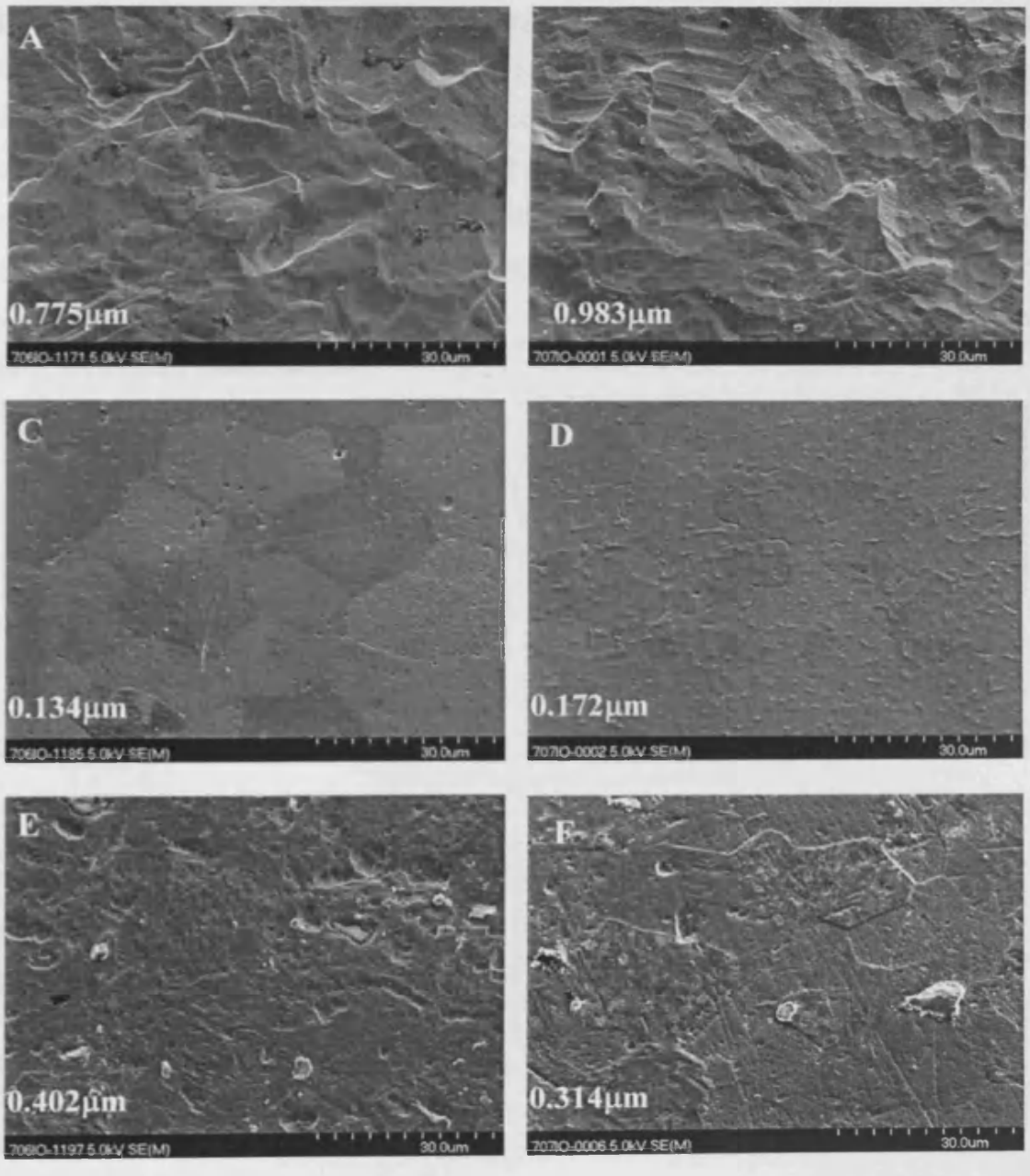

Titanium-6%Aluminium-7%Niobium:

Problems with surface finish reproducibility were experienced with TAN, most likely as a result of efforts to standardise the procedures by the vendors. Upon receipt of new samples, regardless of material or surface preparation, all samples were privy to random profilometry (3 samples were chosen randomly and 2 areas on each of the samples were analysed for average roughness and an overall average taken, conditions in chapter 2 materials and methods) and SEM analysis. It is clear from the images below, while the original standard micro-rough TAN produces the well characterised 'micro-spiked' surface, the new samples (H) are clearly not of similar morphology. In contrast, electropolishing of TAN produced consistent results from the original samples (J), producing a slight decrease in average roughness as desired upon receipt of new samples (K), as standardisation of the samples appeared more readily achievable. Once again, problems were encountered with paste polished samples. Compared to the original samples (L) new samples had a higher average roughness and a distinctly rougher surface morphology (M).When sent back for re-processing, the surfaces were returned to their original form (I,N). Nevertheless, despite quality control measures, it is reasonable to believe that not all samples included in studies were of similar topography. This would therefore, directly influence the reproducibility of any results obtained and possibly mask the true affect of the surface as 'rogue' surfaces would hinder data interpretation.

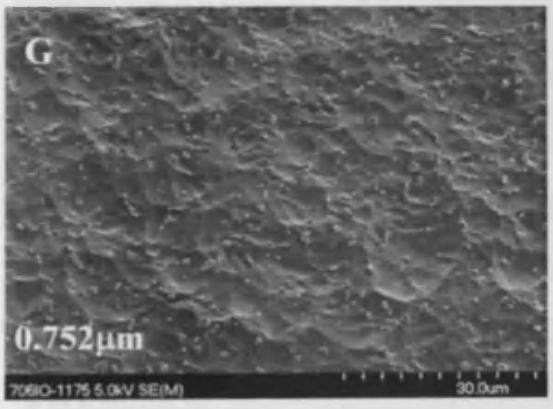

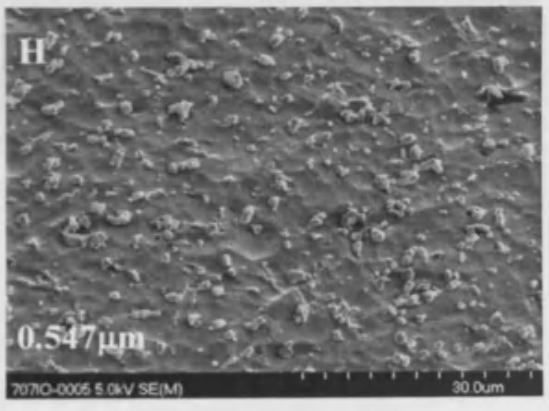

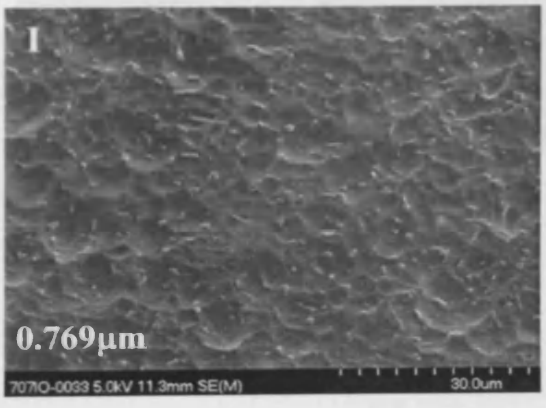

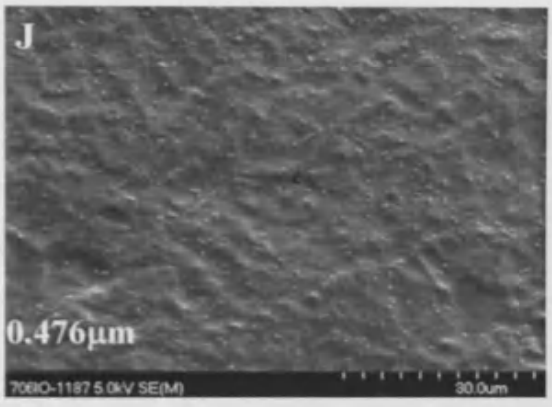
J
0.476μm
7069O-1187 5.0kV SE(M)
30.0um

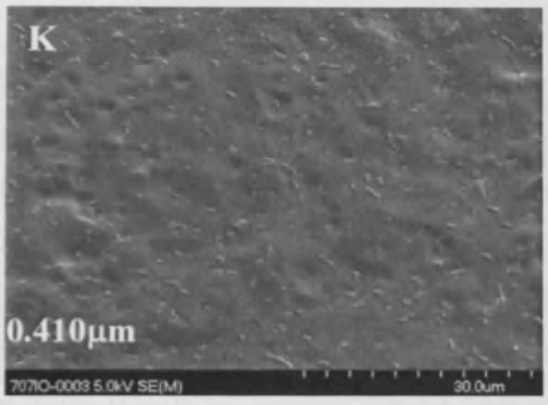
K
0.410μm
7071O-0003 5.0kV SE(M)
30.0um

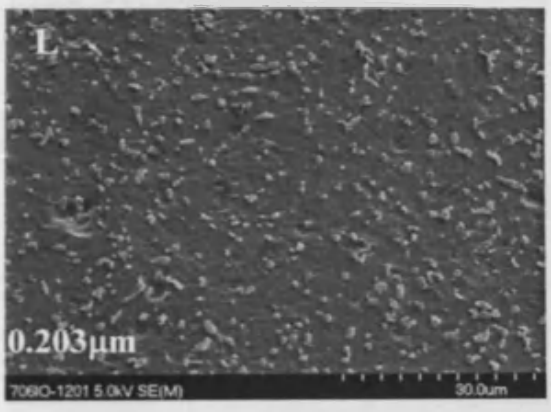
L
0.203μm
7069O-1201 5.0kV SE(M)
30.0um

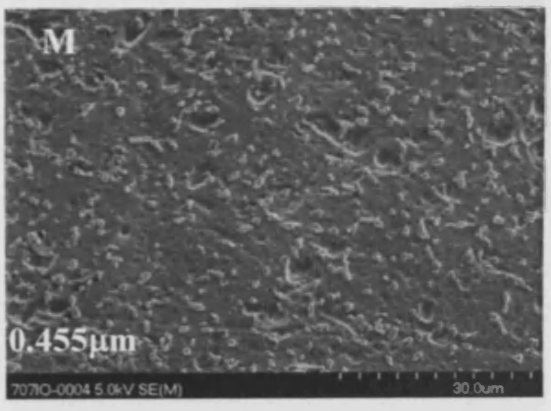
M
0.455μm
7071O-0004 5.0kV SE(M)
30.0um

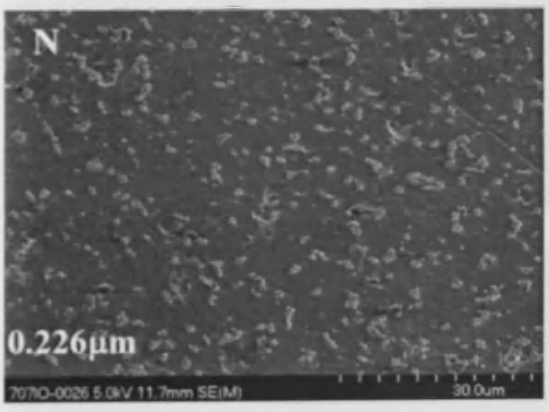
N
0.226μm
7071O-0026 5.0kV 11.7mm SE(M)
30.0um

Titanium-15%Molybdenum

Reproducibility of Ti15Mo samples generally appeared consistent. Some distinction in surface morphology can be distinguished be.ween the original standard micro-rough samples (O) and the newly received ones (P) however the main characteristics of the surface remain similar (grain size, waviness), hence re-processing was not undertaken. Compared to the original electropolished sample (Q), the recently received sample appears much smoother and cleaner (R). Since this was the aim of the technique these samples were retained. As with the standard samples, the differences between the original paste polished samples (S) and the more recent addition (T) were not deemed to require re-processing. However, clearly the basket weave appearance noted for earlier samples (i.e. O, S) seems to be removed in later samples (i.e P, T), suggesting the final processing had changed.

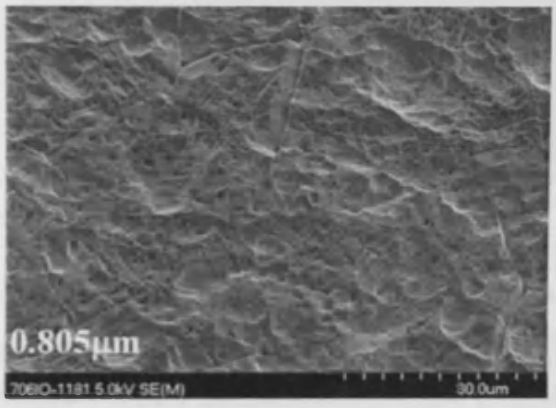

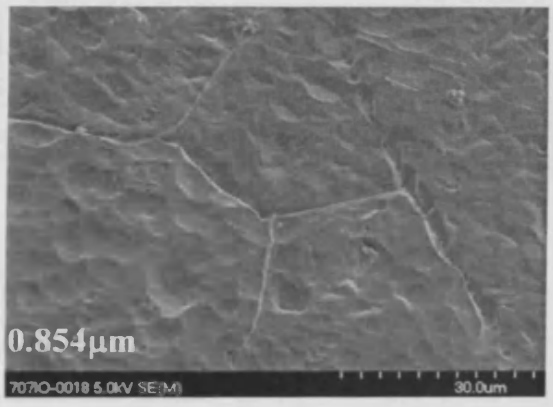

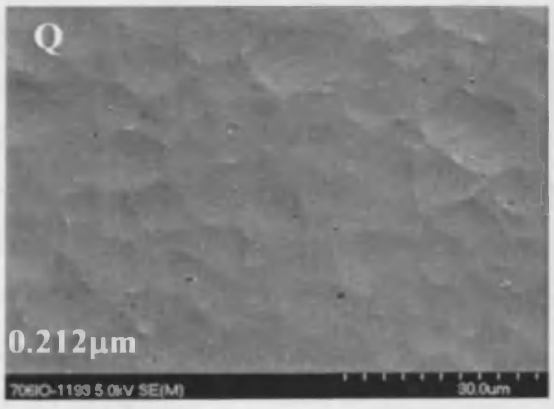

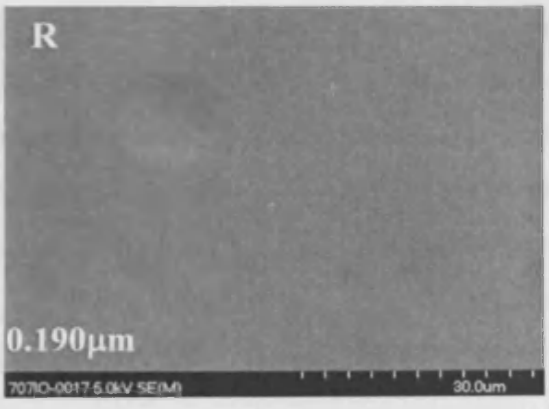

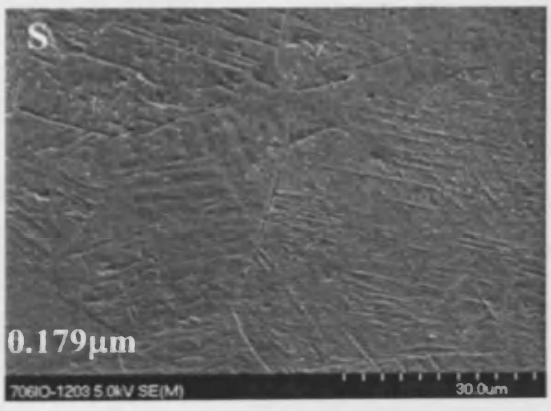

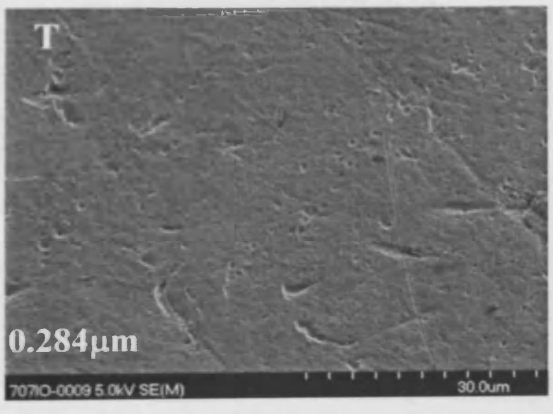

Stainless steel:
Original samples of stainless steel (U) were extremely smooth and continued to be received in this manner until the last batch of samples. As is elucidated below, the new samples are significantly rougher (V) than original samples, and therefore were excluded from the study. Sufficient numbers of stainless steel were available so re-processing was not deemed necessary.

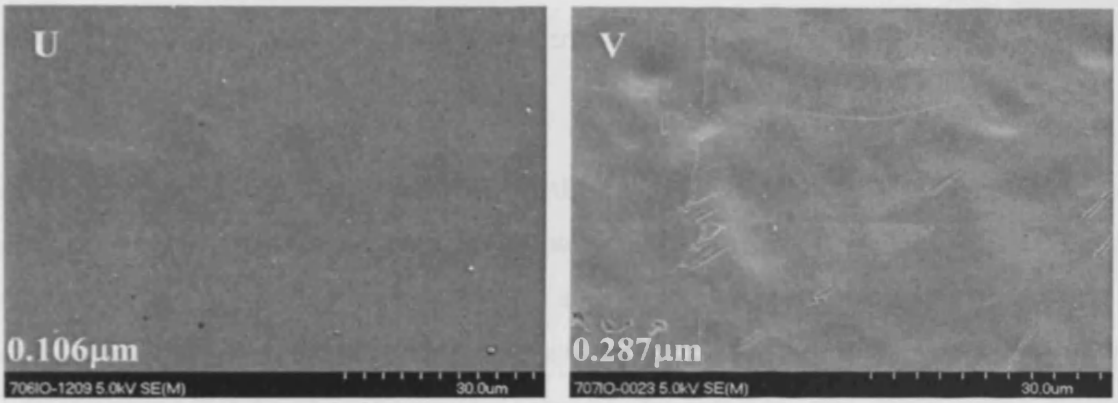

As previously discussed, the matter of surface characterisation is a contentious one since the majority of studies fail to comprehend, or perhaps blatantly ignore, the limitations of surface characterisation methods. One method alone does not suffice in any instance to provide the necessary information regarding the distinctions in surface profile hence several are essential to provide an eclectic, but not definitive overview. With this in mind, a cautious approach should be adopted when one is asked to accept results involving surfaces be it metal, polymer of surface modified. Furthermore, as is clear from the samples provided here, a continuous process of quality control is essential to any study investigating surface control changes for biological application, as well as providing a key insight for data interpretation. This issue is re-visited in Appendix G which covers sample variability for the whole study.

Appendix E – Rat calvaria isolation and subculture

For proliferating cultures, rat calvaria or rat calvarial cells were cultured in Dulbeccos modified eagles medium (DMEM) supplemented with 10% foetal calf serum (FCS; Gibco), 50μg/ml of ascorbic acid (Sigma), penicillin-streptomycin (Gibco), and fungizone (Gibco).

For experimental cultures, such as those in chapter 3, and 4, samples with cells were cultured in the above media supplemented addiotnally with 5mM beta-glycerophosphate and 10nM dexamethasone. This media is referred to DMEM+5mMBGP.

(i) Enzymatic Isolation

Six day old Swiss Wister rats were used for the *in vitro* portion of this study. Subsequent to euthanasia, neonatal rats were transferred into a large container containing Betadine for 5 minutes. The rats were then transferred into a new container and washed 4 times with 70% ethanol (Fluka, Gmbh). Subsequent to washing, neonatal rats were placed in 100mm petri-dishes (Corning, USA). To expose the calvaria, an incision was made using a surgical scissors at the nape of the neck and was continued over the ear, and ended over the orbit. With a sterile forceps and scissors (different to that used for removal of the skin), the frontal and parietal calvarial were removed, taking due care not to disturb the underlying tissue and blood vessels to avoid subsequent contamination. Calvarial were placed in Tyrode buffered salt solution (TBSS)*, pH7.4, until isolation was complete for all rats. For enzymatic digestion, 0.5mg/ml of trypsin (Gibco) and 300U/ml of collagenase type I (Worthington, USA) were dissolved in TBSS, and the mixture was subsequently filtered. In an attempt to exclude any debris from the calvaria, the TBSS solution was aspirated from the calvaria (being careful not to touch the calvaria), and new, sterile TBSS was added. This process was repeated 3 times. Samples were ultimately transferred to a magnetic stirring bottle. The pre-digestion mix of trypsin and collagenase was added, and subsequently were incubated for 70 minutes at 37°C, 5% CO_2, with continuous stirring. Then, DMEM media containing FCS was added to stop the enzymatic reaction. The supernatant was removed, taking care not to disturb the calvaria, and a second digestion was carried out, with TBSS containing 300U/ml of collagenase I. Samples were once again incubated at 37°C, 5% CO_2, for 2 hours. Next, DMEM containing FCS was added to stop the enzymatic reaction, after which, the supernatant was removed, and the nude calvarial were washed 3 times with TBSS. After this, the nude calvaria were transferred to 60x15mm petri-dishes (Corning, USA) containing

4ml of DMEM media containing 25μg/ml of ascorbic acid (Sigma, UK), 10% FCS (Gibco), 1% penicillin-streptomycin (full media). Media was changed every 2 days.

(ii) Subculture Part I

Once cultures containing calvaria were observed to be sub-confluent, the following procedure was followed. Enyzmatic digestion was carried out using 0.5mg/ml of trypsin and 300U/ml of collagenase type I which was dissolved in serum-free DMEM. Cultures were incubated for approximately 1 hour at 37°C, 5% CO_2. DMEM media containing FCS was added to each petri-dish to stop the digestion. If the denuded calvaria were still required, they were removed from the dish, washed with TBSS and, with a sterile forceps, were transferred to a new, sterile 60x15mm petri-dish containing full media. The remaining cell suspension was pipetted into a 50ml falcon tube and centrifuged. Subsequently, the supernatant was removed and the cells were re-suspended in full media, counted using a haemocytometer and seeded into cell culture flasks at the desired densities. Media was changed every 2 days. At each isolation, at 2,7,14 and 21 days, a representative sample dish was taken and stained for alkaline phosphatase (Sigma, UK) and Alizarin Red-S (Chemicon, USA) to test for phenotype.

(iii) Subculture Part II

When cells grown in cell culture flasks were observed to be confluent cells were rinsed 3 times with 0.1M phosphate buffered saline (PBS) solution, and enzymatic digestion was carried out using 1 x trypsin-EDTA (Gibco) suspended in PBS. Flasks were incubated for approximately 5 minutes at 37°C, 5% CO_2. Once the cells had visibly detached, full media was added to stop the reaction. Cell suspensions were transferred to either a 15ml or 50ml Falcon tube, and centrifuged. Next, the supernatant was removed, and the cells were re-suspended in full media. Cells were counted using a haemocytometer, and either re-seeded at a desired density or frozen.

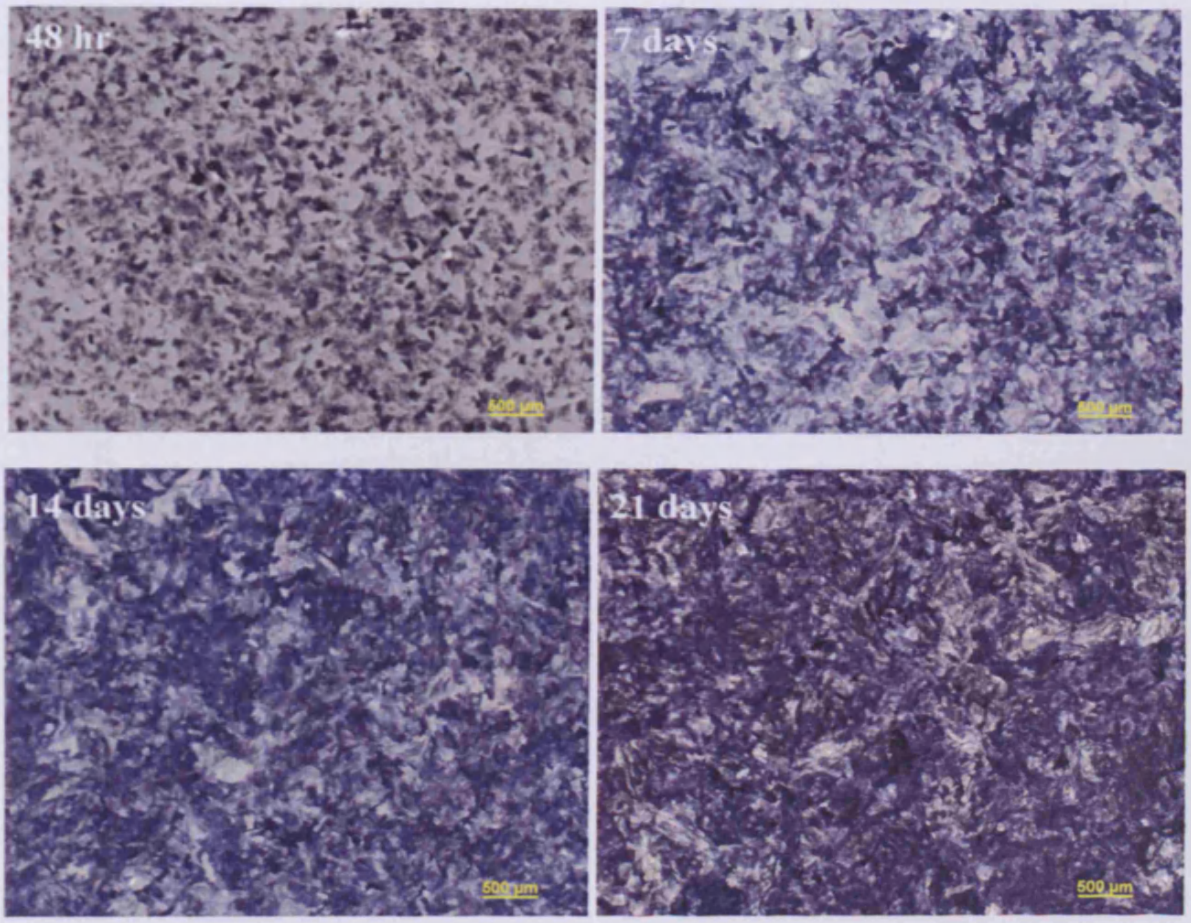

Alkaline phospatase staining of rat calvarial cells after 48 hours, 7, 14 and 21 days culturing in 60x15mm petri-dishes to test for phenotype.

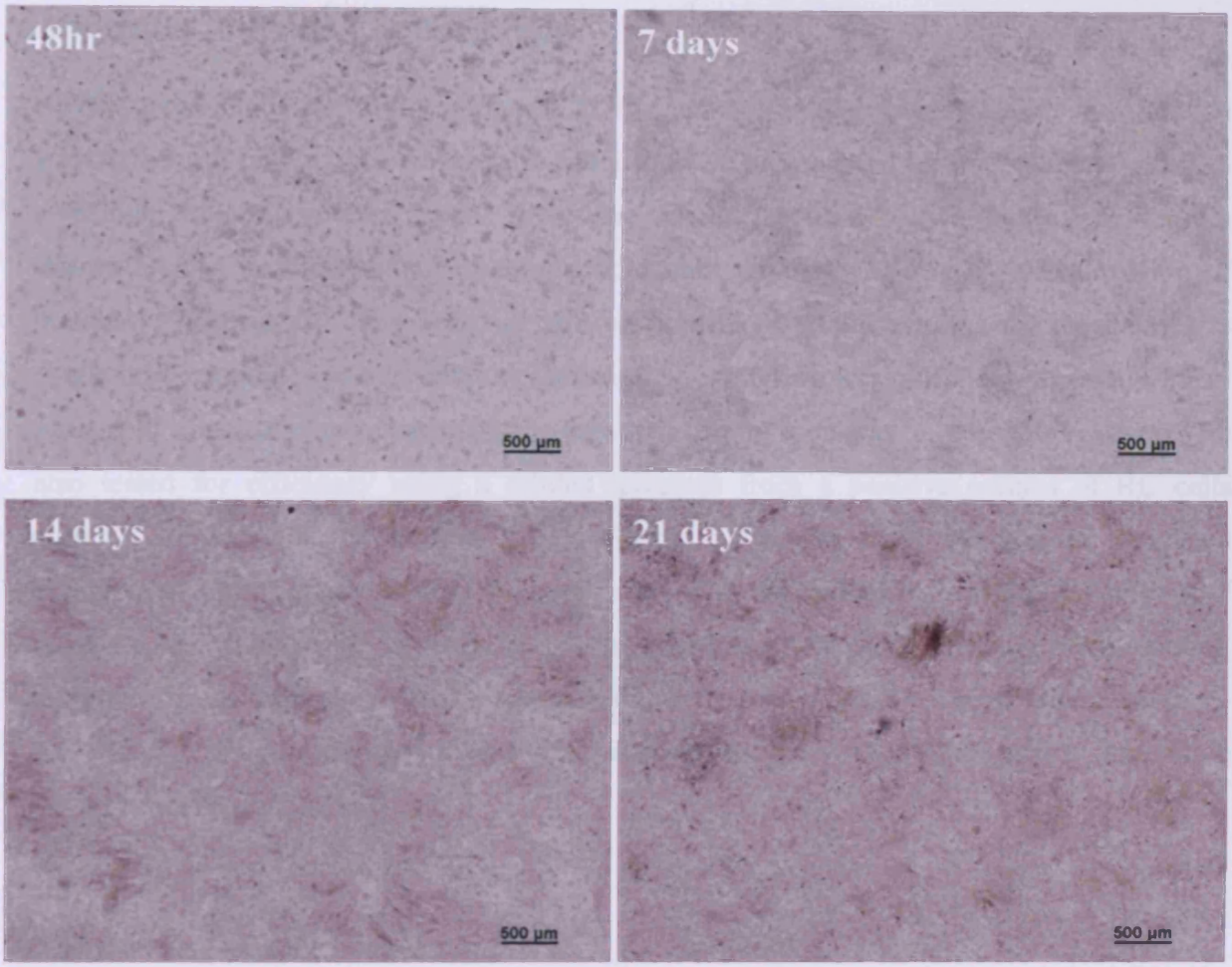

Alizarin Red-S staining of rat calvarial cells after 48 hours, 7, 14 and 21 days culturing in 60x15mm petri-dishes to test for phenotype.

*** Tyrode balanced salt solution:**

Potassium chloride	**0.2g/L**
Sodium chloride	**8.0g/L**
Sodium dihydrogenphosphate	**0.056g/L**
D-glucose	**1.0g/L**
Sodium hydrogencarbonate	**1.0g/L**

Appendix F: Primer optimisation.

SYBR green binds all double stranded DNA, emitting a fluorescent signal of a defined wavelength on binding. However, non-specific PCR products and primer dimers will also contribute to the fluorescent signal. Therefore, when using SYBR green the cycling program should always be followed by melting curve analysis. This allows for identification of potential contaminants. The presence of one prominent peak indicates the presence of a single homogenous product while the inclusion of primer dimers will result in an additional peak with a melting temperature that is less than that of the specific product. Primers were also tested for efficiency using a diluted template from a positive control of RC cells cultured in a $75cm^2$ flask until sub-confluent. Since the PCR reaction is based on exponential amplification, if the efficiency of the PCR amplification is 100% the amount of template will double with each cycle, and the standard curve plot of the log of the starting template versus PCR cycles will generate a linear fit with a slope between approximately -3.1 and -3.6 which represents a 90-110% reaction efficiency which is typically acceptable for accurate quantification.

A

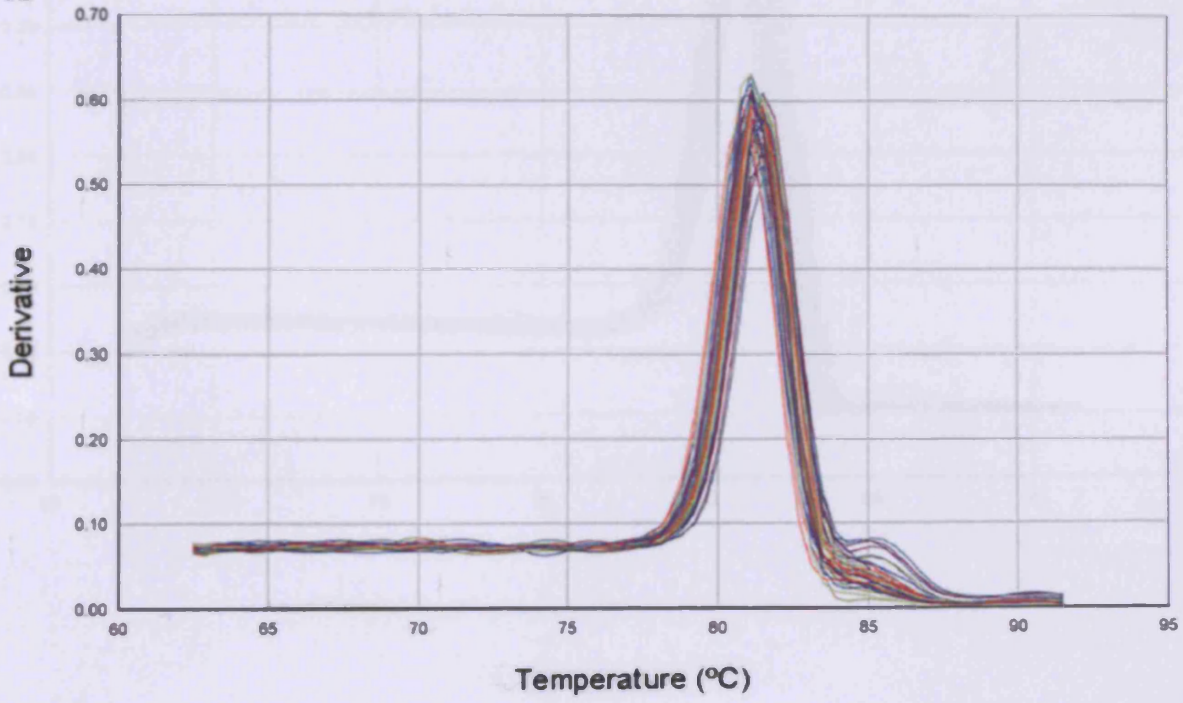

B

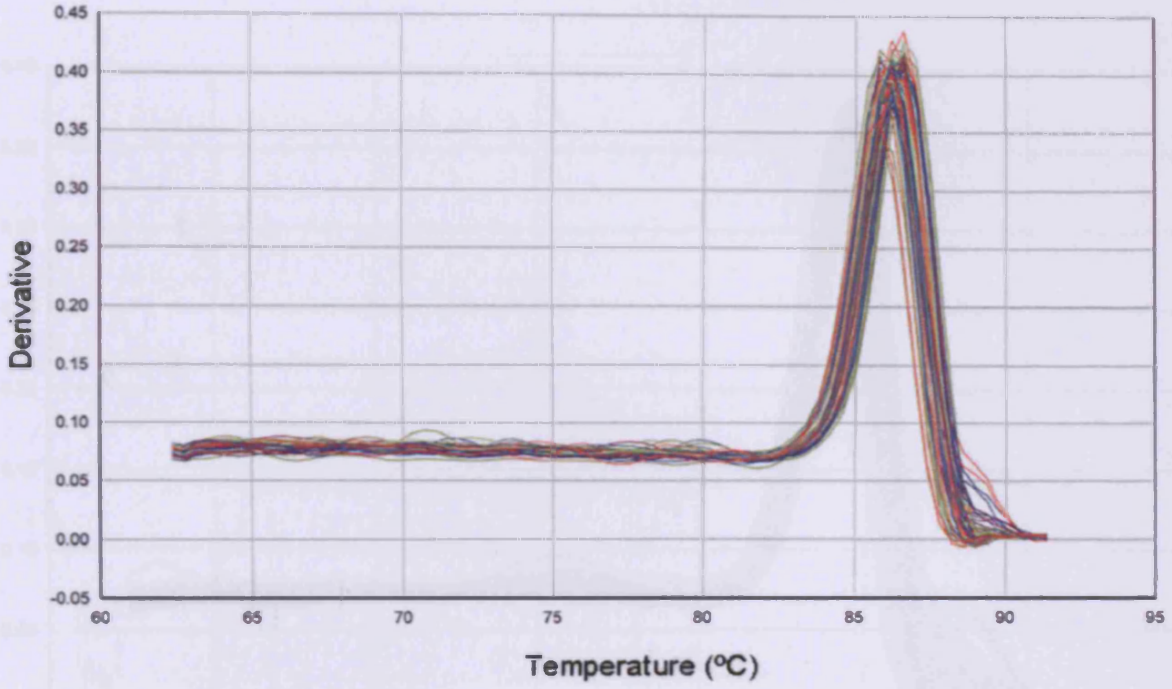
Derivative
0.45
0.40
0.35
0.30
0.25
0.20
0.15
0.10
0.05
0.00
-0.05
60
65
70
75
80
85
90
95
Temperature (°C)

C

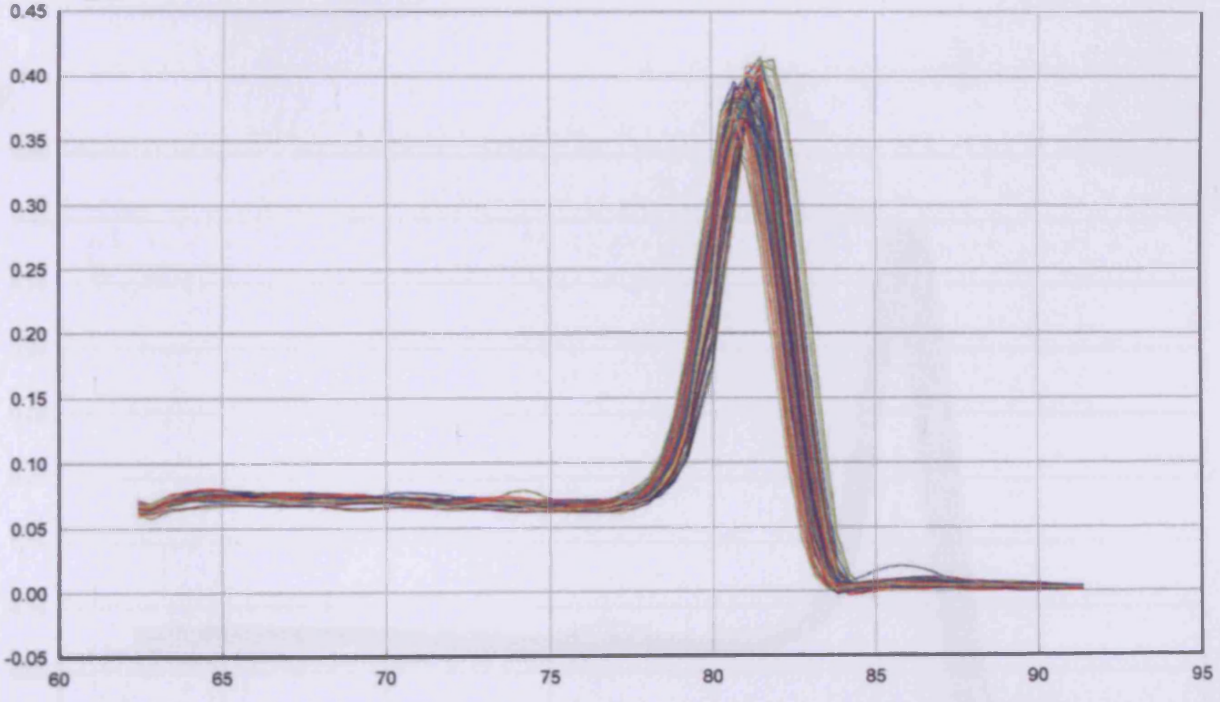
0.45
0.40
0.35
0.30
0.25
0.20
0.15
0.10
0.05
0.00
-0.05
60
65
70
75
80
85
90
95

D

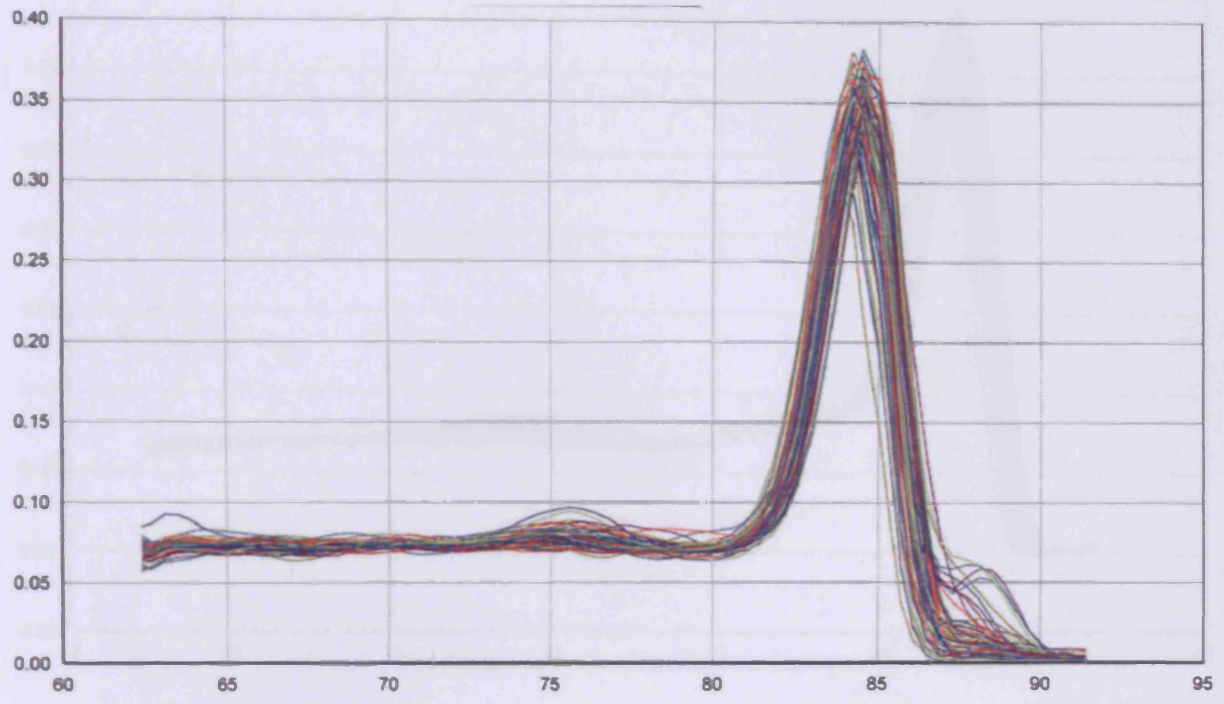
0.40
0.35
0.30
0.25
0.20
0.15
0.10
0.05
0.00
60
65
70
75
80
85
90
95

E

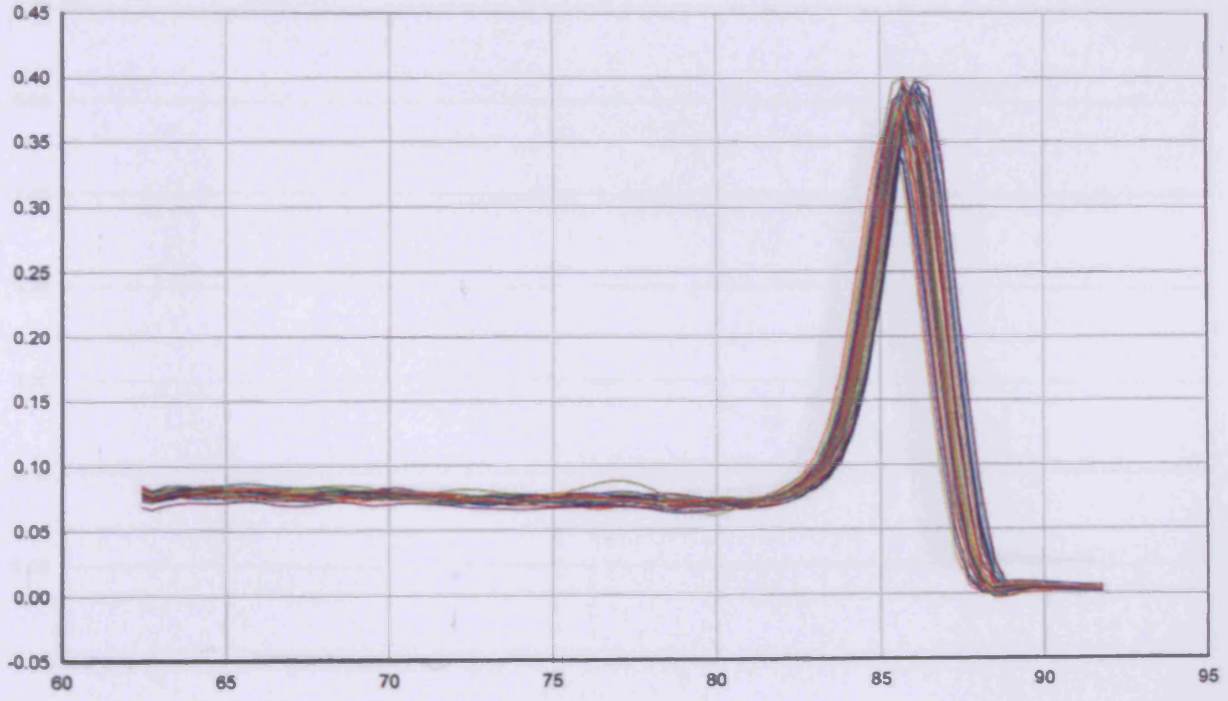
0.45
0.40
0.35
0.30
0.25
0.20
0.15
0.10
0.05
0.00
-0.05
60
65
70
75
80
85
90
95

F

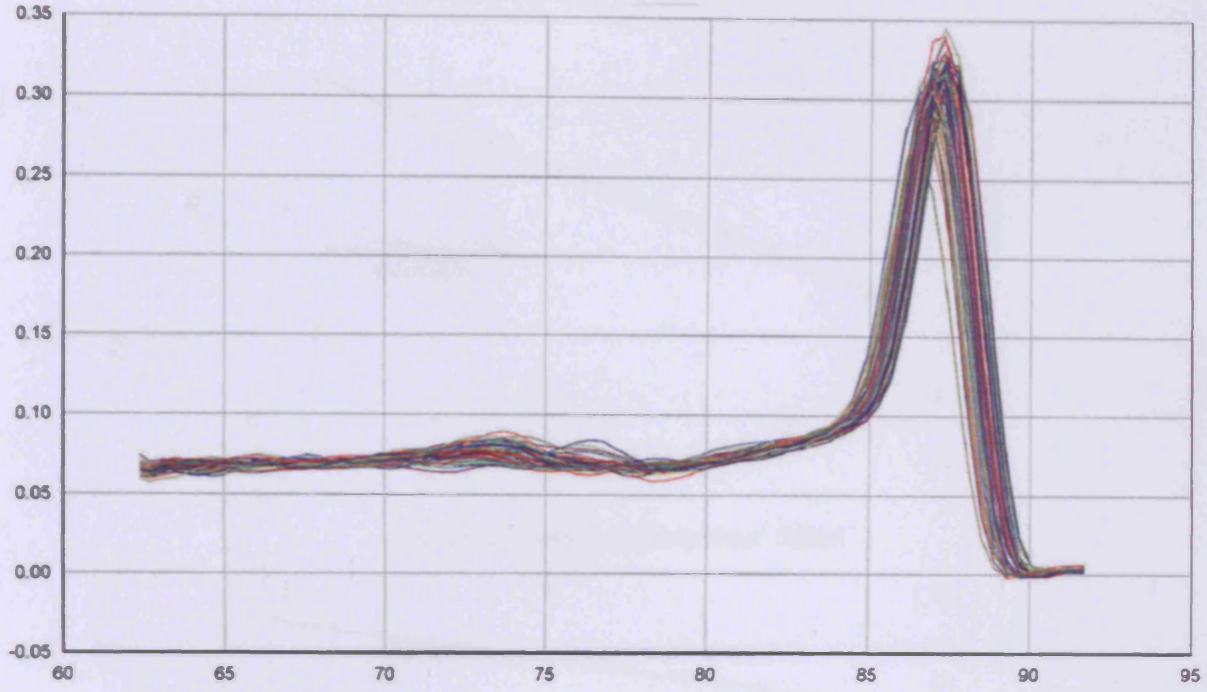

G

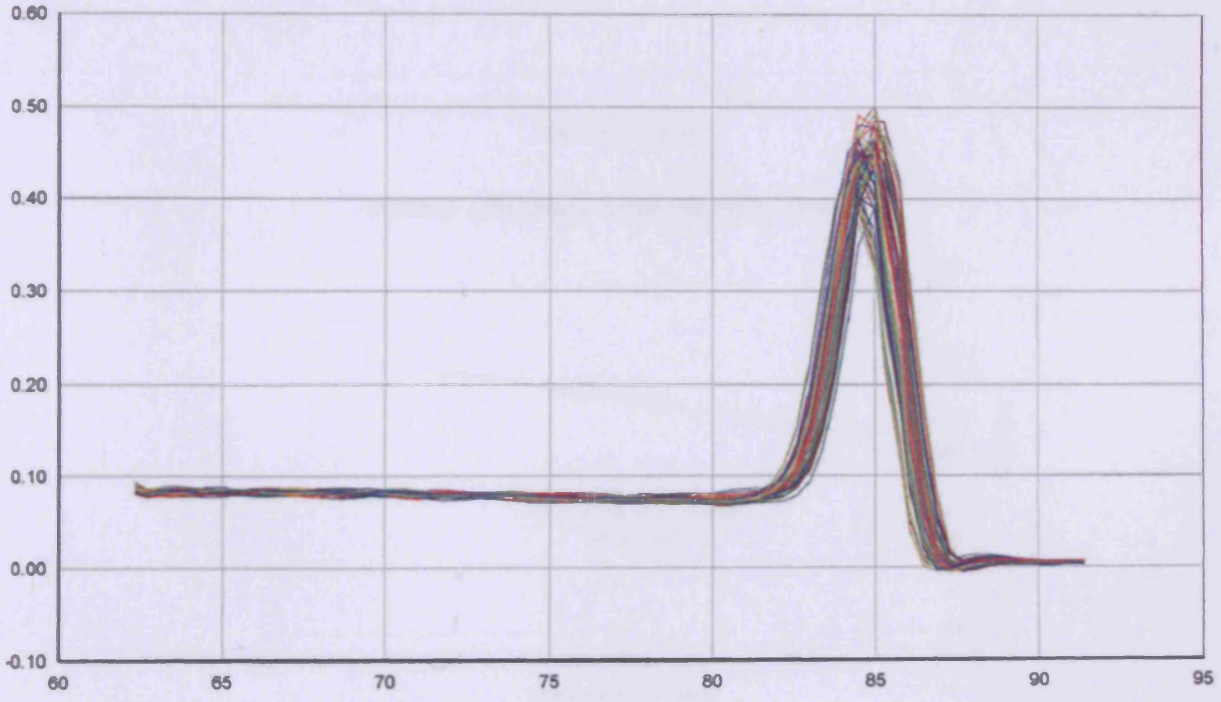

Dissociation curves for the primers used in this study. Note that for each primer one dominant peak is present indicating the presence of one product. A – 18S; B – Type I Collagen; C – Cbfa-1; D – Osterix; E - Alkaline phosphatase; F – Bone sialoprotein II; G – Osteocalcin.

Primer efficiency optimisation: 18S

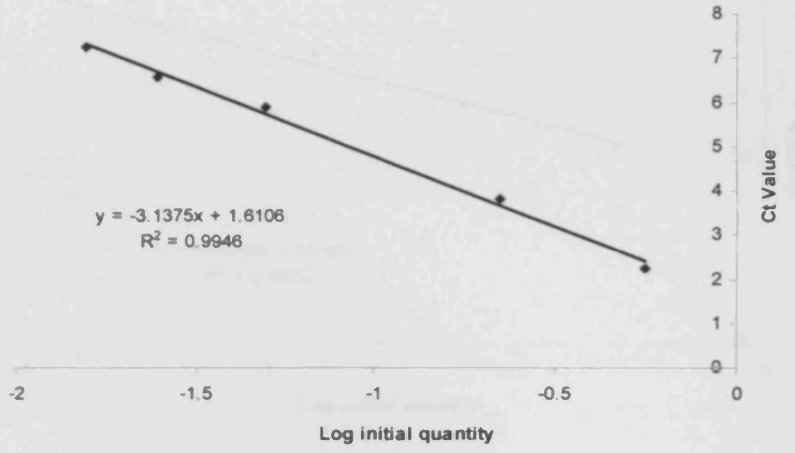

Primer efficiency optimisation: COL1

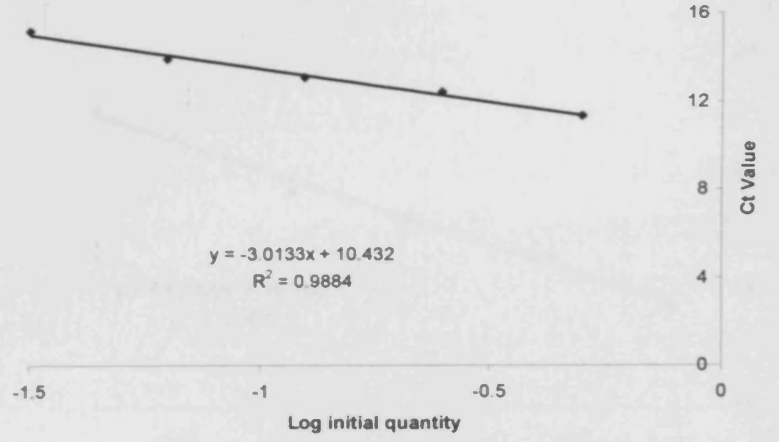

Primer efficiency optimisation: Osterix

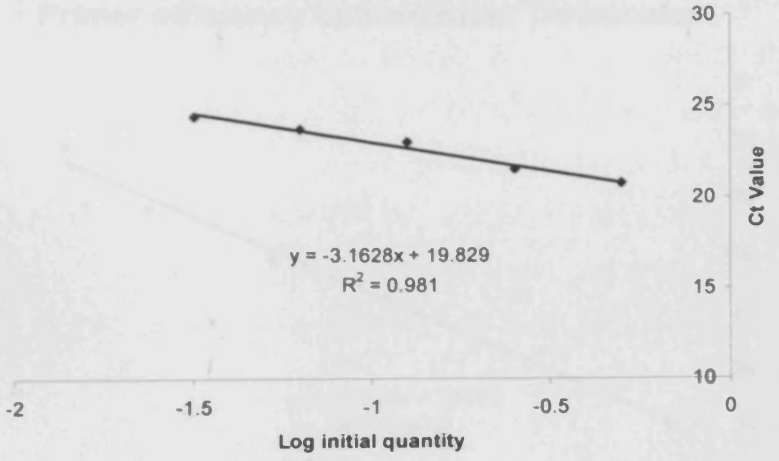

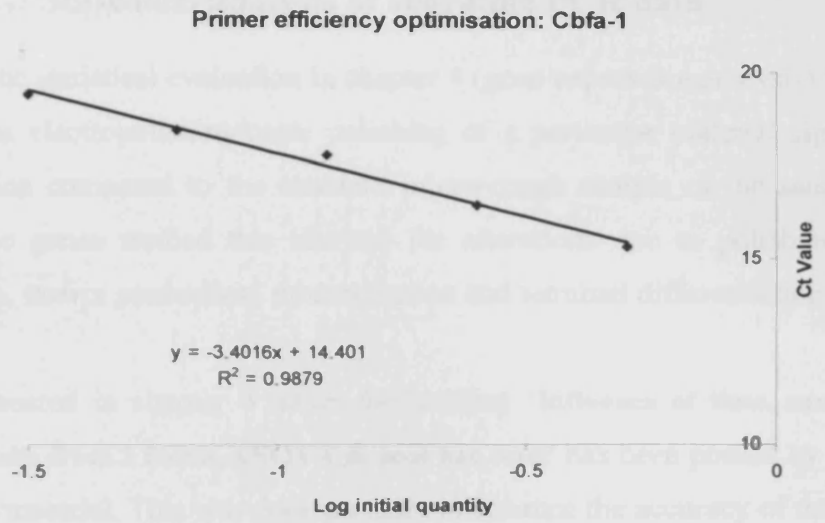
Primer efficiency optimisation: Cbfa-1
y = -3.4016x + 14.401
R² = 0.9879
Ct Value
Log initial quantity
20
15
10
-1.5
-1
-0.5
0

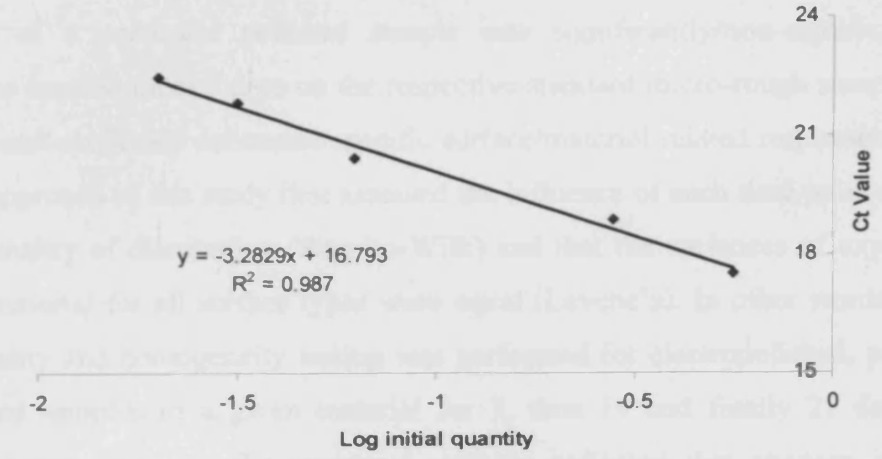
Primer efficiency optimisation: Bone Sialoprotein
y = -3.2829x + 16.793
R² = 0.987
Ct Value
Log initial quantity
24
21
18
15
-2
-1.5
-1
-0.5
0

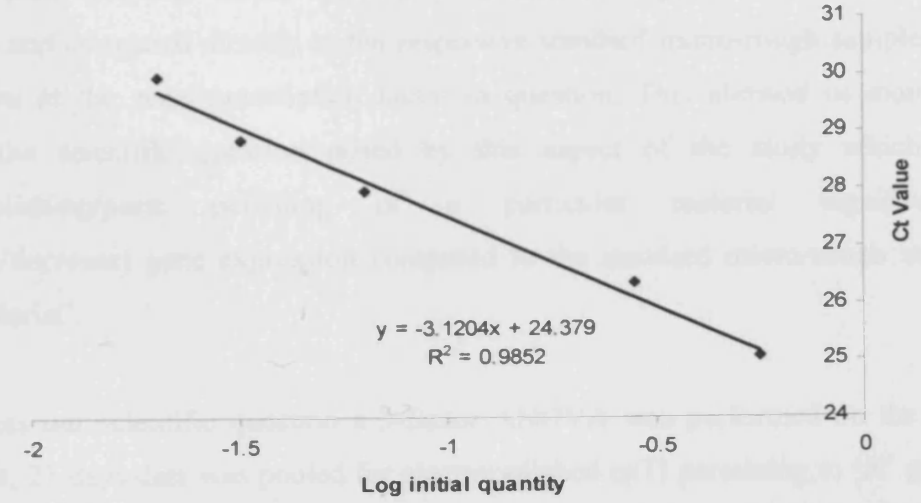
Primer efficiency optimisation: Osteocalcin
y = -3.1204x + 24.379
R² = 0.9852
Ct Value
Log initial quantity
31
30
29
28
27
26
25
24
-2
-1.5
-1
-0.5
0

Appendix G: Statistical analysis of real-time PCR data

The basis of the statistical evaluation in chapter 4 (gene expression analysis) is related to the question 'does electropolishing/paste polishing of a particular material significantly alter gene expression compared to the standard micro-rough sample of the same material'. In context of the genes studied this allowed for alterations due to polishing in osteoblast differentiation, matrix production, mineralisation and terminal differentiation to be assessed.

The data presented in chapter 4 under the heading '**Influence of time, surface finish and material: Results from 3 factor ANOVA & post hoc tests**' has been pooled by timepoint for a given surface/material. This was done partially to enhance the accuracy of the normality and homogeneity testing due to the relatively low 'n' number at each time point for a given sample. The p values quoted represent the significant/non-significant observations relating to whether a particular surface type affected the gene expression, not if the gene expression at 7 days of a particular polished sample was significantly/non-significantly altered compared to expression at 7 days on the respective standard micro-rough sample. While the latter approach obviously delineates specific surface/material related responses at each time point, the approach of this study first assessed the influence of each time point as a factor by testing normality of distribution (Shapiro-Wilk) and that the variances of expression for a particular material for all surface types were equal (Levene's). In other words, for a given gene normality and homogeneity testing was performed for electropolished, paste polished and standard samples of a given material for 7, then 14 and finally 21 days. As these assumptions were met i.e. the statistical analysis indicated that changes in expression between different surface finishes of a given material were similar, it was decided that the data for each timepoint would therefore be pooled for a given surface treatment of each material, and compared directly to the respective standard micro-rough samples for overall expression of the gene/transcription factor in question. This allowed us more broadly to answer the scientific question posed by this aspect of the study which was 'does electropolishing/paste polishing of a particular material significantly alter (increase/decrease) gene expression compared to the standard micro-rough sample of the same material'.

To address our scientific question a 3-factor ANOVA was performed on the pooled data (i.e. 7, 14, 21 days data was pooled for electropolished cpTi pertaining to 'X' gene) relating to the factors surface, material and time. This permitted the individual influence of each

factor to be evaluated on gene expression while also allowing the interaction of the factors to be delineated. Subsequent to global significances being elucidated by the ANOVA, we were able to also perform post-hoc tests to delineate which means contributed to the observed effect on gene expression for a given sample. Two post-hoc tests were employed. The Bonferroni post-hoc test was applied when assumptions relating to normal data distribution and homogeneity were met. When assumptions regarding homogeneity were not met, the Games-Howell post-hoc test was applied. This post hoc test is still applicable in an ANOVA setting as the latter is robust to violations to the assumption of homogeneity. Using the Games-Howell post hoc test adjusts for these violations of homogeneity and therefore can be used with ANOVA.

However, in the interest of providing the most comprehensive view of the effect of polishing on gene expression we also performed analysis relating to the differences in gene expression between surface treatments of a particular material at each time point which are summarised also in chapter 4 under the heading '**Influence of surface over time: Results from Univariate ANOVA and Bonferroni post hoc test**'. Normality and homogeneity tests were performed on data from each time point for a given material. Univariate ANOVA analysis delineated the influence of surface type at specific time points on gene expression and Bonferroni post-hoc tests were carried out for individual comparisons between surfaces of a given material at each time point.

Appendix H: Histological staining methodology

Histological staining of sections with Giemsa-Eosin

Sectioned samples were placed in 1% formic acid for 30 seconds, followed by rinsing in running tap water for approximately 5 minutes. Sections were then rinsed in double distilled water and placed in 15% Giemsa solution, and incubated at 57° on a hot plate, for 75 minutes before being rinsed with dH_2O. Subsequently, the sections were placed in 1% Eosin for 5 minutes. Sections were then placed into 70% ethanol, followed by a rinsing in 96% ethanol and finally, two rinses in absolute ethanol for two minutes and then blotted dry.

Solutions

1% Formic Acid (per 100ml)
98.8ml dH2O
1.2ml Formic acid (85%) (Fluka, 06460)

15% Giemsa (per 100ml)
85ml double dH2O
15ml Giemsa (Fluka, 48900)

1% Eosin (per 100ml)
1g Eosin (Fluka, 45240; CI # 45380)
100ml ddH_2O

Appendix I: Sample variability.

Surface variability has been a major issue through the course of this study. Below, are examples of the varying surface morphologies and roughness profiles accrued for different batches of 13mm sample discs received during the course of this study. For cpTi samples, TE appears to have the most dramatic overall changes in morphology. TP also shows a high variability between batches, while TS remains generally consistent, but differences in surface morphology are clearly apparent. TAN 13mm samples were observed to have some of the greatest inter-batch variability. Again, NE was considered the most variable; however batch C of the TAN samples varied considerably compared to previous batches. The main differences observed between batches of Ti15Mo samples is the changes in nano-topography within the grains of the MS discs, the variation in dimension and frequency of undulations on the ME sample discs, and the loss/reduction of the basket weave pattern of MP samples.

Inter-batch variability of 13mm samples

Commercially pure titanium.

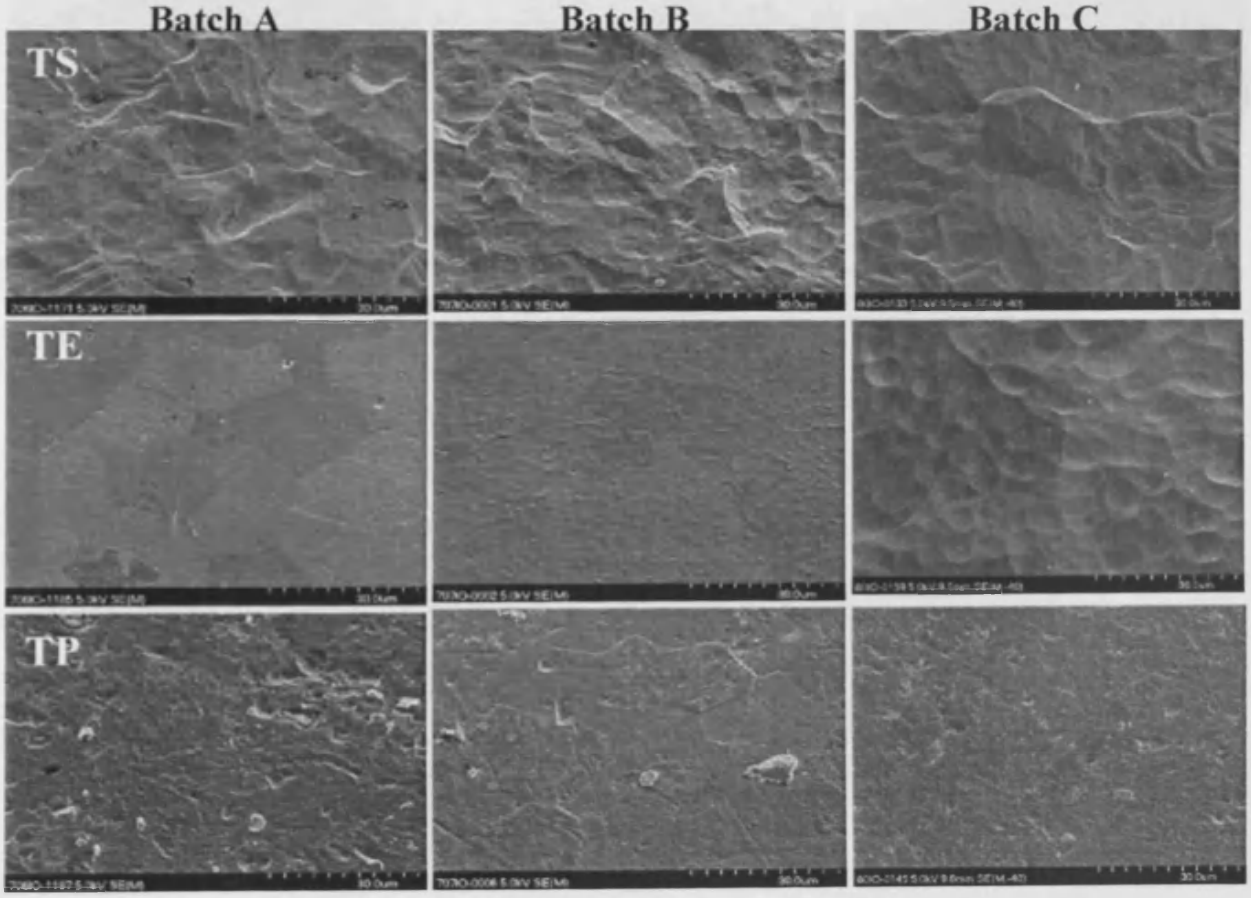

Titanium-6%Aluminium-7%Niobium

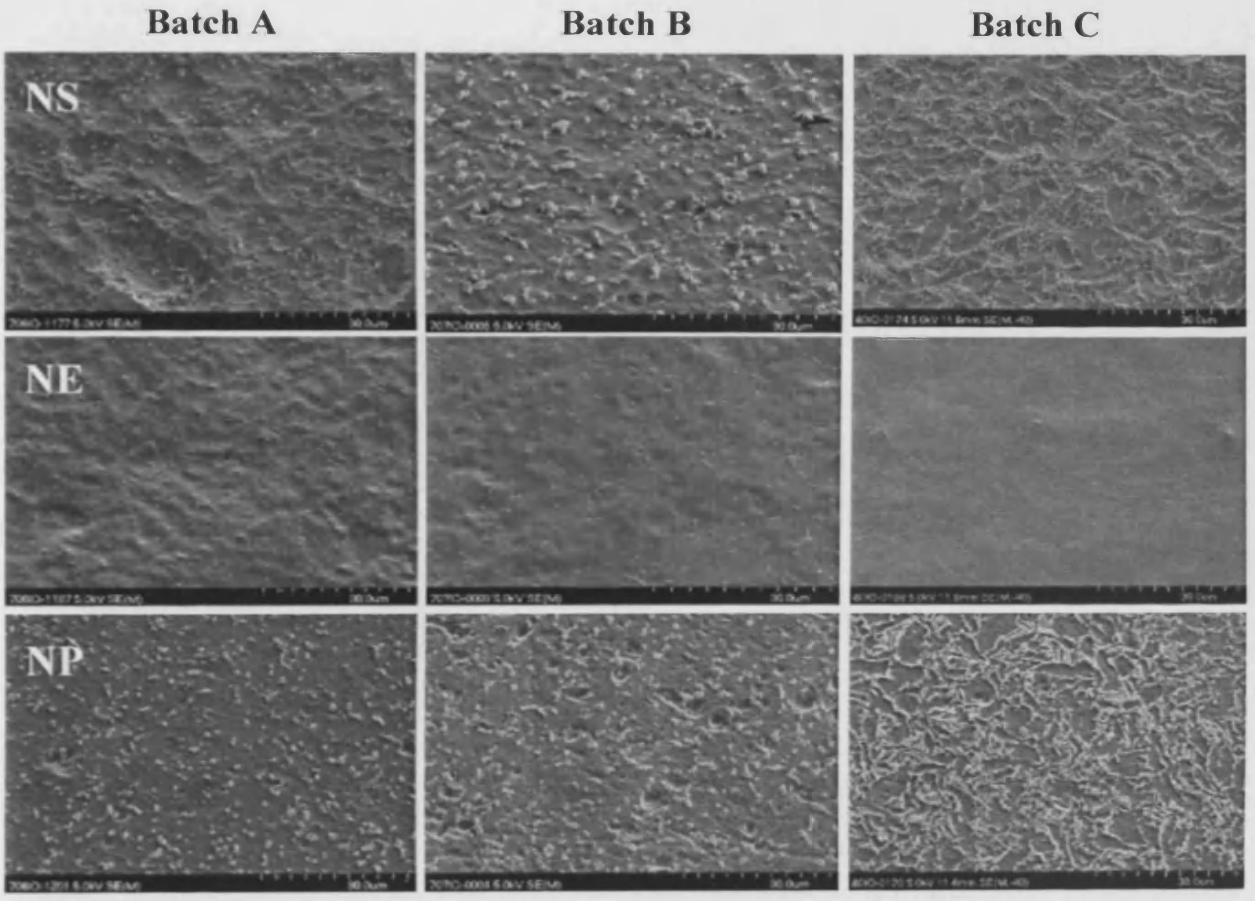

Titanium-15%-Molybdenum

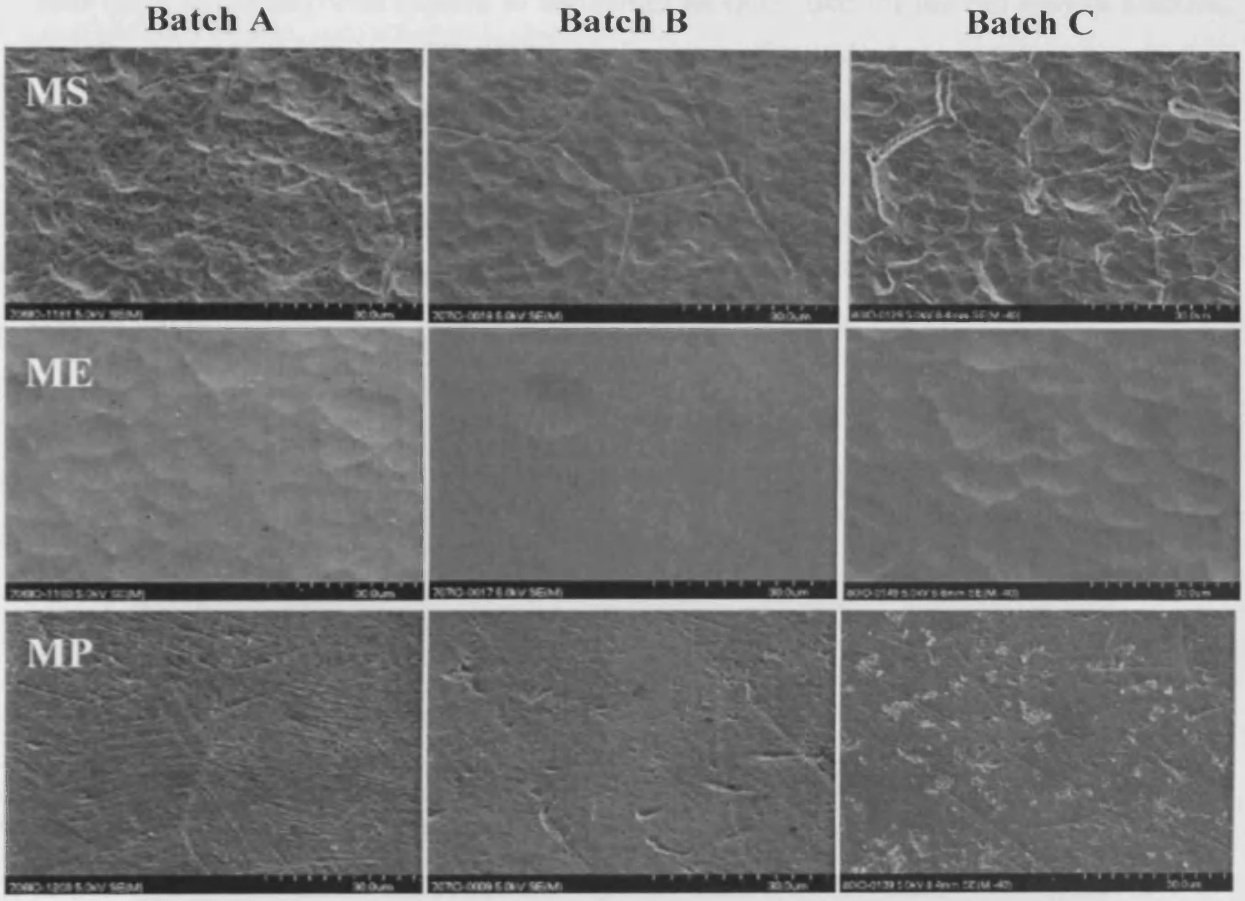

Stainless steel:

Variability between 13mm and 50mm samples:

Inter-batch variability with regards to the 13mm samples used for the cell growth kinetics, viability and cytoskeletal portion of this study, is clearly evident above. However, further variability between these and the large 50mm samples used for real-time PCR experiments, was also evident, which renders comparisons between studies tentative. Although one must note that the samples used for *in vitro* analysis were those from the final batch (image far right), which overall are a good reflection of the surface morphology of their 50mm counterparts.

Commercially pure titanium:

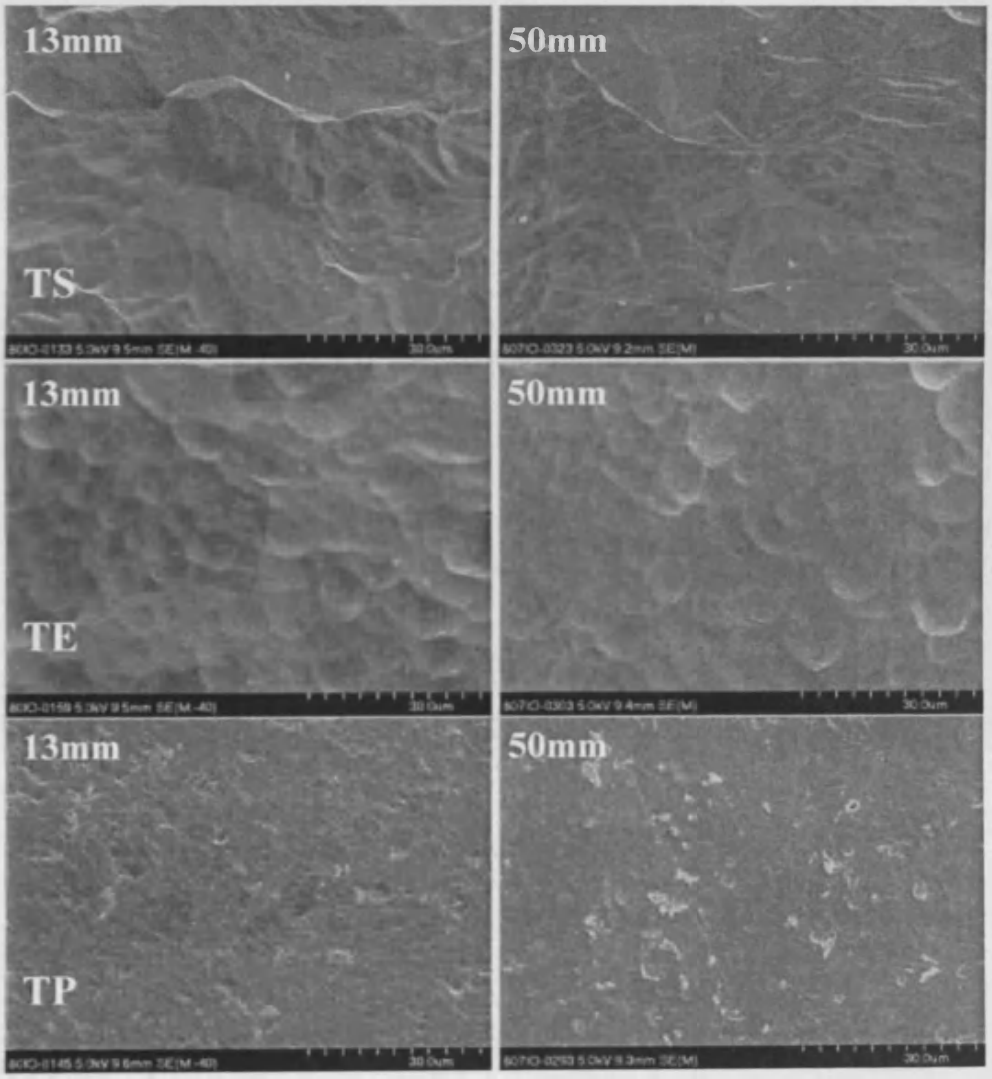

Titanium-6%Aluminium-7%Niobium

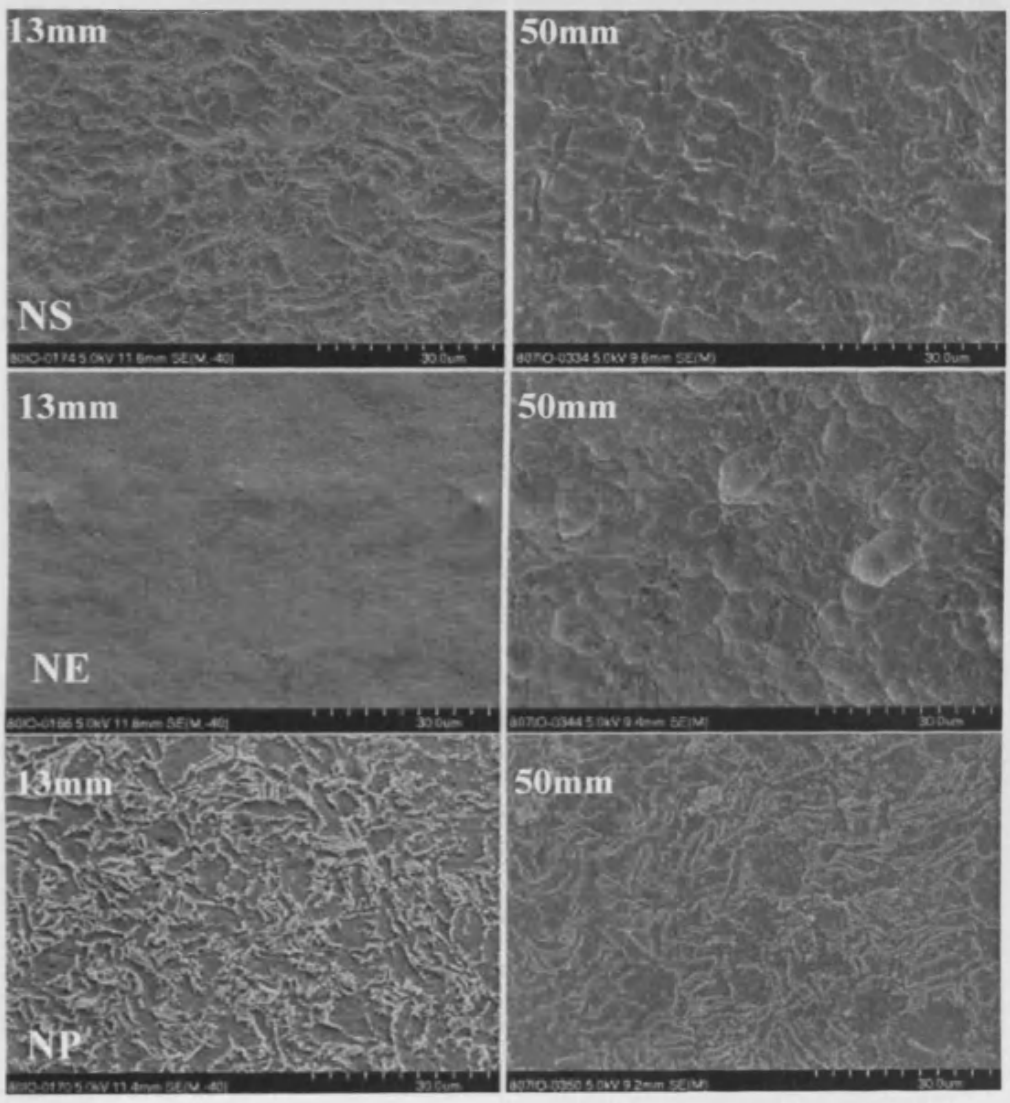

Titanium-15%-Molybdenum

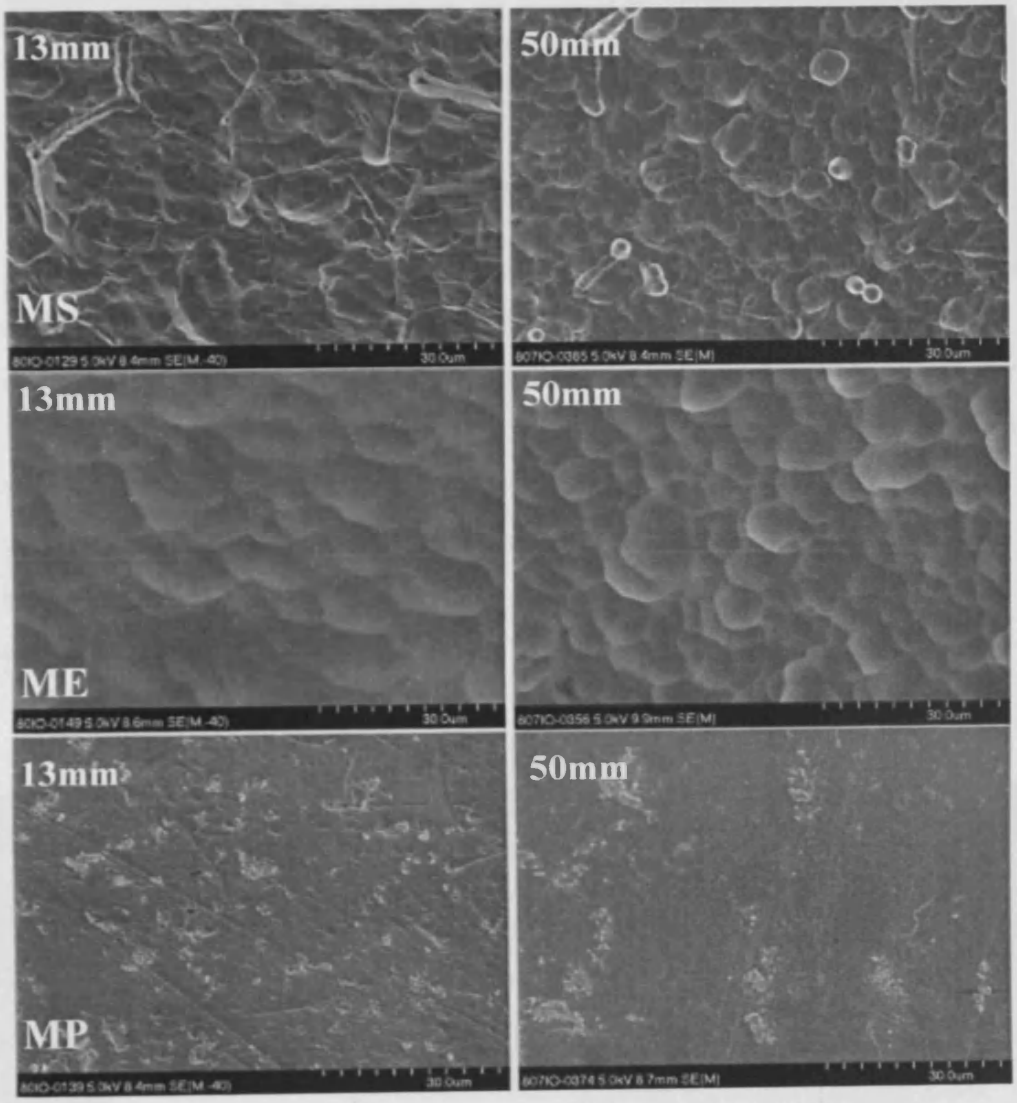

Stainless steel:

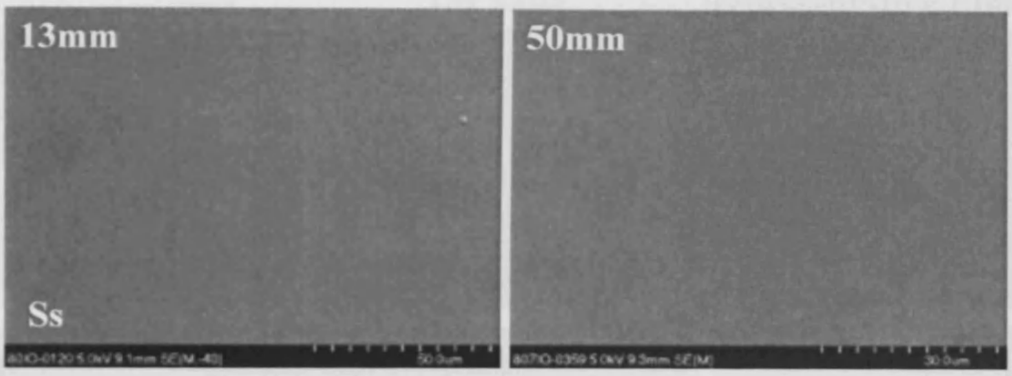

Variability between discs, screws, and nails:

This section is included to highlight the differences in surface morphology between similar materials used for different implant applications. The images below depict the 13mm samples used for *in vitro* work, as well as the TAN cortical screws, cpTi LCPS and TAN IM nails used for *in vivo* work.

Commercially pure titanium:

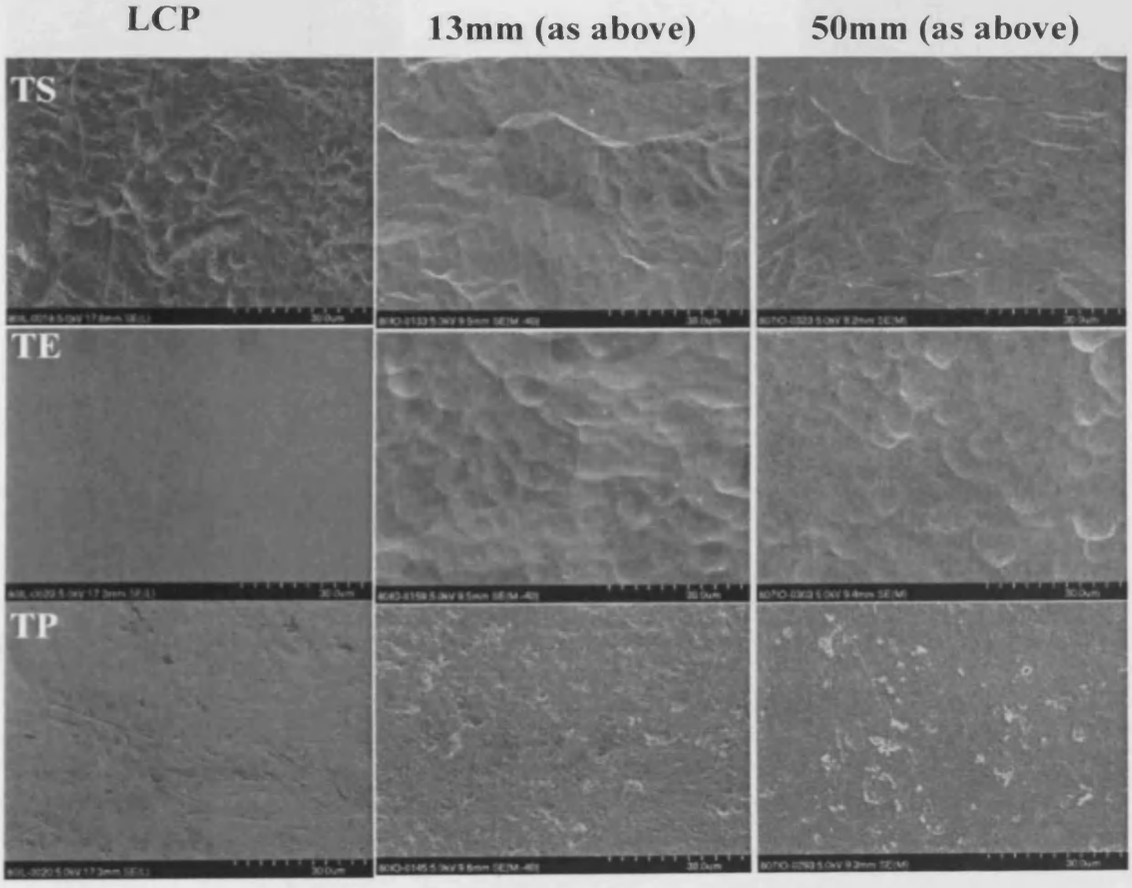

Titanium-6%Aluminium-7%Niobium

Cortical screws	IM nails	Representative 13mm disc
NS 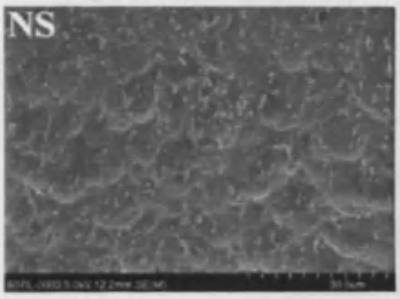	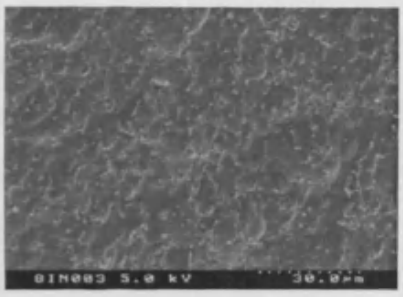	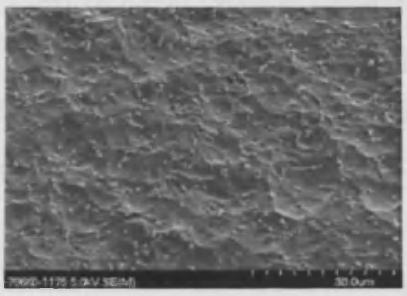
NP 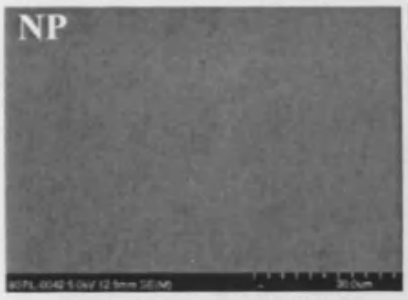	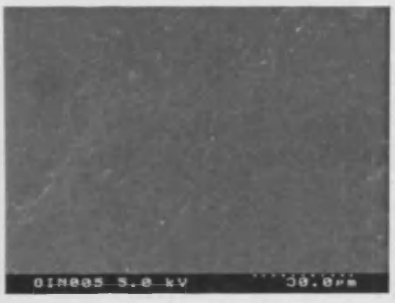	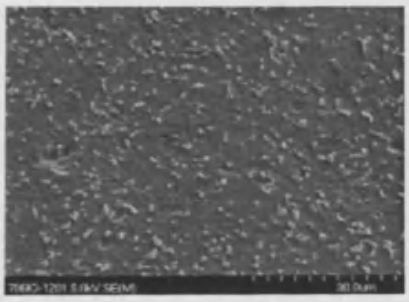
NE 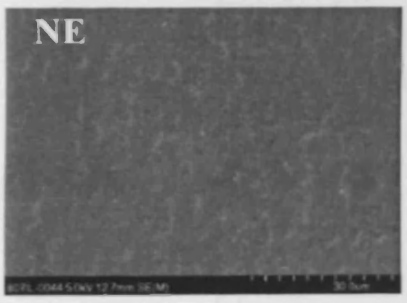	No NE was included in this study.	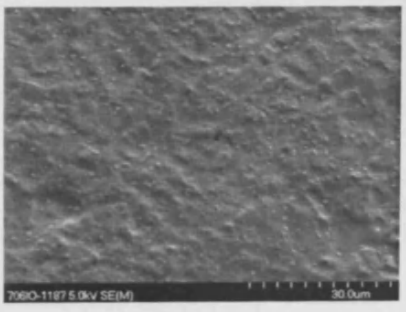

The following box-plot graphs are included to highlight the variability observed for samples used in this study. The values represent average roughness of the various 13mm and 50mm samples. It is clear from these graphs that a many of the values of standard samples overlap with those of polished samples, and therefore, indicates that many of the difficulties encountered with reproducibility, are largely attributable to these roughness variations. Even our Ss control showed a high degree of variability; however this was confined to one particular batch, which was excluded from the study.

Commercially pure titanium

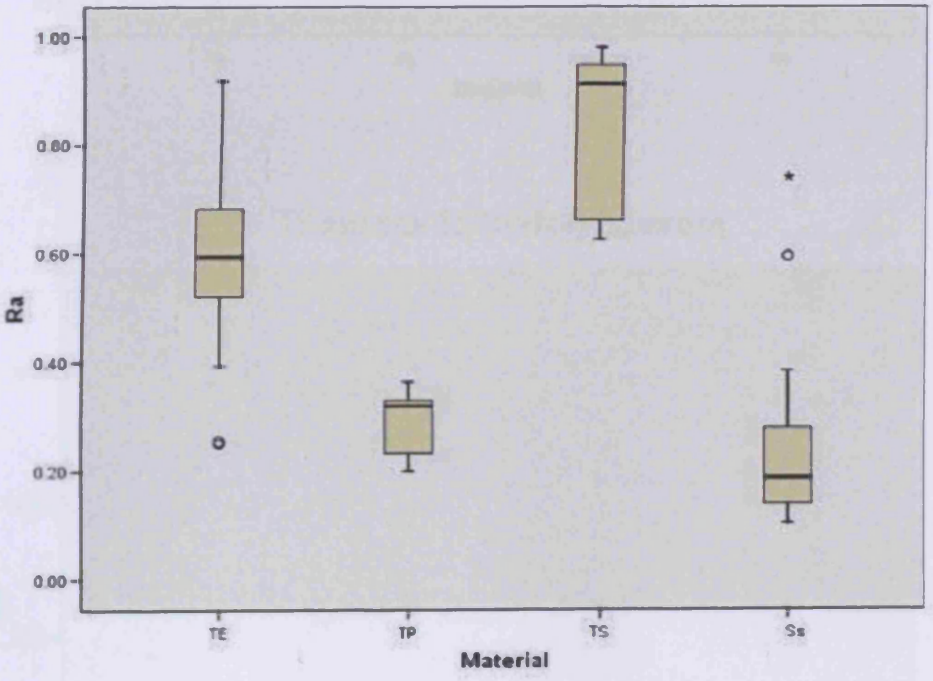

Titanium-6%Aluminium-7%Niobium

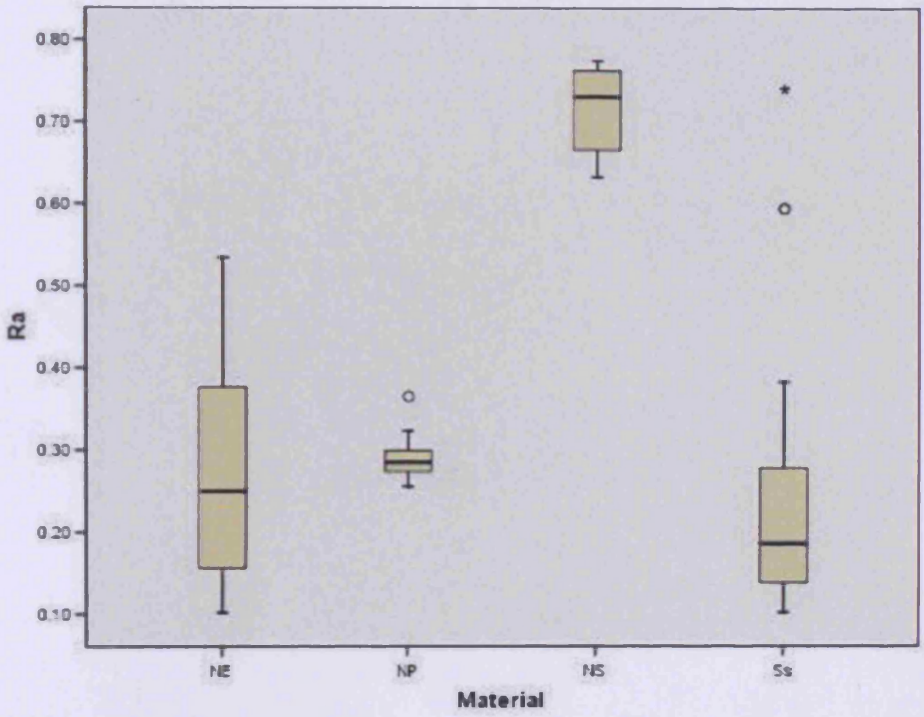

Titanium-15%Molybdenum